frontiers | Research Topics

Advances in diagnostics and management of adrenal tumors

Edited by
Piotr Glinicki, Marta Araujo-Castro and Nadia Sawicka-Gutaj

Published in
Frontiers in Endocrinology

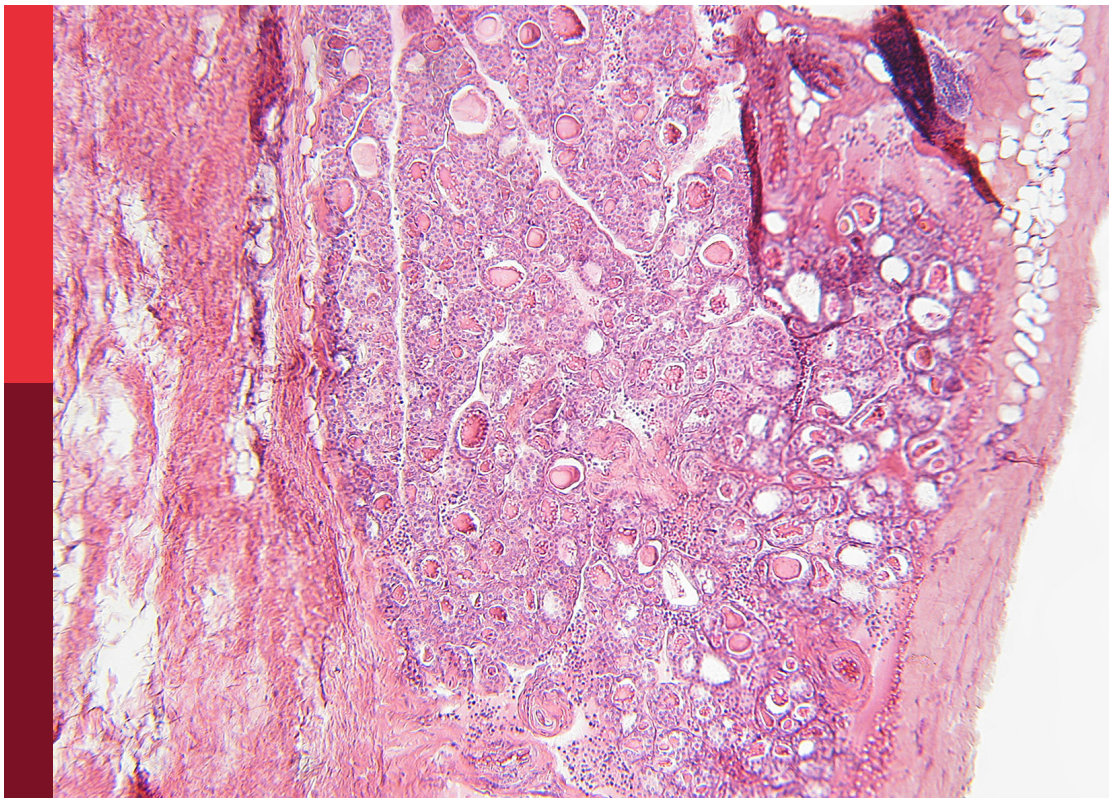

ISSN 1664-8714
ISBN 978-2-8325-5996-3
DOI 10.3389/978-2-8325-5996-3

About Frontiers

Frontiers is more than just an open access publisher of scholarly articles: it is a pioneering approach to the world of academia, radically improving the way scholarly research is managed. The grand vision of Frontiers is a world where all people have an equal opportunity to seek, share and generate knowledge. Frontiers provides immediate and permanent online open access to all its publications, but this alone is not enough to realize our grand goals.

Frontiers journal series

The Frontiers journal series is a multi-tier and interdisciplinary set of open-access, online journals, promising a paradigm shift from the current review, selection and dissemination processes in academic publishing. All Frontiers journals are driven by researchers for researchers; therefore, they constitute a service to the scholarly community. At the same time, the *Frontiers journal series* operates on a revolutionary invention, the tiered publishing system, initially addressing specific communities of scholars, and gradually climbing up to broader public understanding, thus serving the interests of the lay society, too.

Dedication to quality

Each Frontiers article is a landmark of the highest quality, thanks to genuinely collaborative interactions between authors and review editors, who include some of the world's best academicians. Research must be certified by peers before entering a stream of knowledge that may eventually reach the public - and shape society; therefore, Frontiers only applies the most rigorous and unbiased reviews. Frontiers revolutionizes research publishing by freely delivering the most outstanding research, evaluated with no bias from both the academic and social point of view. By applying the most advanced information technologies, Frontiers is catapulting scholarly publishing into a new generation.

What are Frontiers Research Topics?

Frontiers Research Topics are very popular trademarks of the *Frontiers journals series*: they are collections of at least ten articles, all centered on a particular subject. With their unique mix of varied contributions from Original Research to Review Articles, Frontiers Research Topics unify the most influential researchers, the latest key findings and historical advances in a hot research area.

Find out more on how to host your own Frontiers Research Topic or contribute to one as an author by contacting the Frontiers editorial office: frontiersin.org/about/contact

Advances in diagnostics and management of adrenal tumors

Topic editors

Piotr Glinicki — EndoLab Laboratory, Centre of Postgraduate Medical Education, Poland

Marta Araujo-Castro — Ramón y Cajal University Hospital, Spain

Nadia Sawicka-Gutaj — Poznan University of Medical Sciences, Poland

Citation

Glinicki, P., Araujo-Castro, M., Sawicka-Gutaj, N., eds. (2025). *Advances in diagnostics and management of adrenal tumors*. Lausanne: Frontiers Media SA. doi: 10.3389/978-2-8325-5996-3

Table of contents

frontiers | Frontiers in Endocrinology

TYPE Editorial
PUBLISHED 30 January 2025
DOI 10.3389/fendo.2025.1543773

OPEN ACCESS

EDITED AND REVIEWED BY
Henrik Falhammar,
Karolinska Institutet (KI), Sweden

*CORRESPONDENCE
Piotr Glinicki
piotr.glinicki@bielanski.med.pl
Marta Araujo-Castro
marta.araujo@salud.madrid.org

RECEIVED 11 December 2024
ACCEPTED 06 January 2025
PUBLISHED 30 January 2025

CITATION
Glinicki P, Sawicka-Gutaj N and Araujo-Castro M (2025) Editorial: Advances in diagnostics and management of adrenal tumors. *Front. Endocrinol.* 16:1543773. doi: 10.3389/fendo.2025.1543773

Editorial: Advances in diagnostics and management of adrenal tumors

Piotr Glinicki[1,2]*, Nadia Sawicka-Gutaj[3] and Marta Araujo-Castro[4,5]

[1]EndoLab Laboratory, Centre of Postgraduate Medical Education, Warsaw, Poland, [2]Department of Endocrinology, Centre of Postgraduate Medical Education, Warsaw, Poland, [3]Department of Endocrinology, Metabolism and Internal Medicine, Poznań University of Medical Sciences, Poznań, Poland, [4]Endocrinology & Nutrition Department, Hospital Universitario Ramón y Cajal, Madrid, Spain, [5]Instituto de Investigación Biomédica Ramón y Cajal (IRYCIS), Madrid, Spain

KEYWORDS

adrenal tumors, pheochromocytoma, paraganglioma, adrenocortical carcinoma, Cushing syndrome, primary aldosteronism, biomarkers

Editorial on the Research Topic
Advances in diagnostics and management of adrenal tumors

Adrenal tumors are a heterogeneous group of tumors characterized by diverse biology and clinical courses. They may be associated with high malignant potential and/or hormonal activity, leading to multiple complications, with cardiovascular issues being the most prevalent. Diagnosing adrenal tumors often requires complex and costly laboratory and imaging procedures, which, unfortunately, in many cases, do not provide complete certainty about the diagnosis or the nature of the neoplastic process (benign, malignant, or hormonally active). A major challenge is that hormonally active adrenal tumors or potentially malignant adrenal lesions are rare or very rare. As a result, conducting research on them is particularly difficult. One of the current research directions for this group of neoplasms is biochemical research in metabolomics and proteomics, supported by bioinformatics techniques based on artificial intelligence (AI).

The latest in biochemical diagnostics of adrenal tumors

New biochemical methods for the diagnosis and monitoring of patients with adrenal tumors are currently being developed in two parallel directions. The first line of research involves classical immunological (immunochemical) methods based on the antigen-antibody reaction. In particular, automated immunochemical methods based on the chemiluminescence reaction (CLIA, ECLIA) are being evaluated, primarily as widely available, inexpensive, and easy-to-use screening tools (1). These studies include the use of these methods as screening tests in the diagnosis of patients with suspected primary aldosteronism (PA), the feasibility and clinical value of assaying various hormones, e.g. aldosterone, direct renin concentration (DRC), plasma renin activity (PRA), and cortisol in

tests aimed at differentiating between different subtypes of PA, and, thirdly, the feasibility of assaying free hormone fractions in various biological materials (e.g., free cortisol in saliva) (2–4). The other direction involves chromatographic methods. New possibilities for biochemical diagnostics are opened by metabolomics research using modern analytical techniques: Liquid chromatography–mass spectrometry (LC-MS/MS), Gas chromatography/mass spectrometry (GC/MS) and others. The development of various chromatographic techniques, especially the LC-MS/MS technique, makes it possible to determine multiple hormones during a single analysis (e.g., steroid hormone profile in plasma or daily urine collection, free metanephrine profile in plasma, etc.) in routine diagnostics (5, 6). The introduction of the ability to determine hormone panels using various chromatographic techniques (mainly LC-MS/MS and GC/MS) into biochemical diagnostics enables new studies both in screening diagnosis of adrenal tumor lesions and in other diagnostic and therapeutic areas. An additional unique feature of hormonal profile studies in biological material from patients with adrenal tumors is their personalized nature, which can be used in the individual diagnostic-therapeutic process in a given group of patients (7, 8).

The latest in molecular diagnostics of adrenal tumors

Progress in the field of molecular studies in adrenal tumors has been made in the molecular characterization of pheochromocytoma, adrenal Cushing's syndrome, PA, and adrenocortical carcinoma (ACC). F or pheochromocytomas, although some older studies reported a prevalence of germline genetic variants in 10% - 15% of the patients, more recent studies performed with NGS (Next-generation sequencing) technology describe genetic variants in up to 35% - 40% of patients (9–11). The prevalence of genetic variants in these patients has been increasing over the years as new genes such as *CSDE1, H3F3A, MET, MERTK* and *IRP1*, have been discovered (10). Furthermore, recent advances in the study of pheochromocytomas have revealed new molecular events in these tumors. In the context of adrenal Cushing's syndrome, one of the most recent discoveries has taken place in patients with primary bilateral macronodular adrenal hyperplasia (PBMAH): the discovery of the role of variants in *KDM1A* in GIP-mediated cases of Cushing's syndrome. It was reported that 100% of the patients with PBMAH and GIP-responsive Cushing's syndrome had a germline variant in *KDM1A*, compared with 0% of patients from the control group (11). The discovery of genetic alterations such as *ARMC5* and *KDM1A* in PBMAH allows early detection of PBMAH in patients' relatives (12). Regarding PA, several genetic defects in the germline or somatic state have been identified. Although only 5% of PA are familial (13), it is currently known that approximately 90% of aldosterone-producing adenomas (APAs) are due to somatic variants in genes encoding ion channels or transporters including *KCNJ5, CACNA1D, ATP1A1*, and *ATP2B3* (14). In recent years, new somatic variants have been identified, including a new one in *CACNA1H* (15). In addition, more recently, the co-existence of *CTNNB1* with *G Protein Subunit Alpha Q (GNAQ)/G Protein Subunit Alpha 11 (GNA11)* variants has been documented in 59% of APAs (16). Finally, advances in the genetics of ACC have also been reported. Although there are not many current therapeutic options directly targeting reported ACC alterations, some studies have detected variants in *TP53, BRD9, TERT, CTNNB1, CDK4, FLT4* and *MDM2* as potentially targetable genetic alterations in patients with ACC (17). Utilizing blood-based NGS to characterize genomic alterations in advanced ACC is feasible in over 80% of patients, with 50% of them being potentially targetable (18). Thus, in conclusion, advances in the knowledge of the genetic context of functioning adrenal tumors have allowed a better characterization of these tumors, with important implications in the management of these patients, including the personalization of follow-up and treatment, and its importance in the face of genetic counseling for patients and their relatives.

The current Research Topic remains of high scientific and clinical interest and includes 23 articles.

The aim of the first article (Araujo-Castro et al.) was to compare the clinical presentation and laboratory hormonal diagnostics in patients with two forms of PA: familial hyperaldosteronism (FH) and primary hyperaldosteronism (PA). The study was a meta-analysis based on a systematic review of the literature to identify patients with FH. A total of 360 FH cases (246 FH type I, 73 type II, 29 type III and 12 type IV) and 830 sporadic PA patients (from the SPAIN-ALDO registry) were included in the study. Analysis of the results showed a different clinical presentation in patients with FH-I and III compared to sporadic forms of PA. In this regard, FH-I is characterized by a low prevalence of hypokalemia, while FH-III is characterized by severe aldosterone over-secretion causing hypokalemia in more than 85% of patients. The clinical and hormonal phenotype of types II and IV is similar to that of patients with sporadic PA.

Another original article (Liu et al.) focused on the evaluation of postoperative management of patients with pheochromocytoma assessing hemodynamic stability as one of the main causes of serious complications after surgical treatment, and in extreme cases leading to patient death.

The aim of this retrospective study by Canu et al. was to evaluate changes in Luteinizing hormone (LH), sex hormone binding globulin (SHBG), total testosterone (TT) and calculated free testosterone (cFT), the prevalence and type of hypogonadism and sexual function, the latter before and after androgen replacement therapy (ART) in patients with ACC treated with adjuvant mitotane therapy (AMT). The authors suggested monitoring LH, SHBG, TT and cFT and sexual function during AMT, and starting ART in hypogonadal patients with ACC with sexual dysfunction.

The research group of Araujo-Castro et al. sought to evaluate the prevalence of recurrence in patients with pheochromocytomas and sympathetic paragangliomas (PGLs; collectively referred to as PPGLs) and to identify predictors of recurrence (local recurrence and/or metastatic disease). This retrospective multicenter study included information on 303 patients with PPGLs in follow-up in 19 Spanish tertiary hospitals. The conclusions of this study are that since PPGL recurrence can occur at any time after the initial

diagnosis of PPGL, it is recommended to closely follow up with all patients with PPGL, especially those with a higher risk of recurrence.

In a different article, researchers (Vetrivel et al.) performed a transcriptomic analysis of adrenal signaling pathways in different forms of endogenous Cushing's syndrome to define areas of dysregulation and targets that can be treated. NGS analysis was performed on adrenal samples from patients with PBMAH (n = 10) and control adrenal samples (n = 8). Validation groups included cortisol-producing adenoma (CPA, n=9) and samples from patients undergoing bilateral adrenalectomy for Cushing's syndrome (BADX-CD, n=8). This project concluded that the therapeutic effect was independent of the actions of ACTH, postulating a promising application of PPARG activation in endogenous hypercortisolism.

According to Díaz-López et al., severe hypokalemia leading to rhabdomyolysis (RML) in PA is a rare occurrence, with only a few cases reported in the last four decades. Their systematic review and case report aimed to gather all published data regarding hypokalemic RML as a presentation of PA, in order to contribute to the early diagnosis of this extremely rare condition. Early detection and management are essential to reduce the frequency of complications such as acute kidney injury.

Mansour et al. investigated an integrated diagnostic approach to predict the source of aldosterone overproduction in PA. A total of 269 patients with PA from the prospective German Conn Registry were included in this study. The integration of clinical parameters into a radiomics machine learning model improved the prediction of the source of aldosterone overproduction and subtyping in the patients.

Szatko et al. prepared a mini-review summarizing current data on the pathophysiological pathways of cardiac damage caused by catecholamines, the clinical presentation of PPGL-induced cardiomyopathies, and discussion of treatment options.

The aim of another included study (Berndt et al.) was to assess the diagnostic value of salivary cortisol and cortisone in patients with suspected hypercortisolism including 155 patients with adrenal incidentaloma, and 54 patients with suspected Cushing's syndrome. The authors concluded that late-night salivary cortisol is not sufficiently sensitive or specific to be used for screening patients with suspected hypercortisolism. Instead, late-night salivary cortisone appears to be a promising alternative in patients with adrenal incidentaloma and salivary cortisone at 8 a.m. following the dexamethasone suppression test in patients with suspected Cushing's syndrome.

The research group of Choromańska et al. assessed the total antioxidant/oxidant status in the plasma and urine of patients with adrenal tumors. The study group consisted of 60 patients (31 women and 29 men) with adrenal masses, classified into three subgroups: non-functional incidentaloma, pheochromocytoma and Cushing / Conn adenoma. The authors analyzed various biomarkers of antioxidant activity: Total Antioxidant Capacity, Total OxidantStatus, Oxidative Stress Index and Antiradical Activity (Radical-Scavenging Activity Assay, Ferric-Reducing Antioxidant Power). Both plasma and urine redox biomarkers can be used to assess systemic antioxidant status in patients with adrenal tumors.

Sun et al. developed a computed tomography (CT) -based radiological-clinical prediction model for evaluating the surgical difficulty of treatment using RPLA (Retroperitoneal Laparoscopic Adrenalectomy) based on data from 398 patients with adrenal tumors. The authors developed a radiological-clinical prediction model to predict the difficulty of RPLA procedures. This model was suitable, accessible, and helpful for individualized surgical preparation and reduced operative risk.

A meta-analysis by Li et al. focused on comparing the advantages of robotic posterior retroperitoneal adrenalectomy (RPRA) over laparoscopic posterior retroperitoneal adrenalectomy (LPRA). A total of 675 patients were included. It was found that RPRA is associated with a significantly shorter hospital stay compared to LPRA, while showing a comparable operative time, blood loss, conversion rate, and complication rate.

The following article (Sun et al.) described machine learning models for predicting the difficulty of retroperitoneal laparoscopic adrenalectomy by combining clinical and radiomic characteristics. These models can help surgeons evaluate surgical difficulty, reduce risks, and improve patient benefits.

In another study (Urusova et al.), the authors introduced a universal mathematical model for the differential diagnosis of all morphological types of ACC in adults. The method involves determining eight diagnostically significant indicators that enable the calculation of the probability of ACC development using specified formulas.

Zhanghuang et al. presented an interesting case report of a bilateral adrenal giant medullary lipoma and performed a review of the literature. Patients with adrenal myelolipoma complicated with sexual development disorders can be monitored after resection of the myelolipoma, prior to oculoplastic surgery. In some cases, patients with sexual development disorders may experience spontaneous relief of abnormal manifestations of the external genitalia.

Another article (Deng et al.) presented a case of ACC with liver metastases treated with systemic antitumor therapy combined with local therapy for liver lesions (mitotane combined with TACE +MWA). The treatment outcome was a partial response, and the progression free survival of the patient has been extended to approximately 28 months so far, with survival when the study was completed (September 2022).

The Research Group of Enguita et al. found significant differences in the miRNA expression profiles of paragangliomas and pancreatic neuroendocrine tumors, leading to the identification of 6 key miRNAs (miR-10b-3p, miR-10b-5p, and the miRNA families miR-200c/141 and miR-194/192) that can effectively differentiate between the two types of tumors.

A group of authors from Italy (Delbarba et al.) included a total of 24 patients with ACC in their study. Testosterone deficiency was reported in 10 patients (41.7%) at baseline. It was found that mitotane therapy exposes these patients to a further elevated risk of hypogonadism, which should be promptly recognized and treated as it may have a negative impact on quality of life.

Kimura et al. presented a prospective study on mixed corticomedullary tumors of the adrenal gland, which are extremely rare tumors characterized by an admixture of steroidogenic cells and chromaffin cells in a single tumor mass simultaneously producing

adrenocortical hormones and catecholamines; in some cases, it is associated with ectopic adrenocorticotropic hormone.

An included review (Constantinescu et al.) described clinically "silent" PPGLs which are characterized by the absence of signs and symptoms associated with catecholamine excess. "Non-secretory" tumors are those with an absence of clear catecholamine secretory activity, "biochemically negative" PPGLs are those characterized by plasma or urinary metanephrines below the upper cut-offs of reference intervals and "non-functional" tumors are those with no catecholamine synthesis as determined by measurements of catecholamines in the tumor tissue.

Another case report (Weng et al.) highlighted the remarkable response of a patient with an ACC microsatellite instability-high tumor, *MLH1* splice variant, and high tumor mutational burden to treatment with a novel combination of mitotane, etoposide, paraplatin and sintilimab.

The research group of Zhang et al. investigated steroid profiling by LC-MS/MS led us to select DHEA as a candidate reference hormone for cortisol secretion. Lateralization and different steroid ratios showed that each steroid and all three steroidogenic pathways may be affected in patients with PBMAH. In patients with germline *ARMC5* variants, the androgen pathway was particularly dysregulated.

In the final study to be included (Mellid et al.) 23 patients carrying germline *NF1* variants were found to have additional pathogenic germline variants in *DLST* (n=1) and *MDH2* (n=2), and two somatic variants in *H3-3A and PRKAR1A*, revealed by targeted sequencing. Thus, the authors concluded that variants affecting genes involved in different pathways (pseudohypoxic and receptor tyrosine kinase signaling) co-occurring in the same patient could provide a selective advantage for the development of PPGL and explain the variable expressivity and incomplete penetrance observed in some patients.

In summary, this Research Topic illustrates the challenges in the diagnosis and treatment of patients with adrenal tumors along with new diagnostic and therapeutic options.

Author contributions

PG: Conceptualization, Formal analysis, Investigation, Project administration, Supervision, Validation, Writing – original draft, Writing – review & editing. NS-G: Conceptualization, Investigation, Writing – original draft, Writing – review & editing. MA-C: Conceptualization, Formal analysis, Investigation, Project administration, Supervision, Validation, Writing – original draft, Writing – review & editing.

Conflict of interest

The authors declare that the research was conducted in the absence of any commercial or financial relationships that could be construed as a potential conflict of interest.

The handling editor HF declared a past co-authorship with the author PG.

Publisher's note

References

1. Lopez AG, Fraissinet F, Lefebvre H, Brunel V, Ziegler F. Pharmacological and analytical interference in hormone assays for diagnosis of adrenal incidentaloma. *Ann Endocrinol (Paris).* (2019) 80:250–8. doi: 10.1016/j.ando.2018.11.006

2. Taki Y, Kono T, Teruyama K, Ichijo T, Sakuma I, Nagano H, et al. Comparative analysis of aldosterone and renin assays for primary aldosteronism screening. *Sci Rep.* (2024) 14:26040. doi: 10.1038/s41598-024-75645-1

3. Honma KI, Nakayama Y, Tamaki A, Uehara M, Teruya T, Yabiku T, et al. Impact of the transition from radioimmunoassay (RIA) to chemiluminescent enzyme immunoassay (CLEIA) for the measurement of plasma aldosterone concentration (PAC) on the diagnosis of primary aldosteronism (PA) via retrospective analyses in Okinawa. *Japan. Endocr J.* (2024) 71:895–906. doi: 10.1507/endocrj.EJ24-0227

4. Fuld S, Constantinescu G, Pamporaki C, Peitzsch M, Schulze M, Yang J, et al. Screening for primary aldosteronism by mass spectrometry versus immunoassay measurements of aldosterone: A prospective within-patient study. *J Appl Lab Med.* (2024) 9:752–66. doi: 10.1093/jalm/jfae017

5. Knuchel R, Erlic Z, Gruber S, Amar L, Larsen CK, Gimenez-Roqueplo AP, et al. Association of adrenal steroids with metabolomic profiles in patients with primary and endocrine hypertension. *Front Endocrinol (Lausanne).* (2024) 15:1370525. doi: 10.3389/fendo.2024.1370525

6. Reel PS, Reel S, van Kralingen JC, Langton K, Lang K, Erlic Z, et al. Machine learning for classification of hypertension subtypes using multi-omics: A multi-centre, retrospective, data-driven study. *EBioMedicine.* (2022) 84:104276. doi: 10.1016/j.ebiom.2022.104276

7. Vogg N, Müller T, Floren A, Dandekar T, Riester A, Dischinger U, et al. Simplified urinary steroid profiling by LC-MS as diagnostic tool for Malignancy in adrenocortical tumors. *Clin Chim Acta.* (2023) 543:117301. doi: 10.1016/j.cca.2023.117301

8. Schweitzer S, Kunz M, Kurlbaum M, Vey J, Kendl S, Deutschbein T, et al. Plasma steroid metabolome profiling for the diagnosis of adrenocortical carcinoma. *J Endocrinol.* (2019) 180:117–25. doi: 10.1530/EJE-18-0782

9. Pomares FJ, Cañas R, Rodriguez JM, Hernandez AM, Parrilla P, Tebar FJ. Differences between sporadic and multiple endocrine neoplasia type 2A phaeochromocytoma. *Clin Endocrinol (Oxf).* (1998) 48:195–200. doi: 10.1046/J.1365-2265.1998.3751208.X

10. Jhawar S, Arakawa Y, Kumar S, Varghese D, Kim YS, Roper N, et al. New insights on the genetics of pheochromocytoma and paraganglioma and its clinical implications. *Cancers (Basel).* (2022) 14(3):594. doi: 10.3390/CANCERS14030594

11. Liu Z, Ma J, Jimenez C, Zhang M. Pheochromocytoma: A clinicopathologic and molecular study of 390 cases from a single center. *Am J Surg Pathol.* (2021) 45:1155–65. doi: 10.1097/PAS.0000000000001768

12. Chasseloup F, Bourdeau I, Tabarin A, Regazzo D, Dumontet C, Ladurelle N, et al. Loss of KDM1A in GIP-dependent primary bilateral macronodular adrenal hyperplasia with Cushing's syndrome: a multicentre, retrospective, cohort study. *Lancet Diabetes Endocrinol.* (2021) 9:813–24. doi: 10.1016/S2213-8587(21)00236-9

13. Cavalcante IP, Berthon A, Fragoso MC, Reincke M, Stratakis CA, Ragazzon B, et al. Primary bilateral macronodular adrenal hyperplasia: definitely a genetic disease. *Nat Rev Endocrinol.* (2022) 18(11):699–711. doi: 10.1038/S41574-022-00718-Y

14. Araujo-Castro M, Martín Rojas-Marcos P, Parra Ramírez P. Familial forms and molecular profile of primary hyperaldosteronism. *Hipertens y Riesgo Vasc.* (2022) 39:167–73. doi: 10.1016/j.hipert.2022.05.007

15. Fernandes-Rosa FL, Williams TA, Riester A, Steichen O, Beuschlein F, Boulkroun S, et al. Genetic spectrum and clinical correlates of somatic mutations in aldosterone-producing adenoma. *Hypertension.* (2014) 64:354–61. doi: 10.1161/HYPERTENSIONAHA.114.03419

16. Tseng CS, Peng KY, Wang SM, Tsai YC, Huang KH, Lin WC, et al. A novel somatic mutation of CACNA1H p.V1937M in unilateral primary hyperaldosteronism. *Front Endocrinol (Lausanne)*. (2022) 13:816476. doi: 10.3389/FENDO.2022.816476

17. Zhou J, Azizan EAB, Cabrera CP, Fernandes-Rosa FL, Boulkroun S, Argentesi G, et al. Somatic mutations of GNA11 and GNAQ in CTNNB1-mutant aldosterone-producing adenomas presenting in puberty, pregnancy or menopause. *Nat Genet*. (2021) 53:1360–72. doi: 10.1038/S41588-021-00906-Y

18. Nazha B, Zhuang TZ, Dada HI, Drusbosky LM, Brown JT, Ravindranathan D, et al. Blood-based next-generation sequencing in adrenocortical carcinoma. *Oncologist*. (2022) 27:462–8. doi: 10.1093/ONCOLO/OYAC061

frontiers | Frontiers in Endocrinology

TYPE Perspective
PUBLISHED 16 September 2022
DOI 10.3389/fendo.2022.1026918

OPEN ACCESS

EDITED BY
Marta Araujo-Castro,
Ramón y Cajal University Hospital, Spain

REVIEWED BY
Guozhu Hou,
National Cancer Center, Chinese Academy of Medical Sciences and Peking Union Medical College, China

*CORRESPONDENCE
Noriko Kimura
kimura.noriko.sf@mail.hosp.go.jp

SPECIALTY SECTION
This article was submitted to Adrenal Endocrinology, a section of the journal Frontiers in Endocrinology

RECEIVED 24 August 2022
ACCEPTED 30 August 2022
PUBLISHED 16 September 2022

CITATION
Kimura N, Motoyama T, Saito J and Nishikawa T (2022) Mixed corticomedullary tumor of the adrenal gland.
Front. Endocrinol. 13:1026918.
doi: 10.3389/fendo.2022.1026918

Mixed corticomedullary tumor of the adrenal gland

Noriko Kimura[1,2]*, Teiich Motoyama[3], Jun Saito[4] and Tetsuo Nishikawa[4]

[1]Department of Clinical Research, National Hospital Organization Hakodate Hospital, Hakodate, Japan, [2]Department of Diagnostic Pathology, National Hospital Organization Hakodate Hospital, Hakodate, Japan, [3]Department of Pathology, Yamagata University School of Medicine, Yamagata, Japan, [4]Endocrinology and Diabetes Center, Yokohama Rosai Hospital, Yokohama, Japan

Mixed corticomedullary tumor (MCMT) of the adrenal gland is an extremely rare tumor characterized by an admixture of steroidogenic cells and chromaffin cells in a single tumor mass simultaneously producing adrenocortical hormones and catecholamines; it is associated with ectopic adrenocorticotropic hormone (ACTH) in some cases. We reviewed and summarized clinicopathological data of 28 MCMTs, including four metastatic tumors in 26 previous reports. These reports included 21 females and 7 males, and the average tumor sizes were 4.8 $\pm$ 2.5 cm and 12.6 $\pm$ 6.4 cm in the non-metastatic and metastatic groups, respectively ($P<0.001$). The clinical manifestations and laboratory data were as follows: Cushing or subclinical Cushing syndrome, 58% (14/24); hypertension, 71% (17/24); elevated adrenocortical hormones, 75% (18/24); elevated catecholamines, 75% (18/24); and ectopic ACTH, 71% (10/14). All four patients with metastatic MCMTs had poor prognoses and elevated adrenocortical hormone levels; however, only two patients had elevated catecholamine levels. Immunohistochemistry was essential for the pathologic diagnosis of MCMTs. In this study, using an improved technique, we detected ectopic ACTH-producing cells in the same paraffin-embedded sections reported to be negative in our previous reports. As MCMT is composed of cells with embryologically different origins, its pathogenesis has been explained by various hypotheses. We compared MCMT to the adrenal gland of birds and the early stage of human fetuses, in which nests of chromaffin cells and steroidogenic cells admix without the formation of cortex and medulla. MCMT is characterized by the immaturity of organogenesis and might be classified as an adrenal embryonal tumor.

KEYWORDS

mixed corticomedullary tumor, pheochromocytoma, adrenocortical tumor, ectopic ACTH, pathogenesis

Introduction

Mixed corticomedullary tumor (MCMT) of the adrenal gland is an extremely rare tumor characterized by an admixture of cell nests of both adrenal cortical and medullary cells in a single mass that produces adrenocortical steroid hormones and catecholamines (CA). MCMT also sometimes produces ectopic adrenocorticotropic hormone (ACTH) and can induce Cushing syndrome or subclinical Cushing syndrome. To date, less than 40 cases of MCMT have been reported since the first case was diagnosed in 1969. Herein, we reviewed 28 cases in 26 MCMT reports (1–26) and added some experimental data and hypotheses on the pathogenesis of MCMT.

Patients with MCMTs presented with varying levels of CA, adrenocortical hormones, and ACTH. Additionally, careful pathologic diagnosis is necessary to define adrenocortical or medullary cells using immunohistochemistry. All MCMTs previously reported were histologically confirmed. Although MCMTs were initially considered benign, 4 of the 28 patients with MCMT had distant metastases and poor prognoses. Thus, it should be considered that all MCMTs have some metastatic potential, as does pheochromocytoma (PCC).

Most MCMT studies focused on its pathogenesis because it is composed of different cell types: the medullary cells are derived from the neuro-ectodermal cells of the neural crest, and the adrenocortical cells are from the mesodermal layer, which is structurally similar to the adrenal gland. The most important difference between MCMT and the human adrenal gland is that the tumor cell nests of steroidogenic and medullary cells are randomly admixed in MCMT. In contrast, the human adrenal gland has distinct steroidogenic and medullary areas, namely the cortex and medulla. Many authors have attempted to explain the pathogenesis of this peculiar tumor through several hypotheses, including collision tumor, gene mutations, and stemness factors. Herein, we suggest perspective pathogenesis and ectopic ACTH in MCMT based on the comparative anatomy of the adrenal gland in vertebrates and human fetuses.

Clinical manifestations and laboratory findings

We reviewed the characteristics of 26 previous studies involving 28 patients, including 24 patients with non-metastatic MCMTs from 22 studies (group A) (1–14, 16, 17, 19, 21, 22, 24, 26) and 4 patients with metastatic MCMTs from 4 other reports (group B) (15, 18, 20, 23).

The average patient age was 46.4 ± 12.3 years (mean ± standard deviation [SD], range: 25–66 years) in group A and 51.8 ± 26.4 years (range: 16–78 years) in group B. There were 21 female and 7 male patients, with a female:male ratio of 3:1; group A included 19 female and 5 male patients, while group B included 2 female and 2 male patients. The clinical manifestations and laboratory data were as follows: overall, 58% (14/24) had Cushing syndrome or subclinical Cushing syndrome, which was defined as autonomous glucocorticoid production without specific signs and symptoms of Cushing syndrome (27); 71% (17/24) had hypertension, and 75% (18/24) had elevated cortisol and CA levels. Plasma and/or urine CA, including epinephrine, norepinephrine, and dopamine, and their metabolites, such as metanephrine and vanillylmandelic acid, were measured in each institute. The types of elevated CA are as follows: epinephrine plus norepinephrine plus dopamine, one; epinephrine plus norepinephrine, five; metanephrine only, two; dopamine only, one; vanillylmandelic acid, three; and elevated CA with unknown types, six; and the analysis revealed that at least 44% (8/18 cases) were epinephrine-producing. The medullary component in four cases was unassociated with CA secretion (biochemically non-functional) and was identified histopathologically (12, 18, 20, 23). Further, adrenocortical cells produced cortisol in most cases and aldosterone in two cases, and only one case produced dehydroepiandrosterone sulfate (DHEA-sulfate). Seven of 12 previous cases with elevated cortisol had unsuppressed ACTH levels, despite a hypercortisolemic state (19). The detectable ACTH level was not grossly elevated, as is usually seen from pituitary or ectopic sources (19). We added six subsequent cases from the reports after Lwin et al. (19) and found that 71% (10/14) of MCMTs had subclinical Cushing syndrome with ectopic ACTH. In cases with Cushing syndrome, ectopic ACTH syndrome was defined as ACTH dependent when the plasma ACTH level was >15 pg/ml (reference range: 10–50 pg/ml) and ACTH independent when the plasma ACTH level was <5 pg/ml based on a previous report (23). Among the eight ACTH cases examined with immunohistochemistry (2, 3, 9, 19, 22–24, 26), only three cases showed focal positivity for ACTH (2, 23, 26).

Pathology of MCMTs

MCMTs were first defined histologically as cortical cells with round, regularly shaped, and rather small nuclei, and medullary cells with basophilic cytoplasm and nuclei with more varied appearance (1). The adrenocortical and medullary components' ratios may differ between cases. In most cases, the cortical cells have mild abnormality; however, some metastatic MCMTs had cortical cells with malignant features described as Weiss's criteria 7 (20). Both cells of the medullary and cortical components in MCMT are apparently tumor cells similar to PCC and adrenocortical neoplasm morphology and biology. MCMT is a very peculiar tumor, and its histology may vary from case to case, especially if it is metastatic.

The mean ± SD tumor sizes of non-metastatic and metastatic MCMTs were 4.8 ± 2.5 cm (range: 2.5–11.8 cm)

and 12.6 ± 6.4 cm (range: 8–22 cm), respectively. Metastatic MCMTs were larger than non-metastatic MCMTs (P<0.001). In non-metastatic MCMTs, the cortical cells were usually uniformly shaped with mild nuclear atypia and had cortical adenoma features. Meanwhile, the medullary cells had slightly basophilic cytoplasm with hyperchromatic, irregularly shaped nuclei and nucleoli arranged in a zellballen pattern, which are compatible with those of PCC. Thus, MCMT was considered a mixed tumor of cortical adenoma/carcinoma and PCC.

Immunohistochemistry

Immunohistochemistry was performed to distinguish the medullary cells from the cortical cells in the MCMTs. Chromogranin-A (CgA) and synaptophysin (SP) were the most frequently used antibodies to identify the medullary cells in 25 and 10 tumors, respectively. In addition, catecholamine synthesizing enzymes, such as tyrosine hydroxylase (TH), dopamine-b-hydroxylase (DBH), and phenylethanolamine-N-methyltransferase (PNMT), were positive in four cases (2, 9, 22, 26). Insulinoma-associated protein 1 (INSM1) was detected in one (22) case with two recently reported cases after our review (2, 9). CgA and SP were the most frequently used antibodies for confirming neuroendocrine tumors, including PCC. However, both antibodies and INSM1 are also markers for epithelial neuroendocrine tumors (eNETs) and are not specific markers for PCC. The combined use of these antibodies and TH or DBH is suitable for detecting CA-producing cells (28). The adrenocortical component was confirmed by inhibin-alpha in 11 cases, steroidogenic factor 1 (SF-1) in six cases, calretinin in four cases, and melan-A in four cases. Steroidogenic enzymes (3β-hydroxysteroid dehydrogenase; 11 β-hydroxylase [CYP11β1], p450c21, and p450c17) were positive in four cases. Among these antibodies for adrenocortical cells, SF-1 is presently the most universally used antibody to identify adrenocortical cells. The analysis of hormone products showed that the cortical cells and medullary cells were compatible with those present in adrenocortical adenoma and PCC, respectively. Electron microscopic examination was used to identify neuroendocrine granules in the cytoplasm of medullary cells and mitochondria with tubulovesicular cristae for adrenocortical cells (2, 4, 5). Sudan III stain was used for fat globules in adrenocortical cells (2, 3).

Given that Cases # 2, 3, and 9 were our own previously reported cases, we re-examined the immunohistochemical staining of ACTH using novel modalities, including an autoimmunostainer for the same buffered formalin-fixed, paraffin-embedded blocks used before. Briefly, the immunohistochemical procedures for ACTH were performed using an automated immunostainer (Benchmark, Ventana, Tucson, AZ, USA) according to the manufacturer's protocol. The primary antibody for ACTH was mouse monoclonal, clone 02A3 (DAKO), and the final dilution was 1:100. We did not need any enhancement for materials, and the incubation time was 32 minutes. The positive control was a human pituitary gland, and the negative control was phosphate-buffered saline. There was no nonspecific ACTH staining. The results revealed that all three MCMTs clearly demonstrated cell nests of medullary cells positive for ACTH immunoreactivity (Figure 1). This suggested that some medullary cells of MCMT with subclinical Cushing syndrome could produce ectopic ACTH. These ectopic ACTH-producing tumor cells were characteristically bizarre cells with abundant basophilic cytoplasm and irregularly shaped, large nuclei located at the intersection between the nests of cortical cells and smaller medullary cells. The smaller medullary cells with mild atypia did not show ACTH immunoreactivity. It is speculated that morphologically atypical medullary cells with bizarre nuclei have some genetic changes that produce both catecholamines and ACTH simultaneously, as shown in ectopic ACTH-producing PCC (29). The lack of ACTH reactivity in previous reports with subclinical Cushing syndrome may be due to the low levels of ACTH produced by the tumor cells and the lower sensitivity of immunohistochemistry at the time of the study, resulting in false negative staining as suspected by Lwin et al. (19). The reasons of discrepancy between our results of ACTH and the original data are considered as following; Immunohistochemical principle is basically same as before, however, recent progress in immunohistochemistry using an autoimmunostainer contributed to get more sensitive and specific results compared to the years of the original technique was performed. Furthermore, immunohistochemistry is now daily used technique in pathology laboratories but not a special technique for research as used before. Both progress of instruments and human techniques may be the reasons for detecting ACTH this time. However, in the above three cases, medullary cells with mild atypia had very few cells immunoreactive to ACTH, suggesting that the grade of histological atypia of medullary cells is related to the ectopic ACTH production. The immunohistochemical data are summarized in Table 1.

Other concurrent lesions

The previously reported MCMTs had other concurrent lesions, such as neurofibromatosis type 1 (14), myelolipoma (6, 9, 13), aldosterone-producing adrenocortical micronodules (26), and spindle cell sarcoma (4).

Metastatic MCMT

Distant metastasis was observed in four patients (15, 18, 20, 23). The metastatic sites were the liver in four patients, lung in two patients, and posterior stomach in one patient. One patient

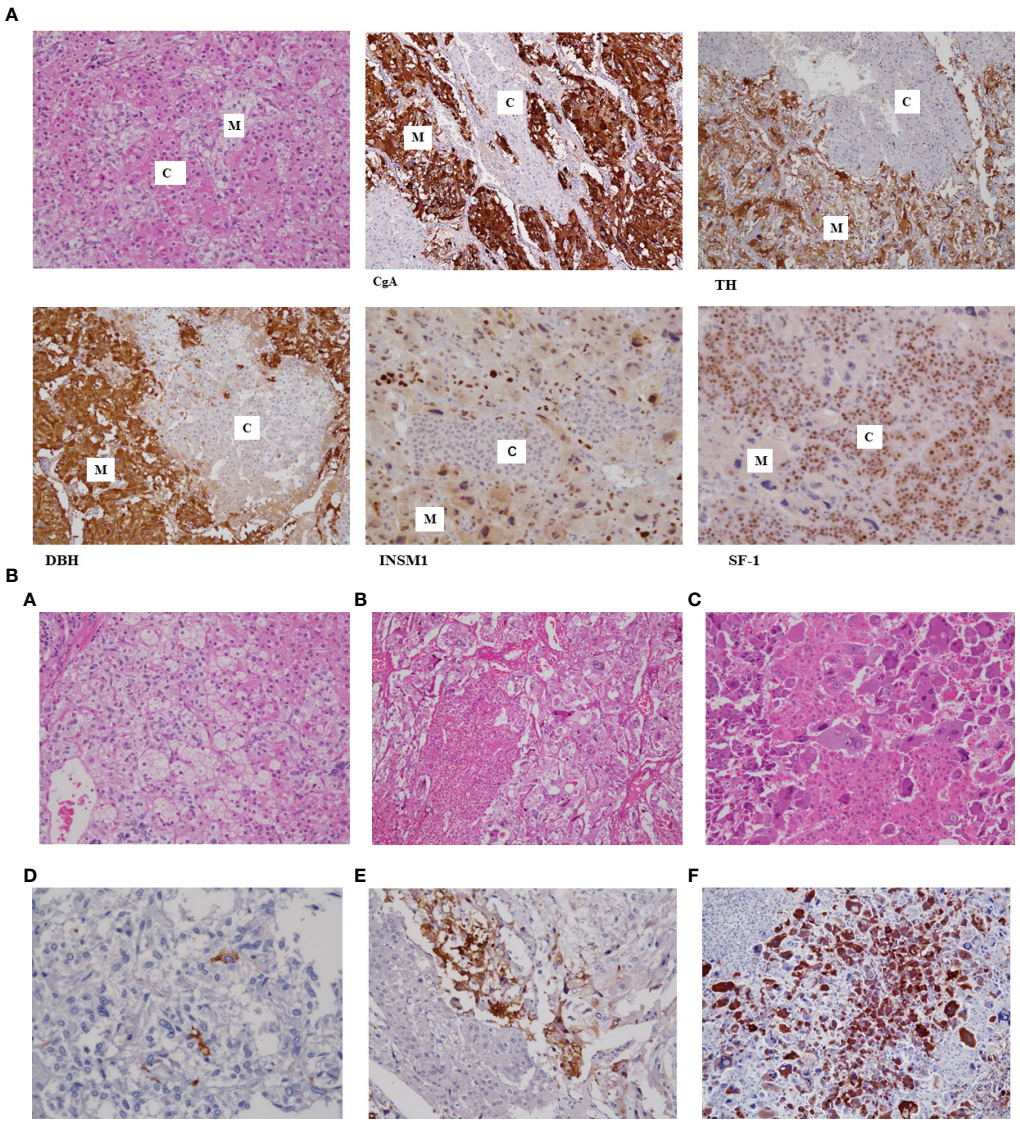

FIGURE 1
(A) Histology of mixed corticomedullary tumor (MCMT) with immunohistochemistry. The tumor is composed of nests of cortical cells with eosinophilic cytoplasm and round nuclei (C) and medullary cells with pale cytoplasm and hyperchromatic, irregularly shaped nuclei (M). Cell nests of medullary cells are positive for chromogranin-A (CgA), tyrosine hydroxylase (TH), dopamine beta-hydroxylase (DBH), and INSM1; however, cortical cells are negative for all these biological markers but positive for SF1. **(B)** Histology of three cases of MCMTs with subclinical Cushing syndrome. Three cases of MCMT are demonstrated. The upper and lower lines are the same cases subjected to hematoxylin-eosin and adrenocorticotropic hormone (ACTH) immunohistochemical staining, respectively. Tumor cells in the left line show mild atypia in both cortical cells and medullary cells (A), and there are few ACTH-positive cells (D). Nests of medullary cells in the middle line show small and large irregular nuclei (B) and stain positively for ACTH in the adjacent area of cortical cells (E). Medullary cells in the right line have irregularly shaped large basophilic cytoplasm and hyperchromatic large nuclei, especially those adjacent to eosinophilic cortical cells (C), and these medullary cell components strongly demonstrate ACTH immunoreactivity (F). Cortical cells in these cases show very mild atypia and are compatible with cortical adenoma.

had local recurrence in addition to liver metastasis. All patients with metastasis had elevated steroid hormones (three patients with cortisol and one patient with DHEA-sulfate); however, two patients had no elevated catecholamines (20, 23). One patient only had elevated cortisol levels at the time of primary tumor diagnosis, following which the CA levels were elevated at the time of liver metastasis (18). Only one patient had both elevated CA and steroid hormone levels from the time of primary diagnosis (15). Metastatic MCMTs produced more adrenocortical hormones than CA.

Histologically, all MCMTs with metastasis had both components of cortical tumor and PCC. The histological

TABLE 1 Immunohistochemical markers used for identifying medullary cells and cortical cells in 28 previous reports of mixed corticomedullary tumors of the adrenal gland.

Antibodies	Medullary cells (Cases)	Cortical cells (Cases)
Chromogranin A	25	0
Synaptophysin	10	0
S100 for sustentacular cells	3	0
Catecholamine synthesizing enzymes: TH, DBH, PNMT	4	0
INSM1	3	0
ACTH for subclinical Cushing syndrome	4	0
Inhibin alpha	0	11
SF-1	0	6
Melan A	0	4
Calretinin	0	4
Steroid hormone synthesizing enzymes (3β-HSD, P450c21, P450c11, P450c17)	0	4
Pancytokeratin	0	5

TH, tyrosine hydroxylase; DBH, dopamine-b-hydroxylase; PNMT, phenylethanolamine N-methyltransferase; INSM1, insulinoma-associated protein 1; ACTH, adrenocorticotropin; 3b-HSD, 3 beta-hydroxysteroid dehydrogenase; P450c21, 21beta hydroxylase; P450c11, 11beta-hydroxylase; P450c17, 17alpha-hydroxylase.

description of the metastatic MCMTs only included information about the primary tumors without any information about the metastatic sites. One case only described the medullary component without describing the cortical component; the tumor cells had marked nuclear pleomorphism, abundant mitotic cells with atypical mitotic figures, confluent geographic tumor necrosis, and vascular invasion in the PCC component (15). Another case was described as a high-grade undifferentiated carcinoma with evident tumor necrosis and focal vascular invasion. Many of the cells were large and pleomorphic, and some were multinucleated and bizarre with frequent mitoses up to 4/high-power field with aberrant forms. A Weiss score 7 was given, indicating adrenocortical carcinoma; however, no description of the medullary component was provided (20). From these descriptions, metastatic MCMTs had features of adrenocortical carcinoma or high-grade PCC (30).

These patients had poor prognoses due to highly progressive tumors. Two patients died 18–24 months postoperatively (18, 20), while two other patients deteriorated with metastatic tumors postoperatively (15, 23).

Discussion

Terminology of MCMT with metastasis

The terms "mixed corticomedullary carcinoma" were used for three cases (15, 18, 20) and "malignant mixed corticomedullary tumor" for the other case (23). The term "corticomedullary" carcinoma provides the impression that metastasis occurs only in the cortical component and not in the medullary component. All four MCMTs with metastasis had histological components of both cortical and medullary cells; however, biologically, all had elevated steroid hormones, while two cases had unelevated CA. The term "mixed corticomedullary carcinoma" seems to be inappropriate because the medullary component is non-epithelial; instead, it should be called sarcoma when it is pathologically diagnosed as malignant. The World Health Organization Endocrine Tumor Classification 4th edition (2017) recommends using metastatic pheochromocytoma and avoiding the terms "benign" or "malignant" to classify PCC. We would like to suggest the term "metastatic MCMT" instead of "mixed corticomedullary carcinoma" or "malignant MCMT." There were only four metastatic MCMTs in the previous reports; however, patient follow-up time was insufficient, especially in the recently reported cases, and life-long follow-up may be necessary as requested for patients with PCC.

Pathogenesis of MCMT

While previous reports have focused on the pathogenesis of MCMT, it remains unclear. The separate embryological origin of the adrenal medulla and cortex was previously suggested to favor a two clonal collision tumor (4, 5, 18). Disruption of the normal cortical-chromaffin cell interactions (paracrine interactions) by unknown mechanisms could theoretically result in trophic stimulation of both cell lineages and provide a possible explanation for the development of MCMTs (7, 14). Genetic testing was negative for *RET, VHL, SDHB, SDHC*, and *SDHD* (8). We detected immunohistochemical reactivity of *SDHB* in MCMTs, which ruled out *SDHx* gene mutations (data not

shown). Only one case had NF1 (14), but majority of the tumor component of this patient was a composite PCC, and only 20% was cortical. A whole exome sequencing analysis using genomic DNA extracted from peripheral leukocytes and paraffin-embedded tumor tissue revealed no germline or somatic gene alterations (22), such as in *PRKACA, CTNNB1, GNAS, ARMC5, PRKAR1A, PDE11A*, or *PDE8B*, which have been reported in adrenal cortisol-producing adenomas (31). Moreover, no germline or somatic gene mutations were found in genes that have been reported in PCC, such as *NF1, RET, VHL, SDHx, TMEM127, MAX, HIF2A, PHD1/PHD2, FH, KIF1B, DNMT3A, IDH1*, or *SLC25A11* (32). Among the 10 genes detected as possible pathogenic candidates, Kanzawa et al. (22) focused on fibroblast growth factor receptor 4 (*FGFR4*). A homozygous *FGFR4-G388R* germline variant was identified in MCMT, which was suggested to influence the development of the adrenocortical component but not the PCC component.

Another hypothesis is based on a genetic event in stem cells which gives rise to cells constituting the cortex and the medulla. Immunohistochemistry using various tumor stem cell-specific markers, including acetaldehyde dehydrogenase 1, CD44, CD133, Nestin, NGFR, and SOX9, revealed short spindle-positive cells scattered within the tumor, suggesting the involvement of tumor stem cells (21). Double-labeling immunohistochemistry identified the presence of a few spindle cells within the tumor immunoreactive for both cortical and medullary antigens (23). Along with the positive immunofluorescence for cancer stem cell biomarkers (OCT4, NANOG, and SOX-2), these findings indicated the involvement of primitive embryonic cells as the origin of MCMT and concluded that MCMT may not come from colliding tumors, but from a single stem cell. Chiou et al. (24) reported that the previously well-known mutations for adrenocortical adenoma (*GNAS, CTNNB1, PRKAR1A, PRKACA, PDE11A, PDE8B, KCNJ5, CACNA1D*) (31) and PCC (*RET, VHL, NF1, SDHA, SDHB, SDHC, SDHD, SDHAF2, TMEM127, MAX, EGLN1 (PHD2), EPAS1(HIF2A), KIF1B, MET, FH*, and *H-RAS*) (32) were not detected in their MCMT. However, immunohistochemistry confirmed that the stemness markers SOX2, CD44, and OCT4 were highly expressed in MCMT with greater adrenocortical adenoma density than in PCC. Several mutations were also identified in membrane receptors, such as *LRP5* p.C1548F, *IGFBP2* p. L21insPLL, *GPR39* p.V230A, *EMR2* p.S523F, which may be associated with MCMT development (24). Stemness activation may drive tumor formation, and the complex proliferative signaling caused by germline and somatic mutations may accelerate tumor growth. The mechanism by which stemness and asymmetrical tumorigenesis in the adrenal gland of MCMT are initiated remains unclear (24). Although cancer stem cells have been observed in MCMT as well as PCCs and paragangliomas (33) but also in other endocrine, non-endocrine, and neural tumors. The precise role of cancer stem cells and mutations in membrane receptors in MCMT tumor formation remains further accumulation of experiments.

MCMT and the bird/fetal adrenal gland

Apart from cancer stem cell analysis, we would like to suggest a different approach to investigate MCMT tumorigenesis based on comparative endocrinology. MCMTs are histologically similar to the adrenal gland of birds, in which the catecholaminergic tissue is dispersed in the corticosteroidogenic tissue (34). A comparative endocrinology study showed evidence of considerable interspersion of the two components of chromaffin cells and corticosteroidogenic tissues in birds and most amphibians. However, the cortex-medulla relationship in most mammals represents a division into two separate tissues through contiguous components (35).

In humans, the fetal adrenal glands are detectable around the 6^{th} week of development, and its morphology is completed around the 7^{th} gestational week (35). The morphological and steroidogenic functions of the fetal adrenal cortex are formed around the 7^{th} gestational week (36). The neural crest-derived chromaffin cells stain positively for CgA and migrate toward the adrenal cortex as islands in the 6^{th}–7^{th} gestational weeks. These chromaffin cells initially appear as small clusters or nests scattered throughout the cortex, where they gradually invade the medial aspect of the cortical tissue along the central vein at the 7^{th}–12^{th} gestational weeks to gain a central position and then form around the adrenal medulla (36). However, the enzymes involved in CA biosynthesis can be detected as early as the 6^{th} gestational week (37, 38). Therefore, the adrenal glands of birds and human fetuses at the 6^{th}–7^{th} gestational weeks are similar, forming an independent organ with admixed corticomedullary cell nests that produce steroid hormones and CAs. MCMT is characterized by the immaturity of organogenesis and might be classified as an embryonal tumor of the adrenal gland.

ACTH production in MCMT

Small amounts of ACTH are released within the adrenal gland during splanchnic nerve stimulation in the functionally hypophysectomized calf (39). The epithelial hypophysis has long been believed to originate from Rathke's pouch (RP). However, experiments on some amphibian species showed that the primordium of the epithelial hypophysis originates from the anterior neural ridge and migrates underneath the brain to form an RP-like structure (40). Further, early rat embryo culture confirmed that adenohypophyseal cells originate from the rostral end of the neural plate before RP formation (41). These animal models suggest that the anterior pituitary gland also exists close to the neural crest in human fetuses. It could be

hypothesized that some anterior pituitary cells may migrate into the neural crest, become part of chromaffin cell nests, and produce ACTH during medullary component formation in early fetal stages as MCMT. However, further investigations are necessary to confirm this hypothesis.

Data availability statement

The datasets presented in this article are not readily available because only immunohistochemical data are added in this manuscript. Requests to access the datasets should be directed to kimura.noriko.sf@mail.hosp.go.jp.

Ethics statement

This study was approved by the institutional review board of the National Hospital Organization Hakodate Hospital (#R4-0730001).

Author contributions

NK and TM contributed to the pathology research, and JS and TN contributed to the clinical research. NK re-examined the immunohistochemistry of ACTH, SF-1, INSM1, TH, DBH using the same paraffin-embedded blocks of the tumors that were used for the original manuscripts of the above references #2, 3, and 9, and confirmed that all those tumors contained cells immunoreactive to ACTH and the other antibodies. NK wrote the manuscript text and prepared Figure 1 and Table 1. All authors reviewed and approved the manuscript.

Acknowledgments

We are grateful to Professor Sakae Kikuyama, Waseda University, Tokyo, Japan, for excellent suggestions for the development of endocrine organs.

Conflict of interest

The authors declare that the research was conducted in the absence of any commercial or financial relationships that could be construed as a potential conflict of interest.

Publisher's note

References

1. Mathison DA, Waterhouse CA. Cushing's syndrome with hypertensive crisis and mixed adrenal cortical adenoma-pheochromocytoma (corticomedullary adenoma). *Am J Med* (1969) 47:635–41. doi: 10.1016/0002-9343(69)90193-4

2. Akai H, Sanoyama K, Namai K, Miura Y, Murakami O, Hanew K, et al. A case of adrenal mixed tumor of pheochromocytoma and adrenocortical adenoma presenting diabetes mellitus and hypertension. *Nihon Naibunpi Gakkai Zasshi* (1993) 69:659–69. doi: 10.1507/endocrine1927.69.7_659

3. Ohta TI, Motoyama T, Imai T. Cortico-medullary mixed tumor (phaeochromocytoma and cortical adenoma) of the adrenal gland. *J Urol Pathol* (1995) 3:157–64.

4. Michal M, Havlicek F. Corticomedullary tumors of the adrenal glands. *Pathol Res Pract* (1996) 192:1082–9. doi: 10.1016/s0344-0338(96)80023-9

5. Wieneke JA, Thompson LDR, Heffess CS. Corticomedullary mixed tumor of the adrenal gland. *Ann Diagn Pathol* (2001) 5:304–8. doi: 10.1053/adpa.2001.28297

6. Chu AY, LiVolsi VA, Fraker DL, Zhang PJ. Corticomedullary mixed tumor of the adrenal gland with concurrent adrenal myelolipoma. *Arch Pathol Lab Med* (2003) 127:e329-32. doi: 10.5858/2003-127-e329-CMTOTA

7. Ma W-Y, Yang A-H, Chang Y-H, Lin L-Y, Lin H-D. Coexistence of adrenal cushing syndrome and pheochromocytoma in a "corticomedullary adenoma": A case report and review of the literature. *Endocrinologist* (2007) 17:341–5. doi: 10.1097/ten.0b013e3181596219

8. Lee P, Bradbury RA, Sy J, Hughes L, Wong L, Falk G, et al. Phaeochromocytoma and mixed corticomedullary tumour – a rare cause of cushing's syndrome and labile hypertension in a primigravid woman postpartum. *Clin Endocrinol (Oxf)* (2008) 68:492–4. doi: 10.1111/j.1365-2265.2007.03038.x

9. Shiba A, Saito J, Yokoo H, Kawaguchi J, Nakamura M, Matsuzawa Y, et al. A case of subclinical cushing syndrome due to mixed corticomedullary tumor associated with myelolipoma. *Folia Endocrinologica Japonica* (2008) 84:894. doi: 10.1507/endocrine1927.84.3_867

10. Kimura T, Usui T, Inamoto S, Minamiguchi S, Okuno H, Sasano H, et al. Pheochromocytoma with subclinical cushing's syndrome caused by corticomedullary mixed tumor of the adrenal gland. *J Clin Endocrinol Metab* (2009) 94:746–7. doi: 10.1210/jc.2008-2013

11. Alexandraki KI, Michail OP, Nonni A, Diamantis D, Giannopoulou I, Kaltsas GA, et al. Corticomedullary mixed adrenal tumor: Case report and literature review. *Endocr J* (2009) 56:817–24. doi: 10.1507/endocrj.k09e-010

12. Trimeche Ajmi S, Chadli Chaieb M, Mokni M, Braham R, Ach K, Maaroufi A, et al. Corticomedullary mixed tumor of the adrenal gland. *Ann Endocrinol (Paris)* (2009) 70:473–6. doi: 10.1016/j.ando.2009.09.003

13. Singh M, Mandal S, Kakkar AK, Khurana N, Garg A. Mixed corticomedullary tumour with myelolipoma: a rare coexistence. *Pathology* (2010) 42:589–91. doi: 10.3109/00313025.2010.508741

14. Lau SK, PG C, Weiss LM. Mixed cortical adenoma and composite pheochromocytoma-ganglioneuroma: an unusual corticomedullary tumor of the adrenal gland. *Ann Diagn Pathol* (2011) 15:185–9. doi: 10.1016/j.anndiagpath.2010.02.005

15. Turk AT, Asad H, Trapasso J, Perilli G, LiVolsi VA. Mixed corticomedullary carcinoma of the adrenal gland: A case report. *Endocr Pract* (2012) 18:e37–42. doi: 10.4158/ep11222.cr

16. Kaneko T, Matsushima H, Homma Y. Dopamine-secreting corticomedullary mixed tumor of the adrenal gland: Letter to the Editor. *Int J Urol* (2012) 19:1123–4. doi: 10.1111/j.1442-2042.2012.03107.x

17. Donatini G, Van Slycke S, Aubert S, Carnaille B. Corticomedullary mixed tumor of the adrenal gland–a clinical and pathological chameleon: case report and review of literature. *Updates Surg* (2013) 65:161–4. doi: 10.1007/s13304-011-0132-118

18. Michalopoulos N, Pazaitou-Panayiotou K, Boudina M, Papavramidis T, Karayannopoulou G, Papavramidis S. Mixed corticomedullary adrenal carcinoma. *Surg Today* (2013) 43:1232–9. doi: 10.1007/s00595-012-0458-4

19. Lwin TM, Galal N, Gera S, Marti JL. Adrenal cushing syndrome with detectable ACTH from an unexpected source. *BMJ Case Rep* (2016) 2016: bcr2016216965. doi: 10.1136/bcr-2016-216965

20. Alsabek MB, Alhmaidi R, Ghazzawi B, Hamed G, Alseoudi A. Mixed corticomedullary adrenal carcinoma – case report: Comparison in features, treatment and prognosis with the other two reported cases. *Int J Surg Case Rep* (2017) 31:254–61. doi: 10.1016/j.ijscr.2017.01.010

21. Duan L, Fang F, Fu W, Fang Z, Wang H, Yu S, et al. Corticomedullary mixed tumour resembling a small adrenal gland-involvement of cancer stem cells: case report. *BMC Endocr Disord* (2017) 17:9. doi: 10.1186/s12902-017-0157-7

22. Kanzawa M, Fukuoka H, Yamamoto A, Suda K, Shigemura K, Hara S, et al. Adrenal corticomedullary mixed tumor associated with the FGFR4-G388R variant. *J Endocr Soc* (2020) 4:bvaa101. doi: 10.1210/jendso/bvaa101

23. Ramírez-Rentería C, Espinosa-De-Los-Monteros AL, Etual E-C, Marrero-Rodríguez D, Castellanos G, Arreola-Rosales R, et al. From ACTH-dependent to ACTH-independent cushing's syndrome from a malignant mixed corticomedullary adrenal tumor: Potential role of embryonic stem cells. *Case Rep Endocrinol* (2020) 2020:1–9. doi: 10.1155/2020/4768281

24. Chiou H-YC, Jiang H-J, Yang S-F, Kuo K-K, Lin P-C, Hsiao P-J. Stemness regulation of the adrenal mixed corticomedullary tumorigenesis-a case-control study. *Neoplasia* (2020) 22:263–71. doi: 10.1016/j.neo.2020.04.003

25. Inoue A, Inoue S, Sawai R, Hamamatsu K, Okazaki K, Nishizawa H, et al. Mixed corticomedullary tumors of the adrenal gland harboring both medullary and cortical properties. *J Endocr Soc* (2021) 5:A143. doi: 10.1210/jendso/bvab048.289

26. Yoshida S, Babaya N, Ito H, Hiromine Y, Taketomo Y, Niwano F, et al. Mixed corticomedullary tumor accompanied by unilateral aldosterone-producing adrenocortical micronodules: A case report. *J Endocr Soc* (2021) 5:bvab140. doi: 10.1210/jendso/bvab140

27. Iacobone M, Citton M, Scarpa M, Viel G, Boscaro M, Nitti D. Systematic review of surgical treatment of subclinical cushing's syndrome. *Br J Surg* (2015) 102:318–30. doi: 10.1002/bjs.9742

28. Kimura N. Dopamine β-hydroxylase: An essential and optimal immunohistochemical marker for pheochromocytoma and sympathetic paraganglioma. *Endocr Pathol* (2021) 32:258–61. doi: 10.1007/s12022-020-09655-w

29. Gabi JN, Milhem MM, Tovar YE, Karem ES, Gabi AY, Khthir RA. Severe cushing syndrome due to an ACTH-producing pheochromocytoma: A case presentation and review of the literature. *J Endocr Soc* (2018) 2:621–30. doi: 10.1210/js.2018-00086

30. Kimura N, Takayanagi R, Takizawa N, Itagaki E, Katabami T, Kakoi N, et al. Pathological grading for predicting metastasis in phaeochromocytoma and paraganglioma. *Endocr Relat Cancer* (2014) 21:405–14. doi: 10.1530/ERC-13-0494

31. Juhlin CC, Bertherat J, Giordano TJ, Hammer GD, Sasano H, Mete O. What did we learn from the molecular biology of adrenal cortical neoplasia? from histopathology to translational genomics. *Endocr Pathol* (2021) 32:102–33. doi: 10.1007/s12022-021-09667-0

32. Tischler AS, de Kreijger RR, Gill A, Kawashima A, Kimura N, Komminoth P, et al. WHO classification of tumours of endocrine organs. In: R Lloyd, RY Osamura, G Kloppel, J Rosai, editors. *Genotype-phenotype correlation of hereditary phaeochromocytoma and paraganglioma susceptibility genes*, *4th ed*, vol. . p . Lyon, France: International Agency for Research on Cancer (2017). p. 181–2.

33. Scriba LD, Bornstein SR, Santambrogio A, Mueller G, Huebner A, Hauer J, et al. Cancer stem cells in pheochromocytoma and paraganglioma. *Front Endocrinol (Lausanne)* (2020) 11:79. doi: 10.3389/fendo.2020.00079

34. Gorbman A, Dickhoff WW, Vigna SR, Clark NB, Ralph CL. Comparative endocrinology. In: *The adrenal medulla*. New York: John Wiley & Sons (1983). p. 373–77.

35. Melau C, Nielsen JE, Frederiksen H, Kilcoyne K, Perlman S, Lundvall L, et al. Characterization of human adrenal steroidogenesis during fetal development. *J Clin Endocrinol Metab* (2019) 104:1802–12. doi: 10.1210/jc.2018-01759

36. Bechmann N, Berger I, Bornstein SR, Steenblock C. Adrenal medulla development and medullary-cortical interactions. *Mol Cell Endocrinol* (2021) 528:111258. doi: 10.1016/j.mce.2021.111258

37. Ehrhart-Bornstein M, Hinson JP, Bornstein SR, Scherbaum WA, Vinson GP. Intraadrenal interactions in the regulation of adrenocortical steroidogenesis. *Endocr Rev* (1998) 19:101–43. doi: 10.1210/edrv.19.2.0326

38. Molenaar WM, Lee VM-Y, Trojanowski JQ. Early fetal acquisition of the chromaffin and neuronal immunophenotype by human adrenal medullary cells. an immunohistological study using monoclonal antibodies to chromogranin a, synaptophysin, tyrosine hydroxylase, and neuronal cytoskeletal proteins. *Exp Neurol* (1990) 108:1–9. doi: 10.1016/0014-4886(90)90001-9

39. Jones CT, Edwards AV. Release of adrenocorticotrophin from the adrenal gland in the conscious calf. *J Physiol* (1990) 426:397–407. doi: 10.1113/jphysiol.1990.sp018145

40. Kikuyama S, Okada R, Hasunuma I, Nakada T. Some aspects of the hypothalamic and pituitary development, metamorphosis, and reproductive behavior as studied in amphibians. *Gen Comp Endocrinol* (2019) 284:113212. doi: 10.1016/j.ygcen.2019.113212

41. Kouki T, Imai H, Aoto K, Eto K, Shioda S, Kawamura K, et al. Developmental origin of the rat adenohypophysis prior to the formation of rathke's pouch. *Development* (2001) 128:959–63. doi: 10.1242/dev.128.6.959

frontiers | Frontiers in Endocrinology

TYPE Original Research
PUBLISHED 30 September 2022
DOI 10.3389/fendo.2022.1011043

OPEN ACCESS

EDITED BY
Piotr Glinicki,
Centre of Postgraduate Medical Education, Poland

REVIEWED BY
Otilia Kimpel,
University Hospital of Wuerzburg, Germany
Mara Carsote,
Carol Davila University of Medicine and Pharmacy, Romania

*CORRESPONDENCE
Mateusz Maciejczyk
mat.maciejczyk@gmail.com

SPECIALTY SECTION
This article was submitted to Adrenal Endocrinology, a section of the journal Frontiers in Endocrinology

RECEIVED 03 August 2022
ACCEPTED 09 September 2022
PUBLISHED 30 September 2022

CITATION
Choromańska B, Myśliwiec P, Kozłowski T, Łukaszewicz J, Vasilyevich HP, Dadan J, Zalewska A and Maciejczyk M (2022) Antioxidant and antiradical activities depend on adrenal tumor type.
Front. Endocrinol. 13:1011043.
doi: 10.3389/fendo.2022.1011043

Antioxidant and antiradical activities depend on adrenal tumor type

Barbara Choromańska[1], Piotr Myśliwiec[1], Tomasz Kozłowski[1], Jerzy Łukaszewicz[1], Harelik Petr Vasilyevich[2], Jacek Dadan[1], Anna Zalewska[3] and Mateusz Maciejczyk[4]*

[1]1st Department of General and Endocrine Surgery, Medical University of Bialystok, Bialystok, Poland, [2]Department of General Surgery, Grodno State Medical University, Grodno, Belarus, [3]Experimental Dentistry Laboratory, Medical University of Bialystok, Bialystok, Poland, [4]Department of Hygiene, Epidemiology and Ergonomics, Medical University of Bialystok, Bialystok, Poland

The aim of the study was to assess the total antioxidant/oxidant status in the plasma and urine of patients with adrenal tumors. The study group consisted of 60 patients (31 women and 29 men) with adrenal masses, classified into three subgroups: non-functional incidentaloma, pheochromocytoma and Cushing's/Conn's adenoma. The number of patients was set *a priori* based on our previous experiment (α = 0.05, test power = 0.9). Antioxidant activity (Total Antioxidant Capacity (TAC), Total Oxidant Status (TOS), Oxidative Stress Index (OSI)) and antiradical activity (Radical-Scavenging Activity Assay (DPPH), Ferric-Reducing Antioxidant Power (FRAP)) were measured using colorimetric methods. FRAP level was decreased in plasma and urine incidentaloma *($p<0.0001$)*, pheochromocytoma *($p<0.0001$)* and Cushing's/Conn's adenoma *($p<0.0001$)*, while DPPH antiradical activity only in plasma of patients with adrenal masses *($p<0.0001$)*. Plasma TAC was increased in incidentaloma patients *($p=0.0192$)*, whereas in pheochromocytoma group *($p=0.0343$)* was decreased. Plasma and urine TOS *($p<0.0001$)* and OSI *($p<0.01$)* were significantly higher in patients with adrenal tumors. In pheochromocytoma patients, plasma and urine TAC *($p=0.001$; $p=0.002$)*, as well as plasma plasma DPPH *($p=0.007$)* and urine FRAP *($p=0.017$)* correlated positively with normethanephrine. We are the first who showed reduced radical scavenging capacity in the plasma/urine of patients with adrenal masses. Nevertheless, plasma TAC was significantly higher in the incidentaloma group compared to controls. Therefore, plasma and urinary antioxidant and antiradical activities depend on the presence of the tumor. Lower levels of TAC, DPPH and FRAP clearly indicate a reduced ability to scavenge free radicals and thus a lack of effective protection against oxidative stress in patients with adrenal tumors. Both plasma and urine redox biomarkers can be used to assess systemic antioxidant status in adrenal tumor patients.

KEYWORDS

adrenal tumors, incidentaloma, pheochromocytoma, cushing's/conn's adenoma, antioxidants, total antiradical activity

Introduction

Although malignant adrenal tumors are rare, with 1-2 cases per 1 million people a year, benign adrenal masses are the most common of all tumors in humans (1). Typically, they are detected incidentally during diagnostic imaging due to other diseases, hence the term incidentaloma (2). Adrenal masses occur in up to 5% of the adult population, with malignancy rates in 1–12% (3). Even though, most of these masses are benign and nonfunctional, 1–15% may cause overproduction of hormones (aldosterone, cortisol or catecholamines) (3–5). Unfortunately, the pathogenesis of adrenal tumors is not fully understood. Currently, it is believed that most of them are caused by genetic abnormalities (6). Hypoxia-induced factor (HIF-1) deregulation has been involved in the pathogenesis of cancer secreting catecholamines (7). Indeed, the VHL/HIF axis mutation is most common in pheochromocytoma (8). Recent research has brought awareness to the key role of oxidative stress (OS) in cancer development (9–11). Reactive oxygen species (ROS) and HIF-1 interact with each other, intensifying the process of carcinogenesis under hypoxic conditions (12–14). In response to hypoxia, HIF-1 activation leads to an increased activity of NADPH oxidase, the main source of ROS in a cell (15). Overproduction of ROS disrupts cellular metabolism including many signaling pathways (NF-κB, PI3 kinase, MAPK or p21RAS) and induces oxidative damage to lipids and proteins (16, 17). The accumulated products of lipid and protein oxidation are cytotoxic increasing the structural and functional damage to cell organelles and inducing apoptosis (18). Further on, overproduction of ROS can damage nucleic acids and lead to cell death through necrosis (16). Therefore, aerobic organisms have developed a defense mechanism in the form of antioxidant barrier (19). Until now, little is known about the interaction of oxidants and antioxidants in the development of adrenal tumors. In our previous study, we have described abnormalities in both enzymatic and non-enzymatic antioxidant barrier (20). However, it is not known how the total antioxidant status changes in patients with adrenal tumors. The compounds with antioxidant properties can interact additively or synergistically with each other (21, 22). Therefore, total antioxidant capacity better characterizes the redox status of the biological system than the determination of individual antioxidants separately (23, 24). Therefore, the aim of this study was to evaluate the total antioxidant potential using various methods: total antioxidant capacity (TAC), iron reducing antioxidant power (FRAP) and the DPPH (2,2′-diphenyl-1-picrylhydrazyl) radical scavenging activity. Redox status was also assessed by measuring the total oxidant status (TOS) and the oxidative stress (OSI) index. Thus, the results of our study will provide an answer to the question: is the oxidation-reduction equilibrium shifted towards the oxidation?

Adrenal tumors may not show specific clinical symptoms and are usually detected accidentally. Due to their diversity, diagnostics are complicated and burdensome for the patient. Therefore, it is important to search new, more specific and sensitive markers in the material collected in a non-invasive manner. Importantly, the total antioxidant potential depending on the biological fluid (plasma, serum, urine, etc.). However, there are no studies characterizing the antioxidant status in different diagnostic biomaterials of patients with adrenal tumors. Therefore, the aim of our study was also a comparative evaluation of the total antioxidant capacity in the plasma and urine to assess their diagnostic utility.

Materials and methods

The study was designed and conducted in accordance with the Guidelines for Good Clinical Practice and the Declaration of Helsinki. The study was also approved by the Bioethics Committee of the Medical University of Bialystok (code of permission: R-I-002/66/2015, APK.002.341.2020). All patients gave their informed consent to participate in this study.

The inclusion criterion for the study group was the presence of an adrenal tumor, while the control group included generally healthy subjects. The diagnosis of adrenal tumor was performed in the departments of internal diseases with an endocrine profile. The subjects from both study and control groups were qualified for the study based on a negative medical history concerning: neoplastic diseases, metabolic diseases (osteoporosis, gout, mucopolysaccharidosis, insulin resistance and type 1 diabetes), cardiovascular diseases, autoimmune diseases (ulcerative colitis, Hashimoto's disease and Crohn's disease), diseases of the genitourinary, digestive and respiratory systems, infectious diseases (HIV/AIDS, hepatitis A, B and C), acute inflammation, as well as pregnancy in women. The participants of the study were not abusing alcohol nor smoking. Additional exclusion criteria were taking nonsteroidal anti-inflammatory drugs, glucocorticosteroids, antibiotics and antioxidant supplements (including iron preparations) for three months before collecting material for the study. Patients in all groups were on a diet (2000 kcal, including 55% carbohydrates, 30% fat, and 15% protein) determined by a dietician.

The study group consisted of 60 patients (31 women and 29 men aged from 50 to 65 years) with adrenal masses diameter > 4 cm and < 8 cm, who were treated using endoscopic adrenalectomy at the First Department of General and Endocrine Surgery at the University Hospital in Bialystok. The patients were classified into three subgroups: patients with non-functional incidentaloma (n=20), pheochromocytoma (n=20) and Cushing's/Conn's adenoma (n=20). In the adenoma subgroup Cushing's syndrome was diagnosed in 11 patients and Conn's syndrome in 9 patients. Preoperatively patients with Conn's syndrome received potassium supplementation or spironolactone (aldosterone receptor blocker). Patients with

phaeochromocytoma took doxazosin (a selective alpha-1-adrenergic receptor blocker) for 10 to 14 days before surgery to avoid intraoperative hypertensive crisis.

The control group included 60 healthy people (31 women and 29 men aged 50 to 65) whose blood counts and biochemical blood tests (Na^+, K^+, ALT, AST, creatinine and INR) were within the reference values. The subjects underwent abdominal ultrasound, which showed no abnormalities. The patients of the controls group were treated at the Specialist Dental Clinic at the Medical University of Bialystok.

The clinical and laboratory characteristics of the control and study groups are shown in Table 1.

Blood and rine collection

All samples from healthy individuals and patients with adrenal mass were collected in a fasting state. The patients declared, that they did not perform intense physical activity twenty-four hours prior to blood sampling. Blood samples were collected into EDTA and serum tubes (SARSTEDT, S-Monovette) and centrifuged at 4°C, 1789 x g for 10 minutes. The urine samples were collected in a sterile disposable container from the first-morning portion of urine from the middle stream immediately after bedtime and centrifuged at 252 x g for 5 minutes. In order to protect against oxidation, the supernatant was added (10 µl of 0.5 M BHT/1 ml of plasma/serum and urine) and stored at -80°C until appropriate determinations were made.

Laboratory measurements

Serum cortisol before 10 a.m., serum aldosterone, Na^+, K^+, glucose, and urine methanephrine and normethanephrine, as well as full blood count were analyzed using an Abbott analyzer (Abbott Diagnostics, Wiesbaden, Germany).

Redox assays

All reagents used to perform the redox assays were obtained from Sigma-Aldrich (Nümbrecht, Germany/Saint Louis, MO, USA). The absorbance of the samples was measured using Mindray MR-96 Microplate Reader (Mindray, Nanshan, China). Determinations of all tested parameters were carried out in triplicate samples. The results were standardized to 1 mg of total protein.

Antioxidant/oxidant activity tests

Total antioxidant capacity

The level of plasma total antioxidant capacity (TAC) was determined using ABTS (2,2-azinobis-3-ethylbenzothiazoline-6-

TABLE 1 Clinical and routine laboratory characteristics of the controls, incidentaloma, pheochromocytoma, and Cushing's/Conn's adenoma patients.

	Controls *(n=60)*	Incidentaloma *(n=20)*	Pheochromocytoma *(n=20)*	Cushing's/Conn's adenoma *(n=20)*	ANOVA
Age	**58** ± 10	**59** ± 12	**57** ± 10	**58** ± 7	*p=0.908*
Size of the tumor (cm)	–	**4.053** ± 1.727	**3.889** ± 1.384	**3.685** ± 1.798	*p=0.7846*
BMI (kg/m^2)	**23.16** ± 0.8042	**29.53** ± 4.97***	**27.58** ± 6.452*	**29.53** ± 3.554****	*p<0.0001*
Na^+ (mmol/l)	**139.1** ± 2.149	**140.5** ± 2.503	**139.1** ± 2.516	**138.8** ± 2.579	*p=0.1015*
K^+ (mmol/l)	**4.411** ± 0.3498	**4.489** ± 0.3129	**4.375** ± 0.351	**4.179** ± 0.5804	*p=0.0895*
WBC ($10^3/\mu L$)	**7.33** ± 1.205	**7.349** ± 2.344	**7.675** ± 2.057	**7.596** ± 2.273	*p=0.926*
RBC ($10^6/\mu L$)	**4.656** ± 0.3412	**4.816** ± 0.3703	**4.483** ± 0.5508	**4.545** ± 0.3733	*p=0.0799*
HGB (g/dL)	**13.62** ± 0.7923	**14.53** ± 1.195	**13.89** ± 1.48	**13.78** ± 1.138	*p=0.0585*
PLT ($10^3/\mu L$)	**288.4** ± 14.08	**242.1** ± 69.22**~	**254.2** ± 49.86	**198.3** ± 46.7****^^	*p<0.0001*
Glucose (mg/dL)	**77.18** ± 6.372	**99.79** ± 21.88***	**91.56** ± 16.91*	**94.94** ± 19.14**	*p<0.0001*
Aldosterone (ng/dL)	**13.86** ± 7.062	**14.46** ± 8.45~	**17.4** ± 8.123	**23.2** ± 13.37***	*p=0.0008*
Serum cortisol before 10 a.m. (µg/dL)	**12.19** ± 4.469	**15.43** ± 5.492	**14.04** ± 5.747	**16.88** ± 5.398**	*p=0.0019*
Urine methanephrine (µg/24h)	**146.5** ± 77.61	**103.7** ± 49.56^^^^	**727.5** ± 544.1****	**152.8** ± 82.38^^^^	*p<0.0001*
Urine normethanephrine (µg/24h)	**237.8** ± 83.04	**248.3** ± 123.7^^^^	**737.5** ± 292.9****	**362.2** ± 128.4**^^^^	*p<0.0001*

Results are presented as mean with standard deviation. *p<0.05, **p<0.01, ***p <0.001, ****p < 0.0001 indicate significant differences from the controls; ^^ p<0.01, ^^^^ p<0.0001 indicate significant differences from the pheochromocytoma group; ~ p<0.05 indicate significant differences from the Cushing's/Conn's group; body mass index (BMI), white blood cell count (WBC), red blood cell count (RBC), hemoglobin (HGB) and platelet count (PLT). Bold indicates mean values.

sulfonic acid) radical cation and Trolox (6-hydroxy-2,5,7,8-tetramethylchroman-2-carboxylic acid) as a standard. Absorbance was read spectrophotometrically at 660 nm (25).

Total oxidant status

In the presence of the oxidants contained in the sample, the level of plasma total oxidant status (TOS) was evaluated bichromatically at 560/800 nm based on the oxidation reaction of Fe^{2+} to Fe^{3+} (26).

Oxidative stress index (OSI)

Oxidative stress index (OSI) was counted as TOS to TAC ratio: OSI = TOS/TAC (27).

Antiradical activity tests

Radical-scavenging activity assay (DPPH)

The antioxidant potential of plasma and urine was also assayed using DPPH (1,1-diphenyl-2- picrylhydrazyl) radical and Trolox as a standard (22). The absorbance of DPPH, after decolorization in the presence of antioxidants, was measured spectrophotometrically at 515 nm.

Ferric-reducing antioxidant power

The level of ferric-reducing antioxidant power (FRAP) was assayed using the reduction reaction of Fe^{2+} to Fe^{3+} an acidic environment. Absorbance of the resulting a colorful ferrous tripyridyltriazine (Fe^{3+}-TPTZ) complex was measured colorimetrically at 592 nm (28).

Hydrophilic antioxidants and hydrogen peroxide

Uric acid (UA)

UA concentration was analyzed using Abbott analyzer (Abbott Diagnostics, Wiesbaden, Germany).

Ascorbic acid

AA concentration was determined colorimetrically using Folin-Ciocalteu reagent. The absorption of the color product formed in the reaction between AA and Folin-Ciocalteu reagent was measured at 760 nm (29).

Albumin

The concentration of albumin was determined colorimetrically using bromocresol green solution. The absorbance was measured at 628 nm wavelength in the reaction between albumin and bromocresol green in succinate buffer.

The total phenolic content

TPC was assayed according to the Folin–Ciocalteu colorimetric method (30). The absorption was measured at 760 nm in the reaction between phenols and Folin–Ciocalteu reagent.

Total thiols

Total thiols concentration was measured colorimetrically at 420 nm using Ellman's reagent (31). The concentration of thiol groups was counted on the basic of the calibration curve using reduced glutathione (GSH) as a standard.

Hydrogen peroxide

The concentration of H_2O_2 was measured using commercially available kit (The Amplex® Red Hydrogen Peroxide/Peroxidase Assay Kit; Invitrogen, Molecular Probes, Paisley, United Kingdom) according to the manufacturer's instructions. The H_2O_2 concentration was determined immediately after centrifuging the sample.

Statistical analysis

Statistical analysis was performed using GraphPad Prism 7.0 (GraphPad Software, La Jolla, USA) and Microsoft Excel 16.49 for MacOS. The Shapiro–Wilk test were used to evaluate the distribution of the results and data were presented as mean ± SD. The homogeneity of variance was checked by Levine's test. The groups were compared using one-way analysis of variance ANOVA with Tukey's *post-hoc* test. Multiplicity adjusted p value was also calculated. Correlations between biomarkers and clinical parameters were assessed based on the Pearson correlation coefficient. Statistically significant value was $p \leq 0.05$.

The number of patients was determined *a priori* based on the previous pilot study ($n = 40$). The power of the test was assumed as 0.9 and $\alpha = 0.05$. Variables used for sample size calculation were plasma and urine TAC, TOS and FRAP. The ClinCalc online calculator provided the sample size for one group. The minimum number of patients was 17.

Results

Table 1 demonstrates a comparison of the clinical and laboratory characteristics of the controls and patients with adrenal masses: incidentaloma, pheochromocytoma, and Cushing's/Conn's adenoma. We found higher BMI values and serum glucose concentration in all study subgroups compared to the healthy controls. The PLT content was decreased in patients with incidentaloma and Cushing's/Conn's adenoma than in the controls and patients with pheochromocytoma. Urinary metanephrine and normetanephrine were increased in the

10.3389/fendo.2022.1011043

pheochromocytoma group than the controls and incidentaloma and Cushing's/Conn's adenoma patients. However, concentration of serum cortisol and aldosterone were higher in Cushing's/Conn's adenoma group as compared to the controls.

Plasma and urine concentration of total antioxidant capacity in patients with adrenal tumors

The TAC test is used to assess total antioxidant activity, especially non-enzymatic antioxidant activity. The TAC test determines the activity of known and unknown antioxidants and detects the synergism between the antioxidants (32, 33). Interestingly, plasma TAC was increased in incidentaloma patients (+29%, $p=0.0192$), whereas in pheochromocytoma group was decreased (-27%, $p=0.0343$) as compared with the controls. Additionally, plasma TAC was greater in incidentaloma group (+77%, $p<0.0001$; +60%, $p=0.0006$; respectively) than the pheochromocytoma and Cushing's/Conn's adenoma patients (Figure 1A). In urine TAC values was significantly diminished in patients with adrenal masses: incidentaloma (-27%, $p=0.0001$), pheochromocytoma (-20%, $p=0.0063$) and Cushing's/Conn's adenoma (-21%, $p=0.0037$) in comparison with the controls (Figure 1B). However, plasma/urine index of TAC was enhanced only in incidentaloma patients (+90%, $p<0.0001$; +101%, $p<0.0001$; +55%, $p=0.0015$; respectively) than the controls, pheochromocytoma and Cushing's/Conn's adenoma (Figure 1C).

Plasma and urine concentration of total oxidant status in patients with adrenal tumors

TOS is indicator to determine all oxidants in the sample, which can more specifically reflect the changes of oxidant capacity than various oxidants measured separately. We found significantly higher values of plasma and urine TOS in all study subgroups: incidentaloma (+214%, $p<0.0001$; +184%, $p<0.0001$), pheochromocytoma (+313%, $p<0.0001$; +375%, $p<0.0001$) and Cushing's/Conn's adenoma (+229%, $p<0.0001$; +200%, $p<0.0001$) than the healthy controls. Moreover, plasma TOS was increased in pheochromocytoma (+31%, $p=0.0082$; +26%, $p=0.0336$; respectively) than the incidentaloma and Cushing's/Conn's adenoma. Similarly to plasma, in urine patients with pheochromocytoma (+67%, $p=0.0245$; +58%, $p=0.0462$; respectively) had greater value than the incidentaloma and Cushing's/Conn's adenoma patients (Figures 1D, E). Plasma/urine index of TOC did not differ between study groups (Figure 1F).

Plasma and urine oxidative stress index in patients with adrenal tumors

We noticed increased OSI in plasma of pheochromocytoma (+421%, $p<0.0001$) and Cushing's/Conn's adenoma (+304%, $p=0.0003$) patients as compared to the healthy controls. Further on, plasma OSI was greater in pheochromocytoma (+123%, $p=0.009$) than incidentaloma patients (Figure 1G). In urine OSI was enhanced in all study subgroups: incidentaloma (+292%, $p=0.0012$), pheochromocytoma (+533%, $p<0.0001$) and Cushing's/Conn's adenoma (+288%, $p=0.0015$) in comparison with the controls (Figure 1H). We did not find any differences in plasma/urine index of OSI in study groups (Figure 1I).

Plasma and urine antiradical activity in patient with adrenal tumors

The antiradical activity is usually determined by measuring the scavenging of the synthetic radical 2,2′-diphenyl-1-picrylhydrazyl (DPPH). It is also measured in ferric reducing antioxidant power (FRAP) assay. The reduction assays assume that antioxidants are reducing agents which react with free radicals (33, 34). We observed markedly lower plasma DPPH in all patients with adrenal masses: incidentaloma (-57%, $p<0.0001$), pheochromocytoma (-65%, $p<0.0001$) and Cushing's/Conn's adenoma (-61%, $p<0.0001$) than the controls (Figure 2A). Whereas, in urine, DPPH was decreased only in Cushing's/Conn's adenoma patients (-37%, $p=0.0056$) as compared to the controls (Figure 2B). However, plasma/urine index of DPPH was diminished in pheochromocytoma (-33%, $p=0.0003$) and Cushing's/Conn's adenoma (-22%, $p=0.0289$) in comparison with the controls (Figure 2C).

The plasma and urine FRAP was significantly decreased in all study subgroups: incidentaloma (-55%, $p<0.0001$; -46%, $p<0.0001$), pheochromocytoma (-54%, $p<0.0001$; -41%, $p<0.0001$) and Cushing's/Conn's adenoma (-53%, $p<0.0001$; -37%, $p<0.0001$) as compared to the controls (Figures 2D, E). However, there were no differences between the study groups in the plasma/urine index of FRAP (Figure 2F).

Serum/plasma and urine concentration of selected antioxidants and hydrogen peroxide

Table 2 presents levels of selected antioxidants and hydrogen peroxide.

We found diminished concentration of UA only in plasma of incidentaloma patients (-19%, $p=0.0056$), while in urine the UA concentration was lower in all study groups: incidentaloma (-25%, $p<0.0001$), pheochromocytoma (-24%, $p<0.0001$) and

10.3389/fendo.2022.1011043

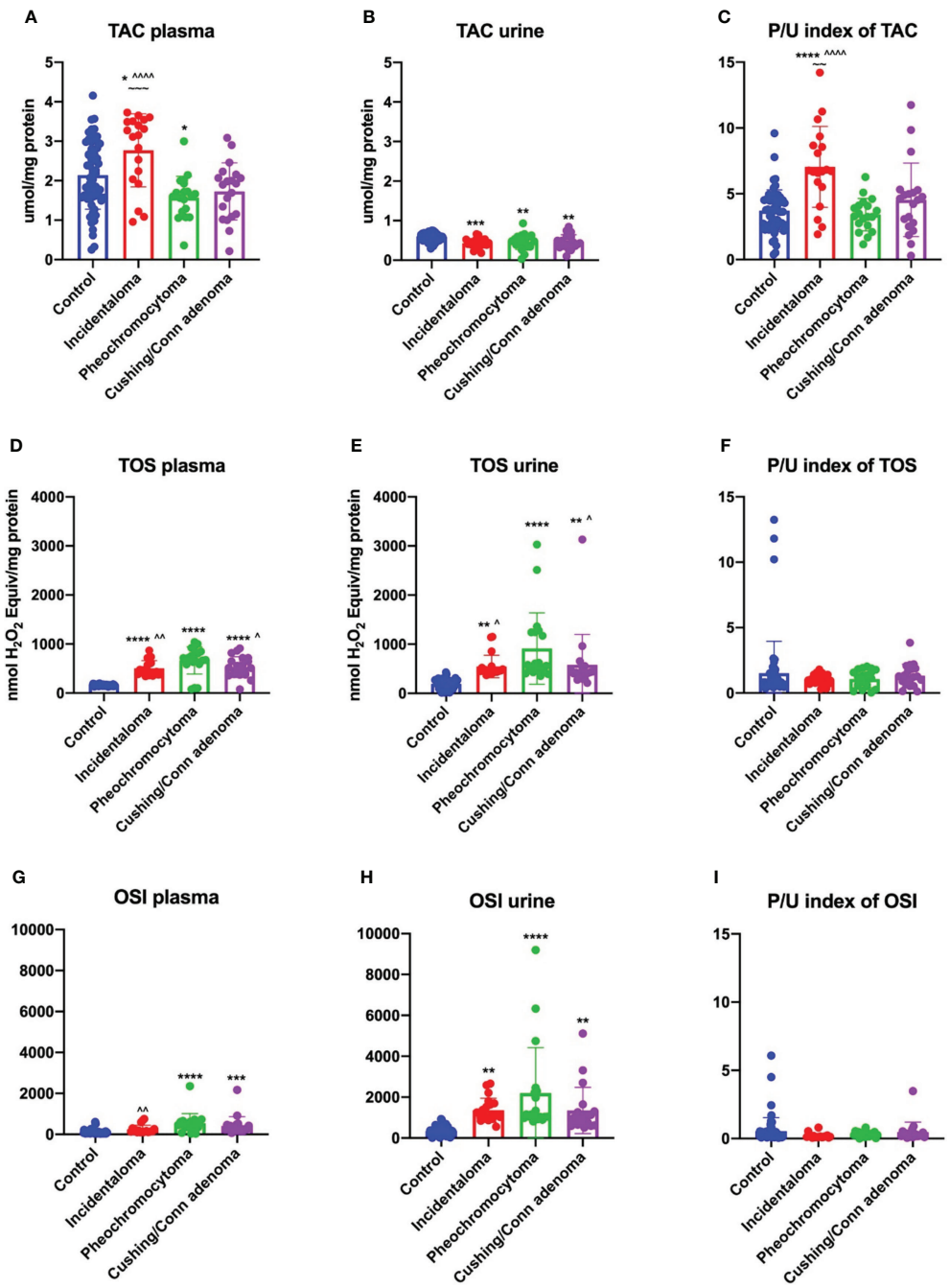

FIGURE 1
Plasma TAC **(A)**, TOS **(D)** and OSI **(G)**, urine TAC **(B)**, TOS **(E)** and OSI **(H)**, and plasma/urine index of TAC **(C)**, TOS **(F)** and OSI **(I)** of the controls, incidentaloma, pheochromocytoma, and Cushing's/Conn's adenoma patients. Results are presented as mean with standard deviation. *p<0.05, **p<0.01, ***p < 0.001, ****p < 0.0001 indicate significant differences from the controls; ^ p<0.05, ^^ p<0.01, ^^^^p<0.0001 indicate significant differences from the pheochromocytoma group; ~~ p<0.01, ~~~ p<0.001 indicate significant differences from the Cushing's/Conn's group; total antioxidant capacity (TAC), total oxidant status (TOS) and oxidative status index (OSI).

10.3389/fendo.2022.1011043

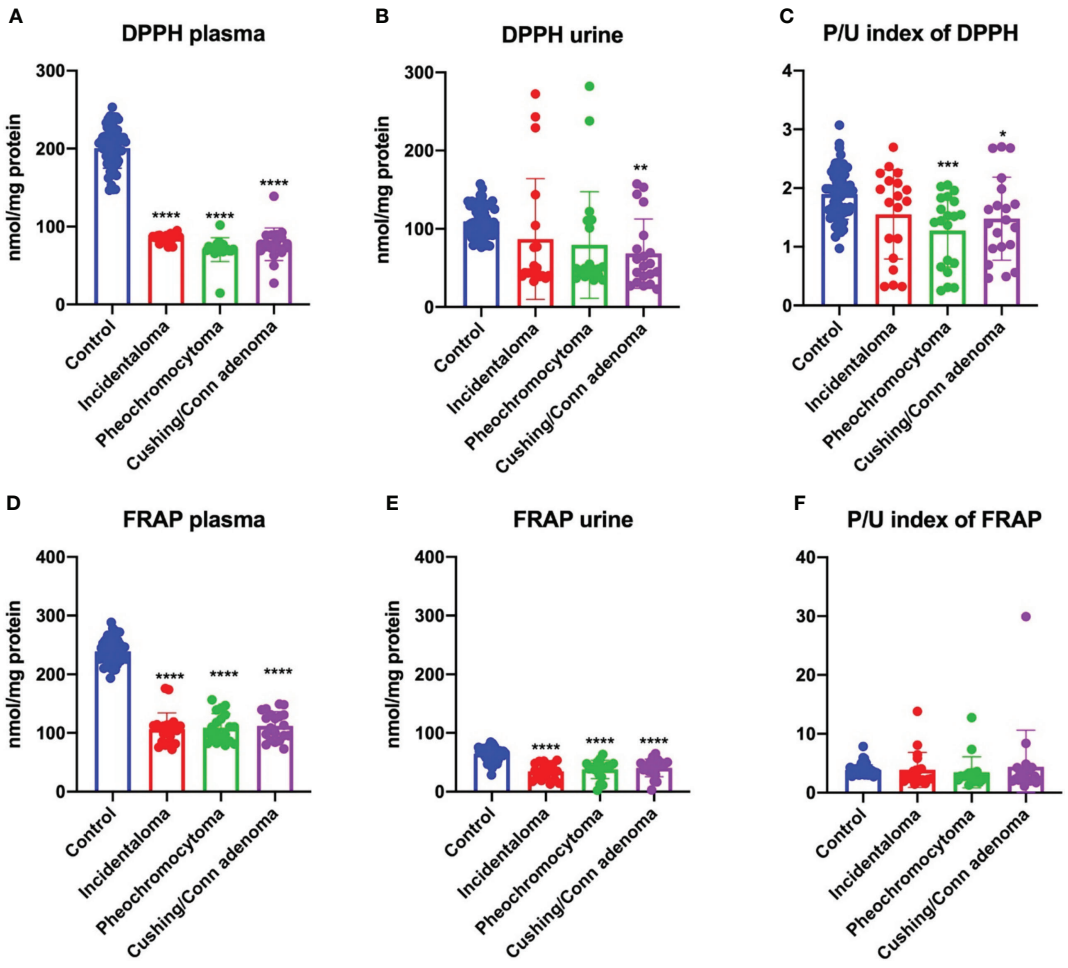

FIGURE 2
Plasma DPPH **(A)** and FRAP **(D)**, urine DPPH **(B)** and FRAP **(E)**, and plasma/urine index of DPPH **(C)** and FRAP **(F)** of the controls, incidentaloma, pheochromocytoma, and Cushing's/Conn's adenoma patients. Results are presented as mean with standard deviation. *p<0.05, **p<0.01, ***p < 0.001, ****p < 0.0001 indicate significant differences from the controls; 2,2′-diphenyl-1-picrylhydrazyl radical (DPPH) and ferric reducing antioxidant power (FRAP).

Cushing's/Conn's adenoma (-29%, *p<0.0001*) in comparison with the controls.

The plasma content of AA was decreased in patients with adrenal incidentaloma (-12%, *p=0.0335*), pheochromocytoma (-16%, *p=0.0031*) and Cushing's/Conn's adenoma (-16%, *p=0.0037*), whereas in urine content of AA was lower in pheochromocytoma (-26%, *p=0.011*) and Cushing's/Conn's adenoma (-27%, *p=0.0085*) than the controls.

We observed decreased concentration of serum albumin in patients with adrenal masses: incidentaloma (-16%, *p=0.0168*), pheochromocytoma (-16%, *p=0.0206*) and Cushing's/Conn's adenoma (-14%, *p=0.0068*) than the controls.

The plasma content of total thiols in patients with incidentaloma was increased (+26%, *p=0.018*) while in pheochromocytoma was diminished (-24%, *p=0.0331*) as compared to the controls. Additionally, patients with incidentaloma had higher plasma total thiols content than pheochromocytoma (+65%, *p<0.0001*) and Cushing's/Conn's adenoma (+42%, *p=0.0033*) groups.

Patients with incidentaloma had lower content of serum and urine (-42%, *p=0.0034*; -23%, *p=0.029*) TPC than the controls, whereas Cushing's/Conn's adenoma had decreased only in serum.

We observed increased concentration of H_2O_2 in plasma and urine of patients with adrenal masses: incidentaloma (+168%, *p<0.0001*; +40%, *p<0.0001*), pheochromocytoma (+60%, *p=0.0004*; +21%, *p=0.0058*) and Cushing's/Conn's adenoma (+48%, *p=0.0082*; +26%, *p=0.0005*) than the controls. Interestingly, plasma concentration of H_2O_2 was greater in incidentaloma patients than pheochromocytoma (+36%, *p<0.0001*) and Cushing's/Conn's adenoma (+82%, *p<0.0001*) groups.

10.3389/fendo.2022.1011043

TABLE 2 The serum/plasma and urine concentration of selected antioxidants and hydrogen peroxide of the controls, incidentaloma, pheochromocytoma, and Cushing's/Conn's adenoma patients.

	Controls *(n=60)*	Incidentaloma *(n=20)*	Pheochromocytoma *(n=20)*	Cushing's/Conn's adenoma *(n=20)*	ANOVA
Serum/plasma					
UA (mg/dL)	**5.427** ± 1.045	**4.393** ± 1.083**	**5.309** ± 1.187	**5.114** ± 1.225	*p=0.011*
AA (µg/mg protein)	**17.03** ± 3.535	**14.98** ± 2.498*	**14.34** ± 1.46**	**14.37** ± 1.733**	*p=0.0001*
Albumin (mg/dL)	**4.934** ± 0.943	**4.223** ± 1.107*	**4.24** ± 0.568*	**4.138** ± 0.896**	*p=0.0005*
TPC (µg/mg protein)	**66.23** ± 27.25	**38.13** ± 24.51**	**52.41** ± 34.65	**49.05** ± 34.21**	*p=0.0032*
Total thiols (µg/mg protein)	**21.07** ± 4.564	**26.47** ± 8.702*^^^^~~	**16.07** ± 7.904*	**18.66** ± 9.837	*p<0.0001*
H_2O_2 (pmol/µL)	**6.319** ± 1.25	**16.96** ± 5.731****^^^^~~~~	**10.14** ± 4.372***	**9.344** ± 4.765**	*p<0.0001*
Urine					
UA (mg/dL)	**54.63** ± 10.47	**40.95** ± 7.78****	**41.26** ± 7.577****	**38.95** ± 10.71****	*p<0.0001*
AA (µg/mg protein)	**17.02** ± 5.294	**13.71** ± 5.902	**12.54** ± 6.243*	**12.42** ± 4.913**	*p=0.0009*
Albumin (µg/mg protein)	**19.87** ± 5.095	**19.76** ± 8.811	**19.93** ± 6.843	**21.47** ± 7.835	*p=0,8016*
TPC (µg/mg protein)	**214.2** ± 61.04	**165.6** ± 74.57*	**175.3** ± 71.74	**190.9** ± 71.1	*p=0.0171*
Total thiols (µg/mg protein)	**1.026** ± 0.4782	**0.9718** ± 0.5693	**0.9658** ± 0.5305	**0.9365** ± 0.465	*p=0.895*
H_2O_2 (pmol/mg protein)	**0.4988** ± 0.0791	**0.699** ± 0.053****	**0.606** ± 0.102**	**0.6283** ± 0.247***	*p<0.0001*

Results are presented as mean with standard deviation. * p<0.05, **p<0.01, *** p <0.001, **** p < 0.0001 indicate significant differences from the controls; ^^^^ p<0.0001 indicate significant differences from the pheochromocytoma group; ~~ p<0.01, ~~~~ p<0.0001 indicate significant differences from the Cushing's/Conn's group; hydrogen peroxide (H_2O_2), ascorbic acid (AA), Total Phenolic Content (TPC) and uric acid (UA). Bold indicates mean values.

Correlations between the analyzed redox biomarkers and clinical parameters in the controls

In the controls, plasma TAC correlated highly positively with urine TAC *(R=0.981, p<0.0001)*, plasma DPPH *(R=0.886, p<0.0001)* and plasma FRAP *(R=0.945, p<0.0001)*, as well as negatively with plasma OSI *(R=-0.724, p<0.0001)*. Plasma OSI was associated positively with urine OSI *(R=0.541, p<0.0001)*, and negatively with plasma DPPH *(R=-0.573, p<0.0001)* and plasma FRAP *(R=-0.604, p<0.0001)*. The positive associations were between plasma DPPH and plasma FRAP *(R=0.858, p<0.0001)*, plasma DPPH and urine DPPH *(R=0.797, p<0.0001)*, plasma FRAP and urine FRAP *(R=0.775, p<0.0001)*, urine TAC and urine DPPH *(R=0.838, P<0.0001)*, urine TAC and urine FRAP *(R=0.812, p<0.0001)*, urine TOS and urine OSI *(R=0.904, p<0.0001)*, and urine DPPH and urine FRAP *(R=0.702, p<0.0001)*. We observed negative correlation between plasma TOS and plasma DPPH *(R=-0.291, p=0.024)*, urine TAC and urine OSI *(R=-0.63, p<0.0001)*, urine TAC and urine TOS *(R=-0.308, p=0.017)*, urine TOS and urine FRAP *(R=-0.27, p=0.037)*, urine OSI and urine DPPH *(R=-0.444, p<0.0001)*, as well as urine OSI and urine FRAP *(R=-0.52, p<0.0001)*. Moreover, BMI correlated positively with cortisol *(R=0.415, p=0.023)*, and negatively with urine TOS *(R=-0.481, p=0.007)* and urine OSI *(R=-0.435, p=0.016)*. Plasma FRAP was positively associated with glucose *(R=0.4, p=0.035)*, while normethanephrine correlated positively with cortisol *(R=0.282, p=0.029)* and methanephrine *(R=0.854, p<0.0001)*. Plasma UA correlated positively with plasma TPC *(R=0.713, p<0.0001)*, plasma and urine TAC *(R=0.879, p<0.0001; R=0.889, p<0.0001)*, plasma and urine DDPH *(R=0.852, p<0.0001; R=0.779, p<0.0001)*, plasma and urine FRAP *(R=0.832, p<0.0001; R=0.705, p<0.0001)*, and negatively with plasma and urine OSI *(R=-0.608, p<0.0001; R=-0.504, p<0.0001)*. Plasma TPC was associated positively with TAC *(R=0.77, p<0.0001; R=0.779, p<0.0001)*, DDPH *(R=0.645, p<0.0001; R=0.618, p<0.0001)*, FRAP *(R=0.772, p<0.0001; R=0.632, p<0.0001)*, and negatively with plasma and urine OSI *(R=-0.6, p<0.0001; R=-0.506)*. Urine UA positively correlated with plasma UA *(R=0.691, p<0.0001)* and plasma TPC *(R=0.495, p<0.0001)*. We observed positive correlation between plasma TPC and plasma UA *(R=0.713, p <0.0001)* and glucose *(R=0.382, p=0.045)*. The urine albumin was positively associated with plasma albumin *(R=0.412, p=0.001)* and BMI *(R=0.415, p=0.023)*. (Figure 3A).

Correlations between the analyzed redox biomarkers and clinical parameters in incidentaloma patients

In incidentaloma patients, plasma TAC was associated positively with plasma DPPH *(R=0.712, p=0.001)*, plasma FRAP

10.3389/fendo.2022.1011043

(R=0.714, p=0.001) and urine TAC *(R=0.943, p<0.0001)*, as well as negatively with plasma OSI *(R=-0.866. p<0.0001)*. The positive correlations were between plasma TOS and plasma OSI *(R=0.733, p<0.0001)*, plasma OSI and urine OSI *(R=0.613, p=0.005)*, plasma FRAP and urine FRAP *(R=0.759, p<0.0001)*, urine TAC and urine DPPH *(R=0.697, p=0.001)*, urine TAC and urine FRAP *(R=0.84, p<0.0001)*, urine TOS and urine OSI *(R=0.594, p=0.006)*, as well as urine DPHA and urine FRAP *(R=0.563, p=0.015)*. Whereas. we found negative associations between plasma TOS and plasma DPPH *(R=-0.498, p=0.025)*, plasma OSI and plasma DPPH *(R=-0.844, p<0.0001)*, plasma OSI and plasma FRAP *(R=-0.493, p=0.032)*, as well as urine TAC and urine OSI *(R=-0.553, p=0.011)*. Further on, plasma TOS negatively correlated with normethanephrine *(R=-0.448, p=0.048)*, whereas urine TOS wit serum albumin *(R=-0.519, p=0.019)*. We observed positive correlations between cortisol and methanephrine *(R=0.485, p=0.03)*, cortisol and urine OSI *(R=0.496, p=0.026)*, methanephrine and normethanephrine *(R=0.781, p<0.0001)*, methanephrine and aldosterone *(R=0.529, p=0.017)*, as well as normethanephrine and aldosterone *(R=0.483, p=0.031)*. Plasma total thiols was positively associated with plasma and urine TAC *(R=0.484, p=0.036; R= 0.482, p=0.032)* as well as with aldosterone *(R=0.549, p=0.12)*, whereas urine total thiols correlated with urine UA *(R=0.464, p=0.039)*. We found negative correlation between plasma AA and plasma FRAP *(R=-0.553, p=0.012)* and urine TOS *(R=-0.501, p=0.024)*. Urine AA was positively associated with TOS *(R=0.722, p<0.0001)* and OSI (R=0.589, p=0.006) in urine. Urine TPC negatively correlated with urine FRAP *(R=-0.552, p=0.014)*. Plasma H_2O_2 was associated positively with urine albumin *(R=0.586, p=0.03)* (Figure 3B).

Correlations between the analyzed redox biomarkers and clinical parameters in pheochromocytoma patients

In pheochromocytoma subgroup, plasma TAC correlated positively with plasma DPPH *(R=0.815, p<0.0001)*, plasma

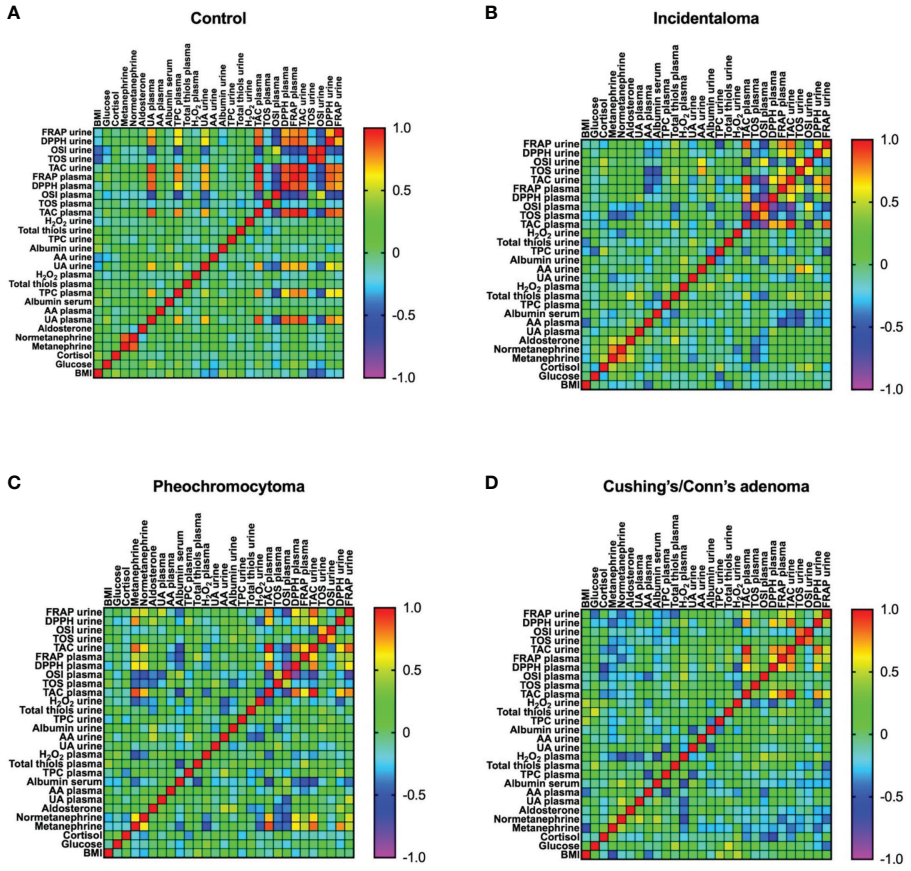

FIGURE 3
Correlations between the analyzed redox biomarkers and clinical parameters in in plasma and urine of the controls **(A)** and patients with incidentaloma **(B)**, pheochromocytoma **(C)**, and Cushing's/Conn's adenoma **(D)**. Ferric reducing antioxidant power (FRAP), 2,2′-diphenyl-1-picrylhydrazyl radical (DPPH), oxidative status index (OSI), total oxidant status (TOS), total antioxidant capacity (TAC), body mass index (BMI).

FRAP *(R=0.61, p=0.004)* and urine TAC *(R=0.973, p<0.0001)*, whereas negatively plasma OSI *(R=-0.711, p<0.0001)*. We found positive associations between plasma TOS and plasma OSI *(R=0.494, p=0.027)*, plasma DPPH and urine DPPH *(R=0.451, p=0.046)*, plasma FRAP and urine FRAP *(R=0.458, p=0.049)*, urine TAC and urine DPPH *(R=0.639, p=0.002)*, urine TAC and urine FRAP *(R=0.835, p<0.0001)*. Methanephrine was associated positively with normethanephrine *(R=0.631, p=0.003)*, plasma and urine TAC *(R=0.877, p<0.0001; R=0.83, p<0.0001)*, as well as negatively with urine H_2O_2 *(R=-0.474, p=0.035)*, DPPH *(R=0.633, p=0.003; R=0.76, p<0.0001)*, and FRAP *(R=0.511, p=0.021; R=0.515, p=0.024)*. We observed that normethanephrine correlated positively with plasma and urine TAC *(R=0.698, p=0.001; R=0.657, p=0.002)*, plasma DPPH *(R=0.586, p=0.007)* and urine FRAP *(R=0.54, p=0.017)*, as well as negatively with plasma OSI *(R=-0.525, p=0.017)*. The negative correlation was also between plasma OSI and plasma DPPH *(R=-0.869, p<0.0001)*. Plasma UA was positively associated with urine FRAP *(R=0.521, p=0.027)* and negatively with plasma OSI *(R=-0.465, p=0.045)*. We observed positive correlation between plasma TPC and urine DPPH *(R=0.462, p=0.047)*. Plasma total thiols was negatively associated with serum albumin *(R=-0.553, p=0.011)*. We found positive correlation between urine AA and aldosterone *(R=0.503, p=0.033)* (Figure 3C).

Correlations between the analyzed redox biomarkers and clinical parameters in Cushing's/Conn's adenoma patients

In Cushing's/Conn's adenoma patients, plasma TAC highly positively correlated with plasma DPPH *(R=0.637, p=0.002)*, plasma FRAP *(R=0.782, p<0.0001)* and urine TAC *(R=0.956, p<0.0001)*. The positive correlations were between plasma DPPH and plasma FRAP *(R=0.58, p=0.007)*, plasma DPPH and urine DPPH *(R=0.674, p=0.001)*, plasma FRAP and urine FRAP *(R=0.516, p=0.02)*, urine TAC and urine DPPH *(R=0.852, p<0.0001)*, urine TAC and urine FRAP *(R=0.527, p=0.017)*, urine TOS and urine OSI *(R=0.821, p<0.0001)*, and urine DPPH and urine FRAP *(R=0.469, p=0.037)*. Additionally, plasma DPPH was associated negatively with cortisol *(R=-0.569, p=0.009)*, whereas methanephrine positively with normethanephrine *(R=0.457, p=0.043)*. We found positive correlation between plasma UA and normethanephrine *(R=0.522, p=0.018)*. Plasma and urine total thiols correlated positively with glucose *(R=0.468, p=0.05; R=0.535, p=0.022)*. The positive correlations were between plasma serum albumin and normethanephrine *(R=0.486, p=0.035)*, as well as urine TPC and BMI *(R=0.461, p=0.041)*, whereas negative correlations were between plasma TPC and plasma AA *(R=-0.542, p=0.017)*, as well as urine albumin and urine UA *(R=-0.49, p=0.028)*. Plasma H_2O_2 was negatively associated with normethanephrine *(R=-0.541, p=0.014)*, plasma UA *(R=-0.45, p=0.046)* and plasma albumin *(R=-0.534, p=0.019)*, while urine H_2O_2 positively associated with BMI *(R=0.477, p=0.033)*. (Figure 3D).

Discussion

In recent years, many studies have been conducted trying to explain the pathogenesis of cancer. The burden of cancer continues to increase worldwide. According to the World Health Organization (WHO), cancer is the second leading cause of death in the world, accounting for approximately 9.6 million deaths in 2018 (35). Numerous studies suggest that redox imbalance may be a factor predisposing to cancer development (9, 36, 37). However, it has not yet been clarified in what direction the redox equilibrium is shifted and whether these disorders may be involved in the development of adrenal tumors. This is the first study to evaluate the total antioxidant potential in patients with adrenal tumors. Additionally, we compared redox status depending on the type of the tumor: incidentaloma, pheochromocytoma and Cushing's/Conn's adenoma.

Antioxidants can act additively or synergistically, and can be absorbed and utilized in the body in different ways (38). Therefore, the assessment of total antioxidant activity provides more reliable information about the biological system than the assessment of individual antioxidants separately (21). There are many different methods for measuring total antioxidant activity. The contribution of individual antioxidants varies, because the same antioxidants have different reactivity in various methods (39, 40). Moreover, in order to correctly measure total antioxidant activity, it is recommended to perform at least two different tests. These methods use the ability of the test compound or product to scavenge free radicals and/or metal ions involved in the oxidation reaction.

It is also important to distinguish between antioxidant and antiradical activity. Antioxidant activity is characterized by the ability to inhibit the oxidation process, while antiradical activity is the ability to react with free radicals (41). In our study, we demonstrated reduced radical scavenging capacity in patients with incidentaloma (↓DPPH and ↓FRAP in plasma), pheochromocytoma (↓DPPH in plasma, ↓FRAP in plasma and urine) and Cushing's/Conn adenoma (↓DPPH and ↓FRAP in plasma and urine) compared to the control group. Antioxidant capacity assessed in the TAC assay was also decreased in the plasma of pheochromocytoma patients and in the urine of all patients with adrenal masses. Nevertheless, plasma TAC levels were also significantly higher in the incidentaloma group compared to controls.

The DPPH test uses stable 1,1-diphenyl-2- picrylhydrazyl free radical and thus reflects the radical scavenging process and antiradical activity (33). The FRAP method is based on the

reduction of iron ions by antioxidants contained in the sample (42). The contribution of individual antioxidants to the total antioxidant potential varies depending on the test used. Due to low pH = 3.6, share of GSH and thiol groups in the total antioxidant potential is significantly lower in the FRAP assay than in DPPH and TAC methods (22, 28). Therefore, plasma FRAP much better reflect the antioxidant potential of the human body (38).

In our study, we observed decreased plasma DPPH and FRAP in all study groups: incidentaloma, pheochromocytoma and Cushing's/Conn's adenoma. This suggests depletion of antioxidant reserves and/or increased free radical production in patients with adrenal masses. This is confirmed by the decrease in blood hydrophilic antioxidants such as AA and albumin compared to controls. TPC content was also significantly reduced in patients with incidentaloma and Cushing's/Conn's adenoma. In contrast, in urine we found a decrease in UA, the most important of the antioxidants in this biological fluid. Urinary AA concentrations were also significantly lower in patients with pheochromocytoma and Cushing's/Conn's adenoma. Although we did not directly evaluate the rate of ROS production in our patients, total oxidative potential (TOS) was significantly higher in adrenal cancer cases as compared to heathy controls. This parameter expresses the total oxidant content in the biological material and may indicate increased ROS formation in patients with adrenal masses. Importantly, this biomarker indicates an increase in both free-radical and non-radical oxidant species.

TAC measures only part of the antioxidant capacity, i.e. non-enzymatic activity, and is mainly influenced by antioxidants present at the highest concentrations. Uric acid and thiol protein groups have the largest share in TAC in human plasma (32). Therefore, the higher plasma TAC in incidentaloma patients may be due to an increased pool of circulating thiols. Indeed, total thiol levels were significantly higher only in patients with incidentaloma. This can be also evidenced by the correlations we found in our study. Plasma thiols was positively associated with plasma and urine TAC *(R=0.484, p=0.036; R= 0.482, p=0.032)* as well as with aldosterone *(R=0.549, p=0.12)*. It also suggests an adaptive response to overproduction of ROS. The strengthening of the antioxidant barrier is the primary protective mechanisms against systemic oxidative stress. In this study, in addition to TOS, we also evaluated hydrogen peroxide production. H_2O_2 is not a free radical. Nevertheless, it has the ability to migrate through cell membranes and, in high concentrations, exhibits a strong cytotoxic effects. Hydrogen peroxide levels were significantly higher in the plasma of incidentaloma group compared to patients with other adrenal masses and healthy controls.

However, we also observed diminished plasma TAC in patients with pheochromocytoma. This may be a result of decreased plasma concentration of GSH, the major non-enzymatic antioxidant in these patients (20). Lower GSH concentrations lead to the intensification of the inflammatory process with an increase in the secretion of inflammatory mediators: IL-1β and TNF-α. Depletion of glutathione reserves also promotes oxidative and carbonyl stress, which may be responsible for the development of metabolic complications of adrenal tumors. However, further studies are needed to clarify the sources of increased ROS production in adrenal tumor cases.

The question now arises: is there a shift in redox equilibrium in favor of oxidation reactions? For this purpose, we calculated the oxidative stress index (OSI), which is the quotient of total antioxidant potential (TAC) to TOS. OSI was significantly higher in all patients with adrenal tumors and therefor antioxidant/oxidant barrier is shifted towards an increased oxidation process. Thus, in patients with adrenal tumors, oxidative damage to proteins, lipids, and DNA may be exacerbated. Although we observed disturbances in the redox homeostasis in all study groups, they were the most severe in patients with pheochromocytoma. Increased oxidative stress in patients with phaeochromocytoma can be associated with HIF-1 (hypoxia-inducible factor 1) activity. Under hypoxic conditions, HIF-1 by stabilizing HIF-1α, increases the activity of NADPH oxidase, contributing to the ROS overproduction. Moreover, most patients with adrenal gland tumors are overweight or obese. It is well known that an excessive amount of adipose tissue leads to increased production of ROS (43). Therefore, the question arises whether the redox disturbances are not the result of increased body weight or metabolic disorders of obesity. Although we have not investigated this directly, it can be speculated that the increased oxidative stress in patients with adrenal tumors may be associated with obesity. It has been described that adipokines secreted by adipose tissue can activate nuclear factor kappa B (NF-κB), which induces the secretion of proinflammatory cytokines (IL-1. IL-6. IL-8), tumor necrosis factor α (TNF-α), as well as impairs the bioavailability of NO and increases the formation of free radicals (43–46). Further on, patients with functional adrenal tumors, especially phaeochromocytomas suffer often from impaired lipid and glucose metabolism, and insulin resistance (47), which may be the result of increased production of catecholamines, obesity, as well as the advantage of the oxidative process over antioxidant (48). In addition, increased cortisol secretion can exacerbate oxidative stress. Although cortisol enhances the process of gluconeogenesis, it also enhances lipolysis of adipose tissue, leading to hyperglycemia and hyperlipidemia (49–51). Thus, we cannot exclude that metabolic abnormalities lead to impaired redox homeostasis in patients with adrenal tumors. Nevertheless, our patients had an adequate glucose profile, indicating that impaired redox balance depends on the presence of the tumor.

It should also be noted that the total antioxidant potential may vary depending on the biological fluid in which it is measured. Parameters that assess redox homeostasis are usually measured in serum or plasma as a stable environment for systemic biomarkers (52). Nevertheless, Il'yasova et al. (53)

argue that urine is a better biological fluid for the evaluation of oxidative stress markers than plasma or serum; and urinary oxidative stress parameters may reflect local and systemic oxidative status (52). The urine has a lower content of metals and ROS promoters, therefore in the urine there is a lower risk of obtaining results with elevated values of oxidative stress markers (53). In this study we observed higher TAC, DPPH and FRAP values in the plasma than in urine. However, it was also observed that urine TAC had similar or higher values than in blood plasma (34). Therefore, it is important to check whether redox biomarkers correlate between different body fluids. Antioxidant status measured in body fluids generally reflect a local, not a systemic, redox homeostasis (54). However, we found positive correlations between plasma FRAP and urine FRAP in patients with incidentaloma. In pheochromocytoma subgroup, plasma TAC correlated positively with urine TAC, as well as plasma DPPH and urine DPPH, plasma FRAP and urine FRAP. In Cushing's/Conn's adenoma, plasma TAC highly positively correlated with urine TAC, plasma DPPH with urine DPPH and plasma FRAP with urine FRAP. This indicates that urinary antioxidant status reflects changes in blood and can be used to assess systemic redox imbalances. These hypotheses are also supported by the correlations between plasma/urinary antioxidant status and the classical biomarkers evaluated to assess disease progression: cortisol, metanephrine, and normetanephrine.

In the study groups, both TAC, DPPH, and FRAP generally did not correlate with UA concentration and total polyphenolic content. Thus, as opposed to healthy people, these compounds may be marginally responsible for plasma/urine antioxidant activity. The weakening of the antioxidant barrier may be due to depletion of other low molecular weight antioxidants such as lipophilic α-tocopherol, β-carotene, retinol, and coenzyme Q10. This issue requires further research and may be of great clinical importance.

Our study confirms previous reports that patients with adrenal tumors are especially vulnerable to oxidative stress and oxidative damage (20, 55). Although our study does not explain this, antioxidant supplementation may be considered in patients with adrenal tumors. Clinical trials evaluating the utility of antioxidant therapy/dietary modifications in patients with adrenal masses are needed. Studies to elucidate the reasons for impaired redox homeostasis in these patients are also essential.

Summarizing, we demonstrated reduced radical scavenging capacity in the plasma/urine of patients with adrenal masses. Nevertheless, plasma TAC was significantly higher in the incidentaloma group compared to controls. Thus, plasma and urinary antioxidant and antiradical activities depend on the presence of the tumor. Both plasma and urine redox biomarkers can be used to assess systemic antioxidant status in adrenal tumor patients. Although antioxidants are the main defense mechanism against ROS overproduction, the reduced levels of TAC, DPPH and FRAP clearly indicate a reduced ability to scavenge free radicals and thus a lack of effective protection against oxidative stress in patients with adrenal tumors.

Data availability statement

The raw data supporting the conclusions of this article will be made available by the authors, without undue reservation.

Ethics statement

The studies involving human participants were reviewed and approved by Bioethics Committee of the Medical University of Bialystok. The patients/participants provided their written informed consent to participate in this study.

Author contributions

Conceptualization, BCh, PM, AZ and MM. Data curation, BCh and MM. Formal analysis, BCh. Funding acquisition, BCh and MM. Investigation, BCh, PM, AZ and MM. Methodology, BCh, AZ and MM. Project administration, BCh. Resources, BCh, PM, HV, and JD. Software, BCh, PM, TK, JL and MM. Supervision, PM, HV, JD and MM. Validation, BCh and MM. Visualization, MM. Writing – original draft, BCh and MM. Writing – review & editing, PM, AZ and MM. All authors contributed to the article and approved the submitted version.

Funding

This work was granted by the Medical University of Bialystok. Poland (grant number: SUB/1/DN/21/002/1140; SUB/1/DN/21/002/3330; SUB/1/DN/21/002/1209; SUB/1/DN/22/002/3330.

Conflict of interest

The authors declare that the research was conducted in the absence of any commercial or financial relationships that could be construed as a potential conflict of interest.

Publisher's note

References

1. Jasim S, Habra MA. Management of adrenocortical carcinoma. *Curr Oncol Rep* (2019) 21:20. doi: 10.1007/s11912-019-0773-7

2. Song JH, Mayo-Smith WW. Incidentally discovered adrenal mass. *Radiol Clin North Am* (2011). doi: 10.1016/j.rcl.2010.10.006

3. Ebbehoj A, Kaur RJ, Li D, Singh S, Zhang C, Atkinson EJ, et al. SAT-176 epidemiology of adrenal tumors: A population based study of 1287 patients. *J Endocr Soc* (2020) 4:SAT-176. doi: 10.1210/jendso/bvaa046.189

4. Jason DS, Oltmann SC. Evaluation of an adrenal incidentaloma. *Surg Clinics North America* (2019) 99(4):721–9. doi: 10.1016/j.suc.2019.04.009

5. Grumbach MM, Biller BMK, Braunstein GD, Campbell KK, Aidan Carney J, Godley PA, et al. Management of the clinically inapparent adrenal mass ("incidentaloma"). *Ann Internal Med* (2003) 56(2):69. doi: 10.7326/0003-4819-138-5-200303040-00013

6. Taïeb D, Pacak K. Genetic determinants of pheochromocytoma and paraganglioma imaging phenotypes. *J Nucl Med* (2020) 61(5):643–5. doi: 10.2967/jnumed.120.245613

7. Vaidya A, Flores SK, Cheng Z-M, Nicolas M, Deng Y, Opotowsky AR, et al. EPAS1 mutations and paragangliomas in cyanotic congenital heart disease. *New Engl J Med* (2018) 378(13):1259–61. doi: 10.1056/nejmc1716652

8. Fishbein L, Leshchiner I, Walter V, Danilova L, Robertson AG, Johnson AR, et al. Comprehensive molecular characterization of pheochromocytoma and paraganglioma. *Cancer Cell* (2017) 31(2):181–93. doi: 10.1016/j.ccell.2017.01.001

9. Zińczuk J, Maciejczyk M, Zaręba K, Romaniuk W, Markowski A, Kędra B, et al. Antioxidant barrier, redox status, and oxidative damage to biomolecules in patients with colorectal cancer. can malondialdehyde and catalase be markers of colorectal cancer advancement? *Biomolecules* (2019) 9:637. doi: 10.3390/biom9100637

10. Zińczuk J, Maciejczyk M, Zaręba K, Pryczynicz A, Dymicka-Piekarska V, Kamińska J, et al. Pro-oxidant enzymes, redox balance and oxidative damage to proteins, lipids and DNA in colorectal cancer tissue. is oxidative stress dependent on tumour budding and inflammatory infiltration? *Cancers (Basel)* (2020) 12 (6):1636. doi: 10.3390/cancers12061636

11. Poprac P, Jomova K, Simunkova M, Kollar V, Rhodes CJ, Valko M. Targeting free radicals in oxidative stress-related human diseases. *Trends Pharmacol Sci* (2017) 38(7):592–607. doi: 10.1016/j.tips.2017.04.005

12. Schroedl C, McClintock DS, Budinger GRS, Chandel NS. Hypoxic but not anoxic stabilization of HIF-1α requires mitochondrial reactive oxygen species. *Am J Physiol Lung Cell Mol Physiol* (2002) 283(5):L922–31. doi: 10.1152/ajplung.00014.2002

13. Wartenberg M, Ling FC, Müschen M, Klein F, Acker H, Gassmann M, et al. Regulation of the multidrug resistance transporter p-glycoprotein in multicellular tumor spheroids by hypoxia-inducible factor (HIF-1) and reactive oxygen species. *FASEB J: Off Publ Fed Am Soc Exp Biol* (2003) 17(3):503-5. doi: 10.1096/fj.02-0358fje

14. Callapina M, Zhou J, Schmid T, Köhl R, Brüne B. NO restores HIF-1α hydroxylation during hypoxia: Role of reactive oxygen species. *Free Radic Biol Med* (2005) 39(7):925–36. doi: 10.1016/j.freeradbiomed.2005.05.009

15. Zhang M, Wu J, Huo L, Luo L, Song X, Fan F, et al. Environmental enrichment prevent the juvenile hypoxia-induced developmental loss of parvalbumin-immunoreactive cells in the prefrontal cortex and neurobehavioral alterations through inhibition of NADPH oxidase-2-Derived oxidative stress. *Mol Neurobiol* (2016) 53(10):7341–50. doi: 10.1007/s12035-015-9656-6

16. Valko M, Rhodes CJ, Moncol J, Izakovic M, Mazur M. Free radicals, metals and antioxidants in oxidative stress-induced cancer. *Chem Biol Interact* (2006) 160 (1):1-40. doi: 10.1016/j.cbi.2005.12.009

17. Li S, Tan HY, Wang N, Zhang ZJ, Lao L, Wong CW, et al. The role of oxidative stress and antioxidants in liver diseases. *Int J Mol Sci* (2015) 16 (11):26087–124. doi: 10.3390/ijms161125942

18. Friguet B. Oxidized protein degradation and repair in ageing and oxidative stress. *FEBS Lett* (2006) 580(12):2910–6. doi: 10.1016/j.febslet.2006.03.028

19. Lushchak VI. Free radicals, reactive oxygen species, oxidative stress and its classification. *Chem Biol Interact* (2014) 224c:164–75. doi: 10.1016/j.cbi.2014.10.016

20. Choromańska B, Myśliwiec P, Kozłowski T, Łuba M, Wojskowicz P, Dadan J, et al. Antioxidant barrier and oxidative damage to proteins, lipids, and DNA/RNA in adrenal tumor patients. *Oxid Med Cell Longev* (2021) 2021:5543531. doi: 10.1155/2021/5543531

21. van der Schaft N, Schoufour JD, Nano J, Kiefte-de Jong JC, Muka T, Sijbrands EJG, et al. Dietary antioxidant capacity and risk of type 2 diabetes mellitus, prediabetes and insulin resistance: the Rotterdam study. *Eur J Epidemiol* (2019) 34(9):853–61. doi: 10.1007/s10654-019-00548-9

22. Janaszewska A, Bartosz G. Assay of total antioxidant capacity: comparison of four methods as applied to human blood plasma. *Scand J Clin Lab Invest* (2002) 62:231–6. doi: 10.1080/003655102317475498

23. Choromańska B, Myśliwiec P, Łuba M, Wojskowicz P, Myśliwiec H, Choromańska K, et al. Impact of weight loss on the total Antioxidant/Oxidant potential in patients with morbid obesity–a longitudinal study. *Antioxidants* (2020) 9(5):376. doi: 10.3390/antiox9050376

24. Toczewska J, Maciejczyk M, Konopka T, Zalewska A. Total oxidant and antioxidant capacity of gingival crevicular fluid and saliva in patients with periodontitis: Review and clinical study. *Antioxidants* (2020) 9(5):450. doi: 10.3390/antiox9050450

25. Erel O. A novel automated direct measurement method for total antioxidant capacity using a new generation, more stable ABTS radical cation. *Clin Biochem* (2004) 37:277–85. doi: 10.1016/j.clinbiochem.2003.11.015

26. Erel O. A new automated colorimetric method for measuring total oxidant status. *Clin Biochem* (2005) 38:1103–11. doi: 10.1016/j.clinbiochem.2005.08.008

27. Skutnik-Radziszewska A, Maciejczyk M, Fejfer K, Krahel J, Flisiak I, Kołodziej U, et al. Salivary antioxidants and oxidative stress in psoriatic patients: Can salivary total oxidant status and oxidative status index be a plaque psoriasis biomarker? *Oxid Med Cell Longev* (2020) 2020:9086024. doi: 10.1155/2020/9086024

28. Benzie IFF, Strain JJ. The ferric reducing ability of plasma (FRAP) as a measure of "Antioxidant power": The FRAP assay. *Anal Biochem* (1996) 239:70–6. doi: 10.1006/abio.1996.0292

29. Jagota SK, Dani HM. A new colorimetric technique for the estimation of vitamin c using folin phenol reagent. *Anal Biochem* (1982) 127(1):178–82. doi: 10.1016/0003-2697(82)90162-2

30. Bobo-García G, Davidov-Pardo G, Arroqui C, Vírseda P, Marín-Arroyo MR, Navarro M. Intra-laboratory validation of microplate methods for total phenolic content and antioxidant activity on polyphenolic extracts, and comparison with conventional spectrophotometric methods. *J Sci Food Agric* (2015) 95:204–9. doi: 10.1002/jsfa.6706

31. Ellman GL. Tissue sulfhydryl groups. *Arch Biochem Biophys* (1959) 82:70–7. doi: 10.1016/0003-9861(59)90090-6

32. Bartosz G. Non-enzymatic antioxidant capacity assays: Limitations of use in biomedicine. *Free Radic Res* (2010) 44(7):711–20. doi: 10.3109/10715761003758114

33. Tirzitis G, Bartosz G. Determination of antiradical and antioxidant activity: Basic principles and new insights. *Acta Biochim Pol* (2010) 57(2):139-42. doi: 10.18388/abp.2010_2386

34. Bartosz G. Total antioxidant capacity. *Adv Clin Chem* (2003) 37:219–92. doi: 10.1016/s0065-2423(03)37010-6

35. Zhuang Q, Lau ZY, Ong WS, Yang GM, Tan KB, Ong MEH, et al. Sociodemographic and clinical factors for non-hospital deaths among cancer patients: A nationwide population-based cohort study. *PloS One* (2020) 15: e0232219–e0232219. doi: 10.1371/journal.pone.0232219

36. Kundaktepe BP, Sozer V, Durmus S, Kocael PC, Kundaktepe FO, Papila C, et al. The evaluation of oxidative stress parameters in breast and colon cancer. *Medicine* (2021) 100:e25104–4. doi: 10.1097/MD.0000000000025104

37. Du X, Li D, Wang G, Fan Y, Li N, Chai L, et al. Chemoprotective effect of atorvastatin against benzo(a)pyrene-induced lung cancer *via* the inhibition of oxidative stress and inflammatory parameters. *Ann Transl Med* (2021) 9:355. doi: 10.21037/atm-20-7770

38. Carrión-García CJ, Guerra-Hernández EJ, García-Villanova B, Serafini M, Sánchez MJ, Amiano P, et al. Plasma non-enzymatic antioxidant capacity (NEAC) in relation to dietary NEAC, nutrient antioxidants and inflammation-related biomarkers. *Antioxidants* (2020) 9(4):301. doi: 10.3390/antiox9040301

39. Arnao MB. Some methodological problems in the determination of antioxidant activity using chromogen radicals: A practical case. *Trends Food Sci Technol* (2000) 11(11):419–21. doi: 10.1016/S0924-2244(01)00027-9

40. Sánchez-Moreno C. Methods used to evaluate the free radical scavenging activity in foods and biological systems. *Food Sci Technol Int* (2002) 8(3):179–83. doi: 10.1106/108201302026770

41. Burlakova EB, Alesenko AV, Molochkina EM, Palmina NP, Khrapova NG. Bioantioxidants in radiation damages and malignant growth. *Nauka (in Russian)* (1975).

42. Honzel D, Carter SG, Redman KA, Schauss AG, Endres JR, Jensen GS. Comparison of chemical and cell-based antioxidant methods for evaluation of foods and natural products: Generating multifaceted data by parallel testing using erythrocytes and polymorphonuclear cells. *J Agric Food Chem* (2008) 56(18):8319–25. doi: 10.1021/jf800401d

43. Furukawa S, Fujita T, Shimabukuro M, Iwaki M, Yamada Y, Nakajima Y, et al. Increased oxidative stress in obesity and its impact on metabolic syndrome. *J Clin Invest* (2004) 114(12):1752–61. doi: 10.1172/JCI21625

44. Förstermann U, Sessa WC. Nitric oxide synthases: Regulation and function. *Eur Heart J* (2012) 33(7):829–37. doi: 10.1093/eurheartj/ehr304

45. Valko M, Leibfritz D, Moncol J, Cronin MTD, Mazur M, Telser J. Free radicals and antioxidants in normal physiological functions and human disease. *Int J Biochem Cell Biol* (2007) 39:44–84. doi: 10.1016/j.biocel.2006.07.001

46. Choromańska B, Myśliwiec P, Łuba M, Wojskowicz P, Dadan J, Myśliwiec H, et al. A longitudinal study of the antioxidant barrier and oxidative stress in morbidly obese patients after bariatric surgery. does the metabolic syndrome affect the redox homeostasis of obese people? *J Clin Med* (2020) 9:976. doi: 10.3390/jcm9040976

47. Erlic Z, Beuschlein F. Metabolic alterations in patients with pheochromocytoma. *Exp Clin Endocrinol Diabetes* (2019) 127(2-03):129–36. doi: 10.1055/a-0649-0960

48. Siraki AG, O'Brien PJ. Prooxidant activity of free radicals derived from phenol-containing neurotransmitters. *Toxicology* (2002) 177(1):81–90. doi: 10.1016/S0300-483X(02)00197-X

49. bin Rubaia'an MA, Alotaibi MK, Alotaibi NM, Alqhtani NR. Cortisol in oral and maxillofacial surgery: A double-edged sword. *Int J Dent* (2021) 2021:7642875. doi: 10.1155/2021/7642875

50. Thuzar M, Stowasser M. The mineralocorticoid receptor–an emerging player in metabolic syndrome? *J Hum Hypertens* (2021) 35:117–23. doi: 10.1038/s41371-020-00467-3

51. Arnaldi G, Scandali VM, Trementino L, Cardinaletti M, Appolloni G, Boscaro M. Pathophysiology of dyslipidemia in cushing's syndrome. *Neuroendocrinology* (2010) 92(suppl 1):86–90. doi: 10.1159/000314213

52. Gyurászová M, Kovalčíková A, Janšáková K, Šebeková K, Celec P, Tóthová L. Markers of oxidative stress and antioxidant status in the plasma, urine and saliva of healthy mice. *Physiol Res* (2018) 67(6):921–34. doi: 10.33549/physiolres.933866

53. , Scarbrough P, Spasojevic I. Urinary biomarkers of oxidative status. *Clin Chim Acta* (2012) 413(19–20):1446–53. doi: 10.1016/j.cca.2012.06.012

54. Maciejczyk M, Zalewska A, Ładny JR. Salivary antioxidant barrier, redox status, and oxidative damage to proteins and lipids in healthy children, adults, and the elderly. *Oxid Med Cell Longev* (2019) 2019:1–12. doi: 10.1155/2019/4393460

55. Choromańska B, Myśliwiec P, Kozłowski T, Łuba M, Wojskowicz P, Dadan J, et al. Cross-talk between nitrosative stress, inflammation and hypoxia-inducible factor in patients with adrenal masses. *J Inflammation Res* (2021) 14:6317–30. doi: 10.2147/JIR.S337910

frontiers | Frontiers in Endocrinology

TYPE Systematic Review
PUBLISHED 17 October 2022
DOI 10.3389/fendo.2022.1021420

OPEN ACCESS

EDITED BY
Marta Araujo-Castro,
Ramón y Cajal University Hospital,
Spain

REVIEWED BY
Thomas Papathomas,
University of Birmingham,
United Kingdom
Ruth Casey,
University of Cambridge,
United Kingdom

*CORRESPONDENCE
Christina Pamporaki
christina.pamporaki@uniklinikum-dresden.de
Georgiana Constantinescu
georgiana.constantinescu@uniklinikum-dresden.de

SPECIALTY SECTION
This article was submitted to Adrenal Endocrinology, a section of the journal Frontiers in Endocrinology

RECEIVED 17 August 2022
ACCEPTED 28 September 2022
PUBLISHED 17 October 2022

CITATION
Constantinescu G, Preda C, Constantinescu V, Siepmann T, Bornstein SR, Lenders JWM, Eisenhofer G and Pamporaki C (2022) Silent pheochromocytoma and paraganglioma: Systematic review and proposed definitions for standardized terminology. *Front. Endocrinol.* 13:1021420. doi: 10.3389/fendo.2022.1021420

Silent pheochromocytoma and paraganglioma: Systematic review and proposed definitions for standardized terminology

Georgiana Constantinescu[1,2,3]*, Cristina Preda[2], Victor Constantinescu[4], Timo Siepmann[3,5], Stefan R. Bornstein[1,6,7], Jacques W. M. Lenders[1,8], Graeme Eisenhofer[1,9] and Christina Pamporaki[1]*

[1]Department of Endocrinology and Diabetes, University Hospital Carl Gustav Carus, Technische Universität Dresden, Dresden, Germany, [2]Department of Endocrinology, Grigore T. Popa University, Iasi, Romania, [3]Department of Health Care Sciences, Center for Clinical Research and Management Education, Dresden Inter-national University, Dresden, Germany, [4]Center of Clinical Neuroscience, University Clinic Carl-Gustav Carus, Dresden University of Technology, Dresden, Germany, [5]Department of Neurology, University Hospital Carl Gustav Carus, Technische Universität Dresden, Dresden, Germany, [6]Department of Health Care Sciences, Center for Clinical Research and Management Education, Dresden International University, Dresden, Germany, [7]Division of Diabetes & Nutritional Sciences, Faculty of Life Sciences & Medicine, King's College London, London, United Kingdom, [8]Department of Internal Medicine, Radboud University Medical Centre, Nijmegen, Netherlands, [9]Institute of Clinical Chemistry and Laboratory Medicine, University of Dresden, Dresden, Germany

Pheochromocytomas and paragangliomas (PPGLs) are rare neuroendocrine tumors with heterogeneous clinical presentations and potential lethal outcomes. The diagnosis is based on clinical suspicion, biochemical testing, imaging and histopathological confirmation. Increasingly widespread use of imaging studies and surveillance of patients at risk of PPGL due to a hereditary background or a previous tumor is leading to the diagnosis of these tumors at an early stage. This has resulted in an increasing use of the term "silent" PPGL. This term and other variants are now commonly found in the literature without any clear or unified definition. Among the various terms, "clinically silent" is often used to describe the lack of signs and symptoms associated with catecholamine excess. Confusion arises when these and other terms are used to define the tumors according to their ability to synthesize and/or release catecholamines in relation to biochemical test results. In such cases the term "silent" and other variants are often inappropriately and misleadingly used. In the present analysis we provide an overview of the literature and propose standardized terminology in an attempt at harmonization to facilitate scientific communication.

KEYWORDS

pheochromocytoma, paragangliomas, silent, clinically silent, biochemically negative

Introduction

Pheochromocytomas and paragangliomas (PPGLs) are neuroendocrine tumors derived from chromaffin cells of the adrenal medulla or extra-adrenal paraganglionic tissue. Clinical presentation of PPGL depends on capacity of the tumors to synthesize and release catecholamines to impact adrenergic receptors in multiple tissues and organs (1). Signs and symptoms vary accordingly and are highly heterogeneous. Biochemical diagnosis depends primarily on measurements of plasma or urinary metanephrines, the O-methylated metabolites of catecholamines (2).

The past several decades have seen increased use of the term "silent PPGL", presumably reflecting increased discovery of tumors that do not produce the usual signs and symptoms of catecholamine excess consequent to their discovery as incidentalomas or during routine surveillance based on hereditary risk or a previous tumor. The term "silent PPGL" or other variants have become common in the literature without any clear or consistent link to the clinical and biochemical presentation of affected patients. In some cases, the term "silent" is used to describe the absence of signs and symptoms of catecholamine excess (3–5). In other cases, use of the terms "silent" and "non-functioning" tumors have been employed equivalently to describe patients with PPGL who present without signs and symptoms but in whom it is not always clear whether the tumors produce catecholamines (6–8). In other cases, the term "non-secretory" or "non-secreting" has been employed to designate patients with absence of secretory symptoms or lack of functional activity (9–11). Appropriate definitions according to the ability of the tumors to synthesize catecholamines (functional/non-functional), release catecholamines (secretory/non-secretory) or according to the presence of positive or negative biochemical test results (biochemically positive/negative) are essential for scientific communication.

The need for unified nomenclature to better describe "silent PPGLs" has become increasingly important given the widespread use of anatomic imaging and expansion of surveillance programs for patients at risk of PPGL due to genetic predisposition or a previous tumor (12, 13). The aim of the present analysis is first to review the relevant literature and then propose standardized terminology in an attempt to improve scientific communication about PPGLs according to their ability to synthesize, store, metabolize and secrete the catecholamines responsible for the heterogeneous clinical presentation of the tumors.

Overview of the literature

Two researchers (GC and VC) independently searched PubMed for articles published in English from 1-1-1980 to 30-08-2021. The following search terms were used: ((pheochromocytoma [MeSH Terms]) or (pheochromocytoma [Title/Abstract]) or (paraganglioma [Title/Abstract])) AND ((silent [Title/Abstract]) or (nonfunctioning [Title/Abstract])). Based on title and abstract, GC and VC independently selected the papers that reported on patients with PPGLs. Subsequently, full text articles were downloaded. Articles without extractable data of individual cases were excluded. GC and VC accessed all papers and extracted data. Items not explicitly reported were noted as 'not mentioned'. Three hundred ten articles were initially identified through PubMed. One hundred twenty-nine articles were excluded for lack of eligibility after review of the title and abstract (not in English, not human related or no abstract available) (Figure 1). Screening by title and article excluded a further 61 articles, while screening after reading the full text reduced the eligible articles to 85, which covered a total of 157 cases in the final analysis. The PRISMA flow diagram is shown in Figure 1. Due to data heterogeneity no meta-analysis was carried out.

Patient characteristics

Among the 157 cases reported in the final analysis (Table 1), 48% were females. Patients presented more often with extra-adrenal (62%) than adrenal tumors, whereas prevalence of metastatic disease was 25%. The most common reasons for biochemical testing were detection of incidental adrenal lesions (62%) due to abdominal or other non-specific complaints. Finally, in 36% of cases, diagnosis was established during surveillance and follow up. There remained only 3 cases (2%) where specific signs and symptoms of catecholamine excess provided the initial reason for the diagnostic work up.

Terminology according to clinical and biochemical phenotypes

In 56 patients (36%) the authors used the term 'clinically silent' (3–9, 14–57) to describe the absence of the "classic triad" and/or hypertension. In eight cases, although patients were defined to have 'clinically silent' tumors, they presented with symptoms that could have been related to catecholamine excess, such as sweating, weight loss, vomiting and nausea (3, 5, 9, 15, 24, 31, 48, 57). In addition to the term "clinically silent" to define the absence of signs and symptoms, other terms were used based on biochemistry. In particular, 55 cases were defined by the authors as "biochemically silent" (4, 11, 16, 18, 21, 22, 58–64), 59 as "non-functional" (6–8, 17, 19, 35–39, 41–50, 52–54, 65–89) and two as "non-secretory" PPGL (9, 10) and 7 patients presented "negative markers" (90).

Among 55 cases defined by the authors as "biochemically silent", test results of plasma metanephrines with respective reference intervals were available in only 15 cases (11, 22, 58,

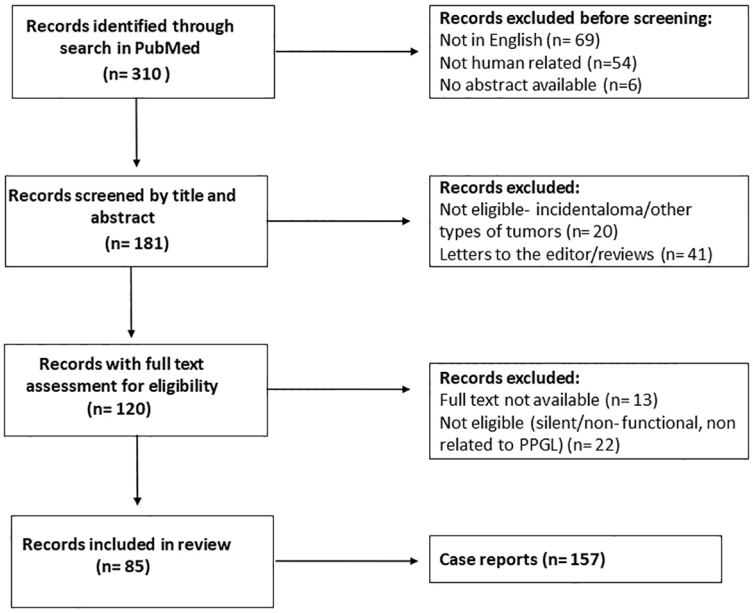

FIGURE 1
Flow chart after review of the literature. After screening and text analysis, 157 cases were included in the final analysis.

TABLE 1 Patient characteristics.

Total Number	**157**
Female, n (%)*	58 (48%)
Age at initial diagnosis, years (SD)	45 (±14.7)
Location	
Extra-adrenal	62% (74/157)
Adrenal	38% (60/157)
Head and Neck	15% (25/157)
Diagnostic setting	
Incidentaloma	62% (97/157)
Abdominal complaints	48.3% (45/93)
Imaging performed for non-specific complaints	51.7% (48/93)
Surveillance/Follow up	36% (57/157)
Specific signs and symptoms	2% (3/157)
Tumor composition (reported in 29 cases)	
Solid	31% (9/29)
Cystic	31% (9/29)
Hemorrhagic and/or necrosis	38% (11/29)
Maximal tumor diameter (cm) (reported in 81 cases)	5.5 (0.25-25)#
Metastatic disease (reported in 68 cases)	25% (17/68)
Plasma free metanephrines (reported in 45 cases)	
Results within the normal range	89% (40/45)
Elevated results	11% (5/45)
Urinary metanephrines (reported in 57 cases)	
Results within the normal range	75.4% (43/57)
Elevated results	24.5% (14/57)

59, 64) (Table 2). Among those 15 cases, test results and reference intervals for plasma catecholamines and metanephrines were reported in five cases (11, 58) and for urinary metanephrines (+/- catecholamines) in 25 cases (16, 21, 22, 58, 59, 61, 63, 64). All plasma results showed values below upper cut-offs of stipulated reference intervals. Urinary metanephrines were below upper cut-offs of reference intervals in all except one case when at the 3 year follow up the patient presented with increased urinary normetanephrine (21). Finally, test results and reference intervals for plasma and urinary metanephrines were available in only eight cases (22, 58, 59, 64), whereas in only four patients test results and reference intervals were available for catecholamines and metanephrines in both plasma and urine (58). In all these patients the results showed normal values.

Similarly, among 59 patients classified by the authors with 'non-functional' tumors (6–8, 17, 19, 35–39, 41–50, 52–54, 65–89), test results and reference intervals for plasma metanephrines were only mentioned in ten cases (65, 86, 89) and for urinary metanephrines in fourteen (65, 79, 86, 87) (Table 2). In one patient referred to as having a non-functional tumor, both plasma and urinary measurements indicated increased concentrations of normetanephrine (65), while in another patient only plasma metanephrines were measured and found to be increased (19). Two patients were referred to as having 'non-secretory' PPGL (9, 10) while 7 patients presented with negative markers according to the authors (90).

10.3389/fendo.2022.1021420

TABLE 2 Biochemical tests in patients according to authors' classification of catecholamine biochemical activity.

	Biochemically silent				Non-functional/Non-secretory/ Negative markers			
	No	TR	RI	References[§]	No	TR	RI	References[§]
Plasma								
Cat	1	1	1	16	9	2	1	87, 90[¥]
Met	36	15	25	22, 59,61*, 64	14	10	10	65[¶], 86, 89,90[¥]
Cat& Met	5	5	5	11, 58	0	0	0	–
CgA	4	3	3	16, 58	1	1	1	9
Urine								
Cat	3	0	0	–	6	1	1	84
Met	36	9	25	21[¶], 22, 61*,64	16	16	14	9[¥], 65[¶], 79, 86, 87,90[¥]
Cat& Met	15	15	15	16, 58, 59, 63	2	1	1	43
VMA	2	0	0	-	9	3	3	36, 41, 88

No, total number of patients with; Cat, catecholamines; Met, metanephrines; CgA, chromogranin A; VMA, vanillylmandelic acid; TR, test result reported; RI, reference interval reported; *referred to RI but had not test results, [§] references of manuscripts presenting RI and TR.
[¶] increased concentration, [¥] referred to TR but had no RI.

The method of measurement for plasma and urinary catecholamines and metanephrines was mentioned only in eight studies, either as high performance liquid chromatography (9, 29, 58, 59, 63) or liquid chromatography with mass spectrometry (23, 61, 86).

Proposed definitions for a standardized approach

Review of the literature revealed that the term "silent" was used in a highly variable fashion according to widely differing circumstances. The term "clinically silent" was mainly used to describe the absence of symptoms of catecholamine excess, which is appropriate. However, definitions according to the ability of tumors to synthesize and/or release catecholamines were inconsistently used according to biochemical test results. In some cases, biochemical test results were not even mentioned. In order to address these shortcomings, we propose use of standardized terminology that may be useful in an attempt for harmonized and more consistent descriptions of how patients may present with silent PPGL.

Clinically silent PPGLs

"Clinically silent" PPGLs are more common than usually appreciated. Starting in the 1980s patients with pheochromocytoma who were both normotensive and asymptomatic began to be identified incidentally upon imaging studies for purposes other than suspicion of the tumor (91), a trend that has increased subsequently with the broadening use of imaging studies (92). Before this, the almost exclusive mode of discovery was based on clinical suspicion according to the presence of signs and symptoms (93).

Starting in the late 1980's, with the advent of surveillance programs involving patients with von Hippel Lindau (VHL) syndrome or multiple endocrine neoplasia (MEN), it became apparent that most patients identified in this way also had clinically silent tumors (94–100). Discovery at an earlier stage by positive biochemical tests and/or imaging studies when tumors are small and secrete insufficient amounts of catecholamines to produce typical manifestations of the tumor provides the main explanation for such presentations. This underlies the likelihood that all PPGLs start out without eliciting signs and symptoms of catecholamine excess. Nevertheless, some PPGLs can be relatively large and/or secrete large amounts of catecholamines and still remain clinically silent, indicating that other factors can contribute to a normotensive and asymptomatic presentation (101–103).

Apart from tumor size and the extent of catecholamine secretion, other factors that may contribute to the absence of signs and symptoms in patients with PPGLs include the types of catecholamines secreted, the sustained or episodic nature of catecholamine secretion and adaptive physiological responses to catecholamine secretion. About half of all pheochromocytomas produce a combination of epinephrine and norepinephrine, while most others and particularly paragangliomas produce nearly exclusively norepinephrine (104). These differences depend on expression of phenylethanolamine-N-methyltransferase (PNMT), the enzyme that converts norepinephrine to epinephrine (105). Some tumors that show minimal expression or complete lack of dopamine-β-hydroxylase, the enzyme that converts dopamine to norepinephrine, may produce and secrete combinations of dopamine and norepinephrine or occasionally in some paragangliomas only dopamine.

Dopamine has negligible actions on α- and ß-adrenoreceptors and primarily elicits vasodepressor responses *via* actions mediated by an array of dopamine receptors particularly important in mesenteric and renal vascular beds (106, 107). This clarifies why patients with dopamine-producing paragangliomas may be asymptomatic and are usually normotensive or may even suffer from hypotension (105, 108). Epinephrine has variably more potent agonist actions on α- and ß-adrenoreceptors than norepinephrine (109). Epinephrine has particularly stronger actions than norepinephrine on $ß_2$-adrenoreceptors responsible for vasodilation in skeletal muscle. According to studies involving intravenous (i.v.) infusions of epinephrine and norepinephrine in healthy subjects, increases in systolic blood pressure relative to the increased plasma catecholamines are larger for epinephrine than norepinephrine (110). On the other hand, diastolic blood pressure shows small decreases compared to increases with norepinephrine.

With the above factors in mind, the lower potency of norepinephrine than epinephrine on adrenoceptors may contribute to the higher proportion of normotensive and clinically silent norepinephrine-producing tumors in patients with VHL syndrome than those with epinephrine-producing tumors in MEN2 (95); however, there are other factors that can contribute to a clinically silent phenotype among patients with PPGLs.

Among various factors to be considered to account for clinically silent PPGL, it should not be overlooked that blood pressure and other responses associated with increased plasma concentrations of norepinephrine are much larger when due to increased secretion of norepinephrine from sympathetic nerves than associated with i.v. infusion of norepinephrine and therefore presumably also secretion of norepinephrine from a PPGL. For example, although a little more than 2-fold increase in plasma norepinephrine to 3.6 nmol/L during sympathetic activation results in a 25 mmHg increase in systolic blood pressure (111), the same increase in norepinephrine during its i.v. infusion results in only a 4 mmHg increase in systolic blood pressure, while a 25 mmHg increase in blood pressure requires circulating concentrations of norepinephrine of over 20 nmol/L (110). These differences reflect concentration gradients of the transmitter between sites of release at neuroeffector junctions in the adventitia of blood vessels compared to the bloodstream and differing geographic locations of adrenoceptors within blood vessels impacted by neuronal versus hormonal secretion (112). More than 80% of norepinephrine in the blood stream is derived from neuronal rather than hormonal sources and circulating norepinephrine is largely irrelevant as a hormone compared to epinephrine, which also targets different populations of adrenoceptors. The above considerations explain why increases in plasma norepinephrine resulting from tumoral secretion of the catecholamine may not evoke signs and symptoms of catecholamine secretion until increases are reasonably large.

In addition to the aforementioned factors, physiological adaptation can also contribute to a clinically silent presentation in the face of high circulating concentrations of catecholamines. This can take the form of both hypovolemia or a redistribution of blood volume as a compensatory response to increased blood pressure or diminished responsiveness of adrenoceptors to activation by catecholamines after prolonged adrenergic stimulation (101, 113). Of additional relevance are repeated observations that tumors that produce exclusively norepinephrine tend to secrete the catecholamine in a sustained manner whereas those that produce epinephrine tend to more often show an episodic pattern of catecholamine secretion (114–116). Sustained secretion of norepinephrine in the former noradrenergic tumors might be expected to contribute to tachyphylaxis more than in tumors that secrete catecholamines in widely spaced episodes.

It should also be appreciated that although noradrenergic tumors show a usually more sustained pattern of catecholamine secretion than adrenergic tumors, these tumors are also characterized by lower secretory stores of catecholamines (117); this might further impact the clinical presentation by limiting overall secretory capacity.

Apart from head and neck paragangliomas that usually do not produce appreciable catecholamines, relatively low tissue catecholamine stores are particularly common in patients with paragangliomas due to mutations of succinate dehydrogenase subunit B and D (*SDHB* and *SDHD*) genes (117). Tumors due to *SDHB* mutations show a particularly immature phenotype that often involves relatively high tissue contents of dopamine. In order to produce and secrete sufficient amounts of catecholamines to cause related signs and symptoms, these tumors often reach a large size before diagnosis, which may contribute to their predisposition to metastasize. Also, occasionally found are tumors that produce only dopamine (108) or those that do not produce any catecholamines and which remain clinically silent until they produce local mass effects.

Finally, and as will be covered in more detail later, although almost all PPGLs produce catecholamines, a significant proportion do not secrete catecholamines in amounts sufficient to produce diagnostically meaningful increases in plasma or urinary catecholamines or related signs and symptoms of catecholamine excess. These tumors typically can only be detected by measurements of metanephrines in urine or more ideally plasma. Most often these tumors are adrenergic in nature and may only become apparent clinically after catecholamine secretion is provoked.

Taking all the above into consideration, several factors may contribute to the absence of clinical manifestations of PPGLs including small tumor size and minimal catecholamine secretion, as well as the type and pattern of catecholamine secretion, adrenoceptor desensitization and other compensatory responses to the disease. However, in many cases patients may present with nonspecific signs and symptoms that are overlooked by clinicians, especially if there

is coexistence of other clinically confusing conditions (e.g., diabetes, menopause, migraine). Based on our review of the literature, most clinicians still focus their interest on the presence or absence of hypertension (6, 8, 19, 21, 28, 30, 47, 56), although it has been repeatedly shown that this feature has rather limited value for triaging patients according to the likelihood of disease (114, 118–120). On the other hand, symptoms such as hyperhidrosis, palpitations, tremor, pallor, nausea or signs such as low body mass index may be more useful in the assessment of the clinical suspicion of a PPGL (120). A detailed medical history for the detection of clinical signs and symptoms related to catecholamine excess, is therefore important before defining a PPGL as "clinically silent".

Non-secretory PPGLs

Although the term "clinically silent" should be used to describe the absence of signs and symptoms of catecholamine excess, the term "non-secretory" is preferably used to describe tumors that consistently show lack of catecholamine secretion as manifest by repeated samplings of blood or 24-hour urine specimens and measurements of catecholamines. Catecholamines are actively secreted from chromaffin cells or tumors, principally by a process involving exocytosis, which can occur episodically or at low rates (121). Independent of their secretion, catecholamines also leak continuously from storage vesicles into the cytoplasm of chromaffin cells. Presence of catechol-O-methyltransferase (COMT) within the cytoplasm then leads to metabolism of norepinephrine to normetanephrine and of epinephrine to metanephrine; the metabolites then diffuse passively from chromaffin cells into circulation (122, 123).

"Non-secretory" PPGLs are most often adrenergic tumors, including those due to mutations of cluster 2 genes, that despite the large amounts of tissue catecholamines (Figure 2A), show dense distributions of both epinephrine and norepinephrine vesicles, associated with low levels of secretory activity (Figure 2B). Secretion is often less than 5% of all catecholamine stores within one day (Figure 2C). Consequently, such tumors may present with consistently normal plasma concentrations or urinary outputs of norepinephrine and epinephrine.

Although patients with adrenergic tumors are often asymptomatic due to circulating catecholamines at entirely normal concentrations, it is important to appreciate that such "non-secretory" PPGLs remain functional with large amounts of tissue catecholamines that continuously leak into cytoplasm. There the catecholamines are metabolized to metanephrines, providing a biochemical signal more useful than the catecholamines for diagnosis (124). Also, although such tumors may be classified as non-secretory in nature, it must be appreciated that any tumor that synthesizes, stores and metabolizes catecholamines to metanephrines also has the capacity to secrete catecholamines if provoked. Indeed, the highly differentiated nature of cluster 2 tumors means that the many components of the secretory apparatus are intact and in place to limit catecholamine secretion unless a signal is received (116). The intact secretory apparatus includes receptors and secondary messenger systems that can respond to many signals including dopamine D2 receptor antagonists and glucagon (125). Provoked secretion of catecholamines from these adrenergic tumors can thereby be more easily achieved than from noradrenergic tumors or those due to mutations of pseudohypoxia genes, which secrete catecholamines more continuously than adrenergic tumors (116, 117).

One illustrative case reported as a "non-secreting" pheochromocytoma, based on consistently negative test results for urinary and plasma catecholamines, involved a woman who presented with hypertensive crises after administration of a dopamine D2 receptor antagonist (9). The patient showed complete recovery after a 2.5 cm adrenal mass was resected. Thus, simply because catecholamines may be normal, this does not imply that there is no tumor capable of secreting catecholamines if provoked. In the above case additional tests included plasma chromogranin A, urinary VMA and total metanephrines, but these are also all insensitive tests of catecholamine excess. Measurements of urinary fractionated metanephrines, or more ideally mass spectrometric measurements of plasma free metanephrines, more appropriately establish functionality, but even the latter can be negative in patients with small tumors (86).

Of course, plasma and urine catecholamines can also be consistently normal in patients with large tumors; these can include rare tumors that lack the biosynthetic machinery required for catecholamine production and that also do not produce increases in urinary fractionated or plasma free metanephrines. Although such tumors might also be labeled as "non-secretory" there are other terms as covered later that may more accurately define the nature of their biochemical and clinical presentation.

Biochemically negative PPGLs

Review of the literature shows that patients with PPGLs and negative biochemical test results are often defined to have "biochemically silent" tumors (4, 11, 16, 18, 21, 22, 58–63). In most of the aforementioned studies, the authors define PPGLs as "biochemically silent" according to measurements of catecholamine-related biomarkers that do not exceed the upper cut-offs. Although this may be appropriate in certain circumstances, the term "biochemically silent" is often used indiscriminately. In particular, a large proportion of patients categorized with "biochemically silent" tumors simply have false-negative biochemical test results as a consequence of

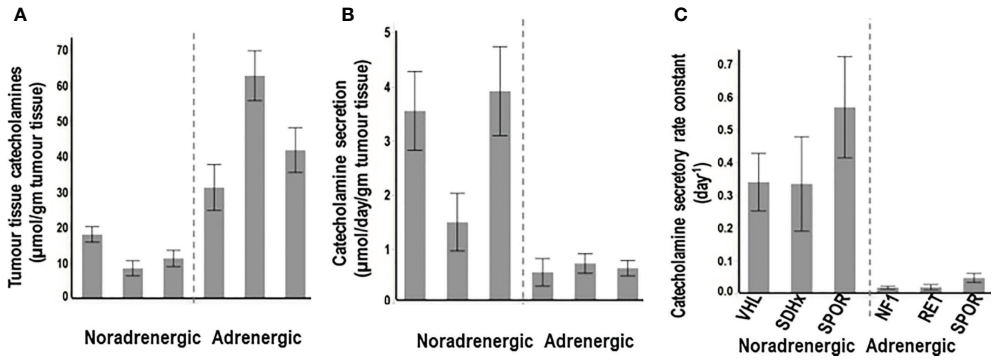

FIGURE 2
Tumor tissue contents of catecholamines **(A)**, rates of secretion of catecholamines from tumors **(B)** and catecholamine secretory rate constants **(C)** for PPGLs from patients with hereditary (*VHL, SDHx*), and sporadic (SPOR) noradrenergic tumors versus hereditary (*NF1, RET*) and sporadic (SPOR) adrenergic tumors. Secretory rate constants illustrate that for noradrenergic tumors over a third of all catecholamines in stores are secreted within one day, whereas for adrenergic tumors less than 5% of stores are secreted within one day. (*Reproduced with permission from Eisenhofer G et al. Clin Biochem Rev 2017*).

inappropriate choice of biochemical markers, measurement methods or even application of reference intervals. The appropriate solution is to define these tumors as "biochemically negative". Such solutions should also clarify the particular test, analytical measurement method and associated reference intervals.

As established in the present literature review, the above information is rarely provided in manuscripts reporting on biochemically silent PPGLs. Even when some or all of the above data are supplied, there may be errors or confusion. The patient presented by Kota et al. (22) with a biochemically silent adrenal incidentaloma that resulted in an intra-operative hypertensive emergency, and was subsequently confirmed to be a pheochromocytoma, provides an illustrative example. The patient was reported to have normal pre-operative urinary fractionated and plasma metanephrines. However, review of the presented data reveals urinary metanephrines reported as a single value with reference intervals in line with spectrophotometric measurements of total metanephrines rather than contemporary measurements of the fractionated metabolites. Even more strikingly, plasma measurements were similarly reported as a single value of 34 µg/dL. Though lower than the reported cut-off of 60 µL/dL, those values are more than three orders of magnitude higher than established plasma concentrations and also well beyond the range of either normetanephrine or metanephrine for patients with pheochromocytoma. Such reports are emblematic of a general lack of clinical understanding of measurement methods and biochemical tests.

Despite recommendations of the Endocrine Society clinical practice guidelines that biochemical diagnosis of PPGLs should be based on measurements of plasma free or urinary fractionated metanephrines (2) many clinicians still rely on measurements of catecholamines, vanillylmandelic acid (VMA) and/or chromogranin A (CgA) for diagnosis of PPGLs. As covered earlier, metanephrines are produced within chromaffin cells by COMT, an enzyme absent in sympathetic nerves. This means that the O-methylated metabolites are much more specific for chromaffin cells and PPGLs than their parent catecholamines or any other catecholamine metabolites. Consequently, about 8-9% of patients with sporadic PPGLs and 21-31% with hereditary PPGLs, have normal plasma concentrations and/or urinary outputs of catecholamines but show elevations of plasma metanephrines (126). Apart from the importance of measuring metanephrines rather than catecholamines, the benefits of additional measurements of methoxytyramine in plasma should also be considered. This assists not only with confirmation of disease but also with detection of predominantly dopamine producing tumors (108, 127).

Although the superiority of metanephrines over catecholamines is clear, superiority of measurements in plasma over urine was only recently clearly established. In particular, Eisenhofer and colleagues (86), showed that urinary fractionated metanephrines and methoxytyramine have a significantly lower sensitivity (92.9%) compared to plasma free metanephrines and methoxytyramine (97.9%). The above findings can be explained by the large amounts of normetanephrine and dopamine formed in the body that are produced and metabolized within mesenteric organs (128). This confuses the diagnostic signal of urinary normetanephrine and methoxytyramine, which are commonly measured in urine after acid hydrolysis catalyzed deconjugation of sulfate conjugated metabolites to free metabolites. The sulfate-conjugated metabolites are the main species present in urine and their synthesis from the actions of a specific sulfotransferase isoenzyme, SULT1A3, localized to gastrointestinal tissues, acts to dilute the signal of the free

metabolites produced elsewhere in the body including in chromaffin cell tumors. The additional substantial impact of dietary derived dopamine on sulfate conjugated metabolites of dopamine and its metabolite methoxytyramine further reduces any diagnostic signal for urinary methoxytyramine measured after acid hydrolysis (129).

Apart from the appropriate choice of biochemical markers, appropriate choice of measurement methods is also crucial for the accurate diagnosis or exclusion of PPGLs. Among analytical methods, liquid chromatography with electrochemical detection (LC-ECD) (122), and liquid chromatography with tandem mass spectrometry (LC-MS/MS) (130) offer superior diagnostic performance compared to immunoassays (131). Although LC-ECD is well established for measurements of urinary fractionated metanephrines, many clinicians continue to rely on immunoassay measurements of plasma metanephrines, which is associated with false negative results in up to a quarter of all patients with PPGL (131). The significant drop in the diagnostic sensitivity is explained by problems with calibration, in particular lack of commercially available L-isomers, which resulted in measurements that are 60% lower than true concentrations. The problem is further compounded by use of inappropriately high upper cut-offs of reference intervals.

Inappropriately high upper cut-offs can also be a problem for other methods used for measurements of plasma free metanephrines. In particular, some laboratories have set cut-offs of reference intervals determined from blood samples obtained from patients in the seated position, which results in an activated sympathetic nervous system and increased plasma concentrations of norepinephrine and normetanephrine. The associated reference intervals are too high for reliable confirmation of PPGL, as well as exclusion of PPGL, which as recommended by Endocrine Society guidelines should be established from samples taken in the supine position.

Although most of the "biochemically silent" PPGLs described in the literature probably involve cases with false negative test results, there are occasional patients with truly "biochemically silent" PPGLs. Apart from the non-functional tumors that are described in detail below, functional PPGLs of small size (usually <1 cm) at an early stage of development may present with negative biochemical test results. Indeed, surveillance programs and widespread use of imaging techniques have led to the increased detection of such small PPGLs, which despite their functionality are still too small to produce sufficient amounts of catecholamines and therefore meaningful increases in plasma or urinary catecholamines and their metabolites. This can be easily understood when the strong association between tumor size and the extent of increases in summed plasma concentrations of metanephrines is considered (89). As mentioned above, this association is based on the continuous production of metanephrines within the tumor cell cytoplasm, which depends on passive leakage of catecholamines from vesicular stores, the size of which relate to tumor burden (123, 124).

Non-functional PPGLs

Correct determination of functionality – in terms of whether PPGL synthesize, store and have potential to secrete catecholamines – can be important in determining need for pre-operative α-adrenoceptor blockade to avoid potential danger of catecholamine hypersecretion that might be provoked during surgical intervention. Even a small PPGL or those associated with normal biochemical test results can produce dangerous increases in blood pressure (132–134). Hypertensive crises during adrenalectomy have been reported in patients with negative biochemical test results (8) including one case involving development of pulmonary edema that required a seven day intensive care unit recovery (4). Increasingly inappropriate use of the term, "non-functional", may be misleading to some who may incorrectly determine lack of need for α-adrenoceptor blockade.

"Non-functional" PPGLs, are tumors that neither synthesize nor secrete catecholamines, often located in the head and neck (HNPGL) or rarely the upper/anterior mediastinum (135). Only 3-4% of HNPGLs produce norepinephrine (136), though as much as 1/3 of all HNPGLs may produce some dopamine (137). In cases of total absence of catecholamine production, HNPGLs can be defined as "non-functional". Abdominal "non-functional" PPGLs are extremely rare, but when found may be due to *SDHB* mutations (58). Lack of catecholamine secretion and metabolism by these tumors may result from a defect in the synthesis of catecholamines due to absence of tyrosine hydroxylase, rather than a defect in the storage or release of catecholamines.

Tyrosine hydroxylase is responsible for conversion of L-dopa to dopamine and represents the rate limiting enzyme in catecholamine synthesis (138). Thus, absence of this or other critical enzymes, such as dopamine beta-hydroxylase (139), is expected to lead to absence of tumor tissue catecholamines and a "non-functional" presentation (Table 3). Such tumors, similar to those that produce predominantly dopamine, tend to reach a large size before diagnosis, which is usually due to local mass effects and incidental discovery on imaging. Biochemically negative PPGL that are characterized by an immature biochemical phenotype and low tissue stores of catecholamines, only some of which may be truly "non-functional" (58), are associated with an aggressive phenotype in terms of higher rates of malignancy (140–144).

With the above considerations in mind, the definitive method to establish absence of functionality in a PPGL is through measurements of tumor tissue catecholamines as illustrated by Timmers et al. (58). Additional measurements of tumor tissue tyrosine hydrolase activity can also be useful, as can

TABLE 3 Expected biochemical test results and features in biochemically negative, non-secretory and non-functional tumors.

Tumor type	Plasma or urinary catecholamines	Plasma or urinary metanephrines	Catecholamine synthesizing enzymes	Tumor tissue catecholamines
Biochemically negative	Normal	Normal	Present if functional	Present if functional
Non-secretory	Normal	Elevated	Present	Present
Non-functional	Normal	Normal*	Absent/undetectable	Undetectable/low†

*If tumor tissue catecholamines and/or catecholamine synthesizing enzymes cannot be assessed, then a non-functional tumor may be defined by plasma or urinary metaneprhrines that are too low according to relationships with tumor size. †Catecholamines are potentially measureable in any human tissue, but for a tumor that is non-functional tissue catecholamines are considerably lower than in functional PPGLs.

be immunohistochemical analyses for the presence of catecholamine-synthesizing enzymes (145, 146). However, immunohistochemical presence of enzymes involved in catecholamine synthesis does not always translate to functional synthesis and storage of catecholamines in secretory granules (121). Lack of secretory granules with electron microscopy can also point to a non-functional paraganglioma. However, presence of secretory granules may not necessarily indicate a tumor with functional capacity to synthesize and store catecholamines, since the electron dense nature of such granules reflects presence of chromogranins and it can be possible for granins to be present in secretory granules without presence of catecholamines (58). Also, as reported in two studies (147, 148), since dopamine is produced in the cytoplasm while production of norepinephrine requires translocation of dopamine into secretory granules, lack of secretory granules but presence of tyrosine hydroxylase might be responsible for some cases of exclusively dopamine-producing tumors. This may also be the situation in HNPGLs that produce methoxytyramine from dopamine (149).

Pre-operatively, lack of functionality may be suspected through considerations of tumor size and plasma metanephrines (89). Since the sum of plasma free metanephrines is positively related to tumor size it can be possible to identify which tumors are likely to be non-functional rather than simply biochemically negative (Figure 3). For instance, in the study of Gruber et al. (64), the authors defined seven patients with pheochromocytomas and biochemical negative results as biochemically "silent". On inspection of the relationship of tumor size with the sum of plasma metanephrines (Figure 3A), it could be determined that for all seven patients the sum of plasma metanephrines falls within the expected relationship with tumor size, indicating that the negative biochemical signal for the tumors in those patients most likely reflected their small size rather than any lack of functional production of catecholamines. In other words, tumor size was small and the associated total catecholamine contents were unlikely sufficient to produce a positive biochemical signal.

In the report that assessed functionality according to tumor size in relation to plasma metanephrines (89), one of 207 patients (0.5%) with pheochromocytoma and another one of 45 patients (2.2%) with paragangliomas were defined as having non-functional tumors based on negative biochemical test results and a mean tumor diameter of larger than 2 cm. This compared to 12 of 43 patients (28%) with HNPGL defined to have non-functional tumors by the same criteria. Other patients with negative biochemical test results and mean diameters less than 2 cm, including 11 of the 43 patients with HNPGL (26%), were defined as having indeterminate catecholamine biochemical phenotypes. Thus, in those patients as well as 3 of 207 patients with pheochromocytoma who had negative biochemistry, functionality could not be excluded. In another report by Heavner et al. (90) in which seven pheochromocytomas were appropriately defined as biomarker negative, there were two patients reported with biochemically negative results for plasma metanephrines, one with a 1.7 cm tumor and the other with a 15 cm tumor. The latter large tumor could therefore be defined as non-functional, while for the former 1.5 cm tumor lack of function could not be determined. There was another patient with a 6.3 cm tumor in whom tests of plasma free metanephrines were indicated as normal, though not reported. That patient most likely also had a non-functional tumor. For the other four cases, either biochemical tests were inadequate or tumors were too small to determine functionality.

As illustrated in Figure 3B, a selection of cases from the above two reports (89, 90) serves to clarify situations, other than those that verify absence of tyrosine hydroxylase and tumor tissue catecholamines, where the term "non-functional" might be applied to patients with PPGL who present with negative biochemical test results for plasma free metanephrines.

Relationships of tumor size with urinary metanephrines have yet to be adequately determined. Therefore, determinations of non-functional versus functional status are more difficult for urinary than plasma measurements. Also, among 236 patients with PPGLs in a previous report (86), 16 patients had negative test results for urinary fractionated metanephrines compared to 5 with negative results for plasma free metanephrines. Thus, negative test results for measurements of urinary metanephrines more usually do not indicate a non-functional tumor, but rather reflect relative

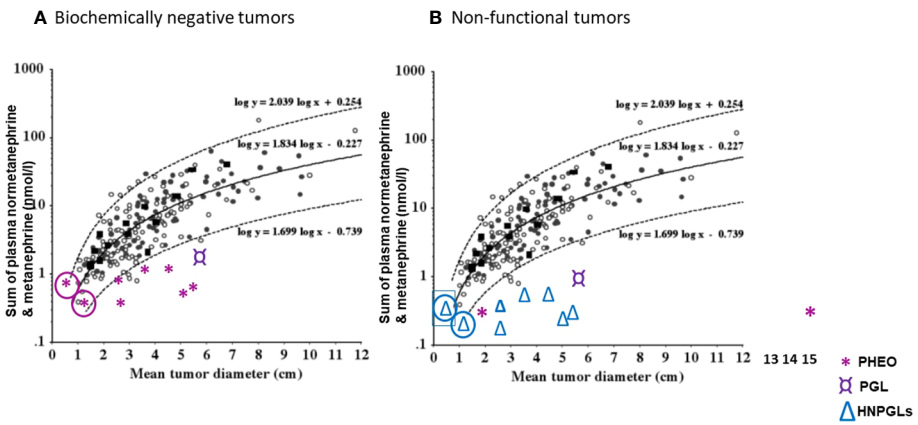

FIGURE 3
(A) Correlation of original tumor size with the sum of plasma normetanephrine and metanephrine (nmol/l) in seven patients (*) with biochemically negative PPGLs from the study of Gruber et al. (64). **(B)** Correlation of original tumor size with the sum of plasma normetanephrine and metanephrine (nmol/l) in seven patients (△) with head and neck paraganglioma (HNPGLs), one (¤) with abdominal paraganglioma (PGL) and two with pheochromocytomas (PHEO), from the study of Eisenhofer et al. (89) and Heavner et al. (90). In circle are shown two patients with questionable tumor functionality. (*Reproduced with permission from Eisenhofer G et al. Clin Chem 2015*).

lack of diagnostic sensitivity. Moreover, in that study two of the five patients with previously negative results for plasma free metanephrines showed positive test results after three to six years of further testing when tumors enlarged.

For plasma or urinary catecholamines such determinations of functionality from relationships with tumor size are not possible. Thus, for these and most other situations involving biochemical test results that fall below upper cut-offs of reference intervals, rather than defining the tumors as non-functional or non-secretory, it is more appropriate to indicate the tumors as biochemically negative.

Summary of proposed nomenclature

To facilitate scientific communication and consistent interpretation, we propose definitions for the various types of "silent" PPGLs as illustrated in Figure 4 and outlined below.

- "Clinically silent" PPGLs are those characterized by the absence of signs and symptoms associated with catecholamine excess.

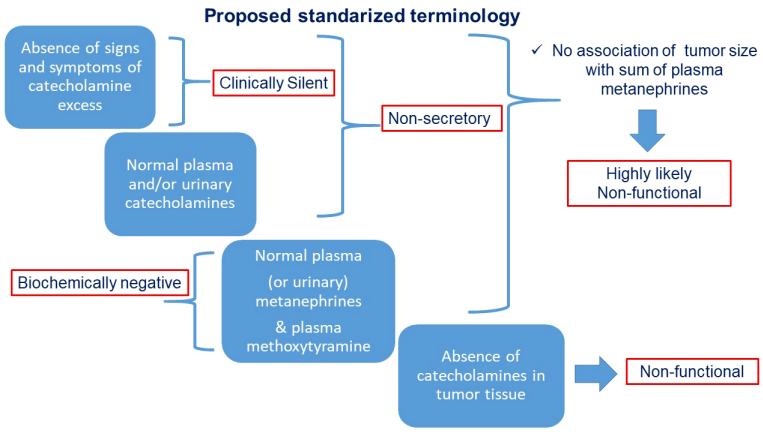

FIGURE 4
Chart flow with proposed standardized terminology for various types of "silent" PPGLs.

- "Non-secretory" tumors are those with absence of clear catecholamine secretory activity, often adrenergic and presenting with normal plasma and/or urinary catecholamines over multiple sampling time points.
- "Biochemically negative PPGLs are those characterized by plasma or urinary metanephrines below the upper cut-offs of reference intervals. If only catecholamines are measured the same term may be used with clarification
- "Non-functional" tumors are those with absent catecholamine synthesis as determined from measurements of catecholamines in the tumor tissue, assessments of tumor tissue tyrosine hydroxylase or large size in association with negative results for plasma or urinary metanephrines.

The above aspects are important to consider in daily clinical practice for individualized management and treatment of patients with PPGLs. In particular, "clinically silent" and "non-secretory" tumors are usually functional, and pre-surgical treatment with α-adrenoceptor blockade is essential to minimize intraoperative hemodynamic instability. In patients presenting with negative biochemical test result, the reliability of measurements should be verified. A negative biochemical test result cannot alone exclude functionality, especially for smaller PPGLs (<2 cm). Unless, functionality is correctly excluded, pre-operative blockade of adrenoreceptors remains important.

Data availability statement

The original contributions presented in the study are included in the article/supplementary material. Further inquiries can be directed to the corresponding authors.

Author contributions

Conceptualization, GC and CP. Methodology, VC, TS. data curation, CPr, TS. Writing—original draft preparation, GC, VC, CP. Writing—review and editing GC, GE, JL, CP. Supervision, GE, JL, CP, SB. All authors contributed to the article and approved the submitted version.

Funding

This work was supported by the Deutsche Forschungs gemeinschaft (CRC/Transregio 205/2; to GC, SB, JL, GE, CP).

Acknowledgments

This work is part of a Master's thesis of the Master's Program in Clinical Research, Dresden International University, Dresden, Germany.

Conflict of interest

The authors declare that the research was conducted in the absence of any commercial or financial relationships that could be construed as a potential conflict of interest.

Publisher's note

References

1. Lenders JW, Eisenhofer G, Mannelli M, Pacak K. Phaeochromocytoma. *Lancet.* (2005) 366(9486):665–75. doi: 10.1016/S0140-6736(05)67139-5

2. Lenders JW, Duh QY, Eisenhofer G, Gimenez-Roqueplo AP, Grebe SK, Murad MH, et al. Pheochromocytoma and paraganglioma: an endocrine society clinical practice guideline. *J Clin Endocrinol Metab* (2014) 99(6):1915–42. doi: 10.1210/jc.2014-1498

3. Li C, Chen Y, Wang W, Teng L. A case of clinically silent giant right pheochromocytoma and review of literature. *Can Urol Assoc J* (2012) 6(6):E267–9. doi: 10.5489/cuaj.132

4. Aggarwal S, Talwar V, Virmani P, Kale S. Anesthetic management of clinically silent familial pheochromocytoma with MEN 2A: A report of four cases. *Indian J Surg* (2016) 78(5):414–7. doi: 10.1007/s12262-016-1539-1

5. Lee PH, Blute RJr., Malhotra R. A clinically "silent" pheochromocytoma with spontaneous hemorrhage. *J Urol* (1987) 138(6):1429–32. doi: 10.1016/S0022-5347(17)43663-9

6. LH A, Geeta KA KA, PA K, Deepa MR. Extra- adrenal silent retroperitoneal paraganglioma: report of a rare case. *J Clin Diagn Res* (2014) 8(11):Fd06–7. doi: 10.7860/JCDR/2014/10133.5138

7. Gannan E, van Veenendaal P, Scarlett A, Ng M. Retroperitoneal non-functioning paraganglioma: A difficult tumour to diagnose and treat. *Int J Surg Case Rep* (2015) 17:133–5. doi: 10.1016/j.ijscr.2015.11.004

8. Gellad F, Whitley J, Shamsuddin AK. Silent malignant intrathoracic pheochromocytoma. *South Med J* (1980) 73(4):513–4. doi: 10.1097/00007611-198004000-00030

9. Montemurro D, Rossi GP. Veralipride-induced acute coronary syndrome unmasking a non-secreting pheochromocytoma. *J Endocrinol Invest* (2006) 29(7):650–2. doi: 10.1007/BF03344166

10. Singh S, Kumar A, Mehrotra A, Rao RN, Behari S. Nonsecretory paraganglioma in cavernous sinus masquerading as meningioma. *World Neurosurg* (2019) 126:399–404. doi: 10.1016/j.wneu.2019.02.111

11. Montebello A, Ceci Bonello E, Giordano Imbroll M, Gruppetta M. Biochemically silent phaeochromocytoma presenting with non-specific loin pain. *BMJ Case Rep* (2021) 14(8):e244258. doi: 10.1136/bcr-2021-244258

12. Amar L, Pacak K, Steichen O, Akker SA, Aylwin SJB, Baudin E, et al. International consensus on initial screening and follow-up of asymptomatic SDHx mutation carriers. *Nat Rev Endocrinol* (2021) 17(7):435–44. doi: 10.1038/s41574-021-00492-3

13. Plouin PF, Amar L, Dekkers OM, Fassnacht M, Gimenez-Roqueplo AP, Lenders JW, et al. European Society of endocrinology clinical practice guideline for long-term follow-up of patients operated on for a phaeochromocytoma or a paraganglioma. *Eur J Endocrinol* (2016) 174(5):G1–g10. doi: 10.1530/EJE-16-0033

14. Munakomi S, Rajbanshi S, Adhikary PS. Case report: A giant but silent adrenal pheochromocytoma - a rare entity. *F1000Res.* (2016) 5:290. doi: 10.12688/f1000research.8168.1

15. Wang Z, Cai Q, Li G, Jiang N, Niu Y. Giant pheochromocytoma with leukemoid reaction: A case report. *Urology.* (2017) 99:e17–e9. doi: 10.1016/j.urology.2016.08.021

16. Sundahl N, Van Slycke S, Brusselaers N. A rare case of clinically and biochemically silent giant right pheochromocytoma: case report and review of literature. *Acta Chir Belg* (2016) 116(4):239–42. doi: 10.1080/00015458.2016.1139838

17. Gupta A, Bains L, Agarwal MK, Gupta R. Giant cystic pheochromocytoma: A silent entity. *Urol Ann* (2016) 8(3):384–6. doi: 10.4103/0974-7796.184886

18. El-Doueihi RZ, Salti I, Maroun-Aouad M, El Hajj A. Bilateral biochemically silent pheochromocytoma, not silent after all. *Urol Case Rep* (2019) 24:100876. doi: 10.1016/j.eucr.2019.100876

19. Ranjan R, Mittal A, Panwar V, Narain TA, Talwar HS, Mammen KJ. Extending horizon of robotic surgery to bladder-preserving approach for vesical paraganglioma: Rare case with unusual presentation. *J Endourol Case Rep* (2020) 6 (4):319–21. doi: 10.1089/cren.2020.0077

20. Petramala L, Concistrè A, Olmati F, Saraceno V, Iannucci G, Ciardi A, et al. Silent adrenal pheochromocytoma coexistent with corticomedullary hyperplasia: A case incidentally discovered. *Eur J Case Rep Intern Med* (2017) 4(10):000714. doi: 10.12890/2017_000714

21. Spiro A, Usman A, Ajmal A, Hoang TD, Shakir MKM. Asymptomatic and biochemically silent pheochromocytoma with characteristic findings on imaging. *Case Rep Endocrinol* (2020) 2020:8847261. doi: 10.1155/2020/8847261

22. Kota SK, Kota SK, Panda S, Modi KD. Pheochromocytoma: an uncommon presentation of an asymptomatic and biochemically silent adrenal incidentaloma. *Malays J Med Sci* (2012) 19(2):86–91.

23. Ohara N, Kaneko M, Yaguchi Y, Ishiguro H, Ishizaki F, Maruyama R, et al. A case of normotensive incidentally discovered adrenal pheochromocytoma. *Clin Case Rep* (2018) 6(12):2303–8. doi: 10.1002/ccr3.1772

24. Babinska A, Peksa R, Sworczak K. Primary malignant lymphoma combined with clinically "silent" pheochromocytoma in the same adrenal gland. *World J Surg Oncol* (2015) 13:289. doi: 10.1186/s12957-015-0711-6

25. Nagashima F, Hayashi J, Araki Y, Sugihara T, Nomura M, Morichika Y, et al. Silent mixed ganglioneuroma/pheochromocytoma which produces a vasoactive intestinal polypeptide. *Intern Med* (1993) 32(1):63–6. doi: 10.2169/internalmedicine.32.63

26. Ren X, Shang J, Ren R, Zhang H, Yao X. Laparoscopic resection of a large clinically silent paraganglioma at the organ of zuckerkandl: a rare case report and review of the literature. *BMC Urol* (2020) 20(1):156. doi: 10.1186/s12894-020-00732-0

27. Kumar S, Parmar KM, Aggarwal D, Jhangra K. Simple adrenal cyst masquerading clinically silent giant cystic pheochromocytoma. *BMJ Case Rep* (2019) 12(9):e230730. doi: 10.1136/bcr-2019-230730

28. Kashyap AS. Phaeochromocytoma unearthed by fluoxetine. *Postgrad Med J* (2000) 76(895):303. doi: 10.1136/pmj.76.895.303

29. Yoshida K, Sasaguri M, Kinoshita A, Ideishi M, Ikeda M, Arakawa K. A case of a clinically "silent" pheochromocytoma. *Jpn J Med* (1990) 29(1):27–31. doi: 10.2169/internalmedicine1962.29.27

30. Suga K, Motoyama K, Hara A, Kume N, Ariga M, Matsunaga N. Tc-99m MIBG imaging in a huge clinically silent pheochromocytoma with cystic degeneration and massive hemorrhage. *Clin Nucl Med* (2000) 25(10):796–800. doi: 10.1097/00003072-200010000-00009

31. Maharaj R, Parbhu S, Ramcharan W, Baijoo S, Greaves W, Harnanan D, et al. Giant cystic pheochromocytoma with low risk of malignancy: A case report and literature review. *Case Rep Oncol Med* (2017) 2017:4638608. doi: 10.1155/2017/4638608

32. Oakes A, Witt B, Adler DG. Metastatic carotid body paraganglioma detected during evaluation for biliary stone disease. *Diagn Cytopathol* (2014) 42(10):868–71. doi: 10.1002/dc.23038

33. Wen J, Li HZ, Ji ZG, Mao QZ, Shi BB, Yan WG. A case of large "silent" extra-adrenal retroperitoneal paraganglioma resected laparoscopically. *Chin Med Sci J* (2010) 25(1):61–4. doi: 10.1016/S1001-9294(10)60023-5

34. Rashid S, Youssef H, Ali A, Apakama I. Previously clinically "silent" adrenal phaeochromocytoma presenting as hypovolemic shock with paradoxical hypertension. *Libyan J Med* (2007) 2(3):150–1. doi: 10.4176/070606.

35. Lin MW, Chang YL, Lee YC, Huang PM. Non-functional paraganglioma of the posterior mediastinum. *Interact Cardiovasc Thorac Surg* (2009) 9(3):540–2. doi: 10.1510/icvts.2009.206169

36. Law NW, Alfano L. Non-functioning retroperitoneal paraganglioma. *J R Soc Med* (1987) 80(4):246–7. doi: 10.1177/014107688708000416

37. Hajri A, Ballati A, Essaidi Z, Errguibi D, Boufettal R, Rifki El Jai S, et al. Non-functional retroperitoneal paraganglioma: A report of case with literature review. *Ann Med Surg (Lond)* (2021) 65:102360. doi: 10.1016/j.amsu.2021.102360

38. AlMarzooqi R, AlJaberi L, Rosenblatt S, Plesec T, Berber E. A rare case of paraganglioma of the cystic duct. *Int J Surg Case Rep* (2018) 52:16–9. doi: 10.1016/j.ijscr.2018.09.041

39. Moslemi MK, Abolhasani M, Vafaeimanesh J. Malignant abdominal paraganglioma presenting as a giant intra-peritoneal mass. *Int J Surg Case Rep* (2012) 3(11):537–40. doi: 10.1016/j.ijscr.2012.07.007

40. Muñoz-Largacha JA, Glocker RJ, Moalem J, Singh MJ, Litle VR. Incidental posterior mediastinal paraganglioma: The safe approach to management, case report. *Int J Surg Case Rep* (2017) 35:25–8. doi: 10.1016/j.ijscr.2017.03.040

41. Khan MR, Raza R, Jabbar A, Ahmed A. Primary non-functioning paraganglioma of liver: a rare tumour at an unusual location. *J Pak Med Assoc* (2011) 61(8):814–6.

42. Hasselager T, Horn T, Rasmussen F. Paraganglioma of the prostate. a case report and review of the literature. *Scand J Urol Nephrol* (1997) 31(5):501–3. doi: 10.3109/00365599709030651

43. Arrabal-Polo MA, Arrabal-Martin M, Lopez-Leon VM, Abad-Menor F, Valle-Diaz de la Guardia F, Mijan-Ortiz JL, et al. Spontaneous retroperitoneal abscess as the first clinical manifestation of a non-functioning retroperitoneal paraganglioma. *Ann R Coll Surg Engl* (2010) 92(3):W17–9. doi: 10.1308/147870810X12659688851555

44. Alataki D, Triantafyllidis A, Gaal J, Rodiou C, Vouros J, Papathanasiou A, et al. A non-catecholamine-producing sympathetic paraganglioma of the spermatic cord: the importance of performing candidate gene mutation analysis. *Virchows Arch* (2010) 457(5):619–22. doi: 10.1007/s00428-010-0966-9

45. Hong SW, Lee WY, Lee HK. Hepatic paraganglioma and multifocal gastrointestinal stromal tumor in a female: Incomplete Carney triad. *World J Gastrointest Surg* (2013) 5(7):229–32. doi: 10.4240/wjgs.v5.i7.229

46. Hudson I, Phillips RK, Williams EJ. Non-functioning paraganglioma in wall of abdominal aortic aneurysm: a source of diagnostic confusion. *J R Soc Med* (1987) 80(10):648–9. doi: 10.1177/014107688708001018

47. Shidei H, Maeda H, Isaka T, Matsumoto T, Yamamoto T, Nagashima Y, et al. Mediastinal paraganglioma successfully resected by robot-assisted thoracoscopic surgery with en bloc chest wall resection: a case report. *BMC Surg* (2020) 20(1):45. doi: 10.1186/s12893-020-00701-2

48. Mohd Slim MA, Yoong S, Wallace W, Gardiner K. A large mesenteric paraganglioma with lymphovascular invasion. *BMJ Case Rep* (2015) 2015: bcr2015209601. doi: 10.1136/bcr-2015-209601

49. Belhamidi MS, Ratbi MB, Tarchouli M, Adioui T, Ali AA, Zentar A, et al. An unusual localization of retroperitoneal paraganglioma: a case report. *Pan Afr Med J* (2015) 22:12. doi: 10.11604/pamj.2015.22.12.7437

50. Matsumoto J, Tanaka N, Yoshida Y, Yamamoto T. Resection of an intrapericardial paraganglioma under cardiopulmonary bypass. *Asian Cardiovasc Thorac Ann* (2013) 21(4):476–8. doi: 10.1177/0218492312459641

51. Tomulic K, Saric JP, Kocman B, Skrtic A, Filipcic NV, Acan I. Successful management of unsuspected retroperitoneal paraganglioma *via* the use of combined epidural and general anesthesia: a case report. *J Med Case Rep* (2013) 7:58. doi: 10.1186/1752-1947-7-58

52. Martinez JD, Zendejas B, Luna JP, Lopez J, Luna SS, Mendoza-Sánchez F, et al. Left subdiaphragmatic paraganglioma supplied by contralateral right renal artery. *Int J Surg Case Rep* (2012) 3(7):333–7. doi: 10.1016/j.ijscr.2012.03.028

53. Hakimian SM, Naimi A, Emami SM, Rozatii G, Goharian V. Large Retroperitoneal paraganglioma concurrent with periampullary adenocarcinoma. *J Res Med Sci* (2013) 18(12):1114–6.

54. Minagawa T, Sato T, Furuhata M, Hirabayashi N, Kato H. Extra-adrenal pheochromocytoma (paraganglioma) of the urinary bladder: a case report. *Hinyokika Kiyo* (2004) 50(11):787–90.

55. Guo Q, Li B, Guan J, Yang H, Wu Y. Intraoperative diagnosis of functional retroperitoneal multiple paraganglioma: A case report. *Oncol Lett* (2012) 4(4):829–31. doi: 10.3892/ol.2012.795

56. Brown H, Goldberg PA, Selter JG, Cabin HS, Marieb NJ, Udelsman R, et al. Hemorrhagic pheochromocytoma associated with systemic corticosteroid therapy and presenting as myocardial infarction with severe hypertension. *J Clin Endocrinol Metab* (2005) 90(1):563–9. doi: 10.1210/jc.2004-1077

57. Shen SJ, Cheng HM, Chiu AW, Chou CW, Chen JY. Perioperative hypertensive crisis in clinically silent pheochromocytomas: report of four cases. *Chang Gung Med J* (2005) 28(1):44–50.

58. Timmers HJ, Pacak K, Huynh TT, Abu-Asab M, Tsokos M, Merino MJ, et al. Biochemically silent abdominal paragangliomas in patients with mutations in the succinate dehydrogenase subunit b gene. *J Clin Endocrinol Metab* (2008) 93 (12):4826–32. doi: 10.1210/jc.2008-1093

59. Havekes B, van der Klaauw AA, Weiss MM, Jansen JC, van der Mey AG, Vriends AH, et al. Pheochromocytomas and extra-adrenal paragangliomas detected by screening in patients with SDHD-associated head-and-neck paragangliomas. *Endocr Relat Cancer* (2009) 16(2):527–36. doi: 10.1677/ERC-09-0024

60. Marzola MC, Chondrogiannis S, Grassetto G, Rampin L, Maffione AM, Ferretti A, et al. 18F-DOPA PET/CT in the evaluation of hereditary SDH-deficiency paraganglioma-pheochromocytoma syndromes. *Clin Nucl Med* (2014) 39(1):e53–8. doi: 10.1097/RLU.0b013e31829aface

61. Turkova H, Prodanov T, Maly M, Martucci V, Adams K, Widimsky JJr., et al. Characteristics and outcomes of metastatic sdhb and sporadic pheochromocytoma/paraganglioma: an national institutes of health study. *Endocr Pract* (2016) 22(3):302–14. doi: 10.4158/EP15725.OR

62. Dreijerink KMA, Rijken JA, Compaijen CJ, Timmers H, van der Horst-Schrivers ANA, van Leeuwaarde RS, et al. Biochemically silent sympathetic paraganglioma, pheochromocytoma, or metastatic disease in SDHD mutation carriers. *J Clin Endocrinol Metab* (2019) 104(11):5421–6. doi: 10.1210/jc.2019-00202

63. van Duinen N, Kema IP, Romijn JA, Corssmit EP. Plasma chromogranin a levels are increased in a small portion of patients with hereditary head and neck paragangliomas. *Clin Endocrinol (Oxf).* (2011) 74(2):160–5. doi: 10.1111/j.1365-2265.2010.03914.x

64. Gruber LM, Hartman RP, Thompson GB, McKenzie TJ, Lyden ML, Dy BM, et al. Pheochromocytoma characteristics and behavior differ depending on method of discovery. *J Clin Endocrinol Metab* (2019) 104(5):1386–93. doi: 10.1210/jc.2018-01707

65. Curfman KR, Di Como JA, Chung TR, Dumire RD. Functionally silent, giant pheochromocytoma presenting with varicocele. *Am Surg* (2021) 87(1):97–100. doi: 10.1177/0003134820945274

66. Gong J, Wang X, Chen X, Chen N, Huang R, Lu C, et al. Adrenal and extra-adrenal nonfunctioning composite pheochromocytoma/paraganglioma with immunohistochemical ectopic hormone expression: comparison of two cases. *Urol Int* (2010) 85(3):368–72. doi: 10.1159/000317312

67. Abou Chaar MK, Khanfer A, Almasri NM, Abu Shattal M, Alibraheem AO, Al-Qudah O. Metastatic non-functional paraganglioma to the lung. *J Cardiothorac Surg* (2020) 15(1):82. doi: 10.1186/s13019-020-01113-2

68. Soomro NH, Zahid AB, Zafar AA. Non-functional paraganglioma of the mediastinum. *J Pak Med Assoc* (2016) 66(5):609–11

69. Chattoraj AK, Rao UM, Sarkar N, Jakka S. Non-functional retroperitoneal paraganglioma: A case report. *J Family Med Prim Care* (2019) 8(4):1497–9. doi: 10.4103/jfmpc.jfmpc_189_19

70. Bacalbasa N, Balescu I, Tanase A, Brezean I, Vilcu M, Brasoveanu V. Successful resection of a non-functional paraganglioma with celiac trunk invasion followed by common hepatic artery reimplantation - a case report and literature review. *In Vivo.* (2018) 32(4):911–4. doi: 10.21873/invivo.11328

71. Verma A, Pandey D, Akhtar A, Arsia A, Singh N. Non-functional paraganglioma of retroperitoneum mimicking pancreatic mass with concurrent urinary bladder paraganglioma: an extremely rare entity. *J Clin Diagn Res* (2015) 9 (2):Xd09–xd11. doi: 10.7860/JCDR/2015/11156.5570

72. Holden A. Non-functional malignant extra-adrenal retroperitoneal paraganglioma. *Australas Radiol* (1995) 39(4):392–5. doi: 10.1111/j.1440-1673.1995.tb00319.x

73. D'John M, Jabbar F. Primary gallbladder paraganglioma: A case report and review of literature. *Int J Surg Case Rep* (2020) 75:451–3. doi: 10.1016/j.ijscr.2020.09.095

74. Peng C, Bu S, Xiong S, Wang K, Li H. Non-functioning paraganglioma occurring in the urinary bladder: A case report and review of the literature. *Oncol Lett* (2015) 10(1):321–4. doi: 10.3892/ol.2015.3222

75. Katiyar R, Dwivedi S, Trivedi S, Patne SC, Dwivedi US. Non-functional paraganglioma of the urinary bladder treated by transurethral resection: Report of two cases. *J Clin Diagn Res* (2016) 10(2):Xd01–xd3. doi: 10.7860/JCDR/2016/17953.7219

76. Tobón A, Velásquez M, Pérez B, Zúñiga V, Sua LF, Fernández-Trujillo L. Pathologic features and clinical course of a non-functioning primary pulmonary paraganglioma: A case report. *Ann Med Surg (Lond)* (2020) 55:185–9. doi: 10.1016/j.amsu.2020.05.027

77. Kapetanakis S, Chourmouzi D, Gkasdaris G, Katsaridis V, Eleftheriadis E, Givissis P. A rare case of spinal cord compression due to cervical spine metastases from paraganglioma of the jugular foramen-how should it be treated? *J Surg Case Rep* (2018) 2018(2):rjy005. doi: 10.1093/jscr/rjy005

78. Yadav R, Das AK, Kumar R. Malignant non-functional paraganglioma of the bladder presenting with azotemia. *Int Urol Nephrol* (2007) 39(2):449–51. doi: 10.1007/s11255-006-9017-5

79. Katsimantas A, Paparidis S, Filippou D, Bouropoulos KSR, Ferakis N. Laparoscopic resection of a non-functional, extra-adrenal paraganglioma: A case report and literature review. *Cureus.* (2020) 12(4):e7753. doi: 10.7759/cureus.7753

80. Lai Y, Chen D, Yu Z, Ni L, Yang S. Non-functioning paraganglioma of the urinary bladder: A case report and review of the literature. *Oncol Lett* (2014) 7 (3):891–3. doi: 10.3892/ol.2014.1790

81. Xu DF, Chen M, Liu YS, Gao Y, Cui XG. Non-functional paraganglioma of the urinary bladder: a case report. *J Med Case Rep* (2010) 4:216. doi: 10.1186/1752-1947-4-216

82. Wang S, Zhang A, Huang S, Ma Y, Yang Y, Liu X, et al. Non functioning paraganglioma in the urinary bladder: a case report. *Urol J* (2020) 17(4):426–8. doi: 10.22037/uj.v0i0.4741

83. Alanee S, Williamson SR, Gupta NS. A rare case of non-functioning bladder paraganglioma treated with robotic assisted partial cystectomy. *Urol Case Rep* (2019) 26:100950. doi: 10.1016/j.eucr.2019.100950

84. Azzarelli B, Felten S, Muller J, Miyamoto R, Purvin V. Dopamine in paragangliomas of the glomus jugulare. *Laryngoscope.* (1988) 98(5):573–8. doi: 10.1288/00005537-198805000-00020

85. Aghakhani N, George B, Parker F. Paraganglioma of the cauda equina region–report of two cases and review of the literature. *Acta Neurochir (Wien)* (1999) 141(1):81–7. doi: 10.1007/s007010050269

86. Eisenhofer G, Prejbisz A, Peitzsch M, Pamporaki C, Masjkur J, Rogowski-Lehmann N, et al. Biochemical diagnosis of chromaffin cell tumors in patients at high and low risk of disease: Plasma versus urinary free or deconjugated O-methylated catecholamine metabolites. *Clin Chem* (2018) 64(11):1646–56. doi: 10.1373/clinchem.2018.291369

87. Mozersky RP, Girdhar R, Palushock S, Patel N, Nolan S, Bahl VK. Malignant nonfunctioning pheochromocytoma occurring in a mixed multiple endocrine neoplasia syndrome. *Endocr Pract* (1997) 3(4):236–9. doi: 10.4158/3.4.236

88. Kimura N, Miura Y, Nagatsu I, Nagura H. Catecholamine synthesizing enzymes in 70 cases of functioning and non-functioning phaeochromocytoma and extra-adrenal paraganglioma. *Virchows Arch A Pathol Anat Histopathol* (1992) 421 (1):25–32. doi: 10.1007/BF01607135

89. Eisenhofer G, Deutschbein T, Constantinescu G, Langton K, Pamporaki C, Calsina B, et al. Plasma metanephrines and prospective prediction of tumor location, size and mutation type in patients with pheochromocytoma and paraganglioma. *Clin Chem Lab Med* (2020) 59(2):353–63. doi: 10.1515/cclm-2020-0904

90. Heavner MG, Krane LS, Winters SM, Mirzazadeh M. Pheochromocytoma diagnosed pathologically with previous negative serum markers. *J Surg Oncol* (2015) 112(5):492–5. doi: 10.1002/jso.24031

91. Zhang J, Li M, Pang Y, Wang C, Wu J, Cheng Z, et al. Genetic characteristics of incidental pheochromocytoma and paraganglioma. *J Clin Endocrinol Metab* (2022) 107(5):e1835–42. doi: 10.1210/clinem/dgac058

92. Grozinsky-Glasberg S, Szalat A, Benbassat CA, Gorshtein A, Weinstein R, Hirsch D, et al. Clinically silent chromaffin-cell tumors: Tumor characteristics and long-term prognosis in patients with incidentally discovered pheochromocytomas. *J Endocrinol Invest* (2010) 33(10):739–44. doi: 10.1007/BF03346680

93. Smithwick RH, Greer WER, Robertsone CW, Wilkins RW. Pheochromocytoma; a discussion of symptoms, signs and procedures of diagnostic value. *N Engl J Med* (1950) 242(7):252–7. doi: 10.1056/NEJM195002162420705

94. Neumann HP, Berger DP, Sigmund G, Blum U, Schmidt D, Parmer RJ, et al. Pheochromocytomas, multiple endocrine neoplasia type 2, and von hippel-lindau disease. *N Engl J Med* (1993) 329(21):1531–8. doi: 10.1056/NEJM199311183292103

95. Eisenhofer G, Walther MM, Huynh TT, Li ST, Bornstein SR, Vortmeyer A, et al. Pheochromocytomas in von hippel-lindau syndrome and multiple endocrine neoplasia type 2 display distinct biochemical and clinical phenotypes. *J Clin Endocrinol Metab* (2001) 86(5):1999–2008. doi: 10.1210/jcem.86.5.7496

96. Telenius-Berg M, Berg B, Hamberger B, Tibblin S. Screening for early asymptomatic pheochromocytoma in MEN-2. *Henry Ford Hosp Med J* (1987) 35 (2-3):110–4.

97. Kotzerke J, Stibane C, Dralle H, Wiese H, Burchert W. Screening for pheochromocytoma in the MEN 2 syndrome. *Henry Ford Hosp Med J* (1989) 37 (3-4):129–31.

98. Aprill BS, Drake AJ3rd, Lasseter DH, Shakir KM. Silent adrenal nodules in von hippel-lindau disease suggest pheochromocytoma. *Ann Intern Med* (1994) 120 (6):485–7. doi: 10.7326/0003-4819-120-6-199403150-00006

99. Pomares FJ, Cañas R, Rodriguez JM, Hernandez AM, Parrilla P, Tebar FJ. Differences between sporadic and multiple endocrine neoplasia type 2A phaeochromocytoma. *Clin Endocrinol (Oxf).* (1998) 48(2):195–200. doi: 10.1046/j.1365-2265.1998.3751208.x

100. Libutti SK, Choyke PL, Alexander HR, Glenn G, Bartlett DL, Zbar B, et al. Clinical and genetic analysis of patients with pancreatic neuroendocrine tumors associated with von hippel-lindau disease. *Surgery.* (2000) 128(6):1022–7. doi: 10.1067/msy.2000.110239

101. Bravo E, Fouad-Tarazi F, Rossi G, Imamura M, Lin WW, Madkour MA, et al. A reevaluation of the hemodynamics of pheochromocytoma. *Hypertension* (1990) 15(2 Suppl):I128–31. doi: 10.1161/01.HYP.15.2_Suppl.I128

102. Clifton-Bligh R. Diagnosis of silent pheochromocytoma and paraganglioma. *Expert Rev Endocrinol Metab* (2013) 8(1):47–57. doi: 10.1586/eem.12.76

103. Mannelli M, Lenders JW, Pacak K, Parenti G, Eisenhofer G. Subclinical phaeochromocytoma. *Best Pract Res Clin Endocrinol Metab* (2012) 26(4):507–15. doi: 10.1016/j.beem.2011.10.008

104. Ito Y, Fujimoto Y, Obara T. The role of epinephrine, norepinephrine, and dopamine in blood pressure disturbances in patients with pheochromocytoma. *World J Surg* (1992) 16(4):759–63. doi: 10.1007/BF02067379

105. Feldman JM, Blalock JA, Zern RT, Wells SAJr. The relationship between enzyme activity and the catecholamine content and secretion of pheochromocytomas. *J Clin Endocrinol Metab* (1979) 49(3):445–51. doi: 10.1210/jcem-49-3-445

106. Goldberg LI. Cardiovascular and renal actions of dopamine: potential clinical applications. *Pharmacol Rev* (1972) 24(1):1–29.

107. Jose PA, Eisner GM, Felder RA. Regulation of blood pressure by dopamine receptors. *Nephron Physiol* (2003) 95(2):p19–27. doi: 10.1159/000073676

108. Eisenhofer G, Goldstein DS, Sullivan P, Csako G, Brouwers FM, Lai EW, et al. Biochemical and clinical manifestations of dopamine-producing paragangliomas: utility of plasma methoxytyramine. *J Clin Endocrinol Metab* (2005) 90(4):2068–75. doi: 10.1210/jc.2004-2025

109. Ahlquist RP. A study of the adrenotropic receptors. *Am J Physiol* (1948) 153(3):586–600. doi: 10.1152/ajplegacy.1948.153.3.586

110. Ensinger H, Weichel T, Lindner KH, Prengel A, Grünert A, Ahnefeld FW. Relationship between arterial and peripheral venous catecholamine plasma catecholamine concentrations during infusion of noradrenaline and adrenaline in healthy volunteers. *Eur J Clin Pharmacol* (1992) 43(3):245–9. doi: 10.1007/BF02333017

111. Grossman E, Rea RF, Hoffman A, Goldstein DS. Yohimbine increases sympathetic nerve activity and norepinephrine spillover in normal volunteers. *Am J Physiol* (1991) 260(1 Pt 2):R142–7. doi: 10.1152/ajpregu.1991.260.1.R142

112. Kopin IJ, Zukowska-Grojec Z, Bayorh MA, Goldstein DS. Estimation of intrasynaptic norepinephrine concentrations at vascular neuroeffector junctions in vivo. *Naunyn Schmiedebergs Arch Pharmacol* (1984) 325(4):298–305. doi: 10.1007/BF00504372

113. Streeten DH, Anderson GHJr. Mechanisms of orthostatic hypotension and tachycardia in patients with pheochromocytoma. *Am J Hypertens* (1996) 9(8):760–9. doi: 10.1016/0895-7061(96)00057-X

114. Lance JW, Hinterberger H. Symptoms of pheochromocytoma, with particular reference to headache, correlated with catecholamine production. *Arch Neurol* (1976) 33(4):281–8. doi: 10.1001/archneur.1976.00500040065011

115. Ito Y, Obara T, Yamashita T, Kanbe M, Iihara M. Pheochromocytomas: tendency to degenerate and cause paroxysmal hypertension. *World J Surg* (1996) 20 (7):923–6. doi: 10.1007/s002689900140

116. Eisenhofer G, Huynh TT, Elkahloun A, Morris JC, Bratslavsky G, Linehan WM, et al. Differential expression of the regulated catecholamine secretory pathway in different hereditary forms of pheochromocytoma. *Am J Physiol Endocrinol Metab* (2008) 295(5):E1223–33. doi: 10.1152/ajpendo.90591.2008

117. Eisenhofer G, Pacak K, Huynh TT, Qin N, Bratslavsky G, Linehan WM, et al. Catecholamine metabolomic and secretory phenotypes in phaeochromocytoma. *Endocr Relat Cancer* (2011) 18(1):97–111. doi: 10.1677/ERC-10-0211

118. Mannelli M, Ianni L, Cilotti A, Conti A. Pheochromocytoma in Italy: a multicentric retrospective study. *Eur J Endocrinol / Eur Fed Endocrine Societies* (1999) 141(6):619–24. doi: 10.1530/eje.0.1410619

119. Baguet JP, Hammer L, Mazzuco TL, Chabre O, Mallion JM, Sturm N, et al. Circumstances of discovery of phaeochromocytoma: a retrospective study of 41 consecutive patients. *Eur J Endocrinol* (2004) 150(5):681–6. doi: 10.1530/eje.0.1500681

120. Geroula A, Deutschbein T, Langton K, Masjkur JR, Pamporaki C, Peitzsch M, et al. Pheochromocytoma and paraganglioma: Clinical feature based disease probability in relation to catecholamine biochemistry and reason for disease suspicion. *Eur J Endocrinol* (2019) 181(4):409–20. doi: 10.1530/EJE-19-0159

121. Berends AMA, Eisenhofer G, Fishbein L, Horst-Schrivers A, Kema IP, Links TP, et al. Intricacies of the molecular machinery of catecholamine biosynthesis and secretion by chromaffin cells of the normal adrenal medulla and in pheochromocytoma and paraganglioma. *Cancers (Basel)* (2019) 11(8):1121. doi: 10.3390/cancers11081121

122. Eisenhofer G, Kopin IJ, Goldstein DS. Catecholamine metabolism: a contemporary view with implications for physiology and medicine. *Pharmacol Rev* (2004) 56(3):331–49. doi: 10.1124/pr.56.3.1

123. Eisenhofer G, Kopin IJ, Goldstein DS. Leaky catecholamine stores: undue waste or a stress response coping mechanism? *Ann N Y Acad Sci* (2004) 1018:224–30. doi: 10.1196/annals.1296.027

124. Crout JR, Sjoerdsma A. Turnover and metabolism of catecholamines in patients with pheochromocytoma. *J Clin Invest* (1964) 43(1):94–102. doi: 10.1172/JCI104898

125. Lenders JW, Pacak K, Huynh TT, Sharabi Y, Mannelli M, Bratslavsky G, et al. Low sensitivity of glucagon provocative testing for diagnosis of pheochromocytoma. *J Clin Endocrinol Metab* (2010) 95(1):238–45. doi: 10.1210/jc.2009-1850

126. Lenders JW, Pacak K, Walther MM, Linehan WM, Mannelli M, Friberg P, et al. Biochemical diagnosis of pheochromocytoma: which test is best? *Jama* (2002) 287(11):1427–34. doi: 10.1001/jama.287.11.1427

127. Rao D, Peitzsch M, Prejbisz A, Hanus K, Fassnacht M, Beuschlein F, et al. Plasma methoxytyramine: clinical utility with metanephrines for diagnosis of pheochromocytoma and paraganglioma. *Eur J Endocrinol / Eur Fed Endocrine Societies* (2017) 177(2):103–13. doi: 10.1530/EJE-17-0077

128. Eisenhofer G, Aneman A, Friberg P, Hooper D, Fåndriks L, Lonroth H, et al. Substantial production of dopamine in the human gastrointestinal tract. *J Clin Endocrinol Metab* (1997) 82(11):3864–71. doi: 10.1210/jcem.82.11.4339

129. Eisenhofer G, Coughtrie MW, Goldstein DS. Dopamine sulphate: an enigma resolved. *Clin Exp Pharmacol Physiol Suppl.* (1999) 26:S41–53. doi: 10.1210/jcem.82.11.4339

130. Grebe SK, Singh RJ. LC-MS/MS in the clinical laboratory - where to from here? *Clin Biochem Rev* (2011) 32(1):5–31.

131. Weismann D, Peitzsch M, Raida A, Prejbisz A, Gosk M, Riester A, et al. Measurements of plasma metanephrines by immunoassay vs liquid chromatography with tandem mass spectrometry for diagnosis of pheochromocytoma. *Eur J Endocrinol* (2015) 172(3):251–60. doi: 10.1530/EJE-14-0730

132. Mizuta E, Hamada T, Taniguchi S, Shimoyama M, Nawada T, Miake J, et al. Small extra-adrenal pheochromocytoma causing severe hypertension in an elderly patient. *Hypertens Res* (2006) 29(8):635–8. doi: 10.1291/hypres.29.635

133. Ng BW, Wong JS, Toh TH. Biochemically normal adrenal pheochromocytoma following extensive central necrosis in a child with von hippel-lindau (VHL) gene mutation. *BMJ Case Rep* (2021) 14(12):635–8. doi: 10.1136/bcr-2021-245154

134. Sharma JB, Naha M, Kumar S. Successful pregnancy outcome in a case of pheochromocytoma presenting as severe pre-eclampsia with normal urinary catecholamine level. *Indian J Endocrinol Metab* (2013) 17(3):540–1. doi: 10.4103/2230-8210.111696

135. Tischler AS. Pheochromocytoma and extra-adrenal paraganglioma: updates. *Arch Pathol Lab Med* (2008) 132(8):1272–84. doi: 10.5858/2008-132-1272-PAEPU

136. Erickson D, Kudva YC, Ebersold MJ, Thompson GB, Grant CS, van Heerden JA, et al. Benign paragangliomas: clinical presentation and treatment outcomes in 236 patients. *J Clin Endocrinol Metab* (2001) 86(11):5210–6. doi: 10.1210/jcem.86.11.8034

137. Richter S, Qiu B, Ghering M, Kunath C, Constantinescu G, Luths C, et al. Head/neck paragangliomas: focus on tumor location, mutational status and plasma methoxytyramine. *Endocr Relat Cancer* (2022) 86(11):5210–6. doi: 10.1530/ERC-21-0359

138. Nagatsu T, Levitt M, Udenfriend S. Tyrosine hydroxylase. the initial step in norepinephrine biosynthesis. *J Biol Chem* (1964) 239:2910–7. doi: 10.1016/S0021-9258(18)93832-9

139. Mete O, Asa SL, Gill AJ, Kimura N, de Krijger RR, Tischler A. Overview of the 2022 WHO classification of paragangliomas and pheochromocytomas. *Endocr Pathol* (2022) 33(1):90–114. doi: 10.1007/s12022-022-09704-6

140. Timmers HJ, Kozupa A, Eisenhofer G, Raygada M, Adams KT, Solis D, et al. Clinical presentations, biochemical phenotypes, and genotype-phenotype correlations in patients with succinate dehydrogenase subunit b-associated pheochromocytomas and paragangliomas. *J Clin Endocrinol Metab* (2007) 92 (3):779–86. doi: 10.1210/jc.2006-2315

141. Kawashima A, Sone M, Inagaki N, Okamoto K, Tsuiki M, Izawa S, et al. Pheochromocytoma and paraganglioma with negative results for urinary metanephrines show higher risks for metastatic diseases. *Endocrine.* (2021) 74 (1):155–62. doi: 10.1007/s12020-021-02816-9

142. Eisenhofer G, Lenders JW, Siegert G, Bornstein SR, Friberg P, Milosevic D, et al. Plasma methoxytyramine: a novel biomarker of metastatic pheochromocytoma and paraganglioma in relation to established risk factors of tumour size, location and SDHB mutation status. *Eur J Cancer* (2012) 48(11):1739–49. doi: 10.1016/j.ejca.2011.07.016

143. Bechmann N, Moskopp ML, Ullrich M, Calsina B, Wallace PW, Richter S, et al. HIF2α supports pro-metastatic behavior in pheochromocytomas/paragangliomas. *Endocr Relat Cancer* (2020) 27(11):625–40. doi: 10.1530/ERC-20-0205

144. Pamporaki C, Prodanov T, Meuter L, Berends AMA, Bechmann N, Constantinescu G, et al. Determinants of disease-specific survival in patients

with and without metastatic pheochromocytoma and paraganglioma. *Eur J Cancer* (2022) 169:32–41. doi: 10.1016/j.ejca.2022.03.032

145. Konosu-Fukaya S, Omata K, Tezuka Y, Ono Y, Aoyama Y, Satoh F, et al. Catecholamine-synthesizing enzymes in pheochromocytoma and extraadrenal paraganglioma. *Endocr Pathol* (2018) 29(4):302–9. doi: 10.1007/s12022-018-9544-5

146. Kimura N, Shiga K, Kaneko KI, Oki Y, Sugisawa C, Saito J, et al. Immunohistochemical expression of choline acetyltransferase and catecholamine-synthesizing enzymes in head-and-Neck and thoracoabdominal paragangliomas and pheochromocytomas. *Endocr Pathol* (2021) 32(4):442–51. doi: 10.1007/s12022-021-09694-x

147. Matsuda Y, Kimura N, Yoshimoto T, Sekiguchi Y, Tomoishi J, Kasahara I, et al. Dopamine-secreting paraganglioma in the retroperitoneum. *Endocr Pathol* (2017) 28(1):36–40. doi: 10.1007/s12022-016-9457-0

148. Miyamoto S, Yoshida Y, Ozeki Y, Okamoto M, Gotoh K, Masaki T, et al. Dopamine-secreting pheochromocytoma and paraganglioma. *J Endocr Soc* (2021) 5(12):bvab163. doi: 10.1210/jendso/bvab163

149. Osinga TE, Korpershoek E, de Krijger RR, Kerstens MN, Dullaart RP, Kema IP, et al. Catecholamine-synthesizing enzymes are expressed in parasympathetic head and neck paraganglioma tissue. *Neuroendocrinology* (2015) 101(4):289–95. doi: 10.1159/000377703

frontiers | Frontiers in Endocrinology

TYPE Original Research
PUBLISHED 23 November 2022
DOI 10.3389/fendo.2022.1028804

OPEN ACCESS

EDITED BY
Nadia Sawicka-Gutaj,
Poznan University of Medical Sciences, Poland

REVIEWED BY
Anna Zalewska,
Medical University of Bialystok, Poland
Mattia Barbot,
University Hospital of Padua, Italy

*CORRESPONDENCE
Oskar Ragnarsson
oskar.ragnarsson@medic.gu.se

SPECIALTY SECTION
This article was submitted to Adrenal Endocrinology, a section of the journal Frontiers in Endocrinology

RECEIVED 26 August 2022
ACCEPTED 09 November 2022
PUBLISHED 23 November 2022

CITATION
Berndt V, Dahlqvist P, de Verdier J, Ryberg H and Ragnarsson O (2022) The diagnostic value of salivary cortisol and salivary cortisone in patients with suspected hypercortisolism. *Front. Endocrinol.* 13:1028804. doi: 10.3389/fendo.2022.1028804

The diagnostic value of salivary cortisol and salivary cortisone in patients with suspected hypercortisolism

Vendela Berndt[1,2], Per Dahlqvist[3], Jennie de Verdier[4], Henrik Ryberg[2,4] and Oskar Ragnarsson[1,2]*

[1]Department of Endocrinology, Sahlgrenska University Hospital, Göteborg, Sweden, [2]Department of Internal Medicine and Clinical Nutrition, Institute of Medicine, Sahlgrenska Academy, University of Gothenburg, Göteborg, Sweden, [3]Department of Public Health and Clinical Medicine, Umeå University, Umeå, Sweden, [4]Department of Clinical Chemistry, Sahlgrenska University Hospital, Göteborg, Sweden

Background: Diagnosing endogenous hypercortisolism remains a challenge, partly due to a lack of biochemical tests with good diagnostic accuracy.

Objectives: To evaluate the diagnostic value of salivary cortisol and cortisone in patients with suspected hypercortisolism.

Methods: Retrospective study including 155 patients with adrenal incidentaloma, and 54 patients with suspected Cushing´s syndrome (CS). Salivary samples were collected at home, at 11 p.m., and at 8 a.m. following an over-night dexamethasone suppression test (DST). Salivary cortisol and cortisone were measured with liquid chromatography-tandem mass spectrometry.

Results: Ten of 155 patients with adrenal incidentaloma were considered to have autonomous cortisol secretion (ACS). Using previously established cut-offs, all patients with ACS had elevated plasma-cortisol (>50 nmol/L) following DST, 9/10 had elevated late-night salivary cortisone (>15 nmol/L) whereas only 4/10 had elevated late-night salivary cortisol (LNSC; >3 nmol/L) compared to 35%, 9% and 8%, respectively, of the 145 patients with non-functioning adrenal incidentaloma. Six (60%) patents with ACS had elevated salivary cortisol and cortisone at 8 a.m. following DST compared to 9% and 8%, respectively, of patients with non-functioning adrenal incidentaloma. One of 6 patients with overt CS had a normal LNSC and one had normal late-night salivary cortisone, while all had increased salivary cortisol and cortisone following DST.

Conclusion: LNSC is not sufficiently sensitive or specific to be used for screening patients with suspected hypercortisolism. Instead, late-night salivary cortisone seems to be a promising alternative in patients with adrenal incidentaloma and salivary cortisone at 8 a.m. following DST in patients with suspected CS. Larger studies are needed to confirm these findings.

KEYWORDS

adrenal incidentaloma, mild autonomous hypercortisolism, Cushing´s syndrome, salivary cortisol, salivary cortisone

Introduction

Diagnosing Cushing's syndrome (CS) and autonomous cortisol secretion (ACS) in patients with adrenal incidentaloma remains a challenge, partly due to a lack of biochemical tests with high diagnostic accuracy (1, 2). Upon clinical suspicion of CS, current guidelines recommend biochemical screening with either a 1 mg overnight dexamethasone suppression test (DST), 24-hour urinary free-cortisol or late-night salivary cortisol (LNSC) (2). For patients with adrenal incidentaloma, DST is the most commonly recommended first-line screening test for ACS (1–5). However, the low specificity of DST for diagnosing CS and ACS is problematic (6).

LNSC is well-established as a first-line screening test for patients with CS (7–10). The diagnostic value of LNSC for detecting ACS in patients with adrenal incidentaloma is, however, less well established (6). The limited number of studies published to date have shown that LNSC has a relatively low sensitivity for predicting ACS, and subsequently conclude that the test is not suitable for screening of this disorder (11–16).

We have recently demonstrated that salivary cortisone at 11 p.m., as well as salivary cortisol and cortisone at 8 a.m. following 1-mg overnight DST, all have high diagnostic accuracy for CS (17). Also, in a recent study from Norway, salivary cortisone at 8 a.m. following 1-mg overnight DST was found to be useful in patients with hypercortisolism, both CS and ACS (18).

The aim of this study was to evaluate the diagnostic value of LNSC, and late-night salivary cortisone, as well as salivary cortisol and salivary cortisone following DST, both in patients with adrenal incidentaloma and in patients with suspected CS.

Methods

Study design

This was a retrospective study performed at the Department of Endocrinology at the Sahlgrenska University hospital. All patients who provided at least one saliva sample for measurement of cortisol and cortisone between April 2018 and November 2020 were identified by a search in an administrative program at the Department of Clinical Chemistry at the hospital. Medical records were reviewed to gather information on clinical characteristics, including information on factors known to affect cortisol concentrations, the indication for testing, and biochemical test results.

Patients

pt?>In total, 398 sets of saliva samples from to 319 patients were analyzed during the study period. In patients that collected more than one set of salivary samples, the first set of samples was used in the final analysis. However, if the earliest set of samples was incomplete, the first complete set was included instead.

The indication for sampling was adrenal incidentaloma in 184 (58%) patients and suspected CS in 69 (22%) (Figure 1). Patients with other or unknown indication for sampling were excluded [n=66 (21%)]. Of 253 patients with either adrenal

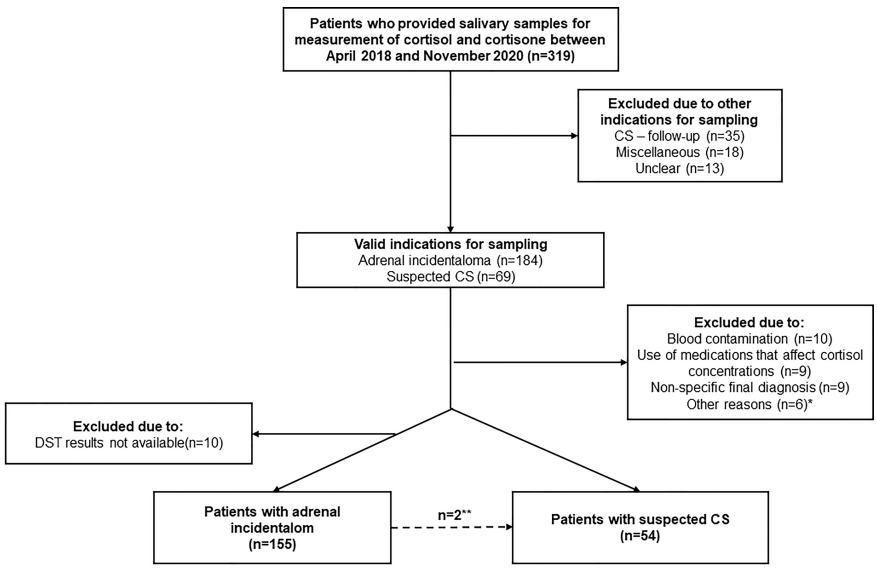

FIGURE 1
Summary of the study population, 319 patients who provided salivary samples for measurement of cortisol and cortisone between April 2018 and November 2020. *Including one patient with pheochromocytoma, one with primary aldosteronism, one with iatrogenic CS, **Two patients with adrenal incidentaloma had clinically overt CS and were included in the analysis of patients with suspected CS.

incidentaloma or suspected CS, 10 were excluded due to suspected contamination of the saliva samples (see below), nine due to use of medications known to affect cortisol concentrations, and 15 due to other reasons (Figure 1). Furthermore, 10 patients with adrenal incidentaloma were also excluded due to unavailable results from DST. Thus, 209 patients were included for the final analysis (Figure 1).

Currently, there is no consensus regarding diagnostic criteria for ACS (6). Therefore, in this study, no predefined diagnostic criteria were used. Instead, the diagnosis was provided through a real-life clinical assessment made by the treating endocrinologist. In general, ACS was diagnosed in patients with adrenal incidentalomas, without overt clinical signs of CS, who had at least two positive diagnostic tests (DST, LNSC, urinary free cortisol and/or plasma-ACTH) indicating abnormal HPA-axis function. Similarly, in patients considered to have non-functioning adrenal incidentaloma, ACS was ruled out based on clinical evaluation showing absence of hypercortisolism-related clinical features and comorbidities, and/or normal biochemical testing (DST, LNSC, urinary free cortisol and/or plasma-ACTH).

The diagnosis of CS was based on clinical symptoms compatible with the syndrome, in combination with at least two biochemical screening tests showing hypercortisolism (2).

Collection of salivary samples

The saliva samples were collected at home using Salivette® Cortisol tubes (Sarstedt, Nümbrecht, Germany) after oral and written instructions on how to properly collect the saliva had been provided (17). The patients were instructed to collect the first salivary sample between 10 and 11 p.m. by chewing on the foam stick until it was completely saturated with saliva. Thereafter, the patients ingested 1 mg dexamethasone. The following day, the second salivary sample was collected between 6 and 8 a.m. The patients were instructed to avoid intense physical exercise during the day of saliva collection, to avoid smoking and use chewing tobacco, eat, or brush their teeth for one hour before saliva collection. Drinking fluids was allowed 30 minutes before the sampling. Minutes before the sampling, the patients were instructed to rinse their mouths with water.

Analytical methods and reference ranges

The cortisol and cortisone concentrations in saliva were measured by liquid chromatography-tandem mass spectrometry (LC-MS/MS). The system used was an Acquity UPLC with a Xevo TQS, equipped with a BEH C18 1.7 µm 2.1 × 100 mm analytical column, all from Waters. As buffer A, 20% methanol and 0.1% formic acid in water was used, buffer B was 20% acetonitrile in methanol. Prior to the analysis, the samples were extracted by using Methyl *tert*-butyl ether and ISOLUTE SLE+ 200 µL Supported Liquid Extraction plates. The coefficients of variation were 6% for cortisol at concentrations between 2.2 and 18.4 nmol/L and 7% for cortisone at concentrations between 4.7 and 26.8 nmol/L. The same LC-MS/MS assay was used to measure UFC. P-cortisol was measured by using a radioimmunoassay (Roche Cobas, Cortisol-II) with a coefficient of variation of 2-3%.

Based on our previous study (17), the upper limit of normal for salivary cortisol and cortisone concentrations, were as follows:

- LNSC <3 nmol/L
- Sa-cortisone at 11 p.m. <15 nmol/L
- Sa-cortisol at 8 a.m. following DST <1 nmol/L
- Sa-cortisone at 8 a.m. following DST <5 nmol/L

In general, p-cortisol following DST <50 nmol/L was considered to exclude hypercortisolism, while values >138 nmol/L were considered to be highly suggestive for hypercortisolism (1, 2).

The upper limit of normal for UFC was 136 nmol/L. In a small minority of patients, another method was used for measuring UFC with a upper limit of normal of 191 nmol/L. The lower limit of normal for p-ACTH was 2.0 pmol/L.

Contamination with exogenous hydrocortisone, or blood, in the salivary samples was determined by calculating the salivary-cortisol:cortisone ratio as previously described (17). Samples with a ratio over the 97.5 percentile for the whole cohort (1.0) were considered to be contaminated.

Statistics

IBM Statistics SPSS version 26 and R were used for statistical analyses.

For comparison of categorical variables, presented as n (%), chi-square test or the Fisher´s exact test were used. Normally distributed numerical variables are described as mean ± standard deviation and non-normally distributed variables as median (interquartile range). Independent t-test was used for comparison between normally distributed variables and the Mann-Whitney U-test for non-normally distributed variables. The level of statistical significance was set at $p < 0.05$.

Receiver-operating characteristic (ROC) analyses were created for each test and presented as area under the curve (AUC) together with 95% confidence intervals (95% CI). DeLong test was used to compare the AUC between the tests, using DST as a reference.

Ethics

This study was approved by the ethical committee of the University of Gothenburg, (Dnr 814-18), and conducted according to the Declaration of Helsinki.

10.3389/fendo.2022.1028804

Results

In total, 209 patients were included in the study, 157 patients with adrenal incidentaloma and 52 patients with suspected CS. Two patients with adrenal incidentaloma had clinically overt CS, one finally diagnosed with Cushing's disease and one with cortisol-producing adrenal adenoma, and were therefore included in the analysis of patients with suspected CS. Thus, in the final analysis, data from 155 patients with adrenal incidentaloma, and 54 patients with suspected CS, were included (Figure 1).

Patients with adrenal incidentalomas

Among the 155 patients with adrenal incidentaloma, 145 (94%) were considered to have non-functioning adrenal adenoma and 10 (6%) to have ACS. Age, gender distribution, BMI, and the prevalence of hypertension, diabetes and tobacco use didn't differ between these groups (Table 1).

Of 145 patients with non-functioning adrenal adenoma, 51 (35%) had P-cortisol >50 nmol/L and 9 (6%) had P-cortisol >138 nmol/L after DST, compared to 10 out of 10 and 6 out of 10 patients with ACS, respectively (Table 1). Eleven of 143 (8%) patients with non-functioning adrenal adenoma had LNSC >3 nmol/L and 13 (9%) had late-night Sa-cortisone >15 nmol/L, compared to 4 out of 10 (40%) and 9 out of 10 (90%) patients with ACS, respectively (Table 1). Six (60%) patents with ACS had elevated salivary cortisol and cortisone at 8 a.m. following DST compared to 9% and 8%, respectively, of patients with non-functioning adrenal incidentalomas. Thus, in patients with adrenal incidentaloma the best diagnostic performance in terms of high sensitivity (90%) in combination with high specificity (91%) for diagnosing ACS was achieved by using late-night Sa-cortisone (Table 1).

In a ROC analysis, the greatest AUC was found for P-cortisol following DST and late-night Sa-cortisone (Figure 2). However, no significant differences were found between the AUCs for the salivary tests and the AUC for P-cortisol following DST. P-cortisol following DST at 107 nmol/L gave the best combination of high sensitivity (90%) and specificity (92%).

One patient with ACS (case 1, Table 2) was treated surgically with unilateral adrenalectomy and one patient, (case 3, Table 2) received pharmacological treatment with Metyrapone. One of these patients had normal LNSC. The remaining 8 patients were treated conservatively.

In a separate analysis, patients with adrenal incidentaloma were instead categorized according to whether P-cortisol following DST was above or below 138 nmol/L. Among the patients with P-cortisol < 138 nmol/L after DST (n=140), LNSC was >3 nmol/L in 11 (8%), late-night Sa-cortisone >15 nmol/L in 14 (10%), salivary cortisol at 8 a.m. following DST >1 nmol/L in 9 (6%) and salivary cortisone at 8 a.m. following DST >3 nmol/L in 32 (23%). In comparison, of patients with P-cortisol >138 nmol/L after DST (n=15), two (13%) had LNSC >3 nmol/L (*P*=0.5 vs patients with P-cortisol < 138 nmol/L after DST), 7 (47%) had late-night Sa-cortisone >15 nmol/L (P<0.001), 6 (40%) had salivary cortisol at 8 a.m. following DST >1 nmol/L (P<0.001) and 10 (67%) had salivary cortisone at 8 a.m. following DST >3 nmol/L (P<0.001).

TABLE 1 Characteristics of patients with non-functioning adrenal incidentaloma and autonomous cortisol secretion who provided salivary samples for analysis of cortisol and cortisone during the study period (April 2018 – November 2020).

	Non-functioning adrenal adenoma (n=145)	Mild autonomous cortisol secretion (n=10)	*p*		
Age (years)	62 ± 12	62 ± 10	1.0		
Women	92 (63)	7 (70)	1.0		
BMI (kg/m^2)	28.5 ± 5.8	27.5 ± 5.4	0.6		
Diabetes	28 (19)	2 (20)	1.0		
Hypertension	67 (47)	6 (60)	0.4		
				Sensitivity	**Specificity**
Post-DST P-cortisol >50 nmol/L	51 (35)	10 (100)	<0.001	100%	65%
Post-DST P-cortisol >138 nmol/L	9 (6)	6 (60)	<0.001	60%	94%
LNSC >3 nmol/L	11 (8)**	4 (40)	0.009	40%	92%
Late-night Sa-cortisone >15 nmol/L	13 (9)**	9 (90)	<0.001	90%	91%
Post-DST Sa-cortisol >1 nmol/L	12 (9)***	6 (60)	<0.001	60%	91%
Post-DST Sa-cortisone >5 nmol/L	11 (8)***	6 (60)	<0.001	60%	92%

Categorical variables are presented as n (%) and continuous variables as mean (± SD). Independent t-test, Chi-square test or Fisher´s exact test were used to analyze statistical differences between the groups. **Not performed in two patients, ***Not performed in three patients.
BMI, body mass index; DST, 1-mg-dexamethasone suppression test; LNSC, late-night salivary cortisol; P, plasma; Sa, salivary.

10.3389/fendo.2022.1028804

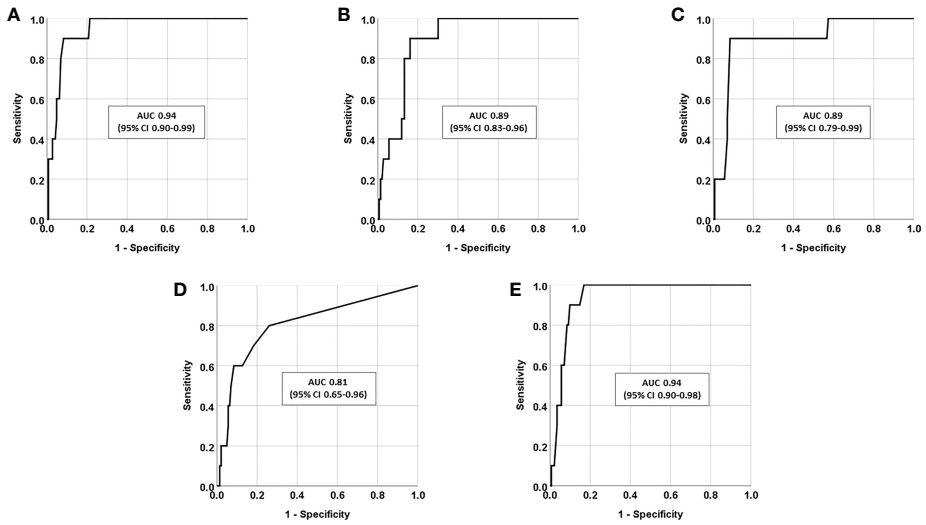

FIGURE 2
Receiver-operating characteristic (ROC) curves presented as area under the curve (AUC) together with 95% confidence intervals (95% CI), in patients with adrenal incidentaloma (n=155) for **(A)** P-cortisol following dexamethasone suppression test (DST), **(B)** late-night Sa-cortisol (LNSC), **(C)** late-night Sa-cortisone, **(D)** Sa-cortisol at 8 a.m. following DST, and **(E)** Sa-cortisone at 8 a.m. following DST.

Patients with suspected Cushing´s syndrome

In total, 54 patients, 45 women (87%) and 9 men (13%), with suspected CS were included in the analysis. CS was ruled out in 47 (87%) patients and confirmed in 7 (13%) patients, 4 with Cushing's disease, two with cortisol-producing adrenal adenoma and one with ectopic CS (Table 3).

One patient with CS had P-cortisol <138 nmol/L following DST, one had normal LNSC and one had normal late-night salivary cortisone (Table 4). Moreover, UFC was normal in three out of six patients (Table 4, cases 1-3). Following DST, all seven patients with CS had Sa-cortisol and cortisone above the normal range. The best diagnostic performance in terms of high sensitivity (100%) in combination with high specificity (91%) for diagnosing CS was achieved by using Sa-cortisone following DST (Table 3).

The greatest AUC in a ROC analysis was found for LNSC and Sa-cortisone following DST (Figure 3), although not significantly different compared to the AUC for P-cortisol following DST.

TABLE 2 Individual data on patients with adrenal incidentalomas diagnosed with autonomous cortisol secretion.

Case no.	Age/ Sex	BMI	Hyper-tension	Diabetes	UFC	P-cortisol after DST	P-ACTH	LNSC	Late-night Sa-cortisone	Sa-cortisol after DST	Sa-cortisone after DST
		Kg/ m^2			*nmol/24-hr**	*nmol/L*	*pmol/ L**	*nmol/ L**	*nmol/L**	*nmol/L**	*nmol/L**
1	35/F	25.1	No	No	147	**150 ˄**	**1.0 ˅**	2.4	**16.0 ˄**	**1.6 ˄**	**9.2 ˄**
2	71/F	17.3	No	No	**191 ˄**	**410 ˄**	**0.3 ˅**	**6.8 ˄**	**36.0 ˄**	**5.1 ˄**	**32.0 ˄**
3	69/F	25.2	Yes	No	92	**110 ˄**	**1.8 ˅**	**5.6 ˄**	**16.0 ˄**	**1.0 ˄**	**5.8 ˄**
4	61/F	31.4	Yes	No	67	**160 ˄**	–	1.4	**16.0 ˄**	0.5	4.4
5	67/M	31.2	No	No	**209 ˄**	**66 ˄**	2.4	**4.2 ˄**	**18.0 ˄**	0.6	4.9
6	66/F	33.9	Yes	Yes	78	**270 ˄**	–	**13.0 ˄**	**38.0 ˄**	**1.7 ˄**	**12.0 ˄**
7	63/M	23.5	Yes	No	131	**260 ˄**	–	2.0	**17.0 ˄**	**1.1 ˄**	**11.0 ˄**
8	59/F	25.2	No	Yes	**236 ˄**	**120 ˄**	**1.6 ˅**	2.1	5.5	**3.4 ˄**	3.5
9	59/M	34.9	Yes	No	80	**120 ˄**	2.9	2.3	**16.0 ˄**	0.7	**5.7 ˄**
10	66/F	26.8	Yes	No	20.2	**190 ˄**	**0.9 ˅**	2.2	**18.0 ˄**	0.5	4.9

*Reference ranges: UFC <136 nmol/L, P-ACTH 2-11 pmol/L, LNSC <3 nmol/L, Late-night Sa-cortisone <15 nmol/L, Sa-cortisol after DST <1 nmol/L, Sa-cortisone <5 nmol/L. Abnormal results are marked in bold style and with ˅ (decreased) or ˄ (increased).
ACTH, adrenocorticotropic hormone; BMI, body mass index; DST, 1-mg-dexamethasone suppression test; F, female; LNSC, late-night salivary cortisol; M, male; P, plasma; Sa, salivary; UFC, urinary free cortisol.

Discussion

In this study, we have evaluated the diagnostic value of measuring cortisol and cortisone in saliva in patients with adrenal incidentaloma, and patients with suspected CS. Our findings suggest that LNSC has a low sensitivity for diagnosing ACS in patients with adrenal incidentaloma whereas Sa-cortisone at 11 p.m. had a high sensitivity and specificity for diagnosing the disorder. Furthermore, in patients with suspected CS, Sa-cortisone following DST seem to be a promising diagnostic alternative.

The diagnostic value of measuring LNSC in patients with adrenal incidentaloma has been studied in a limited number of studies (Table 5) (11–16). In most of these studies LNSC was analyzed with immunochemical methods, i.e. methods with lower analytical specificity than LC-MS/MS due to a risk of cross-reactions between cortisol and other steroid metabolites (19, 20). To our knowledge, LC-MS/MS has only been used three times before for measuring LNSC in patients with adrenal incidentaloma (12, 15, 16). In one of these studies, the sensitivity of Sa-cortisol <2.8 nmol/L at 11 p.m. was 31%, and the specificity was 83%, for diagnosing ACS in 70 patients with adrenal incidentaloma (12), i.e. in line with the current study. Similar results were found in a study from Norway on 165 patients with adrenal incidentaloma (15), and a study from Italy on 106 patients (16). In fact, due to the low sensitivity, all previous studies, regardless of analytical assay, have concluded that LNSC cannot be recommended as an exclusive screening method for ACS (11–16). Instead, LNSC may be used in combination with other tests to confirm the disorder (11).

Bäcklund et al. recently found that Sa-cortisone at 11 p.m. had a higher sensitivity than LNSC for diagnosing CS (17). Our study, showing that 9 of 10 patients with ACS had elevated Sa-cortisone at 11 p.m., suggest that Sa-cortisone may be of greater diagnostic value than LNSC also in patients with adrenal incidentaloma. Similarly, simultaneous measurement of LNSC and Sa-cortisone was recently recommended by Mohamed and colleagues (8). In addition, measuring Sa-cortisol and Sa-cortisone simultaneously enables detection of contamination by exogenous hydrocortisone in the samples. Further studies investigating the value of Sa-cortisone as a part of the diagnostic work-up for adrenal incidentaloma are needed, including efforts to identify biomarkers of clinically relevant ACS that warrants adrenalectomy.

Sa-cortisol and Sa-cortisone were inadequately suppressed following DST in 6 of 10 patients with ACS, whereas inadequate suppression of Sa-cortisol and Sa-cortisone was found only in 9 and 8%, respectively, of patients with non-functioning adrenal incidentalomas, giving a specificity of 91/92%. Sa-cortisol and Sa-cortisone at 8 a.m. following DST has to our knowledge only been studied once before in the context of screening for ACS (18). In that study, 13 of 25 patients with ACS had elevated post-DST Sa-cortisol and 23 of 25 had elevated Sa-cortisone, with 90% and 82% specificity, respectively. Analysis of Sa-cortisol and Sa-cortisone following DST has also been used in two previous studies to screen patients with suspected CS, both showing a high sensitivity (95-100%) and specificity (80-95%) (17, 18), in agreement with our findings. Thus, Sa-cortisol and/or Sa-cortisone following DST are promising diagnostic tools in patients with adrenal incidentaloma as well as patients with suspected CS.

Currently, there is no international consensus on how ACS in patients with adrenal incidentalomas should be diagnosed, and different recommendations have been provided (1–5, 21–

TABLE 3 Characteristics of patients with suspected Cushing's syndrome.

	CS ruled out (n=47)	CS (n=7)	*p*		
Age (years)	40 ± 17	58 ± 8	0.006		
Women	40 (85%)	6 (86%)	1.0		
BMI (kg/m^2)	30.7 ± 8.7	28.8 ± 5.2	0.6		
Diabetes	8 (17%)	2 (29%)	0.6		
Hypertension	15 (32%)	6 (86%)	0.011		
				Sensitivity	**Specificity**
Post-DST P-cortisol >50 nmol/L	18/40 (45%)	6/6 (100%)	0.014	100%	55%
Post-DST P-cortisol >138 nmol/L	4/40 (10%)	5/6 (83%)	0.001	83%	90%
UFC	3/28 (11%)	3/6 (50%)	0.053	50%	89%
LNSC >3 nmol/L	4/45 (9%)	5/6 (83%)	<0.001	83%	91%
Late-night Sa-cortisone >15 nmol/L	3/45 (7%)	5/6 (83%)	<0.001	83%	93%
Post-DST Sa-cortisol >1 nmol/L	7/43 (16%)	7/7 (100%)	<0.001	100%	84%
Post-DST Sa-cortisone >5 nmol/L	4/43 (9%)	7/7 (100%)	<0.001	100%	91%

Categorical variables are presented as n/total n of patients (%) and continuous variables as mean (± SD). Independent t-test, Chi-square test and Fisher´s exact test were used to analyze statistical differences between the groups.
BMI, body mass index; CS, Cushing's syndrome; DST, 1-mg-dexamethasone suppression test; LNSC, late-night salivary cortisol; P, plasma; Sa, salivary; UFC, urinary free cortisol.

10.3389/fendo.2022.1028804

TABLE 4 Individual data on patients diagnosed with Cushing's syndrome.

Case no.	Age/ Sex	UFC	P-cortisol after DST	P-cortisol at 11 p.m.	P-ACTH	LNSC	Late-night Sa-cortisone	Sa-cortisol after DST	Sa-cortisone after DST	Final diagnosis
		*nmol/24-hr**	*nmol/L*	*nmol/L*	*pmol/L**	*nmol/L**	*nmol/L**	*nmol/L**	*nmol/L**	
1	46/F	124	**160 ˄**	**440 ˄**	8.8	**7.0 ˄**	**28.0 ˄**	**1.1 ˄**	**8.7 ˄**	CD
2	57/F	49.6	**170 ˄**	–	**1.6 ˅**	**4.4 ˄**	11.4	**3.2 ˄**	**10.0 ˄**	CPAA
3	69/F	125	–	**250 ˄**	13.0	2.8	**30.0 ˄**	**1.4 ˄**	**18.0 ˄**	CD
4	63/M	–	**830 ˄**	**690 ˄**	**23.0 ˄**	–	–	**27.0 ˄**	**113.0 ˄**	CD
5	62/F	**860 ˄**	**821 ˄**	–	**14.0 ˄**	**27 ˄**	**78 ˄**	**8.4 ˄**	**53.0 ˄**	ECS
6	52/F	**660 ˄**	**430 ˄**	–	**0.2 ˅**	**12.0 ˄**	**56.0 ˄**	**7.2 ˄**	**44.0 ˄**	CPAA
7	58/F	**465 ˄**	**120 ˄**	–	5.9	**21.0 ˄**	**60.0 ˄**	**4.9 ˄**	**27.0 ˄**	CD

*Reference ranges: UFC <136 nmol/L, P-ACTH 2-11 pmol/L, LNSC <3 nmol/L, Late-night Sa-cortisone <15 nmol/L, Sa-cortisol after DST <1 nmol/L, Sa-cortisone <5 nmol/L. Abnormal results are marked in bold style and with ˅ (decreased) or ˄ (increased).

ACTH, adrenocorticotropic hormone; BMI, body mass index; CD, Cushing´s disease; CPAA, Cortisol producing pituitary adenoma; DST, 1-mg-dexamethasone suppression test; ECS, Ectopic Cushing´s syndrome; F, female; LNSC, late-night salivary cortisol; M, male; P, plasma; Sa, salivary; UFC, urinary free cortisol.

23). However, due to the high sensitivity, DST is the most frequently recommended first-line screening method. Indeed, all patients in our study diagnosed with ACS had P-cortisol >50 nmol/L on the DST, supporting a high negative predictive value of P-cortisol <50 nmol/L. The downside of this test is, however, the low specificity. In our study, 35% of patients with non-functioning adrenal incidentaloma had P-cortisol >50 nmol/L following DST, i.e., a "false positive test", in agreement with previous rapports (6). P-cortisol >138 nmol/L following DST has been suggested for diagnosis of ACS by the National Institute of Health (21). In our study, 10% of all patients with adrenal incidentalomas had P-cortisol >138 nmol/L, providing a more reasonable prevalence of ACS in comparison to a cut-off of 50 nmol/L. However, 40% of the patients diagnosed with ACS in our cohort had P-cortisol <138 nmol/L following DST, illustrating a relatively poor ability to confirm the diagnosis by using this cut-off. Our results, therefore, indicate that DST should not be the only biochemical test used to diagnose mild autonomous hypercortisolism, regardless of the cut-off value used.

In a recent meta-analysis including 139 studies, the accuracy of laboratory tests for CS was investigated (24). The sensitivity was high for all tests, lowest for UFC (94%) and highest for DST (99%). In the current study, one patient with overt CS had normal LNSC, another had P-cortisol <138 nmol/L following DST and half of the patients had normal UFC. Interestingly,

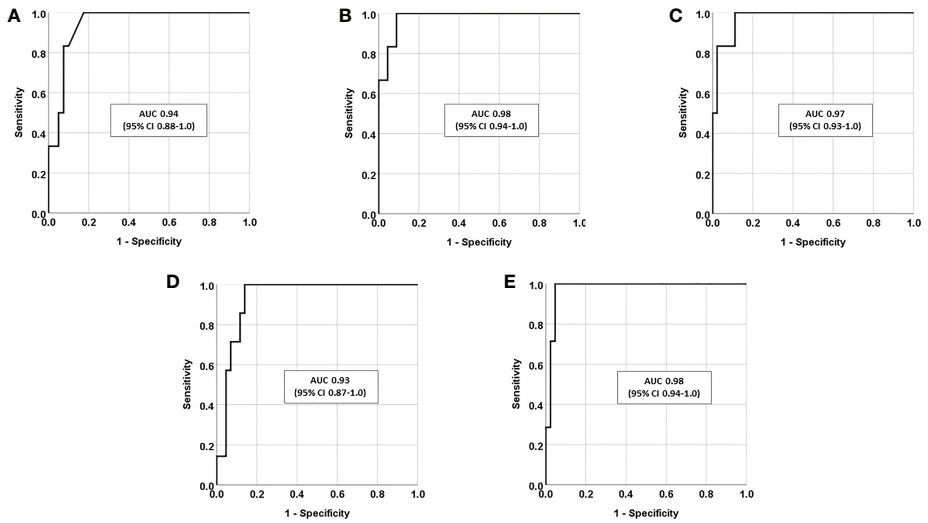

FIGURE 3
Receiver-operating characteristic (ROC) curves presented as area under the curve (AUC) together with 95% confidence intervals (95% CI), in patients with suspected Cushing's syndrome (n=54) for **(A)** P-cortisol following dexamethasone suppression test (DST), **(B)** late-night Sa-cortisol (LNSC), **(C)** late-night Sa-cortisone, **(D)** Sa-cortisol at 8 a.m. following DST, and **(E)** Sa-cortisone at 8 a.m. following DST.

TABLE 5 Summary of studies that have evaluated the diagnostic value of salivary cortisol in patients with adrenal incidentaloma.

	Definition of ACS	No of patients	Main findings	Main conclusion	Comments
Masserini, 2009, Milan, Italy	Two of the following: Cortisol after DST >83 nmol/l, 24-h UFC >193 nmol/24 h, and morning ACTH <2.2 pmol/l.	22 ACS of 103 AI (21%)	LNSC 5.1 nmol/l, had 23% sensitivity and 88% specificity for diagnosis of ACS	LNSC is not suitable as a screening test for ACS. May be used with other tests to confirm ACS	LNSC measured with immunofluorimetrical assay
Palmieri, 2013, Milan, Italy	Two of the following: Cortisol after DST >83 nmol/l, 24-h UFC >193 nmol/24 h, and morning ACTH <2.2 pmol/l.	16 ACS of 70 AI (23%)	LNSC >2.8 nmol/l had 31% sensitivity and 83% specificity for predicting ACS	LNSC useful in combination with DST for diagnosing ACS, but not useful as a single criterion	LNSC measured with LC-MS/MS
Ceccado, 2017, Padova, Italy	S-cortisol >138 nmol/L after DST, or s-cortisol after DST 50–138 nmol/L and one of the following: ACTH <10 ng/L, high LNSC, or high UFC	30 ACS of 164 AI (18%)	Median LNSC higher in patients with ACS than non-ACS, but without a reliable cutoff	Consider UFC together with DST to reduce false-positives. LNSC not suitable as a screening test for ACS	Main focus is on UFC, not LNSC LNSC measured with a radio-immunometric assay
Ueland, 2017, Norway	S-cortisol >50 nmol/L after DST, low morning P-ACTH and at least one ACS related comorbidity.	25 ACS of 131 AI	13 of 25 patients with ACS had elevated post-DST Sa-cortisol and 23 had elevated Sa-cortisone	Post-DST Sa-cortisone useful, especially for diagnosing of hypercortisolism	S-dexamethasone and salivary cortisol and cortisone measured with LC-MS/MS. Controls included and used to calculate reference ranges
Ceccato, 2018, Italy	S-cortisol >50 nmol/L after DST	46 ACS of 106 AI	LNSC similar in patients with or without S-cortisol >50 nmol/L after DST	LNSC not useful to discriminate between non-functioning AI and ACS	Salivary cortisol and cortisone measured with LC-MS/MS
Ueland, 2020, Norway	S-cortisol >50 nmol/L after DST	83 ACS of 165 AI	LNSC false-positive in 23/63 and false-negative in 38/69	LNSC not useful to discriminate between non-functioning AI and ACS	S-dexamethasone and salivary cortisol and cortisone measured with LC-MS/MS. Patients with low dexamethasone bioavailability and patients using oral estrogens excluded
Araujo-Castro, 2021, Spain	S-cortisol after DST >138 nmol/L	19 ACS of 197 AI (10%)	LNSC >157 nmol/l had 88% specificity and 47% sensitivity for identifying ACS. 25% sensitivity for S-cortisol > 50 nmol/L	LNSC has a low reliability for diagnosing ACS	LNSC measured with Electroimmuno-chemiluminescence assay

ACS, Autonomous cortisol secretion; ACTH, adrenocorticotropic hormone; AI, Adrenal incidentaloma; DST, 1-mg over-night dexamethasone suppression test; LC-MS/MS, liquid chromatography tandem mass spectrometry; LNSC, late-night salivary cortisol; P, plasma; S, serum; Sa, salivary; UFC, urinary free cortisol.

however, all patients with overt CS had elevated Sa-cortisol as well as Sa-cortisone at 8 a.m. following DST. Also, in agreement with Bäcklund et al. (17), LNSC and Sa-cortisone at 11 p.m. had a slightly lower sensitivity than salivary samples collected after DST.

The limitations of this study include the limited number of patients, especially the group of patients finally diagnosed with CS, and that two or more saliva samples were not consequently sampled in all patients with suspected CS, emphasizing the need for caution when interpreting the results. Also, due to the retrospective design, the diagnostic criteria for ACS was not predefined. Instead, the diagnosis was based on clinical findings and results from the different cortisol measurement, i.e., a real-life assessment made by several physicians responsible for each patient. Due to the lack of predefined specific criteria, the risk of diagnostic inconsistency cannot be ruled out. Moreover, since the treating clinicians were not blinded to the results of the salivary samples when diagnosing ACS and CS, it is difficult to evaluate independently the diagnostic value of each biochemical test, including salivary cortisol and cortisone. In addition, elevated P-cortisol following DST is often required for diagnosing ACS, which inevitably may have contributed to the high sensitivity of this test. Finally, P-dexamethasone, analysed together with P-cortisol in association with DST, in order to decrease the number of false positive results (18), was not measured in our study. The study has also several strengths, including that all patients who provided salivary samples followed a standardized protocol for collection and a relatively large number of patients with adrenal incidentalomas were included. Furthermore, both salivary cortisol and cortisone were measured, enabling calculation of the cortisol:cortisone ratio and evaluation if the samples were contaminated with exogenous cortisol (hydrocortisone). Another strength is that the salivary samples were analyzed using LC-MS/MS, which is more accurate than other analytical methods used to analyze steroids.

In conclusion, LNSC does not by itself seem to be sufficiently sensitive to screen patients with suspected hypercortisolism,

neither in patients with adrenal incidentalomas, nor in patients with suspected CS. However, Sa-cortisone at 11 p.m. and salivary cortisol and cortisone following DST seem to be promising tests in the same context. Nevertheless, further studies on the diagnostic value of salivary cortisol and cortisone are needed. Ideally, this would be done prospectively with a sufficiently large number of patients, where the criteria for ACS would be predefined, and the investigators would be blinded to the results on salivary cortisol/cortisone when the decision on diagnosis is made.

Data availability statement

The raw data supporting the conclusions of this article will be made available by the authors, without undue reservation.

Ethics statement

This study was approved by the ethical committee of the University of Gothenburg, (Dnr 814-18). Written informed consent for participation was not required for this study in accordance with the national legislation and the institutional requirements.

Author contributions

VB: data curation, formal analysis, investigation, methodology, project administration, software, visualisation and writing - original draft preparation. PD, JV, and HR: writing - reviewing and editing. OR: conceptualisation, formal analysis, funding acquisition, methodology, resources, software, supervision, validation, visualisation, and writing - reviewing and editing. All authors contributed to the article and approved the submitted version.

Acknowledgments

We would like to thank Göran Oleröd and Sara Nadi at the Department of Clinical Chemistry at Sahlgrenska University Hospital, for identifying the eligible patients and providing their salivary test results and Nils Bäcklund for statistical help comparing the ROC curve AUCs.

Conflict of interest

The authors declare that the research was conducted in the absence of any commercial or financial relationships that could be construed as a potential conflict of interest.

Publisher's note

References

1. Fassnacht M, Arlt W, Bancos I, Dralle H, Newell-Price J, Sahdev A, et al. Management of adrenal incidentalomas: European society of endocrinology clinical practice guideline in collaboration with the European network for the study of adrenal tumors. *Eur J Endocrinol* (2016) 175(2):G1–34. doi: 10.1530/EJE-16-0467

2. Nieman LK, Biller BM, Findling JW, Newell-Price J, Savage MO, Stewart PM, et al. The diagnosis of cushing's syndrome: An endocrine society clinical practice guideline. *J Clin Endocrinol Metab* (2008) 93(5):1526–40. doi: 10.1210/jc.2008-0125

3. Yanase T, Oki Y, Katabami T, Otsuki M, Kageyama K, Tanaka T, et al. New diagnostic criteria of adrenal subclinical cushing's syndrome: Opinion from the Japan endocrine society. *Endocr J* (2018) 65(4):383–93. doi: 10.1507/endocrj.EJ17-0456

4. Zeiger MA, Thompson GB, Duh QY, Hamrahian AH, Angelos P, Elaraj D, et al. American Association of clinical endocrinologists and American association of endocrine surgeons medical guidelines for the management of adrenal incidentalomas: executive summary of recommendations. *Endocr Pract* (2009) 15 (5):450–3. doi: 10.4158/EP.15.5.450

5. Lee JM, Kim MK, Ko SH, Koh JM, Kim BY, Kim SW, et al. Clinical guidelines for the management of adrenal incidentaloma. *Endocrinol Metab (Seoul)* (2017) 32 (2):200–18. doi: 10.3803/EnM.2017.32.2.200

6. Sherlock M, Scarsbrook A, Abbas A, Fraser S, Limumpornpetch P, Dineen R, et al. Adrenal incidentaloma. *Endocr Rev* (2020) 41(6):775–820. doi: 10.1210/endrev/bnaa008

7. Raff H, Raff JL, Findling JW. Late-night salivary cortisol as a screening test for cushing's syndrome. *J Clin Endocrinol Metab* (1998) 83(8):2681–6. doi: 10.1210/jc.83.8.2681

8. Mohamed RS, Abuelgasim B, Barker S, Prabhudev H, Martin NM, Meeran K, et al. Late-night salivary cortisol and cortisone should be the initial screening test for cushing's syndrome. *Endocr Connect* (2022) 11(7):e220050. doi: 10.1530/EC-22-0050

9. Kannankeril J, Carroll T, Findling JW, Javorsky B, Gunsolus IL, Phillips J, et al. Prospective evaluation of late-night salivary cortisol and cortisone by EIA and LC-MS/MS in suspected cushing syndrome. *J Endocr Soc* (2020) 4(10):bvaa107. doi: 10.1210/jendso/bvaa107

10. Ponzetto F, Settanni F, Parasiliti-Caprino M, Rumbolo F, Nonnato A, Ricciardo M, et al. Reference ranges of late-night salivary cortisol and cortisone measured by LC-MS/MS and accuracy for the diagnosis of cushing's syndrome. *J Endocrinol Invest* (2020) 43(12):1797–806. doi: 10.1007/s40618-020-01388-1

11. Masserini B, Morelli V, Bergamaschi S, Ermetici F, Eller-Vainicher C, Barbieri AM, et al. The limited role of midnight salivary cortisol levels in the diagnosis of subclinical hypercortisolism in patients with adrenal incidentaloma. *Eur J Endocrinol* (2009) 160(1):87–92. doi: 10.1530/EJE-08-0485

12. Palmieri S, Morelli V, Polledri E, Fustinoni S, Mercadante R, Olgiati L, et al. The role of salivary cortisol measured by liquid chromatography-tandem mass spectrometry in the diagnosis of subclinical hypercortisolism. *Eur J Endocrinol* (2013) 168(3):289–96. doi: 10.1530/EJE-12-0803

13. Ceccato F, Antonelli G, Frigo AC, Regazzo D, Plebani M, Boscaro M, et al. First-line screening tests for cushing's syndrome in patients with adrenal incidentaloma: The role of urinary free cortisol measured by LC-MS/MS. *J Endocrinol Invest* (2017) 40(7):753–60. doi: 10.1007/s40618-017-0644-8

14. Araujo-Castro M, Garcia Cano A, Jimenez Mendiguchia L, Escobar-Morreale HF, Valderrabano P. Diagnostic accuracy of the different hormonal tests used for the diagnosis of autonomous cortisol secretion. *Sci Rep* (2021) 11 (1):20539. doi: 10.1038/s41598-021-00011-4

15. Ueland GA, Grinde T, Methlie P, Kelp O, Lovas K, Husebye ES. Diagnostic testing of autonomous cortisol secretion in adrenal incidentalomas. *Endocr Connect* (2020) 9(10):963–70. doi: 10.1530/EC-20-0419

16. Ceccato F, Barbot M, Albiger N, Antonelli G, Zilio M, Todeschini M, et al. Daily salivary cortisol and cortisone rhythm in patients with adrenal incidentaloma. *Endocrine* (2018) 59(3):510–9. doi: 10.1007/s12020-017-1421-3

17. Backlund N, Brattsand G, Israelsson M, Ragnarsson O, Burman P, Eden Engstrom B, et al. Reference intervals of salivary cortisol and cortisone and their diagnostic accuracy in cushing's syndrome. *Eur J Endocrinol* (2020) 182(6):569–82. doi: 10.1530/EJE-19-0872

18. Ueland GA, Methlie P, Kellmann R, Bjorgaas M, Asvold BO, Thorstensen K, et al. Simultaneous assay of cortisol and dexamethasone improved diagnostic accuracy of the dexamethasone suppression test. *Eur J Endocrinol* (2017) 176 (6):705–13. doi: 10.1530/EJE-17-0078

19. Mészáros K, Karvaly G, Márta Z, Magda B, Tőke J, Szücs N, et al. Diagnostic performance of a newly developed salivary cortisol and cortisone measurement using an LC-MS/MS method with simple and rapid sample preparation. *J Endocrinol Invest* (2018) 41(3):315–23. doi: 10.1007/s40618-017-0743-6

20. Israelsson M, Brattsand R, Brattsand G. 20α- and 20β-dihydrocortisone may interfere in LC-MS/MS determination of cortisol in saliva and urine. *Ann Clin Biochem* (2018) 55(3):341–7. doi: 10.1177/0004563217724178

21. Grumbach MM, Biller BM, Braunstein GD, Campbell KK, Carney JA, Godley PA, et al. Management of the clinically inapparent adrenal mass ("incidentaloma"). *Ann Intern Med* (2003) 138(5):424–9. doi: 10.7326/0003-4819-138-5-200303040-00013

22. Fleseriu M, Auchus R, Bancos I, Ben-Shlomo A, Bertherat J, Biermasz NR, et al. Consensus on diagnosis and management of cushing's disease: a guideline update. *Lancet Diabetes Endocrinol* (2021) 9(12):847–75. doi: 10.1016/S2213-8587(21)00235-7

23. Tabarin A, Assie G, Barat P, Bonnet F, Bonneville JF, Borson-Chazot F, et al. Consensus statement by the French society of endocrinology (SFE) and French society of pediatric endocrinology & diabetology (SFEDP) on diagnosis of cushing's syndrome. *Ann Endocrinol (Paris)* (2022) 83(2):119–41. doi: 10.1016/j.ando.2022.02.001

24. Galm BP, Qiao N, Klibanski A, Biller BMK, Tritos NA. Accuracy of laboratory tests for the diagnosis of cushing syndrome. *J Clin Endocrinol Metab* (2020) 105(6):2081–94. doi: 10.1210/clinem/dgaa105

frontiers | Frontiers in Endocrinology

TYPE Original Research
PUBLISHED 25 November 2022
DOI 10.3389/fendo.2022.1004112

OPEN ACCESS

EDITED BY
Nadia Sawicka-Gutaj,
Poznan University of Medical Sciences, Poland

REVIEWED BY
Claudio Casella,
University of Brescia, Italy
Piotr Glinicki,
Centre of Postgraduate Medical Education, Poland

*CORRESPONDENCE
Yangang Zhang
urozyg@163.com

†These authors have contributed equally to this work

SPECIALTY SECTION
This article was submitted to Adrenal Endocrinology, a section of the journal Frontiers in Endocrinology

RECEIVED 09 August 2022
ACCEPTED 15 November 2022
PUBLISHED 25 November 2022

CITATION
Sun S, Wang J, Yang B, Wang Y, Yao W, Yue P, Niu X, Feng A, Zhang L, Yan L, Cheng W and Zhang Y (2022) A nomogram for evaluation and analysis of difficulty in retroperitoneal laparoscopic adrenalectomy: A single-center study with prospective validation using LASSO-logistic regression. *Front. Endocrinol.* 13:1004112. doi: 10.3389/fendo.2022.1004112

A nomogram for evaluation and analysis of difficulty in retroperitoneal laparoscopic adrenalectomy: A single-center study with prospective validation using LASSO-logistic regression

Shiwei Sun[1†], Jinyao Wang[2,3†], Bin Yang[2,3†], Yue Wang[1], Wei Yao[1], Peng Yue[1], Xiangnan Niu[2,3], Anhao Feng[1], Lele Zhang[4], Liang Yan[2,3], Wei Cheng[2,3] and Yangang Zhang[1,2,3*]

[1]Third Hospital of Shanxi Medical University, Shanxi Bethune Hospital, Shanxi Academy of Medical Sciences, Tongji Shanxi Hospital, Taiyuan, China, [2]Shanxi Bethune Hospital, Shanxi Academy of Medical Sciences, Tongji Shanxi Hospital, Third Hospital of Shanxi Medical University, Taiyuan, China, [3]Tongji Hospital, Tongji Medical College, Huazhong University of Science and Technology, Wuhan, China, [4]Department of Urology, Tangdu Hospital, Air Force Medical University, Xi'an, China

Background: While it is known that inaccurate evaluation for retroperitoneal laparoscopic adrenalectomy (RPLA) can affect the surgical results of patients, no stable and effective prediction model for the procedure exists. In this study, we aimed to develop a computed tomography (CT) -based radiological-clinical prediction model for evaluating the surgical difficulty of RPLA.

Method: Data from 398 patients with adrenal tumors treated by RPLA in a single center from August 2014 to December 2020 were retrospectively analyzed and divided into sets. The influencing factors were selected by least absolute shrinkage and selection operator regression model (LASSO). Additionally, the nomogram was constructed. A receiver operating characteristic curve was used to analyze the prediction efficiency of the nomogram. The C-index and bootstrap self-sampling methods were used to verify the discrimination and consistency of the nomogram.

Result: The following 11 independent influencing factors were selected by LASSO: body mass index, diabetes mellitus, scoliosis, hyperlipidemia, history of operation, tumor diameter, distance from adrenal tumor to upper pole of kidney, retro renal fat area, hyperaldosteronism, pheochromocytoma and paraganglioma, and myelolipoma. The area under the curve (AUC) of the training set was 0.787, and 0.844 in the internal validation set. Decision curve

analyses indicated the model to be useful. An additional 117 patients were recruited for prospective validation, and AUC was 0.848.

Conclusion: This study developed a radiological-clinical prediction model proposed for predicting the difficulty of RPLA procedures. This model was suitable, accessible, and helpful for individualized surgical preparation and reduced operational risk. Thus, this model could contribute to more patients' benefit in circumventing surgical difficulties because of accurate predictive abilities.

KEYWORDS

adrenalectomy, laparoscopy, retroperitoneal space, LASSO, nomogram

Introduction

Adrenal tumors are common among urological conditions, with a median incidence rate of approximately 3.0% (1.05%–8.7%) (1). Involved pathologies include nonfunctional adrenal tumors, primary aldosteronism (PA), Cushing's syndrome, pheochromocytoma and paraganglioma (PPGL), myelolipomas, ganglioneuromas, adrenocortical carcinomas, and adrenal metastasis (2, 3). Computed tomography (CT) is among the preferred localization and diagnostic methods, as it can typically detect adrenal tumors with a diameter of >5 mm (4). In addition, the pathology of lesions can be evaluated preliminarily by CT (5).

As the gold standard treatment for adrenal tumors, laparoscopic surgery has the advantages of accelerating postoperative recovery and shortening postoperative hospital stay (POHS) as compared with open surgery (6–8). Laparoscopic surgery is further divided into transperitoneal laparoscopic adrenalectomy (TPLA) and retroperitoneal laparoscopic adrenalectomy (RPLA), with TLPA first competed in 1992 by Gagner et al. (9) and Higashihara et al. (10) and RPLA first proposed by Gaur et al. (11), later refined by Walz et al. (12). Compared with TLPA, RPLA has less postoperative pain, fewer complications, and lower incidence of intraoperative adverse events such as hemodynamic instability and massive bleeding (13, 14). However, there is currently no effective evaluation system for the difficulties of RPLA. Therefore, exploration of new strategies to improve evaluation efficiency and optimize treatment of adrenal tumors is essential.

Machine learning is a new technique used widely in medical research in recent years. Aside from processing a large amount of data by identifying key factors, it can also capture the relationship between nonlinear variables and accurately predict clinical outcomes. As listed above, this is an indispensable approach to solving complex problems in various fields (15). For instance, current research explored the differences between adrenal pheochromocytoma and lipid-poor adenoma from machine learning (16).

LASSO was established by Tibshirani and found to be one of the most effective classifier construction algorithms to predict clinical outcomes in various classification or regression studies (17). Furthermore, a study used LASSO regression on the preoperative diagnosis of pheochromocytoma, and the model set yielded an AUC of 0.893 (18).

This study used LASSO to retrospectively analyze the influencing factors correlating to the difficulties of RPLA by developing a nomograph. Additionally, this study focused on improving preoperative preparations, reducing the operational risks and improving patients' clinical outcomes.

Methods

Patients and selection criteria

To meet our aim of using LASSO to retrospectively analyze factors influencing the difficulty of RPLA in patients in a single hospital and developing a nomograph to individualize preoperative preparation and reduce operational risk, we retrospectively collected the data of adrenal tumor patients in Shanxi Bethune hospital from August 2014 to December 2020. The models were established based on the retrospective patient data, while adrenal tumor patients from January 2021 to

Abbreviations: APF, adherent perirenal fat; AUC, area under the curve; BMI, body mass index; CI, confidence interval; CT, computed tomography; DAK, distance from adrenal tumor to upper pole of kidney; DARP, distance from adrenal tumor to renal pedicle; DCA, decision curve analysis; LASSO, least absolute shrinkage and selection operator; MAP, Mayo adhesive probability; OR, odds ratio; PA, primary aldosteronism; POHS, postoperative hospital stay; PPGL, pheochromocytoma and paraganglioma; RFA, retrorenal fat area; ROC, receiver operating characteristics; RPLA, retroperitoneal laparoscopic adrenalectomy; TD, tumor diameter; TPLA, transperitoneal laparoscopic adrenalectomy.

December 2021 were prospectively collected for prospective validation. Inclusion criteria included: 1) confirmation of adrenal tumors by abdominal CT examination 1–15 days before operation, 2) routine laboratory examinations (serum aldosterone [supine and erect position], direct renin concentration [supine and erect position], serum cortisol [8:00, 16:00, and 24:00], plasma catecholamine, urine catecholamine, and vanillylmandelic acid) to determine the hormone activity of adrenal tumors performed before operation, and 3) treated by RPLA. Exclusion criteria included: 1) no surgery conducted, 2) multiple operations undergone concurrently, and 3) incomplete CT data. A total of 398 patients were included in the retrospective study, with an additional 117 patients recruited for prospective validation (Figure 1A).

Procedures

As referenced from the previous studies (13, 14, 19–21), patients who meet any of the following conditions are considered to be difficult to operate on: 1) operation time ≥ P_{75} (150 $_{min}$), 2) blood transfusion required during operation due to injury of surrounding organs or blood vessels, 3) convert to open surgery, 4) postoperative complications with Clavien–Dindo grade ≥ 3, 5) POHS ≥ P_{95} (15 d). Otherwise, patients are considered to be easy to operate on.

For this study, patients were divided randomly into training and internal validation sets, with a proportion of 7:3. The data from the training set was used for influencing factor selection and model construction, whereas the data of the internal validation set was used to validate the model (Figure 1B).

Radiological features were obtained using Siemens SOMATOM definition flash or force dual-source CT, with Siemens SOMATOM Definition AS Sliver or GEOptima 660 spiral CT scanning (Siemens, Munich, Germany). CT scanning was performed with 1.0 mm slice thickness and 0.7 mm intervals. The method for measurement of features was as follows. For tumor diameter (TD), we took the larger value of the longest diameter in the largest section of the tumor and the difference between the upper and lower poles of the tumor. For distance from adrenal tumor to upper pole of kidney (DAK), we took the vertical height difference between the lower pole of adrenal tumors and the upper pole of the ipsilateral kidney. For the distance from adrenal tumor to renal pedicle (DARP), we took the vertical height difference between the lower pole of the adrenal tumor and the plane of the ipsilateral renal vein. For the distance from great vessel to the adrenal tumor, we selected the slice closest to the tumor and great vessel (left: abdominal aorta; right: inferior vena cava), and measured the shortest distance between them. For the retrorenal fat area (RFA), we used 3D slicer software to draw the region of interest (ROI) for measurement. The ROI was drawn at the slice of the renal vein in the horizontal view, encompassed by the extended line of the renal vein and its perpendicular line, as well as the visceral tectorial membrane and parietal peritoneum. The above features were measured by two doctors, respectively. If the consistency of the two measurements was >0.75, we took the average of the two values; otherwise, the measurement was re-taken by another senior doctor (Figure 1C).

Statistical analysis

R 4.1.4 (Vienna statistical computing foundation, Austria) and the glmnet (22) package were used to process data. As all continuous variables did not conform to the normal distribution, they are represented by the median [interquartile range]; categorical variables are expressed in frequency and percentage (%). The patients were randomly divided into the training and internal validation sets according to a ratio of 7:3, and the baseline characteristics between each set were compared by analysis of variance. Using the glmnet package, the univariate logistic regression and lasso logistic regression analysis were carried out to verify the independent influencing factors. The nomogram model was then established according to multivariate logistic regression, and the ROC curve and the AUC were used to verify the prediction efficiency of the model. The bootstrap resampling method and calibration curve were used to evaluate the consistency of the model, and the net benefit of patients was evaluated by clinical decision curve analysis (DCA). The prediction model was then verified again in the prospective group. When P-value <0.05, the difference was considered to be statistically significant.

Results

Baseline characteristics

This study involved 398 patients, with all baseline characteristics listed in Table 1. The median patient age is 50.50 [40.00, 58.00] years with 179 male (45.0%) and 219 female (55.0%). A total of 132 patients were considered to be challenging to operate on, with 105 having had an operation time ≥ P_{75}, 13 having required blood transfusion due to intraoperative damage to surrounding organs or vessels, seven having undergone conversion to open surgery, 27 having had complications with a Clavien–Dindo grade ≥ 3 (Table 2), and 19 having had a postoperative hospital stay of ≥ P_{95}. It was discovered by ANOVA that there was no significant difference in preoperative baseline characteristics among the sets.

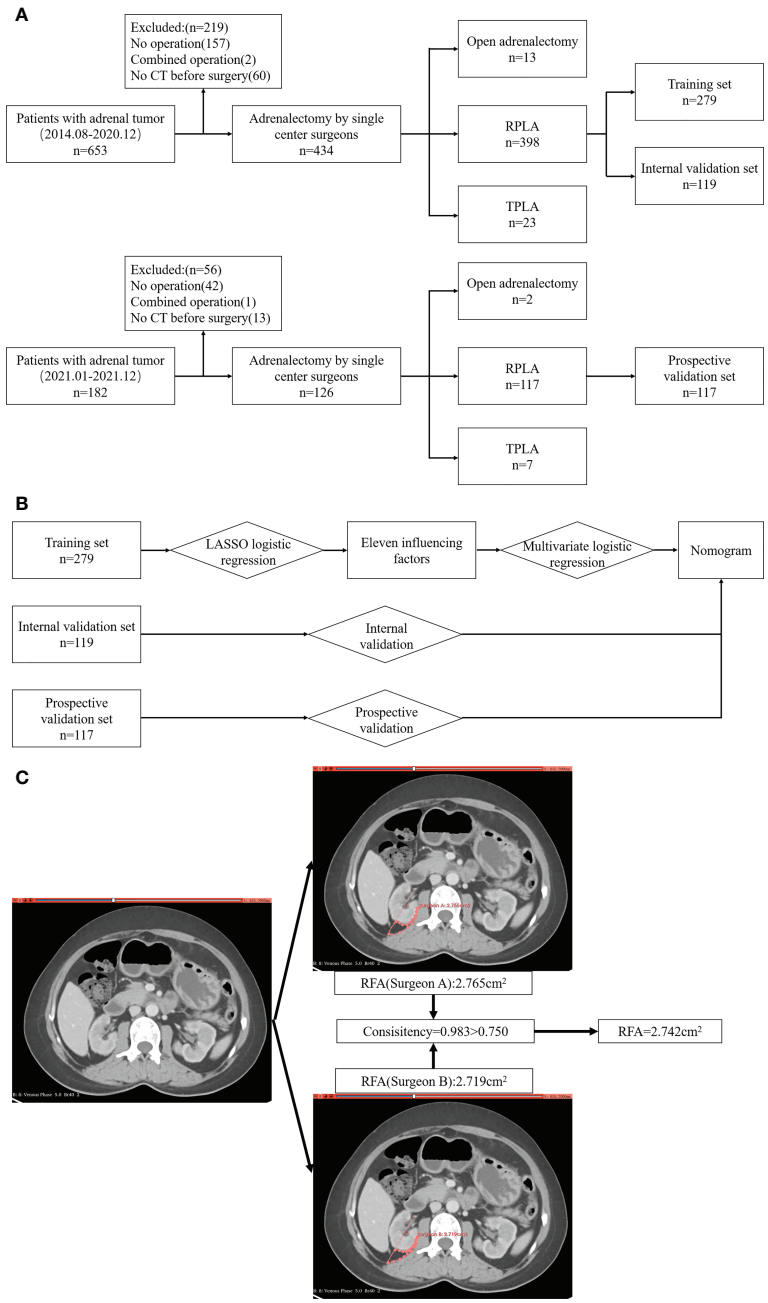

FIGURE 1
Study flowchart. **(A)** Inclusion and exclusion process; **(B)** Analysis and verification process; **(C)** Drawing of ROI and calculation of RFA.

Univariate logistics regression

Univariate logistics regression suggested that there were several influencing factors associated with the difficulty of RPLA, including gender (Odds ratio[OR]: 0.511, 95% Confidence interval[CI]: 0.334–0.779, P=0.002), body mass index (BMI) (OR: 1.076, 95% CI: 1.018–1.138, P=0.01), pathology (OR: 1.185, 95% CI: 1.066–1.320, P=0.002), diabetes mellitus (OR: 2.595, 95% CI: 1.558–4.336, P=0), scoliosis (OR: 2.932, 95% CI: 1.157–7.750, P=0.024), coronary disease (OR: 1.962, 95% CI: 1.008–3.799, P=0.045), hyperlipidemia (OR: 2.595, 95% CI: 1.369–4.962, P=0.004), history of operation (OR: 1.654, 95% CI: 1.048–2.603, P=0.03), TD (OR: 1.022, 95% CI: 1.010–1.035, P=0.001), DAK (OR: 0.979, 95% CI: 0.965–0.993, P=0.004), DARP (OR: 0.983, 95% CI: 0.969–0.997, P=0.015), and RFA (OR: 1.001, 95% CI: 1.000–1.001, P=0.001) (Figure 2).

TABLE 1 Baseline characteristics of the patients.

	Training set (n = 279)	Internal validation set (n = 119)	Prospective validation set (n = 117)	F	P
Gender				1.214	0.298
Male	130 (46.6)	49 (41.2)	60 (51.3)		
Female	149 (53.4)	70 (58.8)	57 (48.7)		
Age (yr)	51.00[42.00,58.50]	50.00[38.50,58.00]	51.00[39.00,58.00]	0.400	0.671
BMI ($kg·m^{-2}$)	24.61[22.84,27.35]	25.35[22.88,27.91]	25.95[23.44,28.32]	2.912	0.055
Pathology				1.536	0.216
NFAT	115 (41.2)	45 (37.8)	38 (32.5)		
PA	81 (29.0)	31 (26.1)	43 (36.8)		
Cushing's syndrome	29 (10.4)	12 (10.1)	17 (14.5)		
PPGL	21 (7.5)	12 (10.1)	7 (6.0)		
Myelolipoma	11 (3.9)	4 (3.4)	4 (3.4)		
Cyst	10 (3.6)	6 (5.0)	3 (2.6)		
Malignant tumor	4 (1.4)	2 (1.7)	2 (1.7)		
Ganglioneuroma	3 (1.1)	1 (0.8)	2 (1.7)		
Others	5 (1.8)	6 (5.0)	1 (0.9)		
Side				0.352	0.703
Left	166 (59.5)	72 (60.5)	65 (55.6)		
Right	113 (40.5)	47 (39.5)	52 (44.4)		
Hypertension				0.369	0.692
No	60 (21.5)	26 (21.8)	21 (17.9)		
Yes	219 (78.5)	93 (78.2)	96 (82.1)		
Diabetes mellitus				1.335	0.264
No	230 (82.4)	92 (77.3)	89 (76.1)		
Yes	49 (17.6)	27 (22.7)	28 (23.9)		
Scoliosis				1.351	0.26
No	267 (95.7)	112 (94.1)	115 (98.3)		
Yes	12 (4.3)	7 (5.9)	2 (1.7)		
Coronary disease				1.957	0.142
No	253 (90.7)	105 (88.2)	98 (83.8)		
Yes	26 (9.3)	14 (11.8)	19 (16.2)		
Cerebral infarction				0.082	0.921
No	253 (90.7)	107 (89.9)	107 (91.5)		
Yes	26 (9.3)	12 (10.1)	10 (8.5)		
Hyperlipidemia				0.184	0.832
No	249 (89.2)	106 (89.1)	102 (87.2)		
Yes	30 (10.8)	13 (10.9)	15 (12.8)		
History of malignancy				2.024	0.133
No	268 (96.1)	117 (98.3)	109 (93.2)		
Yes	11 (3.9)	2 (1.7)	8 (6.8)		
History of operation				0.603	0.547
No	198 (71.0)	89 (74.8)	80 (68.4)		
Yes	81 (29.0)	30 (25.2)	37 (31.6)		
Hb ($g·L^{-1}$)	137.00[127.00,146.00]	135.00[126.00,146.00]	137.00[127.00,146.00]	0.318	0.728
TD (mm)	20.80[15.10,30.40]	22.00[15.50,35.20]	20.00[14.00,28.00]	2.621	0.074
DAK (mm)	-10.00[-20.80,-2.70]	-12.80[-21.20,-5.20]	-9.60[-17.60,-3.50]	1.642	0.195
DARP (mm)	28.80[19.20,37.90]	28.00[18.10,36.80]	28.70[18.40,40.00]	0.587	0.556
DGV (mm)	8.00[3.50,14.00]	6.00[3.00,12.00]	7.00[4.00,12.00]	0.628	0.534
RFA (mm^2)	399.00[203.40,668.50]	429.30[222.00,703.55]	370.30[237.30,635.80]	0.627	0.535

(Continued)

TABLE 1 Continued

	Training set (n = 279)	Internal validation set (n = 119)	Prospective validation set (n = 117)	F	P
Resection range				0.152	0.859
Partial	251 (90.0)	109 (91.6)	105 (89.7)		
Radical	28 (10.0)	10 (8.4)	12 (10.3)		
Operation time (min)	110.00[85.00,150.00]	120.00[95.00,150.00]	98.00[76.00,130.00]	5.015	0.007
Blood loss (ml)	20.00[0.00,50.00]	20.00[10.00,50.00]	15.00[0.00,25.00]	0.763	0.467
POHS (d)	7.00[6.00,9.00]	8.00[7.00,9.50]	6.00[2.00,7.00]	15.683	<0.001

BMI, body mass index; NFAT, non-function adrenal tumor; PA, primary aldosteronism; PPGL, pheochromocytoma and paraganglioma; TD, tumor diameter; DAK, distance from adrenal tumor to upper pole of kidney; DARP, distance from adrenal tumor to renal pedicle; DGV, distance from great vessel to adrenal tumor; RFA, retrorenal fat area.
Others (pathology) include eosinophil tumor, teratoma, schwannoma, hematoma, tuberculoma, foreign body granuloma, retroperitoneal bronchial cyst, hemangioma.

Variable selection

We converted multi-categorical variables into binary-categorical variables through dummy variables; final variable assignments are shown in Table 3. Generalized cross-validation was carried out for all variables through LASSO logistics regression, with the log (lambda) value of the harmonic parameter. The AUC of the model changed along with the change of the lambda. The corresponding number of variables filtered by the model is shown in Figure 3A. We constructed an influencing factor classifier by using the lasso logistic regression model (Figure 3B). After lasso logistic analysis, eleven influencing factors were selected including BMI, diabetes mellitus, scoliosis, hyperlipidemia, history of operation, TD, DAK, RFA, PA, PPGL, and myelolipoma (Table 4).

Nomogram

According to the influencing factors screened by Lasso-logistic regression, multivariate logistic regression was carried out, and the results were displayed by nomogram (Figure 4A). To use the nomogram, we added up the scores corresponding to each prediction index of the patient to calculate the total score, and determined the corresponding risk value from the total score line, which was the probability that the operation would be more complicated in that patient. For example, if a patient's pathological type of tumor were PA, with TD of 40 mm, DAK of -10 mm, RFA of 2000 mm^2, BMI of 26 $kg \cdot m^{-2}$; there was no previous surgery history, scoliosis, history of hyperlipidemia; and there was a history of diabetes, the corresponding scores of each feature were approximately 20, 8, 20, 40, 29, 0, 24, 0, 29, respectively. Thus, the total score was 170, which corresponds to a probability of 80% for increased surgical difficulty and suggests that additional perioperative preparations would be required for an operation.

Validation and performance of nomogram

The C-index of the model was 0.784 (95% CI: 0.736–0.832). After 1000 resampling internal validations, the visible calibration curve fit the ideal curve well, indicating that the probability of

TABLE 2 Classification of complications.

Complications	I	II	IIIa	IIIb	IVa	Summation
Fever	11					11
Hypokalemia	6					6
Hypofunction of cortex	5					5
Hyperkalemia	1					1
Mumps	1					1
Wound infection	1					1
Delayed bleeding	1	1				2
Incomplete ileus		1				1
Deep venous thrombosis		3	1			4
Foreign body granuloma				1		1
Systemic inflammatory response syndrome					1	1
Disturbances of vital signs (requiring ICU management)					24	24
Total	26	5	1	1	25	58

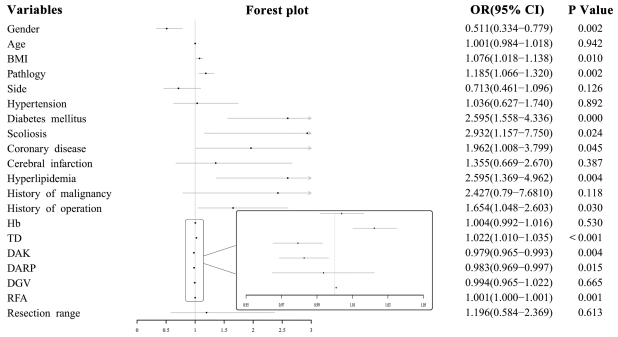

FIGURE 2
Forest plot of influencing factors of surgical difficulty.

the predicted surgical difficulty of the model had good agreement with the actual situation (Figure 4B).

ROC curves were drawn according to the model, with an AUC of 0.787 (95% CI: 0.732–0.843) in the training set and an AUC of 0.844 (95% CI: 0.766–0.923) in the internal validation set. The AUC in the prospective validation set was 0.848 (95% CI: 0.772–0.924) and showed high predictive power for this machine learning model (Figure 4C).

The prediction model based on DCA yielded a net benefit for patients of around 15% when the intervention was performed at approximately 35% probability of difficulty (Figure 4D). The model had a sensitivity of 0.759, a specificity of 0.720, and a Youden index of 0.479, showing high prediction accuracy (Figure 4E).

TABLE 3 Variable assignments.

Variable	Risk Factors	Assignments
X_1	Gender	Male=0, female=1
X_2	Age	Continuous variable
X_3	BMI	Continuous variable
X_4	Side	Left=0, right=1
X_5	Hypertension	No=0, Yes=1
X_6	Diabetes mellitus	No=0, Yes=1
X_7	Scoliosis	No=0, Yes=1
X_8	Coronary disease	No=0, Yes=1
X_9	Cerebral infarction	No=0, Yes=1
X_{10}	Hyperlipidemia	No=0, Yes=1
X_{11}	History of malignancy	No=0, Yes=1
X_{12}	History of operation	No=0, Yes=1
X_{13}	Hb	Continuous variable
X_{14}	TD	Continuous variable
X_{15}	DAK	Continuous variable
X_{16}	DARP	Continuous variable
X_{17}	DGV	Continuous variable
X_{18}	RFA	Continuous variable
X_{19}	Resection range	Partial=0, Radical=1
X_{20}	NFAT	No=0, Yes=1
X_{21}	PA	No=0, Yes=1
X_{22}	Cushing syndrome	No=0, Yes=1
X_{23}	PPGL	No=0, Yes=1
X_{24}	Myelolipoma	No=0, Yes=1
X_{25}	Cyst	No=0, Yes=1
X_{26}	Malignant tumor	No=0, Yes=1
X_{27}	Ganglioneuroma	No=0, Yes=1
X_{28}	Other pathological types	No=0, Yes=1

Discussion

Adrenal tumors are a hot topic in the field of medicine at present. This study outlined the factors in predicting the difficulty of RPLA *via* nomogram regarding BMI, diabetes mellitus, scoliosis, hyperlipidemia, history of surgery, TD, DAK, RFA and pathology. We concluded that the model had a high predictive ability by internal and prospective validation.

Numerous studies have highlighted that TD is a major factor contributing to the difficulty of RPLA (13, 14, 19–21, 23, 24). In a previous analysis of 275 patients who underwent laparoscopic adrenalectomy, Natkaniec et al. posited that type of pathology was a predictor of difficulty and suggested that surgery for malignancy was much more difficult than that for other tumor types (OR, 3.67, 95% CI 1.52–8.87; P = 0.008) (19), while Vidal (21) and Pisarska (25) considered that surgery was more difficult in pheochromocytoma. The effect of DAK on the difficulty of RPLA was first suggested by Wang (23) (OR, 5.76 95% CI, 2.03–16.35; P = 0.001) and Rah (13) (OR, 3.79; 95% CI, 1.66–8.67; P = 0.002), respectively, and DARP was similarly found to affect surgical difficulty in the former study (OR, 6.23; 95% CI, 2.11–18.38; P = 0.001).

Aside from the tumor itself, the surrounding area and surgical site also have an impact on the difficulty, including adherent perirenal fat (APF) (26), peripheral fat distance (27), and posterior adiposity index (13). Previously, Davidiuk et al.

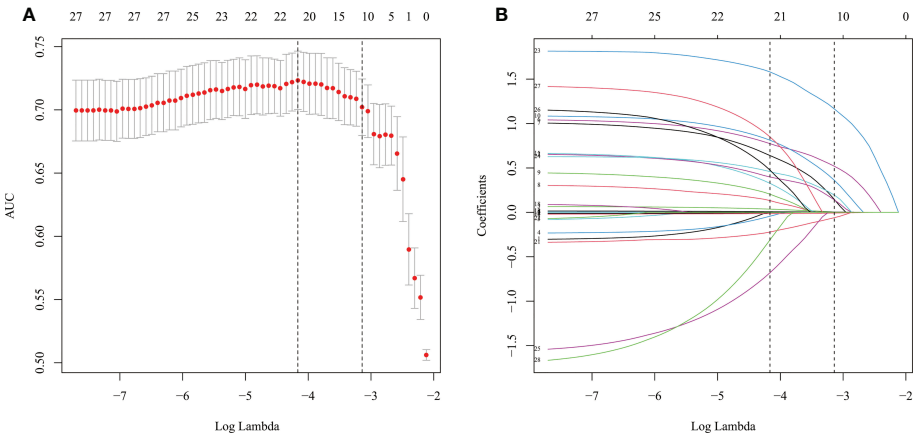

FIGURE 3
LASSO-Logistic regression. **(A)** The cross-validation results. **(B)** LASSO coefficient profiles of the 28 variables.

proposed the Mayo adhesive probability (MAP) to predict APF (26), and Kira et al. (24) confirmed MAP to be related to difficulty of RPLA as the adrenal gland is adjacent to the kidney. At the same time, the surrounding environment, fat thickness, and adhesion degree are related. Hence, it is also effective in adrenalectomy. Rah et al. (13) measured periadrenal fat volume and named it as an independent factor affecting difficulty of RPLA. However, the adrenal gland has minimal surrounding fat and significant measurement inaccuracy. Therefore, we synthesized previous studies and concluded that RFA has a considerable impact on the difficulty of RPLA. Patients with diabetes, hyperlipidemia or previous surgery are often more likely to have APF, and thus present with more difficulty in an RPLA procedure (28). As another factor, while BMI is used to evaluate degree of obesity, it primarily reflects body fat composition, and the distribution of visceral fat, especially perirenal fat, may differ. Therefore, the prediction of BMI on difficulty of RPLA is still controversial, with a limited number of studies suggesting that BMI has a significant impact (1, 14, 21).

TABLE 4 Risk factors selected by LASSO-logistic regression model.

Variable	Risk Factors	Coefficient
X_3	BMI	0.0033
X_6	Diabetes mellitus	0.1469
X_7	Scoliosis	0.5200
X_{10}	Hyperlipidemia	0.3623
X_{12}	History of operation	0.1411
X_{14}	TD	0.0025
X_{15}	DAK	-0.0078
X_{18}	RFA	0.0004
X_{21}	PA	-0.0605
X_{23}	PPGL	1.1655
X_{24}	Myelolipoma	0.1949

For patients with scoliosis, the surgical area is smaller which restricted the movement of laparoscopic instruments during the operation. The intercostal space is narrow while the tumor is adjacent to major blood vessels such as the abdominal aorta and splenic veins, which increase the surgical difficulty and make the operation challenging. However, no current relevant cohort or case-control study has been published, and this issue has only been acknowledged in some medical records or case reports (29).

Based on clinical data and CT features, this study developed a prediction model of the difficulty of RPLA by LASSO. It carried out relevant internal and prospective validation, proving that this model can improve the net benefit rate of patients by up to 15%.

At present, some scholars have worked on the prediction of the surgical difficulty of RPLA, but a lack of precise prediction models has been published. Thus, the innovation of this study is that the influencing factors of difficulty were analyzed by LASSO regression, and a prediction model was established and internally and prospectively validated. Further, this study is currently the largest cohort regarding the prediction of the difficulty of RPLA.

Limitations of this study: 1) this study set up an internal validation set and a prospective validation set, which requires further validation in future multicenter studies, 2) LASSO was used in this study, while other machine learning algorithms such as xGBoost and SVM will be used in the further research.

Conclusion

In this study, independent influencing factors for the difficulty of RPLA included BMI, diabetes mellitus, scoliosis,

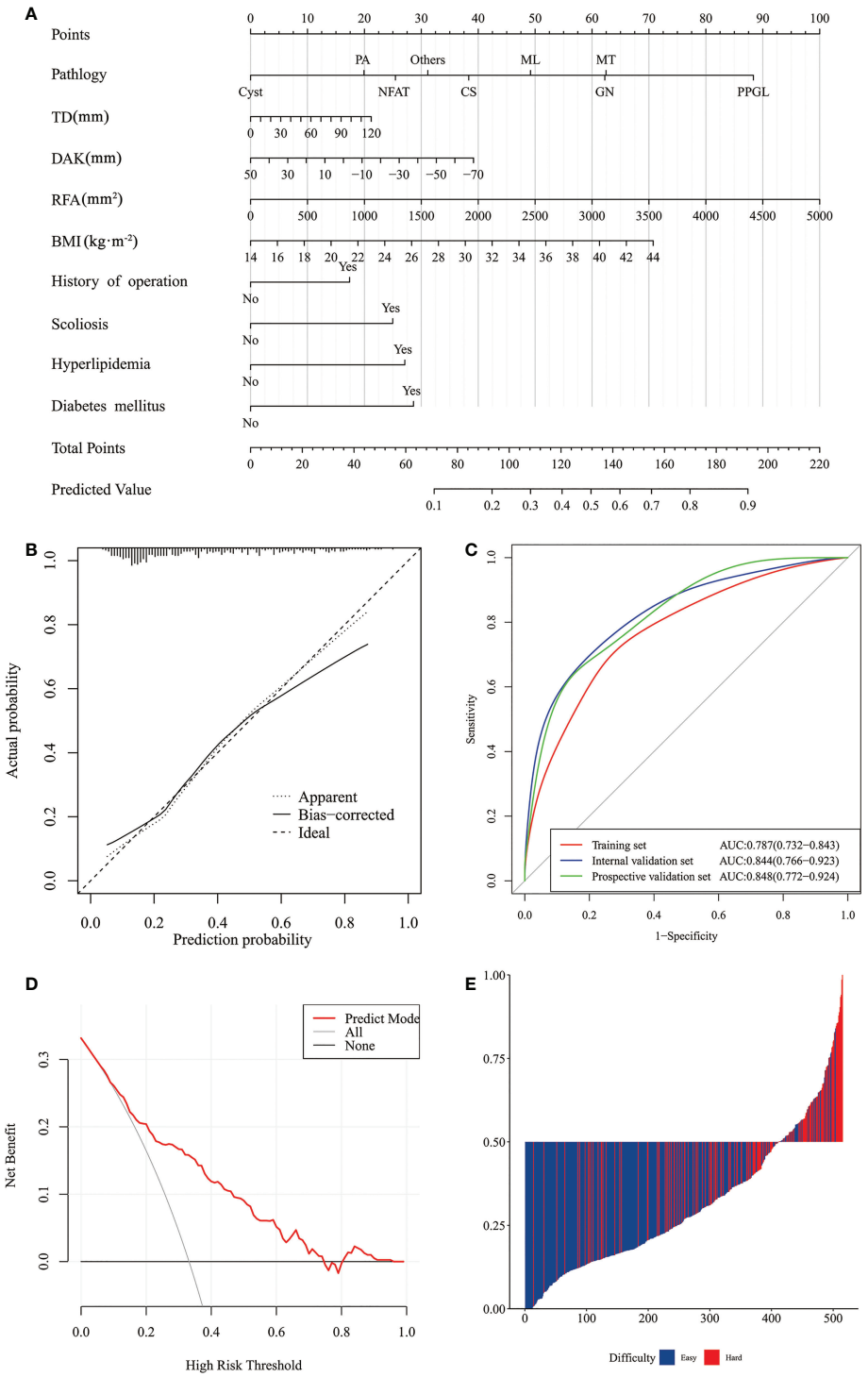

FIGURE 4
Nomogram of prediction model of difficulty of retroperitoneal laparoscopic adrenalectomy and its performance. **(A)** Nomogram. **(B)** Calibration curves of the nomogram in the training and internal validation sets. **(C)** ROC curves of the nomogram in the training, internal and prospective validation sets. **(D)** Clinical decision curve analysis of prediction model. **(E)** The calculated risk scores for each patient within the combined training and external validation datasets.) (NFAT, non-function adrenal tumor; PA, primary aldosteronism; PPGL, pheochromocytoma and paraganglioma; Others, include eosinophil tumor, teratoma, schwannoma, hematoma, tuberculoma, foreign body granuloma, retroperitoneal bronchial cyst, and hemangioma; MT, Malignant tumor, include adrenocortical carcinoma and adrenal metastasis; TD, tumor diameter; DAK, distance from adrenal tumor to upper pole of kidney; RFA, retrorenal fat area; BMI, body mass index.).

hyperlipidemia, history of surgery, TD, DAK, RFA, and pathology. Based on the clinical and radiological characteristics, the machine learning prediction model of the difficulty of RPLA established by LASSO regression had a good predictive performance. Using this model can effectively assist surgeons in evaluating the difficulty of RPLA, facilitating complete individualization of perioperative preparation, thereby reducing surgical risk and benefiting patients.

Data availability statement

The raw data supporting the conclusions of this article will be made available by the authors, without undue reservation.

Author contributions

SS: Project development, Data collection, Data management, Data analysis, Manuscript writing. JW: Project development, Manuscript writing. BY: Project development, Manuscript writing. YW: Data collection, Data management, Data analysis, Manuscript writing. WY, PY, XN, AF, and LZ: Data collection, Data management. LY and WC: Manuscript editing. YZ: Project development, Data analysis, Manuscript editing, Result inspection. All authors contributed to the article and approved the submitted version.

Conflict of interest

The authors declare that the research was conducted in the absence of any commercial or financial relationships that could be construed as a potential conflict of interest.

Publisher's note

All claims expressed in this article are solely those of the authors and do not necessarily represent those of their affiliated organizations, or those of the publisher, the editors and the reviewers. Any product that may be evaluated in this article, or claim that may be made by its manufacturer, is not guaranteed or endorsed by the publisher.

References

1. Bilige W, Wang C, Bao J, Yu D, Min A, Hong Z, et al. Predicting factors related with uncured hypertension after retroperitoneal laparoscopic adrenalectomy for unilateral primary aldosteronism. *Medicine* (2019) 98:e16611. doi: 10.1097/MD.0000000000016611

2. Mansmann G, Lau J, Balk E, Rothberg M, Miyachi Y, Bornstein SR. The clinically inapparent adrenal mass: update in diagnosis and management. *Endocr Rev* (2004) 25:309–40. doi: 10.1210/er.2002-0031

3. Barzon L, Sonino N, Fallo F, Palu G, Boscaro M. Prevalence and natural history of adrenal incidentalomas. *Eur J Endocrinol* (2003) 149:273–85. doi: 10.1530/eje.0.1490273

4. Fassnacht M, Arlt W, Bancos I, Dralle H, Newell-Price J, Sahdev A, et al. Management of adrenal incidentalomas: European society of endocrinology clinical practice guideline in collaboration with the European network for the study of adrenal tumors. *Eur J Endocrinol* (2016) 175:G1–34. doi: 10.1530/EJE-16-0467

5. Zekan D, King RS, Hajiran A, Patel A, Deem S, Luchey A. Diagnostic dilemmas: a multi-institutional retrospective analysis of adrenal incidentaloma pathology based on radiographic size. *BMC Urol* (2022) 22:73. doi: 10.1186/s12894-022-01024-5

6. Gaujoux S, Mihai Rjoint working group of ESES and ENSAT and European Network for the Study of Adrenal Tumours. European Society of endocrine surgeons (ESES) and European network for the study of adrenal tumours (ENSAT) recommendations for the surgical management of adrenocortical carcinoma. *Br J Surg* (2017) 104:358–76. doi: 10.1002/bjs.10414

7. Smith CD, Weber CJ, Amerson JR. Laparoscopic adrenalectomy: new gold standard. *World J Surg* (1999) 23:389–96. doi: 10.1007/pl00012314

8. Pędziwiatr M, Natkaniec M, Kisialeuski M, Major P, Matłok M, Kołodziej D, et al. Adrenal incidentalomas: should we operate on small tumors in the era of laparoscopy? *Int J Endocrinol* (2014) 2014:658483. doi: 10.1155/2014/658483

9. Gagner M, Lacroix A, Bolté E, BOLTé E. Laparoscopic adrenalectomy in cushing's syndrome and pheochromocytoma. *N Engl J Med* (1992) 327:1033. doi: 10.1056/NEJM199210013271417

10. Higashihara E, Tanaka Y, Horie S, Aruga S, Nutahara K, Homma Y, et al. A case report of laparoscopic adrenalectomy. *Nihon Hinyokika Gakkai Zasshi* (1992) 83:1130–3. doi: 10.5980/jpnjurol1989.83.1130

11. Gaur DD. Laparoscopic operative retroperitoneoscopy: use of a new device. *J Urol* (1992) 148:1137–9. doi: 10.1016/s0022-5347(17)36842-8

12. Walz MK, Peitgen K, Hoermann R, Giebler RM, Mann K, Eigler FW. Posterior retroperitoneoscopy as a new minimally invasive approach for adrenalectomy: results of 30 adrenalectomies in 27 patients. *World J Surg* (1996) 20:769–74. doi: 10.1007/s002689900117

13. Rah CS, Kim WW, Lee YM, Chung KW, Koh JM, Lee SH, et al. New predictive factors for prolonged operation time of laparoscopic posterior retroperitoneal adrenalectomy; retrospective cohort study. *Int J Surg* (2021) 94:106113. doi: 10.1016/j.ijsu.2021.106113

14. Alberici L, Paganini AM, Ricci C, Balla A, Ballarini Z, Ortenzi M, et al. Development and validation of a preoperative "difficulty score" for laparoscopic transabdominal adrenalectomy: a multicenter retrospective study. *Surg Endosc* (2022) 36:3549–57. doi: 10.1007/s00464-021-08678-6

15. Obermeyer Z, Emanuel EJ. Predicting the future – big data, machine learning, and clinical medicine. *N Engl J Med* (2016) 375:1216–9. doi: 10.1056/NEJMp1606181

16. Liu H, Guan X, Xu B, Zeng F, Chen C, Yin HL, et al. Computed tomography-based machine learning differentiates adrenal pheochromocytoma from lipid-poor adenoma. *Front Endocrinol* (2022) 13:833413. doi: 10.3389/fendo.2022.833413

17. RT. Regression shrinkage and selection via the lasso. *J R Stat Soc (Series B)* (1996) 58:267–88. doi: 10.1111/j.2517-6161.1996.tb02080.x

18. Shen ZJ, Chen SW, Wang S, Jin XD, Chen J, Zhu Y, et al. Predictive factors for open conversion of laparoscopic adrenalectomy: a 13-year review of 456 cases. *J Endourol.* (2007) 21:1333–7. doi: 10.1089/end.2006.450

19. Natkaniec M, Dworak J, Pędziwiatr M, Pisarska M, Major P, Dembiński M, et al. Patients criteria determining difficulty of the laparoscopic lateral transperitoneal adrenalectomy. A retrospective cohort study. *Int J Surg* (2017) 43:33–7. doi: 10.1016/j.ijsu.2017.05.032

20. Chen Y, Scholten A, Chomsky-Higgins K, Nwaogu I, Gosnell JE, Seib C, et al. Risk factors associated with perioperative complications and prolonged length of stay after laparoscopic adrenalectomy. *JAMA Surg* (2018) 153:1036–41. doi: 10.1001/jamasurg.2018.2648

21. Vidal O, Saavedra-Perez D, Martos JM, de la Quintana A, Rodriguez JI, Villar J, et al. Risk factors for open conversion of lateral transperitoneal laparoscopic adrenalectomy: retrospective cohort study of the Spanish adrenal surgery group (SASG). *Surg Endosc* (2020) 34:3690–5. doi: 10.1007/s00464-019-07264-1

22. Friedman J, Hastie T, Tibshirani R. Regularization paths for generalized linear models *via* coordinate descent. *J Stat Software* (2010) 33:1–22. doi: 10.18637/jss.v033.i01

23. Wang J, Yang B, Sun S, Zhang Y. Perioperative factors influencing the difficulty of retroperitoneal laparoscopic adrenalectomy: a single-center retrospective study. *BMC Urol* (2022) 22:22. doi: 10.1186/s12894-022-00976-y

24. Kira S, Sawada N, Nakagomi H, Ihara T, Furuya R, Takeda M, et al. Mayo Adhesive probability score is associated with the operative time in laparoscopic adrenalectomy. *J Laparoendosc Adv Surg Tech A* (2021) 32(6):595–9. doi: 10.1089/lap.2021.0459

25. Pisarska M, Dworak J, Natkaniec M, Małczak P, Przęczek K, Wysocki M, et al. Risk factors for prolonged hospitalization in patients undergoing laparoscopic adrenalectomy. *Wideochir Inne Tech Maloinwazyjne* (2018) 13:141–7. doi: 10.5114/wiitm.2018.73357

26. Davidiuk AJ, Parker AS, Thomas CS, Leibovich BC, Castle EP, Heckman MG, et al. Mayo Adhesive probability score: an accurate image-based scoring system to predict adherent perinephric fat in partial nephrectomy. *Eur Urol* (2014) 66:1165–71. doi: 10.1016/j.eururo.2014.08.054

27. Lindeman B, Gawande AA, Moore FD, JR, Cho NL, Doherty GM, Nehs MA. The posterior adiposity index: A quantitative selection tool for adrenalectomy approach. *J Surg Res* (2019) 233:26–31. doi: 10.1016/j.jss.2018.07.003

28. Yanishi M, Kinoshita H, Koito Y, Taniguchi H, Mishima T, Sugi M, et al. Adherent perinephric fat is a surgical risk factor in laparoscopic single-site donor nephrectomy: analysis using mayo adhesive probability score. *Transplant Proc* (2020) 52:84–8. doi: 10.1016/j.transproceed.2019.11.027

29. Liu G, Luo G, Tian Y. Thoracoabdominal combined incision treating left adrenal composite pheochromocytoma with severely malformed spine: a case report. *Chin J Urol.* (2020) 41:786–7. doi: 10.3760/cma.j.cn112330-20200302-00147

frontiers | Frontiers in Endocrinology

TYPE Original Research
PUBLISHED 06 December 2022
DOI 10.3389/fendo.2022.1079508

OPEN ACCESS

EDITED BY
Marta Araujo-Castro,
Ramón y Cajal University Hospital, Spain

REVIEWED BY
Juilee Rege,
University of Michigan, United States
Elise Peery Gomez-Sanchez,
University of Mississippi Medical Center, United States

*CORRESPONDENCE
Anna Riester
anna.riester@med.uni-muenchen.de

†These authors share first authorship

SPECIALTY SECTION
This article was submitted to Adrenal Endocrinology, a section of the journal Frontiers in Endocrinology

RECEIVED 25 October 2022
ACCEPTED 21 November 2022
PUBLISHED 06 December 2022

CITATION
Zhang R, Rubinstein G, Vetrivel S, Kunz S, Vogel F, Bouys L, Bertherat J, Kroiss M, Deniz S, Osswald A, Knösel T, Bidlingmaier M, Sbiera S, Reincke M and Riester A (2022) Steroid profiling using liquid chromatography mass spectrometry during adrenal vein sampling in patients with primary bilateral macronodular adrenocortical hyperplasia. *Front. Endocrinol.* 13:1079508. doi: 10.3389/fendo.2022.1079508

Steroid profiling using liquid chromatography mass spectrometry during adrenal vein sampling in patients with primary bilateral macronodular adrenocortical hyperplasia

Ru Zhang[1†], German Rubinstein[1†], Sharmilee Vetrivel[1], Sonja Kunz[1], Frederick Vogel[1], Lucas Bouys[2], Jérôme Bertherat[2], Matthias Kroiss[1,3], Sinan Deniz[4], Andrea Osswald[1], Thomas Knösel[5], Martin Bidlingmaier[1], Silviu Sbiera[3], Martin Reincke[1] and Anna Riester[1*]

[1]Medizinische Klinik und Poliklinik IV, LMU Klinikum, Ludwig-Maximilians-University, Munich, Germany, [2]Institut Cochin, Université Paris-Cité, Paris, France, [3]Department of Internal Medicine I, Division of Endocrinology and Diabetes, University Hospital, University of Würzburg, Würzburg, Germany, [4]Klinik und Poliklinik für Radiologie, LMU Klinikum, Ludwig-Maximilians-University, Munich, Germany, [5]Pathologisches Institut, Ludwig-Maximilians-University, Munich, Germany

Introduction: Adrenal vein sampling (AVS) is not a routine procedure in patients with primary bilateral macronodular adrenocortical hyperplasia (PBMAH), but has been used to determine lateralization of cortisol secretion in order to guide decision of unilateral adrenalectomy. Our aim was to characterize the steroid fingerprints in AVS samples of patients with PBMAH and hypercortisolism and to identify a reference hormone for AVS interpretation.

Method: Retrospectively, we included 17 patients with PBMAH from the German Cushing's registry who underwent AVS. 15 steroids were quantified in AVS and peripheral blood samples using LC-MS/MS. We calculated lateralization indices and conversion ratios indicative of steroidogenic enzyme activity to elucidate differences between individual adrenal steroidomes and in steroidogenic pathways.

Results: Adrenal volume was negatively correlated with peripheral cortisone ($r=0.62$, $p<0.05$). 24-hour urinary free cortisol correlated positively with peripheral androgens (rDHEA=0.57, rDHEAS=0.82, rA=0.73, rT=0.54, $p<0.05$). DHEA was found to be a powerful reference hormone with high selectivity index, which did not correlate with serume cortisol and has a short half-life. All investigated steroids showed lateralization in single patients indicating the heterogenous steroid secretion pattern in patients with PBMAH. The ratios of corticosterone/aldosterone (catalyzed by CYP11B2), androstenedione/dehydroepiandrosterone (catalyzed by HSD3B2) and cortisone/cortisol

(catalyzed by HSD11B2) in adrenal vein samples were higher in smaller adrenals (p<0.05). *ARMC5* mutation carriers (n=6) showed lower androstenedione/17-hydroxyprogesterone and higher testosterone/androstenedione (p<0.05) ratios in peripheral blood, in line with lower peripheral androstenedione concentrations (p<0.05).

Conclusion: Steroid profiling by LC-MS/MS led us to select DHEA as a candidate reference hormone for cortisol secretion. Lateralization and different steroid ratios showed that each steroid and all three steroidogenic pathways may be affected in PBMAH patients. In patients with germline *ARMC5* mutations, the androgen pathway was particularly dysregulated.

KEYWORDS

cortisol, AVS, steroidome, LC-MS/MS, adenoma, DHEA, reference hormone

Introduction

Primary bilateral macronodular adrenocortical hyperplasia (PBMAH) is a benign neoplastic disorder characterized by multiple nodules ≥ 10mm in diameter on both adrenals. The clinical presentation is variable, ranging from asymptomatic to overt symptoms of Cushing's Syndrome (CS), and less commonly mineralocorticoid and/or androgens excess (1–3). This high heterogeneity and lack of specific symptoms renders PBMAH difficult to identify, and criteria for medical treatment or adrenalectomy still remain to be established. Given the complex pathophysiology of PBMAH, analyses of individual adrenal steroidome and comparison of interadrenal differences in steroidogenesis in patients with PBMAH may be of value to better characterize biochemical features and the steroid pathways involved. However, to the best of our knowledge, comprehensive data on steroid fingerprinting of the effluent of adrenal veins, and correlation between steroid patterns and clinical parameters have not yet been published.

Adrenal vein sampling (AVS) is the gold standard used to distinguish unilateral from bilateral forms of primary aldosteronism (PA). Patients with unilateral PA are usually referred to surgery. In selected patients with PBMAH, unilateral adrenalectomy can be a therapeutic approach despite bilateral disease (4–7). This could have the advantage over bilateral adrenalectomy of decreasing the risk for life-threatening adrenal crises and obviate the lifelong adrenocortical hormone replacement (8, 9). Previous studies addressed the application of AVS in PBMAH with CS to guide unilateral adrenalectomy (10–12). However, the variations of AVS protocols in use have been a limiting factor so far, and no consensus on a reference hormone has been achieved, which is required for diagnostic selectivity and to account for sample dilution. Therefore, a reliable reference hormone is necessary for improved interpretation of AVS results. Liquid chromatography-mass spectrometry (LC-MS/MS) for multiple steroids measurements in AVS samples enables a comprehensive appraisal of adrenal steroid output. Calculation of product/precursor ratios provides insights into adrenal steroidogenesis through analysis of the activity of different steroidogenic enzymes and thus allows investigations into alterations of steroidogenic pathways in the adrenal hyperplasia (13).

We hypothesized - based on variability of histopathologic phenotypes - that steroid secretion in PBMAH might be heterogeneous, with differences in steroid fingerprints between individual patients and even between the adrenal glands of the same patient.

To confirm our hypotheses, we followed these steps (1): correlation of steroid profiles with clinical parameters (2); identification of a reference hormone for AVS interpretation in patients with PBMAH using LC-MS/MS; (3) investigation of alterations in inter-adrenal steroidome using lateralization index (LI) and steroidogenic pathways using conversion analysis (product/precursor) in AVS samples.

Methods

Subjects

For this retrospective analysis, we included 17 patients with PBMAH from the German Cushing's registry who underwent AVS between 2006 to 2021 (15 treated at the LMU Klinikum, Ludwig Maximilians University Munich, Germany and 2 at the University Hospital of Würzburg, Julius Maximilians University Würzburg, Germany). These patients had documented ACTH-

independent Cushing's syndrome and bilateral adrenal masses typical for PBMAH. AVS was performed to identify a hormonally dominant side of cortisol production to guide unilateral adrenalectomy. Most of these patients (patients 1 to 12, patient 17 and patient 18) were already part of our study on the clinical role of AVS in PBMAH (14). As described also in that publication, patients underwent biochemical screening for Cushing's syndrome by the three recommended screening tests: 1-mg dexamethasone suppression test (LDDST), late-night salivary cortisol (LNSLC) and 24h urinary free cortisol (UFC), all performed using immunoassay. Germline *ARMC5* (armadillo repeat containing 5) sequencing was performed in 15 patients. Inactivating mutations of *ARMC5*, a putative tumor-suppressor gene, are associated with a more severe hypercortisolism, bigger adrenals with a higher number of nodules (15).The assays for the screening tests, baseline ACTH and *ARMC5* status were described in the online Supplementary Material (14).

The study was approved by the LMU ethics committee (Project number: 152-10) and performed in accordance with the principles of the declaration of Helsinki. All participants gave written informed consent.

Adrenal vein sampling

The decision to perform AVS for patients with bilateral adrenal masses was made independently by the treating endocrinologist before 2012 or by a multidisciplinary endocrine board since 2012. Our group described in detail the exact procedure previously (14). AVS was conducted without ACTH stimulation and peripheral blood samples were collected simultaneously with each of the selective blood samples. Samples were stored at -80°C until analysis. As no guideline is available for AVS performed in PBMAH patients, we interpreted the results in analogy to the Endocrine Society Practice Guideline on primary aldosteronism (PA) (16). Successful catheterization was confirmed in an exploratory analysis by a gradient of steroid concentrations between adrenal vein to peripheral vein (AV/PV, also called selectivity index, SI) greater than 2 (16–18). To analyze lateralization of hormone production we calculated a lateralization index, which is defined by the ratio of the high side to the low side of the corrected steroid of interestlevels (17). Following this definition, LI in our study is defined as:

$$LI = \frac{\left(\frac{steroid}{ipsilateral\ \ reference\ \ hormone}\right) high\ \ side}{\left(\frac{steroid}{ipsilateral\ \ refrence\ \ hormone}\right) low\ \ side}$$

This formula can be used for any steroid of interest, as long as the reference steroid in the denominator position is not affected by the rate of secretion of the steroid in the numerator position. In our PBMAH patient cortisol was used as steroid of interest. Recommendation for unilateral or bilateral adrenalectomy was not based on the results of LC-MS/MS presented in this study. The decision of the interdisciplinary tumour board was guided instead by the severity of CS (clinically and biochemically), the results of radiologic studies, plus AVS results measured with immunoassay as described in our previous study (14).

Steroids analysis by LC-MS/MS

A panel of 15 steroids was quantified in archival AVS and peripheral EDTA-plasma samples using the commercially available MassChrom® Steroid LC-MS/MS kit (Chromsystems, Gräfelfing, Germany) and a 1290 Infinity II ultra-high performance liquid chromatography instrument (Agilent Technologies, Santa Clara, USA) connected to a QTRAP6500+ triple quadrupole mass spectrometer (ABSciex, Framingham, USA). Sample preparation was performed *via* offline solid phase extraction of 500µL sample according to the instructions of the manufacturer. Before extraction, the respective stable isotope labeled steroids were added as internal standards. Twenty microliters were injected to the LC-MS/MS system, ionized with electrospray ionization (ESI) and analyzed in multiple reaction monitoring mode. Aldosterone and DHEA-S were measured in negative ESI mode. All other steroids were measured in positive ESI mode. A six-point calibration with $1/x^2$ weighting was used for quantification of the steroids by the SciexOS software (Version 1.6.1, ABSciex, Framingham, USA). Sample containing steroid concentrations above the highest calibration were re-assayed after dilution in 0.9% saline, and results multiplied by the dilution factor. Quality control samples provided by the manufacturer were measured within each analytical run to continuously monitor performance of the LC-MS/MS measurements. We regularly participated in the national external quality assessment scheme for steroid hormones (Reference Institute for Bioanalytics, RfB, Bonn, Germany) and passed for all included steroids. The kit includes the following steroids: progesterone (Prog), 17-hydroxyprogesterone (17OHP), cortisol (F), 11-deoxycortisol (11dF), 21-deoxycortisol(21dF), cortisone (E), corticosterone (Cort), 11-deoxycorticosterone (DOC), aldosterone (Aldo), dehydroepiandrosterone (DHEA), dehydroepiandrosterone sulfate (DHEAS), dihydrotestosterone (DHT), testosterone (T), androstenedione (A) and estradiol (E2). The low limit of quantification (LLOQ) and up limit of quantification (ULOQ) for each steroid are summarized in Supplemental Data (Table S1). To study the alteration of adrenal steroidogenesis pathways, conversion ratios based on adrenal size and radiological asymmetry were calculated with adrenal vein metabolite/its precursor, and conversion ratios based on *ARMC5* status calculated with peripheral metabolite/its precursor, accordingly (19, 20).

Adrenal size

The adrenal volume was measured in three dimensions and calculated by height x width x depth. One patient provided only axial planes. Therefore, in this patient adrenal size was assessed by the maximum diameter in cm. The definition of adrenal asymmetry was a difference > 30% between adrenal volumes or, if not available, the maximum diameter.

Statistics

We analyzed correlation using a two-tailed Spearman correlation coefficient. Mann Whitney test was used to assess the differences of peripheral steroids and clinical parameters based on *ARMC5* status, and conversion ratios based on adrenal size and *ARMC5* status. The differences of conversion ratios between groups based on radiological asymmetry were evaluated by Wilcoxon test. Steroid concentrations below LLOQ and without peak were calculated as 0.5*LLOQ. A value of $p<0.05$ was considered statistically significant. We used Microsoft Excel 365 for data calculation and GraphPad Prism 8 for the statistical analyses.

Results

Correlation of clinical parameters and peripheral steroidome

16/17 patients were females, 15 patients were older than 55 years (see Supplementary Table S1). The biochemical evaluation demonstrated the typical features of adrenal hypercortisolism. *ARMC5* status was evaluated in 15 patients. 6 patients showed mutations in the *ARMC5* gene, while 9 patients had the wildtype.

Correlations between adrenal volume, baseline ACTH, the three diagnostic tests for CS and the peripheral steroids were analyzed in 15 postmenopausal patients (Figure 1); the male (patient 4) and one premenopausal female (patient 6) were excluded from this analysis. The concentrations of aldosterone (7 patients), 21-deoxycortisol (4 patients), estradiol (8 patients), DHT (8 patients), 11-deoxycorticosterone (2 patients) and progesterone (8 patients) were below LLOQ or detection in >10 % of the samples (Supplementary Table S2). Therefore, we excluded these steroids from further analysis. Adrenal volume showed negative correlations with plasma cortisone concentrations (r=-0.62, $p<0.05$). UFC did not correlate with

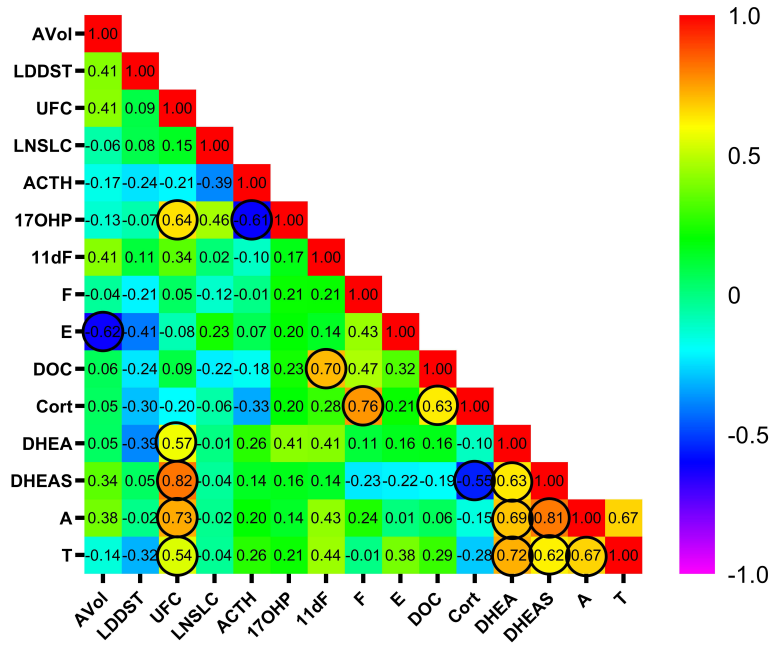

FIGURE 1
Correlation between adrenal volume, the three diagnostic tests of hypercortisolism, and peripheral steroid concentrations as measured by LC-LC/MS. The values in cells are the coefficient r, the circles indicate statistical significance ($p<0.05$). Male and premenopausal female patients were excluded. AVol: adrenal volume; UFC, 24h urinary free cortisol; LDDST, low dose dexamethasone suppression test; LNSLC, late-night salivary cortisol; late-night salivary cortisol; ACTH, adrenocorticotropic hormone. 17OHP, 17-hydroxyprogesterone; 11dF, 11-deoxycortisol; F, cortisol; E, cortisone; DOC, 11-deoxycorticosterone; Cort, corticosterone; DHEA, dehydroepiandrosterone; DHEAS, dehydroepiandrosterone sulfate; A, androstenedione; T, testosterone.

plasma cortisol but did correlate positively with 17-hydroxyprogesterone (r=0.64, $p<0.05$), DHEA (r=0.57, $p<0.05$), DHEAS (r=0.82, $p<0.001$), androstenedione (r=0.73, $p<0.01$) and testosterone (r=0.54, $p<0.05$) in peripheral plasma samples. The association of steroid concentrations with germline *ARMC5* mutation status is presented in Table 1. Patients with germline *ARMC5* mutations had lower plasma androstenedione concentrations than wild-type patients.

Identification of a reference hormone

An ideal reference hormone to be used during AVS for correction of dilution effects in adrenal veins should have a rather short half-life and should be secreted independently of the underlying adrenal pathology. Therefore, the selection of the best reference hormone was based on three steps in our study (1): The candidate hormone should show a concentration gradient between adrenal and peripheral vein (selectivity index) ≥ 2 (2); The candidate hormone should not correlate with cortisol, which would indicate a co-secretion by the cortisol-producing tumor (3); The candidate hormone has a short half-time.

In order to evaluate specific steroids as reference hormones, a ratio of adrenal vein/peripheral vein called selectivity index (SI) was calculated for each steroid. SI > 2 was selected as the traditional cutoff to assess the success of AVS cannulation (16–18), in analogy to AVS for primary aldosteronism (Table 2). In the right AVS of patient 17, only aldosterone showed an SI > 2. We therefore concluded a failure of cannulation of the right adrenal vein of patient 17, and this sample was excluded from further analysis. 17-hydroxyprogesterone, 11-deoxycortisol, corticosterone, DHEA, androstenedione and 11-deoxycorticosterone indicated successful catheterization in >90% of the cases. Thus, correlation analyses between these six steroids and cortisol were performed (Figure 2). Corticosterone (r=0.71, $p<0.0001$), 11-deoxycortisol (r=0.57, $p<0.0005$), 17-hydroxyprogesterone (r=0.59, $p<0.001$) and 11-deoxycorticosterone (r=0.57, $p<0.001$) showed significant correlations with cortisol, indicating a co-secretion with the cortisol-producing tumor. Androstenedione (r=0.27, $p=0.13$) and DHEA (r=0.20, $p=0.27$) had no correlation with cortisol. Compared with androstenedione ($T1/2_A$ is about 30 min) (21), DHEA ($T1/2_{DHEA}$ is 15 to 30 min) (22, 23) has a shorter half-life. As a result, we concluded that DHEA could be a viable reference hormone, meeting all the criteria we defined previously.

Comparison of the steroidome between both adrenals of individual patient and steroidogenic pathways analysis

We calculated the lateralization index to investigate differences in steroid fingerprints between the adrenals of each patient. Figure 3 shows the lateralization indices of the nine steroids, which could be measured adequately, using DHEA as reference hormone. The results indicate that the secretion of all measured steroids could be affected in PBMAH: every measured steroid showed a lateralization (LI above 2) in at least one patient. On the other hand, not every patient with PBMAH showed a lateralization of steroid production: 3 patients (patient 6, 14 and 15) had no lateralization at all when lateralization was defined as LI above 2. If defining LI above 4 as a relevant lateralization in steroid production, only 5 patients fulfilled this criterion by at least one steroid. However, out of these, in two patients (patient 7 and patient 10) the dominant side was inconsistent: In patient 7, the secretion of cortisol was mainly left (LI=82.7), while 11-deoxycortisol (LI=2.0), corticosterone (LI=2.5) and 11-deoxycorticosterone (LI=2.7) were mainly produced by the right adrenal. In patient 10, DHEAS (LI=2.4) production lateralized to the left side, whereas 11-deoxycortisol (LI=2.4), corticosterone (LI=4.8), and 11-deoxycorticosterone (LI=11.5) lateralized to the right side.

TABLE 1 Comparison of peripheral steroids (ng/ml) based on *ARMC5* status.

Peripheral steroids	Wild-type *ARMC5* (n=9)	Mutant *ARMC5* (n=6)	*p* value
F	117.2 [92.8, 153.5]	119.6 [83.0, 163.8]	0.77
E	16.1 [14.1, 17.7]	13.9 [12.3, 18.4]	0.55
Cort	1.8 [0.8, 3.7]	2.5 [1.6, 17.8]	0.18
11dF	0.97 [0.45, 1.19]	0.48 [0.35, 1.04]	0.53
DHEAS	314.0 [221.0, 795.4]	119.0 [45.4, 284.1]	0.06
T	0.13 [0.07, 0.20]	0.06 [0.04, 0.15]	0.18
A	0.77 [0.32, 1.50]	0.27 [0.13, 0.51]	<0.05
DHEA	0.85 [0.33, 1.66]	0.48 [0.13, 0.67]	0.13
17OHP	0.19 [0.15, 0.28]	0.31 [0.12, 0.47]	0.53
DOC	0.07 [0.04, 0.12]	0.04 [0.04, 0.31]	0.75

Data are presented with median [Q1, Q3]. F, cortisol; 11dF, 11-deoxycortisol; 17OHP, 17-hydroxyprogesterone; E, cortisone; DOC, 11-deoxycorticosterone; Cort, corticosterone; DHEA, dehydroepiandrosterone; DHEAS, dehydroepiandrosterone sulfate; A, androstenedione; T, testosterone.

TABLE 2 Concentration gradient (selectivity index, SI) of each steroid from adrenal vein (AV) to peripheral vein (PV) in 17 patients.

Steroids	Successful catheterization*	AV/PV	1	2	3	4	5	6	7	8	9	10	11	12	13	14	15	16	17
Prog	13/17	LAV/PV	6.67	376.74	7.53	18.58	10.06	12.46	3.90	1.56	1047.62	6.47	18.26	1.00	19.96	1.00	23.01	1.60	29.36
	12/17	RAV/PV	4.76	20.23	6.59	22.08	48.39	17.67	19.74	1.62	1841.27	999.75	1.00	1.00	10.90	1.00	30.20	1.40	1.00
17OHP	17/17	LAV/PV	14.22	166.00	11.60	5.12	12.30	162.75	9.83	18.86	46.25	14.34	17.54	8.58	14.14	21.18	25.27	18.26	80.20
	16/17	RAV/PV	9.74	19.13	12.61	8.68	34.48	187.45	38.46	5.04	38.13	162.19	5.25	15.88	9.86	8.80	25.97	19.01	1.90
21dF	13/17	LAV/PV	14.91	0.64	8.13	0.09	2.60	90.11	2.05	47.01	3.47	4.11	19.27	1.00	6.66	8.49	3.70	1.89	9.58
	14/17	RAV/PV	12.50	2.69	6.07	4.27	11.90	123.63	10.73	15.58	4.95	34.88	5.98	1.00	4.20	3.09	1.00	5.00	0.81
11dF	17/17	LAV/PV	13.56	40.62	31.48	12.69	4.58	112.75	13.39	58.08	54.77	11.65	16.07	10.20	9.41	24.27	22.19	13.26	36.08
	16/17	RAV/PV	17.05	7.42	27.34	9.89	16.76	153.92	57.79	12.45	16.38	79.81	5.69	16.50	7.22	10.14	21.48	10.59	1.44
F	16/17	LAV/PV	4.05	5.29	3.05	3.81	1.14	27.52	3.75	15.38	9.48	2.49	3.73	2.17	2.35	3.13	3.99	3.87	9.78
	12/17	RAV/PV	4.31	2.36	1.88	2.24	5.13	33.21	0.10	3.88	1.81	9.04	1.63	2.65	2.07	2.00	3.50	2.51	0.96
E	10/17	LAV/PV	0.83	1.67	3.65	2.80	1.15	6.82	1.34	5.23	2.55	1.89	2.41	0.89	2.04	1.44	2.53	2.30	5.27
	7/17	RAV/PV	0.97	1.39	3.20	3.26	1.72	6.89	3.11	2.14	0.96	3.87	1.45	0.74	1.94	1.17	2.01	1.55	0.93
DOC	16/17	LAV/PV	10.76	75.38	84.50	11.97	7.32	107.28	3.80	41.74	23.38	10.75	17.10	8.96	9.06	10.65	15.45	1.43	33.14
	15/17	RAV/PV	12.33	6.17	68.50	9.10	15.11	161.57	22.50	12.91	29.24	358.06	5.77	10.68	5.30	4.54	19.13	1.29	1.00
Cort	17/17	LAV/PV	16.34	20.43	8.55	10.78	2.49	101.97	10.88	56.65	48.02	7.45	13.45	9.04	5.21	16.17	11.56	12.97	72.42
	16/17	RAV/PV	13.99	2.97	6.37	6.00	12.00	141.45	57.68	16.95	16.55	103.61	3.44	10.49	4.35	6.79	10.52	7.67	1.39
Aldo	14/17	LAV/PV	8.60	29.55	0.14	0.16	524.14	38.98	–	36.97	–	0.88	27.91	11.83	6.88	5.82	6.01	6.94	81.42
	15/17	RAV/PV	7.35	5.45	3.15	0.16	0.38	46.34	–	16.68	–	7.99	5.41	14.52	17.05	5.74	6.01	32.20	6.78
DHEA	17/17	LAV/PV	7.09	8.66	7.77	2.13	2.62	63.38	10.89	4.59	11.39	6.09	17.09	4.12	2.36	10.50	9.99	11.07	19.38
	15/17	RAV/PV	3.74	9.31	16.84	1.69	4.34	63.38	23.50	3.64	29.84	17.66	5.45	3.89	7.46	5.20	8.42	19.62	1.31
DHEAS	0/17	LAV/PV	0.82	1.05	1.19	1.16	1.02	1.95	1.20	0.97	1.03	1.08	1.48	1.25	1.17	1.23	1.30	1.00	1.42
	0/17	RAV/PV	1.10	1.09	1.38	1.11	1.22	1.89	1.32	1.26	1.00	1.33	1.13	1.00	1.11	1.07	1.14	1.00	0.87
A	17/17	LAV/PV	22.11	9.28	5.91	6.76	11.83	159.02	15.17	29.16	25.80	15.26	20.57	7.27	10.53	18.81	25.82	21.80	37.20
	16/17	RAV/PV	17.77	5.83	6.38	10.51	15.41	182.17	52.51	11.17	20.22	46.89	6.01	14.15	14.39	7.32	17.53	26.63	1.24
T	8/17	LAV/PV	1.72	2.46	2.04	0.77	1.62	4.67	1.30	2.62	1.53	1.41	1.84	2.07	0.80	2.14	1.94	2.46	2.62
	5/17	RAV/PV	1.44	1.83	2.82	0.72	3.38	8.22	2.26	1.46	1.30	3.91	1.08	1.53	0.96	1.00	1.95	1.72	1.48
DHT	1/17	LAV/PV	0.74	0.64	2.21	1.19	1.00	1.21	4.86	0.15	0.95	1.00	1.00	1.00	1.00	1.00	1.00	1.00	1.00
	0/17	RAV/PV	1.01	1.12	1.30	1.12	1.00	1.10	1.04	0.15	1.37	1.00	1.00	1.00	1.00	1.00	1.00	1.00	1.00
E2	2/17	LAV/PV	1.35	0.16	1.29	0.94	0.06	0.58	1.61	0.75	2.63	1.00	1.00	1.00	1.00	1.95	7.83	1.00	1.00
	3/17	RAV/PV	1.69	0.08	1.08	0.87	0.30	0.18	4.76	0.94	9.57	1.00	1.00	13.79	1.00	0.30	0.35	1.00	1.00

*Number of samples with successful catheterization (selectivity index>2); AV, adrenal vein; PV, peripheral vein; LAV, left adrenal vein; RAV, right adrenal vein; Prog, progesterone; 17OHP, 17-hydroxyprogesterone; 21dF, 21-deoxycprtisol; 11dF, 11-deoxycortisol; F, cortisol; E, cortisone; DOC, 11-deoxycorticosterone; Cort, corticosterone; Aldo, aldosterone; DHEA, dehydroepiandrosterone; DHEAS, dehydroepiandrosterone sulfate; A, androstenedione; T, testosterone; DHT, dihydrotestosterone; E2, estradiol. The six steroids with the highest SI values are marked in bold.

10.3389/fendo.2022.1079508

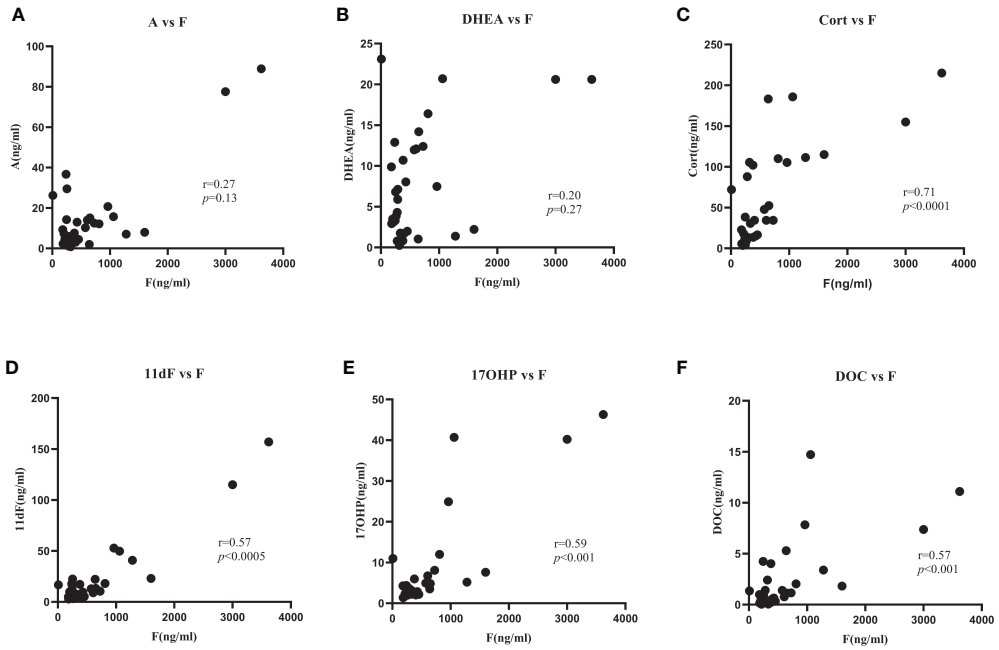

FIGURE 2
Correlation of cortisol vs six steroids with high gradient of concentration from adrenal vein to peripheral vein: androstendione (**A**), DHEA (**B**), corticosterone (**C**), 11-deoxycortisol (**D**), 17-hydroxyprogesteron (**E**), 11-deoxycorticosterone (**F**). F, cortisol; A, androstenedione; DHEA, dehydroepiandrosterone; Cort, corticosterone; 11dF, 11-deoxycortisol; 17OHP, 17-hydroxyprogesterone; DOC, 11-deoxycorticosterone.

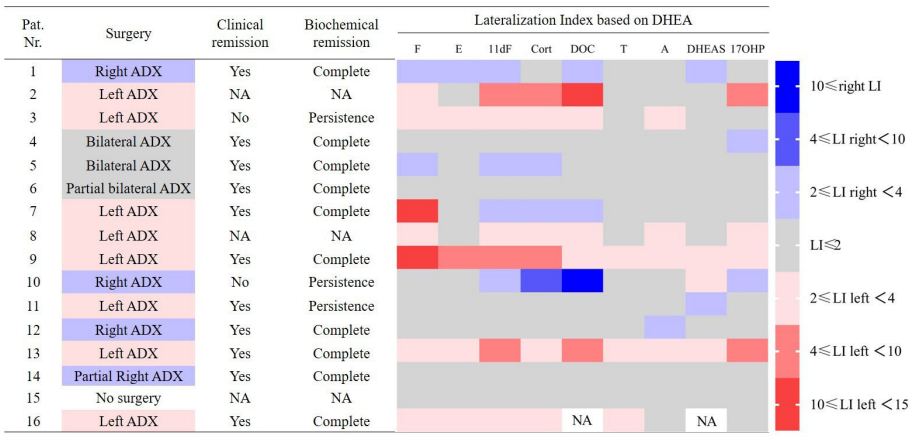

FIGURE 3
Comparison between lateralization index (LI), surgery and outcome in patients with PBMAH. Steroids below LLOQ or dectection were excluded in the figure. Pat. No. 17 was excluded because of failed adrenal vein cannulation. NA, not available; ADX, adrenalectomy; F, cortisol; E, cortisone; 11dF, 11-deoxycortisol; Cort, corticosterone; DOC, 11-deoxycorticosterone; T, testosterone; A, androstenedione; 17OHP, 17-hydroxyprogesterone.

Additionally, conversion ratios (steroid/precursor) based on adrenal size and on *ARMC5* status values were calculated to identify possible differences in affected steroid pathways. All conversion ratios among the pathway of adrenal steroidogenesis were analyzed (Supplementary data, Figure S1). For conversion ratios involving sex hormones, only the values of the postmenopausal women were included. 14 adrenals had a volume ≥ 30 ml, 18 adrenals had a volume< 30 ml, 12 patients showed radiological asymmetry. Aldosterone/corticosterone and cortisone/cortisol were higher in the group of adrenals with volumes< 30 ml (Figures 4A, B) and radiologically small adrenals (Figures 4D, E). Androstenedione/dehydroepiandrosterone was

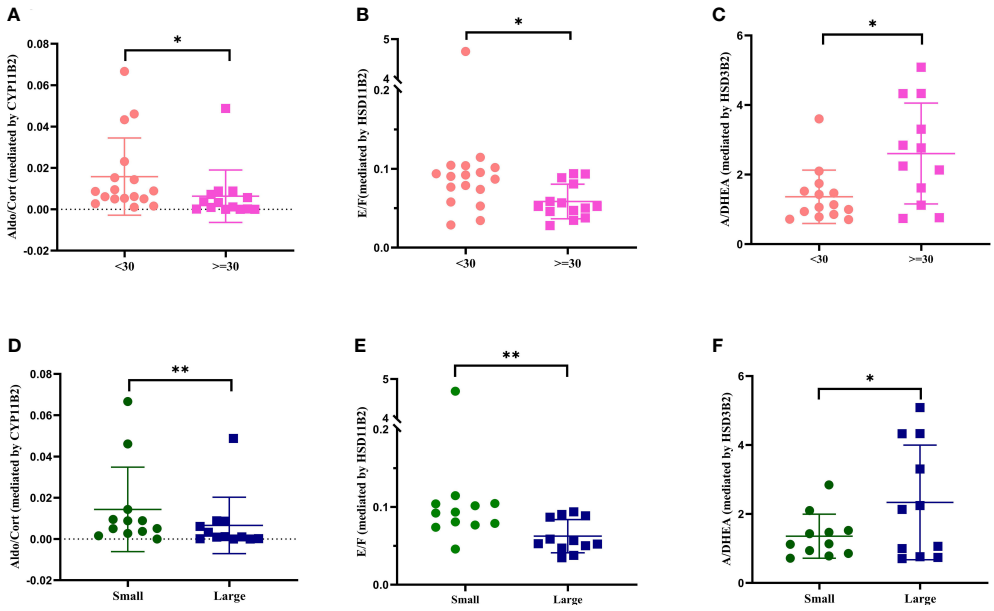

FIGURE 4
Conversion ratio analysis of adrenal vein values based on adrenal volume and radiological asymmetry. Only significant results are shown. Comparisons of Aldo/Cort between groups based on adrenal volume **(A)** and radiological asymmetry **(D)**. Comparison of E/F between groups based on adrenal volume **(B)** and radiological asymmetry **(E)**. Comparison of A/DHEA between groups based on adrenal volume **(C)** and radiological asymmetry **(F)**. Aldo, aldosterone; Cort, corticosterone; A, androstenedione; DHEA, dehydroepiandrosterone; E, cortisone; F, cortisol. *p<0.05, **p<0.01

higher in the group of adrenals with volumes ≥ 30 ml (Figure 4C) and radiologically large adrenals (Figure 4F).

ARMC5 mutation carriers showed lower conversion ratios of androstenedione/17-hydroxyprogesterone and higher testosterone/androstenedione than *ARMC5*-wildtype patients (p<0.05, Figures 5A, B).

Discussion

We performed an exploratory study in patients with PBMAH using LC-MS/MS measurement in peripheral blood and adrenal vein samples to investigate correlations among

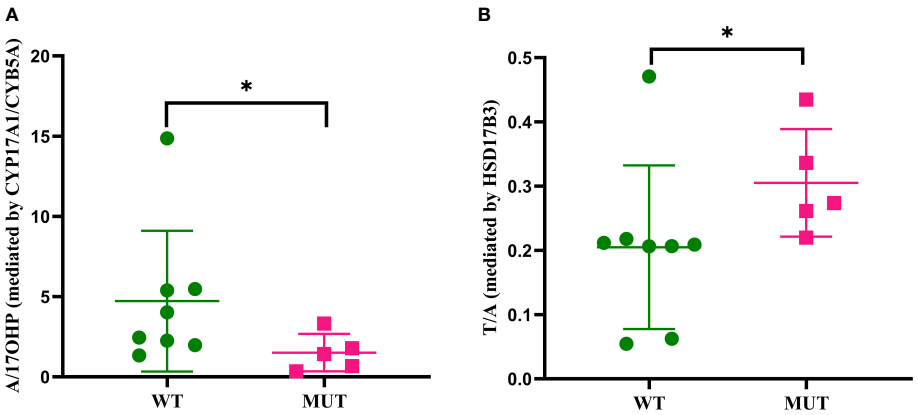

FIGURE 5
Conversion ratio analysis of peripheral steroids based on *ARMC5* status. Only significant conversion ratios are displayed. **(A)** Comparison of A/17OHP between wild-type *ARMC5* patients and mutant *ARMC5* patients. **(B)** Comparison of T/A between wild-type *ARMC5* patients and mutant *ARMC5* patients. A, androstenedione; 17OHP, 17-hydroxyprogesterone; T, testosterone. WT, wild-type *ARMC5* patients; MUT, mutant *ARMC5* patients. *p<0.05

clinical parameters and peripheral steroid concentrations, to identify a potential reference hormone, and to compare the steroidome between both adrenals of individual patients and analyze affected steroidogenic pathways.

Correlations among clinical parameters and peripheral steroids in PBMAH

No correlation between adrenal volume and peripheral cortisol level was found. Even though UFC better reflects the 24-hour time-integrated cortisol secretion compared to random serum cortisol, still no correlation between adrenal volume and UFC was observed indicating variable steroidogenic efficiency between PBMAH cases. This is in line with the findings of Wurth et al. in a cohort of 44 patients with PBMAH, in which adrenal volume was calculated based on computed tomography scans (24). 17-hydroxyprogesterone, DHEA, DHEAS, androstenedione and testosterone showed a positive correlation with UFC. In contrary, no correlation or even negative correlation (DHEAS) with serum cortisol was seen. Also, serum cortisol was not correlated with UFC. A possible explanation could be, that cortisol secretion levels vary throughout the day and UFC reflects the daily cortisol output. As a genetic disease, PBMAH is reported to be associated with germline mutation in *ARMC5* gene. Mutation carriers are found to have an more severe Cushing phenotype than patients with wild-type *ARMC5* (25). In the cohort described by Espiard et al., germline *ARMC5*-mutation is associated with lower ACTH, and higher UFC and higher cortisol after dexamethasone suppression test compared to wild-type PBMAH patients (26). This was not observed in our cohort (Supplementary Table S3), probably due to the relatively small cohort size.

Selection of reference hormone for AVS interpretation

At the moment cortisol is commonly used as a reference hormone to correct for dilution effects during AVS for PA. According to the experience of AVS in PA, a successful adrenal vein cannulation is traditionally defined by a SI >2 when AVS is performed without ACTH stimulation (16–18). In PA, the selection of cortisol as reference hormone is based on the assumption that cortisol is entirely secreted by the normal zona fasciculata and not overproduced by the aldosterone-producing lesion, which however has limitations in case of pronounced aldosterone and cortisol co-secretion (17, 27). Metabolites with long half-life are slowly cleared from circulation, and have decreasing adrenal to peripheral gradients, thus, this will impair the interpretation of AVS results. As a result, we selected the reference hormone based on a three-step approach accounting for these factors. According to our findings, we identified DHEA as the most promising reference hormone in patients with PBMAH.

Alterations in interadrenal steroidome and steroidogenic pathways in PBMAH

AVS was firstly introduced to guide surgical decision making in ACTH-independent Cushing's syndrome by colleagues from the Mayo Clinic (5). In the following years, AVS was performed occasionally in adrenal CS by several centers. Due to the limited sample size and outcome data, our study was not performed to evaluate the optimal LI cut off, rather, the study intended to evaluate the LI of all steroids to evaluate adrenal laterality in patients with PBMAH. Our results nicely illustrate that cortisol lateralization based on AVS is valuable in most patients with PBMAH. Interestingly, corticosterone and 11-deoxycortisol showed also pronounced lateralization effects. So taken together one can say that cortisol is one of the most dysregulated hormones in PBMAH pathology, but all other steroids could be affected, too.

Lower conversion ratios of cortisone/cortisol (catalyzed by HSD11B2) and aldosterone/corticosterone (catalyzed by aldosterone synthase, CYP11B2) were observed in larger adrenals both based on adrenal volumes and radiological asymmetry. HSD11B2 is not expressed in normal adrenals (28), but expressed in adrenal adenomas (28, 29). Therefore, this result is unexpected. However, up to our knowledge the expression status of HSD11B2 in adrenals of PBMAH patients have not been investigated yet.CYP11B2 was undetectable by immunohistochemistry in the tumor of adrenal CS in a study by Nishimoto et al. (30). Similar immunohistochemical analyses have not yet been done in PBMAH, but it could be speculated that lower synthesis of aldosterone in adrenals affected by PBMAH is possibly caused by CYP11B2 repression. Higher conversion ratio of androstenedione/dehydroepiandrosterone (catalyzed by CYP17A1 or CYB5A) in larger adrenals indicates possible dysregulation in androgenic steroids in PBMAH. Taken together, even though PBMAH is primarily associated with cortisol excess, there are co-secretion of steroids of the mineralocorticoid and androgen pathways. In addition, we observed patients with germline *ARMC5* variants have lower androstenedione/17-hydroxyprogesterone and higher testosterone/androstenedione conversion ratios. In line with these findings, peripheral androstenedione concentrations in germline *ARMC5* mutation carriers were decreased, indicating that the androgen steroid pathway is dysregulated in PBMAH patients carrying a germline *ARMC5* mutation, possibly through decreased ACTH. In line with this notion, lower peripheral DHEAS levels measured by LC-MS/MS in germline *ARMC5* mutation carriers were described in another cohort (31). We saw the same tendency in our cohort, but this finding failed to be significant (119 vs 314 ng/ml, p=0.06).

Conclusion

In summary, our study showed some distinct correlations between the adrenal volume, baseline ACTH, the three diagnostic tests for hypercortisolism (LDDST, LNSLC and UFC) and circulating steroids of PBMAH. If AVS is performed in patients with PBMAH, DHEA could be used as reference hormone. Comparative analyses of steroids by LC-MS/MS identified different steroid fingerprints among PBMAH patients and emphasize the heterogeneity of this disease. Germline mutations in the *ARMC5* gene were found to affect the androgen pathway in particular.

Limitations

There are some limitations of our study. (1) The synthesis of sex hormones is affected by gender and age. Due to the limited sample size and biased sex constitution, we were unable to study the correlations between clinical parameters and peripheral steroids based on gender and age. (2) Some patients were lost to follow up after treatment. Therefore, the recurrence of hypercortisolism was not evaluated. (3) AVS is invasive so that having the AVS data from healthy people as control is impossible. (4) Our data is descriptive and further research are needed to confirm our results.

Data availability statement

The original contributions presented in the study are included in the article/Supplementary Material. Further inquiries can be directed to the corresponding author.

Ethics statement

The studies involving human participants were reviewed and approved by LMU ethics committee. The patients/participants provided their written informed consent to participate in this study.

Author contributions

RZ and GR contributed equally to this work and share first authorship. RZ, GR, MR, and AR conceived and planned the experiments. GR, FV, MK, AO, and TK collected the data and provided samples. RZ, GR, SK, LB, JB, and SD performed the experiments. SV, JB, MK, MB, SS, MR and AR contributed to the interpretation of the results. RZ, GR and AR wrote the manuscript. All authors provided critical feedback. All authors contributed to the article and approved the submitted version.

Funding

This work was supported by a grant from the Deutsche Forschungsgemeinschaft (DFG) (within the CRC/Transregio 205/1 "The Adrenal: Central Relay in Health and Disease") to MK, MB, SS, MR and AR. This work is part of the German Cushing's Registry CUSTODES and has been supported by grants from the Else Kröner-Fresenius Stiftung to MR (2012_A103 and 2015_A228).

Acknowledgments

This study was only feasible with the support of the German Cushing Registry team, and clinical assistances in Munich and Würzburg for preparing the samples for LC-MS/MS analysis.

Conflict of interest

The authors declare that the research was conducted in the absence of any commercial or financial relationships that could be construed as a potential conflict of interest.

Publisher's note

Supplementary material

The Supplementary Material for this article can be found online at: https://www.frontiersin.org/articles/10.3389/fendo.2022.1079508/full#supplementary-material

References

1. Bouys L, Chiodini I, Arlt W, Reincke M, Bertherat J. Update on primary bilateral macronodular adrenal hyperplasia (Pbmah). *Endocrine* (2021) 71(3):595–603. doi: 10.1007/s12020-021-02645-w

2. De Venanzi A, Alencar GA, Bourdeau I, Fragoso MC, Lacroix A. Primary bilateral macronodular adrenal hyperplasia. *Curr Opin endocrinol diabetes Obes* (2014) 21(3):177–84. doi: 10.1097/MED.0000000000000061

3. Araujo-Castro M, Marazuela M. Cushing s syndrome due to bilateral adrenal cortical disease: Bilateral macronodular adrenal cortical disease and bilateral micronodular adrenal cortical disease. *Front Endocrinol* (2022) 13:913253. doi: 10.3389/fendo.2022.913253

4. Vassiliadi DA, Tsagarakis S. Diagnosis and management of primary bilateral macronodular adrenal hyperplasia. *Endocrine-related Cancer* (2019) 26(10):R567–R81. doi: 10.1530/ERC-19-0240

5. Young WFJr., du Plessis H, Thompson GB, Grant CS, Farley DR, Richards ML, et al. The clinical conundrum of corticotropin-independent autonomous cortisol secretion in patients with bilateral adrenal masses. *World J Surg* (2008) 32(5):856–62. doi: 10.1007/s00268-007-9332-8

6. Sheikh-Ahmad M, Dickstein G, Matter I, Shechner C, Bejar J, Reut M, et al. Unilateral adrenalectomy for primary bilateral macronodular adrenal hyperplasia: Analysis of 71 cases. *Exp Clin Endocrinol Diabetes Off journal German Soc Endocrinol [and] German Diabetes Assoc* (2020) 128(12):827–34. doi: 10.1055/a-0998-7884

7. Meloche-Dumas L, Mercier F, Lacroix A. Role of unilateral adrenalectomy in bilateral adrenal hyperplasias with cushing's syndrome. *Best Pract Res Clin Endocrinol Metab* (2021) 35(2):101486. doi: 10.1016/j.beem.2021.101486

8. Hahner S, Spinnler C, Fassnacht M, Burger-Stritt S, Lang K, Milovanovic D, et al. High incidence of adrenal crisis in educated patients with chronic adrenal insufficiency: A prospective study. *J Clin Endocrinol Metab* (2015) 100(2):407–16. doi: 10.1210/jc.2014-3191

9. Ritzel K, Beuschlein F, Mickisch A, Osswald A, Schneider HJ, Schopohl J, et al. Clinical review: Outcome of bilateral adrenalectomy in cushing's syndrome: A systematic review. *J Clin Endocrinol Metab* (2013) 98(10):3939–48. doi: 10.1210/jc.2013-1470

10. Acharya R, Dhir M, Bandi R, Yip L, Challinor S. Outcomes of adrenal venous sampling in patients with bilateral adrenal masses and acth-independent cushing's syndrome. *World J Surg* (2019) 43(2):527–33. doi: 10.1007/s00268-018-4788-2

11. Papakokkinou E, Jakobsson H, Sakinis A, Muth A, Wangberg B, Ehn O, et al. Adrenal venous sampling in patients with acth-independent hypercortisolism. *Endocrine* (2019) 66(2):338–48. doi: 10.1007/s12020-019-02038-0

12. Ueland GA, Methlie P, Jossang DE, Sagen JV, Viste K, Thordarson HB, et al. Adrenal venous sampling for assessment of autonomous cortisol secretion. *J Clin Endocrinol Metab* (2018) 103(12):4553–60. doi: 10.1210/jc.2018-01198

13. Genazzani AR, Pluchino N, Begliuomini S, Stomati M, Bernardi F, Pieri M, et al. Long-term low-dose oral administration of dehydroepiandrosterone modulates adrenal response to adrenocorticotropic hormone in early and late postmenopausal women. *Gynecol Endocrinol Off J Int Soc Gynecol Endocrinol* (2006) 22(11):627–35. doi: 10.1080/09513590601024681

14. Rubinstein G, Osswald A, Braun LT, Vogel F, Kroiss M, Pilz S, et al. The role of adrenal venous sampling (Avs) in primary bilateral macronodular adrenocortical hyperplasia (Pbmah): A study of 16 patients. *Endocrine* (2022) 76:434–45. doi: 10.1007/s12020-022-03020-z

15. Assie G, Libe R, Espiard S, Rizk-Rabin M, Guimier A, Luscap W, et al. Armc5 mutations in macronodular adrenal hyperplasia with cushing's syndrome. *New Engl J Med* (2013) 369(22):2105–14. doi: 10.1056/NEJMoa1304603

16. Nieman LK, Biller BM, Findling JW, Murad MH, Newell-Price J, Savage MO, et al. Treatment of cushing's syndrome: An endocrine society clinical practice guideline. *J Clin Endocrinol Metab* (2015) 100(8):2807–31. doi: 10.1210/jc.2015-1818

17. Rossi GP, Auchus RJ, Brown M, Lenders JW, Naruse M, Plouin PF, et al. An expert consensus statement on use of adrenal vein sampling for the subtyping of primary aldosteronism. *Hypertension* (2014) 63(1):151–60. doi: 10.1161/HYPERTENSIONAHA.113.02097

18. Chang CC, Lee BC, Liu KL, Chang YC, Wu VC, Huang KH. Non-stimulated adrenal venous sampling using dyna computed tomography in patients with primary aldosteronism. *Sci Rep* (2016) 6:37143. doi: 10.1038/srep37143

19. Faisal Ahmed S, Iqbal A, Hughes IA. The Testosterone:Androstenedione ratio in Male undermasculinization. *Clin Endocrinol* (2000) 53(6):697–702. doi: 10.1046/j.1365-2265.2000.01166.x

20. Kim SH, Moon JY, Sasano H, Choi MH, Park MJ. Body fat mass is associated with ratio of steroid metabolites reflecting 17,20-lyase activity in prepubertal girls. *J Clin Endocrinol Metab* (2016) 101(12):4653–60. doi: 10.1210/jc.2016-2515

21. Belisle S, Lehoux JG, Brault J. The metabolism of androstenedione in human pregnancy: The use of constant infusion of unlabeled steroid to assess its metabolic clearance rate, its production rate, and its conversion into androgens and estrogens. *Am J obstetrics gynecol* (1980) 136(8):1030–5. doi: 10.1016/0002-9378(80)90632-8

22. Dutheil F, de Saint Vincent S, Pereira B, Schmidt J, Moustafa F, Charkhabi M, et al. Dhea as a biomarker of stress: A systematic review and meta-analysis. *Front Psychiatry* (2021) 12:688367. doi: 10.3389/fpsyt.2021.688367

23. Baulieu EE. Dehydroepiandrosterone (Dhea): A fountain of youth? *J Clin Endocrinol Metab* (1996) 81(9):3147–51. doi: 10.1210/jcem.81.9.8784058

24. Wurth R, Tirosh A, Kamilaris CDC, Camacho J, Faucz FR, Maria AG, et al. Volumetric modeling of adrenal gland size in primary bilateral macronodular adrenocortical hyperplasia. *J Endocr Soc* (2021) 5(1):bvaa162. doi: 10.1210/jendso/bvaa162

25. Cavalcante IP, Berthon A, Fragoso MC, Reincke M, Stratakis CA, Ragazzon B, et al. Primary bilateral macronodular adrenal hyperplasia: Definitely a genetic disease. *Nat Rev Endocrinol* (2022) 18:699–711. doi: 10.1038/s41574-022-00718-y

26. Espiard S, Drougat L, Libe R, Assie G, Perlemoine K, Guignat L, et al. Armc5 mutations in a Large cohort of primary macronodular adrenal hyperplasia: Clinical and functional consequences. *J Clin Endocrinol Metab* (2015) 100(6):E926–35. doi: 10.1210/jc.2014-4204

27. Heinrich DA, Quinkler M, Adolf C, Handgriff L, Muller L, Schneider H, et al. Influence of cortisol cosecretion on non-acth stimulated adrenal venous sampling in primary aldosteronism: A retrospective cohort study. *Eur J Endocrinol* (2022) 187:637–50. doi: 10.1530/EJE-21-0541

28. Mune T, Morita H, Suzuki T, Takahashi Y, Isomura Y, Tanahashi T, et al. Role of local 11 beta-hydroxysteroid dehydrogenase type 2 expression in determining the phenotype of adrenal adenomas. *J Clin Endocrinol Metab* (2003) 88(2):864–70. doi: 10.1210/jc.2001-011335

29. Mazzocchi G, Aragona F, Malendowicz LK, Gottardo L, Nussdorfer GG. Cortisol-secreting adrenal adenomas express 11beta-hydroxysteroid dehydrogenase type-2 gene yet possess low 11beta-Hsd2 activity. *J Invest Med Off Publ Am Fed Clin Res* (2001) 49(2):191–4. doi: 10.2310/6650.2001.34046

30. Nishimoto K, Nakagawa K, Li D, Kosaka T, Oya M, Mikami S, et al. Adrenocortical zonation in humans under normal and pathological conditions. *J Clin Endocrinol Metab* (2010) 95(5):2296–305. doi: 10.1210/jc.2009-2010

31. Hannah-Shmouni F, Berthon A, Faucz FR, Briceno JM, Maria AG, Demidowich A, et al. Mass spectrometry-based steroid profiling in primary bilateral macronodular adrenocortical hyperplasia. *Endocrine-related Cancer* (2020) 27(7):403–13. doi: 10.1530/ERC-20-0102

frontiers | Frontiers in Endocrinology

TYPE Original Research
PUBLISHED 25 January 2023
DOI 10.3389/fendo.2022.1070074

OPEN ACCESS

EDITED BY
Marta Araujo-Castro,
Ramón y Cajal University Hospital, Spain

REVIEWED BY
Delmar Muniz Lourenco Jr.,
Clinical Hospital, University of São Paulo, Brazil
Avinaash Vickram Maharaj,
Queen Mary University of London, United Kingdom

*CORRESPONDENCE
Alberto Cascón
acascon@cnio.es

SPECIALTY SECTION
This article was submitted to Adrenal Endocrinology, a section of the journal Frontiers in Endocrinology

RECEIVED 14 October 2022
ACCEPTED 09 November 2022
PUBLISHED 25 January 2023

CITATION
Mellid S, Gil E, Letón R, Caleiras E, Honrado E, Richter S, Palacios N, Lahera M, Galofré JC, López-Fernández A, Calatayud M, Herrera-Martínez AD, Galvez MA, Matias-Guiu X, Balbín M, Korpershoek E, Lim ES, Maletta F, Lider S, Fliedner SMJ, Bechmann N, Eisenhofer G, Canu L, Rapizzi E, Bancos I, Robledo M and Cascón A (2023) Co-occurrence of mutations in *NF1* and other susceptibility genes in pheochromocytoma and paraganglioma.
Front. Endocrinol. 13:1070074.
doi: 10.3389/fendo.2022.1070074

Co-occurrence of mutations in *NF1* and other susceptibility genes in pheochromocytoma and paraganglioma

Sara Mellid[1], Eduardo Gil[1], Rocío Letón[1], Eduardo Caleiras[2], Emiliano Honrado[3], Susan Richter[4], Nuria Palacios[5], Marcos Lahera[6], Juan C. Galofré[7], Adriá López-Fernández[8], Maria Calatayud[9], Aura D. Herrera-Martínez[10], María A. Galvez[10], Xavier Matias-Guiu[11], Milagros Balbín[12], Esther Korpershoek[13], Eugénie S. Lim[14], Francesca Maletta[15], Sofia Lider[16], Stephanie M. J. Fliedner[17], Nicole Bechmann[4], Graeme Eisenhofer[4,18], Letizia Canu[19], Elena Rapizzi[19], Irina Bancos[20], Mercedes Robledo[1,21] and Alberto Cascón[1,21]*

[1]Hereditary Endocrine Cancer Group, Spanish National Cancer Research Centre (CNIO), Madrid, Spain, [2]Histopathology Core Unit, Spanish National Cancer Research Centre (CNIO), Madrid, Spain, [3]Anatomical Pathology Service, Hospital of León, León, Spain, [4]Institute for Clinical Chemistry and Laboratory Medicine, University Hospital Carl Gustav Carus, Medical Faculty Carl Gustav Carus, Technische Universität Dresden, Dresden, Germany, [5]Endocrinology Department, University Hospital Puerta de Hierro, Madrid, Spain, [6]Endocrinology and Nutrition Department, La Princesa University Hospital, Madrid, Spain, [7]Department of Endocrinology, Clínica Universidad de Navarra, Pamplona, Spain, [8]Hereditary Cancer Genetics Group, Vall d'Hebron Institute of Oncology (VHIO), Barcelona, Spain, [9]Department of Endocrinology and Nutrition, Hospital Universitario 12 de Octubre, Madrid, Spain, [10]Endocrinology and Nutrition Service, Reina Sofia University Hospital, Cordoba, Spain, [11]Department of Pathology, Bellvitge University Hospital, Centro de Investigación Biomédica en Red de Cáncer (CIBERONC), Barcelona, Spain, [12]Molecular Oncology Laboratory, Instituto Universitario de Oncologia del Principado de Asturias, Hospital Universitario Central de Asturias, Oviedo, Spain, [13]Department of Clinical Genetics, Erasmus Medical Center, Rotterdam, Netherlands, [14]Department of Endocrinology, William Harvey Research Institute, Queen Mary University of London, London, United Kingdom, [15]Pathology Unit , Department of Laboratory Medicine, Azienda Ospedaliero-Universitaria (AOU) Città della Salute e della Scienza di Torino, Torino, Italy, [16]Endocrinology Department, National Institute of Endocrinology, Bucharest, Romania, [17]First Department of Medicine, University Medical Center Schleswig-Holstein, Lübeck, Germany, [18]Department of Medicine III, University Hospital Carl Gustav Carus, Technische Universität Dresden, Dresden, Germany, [19]Department of Experimental and Clinical Medicine, University of Florence, Florence, Italy, [20]Division of Endocrinology, Metabolism and Nutrition, Mayo Clinic, Rochester, MN, United States, [21] Centro de Investigación Biomédica en Red de Enfermedades Raras (CIBERER), Instituto de Salud Carlos III, Madrid, Spain

Introduction: The percentage of patients diagnosed with pheochromocytoma and paraganglioma (altogether PPGL) carrying known germline mutations in one of the over fifteen susceptibility genes identified to date has dramatically increased during the last two decades, accounting for up to 35-40% of PPGL patients. Moreover, the application of NGS to the diagnosis of PPGL detects unexpected co-occurrences of pathogenic allelic variants in different susceptibility genes.

10.3389/fendo.2022.1070074

Methods: Herein we uncover several cases with dual mutations in NF1 and other PPGL genes by targeted sequencing. We studied the molecular characteristics of the tumours with co-occurrent mutations, using omic tools to gain insight into the role of these events in tumour development.

Results: Amongst 23 patients carrying germline NF1 mutations, targeted sequencing revealed additional pathogenic germline variants in DLST (n=1) and MDH2 (n=2), and two somatic mutations in H3-3A and PRKAR1A. Three additional patients, with somatic mutations in NF1 were found carrying germline pathogenic mutations in SDHB or DLST, and a somatic truncating mutation in ATRX. Two of the cases with dual germline mutations showed multiple pheochromocytomas or extra-adrenal paragangliomas - an extremely rare clinical finding in NF1 patients. Transcriptional and methylation profiling and metabolite assessment showed an "intermediate signature" to suggest that both variants had a pathological role in tumour development.

Discussion: In conclusion, mutations affecting genes involved in different pathways (pseudohypoxic and receptor tyrosine kinase signalling) co-occurring in the same patient could provide a selective advantage for the development of PPGL, and explain the variable expressivity and incomplete penetrance observed in some patients.

KEYWORDS

pheochromocytoma, NF1, germline mutation, DLST, MDH2, co-occurrent mutations

Introduction

Over the last two decades, the number of genes identified as involved in the hereditary susceptibility to developing pheochromocytoma (PCC) or paraganglioma (PGL), collectively known as PPGLs, has grown to more than fifteen, increasing the percentage of patients carrying known germline predisposing mutations to 35-40% (1). Furthermore, the prevalence and penetrance of PPGL-associated mutations is highly variable and parent-of-origin effects have been identified for at least, three susceptibility genes (*SDHD*, *SDHAF2* and *MAX*), making genetic diagnosis of the disease challenging. Comprehensive gene panels or exome sequencing, which allow the examination of all predisposing genes in one test, have replaced complicated algorithms employed for genetic testing of PPGL patients, and as a result of the shift from sequential gene testing to next-generation sequencing, unexpected genetic variants have been discovered. In this regard, two recent studies describe the presence of pathogenic germline variants in both *NF1* and *SDHD* genes in patients with multiple PPGLs (2, 3), one of whom had no clinical sign of neurofibromatosis type 1 (NF1; MIM #162200). The presence of germline variants in more than one susceptibility gene co-occurring in the same patient adds a further layer of complexity to the genetic diagnosis of the disease, and suggests that a more intricate genetic condition accounts for the development of PPGL in some NF1 patients.

Development of PPGL in patients with NF1 is thought to be very rare (0.1-5.7%) (4–6). A recent study revealed that only 0.3% (1/342) of patients with NF1 developed PPGL (7), while an exhaustive study for the presence of PPGL amongst patients diagnosed with neurofibromatosis (n=156), found that up to 7.7% of patients developed PPGL (8). This percentage could be underestimated since the use of targeted NGS has led to the identification of *NF1* germline mutations in PPGL patients without a clear clinical diagnosis of NF1 (3, 9–12). Nevertheless, the percentage of patients developing PPGL amongst NF1 patients contrasts with that observed for other PPGL syndromes, e.g. 20% in von Hippel-Lindau (VHL; MIM #193300) and 50% in multiple endocrine neoplasia type 2A (MEN2; MIM #171400) (13, 14). Moreover, PPGLs are multifocal or bilateral in 43-45% of VHL cases and in 50-80% of MEN2 cases, compared to 16% in NF1 patients. These differences point to still unknown mechanisms that could account for the development of PPGL in NF1 patients.

We recently identified three patients carrying *NF1* germline mutations and additional variants in other PPGL susceptibility genes. Interestingly, two of the three cases showed quite uncommon clinical findings (bilateral PCC and extra-adrenal PGL). Therefore, herein we analyse, using a comprehensive gene

10.3389/fendo.2022.1070074

panel, a series of NF1 patients with PPGL, enriched in cases with multiple PPGLs, to investigate the co-occurrence of *NF1* mutations with causal variants in other PPGL susceptibility genes. Moreover, we study the molecular characteristics of the tumours with dual mutations, using various omic tools, to gain insight into the role of this genetic event in the development of PPGL.

Methods

Patients and samples

Twenty-three patients diagnosed with PPGL and carrying a germline *NF1* mutation were included in the study (Table 1). The series was enriched with patients developing bilateral PCC or extra-adrenal PGLs. In addition, three patients carrying known germline or somatic mutations in other PPGL susceptibility genes, and a somatic *NF1* alteration were also included for discussion. A summary of the clinical data of the patients included in the study is provided in Table 2. Genomic DNA was extracted from available peripheral-blood leukocytes with the Maxwell Blood DNA-purification system (Promega). Tumour DNA was obtained from all patients with the DNeasy Blood and Tissue kit (QIAGEN) for frozen tissue and the Covaris S2 System (Covaris) for formalin-fixed paraffin-embedded (FFPE) tissue according to the manufacturers' instructions. Informed written consent was obtained for all participants in the study. Ethical approval was granted by local ethical committees with the following reference numbers: 13-004137, 06/Q0104/133, 15/024, 88/11, 2011/0020149, 14/11.06.2020, PI54_2016-v2.

TABLE 1 Molecular findings identified in the patients included in the study.

ID	*NF1* mutation	Varsome/ ClinVar	gnomAD frequency	*NF1* LOH/2nd hit	2nd mutation	Varsome/ ClinVar	gnomAD frequency	LOH
1[#]	p.(His2423GlnfsTer4)	NA; path	–	Yes	p.(Gly374Glu) DLST	18/20 path; path	2/251464	No
2	p.(Leu2323Pro)	19/20 path; VUS	–	Yes	p.(Lys314Met) MDH2	15/20 path; NA	6/251092	No
3	p.(Ser1561Ile)	15/20 path; NA	–	No	p.(Lys314Met) MDH2	15/20 path; NA	6/251092	No
4	p.(Ser1838TyrfsTer23)	NA; NA	–	–	–	–	–	–
5[#]	p.(Thr586ValfsTer18)	NA; path	1/251120	Yes	–	–	–	–
6[#]	p.(Ser260IlefsTer7)	NA; NA	–	Yes	–	–	–	–
7	c.5944-2A>G	6/6 path; path	–	Yes	–	–	–	–
8	c.586+1G>A	6/6 path; path	–	Yes	–	–	–	–
9	p.(Arg2258Ter)	7/8 path; path	–	No	–	–	–	–
10	p.(Met1?)	13/17 path; path	–	Yes	–	–	–	–
11	p.(Leu145GlnfsTer10)	–	–	Yes	–	–	–	–
12	p.(Tyr2285Ter)	7/8 path; path	2/282598	dubious	–	–	–	–
13	p.(Ile429AspfsTer2)	NA; NA	–	Yes	–	–	–	–
14	c.2851-6_2851-3del	NA; path	–	Yes	–	–	–	–
15	p.(His1826Arg)	19/20 path; VUS	–	No	–	–	–	–
16	p.(Gln2589Ter)	7/8 path; path	–	Yes	–	–	–	–
17	c.6147+1G>A	6/6 path; path	–	–	–	–	–	–
18	p.(Tyr628LeufsTer6)	NA; path	–	Yes	–	–	–	–
19	p.(Gln2373Ter)	7/8 path; path	–	Yes	–	–	–	–
20	p.(Arg681Ter)	7/8 path; path	1/250690	Yes	–	–	–	–
21	p.(Gln1086Ter)	7/8 path; path	–	Yes	–	–	–	–
22	c.6820-1G>T	6/6 path; NA	–	Yes	**p.(Arg16Ter) PRKAR1A**	7/8 path; path	–	No
23	p.(Gly2379Arg)	17/20 path; VUS	4/251372	No	**p.(Gly35Trp) H3-3A**	15/19 path; NA	–	No
24	**p.(Leu134GlnfsTer20)**	NA; NA	–	Yes	p.(Gly374Glu) DLST	18/20 path; path	2/251464	No
25	**c.4333-1G>A**	6/6; likely path	1/ 227062	Yes	c.423+1G>A *SDHB*	6/6 path; path	3/ 251374	No
26	**p.(Ser2181ValfrTer19)**	NA; path	–	–	**p.(Arg808Ter) ATRX**	5/5 path; NA	–	No

[#], previously reported case; Path, pathogenic; VUS, variant of uncertain significance; NA, not available; LOH, loss of heterozygosity; bold letters, somatic mutation; we used the ENST00000358273 transcript to name the NF1 variants.

10.3389/fendo.2022.1070074

TABLE 2 Clinical data of the patients included in the study.

ID	Tumor	Distant metastasis	Age	Sex	FH PCC	Clinical features of NF1	FH NF1	Metanephrines
1[#]	Bilateral PCC & MTC	No	56	M	No	Café-au-lait spots, axillary and inguinal freckling, Lisch nodules, macrocephaly, intra- and extra arachnoidal neurofibromas	No	NM
2	PCC	No	25	M	Yes	–	Yes	M>NM
3	TA PGL	No	76	M	No	–	No	NA
4	PCC	No	39	M	No	–	No	NM>M
5[#]	Bilateral PCC	No	45	F	NA	Café-au-lait spots, skin fibromas, multiple GIST and axillary and inguinal freckling	NA	M&NM
6[#]	PCC	No	53	F	No	Unknown NF1 features	Yes	M
7	PCC	Yes	15	F	Yes	Skin neurofibromas	Yes	M
8	PCC	No	59	M	No	–	No	M>NM
9	PCC	No	56	M	No	–	No	M>NM
10	PCC	No	60	M	No	–	No	NM>M
11	PCC	No	43	F	NA	–	NA	NA
12	PCC	No	57	M	No	Neurofibromas, bilateral Lisch nodules, choroidal lesions	Yes	M>NM
13	Bilateral PCC	Yes	60	M	NA	Multiple neurofibromatoma over skin, freckles, intellectual disability (learning difficulties), hearing impairment	NA	M&NM
14	Bilateral PCC	No	56	F	NA	Café-au-lait spots, typical fibromas	NA	M
15	PCC	No	44	M	No	–	No	M
16	PCC	No	51	M	No	–	No	M
17	PCC	No	39	F	No	–	No	NM
18	Bilateral PCC	No	42	F	No	Café-au-lait spots, malignant peripheral nerve sheath tumour, neurofibromas	No	M
19	Bilateral PCC	No	42	F	No	Café-au-ait spots, axillary and inguinal freckling, neurofibroma	No	M&NM
20	Bilateral PCC	No	48	F	No	Café-au-lait spots, neurofibromas, inguinal freckling	No	M&NM
21	Bilateral PCC	No	30	F	No	Café-au-lait, deformity of left forearm, hyperpigmentation , delayed development, grand mal seizures, hamartoma, neurofibroma (plexiform), macrocephaly	No	D&M&NM
22	Bilateral PCC	No	41	F	Yes[‡]	Café-au-lait spots, neurofibroma, axillary freckling	Yes	M&NM
23	PCC	Yes	50	F	No	–	No	NM
24	PCC	No	55	F	No	–	No	M>NM
25	PCC	No	66	F	Yes	–	Yes	M
26	PCC	Yes	63	M	No	–	No	NM

[#], previously reported case (ID 1: Gieldon et al. 2018; ID 5: Barbero et al. 2021; ID 6: Matas-Nadal et al. 2022); PCC, pheochromocytoma; TA, thoracic-abdominal; FH, family history; M, metanephrine; NM, normetanephrine; Path, pathogenic; VUS, variant of uncertain significance; NA, not available; LOH, loss of heterozygosity; [‡], suspicious but not confirmed; MTC, medullary thyroid carcinoma; GIST, gastrointestinal stromal tumor; PGL, paraganglioma; D, dopamine.

Targeted next-generation sequencing (NGS) and loss-of-heterozygosity (LOH) analysis

DNA obtained from blood or tumour samples was used for targeted sequencing. The diagnostic PPGL target panel included all susceptibility genes described so far, and some genes mutated somatically in PPGL, in total 33 genes (*CSDE1*, *KIF1B*, *SDHA*, *SDHB*, *SDHC*, *SDHD*, *SDHAF1*, *SDHAF2*, *EGLN1*, *EGLN2*, *FH*, *MDH2*, *DLST*, *IDH2*, *IDH1*, *TMEM127*, *VHL*, *MET*, *RET*, *PTEN*, *HRAS*, *MEN1*, *KRAS*, *MAX*, *GOT2*, *NF1*, *PRKAR1A*, *ATRX*, *BRAF*, *EPAS1*, *SLC25A11*, *DNMT3A*, *H3F3A*). TruSight (Illumina) oligo probes were designed for the genes of interest. DesignStudio software (Illumina) was used for the design of 891 amplicons. Once the library was prepared, sequencing was performed using a MiSeq sequencer (Illumina). Alignment of sequences was done by MiSeq Reporter and VariantStudio (Illumina), and variant calling was carried out by GATK software. Variants were filtered following standard quality and depth criteria and candidate regions without adequate coverage or quality were amplified by Sanger sequencing. The PredictSNP consensus classifier was used to predict the effect of the amino acid missense substitution identified (15). LOH analysis of the *DLST* locus was performed on tumour DNA from case 1 (see

Figure 1) by high-density SNP-array analysis. Briefly, a genome-wide scan was conducted on 250 ng of tumour DNA with the Illumina Human610-Quad BeadChip (Illumina) and image data was analysed with the Chromosome Viewer tool contained in GenomeStudio 2010.2 (Illumina). The metric we used was the log-R ratio, which is the binary logarithm of the ratio of the observed to expected normalized R values for a given SNP, as previously reported (16).

Methylation arrays

Bisulfite conversion of tumour DNA from case 1 (carrying the germline DLST-p.Gly374Glu mutation) was performed using the EZ DNA Methylation Kit (Zymo Research) and genome-wide DNA methylation was assayed using the Infinium MethylationEPIC BeadChip (Illumina) at the Centro Nacional de Genotipado (CEGEN-ISCIII) (www.cegen.org), as previously described (17). This BeadChip interrogates over 850,000 methylation sites per sample at single-nucleotide resolution. M values were used for statistical analyses. Following, we profiled MethylationEPIC data obtained from the tumour with our series of 12 PPGLs carrying mutations in different susceptibility genes (including three cases with the DLST-p.Gly374Glu mutation). Hierarchical clustering of methylation data was performed using GeneCluster 2.0 (18). The methylome of the tumor carrying co-ocurrent mutations in *DLST* and *NF1* (case 1) was deposited in the National Center for Biotechnology Information GEO database under the accession number GSE217207. Methylation data from the rest of the tumor samples used in this study were previously deposited under the accession numbers GSE111336 and GSE123185 (16).

Liquid chromatographic-tandem mass spectrometric (LC-MS/MS) determination of tricarboxylic acid (TCA) cycle -related metabolites

FFPE tumour tissue (5–10 mg) from three available individuals (cases 1 and 24 with dual *NF1*/*DLST* variants, and case 3 with dual *NF1*/*MDH2* variants) were immersed in 500 mL LC-MS/MS-grade methanol containing isotope-labelled internal standards and processed as previously described (19). An analysis of metabolites was carried out with an AB Sciex 5500 QTRAP mass spectrometer coupled to an Acquity ultra-high-performance liquid chromatographic system (Waters) as previously described (19). We compared the data with that from a series of tumours carrying either *NF1* or *DLST* mutations previously analysed in our laboratory.

Immunohistochemistry (IHC)

Immunohistochemical staining of DLST (11954; rabbit monoclonal 1:150, Cell Signaling Technology), and 5-hydroxymethylcytosine (5-hmC) (Active Motif; 39770) were performed with 3 mm FFPE sections from tumours 1 and 24,

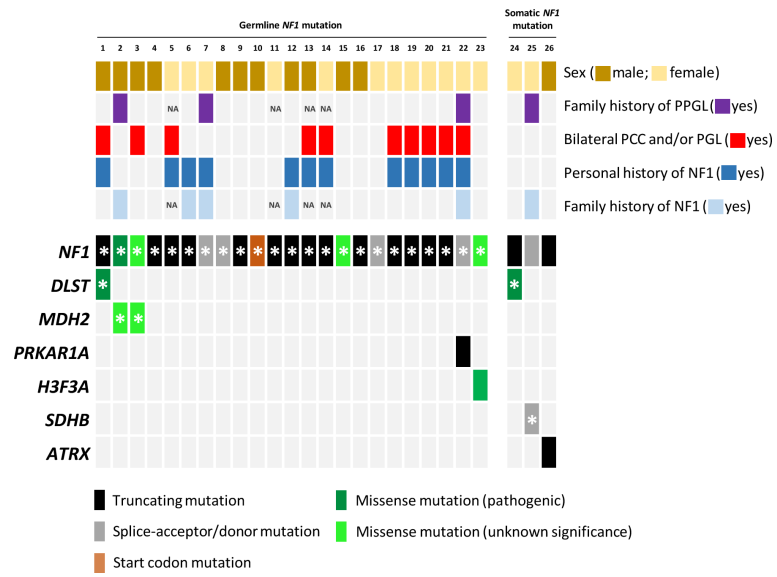

FIGURE 1
Mutational profile of the twenty-six samples included in the study. Each column represents a tumour, with coloured rectangles representing mutations that are germline (denoted with an asterisk) or somatic in each row. Missense variants that ClinVar does not classify as pathogenic mutations and/or that are absent in NF1 patients were categorized as variants of unknown significance. NA, not available.

the two *DLST*/*NF1*-mutated tumour samples, as previously described (16, 20).

RNA sequencing

RNA libraries were built using QuantSeq 3' mRNA-Seq Library Prep Kit FWD for Illumina (Lexogen, 015), following the vendor's protocol for FFPE RNA using 500 ng of total RNA from tumours 1 and 24, carriers of dual mutations in *NF1* and *DLST*. We also used UMI Second Strands Synthesis Module for QuantSeq FWD (Lexogen, 081) and PCR Add-on Kit for Illumina (Lexogen, 020) to adjust the library amplification number of cycles. Libraries were applied to an Illumina flow cell for cluster generation and sequenced on NovaSeq6000. For the hierarchical clustering, performed with GeneCluster 2.0 (18), we used expression data from a list of genes differentially expressed in *DLST* mutated PPGLs (16) from the two *NF1*/*DLST* mutated tumours, three *DLST*- and seven *NF1*-mutated PPGLs. The transcriptomes of the tumors carrying co-ocurrent mutations in *DLST* and *NF1* (cases 1 and 24) were deposited in GEO under the accession number GSE217206. RNA-Seq data for the rest of the tumors used in this study were previously deposited under the EGAS00001006044 accession number in the European Genome-phenome archive (Calsina et al., under review).

Results

NGS analysis

Amongst the twenty-three germline *NF1* mutations included in the study, three missense variants (identified in cases 3, 15 and 23; Table 1; Figure 1) were not classified or were classified as variants of uncertain significance by ClinVar, and have not been found in *NF1* patients. However, most of the predictions included in Varsome suggest a pathological effect of the substitutions, so we took these variants into account throughout the current study. Overall, NF1 clinical features (Table 2) or a family history of NF1 were reported in ~57% of the individuals carrying *NF1* germline mutations.

Targeted sequencing of a panel of 33 PPGL-related genes revealed three germline variants, one in *DLST* and two in *MDH2*, and two somatic mutations in *H3-3A* (previously known as *H3F3A*) and *PRKAR1A* amongst the twenty-three patients carrying *NF1* germline mutations analysed (Table 1; Figure 1). The DLST-p.Gly374Glu variant, previously reported as pathogenic in PPGL patients (16, 21), was found in a patient with bilateral PCC. The MDH2-p.Lys314Met variant, identified in two unrelated patients, has not been previously described in PPGL patients and it is found in 6/251092 controls from gnomAD. Several software (Polyphen/SIFT, Mutation taster, MutationAssessor, CUPSAT, Mutant v3.0) predicted the variant as deleterious. The *H3-3A* variant, p.Gly35Trp, is a known hotspot mutation found in giant cell tumour of bone (22) and PPGL (23).

Three additional patients carrying *NF1* somatic mutations were also included in the study: one patient with PCC, and family history of NF1, carrying a known *SDHB* germline pathogenic mutation (ClinVar ID:29896; LOVD-SDHB ID: 000047), one patient with a *DLST* pathogenic mutation p.Gly374Glu (ClinVar ID:635133) identified in the germline, and one case with an *ATRX* somatic truncating mutation.

All variants were validated by Sanger sequencing.

SNP array

Targeted and Sanger sequencing revealed no LOH of the wild-type (WT) *DLST* allele in the two tumours carrying the p.Gly374Glu mutation. For one of the tumours, a genome-wide SNP array analysis confirmed the absence of LOH and discarded uniparental disomy (UPD) of chromosomal region 14q, on which *DLST* is located, a mechanism described in *DLST*-mutated PPGLs (Supplementary Figure 1) (16). This tumor showed LOH on the long arm of chromosome 17 including the *NF1* locus.

Methylation profiling

It has been reported that the methylation profile observed in *DLST*-mutated tumours is intermediate between the CpG island methylator phenotype (CIMP) described for SDH-mutated PPGLs and the unmethylated profile exhibited by tumours belonging to the so called cluster 2 (i.e. tumours with mutations in *NF1*, *RET*, *MAX* or *HRAS*) (24). When we profiled one of the tumours carrying mutations in *NF1* and *DLST*, it clustered together with *DLST*-mutated tumours and separated from cluster 2 samples (including one *NF1*-mutated PCC) (Figure 2A), suggesting a role of the *DLST* variant in the observed molecular phenotype.

Metabolite analysis

LC-MS/MS analysis of the three tumours available did not reveal conclusive alterations in TCA-cycle metabolites. However, one of the tumours carrying the double mutation in *NF1*/*DLST* exhibited an accumulation of cis-aconitate and a slightly high ketoglutarate/fumarate ratio was observed in the two *NF1*/*DLST*-mutated tumours compared to tumours carrying only an *NF1* mutation (Figure 2B). It is possible that a certain block in the TCA-cycle due to the *DLST* mutation causes this partial accumulation. Finally, a relatively high fumarate to

10.3389/fendo.2022.1070074

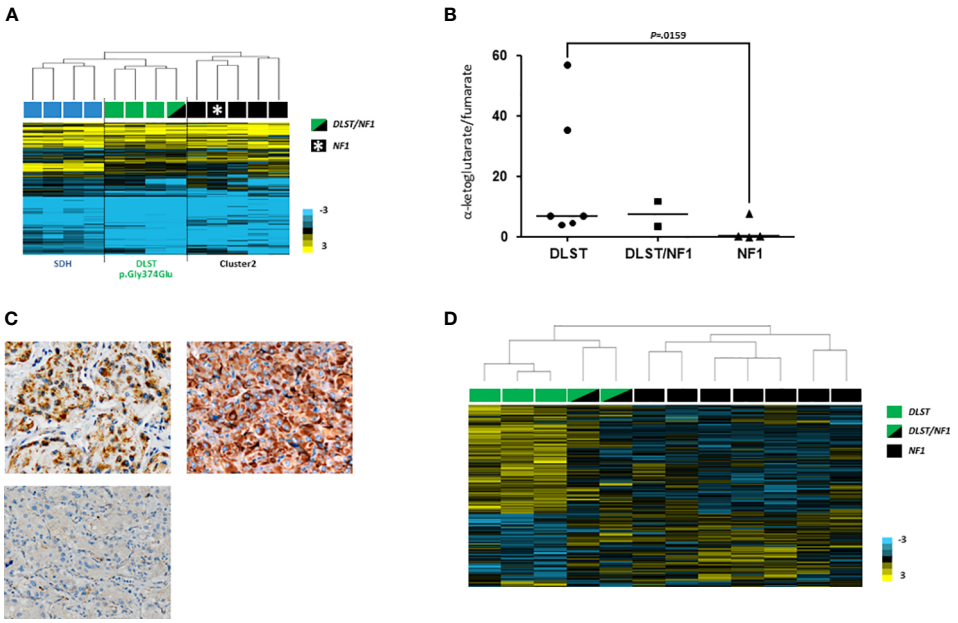

FIGURE 2
(A) Hierarchical clustering performed on the basis of methylation data from PPGLs as follows: one of the two *DLST*/*NF1* (indicated with a green and black rectangle), four SDH-mutated (indicated with blue rectangles), three *DLST*-mutated (indicated with green rectangles) and five cluster 2-mutated (denoted in black rectangles) PPGLs. The DLST/NF1 PPGL was grouped with *DLST*-mutated tumours, and separated from cluster 2-mutated PPGLs. City-block and complete linkage characteristics were used for the analyses. **(B)** α-ketoglutarate/fumarate ratios assessed by LC-MS/MS in *DLST*-mutated tumours (n = 6), *NF1*-mutated PPGLs (n = 4), and the two tumours carrying dual *NF1*/*DLST* mutations. Black lines represent medians. A t test identified significant differences between *DLST*-mutated and *NF1*-mutated tumours. **(C)** Immunostaining for DLST was conducted in the two tumours carrying *DLST*/*NF1* dual mutations (upper panel) revealing the characteristic cytoplasmic aggregates (x20). A VHL-mutated tumor was used as a negative control (lower panel) **(D)** Hierarchical clustering of the two *NF1*/*DLST* mutated tumours, three *DLST*- and seven *NF1*-mutated PPGLs based on gene expression data from a previously reported list of genes differentially expressed in *DLST*-mutated PPGLs. The two tumours carrying the *NF1*/*DLST* mutations were clustered between PPGLs carrying mutations in *NF1* and *DLST*. Uncentered correlation and complete linkage characteristics were used for the analysis.

succinate ratio was observed in the only available tumour carrying dual *NF1*/*MDH2* variants (Supplementary Figure 2), something previously described in *MDH2*-mutated PPGL (19).

IHC assays

In order to investigate whether tumours carrying the *NF1*/DLST-p.Gly374Glu mutations showed other molecular features observed previously in *DLST*-mutated PPGLs, we carried out the IHC for DLST. The two tumours showed a highly positive staining (Figure 2C), something previously reported for PPGLs carrying mutations in *DLST* and other TCA-cycle genes (16, 21), supporting again a role of the *DLST* mutation in tumour development. Another molecular marker described for *DLST*-mutated tumours is the low level of 5-hmC nuclear staining (21), similar to the observed in SDH-mutated PPGLs (25). 5-hmC staining applied to the two *DLST*-mutated tumours were positive in one of the samples and heterogeneous in the second tumour, in which positive regions alternated with regions that had negative IHC (Figuress 3A, B). SDHB IHC carried out in the tumour carrying co-occurrent *SDHB* germline mutation and somatic *NF1* mutation yielded a positive stain, which is atypical for pathogenic *SDHB* mutations (Figure 3C).

Transcriptional profiling

Hierarchical clustering of the two tumours carrying dual mutations in *NF1* and *DLST* based on expression data for genes differentially expressed in *DLST*-mutated PPGLs grouped them in between *DLST* and *NF1* mutated PPGLs, suggesting that an intermediate phenotype was caused by the coexistence of the two alterations (Figure 2D).

Discussion

PPGL is the tumour with the highest degree of heritability attributable to the presence of germline mutations in known genes (up to 40% of cases) (26). Although mutations in some of the susceptibility genes are highly penetrant (e.g. germline mutations in *VHL* or *RET*), variants in other genes such as *SDHB*, *SDHA* (27) or *TMEM127* (28) do not segregate with the

10.3389/fendo.2022.1070074

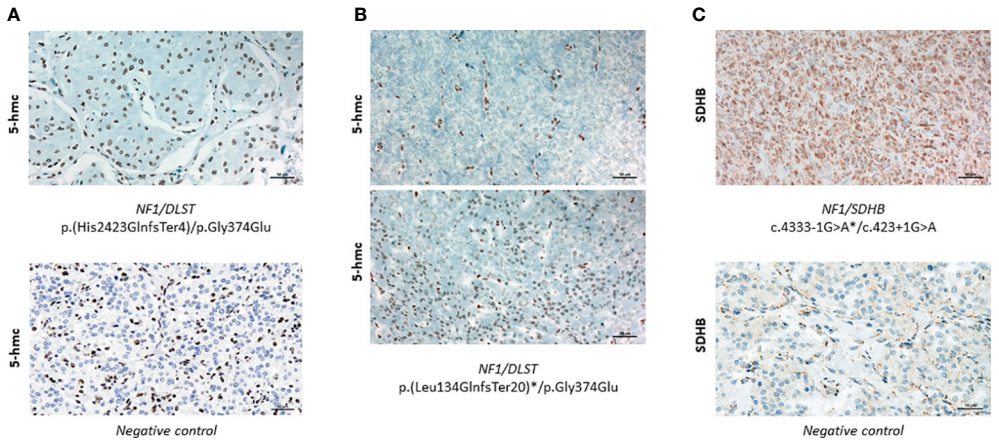

FIGURE 3
(A) Positive 5-hmC IHC performed in case 1 (upper panel) compared to a negative control (lower panel) (x20). **(B)** 5-hmC IHC performed in case 24, showing patches of negative (upper panel) and positive (lower panel) staining (x20)**(C)** Positive SDHB IHC performed in the tumour carrying *SDHB*/*NF1* dual germline mutations (upper panel) compared to a negative control (lower panel) (x20). Asterisks denote a somatic mutation.

disease in some pedigrees due to a low age-dependent penetrance. In this regard, the latest susceptibility genes identified in PPGL patients, *SLC25A11* and *DLST*, have been found in patients with no relatives affected (16, 29), suggesting that these variants have a very low penetrance as well. Though penetrance of *NF1* germline mutations is considered to be virtually complete after childhood, some studies have reported the presence of unexpected *NF1* germline mutations in PPGL patients for whom a clinical diagnosis of the disease was not previously established (3, 9). The finding of 11 additional PPGL patients harbouring germline *NF1* mutations without clinical manifestations of NF1 at diagnosis, underscores the importance of including *NF1* testing in the genetic diagnosis of every PPGL patient, even in the absence of clinical features of the disease.

The penetrance of a given allele can be modified by the simultaneous presence of variants at other gene loci, which may also affect the clinical expressivity of the disease. In the case of NF1, modifier genes have been reported to contribute to the variable expressivity of the disease in a large series of patients (30, 31). The number of café-au-lait macules has been found to be influenced by common SNPs (32), polymorphisms in *ADCY8* correlate with glioma risk in a sex-specific manner (33), and rare germline variants in various genes including *ATM* have been proposed as candidate modifiers of plexiform neurofibroma (34). NF1-associated PPGLs are mostly unilateral (84% of patients) and rarely extra-adrenal (6.1% of patients) (4, 5). Herein we describe two NF1 patients with multiple tumours harboring dual mutations, which, in addition to the previously reported patients carrying *SDHD*/*NF1* mutations, suggest that the co-occurrence of *NF1* mutations with variants affecting other PPGL susceptibility genes (i.e. *DLST*, *MDH2, SDHD*), or still unknown genes, could be responsible of this unusual clinical manifestation in some NF1 patients. In turn, no germline mutations affecting other PPGL susceptibility gene were found in the six exomes from patients with unilateral PCC and constitutive *NF1* mutation included in The Cancer Genome Atlas program (24). Another possible explanation is that the development of PPGL in NF1 is an example of an oligogenic disease caused by the co-occurrence of mutations in two or more genes. In contrast to the thousands of reports in which mutations in single genes cause human diseases, there are only dozens of human disease phenotypes with evidence of digenic inheritance (35–37). The incidence of NF1, approximately 1:2600 to 3000 individuals, could indicate that the findings described in the present study are coincidental.

The DLST-p.Gly374Glu variant has recently been demonstrated to be pathological in PPGL patients (PGL7; MIM # 618475) (16, 21). Despite the absence of LOH affecting the wild-type allele in the two patients in our series, the highly positive IHC for DLST as a molecular marker of TCA-cycle disruption (16), supports its role in tumour development. In addition, the intermediate expression profile of the two tumours between *NF1* and *DLST* mutated PPGLs, the DLST-like methylation profile observed for one of them, and the accumulation of cis-aconitate and the heterogeneous 5-hmC staining observed in the other tumour, reinforces a role of the *DLST* mutation in tumour molecular characteristics. No additional cases with PPGL were identified in the two pedigrees carrying the DLST-p.Gly374Glu mutation, and the finding of the mutation in a healthy 58-year-old relative from one of the families (data not shown) supports the previously described low penetrance of the DLST-p.Gly374Glu variant (16). Interestingly, the patient carrying the *NF1*/*DLST* variants in the germline (case 1) also developed a medullary thyroid carcinoma (MTC) with LOH for the *NF1* mutation (9). Neither *NF1* nor *DLST* are clearly related to medullary thyroid malignancies, but

the co-occurrence of both alterations could account for the presence of bilateral PCC and MTC in the same patient, resembling what happens in multiple endocrine neoplasia type 2. This case is especially intriguing, as clinical features of NF1 were not recognized until the diagnosis of bilateral PCC was made at age 56 years, and in addition the patient developed primary prostate and lung cancers during his lifetime.

The *MDH2* variant, p.Lys314Met, identified in two of the NF1 patients involves one of the four lysines described as playing a role in the activation of MDH2 by acetylation (38, 39). Interestingly, the same lysine was found deleted in another patient with multiple noradrenergic PGLs (40), which supports the relevance of this residue for MDH2 function. The presence of a para-aortic PGL in one of the patients carrying the p.Lys314Met (case 3), reinforces the role of the variant in the disease since a thoracic-abdominal location of PGL, very rare in NF1 patients, is the most frequently found in *MDH2* mutation carriers (19, 40).

The presence of *NF1* somatic mutations is one of the main genetic findings occurring in sporadic PPGLs (accounts for 20-25% of all cases) (41), being mostly tumours with adrenal location and only 4% extra-adrenal (10, 42). It has been repeatedly suggested that there is a mutual exclusivity condition affecting driver events in PPGLs, something that points to the redundancy of the affected signals (43, 44). Finding a mutation in *H3-3A* in a tumour carrying a germline *NF1* variant suggests that perhaps some mutations in *NF1* do need another alteration that confers additional selective advantages to the tumour cells (44). In the majority of NF1 cases, the mutation in *NF1* is sufficient for tumour development and there is no need for accumulation of mutations in other predisposing genes, although it has been suggested that a proportion of apparently NF1-sporadic PPGLs might actually have a germline susceptibility variant in other predisposing genes (44). This is the case of the patient described in the present study carrying a germline *SDHB* mutation and a somatic *NF1* alteration, whose tumour showed no evidence of LOH and a positive SDHB IHC. There is another similar example of co-occurrence of a germline *SDHB* mutation and a somatic *NF1* alteration in a patient who developed a para-aortic PGL (45). Recently, dual *SDHB*/*NF1* loss has been reported as a successful mechanism to force tumour formation in a *SDHB* knockout mouse model (46). *SDHB* loss has been shown to be insufficient for tumour development in SDH-mouse models of PPGL (47), but the concomitant alteration of NF1 finally yielded SDH-like PPGLs, reinforcing the theory for a need of additional genetic events for tumour initiation and maintenance in *SDHB* PPGL, resulting in a lower penetrance of the mutations (48). A similar situation could explain the low penetrance of the p.Gly374Glu *DLST* germline variant observed in our pedigrees. It is noteworthy that all the NF1 cases described herein, as well as those reported in the literature, carry co-occurrent alterations in an apparently unrelated pathway (e.g. pseudohypoxic signalling), suggesting that co-occurrence of alterations in different signalling cascades could provide a selective advantage for the development of PPGL.

Somatic *ATRX* mutations in PPGLs carrying germline mutations in one of the major susceptibility genes (especially in *SDHB*-mutated cases) have been reported (24, 49), and this event has been described as an independent factor of poor prognosis (50). Moreover, a recent study described the co-existence of *NF1* germline mutations and *ATRX* somatic alterations in different tumours from NF1 patients (51). Therefore, finding a PPGL carrying somatic mutations in *NF1* and *ATRX* may not be unexpected, and warns of the malignant potential of the tumour carrying the *ATRX* mutation. Finally, *PRKAR1A*, mapped at 17q22-24, is the gene encoding the protein kinase A regulatory subunit type 1α which can interfere with the ERK1/2 cascade of the MAPK pathway and causes inhibition of cell proliferation (52). *PRKAR1A* is frequently mutated in patients with Carney complex syndrome (MIM #160980) (53), a rare multiple neoplasia syndrome characterized by both endocrine and non-endocrine manifestations. This gene can be rearranged with *RET* to form the thyroid tumour-specific chimeric oncogene PTC2 (54), and it is worth noting that dysregulated protein kinase A has been linked to cancer by activation of mechanisms that overlap but differ from those found in neurofibromatosis tumorigenesis (55). *PRKAR1A* haploinsufficiency is a general tumorigenic signal which may require inactivation of other tumour suppressors to function (56). Another inactivating variant in *PRKAR1A* has been found in a metastatic PCC carrying additional alterations in *ATRX* and *MAML3* (24), but the significance of this somatic event in PPGL etiology is still unknown.

Because of the low penetrance of some mutations, variable expressivity, and parent-of-origin effects associated with some susceptibility genes, a large number of PPGL patients have no family history, masking the hereditary condition and making proper follow-up of individuals at risk for hereditary PPGL difficult. Herein, we propose a new layer of complexity in which mutations affecting genes involved in different pathways (e.g. pseudohypoxic and receptor tyrosine kinase signalling) (Supplementary Figure 3) co-occurring in the same patient, either in the germline or in the tumour, could provide a selective advantage for the development of PPGL. The widespread application of NGS to the diagnosis of PPGL will continue to identify unexpected co-occurrences of pathological mutations, which may provide new insights into the development of these tumors, as well as explain differences in their expressivity and incomplete penetrance.

Data availability statement

The data presented in the study are deposited in the GEO database repository, accession numbers GSE217208, GSE111336

and GSE123185; and in the in the European Genome-phenome archive, accession number EGAS00001006044.

Ethics statement

The studies involving human participants were reviewed and approved by Institutional Review Board of Mayo Clinic: IRB 13-004137; Cambridge East Medical Research Ethics Committee: Ref: 06/Q0104/133; Hospital Universitario 12 de Octubre: 15/024; ENS@T Ethics Committee: 88/11; Azienda Ospedaliera Universitaria Careggi: Prot. N. 2011/0020149; Ethics Committee Institutului National de Endocrinologie: 14/11.06.2020; The Instituto de Salud Carlos III (ISCIII) ethics committee: CEI PI 54_2016-v2. The patients/participants provided their written informed consent to participate in this study.

Author contributions

SM, EG, RL, EC, SR, GE, and EH were involved in data analysis, data interpretation, and final approval of the manuscript. NP, ML, JG, AL-F, MC, AH-M, MG, XM-G, MB, EK, EL, FM, SL, SF, NB, LC, ER, and IB were responsible for data collection and final approval of the manuscript. MR was responsible for study design, data interpretation, manuscript writing, and final approval of the manuscript. AC was responsible for study design, data analysis, data interpretation, manuscript writing, and final approval of the manuscript. All authors contributed to the article and approved the submitted version.

Funding

This work was supported by the Instituto de Salud Carlos III (ISCIII), through the "Acción Estratégica en Salud" (AES) (projects PI18/00454 to AC and PI20/01169 to MR), cofounded by the European Regional Development Fund (ERDF). SM was supported by the Spanish Ministry of Science, Innovation and Universities "Formación del Profesorado Universitario— FPU" fellowship with ID number FPU19/04940.

Conflict of interest

The authors declare that the research was conducted in the absence of any commercial or financial relationships that could be construed as a potential conflict of interest.

Publisher's note

All claims expressed in this article are solely those of the authors and do not necessarily represent those of their affiliated organizations, or those of the publisher, the editors and the reviewers. Any product that may be evaluated in this article, or claim that may be made by its manufacturer, is not guaranteed or endorsed by the publisher.

Supplementary material

The Supplementary Material for this article can be found online at: https://www.frontiersin.org/articles/10.3389/fendo.2022.1070074/full#supplementary-material

SUPPLEMENTARY FIGURE 1
SNP-array study of chromosomes 14 and 17 using tumour DNA from case 1 who carries the DLST-p.Gly374Glu/NF1-p.His2423GlnfsTer4 dual mutation showed no LOH. The lower panel shows the genomic plots of the log R ratio [log 2 (Rpatient/Rreference)], and the upper panel gives the allele frequency parameters along the chromosomes.

SUPPLEMENTARY FIGURE 2
Fumarate/succinate ratios assessed by LC-MS/MS in *MDH2*-mutated PPGLs (n=5), *NF1*-mutated PPGLs (n=5), SDHx-mutated PPGLs (n=11), and one PPGL carrying dual *NF1*/*MDH2* mutation. Black lines represent means. A t test identified differences between means.

SUPPLEMENTARY FIGURE 3
Schematic representation of the three molecular processes involved in the development of PPGL in which we have found co-occurring mutations: pseudohypoxic signalling (shown in purple), receptor tyrosine kinase cascades (shown in green), and epigenetic modifications and chromatin remodelling (shown in blue). The proteins found mutated in PPGL are indicated with dark coloured ovals and white letters, and the proteins whose genes have been found mutated in the present study are indicated with a yellow asterisk.

References

1. Buffet A, Burnichon N, Favier J, Gimenez-Roqueplo AP. An overview of 20 years of genetic studies in pheochromocytoma and paraganglioma. *Best Pract Res Clin Endocrinol Metab* (2020) 34(2):101416. doi: 10.1016/j.beem.2020.101416

2. Chatzikyriakou P, Touska P, Moonim MT, Obholzer R, Afridi S, Sandison A, et al. Case report of a man with multiple paragangliomas and pathogenic germline variants in both NF1 and SDHD. *Cancer Genet* (2021) 256-257:110–4. doi: 10.1016/j.cancergen.2021.05.008

3. Ben Aim L, Pigny P, Castro-Vega LJ, Buffet A, Amar L, Bertherat J, et al. Targeted next-generation sequencing detects rare genetic events in pheochromocytoma and paraganglioma. *J Med Genet* (2019) 56(8):513–20. doi: 10.1136/jmedgenet-2018-105714

4. Jackson BS, De Villiers M, Montwedi D. Association between pheochromocytoma and neurofibromatosis type I: A rare entity in the African population. *BMJ Case Rep* (2021) 14(5):e238380. doi: 10.1136/bcr-2020-238380

5. Gruber LM, Erickson D, Babovic-Vuksanovic D, Thompson GB, Young WFJr., Bancos I. Pheochromocytoma and paraganglioma in patients with neurofibromatosis type 1. *Clin Endocrinol (Oxf)*. (2017) 86(1):141–9. doi: 10.1111/cen.13163

6. Walther MM, Herring J, Enquist E, Keiser HR, Linehan WM. Von recklinghausen's disease and pheochromocytomas. *J Urol.* (1999) 162(5):1582–6. doi: 10.1016/S0022-5347(05)68171-2

7. Darrigo Junior LG, Ferraz VEF, Cormedi MCV, Araujo LHH, Magalhaes MPS, Carneiro RC, et al. Epidemiological profile and clinical characteristics of 491 Brazilian patients with neurofibromatosis type 1. *Brain Behav* (2022) 12(6):e2599. doi: 10.1002/brb3.2599

8. Kepenekian L, Mognetti T, Lifante JC, Giraudet AL, Houzard C, Pinson S, et al. Interest of systematic screening of pheochromocytoma in patients with neurofibromatosis type 1. *Eur J Endocrinol* (2016) 175(4):335–44. doi: 10.1530/EJE-16-0233

9. Gieldon L, Masjkur JR, Richter S, Darr R, Lahera M, Aust D, et al. Next-generation panel sequencing identifies NF1 germline mutations in three patients with pheochromocytoma but no clinical diagnosis of neurofibromatosis type 1. *Eur J Endocrinol* (2018) 178(2):K1–9. doi: 10.1530/EJE-17-0714

10. Burnichon N, Buffet A, Parfait B, Letouze E, Laurendeau I, Loriot C, et al. Somatic NF1 inactivation is a frequent event in sporadic pheochromocytoma. *Hum Mol Genet* (2012) 21(26):5397–405. doi: 10.1093/hmg/dds374

11. Albattal S, Alswailem M, Moria Y, Al-Hindi H, Dasouki M, Abouelhoda M, et al. Mutational profile and genotype/phenotype correlation of non-familial pheochromocytoma and paraganglioma. *Oncotarget* (2019) 10(57):5919–31. doi: 10.18632/oncotarget.27194

12. Parisien-La Salle S, Dumas N, Rondeau G, Latour M, Bourdeau I. Isolated pheochromocytoma in a 73-Year-Old man with no clinical manifestations of type 1 neurofibromatosis carrying an unsuspected deletion of the entire NF1 gene. *Front Endocrinol (Lausanne).* (2019) 10:546. doi: 10.3389/fendo.2019.00546

13. Glasker S, Neumann HPH, Koch CA, Vortmeyer A. *Von Hippel-lindau disease*. Feingold KR, Anawalt B, Boyce A, Chrousos G, de Herder WW, Dhatariya K, editors. South Dartmouth (MA: Endotext (2000).

14. Amodru V, Taieb D, Guerin C, Romanet P, Paladino N, Brue T, et al. MEN2-related pheochromocytoma: current state of knowledge, specific characteristics in MEN2B, and perspectives. *Endocrine* (2020) 69(3):496–503. doi: 10.1007/s12020-020-02332-2

15. Bendl J, Stourac J, Salanda O, Pavelka A, Wieben ED, Zendulka J, et al. PredictSNP: robust and accurate consensus classifier for prediction of disease-related mutations. *PloS Comput Biol* (2014) 10(1):e1003440. doi: 10.1371/journal.pcbi.1003440

16. Remacha L, Pirman D, Mahoney CE, Coloma J, Calsina B, Curras-Freixes M, et al. Recurrent germline DLST mutations in individuals with multiple pheochromocytomas and paragangliomas. *Am J Hum Genet* (2019) 104(4):651–64. doi: 10.1016/j.ajhg.2019.02.017

17. Bibikova M, Le J, Barnes B, Saedinia-Melnyk S, Zhou L, Shen R, et al. Genome-wide DNA methylation profiling using Infinium(R) assay. *Epigenomics* (2009) 1(1):177–200. doi: 10.2217/epi.09.14

18. Reich M, Ohm K, Angelo M, Tamayo P, Mesirov JP. GeneCluster 2.0: An advanced toolset for bioarray analysis. *Bioinformatics* (2004) 20(11):1797–8. doi: 10.1093/bioinformatics/bth138

19. Cascón A, Comino-Méndez I, Currás-Freixes M, De Cubas AA, Contreras L, Richter S, et al. Whole-exome sequencing identifies MDH2 as a new familial paraganglioma gene. *J Natl Cancer Institute* (2015) 107(5):djv053. doi: 10.1093/jnci/djv053

20. Remacha L, Comino-Mendez I, Richter S, Contreras L, Curras-Freixes M, Pita G, et al. Targeted exome sequencing of Krebs cycle genes reveals candidate cancer-predisposing mutations in pheochromocytomas and paragangliomas. *Clin Cancer Res* (2017) 23(20):6315–24. doi: 10.1158/1078-0432.CCR-16-2250

21. Buffet A, Zhang J, Rebel H, Corssmit EPM, Jansen JC, Hensen EF, et al. Germline DLST variants promote epigenetic modifications in pheochromocytoma-paraganglioma. *J Clin Endocrinol Metab* (2021) 106(2):459–71. doi: 10.1210/clinem/dgaa819

22. Behjati S, Tarpey PS, Presneau N, Scheipl S, Pillay N, Van Loo P, et al. Distinct H3F3A and H3F3B driver mutations define chondroblastoma and giant cell tumor of bone. *Nat Genet* (2013) 45(12):1479–82. doi: 10.1038/ng.2814

23. Toledo RA, Qin Y, Cheng ZM, Gao Q, Iwata S, Silva GM, et al. Recurrent mutations of chromatin-remodeling genes and kinase receptors in pheochromocytomas and paragangliomas. *Clin Cancer Res* (2016) 22(9):2301–10. doi: 10.1158/1078-0432.CCR-15-1841

24. Fishbein L, Leshchiner I, Walter V, Danilova L, Robertson AG, Johnson AR, et al. Comprehensive molecular characterization of pheochromocytoma and paraganglioma. *Cancer Cell* (2017) 31(2):181–93. doi: 10.1016/j.ccell.2017.01.001

25. Letouzé E, Martinelli C, Loriot C, Burnichon N, Abermil N, Ottolenghi C, et al. SDH mutations establish a hypermethylator phenotype in paraganglioma. *Cancer Cell* (2013) 23(6):739–52. doi: 10.1016/j.ccr.2013.04.018

26. Wachtel H, Fishbein L. Genetics of pheochromocytoma and paraganglioma. *Curr Opin Endocrinol Diabetes Obes* (2021) 28(3):283–90. doi: 10.1097/MED.0000000000000634

27. Andrews KA, Ascher DB, Pires DEV, Barnes DR, Vialard L, Casey RT, et al. Tumour risks and genotype-phenotype correlations associated with germline variants in succinate dehydrogenase subunit genes SDHB, SDHC and SDHD. *J Med Genet* (2018) 55(6):384–94. doi: 10.1136/jmedgenet-2017-105127

28. Toledo SP, Lourenco DMJr., Sekiya T, Lucon AM, Baena ME, Castro CC, et al. Penetrance and clinical features of pheochromocytoma in a six-generation family carrying a germline TMEM127 mutation. *J Clin Endocrinol Metab* (2015) 100(2):E308–18. doi: 10.1210/jc.2014-2473

29. Buffet A, Morin A, Castro-Vega LJ, Habarou F, Lussey-Lepoutre C, Letouze E, et al. Germline mutations in the mitochondrial 2-Oxoglutarate/Malate carrier SLC25A11 gene confer a predisposition to metastatic paragangliomas. *Cancer Res* (2018) 78(8):1914–22. doi: 10.1158/0008-5472.CAN-17-2463

30. Sabbagh A, Pasmant E, Laurendeau I, Parfait B, Barbarot S, Guillot B, et al. Unravelling the genetic basis of variable clinical expression in neurofibromatosis 1. *Hum Mol Genet* (2009) 18(15):2768–78. doi: 10.1093/hmg/ddp212

31. Pasmant E, Vidaud M, Vidaud D, Wolkenstein P. Neurofibromatosis type 1: from genotype to phenotype. *J Med Genet* (2012) 49(8):483–9. doi: 10.1136/jmedgenet-2012-100978

32. Pemov A, Sung H, Hyland PL, Sloan JL, Ruppert SL, Baldwin AM, et al. Genetic modifiers of neurofibromatosis type 1-associated cafe-au-lait macule count identified using multi-platform analysis. *PloS Genet* (2014) 10(10):e1004575. doi: 10.1371/journal.pgen.1004575

33. Warrington NM, Sun T, Luo J, McKinstry RC, Parkin PC, Ganzhorn S, et al. The cyclic AMP pathway is a sex-specific modifier of glioma risk in type I neurofibromatosis patients. *Cancer Res* (2015) 75(1):16–21. doi: 10.1158/0008-5472.CAN-14-1891

34. Yu Y, Choi K, Wu J, Andreassen PR, Dexheimer PJ, Keddache M, et al. NF1 patient missense variants predict a role for ATM in modifying neurofibroma initiation. *Acta Neuropathol.* (2020) 139(1):157–74. doi: 10.1007/s00401-019-02086-w

35. Kajiwara K, Berson EL, Dryja TP. Digenic retinitis pigmentosa due to mutations at the unlinked peripherin/RDS and ROM1 loci. *Science* (1994) 264 (5165):1604–8. doi: 10.1126/science.8202715

36. Katsanis N, Ansley SJ, Badano JL, Eichers ER, Lewis RA, Hoskins BE, et al. Triallelic inheritance in bardet-biedl syndrome, a mendelian recessive disorder. *Science* (2001) 293(5538):2256–9. doi: 10.1126/science.1063525

37. Mukherjee S, Cogan JD, Newman JH, Phillips JA3rd, Hamid RUndiagnosed Diseases N, et al. Identifying digenic disease genes *via* machine learning in the undiagnosed diseases network. *Am J Hum Genet* (2021) 108(10):1946–63. doi: 10.1016/j.ajhg.2021.08.010

38. Xu W, Li Y, Liu C, Zhao S. Protein lysine acetylation guards metabolic homeostasis to fight against cancer. *Oncogene* (2014) 33(18):2279–85. doi: 10.1038/onc.2013.163

39. Zhao S, Xu W, Jiang W, Yu W, Lin Y, Zhang T, et al. Regulation of cellular metabolism by protein lysine acetylation. *Science* (2010) 327(5968):1000–4. doi: 10.1126/science.1179689

40. Calsina B, Curras-Freixes M, Buffet A, Pons T, Contreras L, Leton R, et al. Role of MDH2 pathogenic variant in pheochromocytoma and paraganglioma patients. *Genet Med* (2018) 20(12):1652–62. doi: 10.1038/s41436-018-0068-7

41. Group NGSiPS, Toledo RA, Burnichon N, Cascon A, Benn DE, Bayley JP, et al. Consensus statement on next-generation-sequencing-based diagnostic testing of hereditary phaeochromocytomas and paragangliomas. *Nat Rev Endocrinol* (2017) 13(4):233–47. doi: 10.1038/nrendo.2016.185

42. Welander J, Larsson C, Backdahl M, Hareni N, Sivler T, Brauckhoff M, et al. Integrative genomics reveals frequent somatic NF1 mutations in sporadic pheochromocytomas. *Hum Mol Genet* (2012) 21(26):5406–16. doi: 10.1093/hmg/dds402

43. Dahia PL. The genetic landscape of pheochromocytomas and paragangliomas: Somatic mutations take center stage. *J Clin Endocrinol Metab* (2013) 98(7):2679–81. doi: 10.1210/jc.2013-2191

44. Dahia PL. Pheochromocytoma and paraganglioma pathogenesis: Learning from genetic heterogeneity. *Nat Rev Cancer.* (2014) 14(2):108–19. doi: 10.1038/nrc3648

45. Choi YM, Lim J, Jeon MJ, Lee YM, Sung TY, Hong EG, et al. Mutation profile of aggressive pheochromocytoma and paraganglioma with comparison of TCGA data. *Cancers (Basel)* (2021) 13(10):2389. doi: 10.3390/cancers13102389

46. Armstrong N, Storey CM, Noll SE, Margulis K, Soe MH, Xu H, et al. SDHB knockout and succinate accumulation are insufficient for tumorigenesis but dual SDHB/NF1 loss yields SDHx-like pheochromocytomas. *Cell Rep* (2022) 38 (9):110453. doi: 10.1016/j.celrep.2022.110453

47. Lussey-Lepoutre C, Buffet A, Morin A, Goncalves J, Favier J. Rodent models of pheochromocytoma, parallels in rodent and human tumorigenesis. *Cell Tissue Res* (2018) 372(2):379–92. doi: 10.1007/s00441-018-2797-y

48. Barbolosi D, Crona J, Serre R, Pacak K, Taieb D. Mathematical modeling of disease dynamics in SDHB- and SDHD-related paraganglioma: Further step in understanding hereditary tumor differences and future therapeutic strategies. *PloS One* (2018) 13(8):e0201303. doi: 10.1371/journal.pone.0201303

49. Fishbein L, Khare S, Wubbenhorst B, DeSloover D, D'Andrea K, Merrill S, et al. Whole-exome sequencing identifies somatic ATRX mutations in pheochromocytomas and paragangliomas. *Nat Commun* (2015) 6:6140. doi: 10.1038/ncomms7140

50. Job S, Draskovic I, Burnichon N, Buffet A, Cros J, Lepine C, et al. Telomerase activation and ATRX mutations are independent risk factors for metastatic pheochromocytoma and paraganglioma. *Clin Cancer Res* (2019) 25(2):760–70. doi: 10.1158/1078-0432.CCR-18-0139

51. Tong S, Devine WP, Shieh JT. Tumor and constitutional sequencing for neurofibromatosis type 1. *JCO Precis Oncol* (2022) 6:e2100540. doi: 10.1200/PO.21.00540

52. Robinson-White A, Hundley TR, Shiferaw M, Bertherat J, Sandrini F, Stratakis CA. Protein kinase-a activity in PRKAR1A-mutant cells, and regulation of mitogen-activated protein kinases ERK1/2. *Hum Mol Genet* (2003) 12(13):1475–84. doi: 10.1093/hmg/ddg160

53. Kirschner LS, Carney JA, Pack SD, Taymans SE, Giatzakis C, Cho YS, et al. Mutations of the gene encoding the protein kinase a type I-alpha regulatory subunit in patients with the Carney complex. *Nat Genet* (2000) 26(1):89–92. doi: 10.1038/79238

54. Romei C, Elisei R. RET/PTC translocations and clinico-pathological features in human papillary thyroid carcinoma. *Front Endocrinol (Lausanne).* (2012) 3:54. doi: 10.3389/fendo.2012.00054

55. Jones GN, Tep C, Towns WH2nd, Mihai G, Tonks ID, Kay GF, et al. Tissue-specific ablation of Prkar1a causes schwannomas by suppressing neurofibromatosis protein production. *Neoplasia* (2008) 10(11):1213–21. doi: 10.1593/neo.08652

56. Martini L. *Encyclopedia of endocrine diseases*. Amsterdam: Elsevier (2004).

frontiers | Frontiers in Endocrinology

TYPE Original Research
PUBLISHED 05 April 2023
DOI 10.3389/fendo.2023.1128061

OPEN ACCESS

EDITED BY
Marta Araujo-Castro,
Ramón y Cajal University Hospital, Spain

REVIEWED BY
Stephen Joel Winters,
University of Louisville, United States
Jaydira Del Rivero,
National Cancer Institute (NIH), United States
Filippo Ceccato,
University of Padua, Italy

*CORRESPONDENCE
Alfredo Berruti
alfredo.berruti@gmail.com

†These authors have contributed equally to this work and share first authorship

‡These authors have contributed equally to this work and share senior authorship

SPECIALTY SECTION
This article was submitted to Adrenal Endocrinology, a section of the journal Frontiers in Endocrinology

RECEIVED 20 December 2022
ACCEPTED 22 March 2023
PUBLISHED 05 April 2023

CITATION
Delbarba A, Cosentini D, Facondo P, Laganà M, Pezzaioli LC, Cremaschi V, Alberti A, Grisanti S, Cappelli C, Ferlin A and Berruti A (2023) Androgen serum levels in male patients with adrenocortical carcinoma given mitotane therapy: A single center retrospective longitudinal study. *Front. Endocrinol.* 14:1128061. doi: 10.3389/fendo.2023.1128061

Androgen serum levels in male patients with adrenocortical carcinoma given mitotane therapy: A single center retrospective longitudinal study

Andrea Delbarba[1†], Deborah Cosentini[2†], Paolo Facondo[1], Marta Laganà[2], Letizia Chiara Pezzaioli[1], Valentina Cremaschi[2], Andrea Alberti[2], Salvatore Grisanti[2], Carlo Cappelli[1], Alberto Ferlin[3‡] and Alfredo Berruti[2*‡]

[1]Department of Experimental Sciences, Unit of Endocrinology and Metabolism, University of Brescia, Azienda Socio Sanitaria Territoriale (ASST) Spedali Civili, Brescia, Italy, [2]Department of Medical and Surgical Specialties, Radiological Sciences, and Public Health, Medical Oncology Unit, University of Brescia, ASST Spedali Civili, Brescia, Italy, [3]Unit of Andrology and Reproductive Medicine, Department of Medicine, University of Padua, Padua, Italy

Objective: Hypogonadism is common in male patients with adrenocortical carcinoma (ACC) who are under treatment with mitotane, but the phenomenon is underestimated, and its prevalence has been poorly studied. This single-center retrospective longitudinal study was undertaken to assess the frequency of testosterone deficiency before and after mitotane therapy, the possible mechanism involved, and the relationship between hypogonadism with serum mitotane levels and prognosis.

Research design and methods: Consecutive male ACC patients followed at the Medical Oncology of Spedali Civili Hospital in Brescia underwent hormonal assessment to detect testosterone deficiency at baseline and during mitotane therapy.

Results: A total of 24 patients entered the study. Of these patients, 10 (41.7%) already had testosterone deficiency at baseline. During follow-up, total testosterone (TT) showed a biphasic evolution over time with an increase in the first 6 months followed by a subsequent progressive decrease until 36 months. Sex hormone binding globulin (SHBG) progressively increased, and calculated free testosterone (cFT) progressively decreased. Based on cFT evaluation, the proportion of hypogonadic patients progressively increased with a cumulative prevalence of 87.5% over the study course. A negative correlation was observed between serum mitotane levels >14 mg/L and TT and cFT.

10.3389/fendo.2023.1128061

Conclusion: Testosterone deficiency is common in men with ACC prior to mitotane treatment. In addition, this therapy exposes these patients to further elevated risk of hypogonadism that should be promptly detected and counteracted, since it might have a negative impact on quality of life.

KEYWORDS

adrenal tumor, mitotane, androgens, hypogonadism, testosterone

Introduction

Mitotane, a derivative of the pesticide dichlorodiphenyltrichloroethane (DDT), is the only systemic therapy approved for the management of adrenocortical carcinoma (ACC) (1), an extremely rare disease with an estimated incidence in western countries ranging between 0.7 and 2 new cases per million population per year (2). The drug, either administered alone (2) or in combination with chemotherapy (3, 4), the EDP regimen (etoposide, doxorubicin, and cisplatin), still represents the only standard systemic therapy for ACC patients with locally advanced or metastatic disease who are not eligible for surgery (5, 6). Mainly thanks to the results of a retrospective study, which compared the outcome of ACC patients using or not using mitotane in adjuvant setting (7, 8), this therapy is recommended by the current international guidelines (5, 6) in patients undergoing radical surgery who are at high risk of relapse and death.

Mitotane is a drug difficult to manage, due to its long half-life, dose-limiting toxicity, and narrow therapeutic window. The strategy of mitotane administration is to achieve and maintain over time circulating drug concentrations ranging between 14 and 20 mg/L (9–11). Unfortunately, mitotane therapy leads to several adverse effects ranging from limited to severe, the most common toxicities involving the endocrine, gastrointestinal, and central nervous systems (12). The side effects are obviously increased when mitotane is administered in association with chemotherapy (13). As regard the endocrine side effects, mitotane therapy induces a deep inhibition of adrenal cortical function resulting in hypoadrenalism and the need in all patients for glucocorticoid supplementation, with individualized dosing, being tapered on the basis of a patient's clinical symptoms and signs of hypoadrenalism (e.g. fatigue, muscle weakness) (14). Moreover, mitotane affects thyroid function, causing central hypothyroidism, burdened by asthenia and concentration deficits, which can ameliorate with the levothyroxine replacement therapy (12, 15).

Hypogonadism (low testosterone) in men is also frequently observed with a reported frequency ranging between 26% and 57% (12). This side effect is potentially relevant, since low testosterone has impacts on many organs (such as the cardiovascular, bones, adipose tissue, and skeletal muscles) and general well-being, and it may worsen asthenia, fatigue, and depression commonly reported by mitotane-treated patients. Although testosterone replacement therapy may ameliorate these symptoms (12), hypogonadism during mitotane treatment is underestimated and poorly characterized, and as a consequence, testosterone therapy is often started late or never considered (12, 13). This is an important issue particularly in ACC patients in whom the drug is administered in adjuvant setting, since they are young, disease free, and potentially cured, and receive the drug for a long period of time. Furthermore, the possible causes and onset timing of hypogonadism have not been well-defined in the literature. In fact, hypogonadism could result from primary deficiency of testosterone production, secondary deficiency from hypothalamus–pituitary dysfunction, or from increased production of sex hormone binding globulin (SHBG) from the liver that reduces the free amount of testosterone (representing the active form).

In this study, we retrospectively assessed the series of ACC male patients treated at the Medical Oncology of the Spedali Civili in Brescia, a reference center for this rare disease in Italy, with the aim of assessing the frequency of testosterone deficiency before and after mitotane therapy, the possible mechanisms involved, and the correlation between hypogonadism with serum mitotane levels and prognosis.

Methods

This is a retrospective longitudinal study. Data of the patients from the Oncology Unit of Spedali Civili in Brescia, from January 2013 to September 2021, were collected, according to the following inclusion criteria: male sex, age ≥ 18 years, histological diagnosis of ACC, availability of data regarding gonadal and adrenal androgens biochemical profiles performed prior to mitotane treatment (alone or in association with chemotherapy) and at least once during therapy, blood samples at fasting in the morning between 8:00 and 10:00 analyzed at the central laboratory of University Hospital of Brescia (chemiluminescence immunoassay).

The primary endpoint of the study was the prevalence of male hypogonadism in men with ACC under adjuvant mitotane therapy. Secondary endpoints were the correlation between serum mitotane levels and gonadal function over time of therapy (up to 36 months), the possible mechanisms involved in the onset of hypogonadism, and the impact of testosterone deficiency on prognosis.

Anthropometric data, smoke and alcohol habits, ACC, and treatment information were collected for all the included patients. ACC hormone secretion was defined as elevated biochemical values of adrenal and gonadal hormones (cortisol, adrenal androgens, aldosterone, and estrogens). In detail, cortisol hypersecretion was

10.3389/fendo.2023.1128061

defined as basal blood values of cortisol > 20 μg/dl and ACTH < 10 pg/ml (not in the course of glucocorticoids therapy). The presence of high-dose glucocorticoids therapy was defined as treatment with cortone acetate ≥50 mg daily or equivalent (due to clinical indication for the management of hypoadrenalism in course of adjuvant treatment).

At baseline (in detail, after adrenal surgery and prior to mitotane therapy) and after 3, 6, 12, 24, and 36 months of this adjuvant treatment, the following were analyzed: serum mitotane levels, total testosterone (TT), SHBG, calculated free testosterone (cFT) using Vermeulen formula (available at http://www.issam.ch/freetesto.htm), estradiol (E2), hemoglobin, hematocrit, creatinine, androstenedione, dehydroepiandrosterone sulfate (DHEAS), and 17-hydroxy progesterone (17OH-P).

To detect hypogonadism, testosterone deficiency was defined based on the biochemical finding of low TT and/or cFT. In details, cut-off values for defined low TT and cFT were <3.5 ng/ml and <63 pg/ml, respectively (16, 17). Eugonadal patients were defined for values of TT ≥3.5 ng/ml and cFT ≥63 pg/ml. In patients receiving testosterone therapy, its possible benefits were evaluated in terms of patient-reported clinical improvement in asthenia, muscle strength, and perceived well-being.

Statistical analysis

Statistical Package for the Social Sciences software IBM SPSS Statistics, Version 25.0, Armonk, (NY) was used for statistical analysis. Since the variables were not normally distributed (Kolmogorov–Smirnov test was used), the comparison between quantitative variables was performed with Wilcoxon test, whereas the comparison between categorial variables was performed with chi-square test. During follow-up, the comparison between quantitative variables over time was performed with ANOVA test. Correlation between serum mitotane levels and biochemical data was performed with Spearman correlation. Kaplan–Meier curves were designed to assess the impact of testosterone deficiency on progression-free survival (PFS, defined as months without metastasis) and overall survival (OS). p-values<0.05 were considered statistically significant.

Results

Of the 61 men evaluated for inclusion, 24 patients met eligibility inclusion criteria (Supplementary Figure S1). Data at baseline (after adrenal surgery and prior to the start of mitotane treatment) are shown in Table 1. At diagnosis, 10 patients (41.7%) were already hypogonadal (nine with low TT and one with low cFT). Of the latter, none had other known testicular–pituitary disease or a recent significant change in body weight or were taking high-dose glucocorticoid therapy or drugs interfering with gonadal function. No differences were observed regarding hypogonadism prevalence in men with secreting (cortisol and/or other adrenal–gonadal hormones) vs. non-secreting ACC and in patients with metastatic vs. non-metastatic tumor.

TABLE 1 Baseline characteristics of the included patients (n=24) prior to the start of mitotane.

Age at diagnosis (years)		52.5 (42.8-58)
BMI (kg/m^2)		24.5 (22-25.8)
Smoking habit	Current smokers	3 (12.5%)
	Past smokers	9 (37.5%)
Alcohol habit	Regular drinkers	7 (29.2%)
	Occasional drinkers	5 (20.8%)
ACC side (left)		15 (62.5%)
ACC secretion	Non-secreting ACC	14 (58.3%)
	Only cortisol	5 (20.8%)
	Cortisol + adrenal androgens	2 (8.3%)
	Cortisol + aldosterone	1 (4.2%)
	Cortisol + estrogens	1 (4.2%)
	Only estrogens	1 (4.2%)
Metastatic ACC		15 (62.5%)
Hypogonadism		10 (41.7%)

Data are expressed as median (IQR) for continuous variables and as absolute number (%) for categorical variables. IQR, interquartile range; BMI, Body Mass Index; ACC, adrenocortical carcinoma.

The comparison between hypogonadal and eugonadal patients at baseline (prior to adjuvant treatment) is shown in Table 2. No significant differences were found in terms of age at diagnosis of ACC, Body Mass Index (BMI), smoke or alcohol habits, and ACC characteristics. At baseline, apart from TT levels, only DHEAS was significantly different between patients with hypogonadism and eugonadism (3.7 vs. 0.3 μg/ml; p=0.001); the two patients affected by secreting adrenal androgens ACC with high DHEAS levels (>6 μg/ml) were present in the hypogonadal group.

Median age at start of mitotane therapy was 52.5 years (43.5–58.8), and median duration of treatment was 23.5 months (11.75–33.75). The median time to attain serum mitotane levels within the therapeutic range (defined as mitotanemia > 14 mg/l) was 4 months (3.5–10.5). In 14 cases (58.3%), mitotane was given alone, whereas in 10 patients (41.6%), it was combined with chemotherapy.

Table 3 shows the variation in biochemical and clinical parameters during treatment with mitotane. TT showed a biphasic evolution with the progressive increase in serum mitotane levels over time: it significantly increased in the first 6 months and then decreased progressively until 36 months. On the contrary, SHBG progressively and significantly increased over the entire follow-up period, and as a consequence, cFT progressively and significantly decreased over time. Therefore, the prevalence of hypogonadism during the follow-up was unchanged when considering TT but significantly increased when considering cFT. Besides the 10 patients with testosterone deficiency before mitotane therapy (considering TT and/or cFT), 11/14 men (78.6%) developed hypogonadism during the treatment, with seven of them showing low cFT with normal TT levels. The cumulative prevalence of testosterone deficiency over the course of the study was therefore 87.5% (21/24 patients).

10.3389/fendo.2023.1128061

TABLE 2 Comparison between hypogonadal and eugonadal patients prior to the start of mitotane.

		Hypogonadal patients (N=10)	Eugonadal patients (N=14)	p
BMI (kg/m^2)		25.0 (22.5-25.0)	23.0 (21.0-27.0)	0.787
Age at diagnosis (years)		49.0 (41.5-57.0)	54.5 (41.8-64.0)	0.463
Smoking habit	Current smokers	3 (30.0%)	0 (0.0%)	0.061
	Past smokers	2 (20.0%)	7 (50.0%)	0.061
Alcohol habit	Regular drinkers	2 (20.0%)	5 (35.7%)	0.243
	Occasional drinkers	1 (10.0%)	4 (28.6%)	0.243
Secreting ACC		5 (50.0%)	5 (35.7%)	0.423
Metastatic ACC		6 (60.0%)	9 (64.3%)	0.825
Haemoglobin (g/dl)		13.5 (11.7-15.4)	13.6 (12.5-14.3)	0.777
Haematocrit (%)		41.1 (36.0-45.3)	39.4 (37.6-42.7)	0.549
Creatinine (mg/dl)		0.7 (0.5-0.9)	0.8 (0.7-1.1)	0.139
TT (ng/ml)		2.4 (1.4-3.1)	5.5 (4.0-6.8)	**0.001**
SHBG (nmol/l)		53.0 (24.8-65.5)	59.5 (30.3-71.5)	0.663
cFT (pg/ml)		65.3 (59.2-98.1)	97.4 (69.6-121.4)	0.125
E2 (pg/ml)		25.0 (18.0-26.0)	23.5 (12.8-32.0)	0.764
Androstenedione (ng/ml)		1.7 (0.9-3.6)	0.8 (0.6-1.1)	0.065
DHEAS (μg/ml)		3.7 (1.4-6.5)	0.3 (0.2-0.7)	**0.001**
17OH-P (ng/ml)		3.4 (1.1-3.7)	1.4 (1.2-1.7)	0.073

Data are expressed as median (IQR) for continuous variables and as absolute number (%) for categorical variables. A comparison between continuous variables was performed with Wilcoxon test; a comparison between categorical variables was performed with chi-square test. IQR, interquartile range; BMI, Body Mass Index; ACC, adrenocortical carcinoma; TT, total testosterone; SHBG, sex hormone binding globulin; cFT, calculated free testosterone; E2, estradiol; DHEAS, dehydroepiandrosterone; 17OH-P, 17-hydroxyprogesterone; significant data in bold.

During mitotane treatment, 91.7% (22/24) of patients required high-dose glucocorticoid therapy. There were no significant differences in hypogonadism prevalence with respect to the presence or absence of high-dose glucocorticoid therapy (20/22 vs. 1/2, p=0.094). At all times of evaluation, there was no significant difference in testosterone deficiency prevalence between men treated with mitotane alone with respect to those with also chemotherapy.

Figure 1 shows the median trend of TT, SHBG, and cFT levels during mitotane treatment. A significant reduction in hemoglobin and hematocrit was found in the first 6 months of treatment. Androstenedione increased in the first 3 months and then progressively decreased, whereas a progressive decrease in DHEAS was observed without statistical significance.

The correlation between serum mitotane levels over time, and gonadal axis variations is shown in Table 4. Within the first 6 months of mitotane treatment, a positive correlation was shown between serum mitotane levels and testosterone deficiency and between serum mitotane levels and SHBG levels, especially when mitotane levels were >14 mg/L. Similarly, a negative correlation was observed between serum mitotane levels >14 mg/L and TT and cFT. The positive correlation between mitotane levels and testosterone deficiency was confirmed at 36 months. No correlations were found between mitotane levels and the other hormones, and between BMI with respect to mitotane levels and gonadal axis (TT, SHBG, and cFT).

By the end of the whole study period (36 months), 21 patients (87.5%) had metastatic ACC and eight (33.3%) died, of which three were hypogonadal prior to the start of mitotane treatment and five had developed testosterone deficiency during follow-up. However, testosterone deficiency (both at baseline and developed during the treatment) had no impact on PFS and OS (Figure 2).

During the study (after 12 or 24 months of mitotane treatment), four men received testosterone replacement therapy (in these four patients, the subsequent serum gonadal hormonal measurements—modified by testosterone therapy—were not considered to calculate the prevalence of hypogonadism). Of them, two were treated with injective undecanoate testosterone 1 g every 3 months and two with transdermal testosterone 20 mg daily. Substitution therapy was started based on the presence of sexual symptoms, severe asthenia, and reduced muscle strength. A slight clinical improvement was reported by these patients after 6 months of testosterone treatment.

Discussion

In this single-center retrospective study involving male ACC patients undergoing treatment with mitotane, we showed a relevant proportion of testosterone deficiency with a cumulative prevalence over the course of the study of 87.5%. These data expand the results of previous studies (12, 15, 18, 19); nevertheless, we found a higher proportion of hypogonadal patients (reported from 26% to 57% in

10.3389/fendo.2023.1128061

TABLE 3 Variation in biochemical and clinical parameters and serum mitotane levels during follow-up.

	Before mitotane (n=24)	3 months (n=21)	6 months (n=22)	12 months (n=17)	24 months (n=14)	36 months (n=10)	p
Haemoglobin (g/dl)	13.5 (12.5-14.8)	13.0 (11.1-13.5)	12.2 (11.1-12.9)	12.4 (11.8-13.8)	13.9 (12.8-14.6)	13.9 (12.9-14.4)	**0.041**
Haematocrit (%)	40.2 (37.7-43.2)	38.5 (33.2-40.6)	36.5 (33.4-37.9)	38.6 (35.6-40.9)	40.9 (36.9-42.7)	41.1 (38.4-42.2)	**0.048**
Creatinine (mg/dl)	0.8 (0.7-1.1)	0.8 (0.5-1.0)	0.7 (0.6-0.8)	0.9 (0.8-1.3)	1.1 (0.8-1.3)	0.8 (0.7-1.0)	0.106
BMI (kg/m^2)	23.6 (22.2-25.9)	24.5 (22.3-25.9)	25.4 (22.4-26.1)	23.8 (21.9-25.2)	23.2 (22.7-26.0)	23.9 (22.4-26.3)	0.322
TT (ng/ml)	3.8 (2.5-5.9)	7.7 (3.9-11.6)	7.8 (3.8-11.7)	4.7 (2.7-8.8)	4.3 (2.9-6.1)	3.6 (2.6-7.4)	**0.043**
SHBG (nmol/l)	55.0 (22.0-66.0)	126.0 (65.5-213.5)	152.5 (78.0-192.5)	157.5 (98.8-234.8)	195.0 (158.8-406.8)	194.0 (126.0-402.0)	**0.010**
cFT (pg/ml)	65.3 (57.2-78.2)	53.5 (23.5-109.9)	47.5 (23.5-87.0)	36.6 (11.5-67.3)	18.3 (5.9-28.5)	17.7 (9.2-25.3)	**0.017**
TT < 3.5 ng/ml	9/24 (37.5%)	4/21 (19.0%)	5/22 (22.7%)	6/17 (35.3%)	5/14 (35.7%)	4/10 (40.0%)	0.538
cFT < 63 pg/ml	1/6 (16.7%)	9/15 (60.0%)	10/14 (71.4%)	9/11 (81.8%)	8/9 (88.9%)	6/6 (100.0%)	**0.037**
E2 (pg/ml)	24.0 (15.5-29.0)	25.0 (14.0-32.8)	27.0 (19.0-39.5)	32.0 (20.5-45.0)	25.0 (16.0-26.0)	25.0 (19.6-29.0)	0.402
Androstenedione (ng/ml)	0.9 (0.8-2.3)	1.2 (0.4-2.7)	0.9 (0.4-2.1)	0.4 (0.3-0.9)	0.3 (0.2-0.7)	0.6 (0.2-0.9)	**0.048**
DHEAS (µg/ml)	0.5 (0.2-3.5)	0.2 (0.2-0.6)	0.2 (0.2-0.5)	0.2 (0.2-1.5)	0.2 (0.2-0.5)	0.2 (0.1-2.1)	0.110
17OH-P (ng/ml)	1.5 (1.2-1.9)	1.9 (1.5-2.6)	2.0 (1.4-3.0)	1.5 (0.9-2.0)	1.2 (0.6-1.6)	1.2 (0.4-1.9)	0.093
Mitotanemia (mg/l)	–	8.0 (3.8-11.2)	9.5 (6.3-13.9)	13.2 (10.8-17.2)	14.4 (11.0-16.5)	14.3 (10.0-19.0)	**0.018**

Data are expressed as median (IQR) for continuous variables and as absolute number (%) for categorical variables. Comparison between continuous variables was performed with ANOVA test for repeated measures (including post-hoc Tukey's analysis); a comparison between categorical variables was performed with chi-square test. IQR, interquartile range; TT, total testosterone; SHBG, sex hormone binding globulin; cFT, calculated free testosterone; E2, estradiol; DHEAS, dehydroepiandrosterone; 17OH-P, 17-hydroxy progesterone; BMI, Body Mass Index; significant data in bold.

the previous studies) (12). This difference could be related to two main factors: the longer follow-up period of our study and the more detailed analysis of hypogonadism based on both TT and cFT.

Noteworthy, 40% of our patients reported testosterone deficiency already before starting mitotane treatment (after adrenal surgery), and the prevalence further increased during the 36 months of follow-up. The proportion of testosterone deficiency in our series did not change in relation to the presence or absence of metastatic disease and the ACC secretory status. These data suggest that neither the tumoral extension nor the tumoral hormonal hypersecretion influenced this phenomenon. Instead, the high prevalence of testosterone deficiency at baseline could be explained by two factors. First of all is the fragility of these patients, given the tumoral condition, with a consequent detrimental effect on gonadal function and reduced production of testosterone. In addition, due to ACC, a possible subversion of adrenal steroidogenesis, with consequent reduction in the amount of testosterone produced by the adrenal glands, cannot be excluded. In particular, an arrest in the last stages of adrenal steroidogenesis (above all due to enzymatic deficiency of 17-beta hydroxysteroid dehydrogenase) can result in the accumulation of androgen precursors (DHEAS, 17-OH progesterone, and androstenedione), reducing the conversion to testosterone (20). Indeed, serum levels of androgen precursors (above all DHEAS) were higher in men with testosterone deficiency than in eugonadal patients at baseline conditions (in part, probably also because of the two patients with secreting adrenal androgens ACC were in the hypogonadal group). This observation confirms the importance of evaluating the androgenic profile also in the male ACC patients, as recommended by international guidelines (5, 6).

On the other hand, the most important factor contributing to the development of testosterone deficiency during the treatment with mitotane is the progressive increase in SHBG levels, produced by the liver through an estrogenic-like effect of mitotane already described (mediated by the induction of transcription factors for SHBG) (12, 15, 21). The increased

10.3389/fendo.2023.1128061

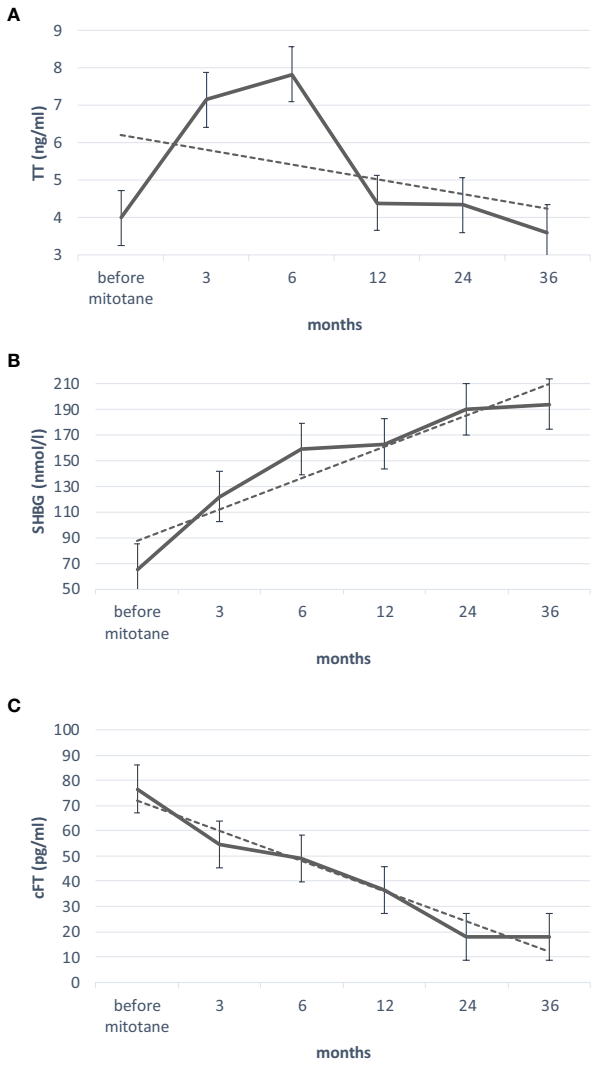

FIGURE 1
Trend of TT **(A)**, SHBG **(B)** and cFT **(C)** levels, during mitotane treatment. Friedman test was used to develop the trend lines. TT, total testosterone; SHBG, sex hormone binding globulin; cFT, calculated free testosterone. Trend lines in dotted.

amount of SHBG binds more testosterone resulting in an increase in TT levels and a decrease in free testosterone (which is the active form of the hormone), with a consequent alteration of testosterone production (22). In fact, during mitotane treatment, most patients were diagnosed with hypogonadism due to low cFT values, with normal, or even elevated, TT levels. Therefore, our results strongly suggest that cFT assessment is essential for the evaluation of the male gonadal status, as also recommended by recent guidelines (17, 23) in the general population. In addition, despite a not significant difference (given the small number of cases), another mechanism that contributes to the development of hypogonadism in these patients is the high-dose glucocorticoid therapy (due to its known interfering effect on male gonadal axis) (15). The latter is necessary in most patients during adjuvant treatment, given the increase in cortisol binding globulin (CBG) induced by mitotane (with a consequent need of further increased therapy) (15).

In details, our data revealed a biphasic change in TT levels with a significant increase in the first 6 months and then a progressive decrease. This initial increase in testosterone levels was also observed in a previous paper by Basile and colleagues (15). However, in that study, the increase in TT levels was maintained throughout an observation period of 24 months, and this observation is in contrast with our data. We do not have an explanation for this discrepancy. More interestingly is the evolution of cFT levels that progressively reduced over time, due to the observed strong increase in SHBG values. From a pathophysiological point of view, our hypothesis is that the reduction in free testosterone induces a pituitary compensation similarly to what has been described in other populations with elevated SHBG, as men with human immunodeficiency virus under retroviral therapy (24). In particular, as SHBG increases, the pituitary production of luteinizing hormone (LH) increases due to lower negative feedback by free testosterone, and therefore, Leydig cells are stimulated to produce higher amount of testosterone to gain a new steady state, as suggested by de Ronde et al. (22). Once this compensation mechanism is exhausted, TT also falls (22, 24). This possible mechanism to explain the observed biphasic TT trend

TABLE 4 Correlations between serum mitotane levels and gonadal function over time.

Serum mitotane levels	3 mo (mg/L)	3 mo > 14 mg/L	6 mo (mg/L)	6 mo > 14 mg/L	12 mo (mg/L)	12 mo. > 14 mg/L	24 mo (mg/L)	24 mo. > 14 mg/L	36 mo (mg/L)	36 mo. > 14 mg/L
TT (ng/ml)	0.298	-0.401	-0.271	**-0.446** *	-0.231	-0.364	0.093	0.301	-0.351	-0.218
SHBG (nmol/l)	0.342	**0.586** *	0.420	**0.626** *	-0.086	0.126	0.429	0.504	0.714	0.577
cFT (pg/ml)	-0.414	-0.537	-0.441	**-0.713** **	-0.200	-0.252	-0.214	-0.126	0.000	-0.707
Hypogonadism	**0,505** *	**0.632** **	0.276	**0.486** *	0.186	0.260	-0.215	0.183	**0.635** *	**0.688** **

Correlation between variables was performed with Spearman correlation. TT, total testosterone; SHBG, sex hormone binding globulin; cFT, calculated free testosterone; mo, months. Number of patients: 3 mo=21; 6 mo=22; 12 mo=17; 24 mo=14; 36 mo=10.
*Correlation is significant at p=0.05 (two-tail).
** Correlation is significant at p=0.01 (two-tail).
significant data in bold.

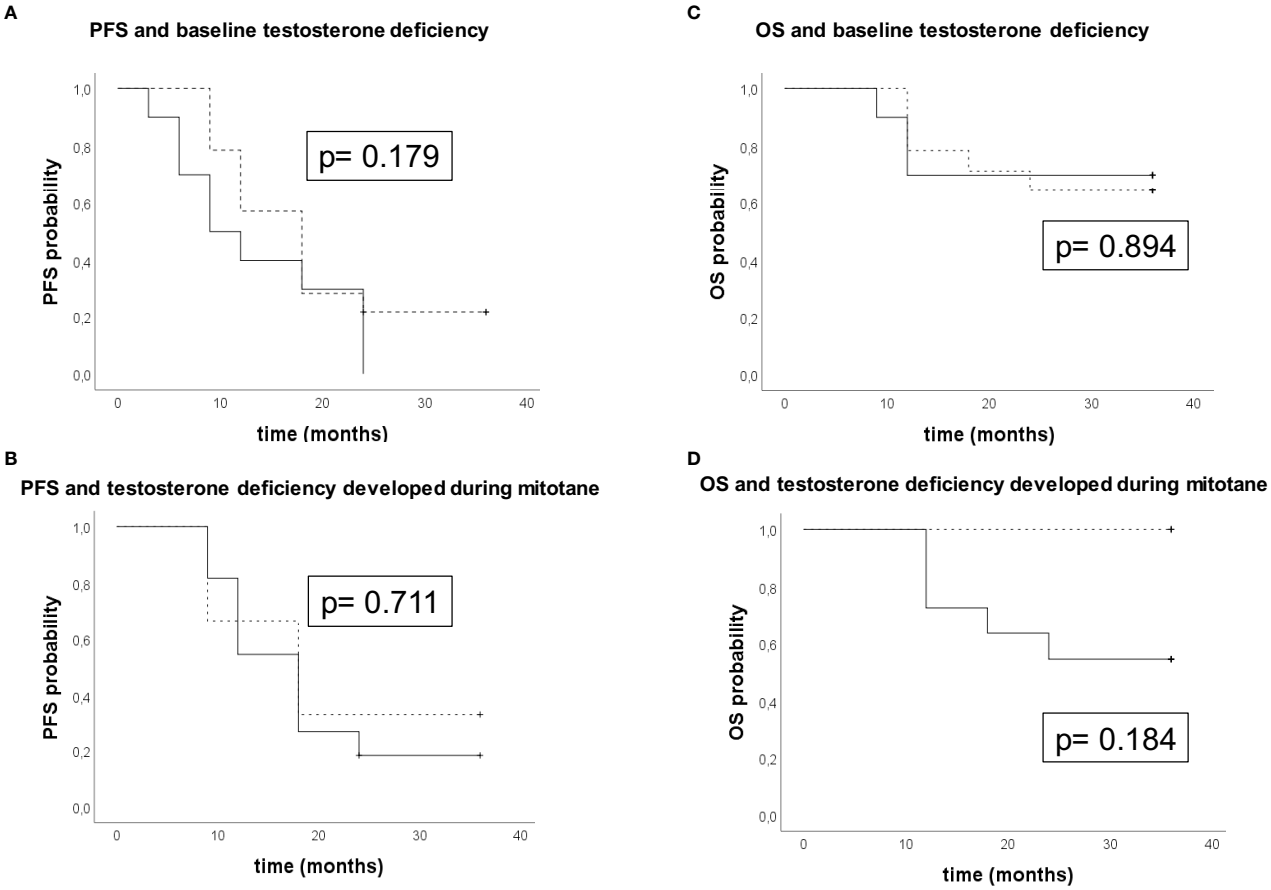

FIGURE 2
Impact of testosterone deficiency on PFS and OS. **(A)** Baseline testosterone deficiency and PFS: cases of metastasis in men with baseline testosterone deficiency (10/10) vs. baseline eugonadal men (11/14); **(B)** testosterone deficiency developed during treatment and PFS: cases of metastasis in men with developed testosterone deficiency (9/11) vs. eugonadal men also during treatment (2/3); **(C)** baseline testosterone deficiency and OS: cases of death in men with baseline testosterone deficiency (3/10) vs. baseline eugonadal men (5/14); **(D)** testosterone deficiency developed during treatment and OS: cases of death in men with developed testosterone deficiency (5/11) vs. eugonadal men also during treatment (0/3). Comparison was performed with chi-square test. Continuous line: testosterone deficiency patients; dotted line: eugonadal men. On the horizontal axis, the months passed. PFS, progression-free survival (as months without metastasis); OS, overall survival (as months without death).

in men treated with mitotane is suggested also by the finding of Basile et al. who observed an increase in LH levels in the first months of treatment (15). Unfortunately, LH was not available in our patients to support these data or, otherwise, to observe an eventual depressing effect of mitotane on LH levels (with consequent possible further drop in TT values).

Interestingly, we observed an inverse correlation between mitotane levels and testosterone concentrations (and a direct relationship with SHBG serum levels) mainly in patients who achieved mitotane concentrations above the lower limit of the therapeutic range (14 mg/L). This underlines that the achievement of therapeutic values is crucial to make the mitotane fully biologically active, but this raises the risk of development of hypogonadism.

The frequency of testosterone replacement therapy is relatively low (four patients) in spite of the high prevalence of testosterone deficiency. This is due to the fact that, according to guidelines, we have addressed in testosterone therapy only patients who spontaneously reported typical symptoms of low testosterone (such as sexual dysfunction) and/or aspecific symptoms as asthenia and reduced muscle strength. However, given the complexity of these patients in whom these symptoms might also be related to the general conditions, it is possible that they under-considered or not reported these symptoms. In light of the results of our study, we stress the need for a more thoughtful andrological evaluation. Although we did not observe a relationship between low testosterone and overall/progression free survival (perhaps also due to the small sample size), we cannot exclude the fact that tumoral prognosis could impair testosterone levels and/or testosterone deficiency might further worsen the outcome of these patients. Therefore, testosterone replacement therapy should be carefully evaluated and proposed in male patients with low testosterone given mitotane therapy. Such therapy could have an impact not only on the quality of life and perceived well-being but also on general symptoms, such as asthenia, muscle strength, bone health, and anemia (23). In addition, testosterone therapy might represent a support care against cancer-related fatigue, inappetence, cachexia, and depression (25).

The strengths of this study rely on the strict selection criteria of a consecutive series of ACC male patients undergoing mitotane

therapy and followed for a long period in a single center. Furthermore, the hormone assessment was performed in the same laboratory and included the complete panel of testicular and adrenal steroids. Furthermore, this is the first study focused on the andrological assessment of patients treated with mitotane with hypogonadism as primary endpoint. The retrospective nature and absence of LH determination (the latter is fundamental for hypogonadism classification) are the main limitations; the use of immunoassay instruments (instead of mass spectrometry) to detect testosterone levels is another limiting point.

In conclusion, testosterone deficiency is common in men with ACC before and in the course of mitotane treatment, and this therapy exposes these patients to an elevated risk of hypogonadism, which might negatively impact the quality of life. This is a relevant issue in this patient setting, since ACC often occurs when patients are at the high of their working and social life, which are significantly affected by complex feelings and lifestyle changes due to the cancer diagnosis.

Based on the results of this study, the evaluation of testosterone deficiency (hypogonadism) should be systematically performed in male ACC patients, and the determination of free testosterone is mandatory in men treated with mitotane. Most of these patients require an andrological evaluation to assess the feasibility and potential utility of testosterone replacement therapy. Collaboration between medical oncologists and andrologists is therefore necessary for the management of these complex patients.

Data availability statement

The raw data supporting the conclusions of this article will be made available by the authors, without undue reservation.

Ethics statement

The studies involving human participants were reviewed and approved by Ethics committee ASST Spedali Civili of Brescia. The patients/participants provided their written informed consent to participate in this study.

Author contributions

AD and DC took the lead in writing the manuscript. AB, AF, and CC conceived the design of the study. AD, DC, PF, ML, LCP, VC, and AA collected and provided the clinical data. SG, AB, AF, and CC supervised the project and contributed to the interpretation of the clinical data. All authors actively revised the manuscript provided critical feedback. All authors contributed to the article and approved the submitted version.

Conflict of interest

The authors declare that the research was conducted in the absence of any commercial or financial relationships that could be construed as a potential conflict of interest.

Publisher's note

Supplementary material

The Supplementary Material for this article can be found online at: https://www.frontiersin.org/articles/10.3389/fendo.2023.1128061/full#supplementary-material

References

1. Cremaschi V, Abate A, Cosentini D, Grisanti S, Rossini E, Laganà M, et al. Advances in adrenocortical carcinoma pharmacotherapy: what is the current state of the art? *Expert Opin Pharmacother* (2022) 23(12):1413–24. doi: 10.1080/14656566.2022.2106128

2. Terzolo M, Daffara F, Ardito A, Zaggia B, Basile V, Ferrari L, et al. Management of adrenal cancer: a 2013 update. *J Endocrinol Invest* (2014) 37(3):207–17. doi: 10.1007/s40618-013-0049-2

3. Fassnacht M, Terzolo M, Allolio B, Baudin E, Haak H, Berruti A, et al. Combination chemotherapy in advanced adrenocortical carcinoma. *N Engl J Med* (2012) 366(23):2189–97. doi: 10.1056/NEJMoa1200966

4. Laganà M, Grisanti S, Cosentini D, Ferrari VD, Lazzari B, Ambrosini R, et al. Efficacy of the EDP-m scheme plus adjunctive surgery in the management of patients with advanced adrenocortical carcinoma: The brescia experience. *Cancers (Basel)* (2020) 12(4): 941. doi: 10.3390/cancers12040941

5. Fassnacht M, Dekkers OM, Else T, Baudin E, Berruti A, de Krijger R, et al. European Society of endocrinology clinical practice guidelines on the management of adrenocortical carcinoma in adults, in collaboration with the European network for the study of adrenal tumors. *Eur J Endocrinol* (2018) 179(4):G1–G46. doi: 10.1530/EJE-18-0608

6. Fassnacht M, Assie G, Baudin E, Eisenhofer G, de la Fouchardiere C, Haak HR, et al. Adrenocortical carcinomas and malignant phaeochromocytomas: ESMO-EURACAN clinical practice guidelines for diagnosis, treatment and follow-up. *Ann Oncol* (2020) 31(11):1476–90. doi: 10.1016/j.annonc.2020.08.2099

7. Terzolo M, Angeli A, Fassnacht M, Daffara F, Tauchmanova L, Conton PA, et al. Adjuvant mitotane treatment for adrenocortical carcinoma. *N Engl J Med* (2007) 356 (23):2372–80. doi: 10.1056/NEJMoa063360

8. Berruti A, Grisanti S, Pulzer A, Claps M, Daffara F, Loli P, et al. Long-term outcomes of adjuvant mitotane therapy in patients with radically resected adrenocortical carcinoma. *J Clin Endocrinol Metab* (2017) 102(4):1358–65. doi: 10.1210/jc.2016-2894

9. Hermsen IG, Fassnacht M, Terzolo M, Houterman S, den Hartigh J, Leboulleux S, et al. Plasma concentrations of o,p'DDD, o,p'DDA, and o,p'DDE as predictors of tumor response to mitotane in adrenocortical carcinoma: results of a retrospective ENS@T multicenter study. *J Clin Endocrinol Metab* (2011) 96(6):1844–51. doi: 10.1210/jc.2010-2676

10. Terzolo M, Baudin AE, Ardito A, Kroiss M, Leboulleux S, Daffara F, et al. Mitotane levels predict the outcome of patients with adrenocortical carcinoma treated

adjuvantly following radical resection. *Eur J Endocrinol* (2013) 169(3):263–70. doi: 10.1530/EJE-13-0242

11. Puglisi S, Calabrese A, Basile V, Ceccato F, Scaroni C, Simeoli C, et al. Mitotane concentrations influence the risk of recurrence in adrenocortical carcinoma patients on adjuvant treatment. *J Clin Med* (2019) 8(11):1850. doi: 10.3390/jcm8111850

12. Bianchini M, Puliani G, Chiefari A, Mormando M, Lauretta R, Appetecchia M. Metabolic and endocrine toxicities of mitotane: A systematic review. *Cancers (Basel)* (2021) 13(19):5001. doi: 10.3390/cancers13195001

13. Turla A, Laganà M, Grisanti S, Abate A, Ferrari VD, Cremaschi V, et al. Supportive therapies in patients with advanced adrenocortical carcinoma submitted to standard EDP-m regimen. *Endocrine* (2022) 77(3):438–43. doi: 10.1007/s12020-022-03075-y

14. Gentilin E, Tagliati F, Terzolo M, Zoli M, Lapparelli M, Minoia M, et al. Mitotane reduces human and mouse ACTH-secreting pituitary cell viability and function. *J Endocrinol* (2013) 218(3):275–85. doi: 10.1530/JOE-13-0210

15. Basile V, Puglisi S, Calabrese A, Pia A, Perotti P, Berruti A, et al. Unwanted hormonal and metabolic effects of postoperative adjuvant mitotane treatment for adrenocortical cancer. *Cancers (Basel)* (2020) 12(9):2615. doi: 10.3390/cancers12092615

16. Bhasin S, Brito JP, Cunningham GR, Hayes FJ, Hodis HN, Matsumoto AM, et al. Testosterone therapy in men with hypogonadism: An endocrine society clinical practice guideline. *J Clin Endocrinol Metab* (2018) 103(5):1715–44. doi: 10.1210/jc.2018-00229

17. Corona G, Goulis DG, Huhtaniemi I, Zitzmann M, Toppari J, Forti G, et al. European Academy of andrology (EAA) guidelines* on investigation, treatment and monitoring of functional hypogonadism in males. *Andrology* (2020) 8(5):970–87. doi: 10.1111/andr.12770

18. Daffara F, De Francia S, Reimondo G, Zaggia B, Aroasio E, Porpiglia F, et al. Prospective evaluation of mitotane toxicity in adrenocortical cancer patients treated adjuvantly. *Endocr Relat Cancer* (2008) 15(4):1043–53. doi: 10.1677/ERC-08-0103

19. Vikner ME, Krogh J, Daugaard G, Andreassen M. Metabolic and hormonal side effects of mitotane treatment for adrenocortical carcinoma: A retrospective study in 50 Danish patients. *Clin Endocrinol (Oxf)* (2021) 94(2):141–9. doi: 10.1111/cen.14345

20. Drucker S, New MI. Disorders of adrenal steroidogenesis. *Pediatr Clin North Am* (1987) 34(4):1055–66. doi: 10.1016/s0031-3955(16)36302-7

21. Winters SJ, Scoggins CR, Appiah D, Ghooray DT. The hepatic lipidome and HNF4α and SHBG expression in human liver. *Endocr Connect* (2020) 9(10):1009–18. doi: 10.1530/EC-20-0401

22. de Ronde W, van der Schouw YT, Muller M, Grobbee DE, Gooren LJ, Pols HA, et al. Associations of sex-hormone-binding globulin (SHBG) with non-SHBG-bound levels of testosterone and estradiol in independently living men. *J Clin Endocrinol Metab* (2005) 90(1):157–62. doi: 10.1210/jc.2004-0422

23. Isidori AM, Aversa A, Calogero A, Ferlin A, Francavilla S, Lanfranco F, et al. Adult- and late-onset male hypogonadism: the clinical practice guidelines of the Italian society of andrology and sexual medicine (SIAMS) and the Italian society of endocrinology (SIE). *J Endocrinol Invest* (2022) 45(12):2385–403. doi: 10.1007/s40618-022-01859-7

24. Pezzaioli LC, Quiros-Roldan E, Paghera S, Porcelli T, Maffezzoni F, Delbarba A, et al. The importance of SHBG and calculated free testosterone for the diagnosis of symptomatic hypogonadism in HIV-infected men: a single-centre real-life experience. *Infection* (2021) 49(2):295–303. doi: 10.1007/s15010-020-01558-6

25. Ruggiero E, Tizianel I, Caccese M, Lombardi G, Pambuku A, Zagonel V, et al. Advanced adrenocortical carcinoma: From symptoms control to palliative care. *Cancers (Basel)* (2022) 14(23):5901. doi: 10.3390/cancers14235901

frontiers | Frontiers in Oncology

TYPE Case Report
PUBLISHED 29 May 2023
DOI 10.3389/fonc.2023.1157740

OPEN ACCESS

EDITED BY
Marta Araujo-Castro,
Ramón y Cajal University Hospital, Spain

REVIEWED BY
Giammaria Fiorentini,
Marche Norde Hospital, Italy
Sarah Allegra,
University of Turin, Italy

*CORRESPONDENCE
Zhigang Ji
jizhigang@pumch.cn

†These authors have contributed equally to this work and share first authorship

RECEIVED 14 February 2023
ACCEPTED 16 May 2023
PUBLISHED 29 May 2023

CITATION
Deng J, Wei L, Fan Q, Wu Z and Ji Z (2023) Long-term partial response in a patient with liver metastasis of primary adrenocortical carcinoma with adjuvant mitotane plus transcatheter arterial chemoembolization and microwave ablation: a case report.
Front. Oncol. 13:1157740.
doi: 10.3389/fonc.2023.1157740

Long-term partial response in a patient with liver metastasis of primary adrenocortical carcinoma with adjuvant mitotane plus transcatheter arterial chemoembolization and microwave ablation: a case report

Jianhua Deng[1†], Lihui Wei[2†], Qihuang Fan[2], Zoey Wu[2] and Zhigang Ji[1*]

[1]Department of Urology, Peking Union Medical College Hospital, Beijing, China, [2]Department of Medicine, Genetron Health (Beijing) Co. Ltd., Beijing, China

Adrenocortical carcinoma (ACC) is a rare, heterogeneous, and aggressive malignancy with a generally poor prognosis. Surgical resection is the optimal treatment plan. After surgery, both mitotane treatment or the etoposide-doxorubicin-cisplatin (EDP) protocol plus mitotane chemotherapy have a certain effect, but there is still an extremely high possibility of recurrence and metastasis. The liver is one of the most common metastatic targets. Therefore, techniques such as transcatheter arterial chemoembolization (TACE) and microwave ablation (MWA) for liver tumors can be attempted in a specific group of patients. We present the case of a 44-year-old female patient with primary ACC, who was diagnosed with liver metastasis 6 years after resection. During mitotane treatment, we performed four courses of TACE and two MWA procedures in accordance with her clinical condition. The patient has maintained the partial response status and has currently returned to normal life to date. This case illustrates the value of the practical application of mitotane plus TACE and MWA treatment.

KEYWORDS

adrenocortical carcinoma, liver metastases, mitotane, TACE, WMA, partial response

Abbreviations: ACTH, Adreno-cortico-tropic-hormone; TSTO: Testosterone; UFC, Urinary free cortisol; DHEA, Prasterone.

Introduction

Adrenocortical carcinoma (ACC) is a rare, heterogeneous, and aggressive malignancy with a generally poor prognosis. At least 50% of patients are detected with metastatic tumors at initial diagnosis. The prognosis for ACC is poor, with a 5-year overall survival (OS) rate of 30% (1), depending on the stage of the disease at diagnosis—5-year survival is 60% to 80% for tumors confined to the adrenal space, 35% to 50% for locally advanced disease, and much lower for metastatic disease with percentages reported ranging from 0% to 28% (2). Although ACC is potentially curable in the early stages, only approximately 30% of malignancies are located in the adrenal gland when diagnosed (3, 4). Most tumors have distant metastases, and this aggressive behavior leads to a poor prognosis. The medical treatment options for ACC are limited and mitotane is the only drug available as its good efficacy on prolongation of RFS (HR = 0.62; 95%CI, 0.42-0.94; P < 0.05) and OS (HR = 0.69; 95%CI, 0.55-0.88, P < 0.05) in patients with ACC after radical surgery (5). For advanced or recurrent patients with poor prognostic parameters, a more aggressive treatment regimen (mitotane with chemotherapy) is recommended according to the result of FIRM-ACT, the only randomized controlled trial designed to evaluate the efficacy of mitotane combination with chemotherapy for ACC (6): patients in the etoposide-doxorubicin-cisplatin-mitotane (EDP-M) group had a significantly higher response rate than those in the streptozocin-mitotane group (23.2% vs. 9.2%, P<0.001) and longer median progression-free survival (PFS, 5.0 months vs. 2.1 months, P<0.001). But EDP-M is more toxic (6) and mitotane has a very poor aqueous solubility (7), there is still limited treatment for advanced or recurrent ACC patients and more exploration is needed.

Combination therapy of transcatheter arterial/transarterial chemoembolization (TACE) and microwave ablation (MWA) is a minimally invasive technique performed by interventional radiologists that delivers embolization chemotherapy, injected through a catheter, into the hepatic artery that directly supplies the tumor. Although TACE+WMA is used frequently to treat hepatocellular carcinoma, intrahepatic cholangiocarcinoma, and intrahepatic colorectal cancer metastases, to our knowledge, it is rarely used for the treatment of metastatic ACC (8–11).

We present a case of a 44-year-old female who was diagnosed with stage III ACC. She underwent a radical adrenalectomy of the left adrenal tumor and then received mono-mitotane chemotherapy. Five years after surgery, she was diagnosed with liver metastasis from ACC. During mitotane treatment, she continued to have persistent liver disease progression and, therefore, underwent four courses of TACE+WMA therapy. Following this treatment, the patient experienced a partial response (PR) to treatment and has remained progression-free for more than 28 months until the last follow-up. We present the following case in accordance with the CARE reporting checklist.

Case description

In 2013, a 36-year-old female Chinese patient presented to the Peking Union Medical College Hospital complaining of infertility, menelipsis for about 4 months, weight gain and facial vellus hair for more than 4 years. She was treated with Yasmin at the local hospital for symptoms of facial vellus hair and elevated testosterone in 2009, then with progesterone due to menopause and reached regular menstruation from July 2011 to 2013 July. In September 2013, she came to Peking Union Medical College Hospital for diagnosis when she developed symptom of menopause again.

Physical examination showed no obvious abnormality, and the patient also denied of family history. Computed tomography (CT) scan and ultrasound examination were preformed that day, which revealed a large mass in the left adrenal gland (Figure 1A). And 3D reconstruction of CT scans showed a significant soft tissue burden in the left adrenal area with the size of approximately 15.9 cm × 15.5 cm, the lesion showed a clear boundary and was supplied by the left adrenal artery and the branches of the left renal artery (Figure 1B). Blood tests revealed plasma ACTH, TSTO, 24-hour UFC and serum total cortisol levels of 42.7 pg/ml, 171.4 ng/dl, 1094 μg/dl, and 16.29 μg/dl, respectively. It is worth mentioning that DHEA value reached an extraordinarily high level, 6779.0 μg/dl. A fine needle aspiration biopsy (FNAB) sample was also taken, andthe pathology showed Ki67 was 3%, excluded pheochromocytoma. Given all these above, her diagnosis was made as "left adrenal gland occupied, with the possibility of ACC" at that time, and was hospitalized for detailed medical treatment.

The timeline of the case including the most important therapeutic procedures is shown in Figure 2. In October 2013, the patient received radical adrenalectomy for ACC. The postoperative pathology examination of the tumor tissue revealed an adrenal cortex adenoma, which invaded the periadrenal tissue, with large leomorphic cells showing high mitotic rate, atypical mitoses, extensive necrosis, and hemorrhage which was consistent with the pathology of FNAB. The tumor grew actively (the malignant potential could not be determined), and the size was 18 cm × 12.5 cm × 10 cm (Figure 1C), determined as stageIII according to the European Network for the Study of Adrenal Tumours (ENSAT) staging system. Tumor immunohistochemistry parameters were CgA (-), Melan-A (+), Syntwo (+), AE1/AE3 (+), P53 (-) (Figure 1D), and Ki-67 approximately 3%. The postoperative blood test results were as follows: plasma ACTH, TSTO, 24-hour UFC levels were 30.2 pg/ml, 15.0 ng/dl, and 36.55 μg/dl, respectively, returned to normal levels. Her menstruation returned to normal 1 month after the operation and she underwent routine follow-up at the local hospital.

In January 2019, the patient was evaluated again due to menopause. The color Doppler ultrasound results from the local hospital showed a moderately echogenic mass in the liver. The patient returned to Peking Union Medical College Hospital for further examination in March 2019. Multiple lesions in the liver were observed through abnormal enhanced CT and multiple low-density nodules and tumor shadows. Liver and kidney function examination revealed that K^+ 5.2 mmol/L, GGT 329 U/L, Alb 45 g/L, ALP 194 U/L, AST 50 U/L, ALT 9 U/L; AFP 2.6 ng/ml. The results described above raised the possibility of ACC liver metastasis. She was treated with hydrocortisone (10 mg q8h) and oral mitotane (1.0 g q8h, plasma concentration 14.1 mg/l) from March 2019. The patient developed diarrhea, sweating, lethargy, and occasional chest tightness after taking mitotane, which was

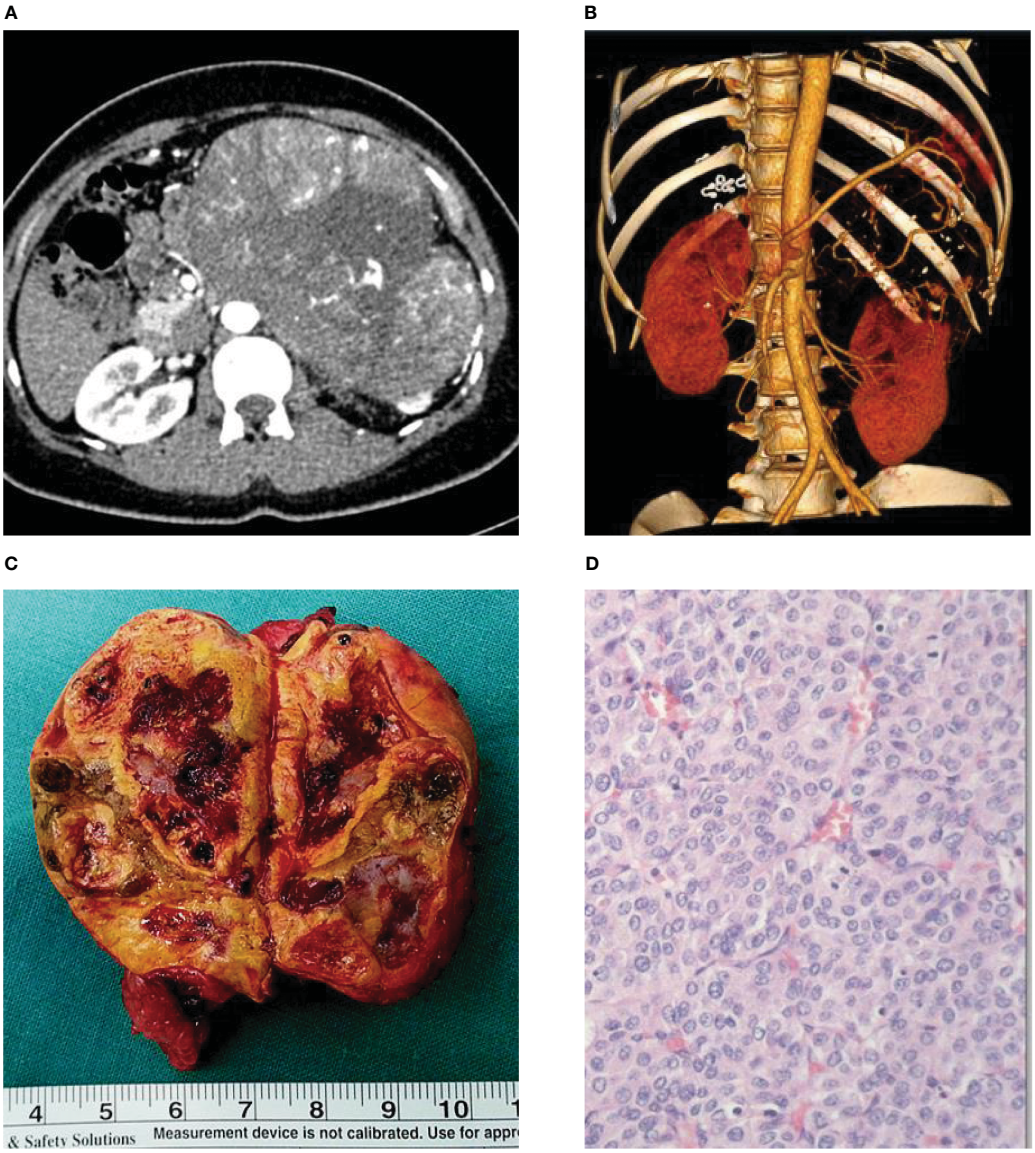

FIGURE 1
Characteristics of primary adrenal cortex tumor. **(A)** CT scan result of the patient revealed left adrenal gland huge mass. **(B)** CT-3D reconstruction of patient's abdomen. **(C)** Surgical removal of adrenal cortex tumor. **(D)** Immunohistochemical results of tumor tissue.

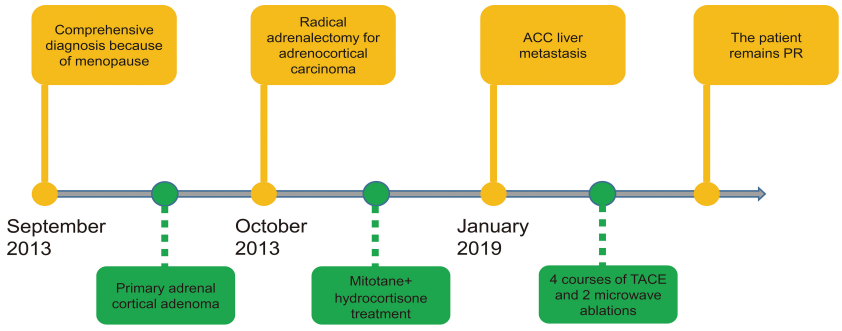

FIGURE 2
Timeline of this case.

considered as common adverse reactions. To prevent liver damage from mitotane, ESSENTIALE 456 mg tid was used at the same time. However, her condition did not improve significantly and her liver lesions was still enlarged. On the basis of the Clinical Practice guidelines of the European Endocrine Society for the treatment of adult ACC, patients with advanced ACC with metastasis may benefit from local treatment (12), we treated her with TACE followed by MWA for the liver lesions.

On 4 March 2019, for the first treatment of TACE, a microcatheter was used to infuse a mixture of 10 ml of lipiodol and 5 ml of leroxatin through the superior mesenteric artery to the blood supply artery of the liver tumor and a good deposition effect was obtained (Figure 3A). The patient did not experience any side effects and continued to receive mitotane and hydrocortisone treatment. In the next 2 months, the patient completed another three courses of TACE on 3 April, 18 April and 9 May, respectively. All the treatment went smoothly, and the mitotane and hydrocortisone treatment was continued during this period (Figure 3B). On 30 May 2019, the patient underwent a CT-guided microwave ablation operation of the liver tumor. Due to pleural hemorrhage in the surgery, peripheral intravenous fluids and a blood transfusion were performed, and pleural effusion drainage and microcatheter super-selected right inferior phrenic artery and right hepatic artery embolization were performed again. On 1 August 2019, the patient completed the second microwave ablation procedure for the liver, and the curative effect was evaluated as partial response(PR) according to RECIST1.1. Subsequently, the patient received continuous mitotane (0.5 g tid) and hydrocortisone treatment. There were no serious adverse reactions for her.

Follow-up examinations were routinely performed after treatment. In the enhanced magnetic resonance imaging (MRI) examination in March and September 2022, her liver showed multiple mass-like abnormal signals, and the lesions were slightly

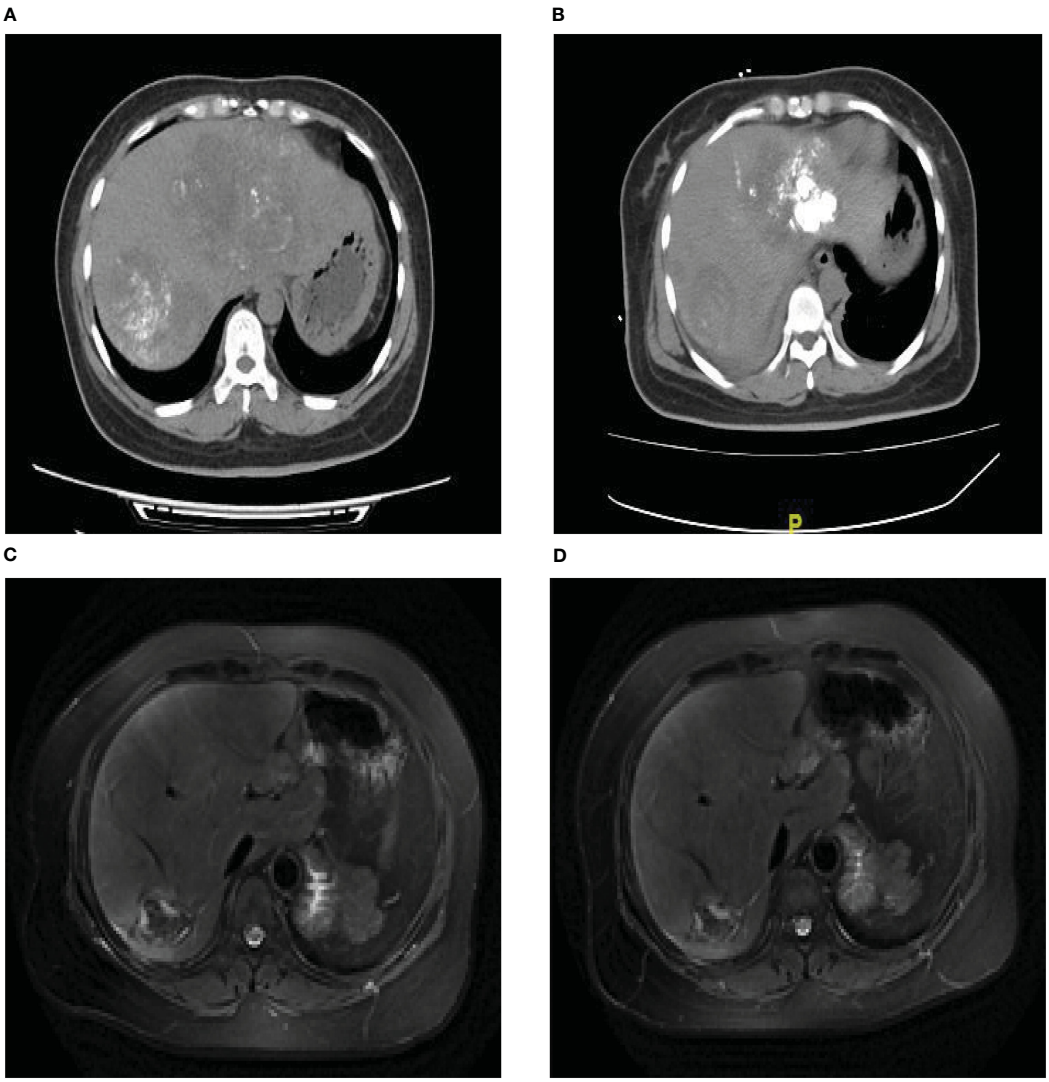

FIGURE 3
TACE perioperative imaging results. **(A)** CT scan picture of patient after the first TACE. **(B)** CT scan picture of patient after four TACE surgeries. **(C)** The abdomen conventional dynamic enhanced MRI image in March 2022. **(D)** The abdomen conventional dynamic enhanced MRI image in September 2022.

smaller (Figures 3C, D). During this period, the patient's treatment was mitotane (0.5g tid) and hydrocortisone. The evaluation of her treatment outcome as TACE+MWA plus mitotane regimen remained PR, and her condition was also stable and comfortable for about 28 months so far.

Discussion and conclusion

Although our understanding of treatments has improved in recent years, patients diagnosed with ACC-metastatic disease after surgery continue to experience poor outcomes, with poor overall survival (13). The liver is one of the most common sites of metastases in ACC and contributes significantly to the mortality and morbidity of patients. The management of ACC requires consideration of oncologic and endocrine simultaneously as the special function of the adrenal gland. But it is regrettable that the level of treatment evidence is grade II to grade IV for ACC up to now, which were based on 1 trial, retrospective studies and nonrandomized trials (14). Treatments for ACC are still being explored and there is limited evidence regarding liver-directed therapy in the treatment of patients with metastatic ACC. Studies have shown that systemic antitumor therapy combined with local therapy is expected to achieve higher tumor response (15).

Mitotane is a commonly used agent preferably for patients with unresectable or recurrent ACC due to its high object response rate. A study evaluated the therapeutic effect of mitotane in the treatment of 391 advanced ACC patients, and found 26 (20.5%) patients had objective response, including 3 complete responses. The overall median PFS and OS was 4.1 and 18.5 months, respectively, demonstrating that mitotane is effective against advanced ACC (16). In recent years, local treatment has been advocated for the treatment of metastatic ACC. Liver-directed therapies have already been proven to improve treatment response in other tumors affecting the liver, such as hepatocellular carcinoma and colorectal tumors (17, 18). There are also some ACC patients with liver metastases benefited from local therapy. A study was reported to treate 29 patients with ACC with liver metastases by TACE. The median PFS was 9 months, and the median OS was 11 months after the first procedure (19). Another study published in 2009 described two patients with liver metastases after being diagnosed with ACC who underwent transcatheter arterial embolization (TAE) for liver lesion. Both patients achieved complete responses after liver-directed therapy (20) and the OS was 77 and 51 months, respectively. The characteristics and outcomes of 3 patients were listed in Table 1. The treatment for liver lesion was different in Hideo's report and ours: we treated liver lesion with TACE with followed by MWA, which was reported could improve local control

TABLE 1 Characteristics and Outcomes of 3 patients with ACC.

	1*	2*	3#
Site	right	right	left
Age	57	54	36
Gender	Female	Male	Female
Symptoms	–	back pain	menopause, weight gain and facial vellus hair
Manifestation of tumor growth	–	+	+
Hypertension	+	–	–
Hormonal activity	Cushing's syndrome	–	–
Size of tumor, cm	7	20	15.9
Ki-67	–	–	3%
DHEA, μg/dl	–	–	6779
Tumor weight, g	32	3080	2150
pT	2	3	3
Postoperative stage	II	III	III
Adjuvant therapy	–	–	–
Interval until recurrence or metastasis, months	33	6	62
Location of recurrence or metastasis	liver (solitary)	liver (solitary)	liver (solitary)
Treatment for recurrence or metastasis	mitotane+cytotoxic chemotherapy→TAE	mitotane+cytotoxic chemotherapy→TAE	mitotane+TACE+MWA

(Continued)

TABLE 1 Continued

	1*	2*	3#
Effect	CR	CR	PR
Survival period, months	77	51	108(still alive as of press time)
Prognosis	AWM	NED	AWM

1.*patients from Hideo's report[];#patient of our case.
2.NED, no evidence of disease; DOD, death of disease; AWM, alive with metastasis; CR, Complete response; PD, progressive disease; PR, partial respons.
3.–, absence; +, presence.

(21), prolong OS (22) and has better clinical effectiveness (23) compared with TACE monotherapy in liver cancer. And mitotane was used for systemic antitumor therapy concomitantly. Beyond that, the site, age, interval until recurrence or metastasis and DHEA are all different between these patients, which may also affect the curative effect in some degree, and more cases are needed to summarize the clinical treatment experience for ACC with liver metastasis.

Here we reported a case that advanced ACC with liver metastases treated with systemic antitumor therapy combined with local therapy for liver lesion (motatine combined with TACE +MWA). The treatment outcome was PR and the PFS of the patient has been extended to about 28 months so far she was still alive up to now (September 2022). Based on our review of the limited literature available, liver-directed therapies such as TACE or SIRT have significant potential as part of treatment regimens in patients with metastatic liver burden in ACC. We consider this to be an emerging area and further research is needed to guide treatment decisions. With systemic antitumor therapy combined with local therapy, such as mitotane plus TACE+MWA we used in this case with less toxicity and side effects in patients with high-grade disease, traditional ACC treatment decisions may achieve better results, which we used in this case. We suggest that there is a need for further research including clinical trials on this topic to further clarify the role of TACE in these patients.

Data availability statement

The original contributions presented in the study are included in the article/supplementary material. Further inquiries can be directed to the corresponding author.

Ethics statement

Written informed consent was obtained from the individual(s) for the publication of any potentially identifiable images or data included in this article.

Author contributions

ZJ designed and supervised the study. JD, LW and QF searched the literatures and participated in clinical data acquisition. JD and LW drafted the manuscript. JD, QF and ZW gave critical revision of the manuscript for important intellectual content. All authors contributed to the article and approved the submitted version.

Conflict of interest

L.W., Q.F. and Z.W. are members of the Genetron Health (Beijing) Technology, Co. Ltd. Beijing, China.

The remaining authors declare that the research was conducted in the absence of any commercial or financial relationships that could be construed as a potential conflict of interest.

Publisher's note

References

1. Fassnacht M, Libé R, Kroiss M, Allolio B. Adrenocortical carcinoma: a clinician's update. *Nat Rev Endocrinol* (2011) 7(6):323–35. doi: 10.1038/nrendo.2010.235

2. Abiven G, Coste J, Groussin L, Anract P, Tissier F, Legmann P, et al. Clinical and biological features in the prognosis of adrenocortical cancer: poor outcome of cortisol-secreting tumors in a series of 202 consecutive patients. *J Clin Endocrinol Metab* (2006) 91(7):2650–5. doi: 10.1210/jc.2005-2730

3. Else T, Kim AC, Sabolch A, Raymond VM, Kandathil A, Caoili EM, et al. Adrenocortical carcinoma. *Endocr Rev* (2014) 35(2):282–326. doi: 10.1210/er.2013-1029

4. Puglisi S, Calabrese A, Basile V, Pia A, Reimondo G, Perotti P, et al. New perspectives for mitotane treatment of adrenocortical carcinoma. *Best Pract Res Clin Endocrinol Metab* (2020) 34(3):101415. doi: 10.1016/j.beem.2020.101415

5. Tang Y, Liu Z, Zou Z, Liang J, Lu Y, Zhu Y. Benefits of adjuvant mitotane after resection of adrenocortical carcinoma: a systematic review and meta-analysis. *BioMed Res Int* (2018) 2018:9362108. doi: 10.1155/2018/9362108

6. Martin F, Massimo T, Bruno A, Eric B, Harm H, Alfredo B, et al. Combination chemotherapy in advanced adrenocortical carcinoma. *N Engl J Med* (2012) 366 (23):2189–97. doi: 10.1056/NEJMoa1200966

7. Malik H, Taufiq A, Jürgen G, Oliver S-C, Matthias K, et al. The challenging pharmacokinetics of mitotane: an old drug in need of new packaging. *Eur J Drug Metab Pharmacokinet* (2021) 46(5):575–93. doi: 10.1007/s13318-021-00700-5

8. Aghamohammadzadeh N, Faraji A, Bozorgi F, Faraji I, Moghadaszadeh M. Primary hyperaldostronisim as initial presentation of adrenal cortical carcinoma

with liver metastasis: a case report. *Int J Hematol Oncol Stem Cell Res* (2013) 7 (2):38–42.

9. Ng L, Libertino JM. Adrenocortical carcinoma: diagnosis, evaluation and treatment. *J Urol* (2003) 169(1):5–11. doi: 10.1097/01.ju.0000030148.59051.35

10. Yang GW, Zhao Q, Qian S, Zhu L, Qu XD, Zhang W, et al. Percutaneous microwave ablation combined with simultaneous transarterial chemoembolization for the treatment of advanced intrahepatic cholangiocarcinoma. *Onco Targets Ther* (2015) 8:1245–50. doi: 10.2147/OTT.S84764

11. Andrasina T, Juracek J, Zavadil J, Cechova B, Rohan T, Vesela P, et al. Thermal ablation and transarterial chemoembolization are characterized by changing dynamics of circulating MicroRNAs. *J Vasc Interv Radiol* (2021) 32(3):403–11. doi: 10.1016/j.jvir.2020.10.024

12. Fassnacht M, Dekkers OM, Else T, Baudin E, Berruti A, de Krijger R, et al. European Society of endocrinology clinical practice guidelines on the management of adrenocortical carcinoma in adults, in collaboration with the European network for the study of adrenal tumors. *Eur J Endocrinol* (2018) 179(4):G1–G46. doi: 10.1530/EJE-18-0608

13. Libé R, Borget I, Ronchi CL, Zaggia B, Kroiss M, Kerkhofs T, et al. Prognostic factors in stage III-IV adrenocortical carcinomas (ACC): an European network for the study of adrenal tumor (ENSAT) study. *Ann Oncol* (2015) 26(10):2119–25. doi: 10.1093/annonc/mdv329

14. Kendrick ML, Lloyd R, Erickson L, Farley DR, Grant CS, Thompson GB, et al. Adrenocortical carcinoma: surgical progress or status quo? *Arch Surg* (2001) 136 (5):543–9. doi: 10.1001/archsurg.136.5.543

15. He MK, Liang RB, Zhao Y, Xu YJ, Chen HW, Zhou YM, et al. Lenvatinib, toripalimab, plus hepatic arterial infusion chemotherapy versus lenvatinib alone for advanced hepatocellular carcinoma. *Ther Adv Med Oncol* (2021) 13. doi: 10.1177/17588359211002720

16. Hong J, Hatchell KE, Bradfield JP, Bjonnes A, Chesi A, Lai C, et al. Transethnic evaluation identifies low-frequency loci associated with 25-hydroxyvitamin d concentrations. *J Clin Endocrinol Metab* (2018) 103(4):1380–92. doi: 10.1210/jc.2017-01802

17. Massmann A, Rodt T, Marquardt S, Seidel R, Thomas K, Wacker F, et al. Transarterial chemoembolization (TACE) for colorectal liver metastases–current status and critical review. *Langenbecks Arch Surg* (2015) 400(6):641–59. doi: 10.1007/s00423-015-1308-9

18. Baere T, Deschamps F, Tselikas L, Ducreux M, Planchard D, Pearson E, et al. GEP-NETS update: interventional radiology: role in the treatment of liver metastases from GEP-NETs. *Eur J Endocrinol* (2015) 172(4):R151–66. doi: 10.1530/EJE-14-0630

19. Cazejust J, Baère T, Auperin A, Deschamps F, Hechelhammer L, Abdel-Rehim M, et al. Transcatheter arterial chemoembolization for liver metastases in patients with adrenocortical carcinoma. *J Vasc Interv Radiol* (2010) 21(10):1527–32. doi: 10.1016/j.jvir.2010.05.020

20. Soga H, Takenaka A, Ooba T, Nakano Y, Miyake H, Takeda M, et al. A twelve-year experience with adrenal cortical carcinoma in a single institution: long-term survival after surgical treatment and transcatheter arterial embolization. *Urol Int* (2009) 82:222–6. doi: 10.1159/000200804

21. Smolock A, Cristescu M, Hinshaw A, Woo K, Wells S, Ziemlewicz T, et al. Combination transarterial chemoembolization and microwave ablation improves local tumor control for 3- to 5-cm hepatocellular carcinoma when compared with transarterial chemoembolization alone. *Abdom Radiol (NY)* (2018) 43(9):2497–504. doi: 10.1007/s00261-018-1464-9

22. Zheng L, Li HL, Guo CY, Luo SX. Comparison of the efficacy and prognostic factors of transarterial chemoembolization plus microwave ablation versus transarterial chemoembolization alone in patients with a Large solitary or multinodular hepatocellular carcinomas. *Korean J Radiol* (2018) 19(2):237–46. doi: 10.3348/kjr.2018.19.2.237

23. Zhang R, Shen L, Zhao L, Guan Z, Chen Q, Li W. Combined transarterial chemoembolization and microwave ablation versus transarterial chemoembolization in BCLC stage b hepatocellular carcinoma. *Diagn Interv Radiol* (2018) 24(4):219–24. doi: 10.5152/dir.2018.17528

frontiers | Frontiers in Endocrinology

TYPE Original Research
PUBLISHED 13 June 2023
DOI 10.3389/fendo.2023.1162725

OPEN ACCESS

EDITED BY
Marta Araujo-Castro,
Ramón y Cajal University Hospital, Spain

REVIEWED BY
Calin Cainap,
University of Medicine and Pharmacy Iuliu Hatieganu, Romania
Filomena De Nigris,
University of Campania Luigi Vanvitelli, Italy

*CORRESPONDENCE
Nuria Valdés
nuria.valdesg@sespa.es
María-Dolores Chiara
mdchiara.uo@uniovi.es

†These authors have contributed equally to this work and share first authorship

‡These authors have contributed equally to this work and share senior authorship

RECEIVED 09 February 2023
ACCEPTED 18 May 2023
PUBLISHED 13 June 2023

CITATION
Enguita JM, Díaz I, García D, Cubiella T, Chiara M-D and Valdés N (2023) Visual analytics identifies key miRNAs for differentiating peripancreatic paraganglioma and pancreatic neuroendocrine tumors.
Front. Endocrinol. 14:1162725.
doi: 10.3389/fendo.2023.1162725

Visual analytics identifies key miRNAs for differentiating peripancreatic paraganglioma and pancreatic neuroendocrine tumors

Jose María Enguita[1†], Ignacio Díaz[1†], Diego García[1], Tamara Cubiella[2,3,4], María-Dolores Chiara[2,3,4*‡] and Nuria Valdés[2,5*‡]

[1]Department of Electrical Engineering, University of Oviedo, Gijón, Spain, [2]Department of Cancer, Health Research Institute of the Principality of Asturias, Oviedo, Spain, [3]Respiratory Tract Tumors, CIBERONC (Network of Biomedical Research in Cancer), Madrid, Spain, [4]Institute of Oncology of the Principality of Asturias, University of Oviedo, Oviedo, Spain, [5]Department of Internal Medicine, Section of Endocrinology and Nutrition, Cabueñes University Hospital, Gijón, Spain

Introduction: Paragangliomas (PGL), a type of neuroendocrine tumor, pose a significant diagnostic challenge due to their potential for unpredictable locations and asymptomatic presentation. Misdiagnosis of peripancreatic PGLs, particularly as pancreatic neuroendocrine tumors (PANNETs), is a pressing issue as it can negatively impact both pre- and post-treatment decision-making. The aim of our study was to identify microRNA markers for the reliable differential diagnosis of peripancreatic PGLs and PANNETs, addressing a crucial unmet need in the field and advancing the standard of care for these patients.

Methods: Morphing projections tool was used to analyze miRNA data from PGL and PANNET tumors present in the TCGA database. The findings were validated using two additional databases: GSE29742 and GSE73367.

Results: Our research uncovered substantial differences in the miRNA expression profiles of PGL and PANNET, leading to the identification of 6 key miRNAs (miR-10b-3p, miR-10b-5p, and the miRNA families miR-200c/141 and miR-194/192) that can effectively differentiate between the two types of tumors.

Discussion: These miRNA levels hold potential as biomarkers for improved diagnosis, offering a solution to the diagnostic challenge posed by these tumors and potentially improving the standard of care for patients.

KEYWORDS

paraganglioma, pancreatic neuroendocrine tumors, microRNA, diagnosis, visual analytic

1 Introduction

Paragangliomas (PGLs) are neuroendocrine tumors with high genetic predisposition. They originate from catecholamine-secreting paraganglionic cells that have a widespread distribution in humans. PGL can have or not a hypersecretory phenotype. They are categorized based in their origin as either parasympathetic or sympathetic. Parasympathetic PGLs are typically found near the aortic arch, neck, and skull base, while sympathetic PGLs arise along the paravertebral axis, retroperitoneum, in the abdomen and pelvis, with the largest forming the adrenal medulla. The term "pheochromocytoma" specifically refers to intra-adrenal sympathetic PGLs according to the latest WHO guidelines (1). PGLs are highly heritable, with approximately 50% of cases associated with a germline mutation in one of at least 15 genes, making them the most heritable tumours in humans. They can occur as part of well-established hereditary syndromes, including multiple endocrine neoplasia type 2A and 2B, von Hippel–Lindau syndrome, neurofibromatosis type 1 and familial paraganglioma syndromes, caused by pathogenic variants in genes encoding Ret Proto-Oncogene (RET), Von Hippel Lindau protein (VHL), Neurofibromin 1 (NF1), or components of the succinate dehydrogenase (SDH) complex, respectively.

Given the widespread distribution of paraganglia, PGL can occur at virtually all locations in the body except the brain and bones. The emergence of PGL in atypical locations can cause confusion and result in missed diagnoses (2). The histopathologic diagnosis is straightforward for PGLs that present in an expected location with classic catecholamine excess symptoms. However, missed diagnoses can occur when the PGLs are in unusual locations, the patient is asymptomatic, or the PGLs do not secrete catecholamines.

Diagnosing peripancreatic PGLs that resemble primary pancreatic lesions can be difficult as they often lack typical PGL symptoms (3, 4). This can be further complicated by the fact that around 10% of pancreatic neuroendocrine tumors are associated with hereditary syndromes like multiple endocrine neoplasia type I (MEN1), von Hippel–Lindau syndrome, neurofibromatosis type 1, and tuberous sclerosis complex (TSC). Preoperative diagnosis can be done through fine-needle aspiration and biopsy, but PGLs and PANNET can have similar morphologic characteristics, leading to misdiagnosis (5–8). Accurate diagnosis is crucial for proper pre- and post-treatment decision-making (9). Therefore, differentiating peripancreatic PGLs from PANNETs is a crucial aspect of clinical practice. Our previous study revealed similarities in genetic profiles but differences in microRNA profiles between the two neoplasms (10). The goal of the present study was to identify microRNA markers that enable differential diagnosis of peripancreatic PGL and PANNET.

2 Materials and methods

2.1 TCGA database

The Cancer Genome Atlas (TCGA) provides gene expression measurements and other transcription data, including more than 20,000 mRNA and hundreds of miRNA expression levels for more than 10,000 tumors from 33 different cancer types. In this study we consider gene expression RNAseq data of cancer cohorts identified as primary paraganglioma (abbreviated here as PGL: pheochromocytoma and paraganglioma, n=149) and pancreatic neuroendocrine tumors (PANNET; 7 samples) (11) from the TCGA Hub. Data were downloaded from the *Xenabrowser* portal https://xenabrowser.net/datapages/. For every cohort we merged: (a) data containing experimental measurements using the Illumina HiSeq 2000 RNA Sequencing platform and mean-normalized per gene across all cohorts; and (b) data with miRNA mature strand expression RNAseq. The resulting table including gene and miRNA expression levels in units of log2(RPM+1) (RPM=Reads per million), was curated by dropping genes and miRNA with invalid values, and later merged with clinical metadata (downloadable from https://portal.gdc.cancer.gov). This allowed for the analysis of 294 miRNAs.

2.2 Interactive data visualization: morphing projections

We used the *t-Distributed Stochastic Neighbor Embedding* (*t*-SNE) algorithm, which is a highly effective method for dimensionality reduction, to visually depict the analyzed tissues according to their genetic signature (12). This approach organizes the samples spatially based on their similarities in gene and miRNA expression, resulting in a visual map containing clusters of samples that exhibit similar genetic characteristics, thereby providing a comprehensive understanding of the predominant genetic profiles present within the analyzed samples.

For the exploratory analysis of the TCGA data we used an in-house developed application that implements the *Morphing Projections* technique (10). This tool facilitates a user-controlled arrangement of the data to enhance the exploration process, which permits a swift comparison of t-SNE plots constructed with diverse gene and/or miRNA lists, thereby enabling the visual identification of varying genetic patterns based on the chosen lists. Additionally, the tool is highly effective for selecting the samples to be examined, which helps to effectively categorize the data for differential genetic analysis.

2.3 Statistical analysis

Along with the morphing projections technique, the tool features statistical functionality, including the use of logistic regression to find genes or miRNA that best explain the differentiation between two groups selected by the user: miRNAs with higher estimated coefficients, as determined by the logistic regression model, have a greater impact on differentiation. This idea was originally introduced by Clark et al. in 2014 (13), in which they aimed to obtain the "characteristic direction" vector in the multidimensional space, and then to select the main components. However, given the limited number of samples in this case, it is crucial to take additional steps to verify the results. To this end,

ANOVA tests are conducted to evaluate the statistical significance of the difference in expression level of the miRNA in the two groups.

3 Results

The morphing projections tool was used to analyze the PANNET and PGL included in TCGA. Smooth animated transitions from gene expression and miRNA expression *t*-SNE maps revealed a remarkably different genetic behavior of 7 samples that had been originally labelled as pancreatic adenocarcinoma. In the gene expression *t*-SNE view, these samples were grouped with PGL; however, when weight was given to a miRNA expression t-SNE view, they were found to move away. This suggests a similar gene expression profile, but different miRNA profile, as shown in Figure 1.

To further investigate this differential expression, data was divided into five groups as shown in Figure 2. First, samples not classified as primary tumors (those with TCGA codes not ending in -01) were eliminated to form the main analysis group #1. Groups #2 and #3 were separated based on gender, with "male" and "female" samples analyzed separately to prevent bias due to unequal proportions of both genders in the PGL set (64 vs. 85). Similarly, groups #4 and #5 were created using race "white" (all 7 available PANNET samples are "white") and ethnicity "not hispanic or latino" (6 of the 7 PANNET samples belong to this ethnicity, except one that is unclassified).

A logistic regression was conducted in each group to identify the most significant miRNAs, as explained in section 2.3, and ANOVA tests were performed to determine the statistical significance. As a result, six miRNAs (-141-3p, -200c-3p, -192-5p, -194-5p, -10b-5p and -10b-3p) were repeatedly found among the top eight positions in all lists and were selected for further analysis (Table 1 and Figure 3). Although more miRNAs could be considered, the six selected adequately explain the difference between both groups.

To validate these data, we used the following datasets: GSE29742 (14), which includes miRNA data from fresh-frozen samples of 48 PGL: 37 pheochromocytomas and 11 paragangliomas; and GSE73367 (15) consisting of miRNA data from fresh-frozen samples of PANNET (n=50). By incorporating these datasets into our analysis, we also aimed to address the limitation of having only 7 PANNET samples. However, the use of various methodologies and normalization protocols complicates direct comparisons between different datasets (16). To address this issue, we applied percentile normalization to the data. In the absence of control samples, each value's percentile was determined based on the full expression levels across all samples in the dataset. This approach allowed us to identify miRNAs that are overexpressed (high percentile values) or underexpressed (low percentile values) relative to the rest of the data.

Results are shown in Figure 4 and clearly confirm our findings for miR-141-3p, -200c-3p, -192-5p and -194-5p, which are clearly overexpressed in PANNETs versus PGL. Additionally, miRNA-10b-5p and miR-10b-3p are overexpressed in PGL compared to PANNET, and although the magnitude of the difference is lower, it is still statistically significant.

4 Discussion

Our research has uncovered a remarkable similarity at the genetic level between PANNETs and PGLs, yet a striking dissimilarity in their miRNA expression profiles. We have identified 6 key miRNAs that can effectively distinguish between the two types of tumors, addressing a crucial need for more accurate diagnosis in the medical community.

We report here that 4 of the 6 identified miRNAs are elevated in PANNETs compared to PGLs. Interestingly, these microRNAs are members of two miRNA families: miR-200c/141-3p and miR-192/194. miRNA families often share similar sequences and structures, indicating a shared function (17). The miR-200c/141-3p family, located on chromosome 11p, has a complex role in cancer, acting as either an onco-miRNA or tumor suppressor depending on the type of cancer. It regulates epithelial-mesenchymal transition through targeting ZEB1/2 (18, 19) and has been linked to pro-apoptotic and anti-proliferative effects in several cancers, yet it also promotes tumor growth, invasion, and migration in others (20). High expression of miR-200c is associated with poor overall survival in gastric and non-small cell lung carcinomas (21, 22), but with better prognosis in ovarian and bladder cancer (23, 24). In pancreatic neuroendocrine cells, the promotion of beta cell survival by miR-200c has been demonstrated to be essential (25, 26). Meanwhile, miR-141 has demonstrated tumor suppressive effects in multiple

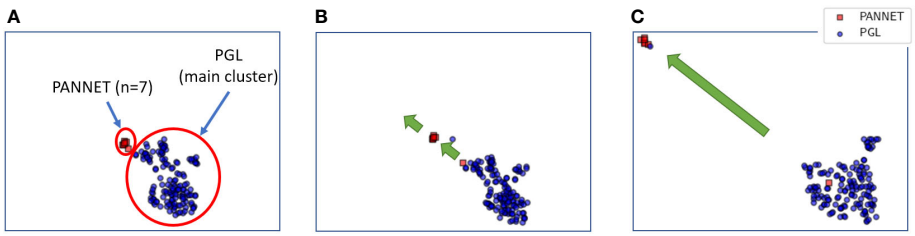

FIGURE 1
Smooth transition of t-SNE maps from gene expression profile **(A)** to miRNA expression profile **(B, C)**. In the gene expression profile **(A)**, PANNET samples cluster with PGL samples. However, as the weight of the t-SNE map shifts from gene expression to miRNA expression **(B, C)**, the PANNET samples move away from the PGL samples.

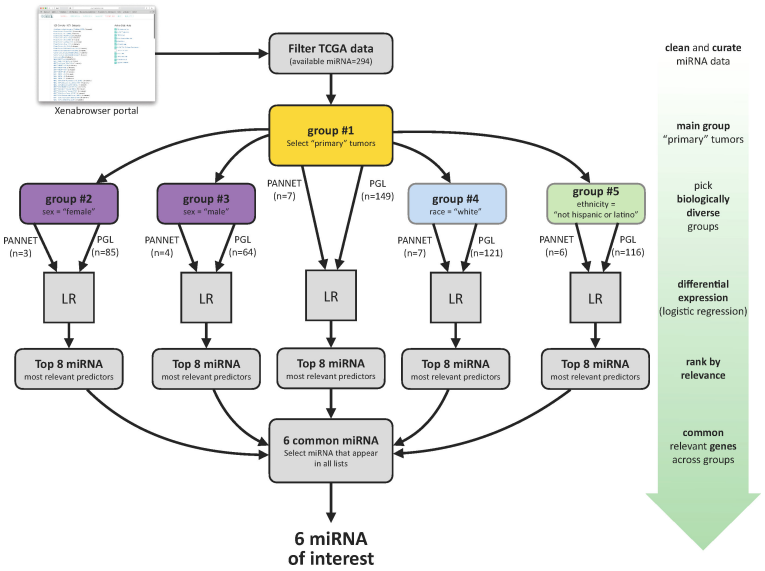

FIGURE 2
Summary of the data segregation and analysis pipeline for analysis between PANNET and PGL.

cancers, including pancreatic adenocarcinomas (27). The role of miR-192/194 family in cancer is complex and still debated, with evidence supporting both oncogenic and tumor-suppressive effects (28). miR-192 has been shown to inhibit tumor angiogenesis (29), while miR-194 suppresses proliferation, migration, and metastasis and induces apoptosis in cancer cells (30–33). The functional significance and mechanisms of action of these two families of miRNAs in neuroendocrine tumors, such as PANNET and PGL, remains unclear. Further research is needed to fully understand their impact on these tumors.

Our study also showed that PGLs express higher levels of both the -3p and -5p strands of the miR-10b duplex compared to PANNETs. Traditionally, only one strand of the miRNA duplex, known as the functional strand, was thought to target specific mRNAs, while the other strand was degraded. However, recent research has revealed that both strands of the duplex can be functional (34), which could account for the accurate detection of both miR-10b strands in both PANNET and PGL. One study has reported that miR-10b can differentiate PGL from neuroblastoma (35). Our results further support its potential as a biomarker for differentiating PANNET from PGL. miR-10b has been shown to be de-regulated in several types of cancer, but it is still unclear if it is causally related to cancer initiation or progression (36–39). To date, many studies have shown that miR-10b could be involved on metastasis in a wide range of cancer types supporting a role for this miRNA in cancer progression (36).

Retroperitoneal PGLs, although rare, can occur in the vicinity of or within the pancreas, resembling primary pancreatic lesions. To date, literature records have documented approximately 56 peripancreatic PGLs (2, 6, 40–46). Distinguishing between PANNETs and PGLs is crucial for appropriate patient management, both preoperatively and postoperatively. An accurate diagnosis of PGLs is essential for preoperative planning as previous research has shown that perioperative mortality and morbidity can be high if a PGL is diagnosed during surgery. This is because induction of anesthesia and manipulation of the tumor during surgery can trigger catecholamine release. In addition, the majority of PGLs are benign; however, the risk of developing metastatic disease is higher in abdominal PGLs, with rates ranging from 11-36%. Currently, there are no reliable markers to

TABLE 1 Selected miRNAs of interest.

miRNA	PANNET (mean ± std)	PGL (mean ± std)	ANOVA (p-value)
hsa-miR-141-3p	10.7 ± 0.76	1.66 ± 0.87	$p < 0.0001$
hsa-miR-200c-3p	13.4 ± 0.80	4.33 ± 1.09	$p < 0.0001$
hsa-miR-10b-5p	13.4 ± 1.0	17.8 ± 0.50	$p < 0.0001$
hsa-miR-192-5p	13.7 ± 0.6	8.78 ± 0.87	$p < 0.0001$
hsa-miR-194-5p	12.4 ± 0.72	7.65 ± 0.86	$p < 0.0001$
hsa-miR-10b-3p	2.65 ± 0.96	6.17 ± 0.65	$p < 0.0001$

Expression levels are given as log2(RPM+1).

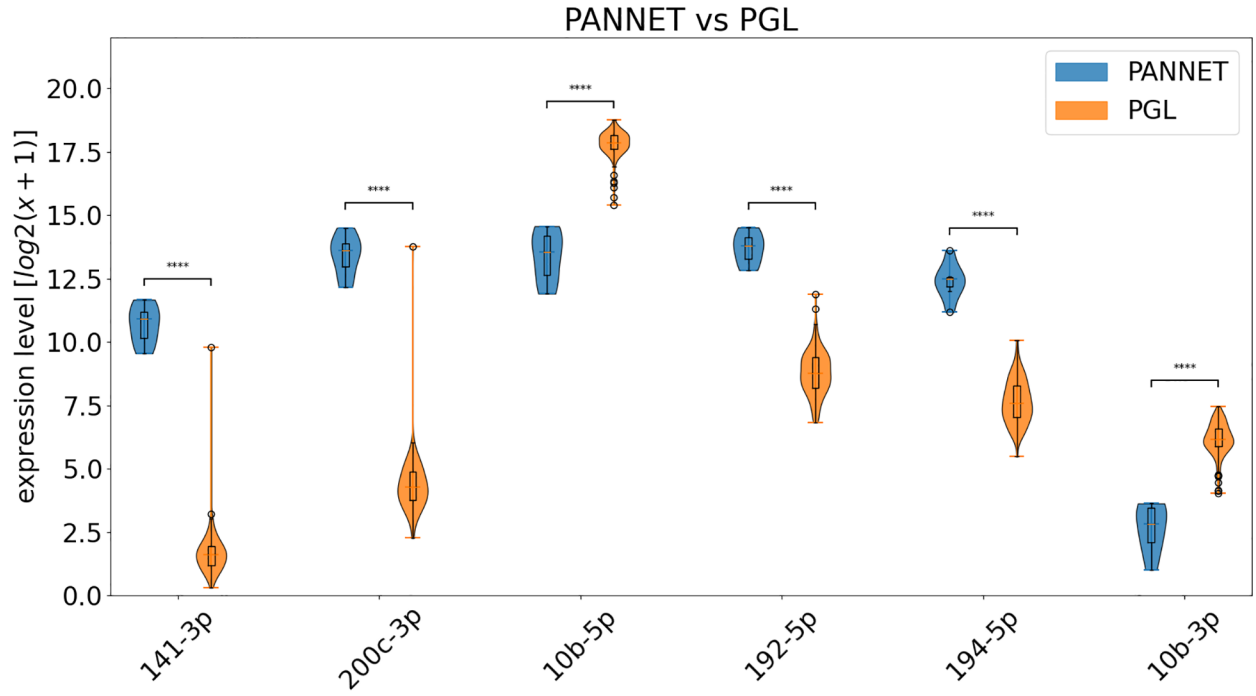

FIGURE 3
Violin diagrams showing the differential expression of the indicated miRNAs in PANNET and PGL included in the TCGA database. **** = p ≤ 0.0001.

predict malignancy, except for the presence of metastases. This highlights the need for follow-up for patients with PGLs as metastatic disease can appear years after diagnosis. Singhi et al (6), reported that 3 of 9 (33%) of patients diagnosed with peripancreatic PGL developed metastases within 5 years of surgery, and 2 of them died because of their disease. In another report (47), 13.9% exhibited a recurrence or widespread disease and one patient died 48 months following diagnosis. Additionally, it is

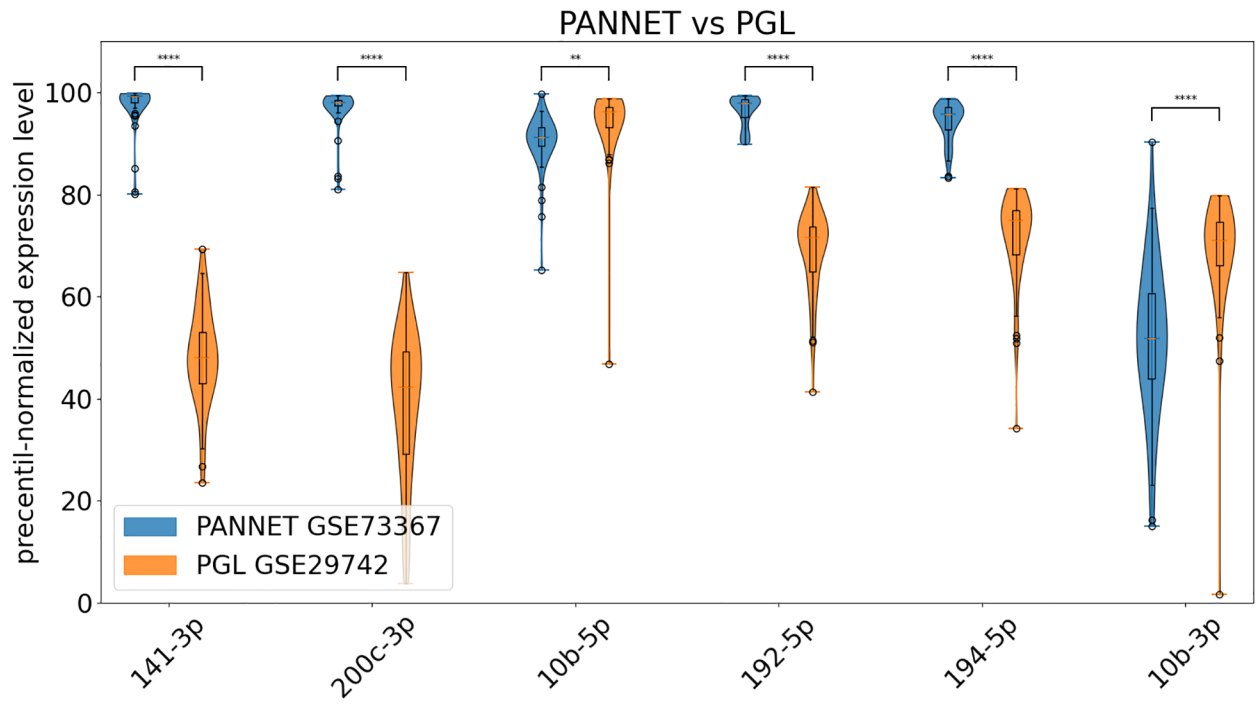

FIGURE 4
Percentile-normalized expression levels of the indicated miRNAs in PANNET, PGL from datasets GSE73367 and GSE29742 (** = p ≤ 0.01, **** = p ≤ 0.0001).

important to note that more than 40% of abdominal PGLs carry a germline pathogenic gene variant, which has significant clinical implications for personalized surveillance and treatment and for the patient's family.

Peripancreatic PGLs not only confound diagnosis through their clinical presentation and imaging characteristics, but also pose a significant challenge for even the most experienced pathologists. On surgical resection, both neoplasms are usually solitary, well-demarcated lesions with a fibrous border. In contrast to the peripancreatic PGLs, PANNETs are typically located inside the pancreatic parenchyma. However, parenchymal invasion was observed in many cases of peripancreatic PGLs with loss of zellballen architecture in these areas making accurate assessment of tumor location challenging. Moreover, PANNETs may display a variety of architectural patterns, including nested and solid growth, which may resemble a zellballen architecture.

By immunohistochemistry, both PGLs and some well-differentiated PANNETs demonstrate S-100-positive sustentacular cells. PANNETs are generally positive for cytokeratins AE1/AE3 and CAM 5.2, whereas PGLs are distinctly negative. Nevertheless, a more comprehensive panel of immunohistochemical stains, including cytokeratins, Vimentin, GATA-3 and/or Pax 8, has been recommended for accurate differentiation between the two types of tumors (6, 48, 49) as a single defining feature is not sufficient. In the absence of clear clinical indications, a diagnosis of a primary pancreatic neoplasm may be more likely than PGL. Ultimately, it is the responsibility of the pathologist to arrive at a definitive diagnosis of PGL. Our findings of using miR-200c/141-3p, miR-192/194 and miR-10b levels as potential biomarkers offer a promising solution to this challenge and hold significant implications for accurate diagnosis of PANNET and PGL.

4.1 Limitations of this study

The TCGA data, while balanced in terms of gender representation, lacks diversity in terms of race and ethnicity, as most samples are from the 'white' or 'non-hispanic-or-latino' groups. This could introduce bias, especially in the case of PANNET where all samples come from these groups. Moreover, the TCGA study only included data from a small number of PANNET samples (7), further limiting its representativeness. By incorporating additional datasets into our analysis, we aimed to address the constraint of a small sample size. However, it's important to acknowledge that these validation datasets lack clinical data, preventing us from exploring variations in the expression levels of the identified microRNAs across different stages of the disease or determining whether the tumors with different behaviours (benign or malignant) exhibit distinct miRNA expression profiles. Therefore, it is crucial to validate the findings of this study using larger sample sizes that encompass diverse racial and ethnic backgrounds and include comprehensive clinical data to facilitate a broader analysis.

5 Conclusions

This study uncovered six key microRNAs (miR-10b-3p, miR-10b-5p, and the miRNA families miR-200c/141 and miR-194/192) that can effectively differentiate peripancreatic PGLs from PANNETs. These findings suggest that measuring the levels of these miRNAs in tumor tissue samples could serve as potential biomarkers for more accurate diagnosis, potentially improving the standard of care for patients.

Data availability statement

Publicly available datasets were analyzed in this study. This data can be found here: https://portal.gdc.cancer.gov and in https://www.ncbi.nlm.nih.gov/ for the Gene Expression Omnibus: GSE29742 and GSE73367.

Author contributions

JE and ID designed and managed the data study. JE, ID and DG performed the data curation and analysis. The biomedical study was designed and managed by M-DC and NV. TC performed bioinformatics analysis. JE, ID, M-DC and NV wrote and reviewed the paper. All authors contributed to the article and approved the submitted version.

Funding

This research has been funded by the Spanish National Research Agency under grant number PID2020-115401GB-I00/AEI/10.13039/501100011033), the Instituto de Salud Carlos III through the project PI20/01754 co-funded by the European Union, the Network Biomedical Research Center–Cancer (CIBERONC), the Spanish Group of Orphan and Infrequent Tumors (GETHI) and the PHEiPAS Association.

Conflict of interest

The authors declare that the research was conducted in the absence of any commercial or financial relationships that could be construed as a potential conflict of interest.

Publisher's note

References

1. Mete O, Asa SL, Gill AJ, Kimura N, de Krijger RR, Tischler A. Overview of the 2022 WHO classification of paragangliomas and pheochromocytomas. *Endocr Pathol* (2022) 33:90–114. doi: 10.1007/s12022-022-09704-6

2. Asa SL, Ezzat S, Mete O. The diagnosis and clinical significance of paragangliomas in unusual locations. *J Clin Med* (2018) 7(9):280. doi: 10.3390/jcm7090280

3. Lightfoot N, Santos P, Nikfarjam M. Paraganglioma mimicking a pancreatic neoplasm. *J Pancreas* (2011) 12:259–61.doi: 10.6092/1590-8577/3293

4. Zamir O, Amir G, Lernau O, Ne'eman Z, Nissan S. Nonfunctional paraganglioma of the pancreas. *Am J Gastroenterol* (1984) 79(10):761–3.

5. Lanke G, Stewart JM, Lee JH. Pancreatic paraganglioma diagnosed by endoscopic ultrasound-guided fine needle aspiration: a case report and review of literature. *World J Gastroenterol* (2021) 27(37):6322–31. doi: 10.3748/wjg.v27.i37.6322

6. Singhi AD, Hruban RH, Fabre M, Imura J, Schulick R, Wolfgang C, et al. Peripancreatic paraganglioma: a potential diagnostic challenge in cytopathology and surgical pathology. *Am J Surg Pathol* (2011) 35(10):1498–504. doi: 10.1097/PAS.0b013e3182281767

7. Nguyen E, Nakasaki M, Lee TK, Lu D. Diagnosis of paraganglioma as a pancreatic mass: a case report. *Diagn Cytopathol* (2018) 46(9):804–6. doi: 10.1002/dc.23974

8. Baumrucker C, Kalavar M, Barkin JA, Franceschi D. The case of an asymptomatic pheochromocytoma masquerading as a pancreatic neuroendocrine tumor. *Pancreas* (2020) 49(7):e65–6. doi: 10.1097/MPA.0000000000001618

9. Straka M, Soumarova R, Migrova M, Vojtek C. Pancreatic paraganglioma - a rare and dangerous entity. vascular anatomy and impact on management. *J Surg Case Rep* (2014) 2014(7):rju074. doi: 10.1093/jscr/rju074

10. Díaz I, Enguita JM, González A, García D, Cuadrado AA, Chiara MD, et al. Morphing projections: a new visual technique for fast and interactive large-scale analysis of biomedical datasets. *Bioinformatics* (2021) 37(11):1571–80. doi: 10.1093/bioinformatics/btaa989

11. Peran I, Madhavan S, Byers SW, McCoy MD. Curation of the pancreatic ductal adenocarcinoma subset of the cancer genome atlas is essential for accurate conclusions about survival-related molecular mechanisms. *Clin Cancer Res* (2018) 24(16):3813–9. doi: 10.1158/1078-0432.CCR-18-0290

12. Van Der Maaten I, Hinton G. Visualizing data using t-SNE. *J Mach Learn Res* (2008) 9(86):2579–625.

13. Clark NR, Hu KS, Feldmann AS, Kou Y, Chen EY, Duan Q, et al. The characteristic direction: a geometrical approach to identify differentially expressed genes. *BMC Bioinf* (2014) 15:79. doi: 10.1186/1471-2105-15-79

14. de Cubas AA, Leandro-García LJ, Schiavi F, Mancikova V, Comino-Méndez I, Inglada-Pérez L, et al. Integrative analysis of miRNA and mRNA expression profiles in pheochromocytoma and paraganglioma identifies genotype-specific markers and potentially regulated pathways. *Endocr Relat Cancer* (2013) 20(4):477–93. doi: 10.1530/ERC-12-0183

15. Sadanandam A, Grotzinger C, Wiedenmann B, Hanahan D. A cross species and multi-omics (including metabolomics) analysis in pancreatic neuroendocrine tumours (miRNA). *NCBI GEO Database: Accession GSE73367* (2015).

16. Malczewska A, Kidd M, Matar S, Kos-Kudla B, Modlin IM. A comprehensive assessment of the role of miRNAs as biomarkers in gastroenteropancreatic neuroendocrine tumors. *Neuroendocrinology* (2018) 107(1):73–90. doi: 10.1159/000487326

17. Kaczkowski B, Torarinsson E, Reiche K, Havgaard JH, Stadler PF, Gorodkin J. Structural profiles of human miRNA families from pairwise clustering. *Bioinformatics* (2009) 25(3):291–4. doi: 10.1093/bioinformatics/btn628

18. Korpal M, Lee ES, Hu G, Kang Y. The miR-200 family inhibits epithelial-mesenchymal transition and cancer cell migration by direct targeting of e-cadherin transcriptional repressors ZEB1 and ZEB2. *J Biol Chem* (2008) 283:14910–4. doi: 10.1074/jbc.C800074200

19. Park SM, Gaur AB, Lengyel E, Peter ME. The miR-200 family determines the epithelial phenotype of cancer cells by targeting the e-cadherin repressors ZEB1 and ZEB2. *Genes Dev* (2008) 22:894–907. doi: 10.1038/ncb1722

20. Klicka K, Grzywa TM, Mielniczuk A, Klinke A, Włodarski PK. The role of miR-200 family in the regulation of hallmarks of cancer. *Front Oncol* (2022) 8:965231(12). doi: 10.3389/fonc.2022.965231

21. Huang ZS, Guo XW, Zhang G, Liang LX, Nong B. The diagnostic and prognostic value of miR-200c in gastric cancer: a meta-analysis. *Dis Markers* (2019) 2019:8949618. doi: 10.1155/2019/8949618

22. Tejero R, Navarro A, Campayo M, Viñolas N, Marrades RM, Cordeiro A. miR-141 and miR-200c as markers of overall survival in early stage non-small cell lung cancer adenocarcinoma. *PloS One* (2014) 9:e101899. doi: 10.1371/journal.pone.0101899

23. Shi C, Zhang Z. The prognostic value of the miR-200 family in ovarian cancer: a meta-analysis. *Acta Obstet Gynecol Scand* (2016) 95:505–12. doi: 10.1111/aogs.12883

24. Mei Y, Zheng J, Xiang P, Liu C, Fan Y. Prognostic value of the miR-200 family in bladder cancer: a systematic review and meta-analysis. *Med (Baltimore)* (2020) 99:e22891. doi: 10.1097/MD.0000000000022891

25. Belgardt BF, Ahmed K, Spranger M, Latreille M, Denzler R, Kondratiuk N. The microRNA-200 family regulates pancreatic beta cell survival in type 2 diabetes. *Nat Med* (2015) 21(6):619–27. doi: 10.1038/nm.3862

26. Title AC, Silva PN, Godbersen S, Hasenöhrl L, Stoffel M. The miR-200-Zeb1 axis regulates key aspects of β-cell function and survival in vivo. *Mol Metab* (2021) 53:101267. doi: 10.1016/j.molmet.2021.101267

27. Zhao G, Wang B, Liu Y, Zhang JG, Deng SC, Qin Q. miRNA-141, downregulated in pancreatic cancer, inhibits cell proliferation and invasion by directly targeting MAP4K4. *Mol Cancer Ther* (2013) 12:2569–80. doi: 10.1158/1535-7163.MCT-13-0296

28. Mishan MA, Tabari MAK, Parnian J, Fallahi J, Mahrooz A, Bagheri A. Functional mechanisms of miR-192 family in cancer. *Genes Chromosomes Cancer* (2020) 59:722–35. doi: 10.1002/gcc.22889

29. Wu SY, Rupaimoole R, Shen F, Pradeep S, Pecot CV, Ivan C, et al. A miR-192-EGR1-HOXB9 regulatory network controls the angiogenic switch in cancer. *Nat Commun* (2016) 7:11169. doi: 10.1038/ncomms11169

30. Meng Z, Fu X, Chen X, Zeng S, Tian Y, Jove R, et al. miR-194 is a marker of hepatic epithelial cells and suppresses metastasis of liver cancer cells in mice. *Hepatology* (2010) 52(6):2148–57. doi: 10.1002/hep.23915

31. Ran RZ, Chen J, Cui LJ, Lin XL, Fan MM, Cong ZZ, et al. miR-194 inhibits liver cancer stem cell expansion by regulating RAC1 pathway. *Exp Cell Res* (2019) 378(1):66–75. doi: 10.1016/j.yexcr.2019.03.007

32. Wang J, Zhang M, Hu X, She J, Sun R, Qin S, Li D. miRNA-194 predicts favorable prognosis in gastric cancer and inhibits gastric cancer cell growth by targeting CCND1. *FEBS Open Bio* (2021) 11(7):1814–1826. doi: 10.1002/2211-5463.13125

33. Wu X, Liu T, Fang O, Leach L, Hu X, Luo Z. miR-194 suppresses metastasis of non-small cell lung cancer through regulating expression of BMP1 and p27 kip1. *Oncogene* (2014) 33(12):1506–14. doi: 10.1038/onc.2013.108

34. Mitra R, Adams CM, Jiang W, Greenawalt E, Eischen CM. Pan-cancer analysis reveals cooperativity of both strands of microRNA that regulate tumorigenesis and patient survival. *Nat Commun* (2020) 11(1):968. doi: 10.1038/s41467-020-14713-2

35. Korotaeva A, Mansorunov D, Apanovich N, Kuzevanova A, Karpukhin A. MiRNA expression in neuroendocrine neoplasms of frequent localization localizations. *Noncoding RNA* (2021) 7(3):38. doi: 10.3390/ncrna7030038

36. Huang L, Lin JX, Yu YH, Zhang MY, Wang HY, Zheng M. Downregulation of six microRNAs is associated with advanced stage, lymph node metastasis and poor prognosis in small cell carcinoma of the cervix. *PloS One* (2012) 7:e33762. doi: 10.1371/journal.pone.0033762

37. Fritz HK, Lindgren D, Ljungberg B, Axelson H, Dahlbäck B. The miR(21/10b) ratio as a prognostic marker in clear cell renal cell carcinoma. *Eur J Cancer* (2014) 50:1758–65. doi: 10.1016/j.ejca.2014.03.281

38. Khella HWZ, Daniel N, Youssef L, Scorilas A, Nofech-Mozes R, Mirham L, et al. miR-10b is a prognostic marker in clear cell renal cell carcinoma. *J Clin Pathol* (2017) 70:854–9. doi: 10.1136/jclinpath-2017-204341

39. Sheedy P, Medarova Z. The fundamental role of miR-10b in metastatic cancer. *Am J Cancer Res* (2018) 8(9):1674–88.

40. Sangster G, Do D, Previgliano C, Li B, LaFrance D, Heldmann M. Primary retroperitoneal paraganglioma simulating a pancreatic mass: a case report and review of the literature. *HPB Surg* (2010) 2010:645728. doi: 10.1155/2010/645728

41. Tsukada A, Ishizaki Y, Nobukawa B, Kawasaki S. Paraganglioma of the pancreas: a case report and review of the literature. *Pancreas* (2008) 36(2):214–6. doi: 10.1097/01.MPA.0000311841.35183.45

42. Zeng J, Simsir A, Oweity T, Hajdu C, Cohen S, Shi Y. Peripancreatic paraganglioma mimics pancreatic/gastrointestinal neuroendocrine tumor on fine needle aspiration: report of two cases and review of the literature. *Diagn Cytopathol* (2017) 45:947–52. doi: 10.1002/dc.23761

43. Inzani F, Rindi G, Tamborrino E, Cobelli R, Bordi C. Extra-adrenal composite paraganglioma with ganglioneuroma component presenting as a pancreatic mass. *Endocr Pathol* (2009) 20(3):191–5. doi: 10.1007/s12022-009-9085-z

44. Zhao Z, Guo Y, Liu L, Zhang L, Li S, Yang J. Primary non-functional pancreatic paraganglioma: a case report and review of the literature. *J Int Med Res* (2022) 50 (12):3000605221143023. doi: 10.1177/03000605221143023

45. Li T, Yi RQ, Xie G, Wang DN, Ren YT, Li K. Pancreatic paraganglioma with multiple lymph node metastases found by spectral computed tomography: a case report and review of the literature. *World J Clin Cases* (2022) 10(31):11638–45. doi: 10.12998/wjcc.v10.i31.11638

46. Jiang CN, Cheng X, Shan J, Yang M, Xiao YQ. Primary pancreatic paraganglioma harboring lymph node metastasis: a case report. *World J Clin Cases* (2021) 9(27):8071–81. doi: 10.12998/wjcc.v9.i27.8071

47. Nikas IP, Ishak A, AlRawashdeh MM, Klapsinou E, Sepsa A, Tzimas GN, et al. Preoperative diagnosis of abdominal extra-adrenal paragangliomas with fine-needle biopsy. *Diagnostics (Basel)* (2022) 12(8):1819. doi: 10.3390/diagnostics12081819

48. So JS, Epstein JI. GATA3 expression in paragangliomas: a pitfall potentially leading to misdiagnosis of urothelial carcinoma. *Mod Pathol* (2013) 26:1365–70. doi: 10.1038/modpathol.2013.76

49. Koo J J, Mertens RB, Mirocha JM, Wang HL, Dhall D. Value of Islet1 and PAX8 in identifying metastatic neuroendocrine tumors of pancreatic origin. *Mod Pathol* (2012) 25:893–901. doi: 10.1038/modpathol.2012.34

frontiers | Frontiers in Endocrinology

TYPE Mini Review
PUBLISHED 13 July 2023
DOI 10.3389/fendo.2023.1204851

OPEN ACCESS

EDITED BY
Valentina Morelli,
Istituto Auxologico Italiano, Italy

REVIEWED BY
Bojana Popovic,
University of Belgrade, Serbia

*CORRESPONDENCE
Alicja Szatko
alicja.szatko@gmail.com
Małgorzata Gietka-Czernel
malgietka@vp.pl

RECEIVED 12 April 2023
ACCEPTED 26 June 2023
PUBLISHED 13 July 2023

CITATION
Szatko A, Glinicki P and Gietka-Czernel M (2023) Pheochromocytoma/paraganglioma-associated cardiomyopathy. *Front. Endocrinol.* 14:1204851. doi: 10.3389/fendo.2023.1204851

Pheochromocytoma/paraganglioma-associated cardiomyopathy

Alicja Szatko[1,2]*, Piotr Glinicki[1,2] and Małgorzata Gietka-Czernel[1]*

[1]Department of Endocrinology, Centre of Postgraduate Medical Education, Warsaw, Poland, [2]EndoLab Laboratory, Centre of Postgraduate Medical Education, Warsaw, Poland

Pheochromocytoma/paraganglioma (PPGL) are neuroendocrine tumors that frequently produce and release catecholamines. Catecholamine excess can manifest in several cardiovascular syndromes, including cardiomyopathy. PPGL-induced cardiomyopathies occur in up to 11% of cases and are most often associated with an adrenal pheochromocytoma (90%) and rarely with a paraganglioma derived from the sympathetic ganglia (10%). PPGL-associated cardiomyopathies can be chronic or acute, with takotsubo cardiomyopathy being the most often reported. These two types of PPGL-induced cardiomyopathy seem to have different pathophysiological backgrounds. Acute catecholaminergic stress inundates myocardial β-adrenoceptors and leads to left ventricle stunning and slight histological apoptosis. In chronic cardiomyopathy, prolonged catecholamine exposure leads to extended myocardial fibrosis, inflammation, and necrosis, and ultimately it causes dilated cardiomyopathy with a low ejection fraction. Sometimes, especially in cases associated with hypertension, hypertrophic cardiomyopathy can develop. The prognosis appears to be worse in chronic cases with a higher hospital mortality rate, higher cardiogenic shock rate at initial presentation, and lower left ventricular recovery rate after surgery. Therefore, establishing the correct diagnosis at an early stage of a PPGL is essential. This mini-review summarizes current data on pathophysiological pathways of cardiac damage caused by catecholamines, the clinical presentation of PPGL-induced cardiomyopathies, and discusses treatment options.

KEYWORDS

pheochromocytoma, paraganglioma, dilated cardiomyopathy, hypertrophic cardiomyopathy, takotsubo cardiomyopathy

1 Introduction

In recent years, we have witnessed remarkable progress in understanding the rare type of neuroendocrine tumors that produce catecholamines, which arise from chromaffin cells within the adrenal medulla (pheochromocytoma) and extra-adrenal sympathetic ganglia (paraganglioma), collectively referred to as pheochromocytoma-paraganglioma (PPGL).

According to the 5th series of the World Health Organization (WHO) Classification of Endocrine and Neuroendocrine Tumors, the term paraganglioma is used for both neoplasms, while pheochromocytoma is classified as an "intra-adrenal paraganglioma" (1). The annual incidence of PPGL increased during the past two decades, reaching an annual incidence of approximately 8 cases per million, mainly due to the increase in the number of imaging studies conducted in clinical practice (2). Despite higher awareness among clinicians and widely used imaging procedures, there are still PPGL cases that remain undetected, often leading to the fatal consequences of catecholamines excess, mainly cardiovascular complications (3).

The effect of supraphysiological levels of epinephrine and norepinephrine on the heart and vessels highly depend on the secretory profile of the PPGL (adrenergic vs. noradrenergic phenotype, episodic via. continuous release) (4). The most common, yet alone nonspecific sign of PPGL: hypertension, among other factors, may lead to myocardial hypoxia with various clinical manifestations: acute (takotsubo, ischemic) and chronic (dilated, hypertrophic) cardiomyopathy (5–8). Catecholamine-induced cardiomyopathy in PPGL (CICMPP) is potentially fatal, but an uncommon complication, with a prevalence of 8–11% of patients with a PPGL (9, 10). Although CICMPP is rarely the initial manifestation of PPGL, it is obligatory to rule out PPGL in patients with heart failure and paroxysmal symptoms: profuse diaphoresis, headaches, pallor, tremor, palpitations, and episodic hypertension, but also hyperglycemia in young patients with normal body mass index (BMI) (4, 10–12).

This review summarizes the pathophysiology of CICMPP, risk factors, the clinical presentation of takotsubo, dilated and hypertrophic CICMPP, treatment options, and future perspectives regarding recent advances in PPGL.

2 Pathophysiology of catecholamine-induced cardiomyopathy in PPGL

To understand the mechanisms leading to the diverse clinical manifestations of CICMPP, it is essential to comprehend how catecholamines affect the cardiovascular system. Catecholamines (epinephrine, norepinephrine, and dopamine) are tyrosine-derived hormones, and neurotransmitters synthesized predominantly in the adrenal medulla, sympathetic nerves, and brain (13, 14). Norepinephrine and epinephrine bind to adrenoceptors, while the effect of dopamine on adrenoceptors is negligible, but in high levels, dopamine may lead to hypotension mainly due to interaction with dopamine receptors present in mesenteric and renal vascular beds (15–17).

Adrenoceptors are a family of transmembrane G protein–linked receptors. There are two main types of adrenoceptors: α and β, which are further divided into nine subtypes: α1A, α1B, α1D, α2A, α2B, α2C, β1, β2, and β3. Binding the physiological ligands (norepinephrine and epinephrine) to adrenoceptors result in G protein–mediated transduction of the signal, activation of second messengers or ion channels, evoking a response in the cell, highly dependent on the type of adrenoceptor and target tissue (18).

α1-adrenoceptors are mostly found in vascular smooth muscle but are also present in the myocardium (subtype α1A) (19, 20). α1-adrenoceptors signal transduction leads to protein kinase C (PKC) activation, 1,4,5-inositol triphosphate production, and intracellular calcium flow (6, 19). This results in smooth muscle contraction, and increased cardiac output, while persistent α1-adrenoceptors stimulation leads to the hypertrophic phenotype (6, 19). α2-adrenoceptors can be found in vascular smooth muscle distally from the sympathetic nerve (mainly α-2B subtype), leading to vasoconstriction, while presynaptic α2-adrenoceptors inhibit norepinephrine release resulting in the reduction of the sympathetic stress response (20, 21). β1-adrenoceptors are expressed in the sinoatrial node, atrioventricular node, and cardiomyocytes, resulting in calcium-mediated increased contractility, heart rate, and enhanced conduction of electrical stimulus (20). In the cardiovascular system, stimulation of β2-adrenoceptors, through inhibition of cAMP production, leads to vasodilatation and relaxation of the myocardium (20, 22).

Norepinephrine has a stronger affinity to α-adrenoceptors than β-adrenoceptors, leading to increased cardiac output and vasoconstriction, which manifests as elevated blood pressure (6). Early response to norepinephrine includes a rise in heart rate, but activation of the baroreflex by the increased blood pressure causes the heart rate to decrease (6). Considering the affinity of norepinephrine to adrenoceptors and the typically continuous pattern of catecholamine release, persistent hypertension and arrhythmias are part of the clinical presentation (22–24). Epinephrine binds to all major adrenoceptors: α1, α2, β1, and β2 (20). At low concentrations, epinephrine is selective for β2-adrenoceptors. The ability to stimulate peripheral β2-adrenoceptors manifests in patients with a PPGL secreting epinephrine as hypotension, once α1-adrenoceptors are pharmacologically blocked (20, 22, 25, 26). At higher concentrations, epinephrine stimulates α-adrenoceptors resulting in vasoconstriction (20). Epinephrine at higher concentrations also has a strong affinity for β1-adrenoceptor, which results in positive inotropic, chronotropic, and dromotropic effects (20). Typically, a PPGL secreting epinephrine in an episodic release pattern is often experienced by the patients as tachyarrhythmias (22, 25, 26). Furthermore, life-threatening, excessive amounts of catecholamines lead to vasoconstriction (including coronary arteries), myocardial ischemia, and necrosis (27). Conditions (e.g., hyperthyroidism, hypercortisolism, hypokalemia, hypocalcemia) that increase the expression and sensitivity of the adrenoceptor amplify the devastating impact of catecholamine excess (3, 28–30).

Acute, uncontrolled release of catecholamines in PPGL causes hyperstimulation of β1-adrenoceptors, increasing heart rate and contractility (31). Furthermore, it significantly raises myocardial oxygen demand, especially when combined with coronary artery spasms due to the activation of α1-adrenoceptors, exposing the myocardium to hypoxia (31). Catecholamine surge also leads to microvascular alterations combined with calcium overload, which according to Wittstein et al., may contribute to reversible coronary

vasoconstriction, as observed in patients with takotsubo CICMPP (6, 32).

Myocardial cytosolic and mitochondrial calcium overload, one of the most prominent features of persistent catecholamine excess, promotes oxidative stress and mitochondrial permeability, leading to cell death (33). Mitochondrial calcium excess promotes hydrogen peroxide synthesis during oxidative deamination of catecholamines (31). The production of superoxide anion radicals is also enhanced by α1-adrenoceptor stimulation: they are products of nicotinamide adenine dinucleotide phosphate (NADPH) reactions (34). Another process that contributes to catecholamine-induced oxidative stress in cardiomyocytes is auto-oxidation of catecholamines producing highly reactive, toxic, and unstable "aminochromes" and inactive, more stable "aminolutins" which can be measured in the plasma (6, 35, 36). The reaction is accelerated by oxygen free radicals and various enzymes, e.g., myeloperoxidase, cytochrome oxidase (6). The toxicity of oxidized catecholamines was proven in the study of Yates et al., in which perfusion with oxidized isoproterenol in isolated rat hearts was found to induce ultrastructural mitochondrial damage in cardiomyocytes — the phenomenon was not observed when fresh isoproterenol was used (37). Furthermore, adrenochrome (50 mg/L) infusion of isolated rat hearts ceased contractile activity in 30 minutes, whereas epinephrine or metanephrine infusions had a positive impact on cardiac contractile activity (38). However, studies concerning the role of "aminochromes" in CICMPP are still missing.

Chronic exposure to catecholamine excess leads to desensitization of β-adrenoceptors (39). Desensitization occurs through the phosphorylation of the adrenoceptor by the G protein–coupled receptor kinase (GRK) and binding to the protein called β-arrestin2. GRK2/β-arrestin2 complexes promote β1-adrenoceptor uncoupling and internalization (40). Furthermore, high catecholamine stress causes β2-adrenoceptors to switch from the Gs to Gi signaling pathway, leading to decreased cardiac contractility (41). Interestingly, not only is the density of β2/β1-adrenoceptors higher at the apex than at the base, but also apical adrenoceptors show higher sensitivity to catecholamines than those at the base (41). The apex–base gradient of β-adrenoceptors and described switch from Gs to Gi of β2-adrenoceptors (also mainly observed in the apex) explain the impaired regional contractility and typical clinical presentation of takotsubo cardiomyopathy: apical hypokinesia and ballooning (41). The negative inotropic effect depends on β2-adrenoceptor phosphorylation by both protein kinase A (PKA) and GRKs (42). It is noteworthy that L41Q GRK5 polymorphism is associated with enhanced desensitization and impaired β-adrenoceptor response, and it is more prevalent among patients with takotsubo cardiomyopathy (43).

3 Predisposing factors and clinical presentation

Given the fact that one in ten patients with PPGL will develop CICMPP, a potentially fatal complication, it is essential to identify and closely monitor predisposed individuals. The results of the study by Wang et al. on 50 patients with CICMPP and 152 patients with PPGL without diagnosed CICMPP, identified five risk factors for CICMPP, namely maximum resting heart rate ≥ 115 per minute, maximum resting systolic blood pressure ≥ 180 mmHg, blood glucose ≥ 8.0 mmol/L, 3 or more reported symptoms (headache, sweating, hypertension, hypotension, palpitation, chest pain, dyspnea, impaired tip perfusion, syncope, nausea, and vomiting), and early onset ≤ 40 years (44). Interestingly, in the study by Zhao et al., among patients with PPGL, female sex, paroxysmal symptoms, PPGL secreting more than one catecholamine, and higher white blood cell and platelet counts were significantly more prevalent in patients developing cardiovascular complications (45). The link between the higher cardiovascular risk in patients with PPGL and increased platelet count may be explained by catecholamine-mediated modulation of platelet function and aggregation via stimulation of dopaminergic and α2-adrenoceptors expressed on platelets, since the activation of platelets is crucial in the pathogenesis of various cardiovascular diseases, e.g., hypertension and atherosclerosis (46–51). Genetic biomarkers may also help to determine the risk of CICMPP. In the recent study by Amar et al., the α2-adrenoceptor variant (alpha 2CDel322–325) was more prevalent among patients with CICMPP (52).

3.1 Takotsubo cardiomyopathy

Excess of catecholamines, apart from other stress factors, may lead to acute, reversible left ventricular wall motion abnormalities (LVWMA) with a regional or circumferential pattern extending beyond the coronary artery supply, named after the Japanese fishing pot used to catch octopus — takotsubo cardiomyopathy (53–56). LVWMA in takotsubo cardiomyopathy results in characteristic left ventricle ballooning during systole (56). LVWMA may affect the apical, mid-apical, mid-ventricular, mid-basal, and basal segments of the left ventricle (57). The clinical presentation of takotsubo CICMPP does not differ from acute coronary syndrome: patients usually report chest and/or abdominal pain, dyspnea, and the majority of patients also experience symptoms that should raise the suspicion of PPGL (e.g., palpitations, profuse sweating, headache) (53). The most common electrocardiogram (ECG) changes in takotsubo CICMPP include ST-elevation myocardial infarction (STEMI)–like changes (more than one-third of the patients), ST segment depression, T-wave inversion, and QT-prolongation (53, 58). Although elevated troponin concentrations were observed in 71–95% of patients with takotsubo cardiomyopathy, the peak values in myocardial infarction biomarkers are usually lower compared to patients with acute coronary syndrome and not proportional to left ventricle impairment (53, 58, 59).

On echocardiography, apical ballooning, hypokinesia, akinesia, dyskinesia of apical segments, and the occasional hypokinetic mid-segments, are the classic presentation of takotsubo cardiomyopathy (6, 59). However, it occurs also in reversed (inverted) form when basal segments are akinetic, while the apex is hyperkinetic (6, 59–61). The latter phenotype is rare, yet more prevalent in patients with takotsubo CICMPP than in the overall group of takotsubo

cardiomyopathy patients: 28.8% vs. 2.2% in the meta-analysis presented by Y-Hassan et al. (62). Moreover, a global pattern is more frequently present in takotsubo CICMPP (62). Compared to the overall takotsubo cardiomyopathy group, takotsubo CICMPP was characterized by higher complication rates: 68.2% vs. 21.8% (i.e., heart failure, pulmonary edema, and cardiogenic shock) and recurrence rate, whereas mortality was reported in 4% of cases and did not differ between the groups (62). In the takotsubo CICMPP group, death occurred in 7% of men and 2.7% of women ($p = 0.35$) (62). Mortality increased significantly during the recurrence of takotsubo CICMPP (11%, 2/18) (62).

3.2 Hypertrophic cardiomyopathy

Longstanding hypertension in undetected PPGL may lead to left ventricle outflow tract obstruction: a hallmark of hypertrophic CICMPP. Patients with hypertrophic cardiomyopathy usually report exertional dyspnea and fatigue with or without chest pain or presyncope (6, 63). In advanced stages, patients may experience orthopnea and/or fluid retention with peripheral/pulmonary edema (63). The typical symptoms of patients with hypertrophic CICMPP may also be complemented with PPGL-suggestive symptoms, namely profuse sweating, and palpitations (64, 65). ECG alterations often meet the criteria of left ventricle hypertrophy (64). Echocardiography shows systolic anterior motion of the anterior mitral valve leaflet, increased left ventricle outflow tract gradient with persisted ejection fraction (EF), and septal and posterior wall hypertrophy (64, 66, 67).

Interestingly, the results of the study by Dobrowolski et al. prove that subclinical impairment of systolic function in PPGL patients was independent of the presence of left ventricle hypertrophy (LVH) (68). In the abovementioned study, the assessment included a global longitudinal strain (GLS) — a parameter derived from two-dimensional speckle-tracking echocardiography — allowing to assess the function of longitudinally-oriented subendocardial fibers, which are the most susceptible to ischemia and wall stress. GLS more accurately reflects intrinsic myocardial function and early systolic dysfunction than EF (68, 69). The patients with PPGL had lower GLS (median 17.2%) than in the control group, while EF did not differ significantly (68). Early systolic dysfunction was confirmed in the meta-analysis, including 252 patients with PPGL, speckle tracking echocardiography (STE) revealed worse GLS in the pooled PPGL group when compared to the control group (-17.3 ± 1.2 vs. -20.0 ± 0.6), differences in EF were not observed between the groups (70). In the study by Dobrowolski et al., the adrenergic biochemical phenotype was associated with worse systolic function and nonsignificantly higher left ventricle mass index compared to BP-matched controls, indicating that apart from pressure overload, epinephrine per se may contribute to LVH (68). Experimental findings suggested the role of catecholamines in the induction of protein synthesis (71). Both systolic and diastolic alterations in patients with PPGL reversed significantly after curative surgery (68).

3.3 Dilated cardiomyopathy

Patients with dilated cardiomyopathy typically experience symptoms of progressive systolic dysfunction, often after a latent period when they are clinically asymptomatic (72, 73). Interestingly, in the analysis by Zhang et al., among all CICMPP cases, PPGL associated with genetic syndromes or metastatic PPGL were found predominantly in patients with dilated PPGL (23% of cases, i.e., multiple endocrine neoplasia type 2, neurofibromatosis type 1, and von Hippel-Lindau syndrome) (72). However, the abovementioned retrospective study has several limitations, including incomplete data regarding imaging findings (e.g., missing echocardiographic parameters leading to the categorization of 14 cases under unspecified cardiomyopathy) and the results of molecular analysis (e.g., SDHB mutations were not included) (72). In dilated CICMPP, ECG may be normal, although alterations ranging from T wave changes and left bundle branch block to disturbances in atrioventricular conduction may occur (73). Echocardiography reveals increased left ventricle end-diastolic volumes or diameters (> 2 Standard Deviations (SDs) from normal) with global systolic dysfunction not attributable to ischemic or valvular disease (73). Cardiovascular magnetic resonance (CMR) shows left ventricle dilatation, and it is also of use to rule out inflammatory processes, to assess rest stress myocardial perfusion, myocardial perfusion, iron, and fat deposition, and aortic distensibility in CICMPP (73, 74). The key to the successful management of dilated CICMPP is complete PPGL resection, which leads to the improvement of EF and lower mortality rate: death occurred in 4% (2/52) of patients who underwent surgical resection of a PPGL and 22% (2/9) of patients not treated surgically (72). The importance of precise screening and prompt diagnosis is highlighted by two case reports of heart transplants undertaken before the diagnosis of PPGL was established (75, 76).

The catecholamine binding affinities to adrenoceptors and pathophysiologic mechanisms leading to different subtypes of CICMPP are presented in Figure 1.

4 Treatment

The early diagnosis, confirmed by biochemical tests (elevated free or fractionated plasma or urine metanephrines), followed by localization of the lesion and complete PPGL resection is the mainstay of the successful treatment of patients with CICMPP. The analysis by Zhang et al. showed that PPGL resection was associated with an improved EF in 96% of CICMPP cases (72). Prior to surgery, α-adrenoceptor blockade should be initiated for 7–14 days (77). Some studies favor α1-selective over nonselective α-adrenoceptor blockers due to lower preoperative diastolic pressure, lower intraoperative heart rate, and better postoperative outcome (77, 78). However, the results of the randomized controlled PRECIST trial showed no differences between phenoxybenzamine and doxazosin in the duration of blood pressure being outside the target range during operation, but phenoxybenzamine was more efficient in preventing intraoperative hemodynamic instability (79). The addition of metyrosine (tyrosine hydroxylase inhibitor) should

10.3389/fendo.2023.1204851

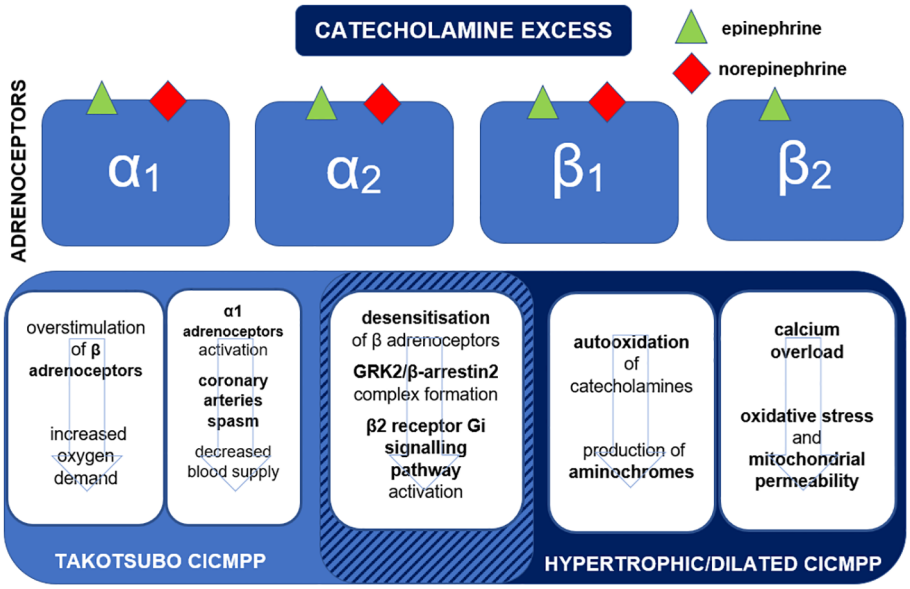

FIGURE 1
Binding affinities of epinephrine and norepinephrine to adrenoceptors and mechanisms leading to the development of subtypes of catecholamine-induced cardiomyopathy in pheochromocytoma-paraganglioma (CICMPP). G_i, inhibiting G protein; GRK, G protein–coupled receptor kinase.

be considered for patients at high risk of catecholamine surge (e.g., with symptomatic, multifocal, or metastatic disease intolerance of α-adrenoceptor blockers or when difficult surgery of PPGL encroaching neighboring vascular structures is anticipated) (80). However, the availability of metyrosine is limited (11).

Once the α-adrenoceptor blockade is assured and the target heart rate (of 60–70 bpm seated and 70–80 bpm standing) is not achieved, a β-adrenoceptor blocker should be initiated (not earlier than 3–4 days after initiation of an α-adrenoceptor blocker) (22, 77). Selective β1-adrenoceptor blockers are favored (since β2-adrenoceptor blockade may result in hypertension). In the emergency setting, intravenous fast-acting esmolol or alternatively metoprolol may allow to optimally react to hemodynamic alterations (3). Among oral β-adrenoceptor blockers, metoprolol succinate (controlled-release) or atenolol are preferred (3). The choice of β-adrenoceptor blockers in the treatment of CICMPP should also include subtype-specific recommendations: preferred non-vasodilating β-adrenoceptor blockers (atenolol, metoprolol, bisoprolol) in hypertrophic cardiomyopathy (81).

The preoperative aim is a blood pressure of less than 130/80 mm Hg while seated and greater than 90 mm Hg systolic while standing (77). If blood pressure is not optimally controlled calcium channel blockers may be added (77). If heart failure is confirmed, angiotensin-converting enzyme inhibitors (ACEI) or angiotensin receptor blockers (ARBs) are a part of pharmacological therapy. There are also novel, potential therapeutic options for patients with PPGL cardiomyopathy and heart failure, namely sodium-glucose cotransporter 2 inhibitors (SGLT2i) and angiotensin receptor/neprilysin inhibitor (ARNI). Multiple trials proved their efficacy in patients with heart failure, but in PPGL data are limited and further studies are needed (82, 83). Before the resection of PPGL, a high-sodium diet and fluid intake should be assured to prevent severe hypotension after PPGL removal (77). Preoperative assessment should also include an electrocardiogram and echocardiogram, which may identify the features of CICMPP (84).

Patients with PPGL are more prone to develop acute cardiovascular complications. In case of hypertensive crisis, intravenous administration of phentolamine, sodium nitroprusside, or nicardipine should be initiated. Once the state of the patient is stable, titration of the phenoxybenzamine dosage can be initiated to reach the target blood pressure (85). Fluid status should be monitored, diuretics are to be avoided unless the patient has fluid congestion, and even then, administered judiciously (6). In the management of hemodynamic instability, vasoactive amines are often administered, but their efficacy may be limited due to sympathetic receptor down-regulation, and they may even exacerbate PPGL-induced cardiac dysfunction (6, 86–88). If hypotension persists despite pharmacological treatment, mechanical circulatory support (MCS) may be needed. In the systematic review of 62 patients with severe systolic dysfunction (median left ventricular ejection fraction (LVEF) of 16% (range 5–32%)) requiring extracorporeal life support (ECLS) due to intractable pheochromocytoma crisis, full recovery of left ventricle function (LVEF >50%) was observed in most patients and 54 (87%) of 62 reported cases survived (89). Also, there are reports of successful left ventricular assist device (LVAD) use in PPGL-induced heart failure and perioperative management (90–92). An intra-aortic balloon pump (IABP) has been used for unresponsive patients but was not effective (93).

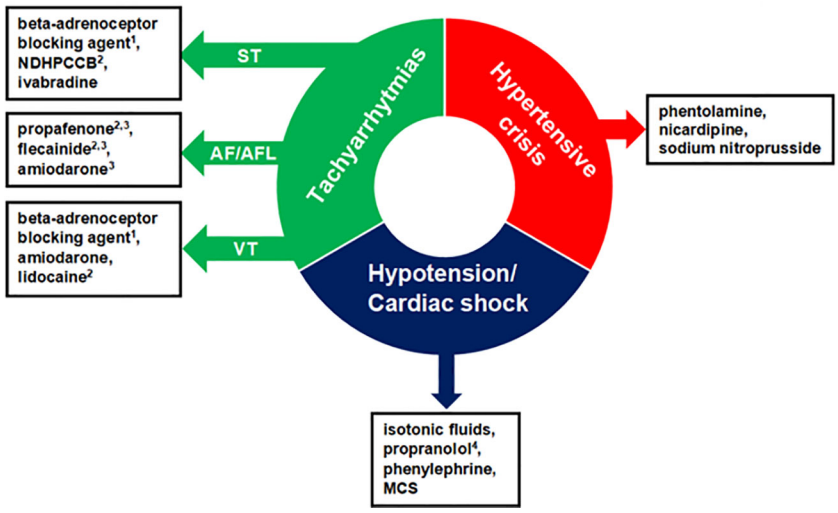

FIGURE 2
Pharmacological management of acute cardiovascular complications in patients with pheochromocytoma-paraganglioma. The order of presented drugs does not correspond to first-, second-, and third-line therapy and the choice of administered drugs should be individualized. [1]With alpha-adrenoceptor blockade, otherwise, it can precipitate a hypertensive crisis. [2]Antiarrhythmic agent not recommended in systolic dysfunction. [3]Used to restore sinus rhythm. [4]In case of hypotension and suspected beta2-adrenoceptor overstimulation. NDHPCCB, Nondihydropyridine Calcium Channel Blockers; ST, Sinus Tachycardia; AF/AFL, Atrial Fibrillation/Atrial Flutter; VT, Ventricular Tachycardia; MCS, Mechanical Circulatory Support.

The general pharmacological management of hypertensive crisis, hypotension/cardiac shock, and the most common tachyarrhythmias in PPGL are summarized in Figure 2.

5 Conclusions

CICMPP is a potentially fatal complication of PPGL, but there are still patients with CICMPP not diagnosed early enough. Thus, it is essential to broaden awareness about the clinical course and adequate management of CICMPP among clinicians and underline the importance of accurate cardiac assessment of PPGL patients.

Currently, the management of CICMPP is based on the guidelines for PPGL treatment, recommended general cardiological interventions, published case series, and few systematic reviews or meta-analyses. Dedicated guidelines of CICMPP management addressing specific features of this rare entity and integrating novel advances in pharmacotherapy and MCS could help to optimally treat patients with CICMPP.

Probably the ongoing progress in genetics and metabolomics in PPGL, completed by integration of the results using artificial intelligence, may contribute to a better understanding of the diverse effects of catecholamine excess on the cardiovascular system, identify predisposing factors (also among asymptomatic carriers of pathogenic mutations in genes predisposing to PPGL development), biomarkers, and establish the prognosis.

Author contributions

MG-C provided the idea for the manuscript. AS, PG, and MG-C reviewed the relevant literature and drafted the manuscript. AS drafted the figures. MG-C and PG reviewed critically the manuscript. All authors have made substantial contributions to the manuscript and have read and approved the final version of the manuscript.

Conflict of interest

The authors declare that the research was conducted in the absence of any commercial or financial relationships that could be construed as a potential conflict of interest.

Publisher's note

References

1. Mete O, Asa SL, Gill AJ, Kimura N, de Krijger RR, Tischler A. Overview of the 2022 who classification of paragangliomas and pheochromocytomas. *Endocr Pathol* (2022) 33(1):90–114. doi: 10.1007/s12022-022-09704-6

2. Berends AMA, Buitenwerf E, de Krijger RR, Veeger N, van der Horst-Schrivers ANA, Links TP, et al. Incidence of pheochromocytoma and sympathetic paraganglioma in the Netherlands: a nationwide study and systematic review. *Eur J Intern Med* (2018) 51:68–73. doi: 10.1016/j.ejim.2018.01.015

3. Nazari MA, Rosenblum JS, Haigney MC, Rosing DR, Pacak K. Pathophysiology and acute management of tachyarrhythmias in pheochromocytoma: jacc review topic of the week. *J Am Coll Cardiol* (2020) 76(4):451–64. doi: 10.1016/j.jacc.2020.04.080

4. Pacak K. New biology of pheochromocytoma and paraganglioma. *Endocr Pract* (2022) 28(12):1253–69. doi: 10.1016/j.eprac.2022.09.003

5. Soltani A, Pourian M, Davani BM. Does this patient have pheochromocytoma? a systematic review of clinical signs and symptoms. *J Diabetes Metab Disord* (2015) 15:6. doi: 10.1186/s40200-016-0226-x

6. Santos JRU, Brofferio A, Viana B, Pacak K. Catecholamine-induced cardiomyopathy in pheochromocytoma: how to manage a rare complication in a rare disease? *Horm Metab Res* (2019) 51(7):458–69. doi: 10.1055/a-0669-9556

7. Zuber SM, Kantorovich V, Pacak K. Hypertension in pheochromocytoma: characteristics and treatment. *Endocrinol Metab Clin North Am* (2011) 40(2):295–311. doi: 10.1016/j.ecl.2011.02.002

8. Kobayashi Y, Kobayashi Y, Hirohata A. Pheochromocytoma found in takotsubo cardiomyopathy patients. *J Invasive Cardiol* (2014) 26(6):E76–7.

9. Park JH, Kim KS, Sul JY, Shin SK, Kim JH, Lee JH, et al. Prevalence and patterns of left ventricular dysfunction in patients with pheochromocytoma. *J Cardiovasc Ultrasound* (2011) 19(2):76–82. doi: 10.4250/jcu.2011.19.2.76

10. Giavarini A, Chedid A, Bobrie G, Plouin PF, Hagege A, Amar L. Acute catecholamine cardiomyopathy in patients with phaeochromocytoma or functional paraganglioma. *Heart* (2013) 99(19):1438–44. doi: 10.1136/heartjnl-2013-304073

11. Lenders JWM, Kerstens MN, Amar L, Prejbisz A, Robledo M, Taieb D, et al. Genetics, diagnosis, management and future directions of research of phaeochromocytoma and paraganglioma: a position statement and consensus of the working group on endocrine hypertension of the European society of hypertension. *J Hypertens* (2020) 38(8):1443–56. doi: 10.1097/HJH.0000000000002438

12. La Batide-Alanore A, Chatellier G, Plouin PF. Diabetes as a marker of pheochromocytoma in hypertensive patients. *J Hypertens* (2003) 21(9):1703–7. doi: 10.1097/00004872-200309000-00020

13. Eisenhofer G, Kopin IJ, Goldstein DS. Catecholamine metabolism: a contemporary view with implications for physiology and medicine. *Pharmacol Rev* (2004) 56(3):331–49. doi: 10.1124/pr.56.3.1

14. Schulz C, Eisenhofer G, Lehnert H. Principles of catecholamine biosynthesis, metabolism and release. *Front Horm Res* (2004) 31:1–25. doi: 10.1159/000074656

15. Contreras F, Fouillioux C, Bolivar A, Simonovis N, Hernandez-Hernandez R, Armas-Hernandez MJ, et al. Dopamine, hypertension and obesity. *J Hum Hypertens* (2002) 16 Suppl 1:S13–7. doi: 10.1038/sj.jhh.1001334

16. Goldberg LI. Cardiovascular and renal actions of dopamine: potential clinical applications. *Pharmacol Rev* (1972) 24(1):1–29.

17. Jose PA, Eisner GM, Felder RA. Regulation of blood pressure by dopamine receptors. *Nephron Physiol* (2003). 95(2):19–27 doi: 10.1159/000073676

18. Docherty JR. The pharmacology of alpha(1)-adrenoceptor subtypes. *Eur J Pharmacol* (2019) 855:305–20. doi: 10.1016/j.ejphar.2019.04.047

19. Brodde OE, Michel MC. Adrenergic and muscarinic receptors in the human heart. *Pharmacol Rev* (1999) 51(4):651–90.

20. Gordan R, Gwathmey JK, Xie LH. Autonomic and endocrine control of cardiovascular function. *World J Cardiol* (2015) 7(4):204–14. doi: 10.4330/wjc.v7.i4.204

21. Giovannitti JAJr., Thoms SM, Crawford JJ. Alpha-2 adrenergic receptor agonists: a review of current clinical applications. *Anesth Prog* (2015) 62(1):31–9. doi: 10.2344/0003-3006-62.1.31

22. Gupta G, Pacak K, Committee AAS. Precision medicine: an update on Genotype/Biochemical phenotype relationships in Pheochromocytoma/Paraganglioma patients. *Endocr Pract* (2017) 23(6):690–704. doi: 10.4158/EP161718.RA

23. Pacak K. Preoperative management of the pheochromocytoma patient. *J Clin Endocrinol Metab* (2007) 92(11):4069–79. doi: 10.1210/jc.2007-1720

24. Eisenhofer G, Huynh TT, Elkahloun A, Morris JC, Bratslavsky G, Linehan WM, et al. Differential expression of the regulated catecholamine secretory pathway in different hereditary forms of pheochromocytoma. *Am J Physiol Endocrinol Metab* (2008) 295(5):E1223–33. doi: 10.1152/ajpendo.90591.2008

25. Kantorovich V, Pacak K. A new concept of unopposed beta-adrenergic overstimulation in a patient with pheochromocytoma. *Ann Intern Med* (2005) 142 (12 Pt 1):1026–8. doi: 10.7326/0003-4819-142-12_part_1-200506210-00023

26. Baxter MA, Hunter P, Thompson GR, London DR. Phaeochromocytomas as a cause of hypotension. *Clin Endocrinol (Oxf)* (1992) 37(3):304–6. doi: 10.1111/j.1365-2265.1992.tb02326.x

27. Rona G. Catecholamine cardiotoxicity. *J Mol Cell Cardiol* (1985) 17(4):291–306. doi: 10.1016/s0022-2828(85)80130-9

28. Motulsky HJ, Insel PA. Adrenergic receptors in man: direct identification, physiologic regulation, and clinical alterations. *N Engl J Med* (1982) 307(1):18–29. doi: 10.1056/NEJM198207013070104

29. Ciaraldi TP, Marinetti GV. Hormone action at the membrane level. viii. adrenergic receptors in rat heart and adipocytes and their modulation by thyroxine. *Biochim Biophys Acta* (1978) 541(3):334–46. doi: 10.1016/0304-4165(78)90193-9

30. Leon AS, Abrams WB. The role of catecholamines in producing arrhythmias. *Am J Med Sci* (1971) 262(1):9–13. doi: 10.1097/00000441-197107000-00002

31. Costa VM, Carvalho F, Bastos ML, Carvalho RA, Carvalho M, Remiao F. Contribution of catecholamine reactive intermediates and oxidative stress to the pathologic features of heart diseases. *Curr Med Chem* (2011) 18(15):2272–314. doi: 10.2174/092986711795656081

32. Wittstein IS, Thiemann DR, Lima JA, Baughman KL, Schulman SP, Gerstenblith G, et al. Neurohumoral features of myocardial stunning due to sudden emotional stress. *N Engl J Med* (2005) 352(6):539–48. doi: 10.1056/NEJMoa043046

33. Khan MU, Cheema Y, Shahbaz AU, Ahokas RA, Sun Y, Gerling IC, et al. Mitochondria play a central role in nonischemic cardiomyocyte necrosis: common to acute and chronic stressor states. *Pflugers Arch* (2012) 464(1):123–31. doi: 10.1007/s00424-012-1079-x

34. Amin JK, Xiao L, Pimental DR, Pagano PJ, Singh K, Sawyer DB, et al. Reactive oxygen species mediate alpha-adrenergic receptor-stimulated hypertrophy in adult rat ventricular myocytes. *J Mol Cell Cardiol* (2001) 33(1):131–9. doi: 10.1006/jmcc.2000.1285

35. Dhalla NS. Formation of aminochrome leads to cardiac dysfunction and sudden cardiac death. *Circ Res* (2018) 123(4):409–11. doi: 10.1161/CIRCRESAHA.118.313416

36. Dhalla KS, Ganguly PK, Rupp H, Beamish RE, Dhalla NS. Measurement of adrenolutin as an oxidation product of catecholamines in plasma. *Mol Cell Biochem* (1989) 87(1):85–92. doi: 10.1007/BF00421086

37. Yates JC, Dhalla NS. Induction of necrosis and failure in the isolated perfused rat heart with oxidized isoproterenol. *J Mol Cell Cardiol* (1975) 7(11):807–16. doi: 10.1016/0022-2828(75)90132-7

38. Yates JC, RE B, Dhalla NS. Ventricular dysfunction and necrosis produced by adrenochrome metabolite of epinephrine: relation to pathogenesis of catecholamine cardiomyopathy. *Am Heart J* (1981) 102(2):210–21. doi: 10.1016/s0002-8703(81)80012-9

39. Kassim TA, Clarke DD, Mai VQ, Clyde PW, Mohamed Shakir KM. Catecholamine-induced cardiomyopathy. *Endocr Pract* (2008) 14(9):1137–49. doi: 10.4158/EP.14.9.1137

40. Kumar A, Pappachan JM, Fernandez CJ. Catecholamine-induced cardiomyopathy: an endocrinologist's perspective. *Rev Cardiovasc Med* (2021) 22 (4):1215–28. doi: 10.31083/j.rcm2204130

41. Paur H, Wright PT, Sikkel MB, Tranter MH, Mansfield C, O'Gara P, et al. High levels of circulating epinephrine trigger apical cardiodepression in a Beta2-adrenergic Receptor/Gi-dependent manner: a new model of takotsubo cardiomyopathy. *Circulation* (2012) 126(6):697–706. doi: 10.1161/CIRCULATIONAHA.112.111591

42. Liu R, Ramani B, Soto D, De Arcangelis V, Xiang Y. Agonist dose-dependent phosphorylation by protein kinase a and G protein-coupled receptor kinase regulates Beta2 adrenoceptor coupling to G(I) proteins in cardiomyocytes. *J Biol Chem* (2009) 284(47):32279–87. doi: 10.1074/jbc.M109.021428

43. Spinelli L, Trimarco V, Di Marino S, Marino M, Iaccarino G, Trimarco B. L41q polymorphism of the G protein coupled receptor kinase 5 is associated with left ventricular apical ballooning syndrome. *Eur J Heart Fail* (2010) 12(1):13–6. doi: 10.1093/eurjhf/hfp173

44. Wang Y, Yu X, Huang Y. Predictive factors for catecholamine-induced cardiomyopathy in patients with pheochromocytoma and paraganglioma. *Front Endocrinol (Lausanne)* (2022) 13:853878. doi: 10.3389/fendo.2022.853878

45. Zhao L, Meng X, Mei Q, Fan H, Liu Y, Zhou X, et al. Risk factors for cardiac complications in patients with pheochromocytoma and paraganglioma: a retrospective single-center study. *Front Endocrinol (Lausanne)* (2022) 13:877341. doi: 10.3389/fendo.2022.877341

46. Ricci A, Bronzetti E, Mannino F, Mignini F, Morosetti C, Tayebati SK, et al. Dopamine receptors in human platelets. *Naunyn Schmiedebergs Arch Pharmacol* (2001) 363(4):376–82. doi: 10.1007/s002100000339

47. Anfossi G, Trovati M. Role of catecholamines in platelet function: pathophysiological and clinical significance. *Eur J Clin Invest* (1996) 26(5):353–70. doi: 10.1046/j.1365-2362.1996.150293.x

48. Tschuor C, Asmis LM, Lenzlinger PM, Tanner M, Harter L, Keel M, et al. *In vitro* norepinephrine significantly activates isolated platelets from healthy volunteers and critically ill patients following severe traumatic brain injury. *Crit Care* (2008) 12(3): R80. doi: 10.1186/cc6931

49. Amadio P, Zara M, Sandrini L, Ieraci A, Barbieri SS. Depression and cardiovascular disease: the viewpoint of platelets. *Int J Mol Sci* (2020) 21(20):7560. doi: 10.3390/ijms21207560

50. Ouvina SM, La Greca RD, Zanaro NL, Palmer L, Sassetti B. Endothelial dysfunction, nitric oxide and platelet activation in hypertensive and diabetic type ii patients. *Thromb Res* (2001) 102(2):107–14. doi: 10.1016/s0049-3848(01)00237-7

51. Beckman JA, Creager MA, Libby P. Diabetes and atherosclerosis: epidemiology, pathophysiology, and management. *JAMA* (2002) 287(19):2570–81. doi: 10.1001/jama.287.19.2570

52. Amar J, Brunel J, Cardot Bauters C, Jacques V, Delmas C, Odou MF, et al. Genetic biomarkers of life-threatening pheochromocytoma-induced cardiomyopathy. *Endocr Relat Cancer* (2022) 29(5):267–72. doi: 10.1530/ERC-21-0373

53. YH S. Clinical features and outcome of pheochromocytoma-induced takotsubo syndrome: analysis of 80 published cases. *Am J Cardiol* (2016) 117(11):1836–44. doi: 10.1016/j.amjcard.2016.03.019

54. YH S, Falhammar H. Pheochromocytoma- and paraganglioma-triggered takotsubo syndrome. *Endocrine* (2019) 65(3):483–93. doi: 10.1007/s12020-019-02035-3

55. Dote K, Sato H, Tateishi H, Uchida T, Ishihara M. [Myocardial stunning due to simultaneous multivessel coronary spasms: a review of 5 cases]. *J Cardiol* (1991) 21 (2):203–14.

56. YH S, Tornvall P. Epidemiology, pathogenesis, and management of takotsubo syndrome. *Clin Auton Res* (2018) 28(1):53–65. doi: 10.1007/s10286-017-0465-z

57. YH S, De Palma R. Contemporary review on the pathogenesis of takotsubo syndrome: the heart shedding tears: norepinephrine churn and foam at the cardiac sympathetic nerve terminals. *Int J Cardiol* (2017) 228:528–36. doi: 10.1016/j.ijcard.2016.11.086

58. Gagnon N, Mansour S, Bitton Y, Bourdeau I. Takotsubo-like cardiomyopathy in a Large cohort of patients with pheochromocytoma and paraganglioma. *Endocr Pract* (2017) 23(10):1178–92. doi: 10.4158/EP171930.OR

59. Ghadri JR, Wittstein IS, Prasad A, Sharkey S, Dote K, Akashi YJ, et al. International expert consensus document on takotsubo syndrome (Part ii): diagnostic workup, outcome, and management. *Eur Heart J* (2018) 39(22):2047–62. doi: 10.1093/eurheartj/ehy077

60. Tagawa M, Nanba H, Suzuki H, Nakamura Y, Uchiyama H, Ochiai S, et al. Ventricular rhythm and hypotension in a patient with pheochromocytoma-induced myocardial damage and reverse takotsubo cardiomyopathy. *Intern Med* (2015) 54 (18):2343–9. doi: 10.2169/internalmedicine.54.4732

61. Di Valentino M, Balestra GM, Christ M, Raineri I, Oertli D, Zellweger MJ. Inverted takotsubo cardiomyopathy due to pheochromocytoma. *Eur Heart J* (2008) 29 (6):830. doi: 10.1093/eurheartj/ehm449

62. YH S, Falhammar H. Clinical features, complications, and outcomes of exogenous and endogenous catecholamine-triggered takotsubo syndrome: a systematic review and meta-analysis of 156 published cases. *Clin Cardiol* (2020) 43 (5):459–67. doi: 10.1002/clc.23352

63. Maron BJ, Desai MY, Nishimura RA, Spirito P, Rakowski H, Towbin JA, et al. Management of hypertrophic cardiomyopathy: jacc state-of-the-Art review. *J Am Coll Cardiol* (2022) 79(4):390–414. doi: 10.1016/j.jacc.2021.11.021

64. Wani A, Adil A, Gardezi SAA, Jain R, Galazka P, Waples MJ, et al. Pheochromocytoma presenting as hypertrophic obstructive cardiomyopathy. *JAMA Cardiol* (2021) 6(8):974–6. doi: 10.1001/jamacardio.2021.0944

65. Alamri A, Oriez C, Brenier M, Voican A, Banu I, Mourad JJ, et al. A case of late-detected pheochromocytoma in a young patient with resistant hypertension and hypertrophic cardiomyopathy. *Am J Hypertens* (2020). doi: 10.1093/ajh/hpaa126

66. Jacob JL, da Silveira LC, de Freitas CG, Centola CA, Nicolau JC, Lorga AM. Pheochromocytoma with echocardiographic features of obstructive hypertrophic cardiomyopathy. a case report. *Angiology* (1994) 45(11):985–9. doi: 10.1177/000331979404501113

67. Huddle KR, Kalliatakis B, Skoularigis J. Pheochromocytoma associated with clinical and echocardiographic features simulating hypertrophic obstructive cardiomyopathy. *Chest* (1996) 109(5):1394–7. doi: 10.1378/chest.109.5.1394

68. Dobrowolski P, Januszewicz A, Klisiewicz A, Gosk-Przybylek M, Peczkowska M, Kabat M, et al. Left ventricular structural and functional alterations in patients with Pheochromocytoma/Paraganglioma before and after surgery. *JACC Cardiovasc Imaging* (2020) 13(12):2498–509. doi: 10.1016/j.jcmg.2020.07.017

69. Joseph G, Zaremba T, Johansen MB, Ekeloef S, Heiberg E, Engblom H, et al. Echocardiographic global longitudinal strain is associated with infarct size assessed by cardiac magnetic resonance in acute myocardial infarction. *Echo Res Pract* (2019) 6 (4):81–9. doi: 10.1530/ERP-19-0026

70. Cuspidi C, Gherbesi E, Faggiano A, Sala C, Carugo S, Grassi G, et al. Targeting left ventricular mechanics in patients with Pheochromocytoma/Paraganglioma: an updated meta-analysis. *Am J Hypertens* (2023) 36(6):333–340. doi: 10.1093/ajh/hpad006

71. Prejbisz A, Lenders JW, Eisenhofer G, Januszewicz A. Cardiovascular manifestations of phaeochromocytoma. *J Hypertens* (2011) 29(11):2049–60. doi: 10.1097/HJH.0b013e32834a4ce9

72. Zhang R, Gupta D, Albert SG. Pheochromocytoma as a reversible cause of cardiomyopathy: analysis and review of the literature. *Int J Cardiol* (2017) 249:319–23. doi: 10.1016/j.ijcard.2017.07.014

73. Schultheiss HP, Fairweather D, Caforio ALP, Escher F, Hershberger RE, Lipshultz SE, et al. Dilated cardiomyopathy. *Nat Rev Dis Primers* (2019) 5(1):32. doi: 10.1038/s41572-019-0084-1

74. Mavrogeni S, Markousis-Mavrogenis G, Markussis V, Kolovou G. The emerging role of cardiovascular magnetic resonance imaging in the evaluation of metabolic cardiomyopathies. *Horm Metab Res* (2015) 47(9):623–32. doi: 10.1055/s-0035-1555913

75. Wilkenfeld C, Cohen M, Lansman SL, Courtney M, Dische MR, Pertsemlidis D, et al. Heart transplantation for end-stage cardiomyopathy caused by an occult pheochromocytoma. *J Heart Lung Transplant* (1992) 11(2 Pt 1):363–6.

76. Dalby MC, Burke M, Radley-Smith R, Banner NR. Pheochromocytoma presenting after cardiac transplantation for dilated cardiomyopathy. *J Heart Lung Transplant* (2001) 20(7):773–5. doi: 10.1016/s1053-2498(00)00233-3

77. Lenders JW, Duh QY, Eisenhofer G, Gimenez-Roqueplo AP, Grebe SK, Murad MH, et al. Pheochromocytoma and paraganglioma: an endocrine society clinical practice guideline. *J Clin Endocrinol Metab* (2014) 99(6):1915–42. doi: 10.1210/jc.2014-1498

78. Prys-Roberts C, Farndon JR. Efficacy and safety of doxazosin for perioperative management of patients with pheochromocytoma. *World J Surg* (2002) 26(8):1037–42. doi: 10.1007/s00268-002-6667-z

79. Buitenwerf E, Osinga TE, Timmers H, Lenders JWM, Feelders RA, Eekhoff EMW, et al. Efficacy of alpha-blockers on hemodynamic control during pheochromocytoma resection: a randomized controlled trial. *J Clin Endocrinol Metab* (2020) 105(7):2381–91. doi: 10.1210/clinem/dgz188

80. Gruber LM, Jasim S, Ducharme-Smith A, Weingarten T, Young WF, Bancos I. The role for metyrosine in the treatment of patients with pheochromocytoma and paraganglioma. *J Clin Endocrinol Metab* (2021) 106(6):e2393–e401. doi: 10.1210/clinem/dgab130

81. Authors/Task Force m, PM E, Anastasakis A, MA B, Borggrefe M, Cecchi F, et al. ESC Guidelines on diagnosis and management of hypertrophic cardiomyopathy: the task force for the diagnosis and management of hypertrophic cardiomyopathy of the European society of cardiology (ESC). *Eur Heart J* (2014) 35(39):2733–79. doi: 10.1093/eurheartj/ehu284

82. Yu M, Du B, Yao S, Ma J, Yang P. Von Hippel-lindau syndrome with a rare complication of dilated cardiomyopathy: a case report. *BMC Cardiovasc Disord* (2022) 22(1):489. doi: 10.1186/s12872-022-02913-1

83. Wang FZ, Wei WB, Li X, Huo JY, Jiang WY, Wang HY, et al. The cardioprotective effect of the sodium-glucose cotransporter 2 inhibitor dapagliflozin in rats with isoproterenol-induced cardiomyopathy. *Am J Transl Res* (2021) 13 (9):10950–61.

84. Fagundes GFC, Almeida MQ. Perioperative management of pheochromocytomas and sympathetic paragangliomas. *J Endocr Soc* (2022) 6(2): bvac004. doi: 10.1210/jendso/bvac004

85. Casey RT, Challis BG, Pitfield D, Mahroof RM, Jamieson N, Bhagra CJ, et al. Management of an acute catecholamine-induced cardiomyopathy and circulatory collapse: a multidisciplinary approach. *Endocrinol Diabetes Metab Case Rep* (2017) 2017:17-0122. doi: 10.1530/EDM-17-0122

86. Grasselli G, Foti G, Patroniti N, Rona R, Perlangeli MV, Pesenti A. Extracorporeal cardiopulmonary support for cardiogenic shock caused by pheochromocytoma: a case report and literature review. *Anesthesiology* (2008) 108 (5):959–62. doi: 10.1097/ALN.0b013e31816c8a78

87. Dominedo C, D'Avino E, Martinotti A, Cingolani E. A rare pheochromocytoma complicated by cardiogenic shock and posterior reversible encephalopathy syndrome: case report. *Eur Heart J Case Rep* (2021) 5(2):ytaa513. doi: 10.1093/ehjcr/ytaa513

88. Cohen CD, Dent DM. Phaeochromocytoma and acute cardiovascular death (with special reference to myocardial infarction). *Postgrad Med J* (1984) 60(700):111–5. doi: 10.1136/pgmj.60.700.111

89. Matteucci M, Kowalewski M, Fina D, Jiritano F, Meani P, Raffa GM, et al. Extracorporeal life support for phaeochromocytoma-induced cardiogenic shock: a systematic review. *Perfusion* (2020) 35(1_suppl):20–8. doi: 10.1177/0267659120908413

90. Nakamura M, Imamura T, Fukui T, Oshima A, Ueno H, Kinugawa K. Successful management of pheochromocytoma crisis with cardiogenic shock by percutaneous left ventricular assist device. *J Cardiovasc Dev Dis* (2022) 9(3):71. doi: 10.3390/jcdd9030071

91. Albulushi A, Zolty R, Lowes B, Duhacheck-Stapleman AL, Sandler T, Sullivan JN, et al. Perioperative management of pheochromocytoma resection in a patient with a continuous flow left ventricular assist device. *J Saudi Heart Assoc* (2020) 32(2):233–5. doi: 10.37616/2212-5043.1026

92. Westaby S, Shahir A, Sadler G, Flynn F, Ormerod O. Mechanical bridge to recovery in pheochromocytoma myocarditis. *Nat Rev Cardiol* (2009) 6(7):482–7. doi: 10.1038/nrcardio.2009.58

93. De Wilde D, Velkeniers B, Huyghens L, Diltoer M. The paradox of hypotension and pheochromocytoma: a case report. *Eur J Emerg Med* (2004) 11(4):237–9. doi: 10.1097/01.mej.0000134729.95226.e7

frontiers | Frontiers in Endocrinology

TYPE Original Research
PUBLISHED 24 July 2023
DOI 10.3389/fendo.2023.1218686

OPEN ACCESS

EDITED BY
Marta Araujo-Castro,
Ramón y Cajal University Hospital, Spain

REVIEWED BY
Pietro Locantore,
Catholic University of the Sacred Heart, Rome, Italy
Roberto Novizio,
Agostino Gemelli University Polyclinic (IRCCS), Italy

*CORRESPONDENCE
Nano Pachuashvili
npachuashvili@bk.ru

RECEIVED 07 May 2023
ACCEPTED 03 July 2023
PUBLISHED 24 July 2023

CITATION
Urusova L, Porubayeva E, Pachuashvili N, Elfimova A, Beltsevich D and Mokrysheva N (2023) The new histological system for the diagnosis of adrenocortical cancer. *Front. Endocrinol.* 14:1218686. doi: 10.3389/fendo.2023.1218686

The new histological system for the diagnosis of adrenocortical cancer

Liliya Urusova, Erika Porubayeva, Nano Pachuashvili*, Alina Elfimova, Dmitry Beltsevich and Natalia Mokrysheva

Department of Fundamental Pathology, Endocrinology Research Centre, Moscow, Russia

Introduction: Adrenocortical cancer (ACC) is a rare malignant tumor that originates in the adrenal cortex. Despite extensive molecular-genetic, pathomorphological, and clinical research, assessing the malignant potential of adrenal neoplasms in clinical practice remains a daunting task in histological diagnosis. Although the Weiss score is the most prevalent method for diagnosing ACC, its limitations necessitate additional algorithms for specific histological variants. Unequal diagnostic value, subjectivity in evaluation, and interpretation challenges contribute to a gray zone where the reliable assessment of a tumor's malignant potential is unattainable. In this study, we introduce a universal mathematical model for the differential diagnosis of all morphological types of ACC in adults.

Methods: This model was developed by analyzing a retrospective sample of data from 143 patients who underwent histological and immunohistochemical examinations of surgically removed adrenal neoplasms. Statistical analysis was carried out on Python 3.1 in the Google Colab environment. The cutting point was chosen according to Youden's index. Scikit-learn 1.0.2 was used for building the multidimensional model for Python. Logistical regression analysis was executed with L1-regularization, which is an effective method for extracting the most significant features of the model.

Results: The new system we have developed is a diagnostically meaningful set of indicators that takes into account a smaller number of criteria from the currently used Weiss scale. To validate the obtained model, we divided the initial sample set into training and test sets in a 9:1 ratio, respectively. The diagnostic algorithm is highly accurate [overall accuracy 100% (95% CI: 96%-100%)].

Discussion: Our method involves determining eight diagnostically significant indicators that enable the calculation of ACC development probability using specified formulas. This approach may potentially enhance diagnostic precision and facilitate improved clinical outcomes in ACC management.

KEYWORDS

adrenocortical carcinoma, adrenocortical tumor, diagnostic criteria, scoring systems, histological system

1 Introduction

Adrenocortical cancer (ACC) is a rare malignant tumor of the adrenal cortex. The reported incidence is 0.5 - 2 cases per 1,000,000 population per year. ACC occurs at any age; however, there is a tendency of increase in the incidence rate in the first and fourth to fifth decades of life, with gender deviations towards the female sex. ACC is mainly sporadic and less often observed as part of hereditary syndromes (1, 2).

There are several histological variants of ACC based on their characteristic cytomorphological features, including conventional, oncocytic, myxoid, and sarcomatoid features (3).

In recent years, ACC has been considered as a heterogeneous group of diseases with various pathomorphological and genomic features, which causes variability in the clinical picture and prognosis for patients (4). An accurate scale for assessing the malignant potential of a tumor is extremely important for deciding on the appointment of adjuvant therapy and determining the features of follow-up of the patient, as well as for predicting immediate and long-term outcomes (5).

Despite the fact that ACC often has a clinically aggressive course, its differential diagnosis from benign adrenocortical adenoma (ACA) can cause difficulties, especially in patients at an early stage with a highly differentiated tumor (6).

In recent decades, the criteria for detecting adrenocortical neoplasms have been improved, which has somewhat simplified the differential diagnosis of ACC and ACA, but diagnostic errors occur in 10-15% of cases (7). Despite the seemingly small percentage of errors, it has a high social significance: it is associated with exhausting regular monitoring and examination, material costs, and is actually unreasonable in the case of overdiagnosis. On the other hand, underdiagnosis does not allow determination of the correct tactics of patient management and prescribing therapy in time, which threatens a fatal outcome.

Currently, there is no single histological criterion that allows the establishment of the malignant nature of an adrenocortical tumor. In the latest clinical guidelines developed jointly by the European Society of Endocrinology (ESE) and the European Network for the Study of Adrenal Tumors (ENSAT), the Weiss system is recommended as the preferred system for determining the malignant potential of ACC in adults and is by far the most widely used system (8).

The aim of this work was to develop a mathematical model with high sensitivity and specificity for determining the malignant potential of adrenocortical tumors, which can be used to diagnose all morphological variants of ACC in adults.

2 Materials and methods

2.1 Patients and samples

The study included tumor tissue samples from patients with adrenal neoplasms who were treated at the Endocrinology Research Centre. All patients underwent adrenalectomy in the period from 2005 to 2022. Patients under the age of 18 at the time of surgical treatment were not included in the study. A total of 143 cases of adrenal tumors were selected for the study.

2.2 Morphological examination

Tumor tissue samples obtained during surgical treatment of patients at the Endocrinology Research Center were fixed in 10% buffered formalin, processed in the histological wiring system of a Leica ASP200, and poured into paraffin. Further, paraffin sections with a thickness of 3 μm were made from the paraffin-embedded tumor tissue samples on a microtome, and applied to slides treated with poly(l-lysine). Then the slides were stained with hematoxylin and eosin according to the standard procedure.

All tumor tissue samples were verified in accordance with the 2022 WHO classification of adrenal cortical tumors.

2.3 Immunohistochemistry imaging

Immunohistochemical analysis of the tumor tissue sections was carried out according to the standard technique with a peroxidase detection system with DAB on an automatic Leica BOND III IHC staining system using Leica reagents. Ki-67 (ACK02, Leica) and PHH3 (PA0817, Leica) antibodies were used. All histological slides were scanned using a Leica Aperio AT2 system at 20x magnification for further analysis. The Ki-67 proliferation index was calculated according to the formula: number of stained nuclei/2,000 cells x 100%, the area of greatest Ki-67 positivity (hot spot). Mitotic count was carried out in ten fields of view with 400x magnification. The most representative fields of view were selected.

2.4 Statistical analysis

Statistical analysis was carried out on Python 3.1 in the Google Colab environment. The cutting point was chosen according to Youden's index. Scikit-learn 1.0.2 was used for building the multidimensional model for Python. Logistical regression analysis was executed with L_1-regularization, which is an effective method for extracting the most significant features of the model.

Model equation:

$$p = 1/(1 + e^{-z})$$

$$Z = \beta_0 + \beta_1 * X_1 + \beta_2 * X_2 + \ldots + \beta_i * X_i$$

Z – dependent binary target,
$X_1, \ldots, X_i$ – independent features,
$\beta_0, \ldots, \beta_i$ – coefficients.
The loss function for the logistical regression model:
Loss_Function = logloss + $\lambda_1 || \beta ||_1$, where
logloss – function logloss;
β – weight of parameters;
λ_1 – L_1-regularization coefficient;

$|| \beta ||_1$ – L_1 – weight norm;
L1-norm:

$$|| \beta ||_1 = \sum_{i=1}^{n} |\beta_i|$$

To validate the obtained model, we divided the initial sample set into training and test sets in a 9:1 ratio, respectively. The operational characteristics used were: diagnostic sensitivity (DS), diagnostic specificity (DSp), positive predictive value of result (PPV), and negative predictive value of result (NPV).

3 Results

3.1 Design of the system for the risk stratification of adrenocortical tumors

The sample size was 143 patients, who were divided into training (n=128) and testing (n=15) groups. The features were analyzed in terms of their informativeness in relation to the diagnosis of ACC. The first stage executed was to assess whether tumor size > 10cm and/or tumor size >200g. If the tumor corresponded to these criteria, the histological diagnosis was consistent with ACC in 100% of cases.

At the second stage, patients with negative values of this criteria were analyzed, that is, tumor size ≤10 cm and tumor weight ≤ 200 g, and Receiver Operating Characteristic (ROC) analysis of the Ki-67 index was performed (Figure 1).

The Area under the ROC Curve (AUC) was 0.987 (95% CI: 0.969-1.000), which corresponds to a high diagnostic efficiency for this feature. According to the Youden's index, a Ki-67 cut-off point was chosen equal to 5%. The confusion matrix of this point is presented in Table 1.

Thus, in all patients with Ki-67<5%, the histological diagnosis is ACA. At the next stage, an ROC-analysis of the Ki-67 was also performed for patients whose Ki-67 level was greater or equal to 5% (Figure 2).

The AUC was 0.830 (95% CI: 0.696-0.964), which corresponds to a satisfactory diagnostic efficiency for this feature. According to Youden's index, a Ki-67 cut-off point was chosen equal to 11%. The classification matrix for a given point is presented in Table 2.

The final stage was to create a mathematical model for the purpose of differential diagnosis of ACC and ACA/neoplasms of undetermined malignant potential for patients with a Ki-67 value in

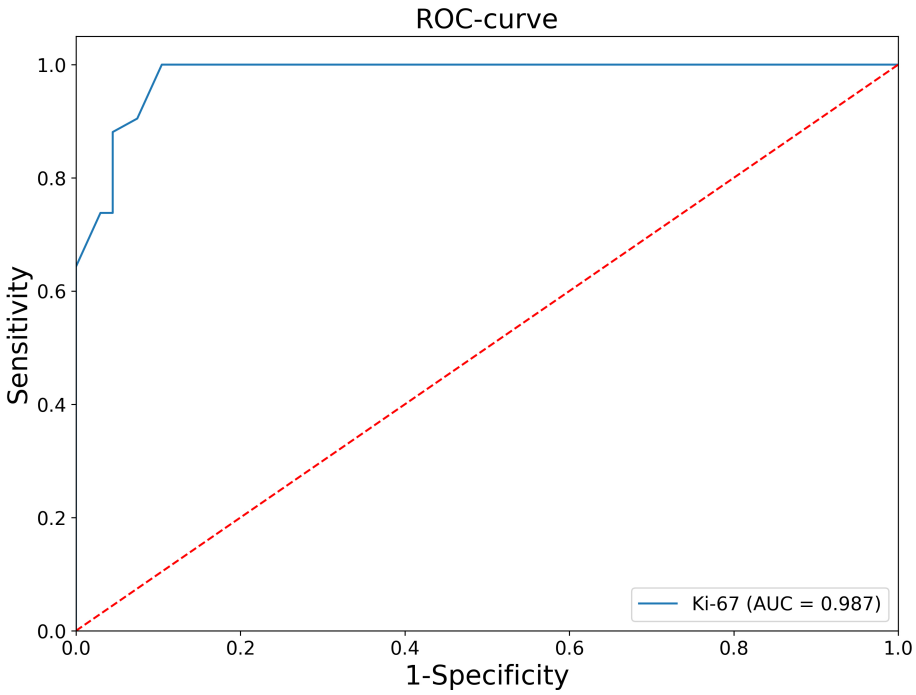

FIGURE 1
ROC analysis of the Ki-67 levels in relation to the diagnosis of ACC.

TABLE 1 Confusion matrix for diagnostics of ACC using a Ki-67 cut-off point of 5% (n= 95).

	ACC	ACA/tumor of uncertain malignant potential
Ki-67 ≥ 5%	36	6
Ki-67< 5%	0	53

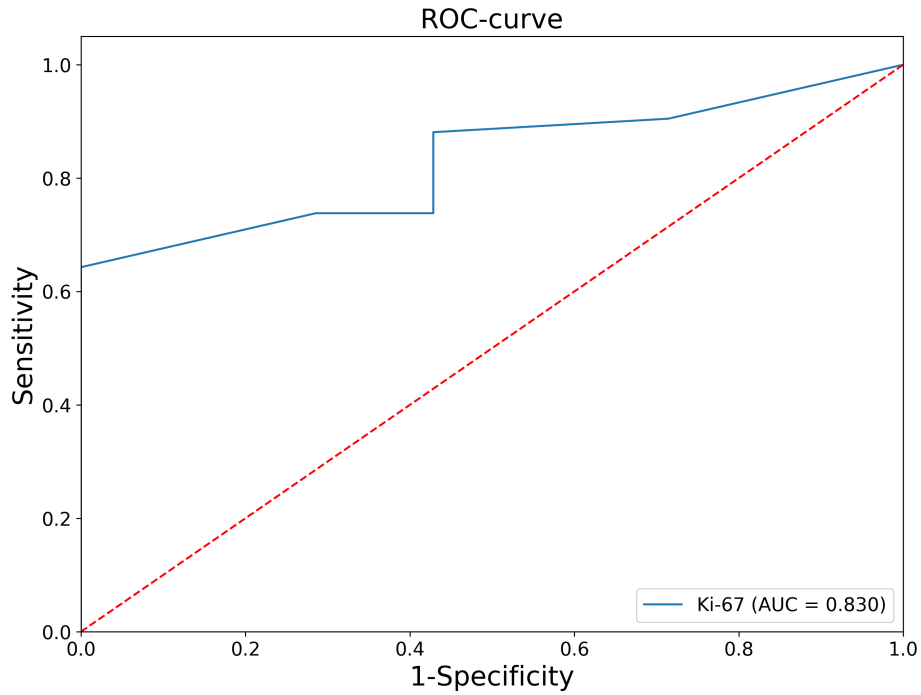

FIGURE 2
ROC analysis of the Ki-67 levels for patients whose Ki-67 level was greater or equal to 5%.

the range of 5% to 10% inclusive. Logistic regression analysis with L1-regularization was used. The response was histological diagnosis. The set of predictors used were:

1. Size of tumor (max) – numeric parameter;
2. Phosphohistone H3 (PHH3) – numeric parameter;
3. Ki-67 – numeric parameter;
4. Mitoses – binary parameter in format (1/0, which corresponds yes/no);
5. Nuclear grade – binary parameter in format (1/0, which corresponds yes/no);
6. Atypical mitoses – binary parameter in format (1/0, which corresponds yes/no);
7. Invasion of capsule – binary parameter in format (1/0, which corresponds yes/no);
8. Diffuse architecture of tumor – binary parameter in format (1/0, which corresponds yes/no);
9. Invasion of venous structures – binary parameter in format (1/0, which corresponds yes/no);
10. Necroses – binary parameter in format (1/0, which corresponds yes/no);
11. Eosinophilic cells – binary parameter in format (1/0, which corresponds yes/no).

As a result, the following regression model was obtained:

$$Z = -0.018 * \text{Xsize} + 0.278 * \text{Xmitoses} - 0.261 * \text{Xnuclear grade} + 0.297 * \text{Xpathological mitoses} + 0.816 * \text{Xinvasion of capsule} + 0.565 * \text{Xnecroses}$$

$$p = 1/(1 + e^{-z})$$

The weight of the remaining features of the model was equal to 0, that is, the remaining features are not taken into account when making a diagnosis. If the p-value is ≥0.5, then histological diagnosis will correspond to ACC; if the p-value is<0.5, it corresponds to ACA. The classification matrix is represented in Table 3.

3.2 The stages of diagnostics

Thus, eight parameters are used in ACC diagnostics (Figures 3–5):

1. Tumor size
2. Tumor weight

TABLE 2 Classification matrix for diagnostics of ACC using a Ki-67 cut-off point equal to 11% (n= 42).

	ACC	ACA/tumor of uncertain malignant potential
Ki-67 ≥ 11%	23	0
Ki-67< 11%	13	6

TABLE 3 Classification matrix for diagnostics of ACC using a logistic regression model (n= 19).

	ACC	ACA/tumor of uncertain malignant potential
Result of the model – ACC	13	3
Result of the model – ACA	0	3

3. Ki-67
4. Mitoses
5. Nuclear grade
6. Atypical mitoses
7. Invasion of capsule
8. Necroses

Diagnostics are carried out in three stages (Figure 6):

1. Size >10 cm and/or weight >200 g → Diagnosis: ACC
2. Ki-67<5% → Diagnosis: ACA
Ki-67 ≥11% → Diagnosis: ACC
3. Ki-67 = 5-10%

$$Z = -0.018 * Xsize + 0.278 * Xmitoses - 0.261 * Xnuclear\ grade + 0.297 * Xpathological\ mitoses + 0.816 * Xinvasion\ of\ capsule + 0.565 * Xnecroses$$

$$p = 1/(1 + e^{-z})$$

p ≥0.5 → Diagnosis: ACC
p<0.5 → Diagnosis: ACA
The final classification matrix is presented in Table 4.
The operational characteristics of the test set were:
DS = 100%
DSp= 100%
PPV =100%
NPV = 100%

There were three false-positive results. The model classified these three cases with tumor of uncertain malignant potential as ACC. However, metastases were developed in these three patients, which allowed them to be attributed to the ACC group. Thus, the model classified all patients correctly.

3.3 Examples

Example 1. Patient L., 66 years old. She complained of episodes of increased blood pressure up to 200/120 mm Hg, general weakness, and increased fatigue. Ultrasound examination revealed a mass in the region of the left adrenal gland.

Multispiral computed tomography (MSCT) revealed a solid lesion of the left adrenal gland with a maximum diameter of 37 mm and a native density of 25-35 Hounsfield Units (HU). Aldosterone – 120 pg/ml, renin – 0.22 ng/mL/hr (2.79 – 61.83), ARR – 545 (<300). In a 24-hour urine test, methylated catecholamines were normal. During the examination of dynamics, aldosterone – 218 pg/ml (<199), renin – 1.566 ng/mL/hr (2.79 – 61.83), and ARR – 545 (<100). In an overnight cortisol suppression test with 1 mg dexamethasone – 2 µg/dL, ACTH – 8.9 pg/ml (7.2 – 63.3).

18F-FDG PET/CT revealed hyperfixation of the radiopharmaceutical in the formation of the left adrenal gland, SUV max 21.33. A preliminary diagnosis was made as a tumor of uncertain malignant potential.

The patient was admitted to the surgical department, where a planned endoscopic left-sided adrenalectomy was performed. The results of the pathoanatomical study are presented in Table 5.

In January 2023, the spread of the tumor process was diagnosed as locoregional recurrence. Relapse-free survival was 12 months.

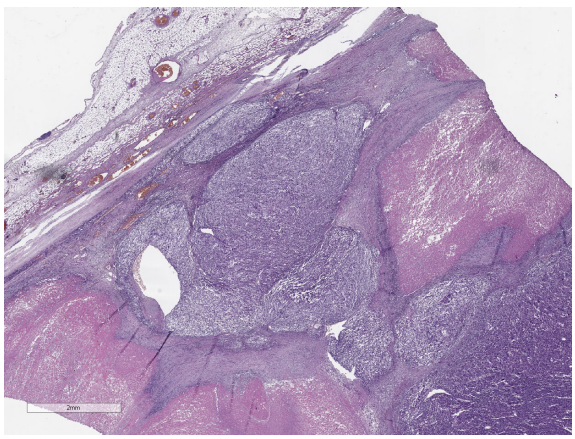

FIGURE 3
ACC, the area of necrosis. Hematoxylin and eosin stain. Scale x100.

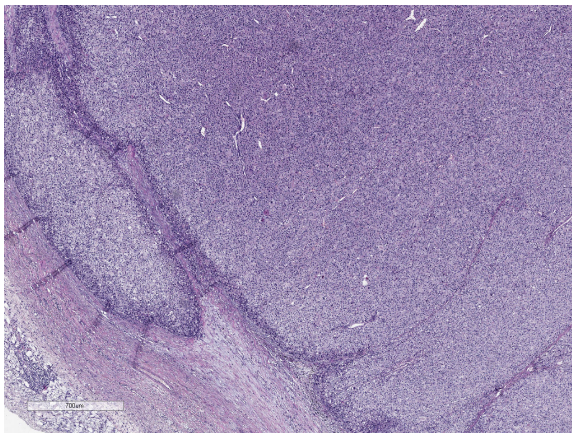

FIGURE 4
ACC, invasion of capsule. Hematoxylin and eosin stain. Scale x100.

Example 2. Patient P., 58 years old. She complained of episodes of increased blood pressure up to 180/120 mm Hg. According to the patient, in 2012, a formation in the left adrenal gland with dimensions of 27x15x17 mm was diagnosed for the first time.

According to MSCT from 2018, a formation with dimensions of 67x46x46 mm, ovoid in shape, and with a native density of 39-57 HU was found in the left adrenal gland.

According to the results of examination, the tumor produces hormones (hypercorticism): cortisol – 375.7 nmol/l, ACTH – 4.1 pmol/l (6 – 58), aldosterone – 130.7 pg/ml (<199), and renin – 3.9 ulU/ml (2.79 – 61.83).

Given the high malignant potential of the formation in the projection of the right adrenal gland, planned surgical treatment was performed in the volume of left-sided adrenalectomy with a tumor. The results of the pathoanatomical study are presented in Table 5.

At the moment, the patient is alive with no signs of disease progression, is disease-free, and overall survival is 15 months.

Example 3. Patient S., 53 years old. During examination in May 2015, according to ultrasound data, a mass of about 44 mm in size was found in the right adrenal gland. During a second examination in May 2016, the mass was measured to be about 41 mm in size.

MSCT revealed a lesion of the right adrenal gland of 42x33x25 mm with a native density of 38-56 HU. According to the results of the survey, no data in favor of hormonal activity was obtained.

The patient was provisionally diagnosed with a tumor with uncertain malignant potential. Surgical treatment was performed in in the volume of right-sided adrenalectomy with a tumor. The results of the pathoanatomical study are presented in Table 5.

At the time of the survey, the patient's relapse-free and overall survival time were 13 and 37 months, respectively. However, a systemic relapse was later established, and the patient died.

Example 4. Patient Y., 49 years old. Complained of increased blood pressure to 280/160 mm Hg., against a background of constant multicomponent antihypertensive therapy, back pain with irradiation to the lower limbs, severe weakness, and a weight gain of 12 kg over the past 3 months.

According to the results of examination: aldosterone – 644 pg/ml (<199), renin – 1.67 ng/mL/hr (2.79 – 61.83), and cortisol – 1351.89 nmol/l, ACTH – 24.8 pmol/L (6 – 58).

According to MSCT, a formation with the dimensions 53x27x21mm with a native density of 32-52 HU was found in the left adrenal gland.

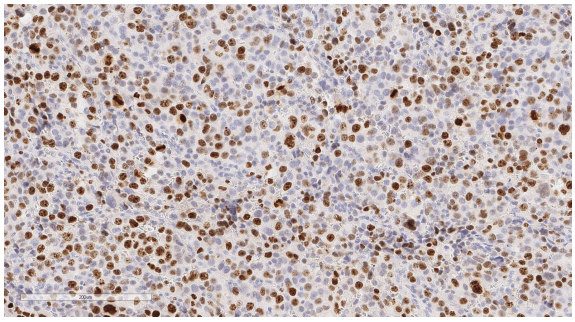

FIGURE 5
ACC, immunohistochemical stain with Ki-67 antibody. Scale x100.

10.3389/fendo.2023.1218686

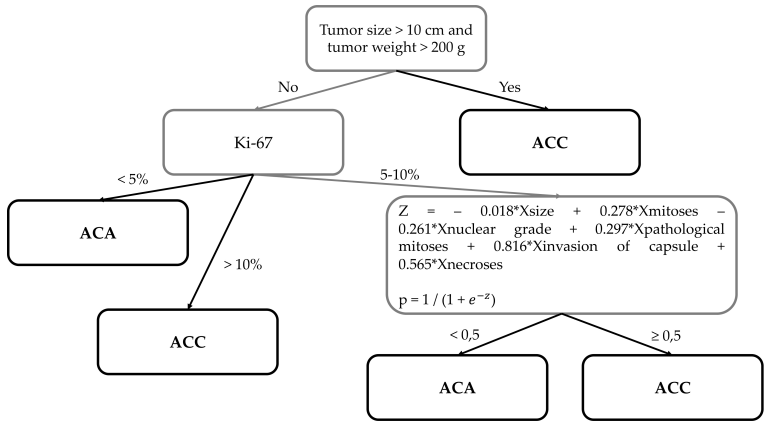

FIGURE 6
The new histological system for the diagnosis of adrenocortical cancer of the Moscow Endocrinology Research Centre.

Performed surgical treatment in the volume of of left-sided adrenalectomy with a tumor. The results of the pathoanatomical study are presented in Table 5.

4 Discussion

In 1984, Louis Weiss proposed a histopathologic classification system for adrenocortical tumors, based on nine criteria (Table 6). The presence of more than three or more features is consistent with adrenocortical carcinoma (9, 10).

In most adrenocortical adenomas, Weiss parameters are not detected, whereas in most cases of ACC (62% in a series of 201 cases in Turin, Italy), 6 or more points are noted, and their malignant nature is beyond doubt (11). However, cases of neoplasms of the adrenal cortex, in which only 1-2 points are detected according to Weiss parameters (approximately 10% of cases), are neoplasms with uncertain malignant potential. At this stage, the determination of their clinical course is an unsolved problem, and calls into question the reliability of the Weiss system and emphasizes the necessity of a more unambiguous scale for the verification of ACC.

In most of the "borderline" cases of Weiss score, the following parameters are most often identified: nuclear grade, diffuse architecture, or sinusoidal invasion. At the same time, it is these parameters that usually have the lowest specificity relative to the correlation with malignant behavior. Other parameters associated with malignant potential, such as a high mitotic rate, atypical mitoses, necrosis, and venous and capsular invasion, are most often not detected in isolation, but are combined with other parameters, thus demonstrating higher scores on the Weiss scale.

The reproducibility of the scale between different pathologists is another factor affecting the diagnostic effectiveness of the Weiss score, since the determination of some parameters, namely, diffuse architecture and sinusoidal and vascular invasion, are very subjective (12).

It is important to note that some parameters of the Weiss system (for example, the absence of diffuse architecture, nuclear atypia, or the invasion of lymphatic vessels) are difficult to assess in the case of a myxoid histological subtypes, since a large amount of myxoid substance makes it difficult to assess the stromal elements of the tumor (13). This may lead to the underestimation of the malignant potential of neoplasms.

Moreover, the use of the Weiss score for oncocytic tumors is not recommended, since oncocytic neoplasms consist of cells with eosinophilic cytoplasm, high nuclear grade, and diffuse architecture, which will inevitably lead to an erroneous diagnosis of ACC, which in turn contradicts their more frequent benign biological behavior (14). Therefore, the Lin–Weiss–Bisceglia system was developed to assess the malignancy of oncocytic variants of adrenal cortical tumors (15).

The Lin–Weiss–Bisceglia system includes "major criteria" and "minor criteria". The diagnosis of ACC is established in the

TABLE 4 Final classification matrix for diagnostics of ACC (n= 143).

Training sample	ACC	ACA/tumor of uncertain malignant potential
Result of the diagnostics – ACC	68	3
Result of the diagnostics – ACA	0	57
Testing sample		
Result of the diagnostics – ACC	8	0
Result of the diagnostics – ACA	0	7

10.3389/fendo.2023.1218686

TABLE 5 Results of a pathoanatomical study of patients with adrenal tumors.

	1	2	3	4
Tumor size, cm	3.7	6.7	4.0	5.0
Tumor weight, g	40	70	30	40
Ki-67, %	10	15	10	6
Mitoses	No	Yes	No	No
Nuclear grade	No	No	No	Yes
Atypical mitoses	No	Yes	Yes	No
Capsular invasion	No	Yes	Yes	No
Necrosis	Yes	Yes	No	No
Diffuse architecture	No	No	Yes	No
Sinusoidal invasion	No	No	No	No
Vascular invasion	No	No	No	No
Eosinophilic cells	No	Yes	Yes	No
Weiss/Lin— Weiss—Bisceglia	1 minor criteria	5 points	1 major and 1 minor criteria	1 point
Diagnosis according to the Weiss/Lin—Weiss—Bisceglia system	Tumor of uncertain malignant potential	ACC, myxoid variant	ACC, oncocytic variant	ACA
Diagnosis according to the system	ACC	ACC	ACC	ACA

presence of at least one of the "major criteria". In case of the presence of at least one "minor criterion" the tumour is considered as an oncocytic adrenal cortical neoplasm with uncertain malignant potential. If there are no both "major criteria" and "minor criteria", an oncocytic tumor is regarded as benign.

At the same time, for the application of this system, it is important that oncocytic adrenal cortical neoplasms are extensively sampled to be certain that they do fit into the category of pure oncocytic tumors. This means that greater than 90% of the tumor must be oncocytic (16). If it is not a pure oncocytic adrenal cortical neoplasm, then the system applied to conventional adrenal cortical carcinomas should be used.

The updated classification of the 2022 World Health Organization (WHO) also suggests using other multiparametric diagnostic algorithms for morphological assessment of neoplasms of the adrenal cortex in adults. These include the reticulin algorithm (17) and the Helsinki score (18), which, according to the literature, can be used for conventional, oncocytic, and myxoid variants of neoplasms.

The reticulin algorithm is based on the detection of changes in the normal structure of the reticulin network (Gordon and Sweet's silver histochemical stain) in combination with one of the following parameters: the presence of mitotic rate more than 5 per 10 mm^2 (50 high-power fields), tumor necrosis, or vascular invasion. However, this method has not found wide application in pathomorphological practice due to its technical complexity.

The Helsinki Score proposes to summarize the numeric value of the Ki-67 labeling index and the scores assigned to increased mitotic rate (a score of 3 is given for a mitotic rate greater than 5 mitoses per 10 mm^2) and tumor necrosis (5 points). A Helsinki score of > 8.5 is a diagnostic sign of ACC, and a score of > 17 makes it possible to regard the tumor as prognostically unfavorable.

Among all the proposed assessment systems, according to the latest data, the Helsinki score is the most reliable (19). However, it should be borne in mind that the assessment of mitoses in the cells of myxoid and oncocytic variants of ACC may be difficult, which may also lead to underestimation of the malignant potential of the tumor. At the same time, the clinical course of the myxoid variant in some cases is much more aggressive in comparison with other ACC variants. In this regard, it is necessary to be wary of the malignant nature of myxoid tumors.

Thus, the Weiss system, which is a standard of diagnosis, cannot be regarded as a universal system, which significantly complicates the diagnostic process because additional algorithms are required for specific histological variants. The system we have developed is a diagnostically meaningful set of indicators that takes into account a smaller number of criteria from the currently used Weiss scale. The diagnostic algorithm is highly accurate [overall accuracy 100% (95% CI: 96%-100%)]. Its main benefit is its universal applicability to all morphological variants of ACC in adult patients, which distinguishes this approach from the current known methods. Importantly, it is also applicable in standard conditions of medical pathomorphological laboratories, i.e., it does not require any parameters that are not assessed in routine examination of histological material.

The developed method includes evaluation of a set of eight diagnostically relevant parameters: tumor size (cm), tumor weight (g), Ki-67 index (%), presence/absence of mitoses, nuclear polymorphism, abnormal mitoses, invasion into the capsule, and necroses. Based on the data obtained, the

10.3389/fendo.2023.1218686

TABLE 6 Systems for assessing the malignant potential of adrenocortical tumors.

Weiss System		Lin— Weiss—Bisceglia System		Helsinki Score	
Parameter	Score	Criteria	Parameter	Parameter	Score
Nuclear grade* ≥ 3		Criteria for inclusion in a group of oncocytic tumors	Eosinophilic cytoplasm	> 5 mitoses/50 HPF	3
	1		High nuclear grade	Necrosis	5
			Diffuse architecture	Proliferative Index (Ki-67 IHC)	Numeric value
> 5 mitoses/50 HPF 1	1	Major criteria	> 5 mitoses/50 HPF 1		
Atypical mitoses	1		Atypical mitoses		
Clear cells ≤ 25%	1		Venous invasion		
Diffuse architecture > 33%	1	Minor criteria	Large size (> 10 cm) or weight (> 200 g)		
Confluent necrosis	1		Necrosis		
Vascular invasion	1		Sinusoidal invasion		
Sinusoidal invasion	1		Capsular invasion		
Capsular invasion	1				
Interpretation		**Interpretation**		**Interpretation**	
Final score ≥ 3	ACC	One more major criterion	ACC	Final score = 0-8.5	ACA
		One more minor criteria	Tumor of uncertain malignant potential	Final score > 8.5	ACC
		The absence of all major and minor criteria	Benign tumor	Final score > 17	Unfavorable prognosis

* The nuclear grade is assessed according to the Fuhrman criteria as follows: grade 1: small and round nuclei, non-visible nucleoli; grade 2: slightly larger and irregularly shaped nuclei, nucleoli visible with a high-magnification lens; grade 3: irregular and enlarged nuclei, nucleoli visible with a low magnification lens; grade 4: bizarre and extremely irregular nuclei, including monstrous cells. ACA, adrenal cortical adenoma; HPF, high-power fields (equivalent to almost 10 mm2).

probability of ACC development is calculated according to formulas in three steps.

It is worth noting that three false-positive results (classified as ACC) were detected, but these cases were diagnosed as tumors of uncertain malignant potential rather than a confirmed ACC. Therefore, it is incorrect to consider this a diagnostic error, as this group of patients required dynamic monitoring to determine their final diagnosis. Moreover, one of these three cases has a locoregional recurrence at the time of writing (January 2023), which confirms the presumed malignant course of the disease according to the new reclassification system.

5 Conclusions

Thus, for patients with a verified histological diagnosis, the developed mathematical model showed 100% accuracy in the training and test samples. The application of the new model could solve the problem of subjectivity and complexity in interpretation of certain criteria of the diagnostic algorithms currently used in clinical practice. Furthermore, the new model is unique in that, unlike others, it allows verification of all morphological variants of ACC. Thus, the results of our study suggest that the application of the new system will improve and standardize the differential diagnosis of adrenocortical tumors.

Data availability statement

The original contributions presented in the study are included in the article/supplementary material. Further inquiries can be directed to the corresponding author.

Ethics statement

The studies involving human participants were reviewed and approved by Institutional Ethics Committee of Endocrinology Research Centre (protocol code 10, 26.05.2020). The patients/participants provided their written informed consent to participate in this study.

Author contributions

LU, AE, DB, and NM designed the research. LU and AE performed the experiments. LU and AE analyzed the data. LU, EP, NP, and AE discussed the data. LU, EP, and NP wrote the paper. All authors contributed to the article and approved the submitted version.

Funding

The study was supported by the Ministry of Science and Higher Education of the Russian Federation (agreement no. 075-15-2022-310).

Conflict of interest

The authors declare that the research was conducted in the absence of any commercial or financial relationships that could be construed as a potential conflict of interest.

Publisher's note

References

1. Chandrasekar T, Goldberg H, Klaassen Z, Wallis CJD, Woon DTS, Herrera-Caceres JO, et al. The who, when, and why of primary adrenal malignancies: Insights into the epidemiology of a rare clinical entity. *Cancer* (2019) 125:1050–9. doi: 10.1002/cncr.31916

2. Sharma E, Dahal S, Sharma P, Bhandari A, Gupta V, Amgai B, et al. The characteristics and trends in adrenocortical carcinoma: a United States Population Based Study. *J Clin Med Res* (2018) 10(8):636–40. doi: 10.14740/jocmr3503w

3. Mete O, Erickson LA, Juhlin CC, Krijger RR, Sasano H, Volante M, et al. Overview of the 2022 WHO classification of adrenal cortical tumors. *Endocr Pathol* (2022) 33:155–96. doi: 10.1007/s12022-022-09710-8

4. Tkachuk AV, Tertychnyi AS, Beltsevich DG, Roslyakova AA, Belousov PV, Selivanova LS. Adrenocortical cancer: morphological variants, immunohistochemical characteristics. *Arkh Patol* (2021) 83(3):10–8. doi: 10.17116/patol20218302110

5. Clay MR, Pinto EM, Fishbein L, Else T, Kiseljak-Vassiliades K. Pathological and genetic stratification for management of adrenocortical carcinoma. *J Clin Endocrinol Metab* (2022) 107(4):1159–69. doi: 10.1210/clinem/dgab866

6. Erickson LA. Challenges in surgical pathology of adrenocortical tumours. *Histopathology* (2018) 72(1):82–96. doi: 10.1111/his.13255

7. Gambella A, Volante M, Papotti M. Histopathologic features of adrenal cortical carcinoma. *Adv Anat Pathol* (2023) 30(1):34–46. doi: 10.1097/PAP.0000000000000363

8. Fassnacht M, Dekkers OM, Else T, Baudin E, Berruti A, Krijger R, et al. European Society of Endocrino;logy Clinical Practice Guidelines on the management of adrenocortical carcinoma in adults, in collaboration with the European Network for the Study of Adrenal Tumors. *Eur J Endocrinol* (2018) 179(4):G1–G46. doi: 10.1530/EJE-18-0608

9. Weiss LM, Medeiros LJ, Vickery AL. Pathologic features of prognostic significance in adrenocortical carcinoma. *Am J Surg Pathol* (1989) 13:202–6. doi: 10.1097/00000478-198903000-00004

10. Weiss LM. Comparative histologic study of 43 metastasizing and nonmetastasizing adrenocortical tumors. *Am J Surg Pathol* (1984) 8:163–9. doi: 10.1097/00000478-198403000-00001

11. Bellantone R, Ferrante A, Boscherini M, Lombardi CP, Crucitti P, Crucitti F, et al. Role of reoperation in recurrence of adrenal cortical carcinoma: results from 188 cases collected in the Italian National Registry for Adrenal Cortical Carcinoma. *Surgery* (1997) 122(6):1212–8. doi: 10.1016/s0039-6060(97)90229-4

12. Wong CL, Fok CK, Chan YK, Tam VH, Fung LM. Was it an adrenocortical adenoma or an adrenocortical carcinoma? Limitation of the weiss scoring system in determining the malignant potential of adrenocortical tumor: report on two cases. *Case Rep Endocrinol* (2022) 7395050. doi: 10.1155/2022/7395050

13. Lam AK. Adrenocortical carcinoma: updates of clinical and pathological features after renewed World Health Organisation classification and pathology staging. *Biomedicines* (2021) 9(2):175. doi: 10.3390/biomedicines9020175

14. Selivanova LS, Abdulkhabirova FM, Voronkova IA, Kuznetsov NS, Troshina EA, Raĭkhman AO, et al. Adrenocortical oncocytoma. *Arkhiv Patologii* (2015) 77 (1):5559. doi: 10.17116/patol201577155-

15. Bisceglia M, Ludovico O, Di Mattia A, Ben-Dor D, Sandbank J, Pasquinelli G, et al. Adrenocortical oncocytic tumors: report of 10 cases and review of the literature. *Int J Surg Pathol* (2004) 12:231–43. doi: 10.1177/106689690401200304

16. Selivanova LS, Roslyakova AA, Kovalenko YA, Bogolyubova AV, Tertychny AS, Bel'tsevich DG, et al. Current criteria for the diagnosis of adrenocortical carcinoma. *Arkhiv Patologii* (2019) 81(3):6673. doi: 10.17116/patol20198103166

17. Mete O, Gucer H, Kefeli M, Asa SL. Diagnostic and prognostic biomarkers of adrenal cortical carcinoma. *Am J Surg Pathol* (2018) 42:201 213. doi: 10.1097/PAS.0000000000000943

18. Pennanen M, Heiskanen I, Sane T, Remes S, Mustonen H, Haglund C, et al. Helsinki score-a novel model for prediction of metastases in adrenocortical carcinomas. *Hum Pathol* (2015) 46:404–10. doi: 10.1016/j.humpath.2014.11.015

19. Minner S, Schreiner J, Saeger W. Adrenal cancer: relevance of different grading systems and subtypes. *Clin Transl Oncol* (2021) 23:1350–7. doi: 10.1007/s12094-020-02524-2

frontiers | Frontiers in Oncology

TYPE Case Report
PUBLISHED 23 August 2023
DOI 10.3389/fonc.2023.1210679

OPEN ACCESS

EDITED BY
Marta Araujo-Castro,
Ramón y Cajal University Hospital, Spain

REVIEWED BY
Giovanni Cochetti,
University of Perugia, Italy
Tao Zhennan,
Nanjing Drum Tower Hospital, China

*CORRESPONDENCE
Yucheng Xie
xieyucheng@etyy.cn

†These authors have contributed equally to this work and share first authorship

RECEIVED 23 April 2023
ACCEPTED 31 July 2023
PUBLISHED 23 August 2023

CITATION
Zhanghuang C, Long N, Yang Z and Xie Y (2023) Bilateral adrenal giant medullary lipoma combined with disorders of sex development: a rare case report and literature review. *Front. Oncol.* 13:1210679. doi: 10.3389/fonc.2023.1210679

Bilateral adrenal giant medullary lipoma combined with disorders of sex development: a rare case report and literature review

Chenghao Zhanghuang[1,2†], Na Long[3†], Zhen Yang[4] and Yucheng Xie[5,6*]

[1]Department of Urology, Kunming Children's Hospital, Yunnan Province Clinical Research Center for Children's Health and Disease, Kunming, China, [2]Yunnan Key Laboratory of Children's Major Disease Research, Yunnan Clinical Medical Center for Pediatric Diseases, Kunming Children's Hospital, Kunming, China, [3]Special Ward, Kunming Children's Hospital, Yunnan Province Clinical Research Center for Children's Health and Disease, Kunming, China, [4]Department of Oncology, Yunnan Children Solid Tumor Treatment Center, Kunming Children's Hospital, Kunming, China, [5]Department of Pathology, Kunming Children's Hospital, Kunming, China, [6]Department of Pathology, The Second People's Hospital of Yunnan Province, Kunming, China

Bilateral adrenal myelolipoma is rare in clinics and patients with disorders of sex development (DSDs). One case was reported in our center. A 45-year-old patient was admitted to the hospital after discovering a left abdominal mass for more than a year and worsening abdominal pain for 18 days. An imaging examination showed bilateral adrenal masses. Physical examination showed clitoris hypertrophy with patelliform changes, thick and dense pubic hair, normal development of bilateral labia majora without labia minora, and urethral opening. After the relevant preoperative examinations, bilateral adrenal mass resection was performed under general anesthesia. The postoperative pathology confirmed adrenal myelolipoma. The incision healed well without recurrence over 10 years after the operation. Her enlarged clitoris decreased in size. This case report has a detailed diagnosis and treatment process and sufficient examination results. It can provide a reference for diagnosing and treating patients with bilateral adrenal myelolipoma and DSD and reduce the risk of misdiagnosis and mistreatment.

KEYWORDS

adrenal myelolipoma, adrenal gland, disorders of sex development (DSD), diagnosis, pathology

Background

Myelolipoma is a rare non-functional benign tumor formed by the proliferation of mature adipose tissue and hematopoietic components of bone marrow. It was first described histologically by Gierke in 1905 and named myelolipoma by Oberling in 1929 (1). The incidence rate is 0.08%–0.2% (2); clinically, most are asymptomatic, whereas large

tumors will cause waist and abdominal pain or rupture and bleeding, etc. In general, there is no endocrine function, and hypertension can also occur (3). Bilateral giant adrenal myelolipoma is rare. A case of bilateral adrenal giant myelolipoma with disorders of sex development (DSDs) was treated in our center, and the following is reported.

Case report

The patient was 45 years old, and the social gender was female. The patient was admitted to the hospital after discovering a left abdominal mass for over a year and aggravation of abdominal pain for 18 days. In January 2008, the patient developed abdominal pain and discomfort without obvious causes. A left abdominal mass, about 4 cm × 3.5 cm × 3 cm in size, was found in the local hospital. In January 2009, the patient touched the left abdomen while bathing and felt that the mass was enlarged and hard, and abdominal pain recurred simultaneously. She was admitted to our hospital with a left abdominal mass of unknown etiology in February 2009. The patient had no fever, night sweats, jaundice, or emaciation. She had no menses since puberty. There was no family history.

Physical examination revealed a temperature of 37.2°C, respiration of 18 beats per minute, pulse of 72 beats per minute, and blood pressure of 120/80 mmHg. The patient had a body weight of 52 kg and a male face with visible whiskers and throat segments and a coarse, deep voice. The axillary hair was thick and dense, the chest was symmetrical without deformity, the breasts were not developed, and a physical examination of the heart and lungs showed no positive signs. The abdomen was soft with no palpable liver. However, a large mass was palpable in the left abdomen with a slightly hard texture and poor mobility, and there was no percussion pain in both renal region. The vulva showed hermaphroditism, thick and dense pubic hair, normal development of bilateral labia majora, no labia minora, hypertrophy of the clitoris like a short penis (4 cm long), no opening at the top, the urethral opening in the vestibule below the clitoris, and no vagina. On digital rectal examination, there was no palpable uterus or prostate-like tissue, no palpable mass in the pelvic cavity, and no testis-like tissue in the inguinal canal area: scoliosis deformity and free movement of limbs.

Abdominal CT examination showed a huge mixed-density lesion (18 cm × 15 cm) in the left retroperitoneal space, including many irregular fat density shadows. The upper boundary of the mass was below the diaphragm, and the lower boundary was at the level of the iliac crest. The pancreas, stomach, and spleen were all compressed and displaced anteriorly, and the left kidney was compressed into the pelvis. A mixed-density shadow of 8 cm × 4 cm with clear borders was seen above the right kidney. On enhancement, the parenchymal portion of the left retroperitoneal mass showed variable enhancement that appeared to be encapsulated (Figures 1A–E). Abdominal and pelvic ultrasound showed a mixed echogenic mass in the left adrenal gland and a solid mass in the right upper abdomen. No definite sonograms of the uterus, prostate, or testis were found. Laboratory tests showed white blood cells of 4.39 × 10^9/L, neutrophils of 74.7%, lymphocytes decreased by 13.9%, and monocytes increased by 10.5%. The red blood cell count was 5.30 × 10^{12}/L, and the hemoglobin was 177 g/L. Total bilirubin, direct bilirubin, and indirect bilirubin increased to 30, 11.3, and 18.7 μmol/L, respectively. Total cholesterol decreased to 2.55 mmol/L, and high-density lipoprotein decreased to 0.95 mmol/L. Other parameters, such as blood glucose and renal function, were normal. Tumor markers such as alpha-fetoprotein, human chorionic gonadotropin, neuron-specific enolase, and carcinoembryonic antigen were negative. Karyotype analysis of the patient's peripheral blood showed that the patient was 46, XX.

The patient underwent open bilateral adrenalectomy under general anesthesia. During the operation, bilateral subcostal transverse incisions were made, the liver and transverse colon were pulled away to expose the retroperitoneal space, and the left retroperitoneal space was dissected after careful mobilization. There was a solid cystic mass (about 24 cm × 16 cm in size), dark, and hard in texture. The mass was dissected carefully to avoid injury to the renal vein. The huge mass was completely removed, and the other

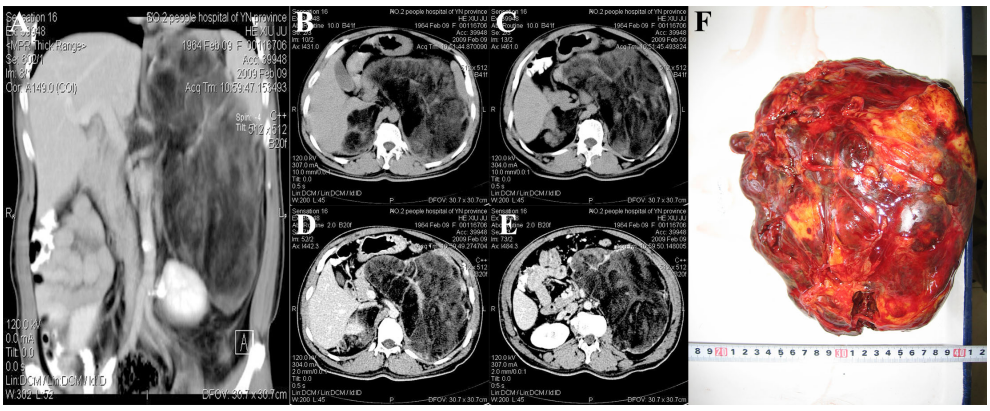

FIGURE 1
CT and gross specimens of the patient. **(A)** The left retroperitoneal mass was huge, and the left kidney was compressed and moved down. No enhancement was found in contrast-enhanced scan. **(B, C)** CT plain scan showed bilateral inhomogeneous density mass. **(D, E)** Bilateral adrenal enhanced CT findings. **(F)** Intraoperative gross specimen of a huge mass in the left adrenal gland.

side was about 9 cm × 5 cm removed. A part of the bilateral mass after complete resection was sent for intraoperative rapid frozen section diagnosis. Intraoperative frozen report: The tumor was derived from adipose tissue and tended to be benign. Lymph node dissection was not performed. After sufficient hemostasis of the operative field, a drainage tube was placed, and the abdominal incision was sutured layer by layer. The intraoperative blood loss was about 500 mL. The operation time was 3 h and 15 min. The operation was uneventful, and anesthesia was stable without a blood transfusion. The patient returned to the ward safely after the operation. The drainage tube was removed 7 days after the operation, and the incision healed well 14 days after the suture was removed. The patient was discharged.

Pathological examination: gross observation: The left side was a yellow-red or dark-red mass, weighing 2.3 kg, measuring 24 cm × 18 cm × 10 cm, with a complete capsule, solid cut surface, and pale yellow fat mixed with reddish-brown (Figure 1F). The right side was a yellow mass measuring 8.5 cm × 4.3 cm × 2.8 cm with an intact capsule and fatty cut surface. Microscopic examination showed that the left tumor mainly showed erythroid, granulocytic, and megakaryocytic bone marrow hematopoietic cells without atypia. The erythroid lineage was dominated by mid- and late-stage erythrocytes, whereas the granulocyte was dominated by mid- and late-young rod and lobulated nuclei. Lymphocytes were scattered or aggregated, and megakaryocytes were scattered, one to three per high-power field. Hemosiderin phagocytosed histiocytes and slight hyperplasia of fibrous tissue were seen locally. A large amount of mature adipose tissue was intermingled. At the edge of the tumor, adrenal globular zone cell clusters of different sizes were seen, and massive hemorrhage was seen in some areas. On the right side, the tumor mainly comprised mature adipose tissue mixed with bone marrow hematopoietic tissue. Under the tumor capsule, the adrenal zona glomerular cells were rarely compressed. The pathological diagnosis was bilateral adrenal myelolipoma with hemorrhage (the left tumor was huge). The adrenal myelolipoma was considered a benign tumor without secretory function, and no chemotherapy, radiotherapy, or endocrine therapy was given after the operation. The patient was followed up for 14 years and 2 months, and the general condition was good, without discomfort and tumor recurrence.

Discussion

The myelolipoma was composed of a mixture of mature fat and bone marrow in varying proportions. In this case, the multifocal dark red area on the left side was dominated by bone marrow hematopoietic tissue, and a few residual zona glomerulus cells were found under the tumor capsule (Figures 2A, B). The right side was dominated by adipose tissue, and only a little bone marrow hematopoietic tissue was scattered among adipocytes (Figures 2C, D). Myelolipoma is more common in the adrenal gland than in the thoracic cavity, retroperitoneum, presacral area (4), mediastinum, spleen, lung, testis, soft tissue, and other parts. It has been reported that (5) occurs simultaneously in the adrenal gland and the contralateral pelvic cavity, and it is extremely rare that the primary tumor occurs in the liver (6, 7). The most common age of adrenal myelolipoma was 50 to 70, and most patients were adults. The incidence of male and female patients was roughly equal. Most

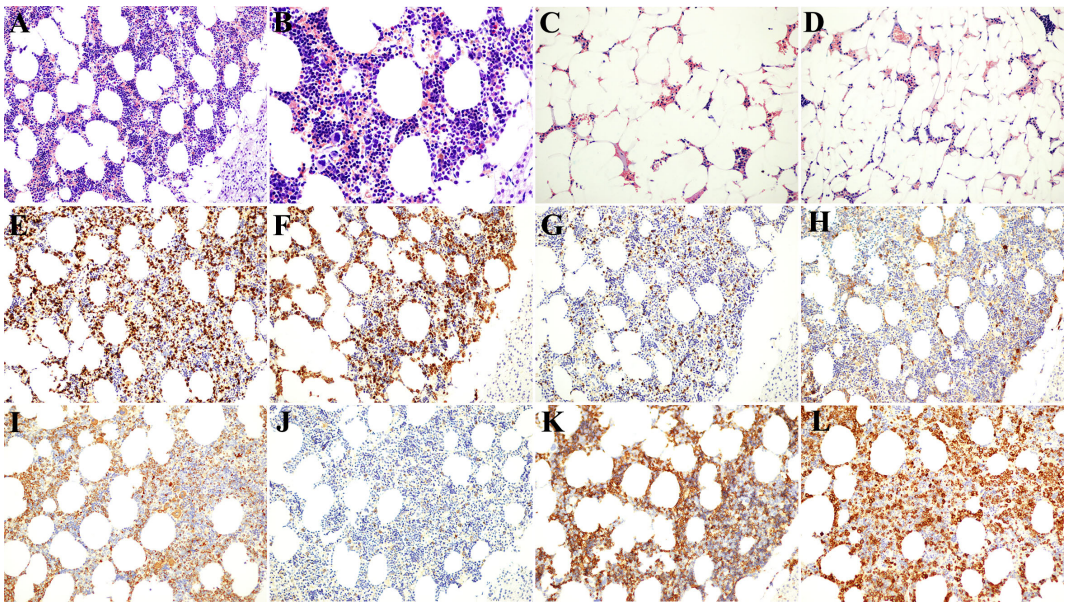

FIGURE 2
Postoperative pathological and immunohistochemical results. **(A, B)** The left tumor was composed of fat cells and various hematopoietic cells, and the lower right was the residual adrenal cortex [Immunohistochemistry (HE); **(A)** 200× and **(B)** 400×]. **(C, D)** The right mass was dominated by adipocytes, with scattered small foci of hematopoietic cells (HE; 200×). **(E)** CD3-positive T lymphocytes (200×). **(F)** CD15-positive granulocytes (200×). **(G)** CD20-positive B lymphocytes (200×). **(H)** CD38-positive plasma cells (200×). **(I)** CD63-positive monocytes and plate-producing cells (200×). **(J)** CD117-positive mast cells (200×). **(K)** CD235a-positive nucleated erythrocytes and mature erythrocytes (200×). **(L)** Myeloperoxidase (MPO)-positive myeloid cells (200×).

tumors are solitary, with a slightly higher incidence on the right side than on the left side and rare on both sides (8). There were no atypia or lip blasts in the adipocytes. Hematopoietic tissue was sparsely or widely distributed, and lymphocytes were scattered or aggregated. Immunohistochemical markers showed granulocytic, erythroid, lymphoid, and megakaryocytic hematopoietic cells at various stages of differentiation (Figures 2E–L).

Differential diagnosis with the following tumors is required: 1. The common type of lipoma has no hematopoietic component, which differs from the location of myelolipoma. It should be noted that some myelolipomas may have fewer hematopoietic components and can be misdiagnosed as lipomas. 2. For well-differentiated liposarcoma, overlapping with myelolipoma but without hematopoietic components, a careful search for immunohistochemical markers can help. Atypical stromal cells with hyperchromatic chromatin or lip blasts can be found. 3. Myeloid neoplasms, often multiple lesions, accompanied by the liver and spleen enlargement and blood system abnormalities. The tumor showed diffuse infiltration of primitive tumor cells, which were atypical and monomorphic. Immunohistochemical staining showed the absence of normal multilineage hematopoietic components of bone marrow. 4. Extramedullary hematopoiesis, usually in the liver, spleen, and lymph nodes, is associated with lymphohematopoietic disease, and the lesions are often multifocal rather than isolated, well-defined nodules.

Endocrine dysfunction can promote the occurrence of adrenal myelolipoma. Statistics show that about 10% of myelolipoma cases are complicated by endocrine insufficiency, including Cushing syndrome, primary aldosteronism, congenital adrenal hyperplasia (CAH), and hyperparathyroidism (9). CAH is an autosomal negative genetic disease caused by defects in adrenocortical hormone synthase, such as 21-hydroxylase, 17-hydroxylase, or 11-hydroxylase (10). Because of the disorder of the glucocorticoid synthesis pathway, such diseases can lead to obvious hyperandrogenism and hyper-adrenocorticotropic hormone (11). According to statistics, the incidence of adrenal myelolipoma in patients with CAH is significantly higher than that in normal people (about 6%). Its incidence is positively correlated with the level of serum adrenocorticotropic hormone (12). Cases of adrenal myelolipoma with obvious hyperandrogenism have also been reported in the literature (13). Therefore, the pathogenesis of adrenal myelolipoma is closely related to the overexpression of androgen and adrenocorticotropic hormone. The patient was diagnosed with male pseudohermaphroditism, accompanied by amenorrhea and clitoral hypertrophy after puberty, which was considered to be related to the excessive expression of androgens caused by adrenal myelolipoma. The symptoms of clitoral hypertrophy were relieved after surgical resection.

There are many studies on the nature of myelolipomas. Bishop et al. (9) found that most myelolipomas have non-random X chromosome inactivation, suggesting that myelolipomas are of monoclonal origin and belong to genuine tumors. The etiology and pathogenesis of adrenal myelolipoma are still unclear. They may be related to adrenal cortical metaplasia induced by necrosis, infection, stress, and other factors (14–16). Cytogenetic examination of adrenal myelolipoma has been reported with chromosome (3; 21) (q25; 11) translocation, which also suggests a true tumor (17). Some authors point out that adrenal myelolipoma often occurs in endocrine diseases or chronic wasting diseases, which may stimulate the differentiation of adrenal cortical mesenchymal cells into myelocytes or adipocytes (18). At present, the presence of bone tissue in myelolipoma is controversial, and most scholars state that bone tissue is metaplasia.

Myelolipoma is generally asymptomatic, with a volume of less than 5 cm and rarely larger than 10 cm (19). The large volume can cause abdominal distension, pain, or other compression symptoms. There are reports of giant adrenal myelolipoma with a maximum diameter of 15–16 cm (20). In this case, the patient had myelolipoma in both adrenal glands, and the left tumor was huge, with a maximum diameter of 24 cm, accompanied by DSD, manifested as clitoral hypertrophy and no vagina. The principle of myelolipoma treatment is small, and asymptomatic can be conservative follow-up. Yalagachin et al. (21) considered that adrenal myelolipoma with function or diameter ≥6 cm should be treated with adrenal tumor resection, and surgical resection of huge tumors can relieve symptoms and prevent complications such as bleeding and rupture. In the past, open surgery was the main clinical operation for giant myelolipoma. However, with the development of laparoscopic technology, laparoscopic adrenalectomy has become the first choice for adults. Of note, is the transabdominal or retroperitoneal approach more advantageous? It is still controversial (22). In recent years, good results of robotic surgical treatment have also been reported (23). In addition, studies have shown that minimally invasive surgery can effectively reduce surgical site infection caused by open surgery so that patients can obtain better perioperative outcomes (24).

Conclusion

In conclusion, myelolipoma is rare in clinical practice, and it is rare to present a huge mass in both adrenal glands with DSD. Adrenal myelolipoma is a benign non-secretory tumor. The tumor was named for the presence of mature adipocytes and bone marrow cells. The disease may result from abnormal cortical reticular endothelial cell metaplasia development or aberrant embryonic residues. However, patients with adrenal myelolipoma that produce compression symptoms such as hypertension need surgical resection of the tumor to relieve the symptoms. Adrenal myelolipoma is considered a benign tumor without secretory function, and postoperative chemoradiotherapy and endocrine therapy are not needed. Patients with adrenal myelolipoma complicated with disorders of sexual development can be followed up after resection of adrenal myelolipoma before oculoplastic surgery, and some patients with disorders of sexual development can spontaneously relieve the abnormal manifestations of external genitalia.

Data availability statement

The original contributions presented in the study are included in the article/supplementary material. Further inquiries can be directed to the corresponding author.

Ethics statement

The studies involving human participants were reviewed and approved by the Ethical Committee of Kunming Children's Hospital (2022-12-001-K01). This study is by the relevant guidelines and regulations. The data in this study were obtained from this patient and his legal guardian. Written informed consent was obtained from the patient's parents.

Author contributions

CZ designed the study. CZ, NL, and ZY collected and analyzed the data. CZ drafted the initial manuscript. CZ revised the article critically. CZ, ZY, NL, BY, and YX reviewed and edited the article. NL and CZ are co-first authors. All authors approved the final manuscript.

Funding

This study was supported by Yunnan Education Department of Science Research Fund (Nos. 2023 J0295 and 2020J0228), Kunming City Health Science and Technology Talent "1000" training Project [No. 2020-SW (Reserve)-112], Kunming Health and Health Commission Health Research Project (No. 2020-0201-001), Kunming Medical Joint Project of Yunnan Science and Technology Department (No. 202001 AY070001-271), Department of Science and Technology of Yunnan province Kunming medicine Joint Special project (No.202301AY070001-108), and Open Research Fund of Clinical Research Center for Children's Health and Diseases of Yunnan Province (No.2022-ETYY-YJ-03). The funding bodies played no role in the study's design and collection, data analysis and interpretation, and manuscript writing.

Conflict of interest

The authors declare that the research was conducted in the absence of any commercial or financial relationships that could be construed as a potential conflict of interest.

Publisher's note

All claims expressed in this article are solely those of the authors and do not necessarily represent those of their affiliated organizations, or those of the publisher, the editors and the reviewers. Any product that may be evaluated in this article, or claim that may be made by its manufacturer, is not guaranteed or endorsed by the publisher.

References

1. Meaglia JP, Schmidt JD. Natural history of an adrenal myelolipoma. *J Urol* (1992) 147(4):1089–90. doi: 10.1016/S0022-5347(17)37482-7

2. Hasan M, Siddiqui F, Al-Ajmi M. FNA diagnosis of adrenal myelolipoma: a rare entity. *Diagn Cytopathol* (2008) 36(12):925–6. doi: 10.1002/dc.20941

3. Jakka N, Venkateshwarlu J, Satyavani N, Neelaveni K, Ramesh J. Functioning adrenal myelolipoma: A rare cause of hypertension. *Indian J Endocrinol Metab* (2013) 17(Suppl 1):S249–51. doi: 10.4103/2230-8210.119588

4. Rizzo G, Coramusi C, Pietricola G, Sionne F, Castri F, Pafundi DP, et al. Laparoscopic approach for a presacral myelolipoma resembling a liposarcoma. *J Surg Case Rep* (2018) 2018(7):rjy156. doi: 10.1093/jscr/rjy156

5. Wadood DQ, Qureshi DSA, Singh DP, Freedman DJ. A rare case of co-existing adrenal and pelvic myelolipomas. *Radiol Case Rep* (2018) 13(5):999–1002. doi: 10.1016/j.radcr.2018.07.008

6. Gallo M, Mineur L, Emptas H, Costes V, Ramos J. Myélolipome hépatique : une entité rare, à propos d'un cas et revue de la littérature [Hepatic myelolipoma: A rare entity, case report and review of the literature]. *Ann Pathol* (2017) 37(5):415–9. doi: 10.1016/j.annpat.2017.06.010

7. Menozzi G, Maccabruni V, Marini G, Froio E, Garlassi E. Contrast-enhanced ultrasound (CEUS) appearance of hepatic myelolipoma. *J Ultrasound* (2014) 19(1):61–5. doi: 10.1007/s40477-014-0137-y

8. Zieker D, Königsrainer I, Miller S, Vogel U, Sotlar K, Steurer W, et al. Simultaneous adrenal and extra-adrenal myelolipoma - an uncommon incident: case report and review of the literature. *World J Surg Oncol* (2008) 6:72. doi: 10.1186/1477-7819-6-72

9. Bishop E, Eble JN, Cheng L, Wang M, Chase DR, Orazi A, et al. Adrenal myelolipomas show nonrandom X-chromosome inactivation in hematopoietic elements and fat: support for a clonal origin of myelolipomas. *Am J Surg Pathol* (2006) 30(7):838–43. doi: 10.1097/01.pas.0000202044.05333.17

10. Fowler MR, Williams RB, Alba JM, Byrd CR. Extra-adrenal myelolipomas compared with extramedullary hematopoietic tumors: a case of presacral myelolipoma. *Am J Surg Pathol* (1982) 6(4):363–74. doi: 10.1097/00000478-198206000-00009

11. Shalaby M, Chandran H, Elford S, Kirk J, McCarthy L. Recommendations of patients and families of girls with 46XX congenital adrenal hyperplasia in the United Kingdom regarding the timing of surgery. *Pediatr Surg Int* (2021) 37(1):137–43. doi: 10.1007/s00383-020-04780-3

12. Nermoen I, Rørvik J, Holmedal SH, Hykkerud DL, Fougner KJ, Svartberg J, et al. High frequency of adrenal myelolipomas and testicular adrenal rest tumours in adult Norwegian patients with classical congenital adrenal hyperplasia because of 21-hydroxylase deficiency. *Clin Endocrinol (Oxf)* (2011) 75(6):753–9. doi: 10.1111/j.1365-2265.2011.04151.x

13. Su HC, Huang X, Dai J, Sun FK. Adrenal myelolipoma associated with hyperandrogenemia. *Int J Urol* (2012) 19(11):1026–8. doi: 10.1111/j.1442-2042.2012.03100.x

14. Calissendorff J, Juhlin CC, Sundin A, Bancos I, Falhammar H. Adrenal myelolipomas. *Lancet Diabetes Endocrinol* (2021) 9(11):767–75. doi: 10.1016/S2213-8587(21)00178-9

15. Alvarez JF, Goldstein L, Samreen N, Beegle R, Carter C, Shaw A, et al. Giant adrenal myelolipoma. *J Gastrointest Surg* (2014) 18(9):1716–8. doi: 10.1007/s11605-014-2553-x

16. Wrightson WR, Hahm TX, Hutchinson JR, Cheadle W. Bilateral giant adrenal myelolipomas: a case report. *Am Surg* (2002) 68(6):588–9. doi: 10.1177/000313480206800615

17. Chang KC, Chen PI, Huang ZH, Lin YM, Kuo PL. Adrenal myelolipoma with translocation (3;21)(q25;p11). *Cancer Genet Cytogenet* (2002) 134(1):77–80. doi: 10.1016/S0165-4608(01)00592-1

18. Luo L, Wang T, Cheng M, Ge X, Song S, Zhu G, et al. Rare benign liver tumors that require differentiation from hepatocellular carcinoma: focus on diagnosis and treatment. *J Cancer Res Clin Oncol* (2023) 149(7):2843–54. doi: 10.1007/s00432-022-04169-w

19. Gupta P, Mondal S, Datta C, Pal DK. Bilateral giant adrenal myelolipoma: A rare scenario. *Indian J Pathol Microbiol* (2022) 65(3):689–91. doi: 10.4103/ijpm.ijpm_182_21

20. Posses SP, Prado BC, Bechara GR, Puppim AR, Carli CRS, MIranda MML. Giant bilateral adrenal myelolipoma:Case presentation and a brief literature review. *Urol Case Rep* (2018) 18:67–9. doi: 10.1016/j.eucr.2018.03.008

21. Yalagachin GH, Bhat BK. Adrenal incidentaloma does it require surgical treatment? Case report and review of literature. *Int J Surg Case Rep* (2013) 4(2):192–4. doi: 10.1016/j.ijscr.2012.09.014

22. Arezzo A, Bullano A, Cochetti G, Cirocchi R, Randolph J, Mearini E, et al. Transperitoneal versus retroperitoneal laparoscopic adrenalectomy for adrenal tumours in adults. *Cochrane Database Syst Rev* (2018) 12(12):CD011668. doi: 10.1002/14651858.CD011668.pub2

23. Cochetti G, Paladini A, Boni A, Silvi E, Tiezzi A, De Vermandois JAR, et al. Robotic treatment of giant adrenal myelolipoma: A case report and review of the literature. *Mol Clin Oncol* (2019) 10(5):492–6. doi: 10.3892/mco.2019.1823

24. de Vermandois JAR, Cochetti G, Zingaro MD, Santoro A, Panciarola M, Boni A, et al. Evaluation of surgical site infection in mini-invasive urological surgery. *Open Med (Wars)* (2019) 14:711–8. doi: 10.1515/med-2019-0081

frontiers | Frontiers in Endocrinology

TYPE Original Research
PUBLISHED 24 August 2023
DOI 10.3389/fendo.2023.1244342

OPEN ACCESS

EDITED BY
Piotr Glinicki,
Centre of Postgraduate Medical Education, Poland

REVIEWED BY
Jacopo Burrello,
University of Turin, Italy
Luigi Petramala,
Sapienza University of Rome, Italy

*CORRESPONDENCE
Moritz Wildgruber
moritz.wildgruber@med.uni-muenchen.de

†These authors have contributed equally to this work and share first authorship

‡These authors have contributed equally to this work and share last authorship

RECEIVED 22 June 2023
ACCEPTED 08 August 2023
PUBLISHED 24 August 2023

CITATION
Mansour N, Mittermeier A, Walter R, Schachtner B, Rudolph J, Erber B, Schmidt VF, Heinrich D, Bruedgam D, Tschaidse L, Nowotny H, Bidlingmaier M, Kunz SL, Adolf C, Ricke J, Reincke M, Reisch N, Wildgruber M and Ingrisch M (2023) Integration of clinical parameters and CT-based radiomics improves machine learning assisted subtyping of primary hyperaldosteronism. *Front. Endocrinol.* 14:1244342. doi: 10.3389/fendo.2023.1244342

Integration of clinical parameters and CT-based radiomics improves machine learning assisted subtyping of primary hyperaldosteronism

Nabeel Mansour[1†], Andreas Mittermeier[1†], Roman Walter[1], Balthasar Schachtner[1], Jan Rudolph[1], Bernd Erber[1], Vanessa F. Schmidt[1], Daniel Heinrich[2], Denise Bruedgam[2], Lea Tschaidse[2], Hanna Nowotny[2], Martin Bidlingmaier[2], Sonja L. Kunz[2], Christian Adolf[2], Jens Ricke[1], Martin Reincke[2], Nicole Reisch[2], Moritz Wildgruber[1*‡] and Michael Ingrisch[1‡]

[1]Department of Radiology, LMU University Hospital, LMU Munich, Munich, Germany, [2]Department of Medicine IV, LMU University Hospital, LMU Munich, Munich, Germany

Objectives: The aim of this study was to investigate an integrated diagnostics approach for prediction of the source of aldosterone overproduction in primary hyperaldosteronism (PA).

Methods: 269 patients from the prospective German Conn Registry with PA were included in this study. After segmentation of adrenal glands in native CT images, radiomic features were calculated. The study population consisted of a training (n = 215) and a validation (n = 54) cohort. The k = 25 best radiomic features, selected using maximum-relevance minimum-redundancy (MRMR) feature selection, were used to train a baseline random forest model to predict the result of AVS from imaging alone. In a second step, clinical parameters were integrated. Model performance was assessed via area under the receiver operating characteristic curve (ROC AUC). Permutation feature importance was used to assess the predictive value of selected features.

Results: Radiomics features alone allowed only for moderate discrimination of the location of aldosterone overproduction with a ROC AUC of 0.57 for unilateral left (UL), 0.61 for unilateral right (UR), and 0.50 for bilateral (BI) aldosterone overproduction (total 0.56, 95% CI: 0.45-0.65). Integration of clinical parameters into the model substantially improved ROC AUC values (0.61 UL, 0.68 UR, and 0.73 for BI, total 0.67, 95% CI: 0.57-0.77). According to permutation feature importance, lowest potassium value at baseline and saline infusion test (SIT) were the two most important features.

10.3389/fendo.2023.1244342

Conclusion: Integration of clinical parameters into a radiomics machine learning model improves prediction of the source of aldosterone overproduction and subtyping in patients with PA.

KEYWORDS

machine learning, hyperaldosteronism, adrenal venous sampling, integrated diagnostics, venous interventions

1 Introduction

Arterial hypertension is the leading underlying cause of cardiovascular disease and the worldwide leading modifiable risk factor for premature death (1). Its early detection, treatment and prevention of major cardiovascular events such as stroke or myocardial infarction allows to reduce both morbidity and mortality (1, 2).

Primary hyperaldosteronism (PA), also known as Conn's syndrome, has been recognized as the most frequent cause of endocrine hypertension, characterized by an excess of aldosterone production, autonomous of major regulators of aldosterone secretion (3). PA is often underdiagnosed because of the lack of specific, easily identifiable features (4). Compared to patients with essential hypertension as well as to the general population, patients with PA have an increased risk of cerebrovascular and cardiovascular events and target organ damage (5–8).

The diagnostic workup of PA consists of a sequence of screening, confirmatory testing and differentiation of the source of aldosterone overproduction (lateralization) (9). The distinction between unilateral and bilateral primary hyperaldosteronism is crucial, because unilateral PA, most often caused by an aldosterone-producing adenoma (APA), can be cured with laparoscopic unilateral adrenalectomy, whereas bilateral PA, most often caused by bilateral hyperplasia (BHA), is routinely treated with mineralocorticoid receptor antagonists (MRA) (9).

Adrenal venous sampling (AVS) is currently considered the gold standard to distinguish unilateral from bilateral disease in patients with PA (10). AVS is technically demanding, especially because the right adrenal vein is small and may be difficult to cannulate; the success rate highly depends on the expertise of the interventional radiologist (11). AVS comes at high cost, is associated with considerable radiation exposure and is variable across different centers due to insufficient standardization of the procedure (12). Due to these challenges, AVS is not consistently available even across high-income countries.

Non-invasive imaging via computed tomography and magnetic resonance imaging (CT/MRI) has not been proven to be a reliable alternative to AVS, as micro-APA (≤10 mm in diameter) remain often undetected by those imaging methods (13–15). Another challenge in non-invasive imaging is the proportion of patients with hormonally inactive adrenal incidentalomas increasing with age, leading to an increased rate of false-positive imaging findings and reduced specificity. A meta-analysis by Zhou et al. (14) revealed that CT/MRI interpretation by radiologists has a modest pooled sensitivity and specificity in identifying unilateral PA (68% and 57%). Functional imaging techniques with C11-metomidate and imaging-based clinical scores showed inconsistent results or were not feasible on a large scale (16). Therefore, current US Endocrine Society as well as the Japan Endocrine Society guidelines recommend performance of AVS as reference standard in all patients eligible for surgical treatment (17, 18).

Quantitative image analysis offers potential solutions by introducing novel imaging biomarkers. A recent pilot study with a small patient cohort (19) demonstrated that quantitative texture analysis might allow for PA subtyping. The combination of quantitative image analysis with machine learning leads to "radiomics", which plays an increasingly important role in the establishment of imaging biomarkers (20–23).

The aim of this study was to investigate the value of a radiomics approach supplemented by clinical and laboratory data for the prediction of the source of aldosterone overproduction and disease subtyping in patients with primary hyperaldosteronism.

2 Materials and methods

2.1 Patients

269 patients with confirmed primary hyperaldosteronism and CT-imaging from the German Conn Registry with diagnosed PA were enrolled (Figure 1). All patients underwent clinical testing, CT imaging and selective AVS performed by experienced interventional radiologists at the university hospital at LMU Munich, Germany. Inclusion criteria were successful bilateral AVS sampling and sufficient CT image quality, including pre-contrast images; exclusion criteria were equivocal AVS results and/or no suitable CT imaging or laboratory data. Patients were included prospectively in the registry; the present study was performed retrospectively as a *post-*

Abbreviations: ACR, aldosterone to cortisol ratio; APA, aldosterone-producing adenoma; AVS, Adrenal venous sampling; BHA, bilateral hyperplasia; BL, bilateral; BMI, body mass index; CI, confidence interval; GLCM, gray level co-occurrence matrix; IBSI, image biomarker standardization initiative; IVC, inferior vena cava; MRMR, maximum-relevance minimum-redundancy; PA, Primary hyperaldosteronism; ROC, AUC area under the receiver operating characteristic curve; SIT, saline infusion test; UL, unilateral left; UR, unilateral right.

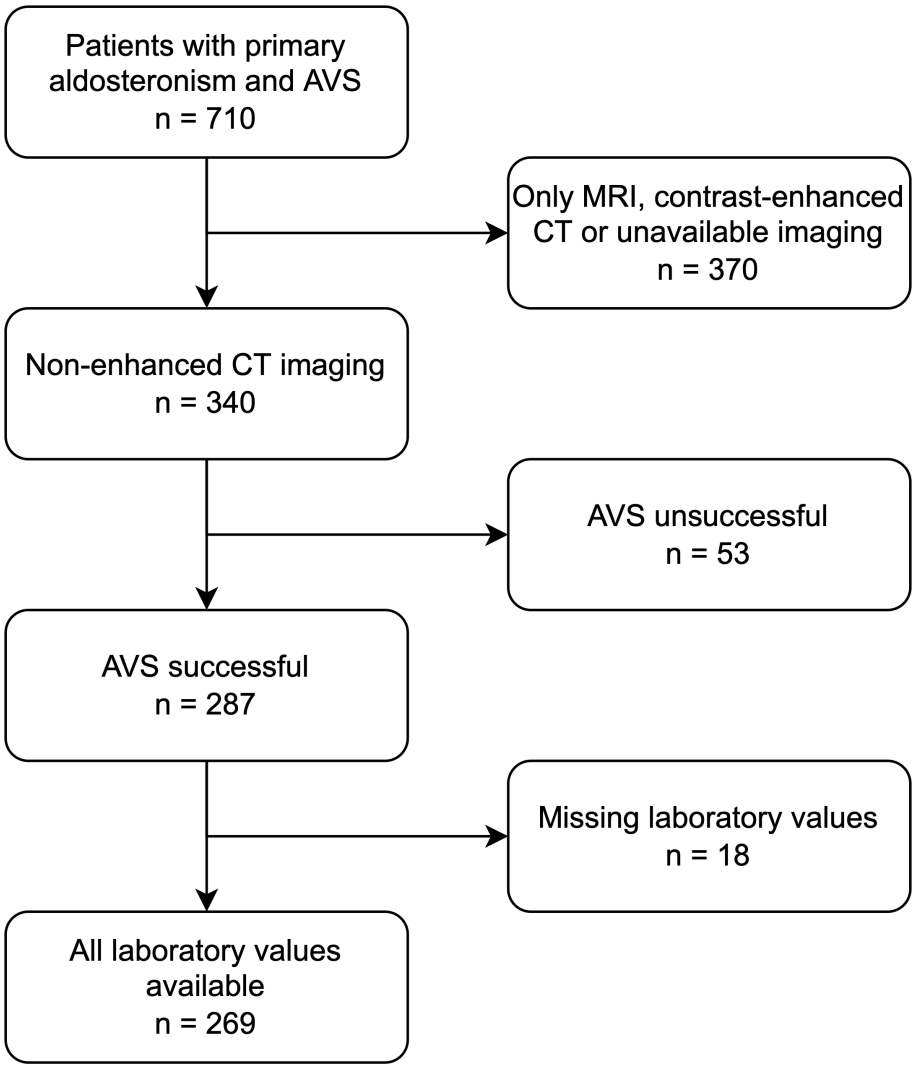

FIGURE 1
Flowchart showing the selection of the final cohort.

hoc analysis. All patients gave written informed consent, and the protocol of the German Conn Registry was approved by the Ethics Committee of the medical faculty of the Ludwig Maximilians University Munich. The diagnostic procedures were performed according to the Endocrine Society Practice Guidelines (17).

2.2 Clinical and laboratory data

Laboratory data and blood pressure values used for analysis were acquired during the baseline visit. Blood samples were drawn in a fasting state in a sitting position in the morning. Plasma aldosterone and renin concentration were measured using the DiaSorin LIAISON® (DiaSorin Ltd, Wokingham, Berkshire, UK). Blood pressure measurements were performed in the sitting position with uncrossed legs, and the arm cuff was placed at the heart level. Blood pressure readings were obtained at the same site after not less than ten minutes of rest using a validated automatic oscillometric device. Lowest potassium concentration was defined as the lowest recorded potassium concentration in the patient's history within two years before therapy. The establishment of the diagnosis PA took place after at least one positive confirmatory test (volume overload test or captopril test). Before testing, the antihypertensive medication was adapted according to guidelines (17). For the measurement of aldosterone post saline infusion test (SIT), 2 liters of 0.9% saline IV are given over a period of 4 hours (08:00-12:00 am). Blood samples for aldosterone, renin, cortisol, and electrolytes are drawn at time zero and after 4h. Patients remain in a seated position for at least 30 min during the infusion. If the aldosterone after saline infusion is ≥60 pg/ml, the diagnosis of PA is confirmed (with parallel suppressed renin). After confirmation further diagnosis (imaging) is required.

2.3 Adrenal venous sampling

In all cases, AVS was performed without adrenocorticotropic hormone stimulation in a sequential manner. During AVS, both

plasma cortisol and plasma aldosterone concentration (PAC) were determined in blood collected selectively from the adrenal veins and simultaneously from the inferior vena cava (IVC). To evaluate the success of adrenal vein catheterization, selectivity index (SI) was defined as the ratio of plasma cortisol concentration for each adrenal vein and IVC (24):

$$SI = \frac{PAC\ adrenal\ veins}{PAC\ IVC}$$

If the selectivity index exceeded two, catheterization was considered successful. The lateralization index (LI) was defined as the aldosterone to cortisol ratio (ACR) on the dosssminant side with excess aldosterone secretion over ACR on the non-dominant side (25):

$$LI = \frac{ACR\ dominant\ adrenal\ vein}{ACR\ non-dominant\ adrenal\ vein}$$

If the LI exceeded four, the patient was judged to have unilateral PA. Otherwise, a diagnosis of bilateral PA was made. The results of AVS then served as the standard of truth.

2.4 Image analysis

For *post-hoc* analyses of CT images, we performed manual whole organ segmentation of the adrenal glands in non-contrast-enhanced CT-images (slice thickness 3-5 mm) on both sides using a dedicated segmentation software (mint lesion™, Mint Medical, Heidelberg, Germany). Non-contrast enhanced CT images were used for the purpose of unifying the study protocol as the impact of contrast enhancement in different phases on density and therefore on some of the radiomic features is not known. Adrenal glands were segmented manually by one radiologist with extensive experience in abdominal CT-imaging. To assess the inter-reader variability of the segmentations, a second reader with comparable experience annotated 50 randomly selected patients within the cohort in a second round, blinded to the results of the first reader. The agreement of segmentations of both readers were assessed via the Dice coefficient.

During pre-processing, each slice was resampled to an in-plane resolution of 1x1 mm^2. No resampling in the z-axis was performed. We performed thresholding on pixel intensities in the range of (-300 to 300) Hounsfield Units (HU) to exclude outliers in the segmentation. A Laplacian of Gaussian filter for edge enhancement was applied to the images with $\sigma = 1$. For gray value discretization, a fixed bin size of FBS = 25 HU was used.

We extracted 144 independent radiomic features from the segmentation of each adrenal gland using the dedicated segmentation software (mint lesion™, Mint Medical GmbH, Heidelberg, Germany), resulting in 288 features per patient (for left and right adrenal gland). The extracted features are a subset of standardized features according to the image biomarker standardization initiative (IBSI) (26). The workflow of the radiomics analysis including segmentation, filter application, feature selection and model training, and evaluation is illustrated in Figure 2.

2.5 Statistical analysis

Continuous variables were presented as mean (± standard deviation), categorical variables as the count in each subgroup. Kruskal-Wallis H-test and Chi-square test were used for global comparison of the patients' characteristics, as appropriate, using the Python package *scipy* (version 1.9.3). Dunn's test with Benjamini-

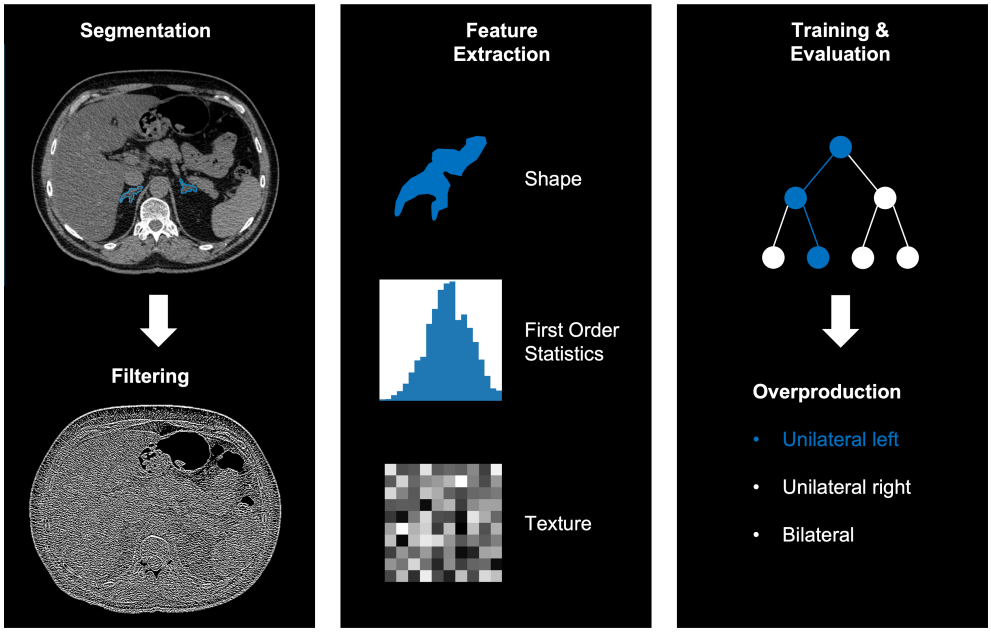

FIGURE 2
Example workflow of image segmentation and filtering (left), radiomics feature extraction (middle) and training and evaluation using a random forest (right).

Hochberg corrections was used for pairwise comparisons using the Python package *scikit-posthocs* (version 0.7.0).

The complete dataset was split into a stratified training and test set, according to an 80:20 split ratio. The features were standardized to zero mean and scaled to unit variance. To reduce the dimensionality, k = 25 features were selected using maximum-relevance minimum-redundancy feature selection (MRMR). These features were used to train a random forest classifier with n = 1000 estimators (implemented in Python 3.9.5 using scikit-learn 1.1.0) to predict the results of AVS, with the three target classes "unilateral left" (UL), "unilateral right" (UR), "bilateral" (BL) overproduction. A random forest classifier is an ensemble machine learning method that combines multiple decision trees to make predictions and classify data by aggregating the results of the individual trees. The predictive performance of the model was assessed with the one-versus-all area under the receiver operating characteristic curve (ROC AUC) evaluated on the hold-out test set. Confidence intervals (CI) were assessed using a bootstrap approach. Feature importance was determined for the test set using permutation feature importance which defines the decrease in model score after random shuffling of a single feature value.

For the baseline setting, we used radiomics features alone to train the model and predict the AVS result for the test set. Then, we included clinical and laboratory parameters into the model and repeated the training and evaluation process.

3 Results

3.1 Patients

According to AVS results, 133/269 (49%) patients were diagnosed with bilateral hyperplasia, and 136 (51%) patients with unilateral aldosterone producing adenoma (n = 76 affecting the left adrenal gland, n = 60 the right). Patients with equivocal AVS results and/or no suitable CT imaging or laboratory data (n= 71) were excluded. There were no significant differences in patients' age, sex and body mass index (BMI) between the three groups, as summarized in Table 1. The cohort was divided by a ratio of 80:20 into training (n = 215) and test set (n = 54) with stratified distributions of subtypes of PA, as illustrated in Figure 3.

The interreader variability for the segmentations of 50 randomly selected patients yielded a mean Dice coefficient of 0.919, indicating a very high agreement between readers.

3.2 Radiomics analysis

With the results of AVS as ground truth, the model trained with radiomics features alone discriminated the location of aldosterone overproduction with ROC AUC of 0.57 for unilateral producing adenoma affecting the left adrenal gland (UL), 0.61 affecting the right adrenal gland (UR) and 0.50 for bilateral hyperplasia (BL) (total 0.56, 95% CI: 0.45-0.65) as illustrated in Figure 4A. Integration of clinical and biochemical data into the machine learning model yielded better ROC AUC values regarding subtype classification for lateralization (0.61 UL, 0.68 UR, and 0.73 for BI, total 0.67, 95% CI: 0.57-0.77), displayed in Figure 4B.

Using MRMR feature selection, a mix of clinical and radiomic features were selected for model training. Permutation feature importance (Figure 5) reveals that the most important features for the model are clinical or biochemical parameters: lowest potassium level recorded, SIT after 4 hours, aldosterone/renin ratio (ARR) and mean diastolic blood pressure measured over 24 hours are the most important distinguishing factors in subtype classification. Radiomic features, including gray level co-occurrence matrix (GLCM) features and first order features were amongst the ten most important features.

4 Discussion

In this explorative study, we have evaluated the value of a radiomics based approach for radiological analysis in patients with primary hyperaldosteronism. We found that the combination of quantitative image features together with clinical and laboratory parameters improves the prediction of the source of aldosterone overproduction as compared to prediction with image features alone. Our model thereby was not limited to the differentiation of aldosterone producing adenoma versus bilateral hyperplasia, but additionally aided in lateralization of the source of aldosterone overproduction. Specifically, the integration of clinical parameters (i.e. serological and clinical tests) into the prediction model led to a marked increase of ROC AUC values, with the best results achieved in the detection of BL hyperplasia. The difference in performance between UL and UR is within the statistical uncertainty, as the confidence intervals of the calculated ROC AUC values overlap due to the small sample size. Of the ten most important features, six were clinical and laboratory parameters, with lowest potassium level as the most important parameter. For the given three-class setting, this is reasonable, since spontaneous hypokalemia is a typical feature of PA, which has been shown to be present in 50% of patients with aldosterone-producing adenoma and in only 15% of patients with bilateral hyperplasia (27).

We computed radiomics features from manual segmentations of the adrenal glands. Our results indicate that these image features alone have only limited predictive value for the discrimination of PA subtypes, yet they are still represented in the top ten features for the integrated model. While the predictive value of image features might be improved, e.g. through optimized and standardized image acquisition or automated adrenal gland segmentation, our findings highlight the value of an integrated diagnostics approach. This observation is in line with a recent study which demonstrated that discrimination of tumor recurrence from radiation necrosis in glioma patients is improved with an integrated model approach (28).

Several prediction models have been investigated in the past to improve the diagnostics of PA. Models analyzing clinical and laboratory data have been proven to be successful in predicting the subtype of PA. Shi et al. (29) investigated 10 clinical/laboratory features and found the primary aldosterone concentration after SIT, aldosterone-to-renin-ratio and ARR after captopril challenge test,

10.3389/fendo.2023.1244342

TABLE 1 Patient characteristics and clinical data.

	Bilateral disease	Unilateral disease (left)*	Unilateral disease (right)*	*p*-value
Age at diagnosis [years]	51.14 (10.64)	51.58 (11.63)	52.07 (11.98)	0.703
Sex [m/f]	75/58	48/28	44/16	0.078
BMI [kg/m^2]	28.33 (4.7)	27.88 (4.89)	27.87 (4.45)	0.722
Laboratory parameters				
Lowest level of potassium [mmol/L]	3.53 (0.46)	3.03 (0.59)^{bi}	3.22 (0.5)^{bi}	**< 0.001**
Sodium [mmol/L]	141.17 (2.29)	140.61 (2.97)^{ur}	141.68 (2.14)	**0.031**
Total cholesterol [mg/dL]	195.9 (40.15)	191.46 (33.76)	185.13 (35.16)	0.207
HDL-C [mg/dL]	54.54 (15.14)	57.2 (15.47)	51.2 (13.36)	0.074
LDL-C [mg/dL]	121.42 (35.82)	114.7 (32.76)	111.95 (32.52)	0.206
Triglycerides [mg/dL]	120.4 (67.51)	111.61 (69.61)	124.97 (69.47)	0.18
GFR [mL/min/1,73m^2]	82.55 (21.13)	88.06 (20.19)	83.89 (17.19)	0.16
Creatinine [mg/dL]	0.96 (0.37)	0.89 (0.23)	0.94 (0.16)	0.054
UA [mg/dL]	28.05 (11.67)	22.2 (8.88)^{bi}	23.1 (9.02)^{bi}	**< 0.001**
Aldosterone baseline [ng/L]	189.56 (108.07)	283.97 (275.46)^{bi}	223.05 (127.78)^{bi}	**< 0.001**
Aldosterone 4h after SIT [ng/L]	119.09 (70.16)	209.69 (213.39)^{bi}	159.19 (117.37)^{bi}	**< 0.001**
Direct Renin Concentration 4h after SIT [mU/L]	5.05 (5.65)	4.94 (4.63)	6.44 (9.56)	0.822
Mean systolic 24h-BP [mmHg]	155.2 (17.23)	151.91 (21.88)	152.08 (20.42)	0.423
Mean diastolic 24h-BP [mmHg]	96.21 (12.32)	91.8 (12.5)	94.56 (12.53)	0.059
Aldosterone-renin-ratio [ng/mU]	58.83 (46.02)	123.31 (197.75)^{bi}	85.98 (106.47)	**0.049**
Aldosterone-ratio (before/after SIT)	1.74 (0.88)	1.58 (0.91)^{bi}	1.73 (0.97)	**0.032**
Treatment, n (%)				
Adrenalectomy	/	53 (70%)	41 (69%)	NA
MRA	133 (100%)	17 (23%)	16 (26%)	NA
Pending adrenalectomy	/	6 (7%)	3 (5%)	NA

Data are presented as mean (± SD) unless indicated otherwise. Kruskal-Wallis H-test was used for global p-values, Dunn's test with Benjamini-Hochberg corrections for pairwise comparisons. 24h-BP, 24-hour blood pressure; ARR, aldosterone/renin ratio; MRA, mineralocorticoid receptor antagonist; PA, primary hyperaldosteronism; HDL, high density lipoprotein cholesterol, LDL, low density lipoprotein cholesterol; GFR, glomerular filtration rate; SIT, saline infusion test; SD, standard deviation; UR, uric acid.

* A lateralization index greater than 4.0, or a lateralization index between 3 and 4 together with a contralateral index below 1.0 were considered to be compatible with unilateral disease.

^{bi} Compared to patients with bilateral disease, p< 0.05.

^{ur} Compared to patients with unilateral disease (right), p< 0.05.

Bold values indicate a p-value under < 0.05.

as the most important variables contributing to the model. Tamaru and colleagues (30) proposed a similar model to predict PA subtype (bilateral vs. unilateral). Both models thus successfully aided in subtype differentiation – localized adenoma versus hyperplasia - however without imaging information lateralization of a unilateral aldosterone producing adenoma is not possible.

We found that the top ten overall features for the integrated model comprise clinical, laboratory and imaging features. In particular, potassium level and aldosterone-to-renin ratio are relevant for PA subtyping (i.e. hyperplasia yes or no), whereas imaging features are relevant for prediction of disease lateralization. These results agree with findings from a recent study (31), which aimed to predict which unilateral adenomas over-produce aldosterone. Similar to our findings, age, sex, serum potassium level and aldosterone-to-renin ratio remained as independent predictors after variable selection. Furthermore, aldosterone concentration after a four-hour SIT contributed substantially to an improvement of the prediction model. This is in line with Nagano et al. (32) who found plasma aldosterone concentrations below 87.9 pg/ml after a SIT as discriminatory predictor for bilateral primary aldosteronism. When comparing several confirmatory tests, a recent meta-analysis showed that the SIT had the best sensitivity and specificity for predicting the subtype of primary aldosteronism (33). In another integrated prediction model, aldosterone levels at screening and after confirmatory testing, as well as lowest potassium level were shown to be the most important clinical parameters predicting subtype diagnosis in primary aldosteronism (34). However, dichotomization into lateralized and bilateral disease in this prediction model does not represent the complexity of the disease as it fails to define with certainty the

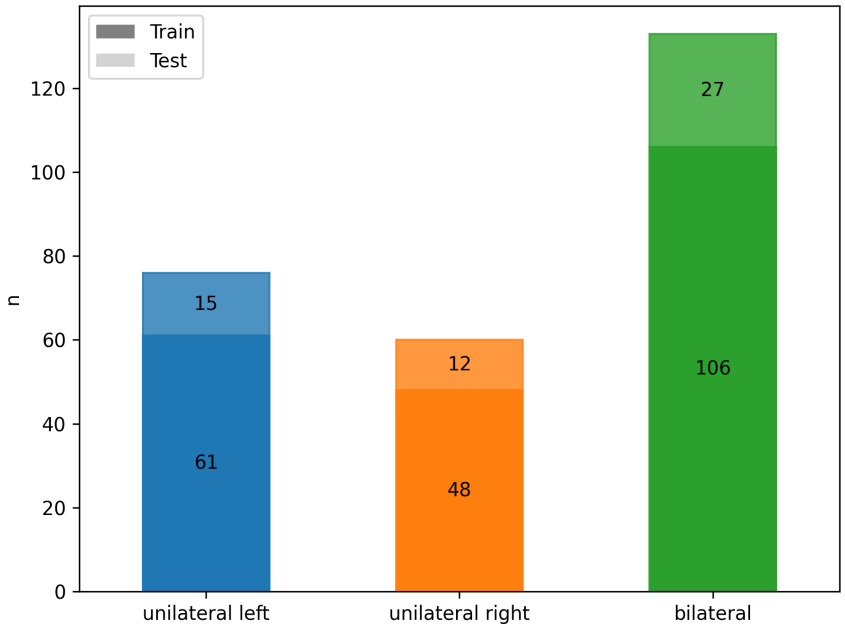

FIGURE 3
Class frequency n for the whole cohort divided by classes (color) and training (n = 215, darker) and testing (n = 54, lighter) data.

side of aldosterone hypersecretion, which is highly relevant in lateralized cases eligible for surgical treatment. Furthermore, the presence of visible nodules in CT-imaging in approximately 86% of the lateralized cases possibly caused a preselection bias.

The SPARTACUS trial (35) compared the outcome of CT-based diagnosis combined with AVS-based management in patients with PA who were treated with either adrenalectomy or MRA and were followed one year. The study did not find significant differences in intensity of antihypertensive medication or clinical benefits. Due to multiple limitations of the study, however, the only randomized prospective trial in this field could not refute the view that AVS is the gold standard for subtyping PA. In light of the SPARTACUS trial, conducting treatment decisions in primary aldosteronism on AVS results alone is challenged without offering a suitable alternative. With a nearly 50% discordance between the diagnostic conclusions derived from the CT and AVS (35), the portion of patients with aldosterone-producing micronodules treated permanently with MRA instead of surgical treatment remains unknown. Recent data by Williams et al. (36) also displayed beneficial outcomes of adrenal surgery for selected patients with bilateral primary aldosteronism, challenging the current dogma of routine medical management of this disease subtype.

Our data indicate that aldosterone overproduction caused by micronodules still may not be detectable by a quantitative analysis

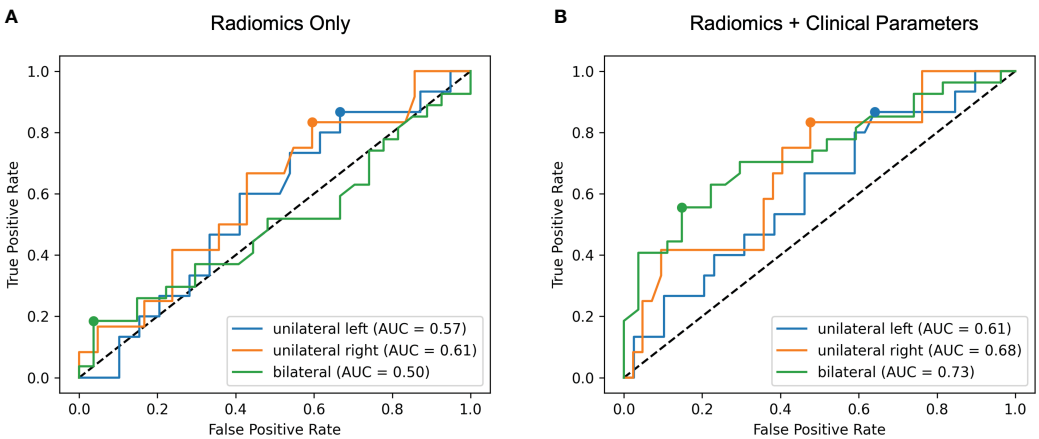

FIGURE 4
Receiver operating characteristic (ROC) curves for radiomics only **(A)** and radiomics + clinical parameters **(B)**. The area under the ROC curve (AUC) for each of the three classes unilateral left, unilateral right and bilateral is calculated in a one-versus-rest manner. Including clinical features results in higher ROC AUC values for all classes.

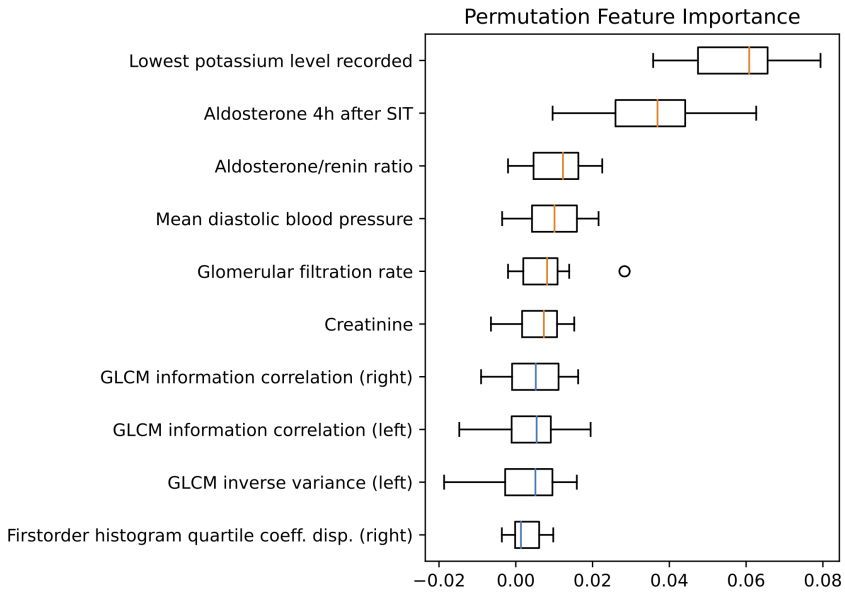

FIGURE 5
Permutation feature importance evaluated for the test set. Boxplots show the feature importance for the ten most important features. The vertical orange lines in the boxplots represent the median value of clinical features and the blue of radiomic features. GLCM, Gray level co-occurrence matrix; SIT, saline infusion test.

of medical imaging like radiomics in a substantial number of patients. This is consistent with findings at our center that reported a prevalence of nonclassical histopathology of unilateral PA in 25% of the unilateral cases, which were mainly attributed to multiple aldosterone-producing micronodules (37).

This study is not without limitations. As a consequence of non-standardized imaging protocols, imaging data is heterogeneous and introduces noise in quantitative image features. Further studies would benefit from standardized CT imaging or even MR imaging with a superior soft-tissue contrast. Moreover, functional imaging techniques, such as Positron Emission Tomography (PET), potentially hybridized with CT or MRI would allow more advanced contrast options with the possibility of molecular imaging (38). Combing those advanced imaging technologies with functional testing such as provocative or inhibitory test may allow for non-invasive diagnostics of PA in the future. Manual segmentation of adrenal glands is tedious; Although we observed very good inter-reader agreement, reproducibility might be further increased through automated approaches, e.g. with U-net based deep learning approaches. We did not perform hyperparameter tuning or benchmarking for our prediction model, simply because the sample size did not allow for the necessary additional test dataset. However, we used a random forest model with robust default settings which has proven to be suitable for classification tasks with a large number of features (39). Our reference standard for PA subtype differentiation in this study was AVS. Although AVS is the current reference standard recommended by experts and guidelines for subtype diagnosis in PA (17), its role in the management of patients PA is currently under debate (35). Additionally, a subgroup of patients affected by non-secreting adrenal incidentalomas of various size would have been an interesting comparison, however within the German Conn registry this group was not available.

5 Conclusion

This study revealed that an integrated diagnostics approach can notably improve the non-invasive identification of the source of aldosterone overproduction and subtype differentiation in PA, when compared to a radiomics approach using CT-imaging data alone. Before such an integrated approach can replace invasive AVS, the predictive value must be further improved and needs to be validated in prospective interventional studies, where machine learning approaches guide clinical decision making.

Data availability statement

The raw data supporting the conclusions of this article will be made available by the authors, without undue reservation.

Ethics statement

All procedures performed in studies involving human participants were in accordance with the ethical standards of the institutional research committee and with the 1964 Helsinki declaration and its later amendments or comparable ethical standards. Data collection was according to the protocol of the German Conn's Registry approved by the Ethics Committee of the Medical Faculty of the Ludwig Maximilians University of Munich.

All patients gave written informed consent, and the protocol of the German Conn's Registry was approved by the Ethics Committee of the University of Munich.

Author contributions

NM, AM, RW, MW, and MI: conception and design of the study, generation, collection, assembly, analysis, and/or interpretation of data, drafting or revision of the manuscript, and approval of the final version of the manuscript. BS, JaR, DH, DB, LT, HN, MB, SK, CA, JeR, MR, and NR: generation, collection, assembly, analysis, and/or interpretation of data; drafting or revision of the manuscript; approval of the final version of the manuscript.

Conflict of interest

The authors declare that the research was conducted in the absence of any commercial or financial relationships that could be construed as a potential conflict of interest.

Publisher's note

References

1. Mills KT, Stefanescu A, He J. The global epidemiology of hypertension. *Nat Rev Nephrol.* (2020) 16:1–15. doi: 10.1038/s41581-019-0244-2

2. Trompeter R, Smith R, Hoare R, Neville B, Chantler C. Neurological complications of arterial hypertension. *Arch Dis Childhood.* (1982) 57(12):913–7. doi: 10.1136/adc.57.12.913

3. Williams TA, Reincke M. MANAGEMENT OF ENDOCRINE DISEASE: Diagnosis and management of primary aldosteronism: the Endocrine Society guideline 2016 revisited. *Eur J endocrinol.* (2018) 179(1):R19–29. doi: 10.1530/EJE-17-0990

4. Gkaniatsa E, Ekerstad E, Gavric M, Muth A, Trimpou P, Olsson DS, et al. Increasing incidence of primary aldosteronism in Western Sweden during 3 decades–yet an underdiagnosed disorder. *J Clin Endocrinol Metab* (2021) 106(9):e3603–e10. doi: 10.1210/clinem/dgab327

5. Rossi GP, Cesari M, Cuspidi C, Maiolino G, Cicala MV, Bisogni V, et al. Long-term control of arterial hypertension and regression of left ventricular hypertrophy with treatment of primary aldosteronism. *Hypertension* (2013) 62(1):62–9. doi: 10.1161/HYPERTENSIONAHA.113.01316

6. Sechi LA, Novello M, Lapenna R, Baroselli S, Nadalini E, Colussi GL, et al. Long-term renal outcomes in patients with primary aldosteronism. *Jama* (2006) 295 (22):2638–45. doi: 10.1001/jama.295.22.2638

7. Mulatero P, Monticone S, Bertello C, Viola A, Tizzani D, Iannaccone A, et al. Long-term cardio-and cerebrovascular events in patients with primary aldosteronism. *J Clin Endocrinol Metab* (2013) 98(12):4826–33. doi: 10.1210/jc.2013-2805

8. Savard S, Amar L, Plouin P-F, Steichen O. Cardiovascular complications associated with primary aldosteronism: a controlled cross-sectional study. *Hypertension* (2013) 62(2):331–6. doi: 10.1161/HYPERTENSIONAHA.113.01060

9. Reincke M, Bancos I, Mulatero P, Scholl UI, Stowasser M, Williams TA. Diagnosis and treatment of primary aldosteronism. *Lancet Diabetes Endocrinol.* (2021) 9 (12):876–92. doi: 10.1016/S2213-8587(21)00210-2

10. Young J. Diagnosis and treatment of primary aldosteronism: practical clinical perspectives. *J Internal Med* (2019) 285(2):126–48. doi: 10.1111/joim.12831

11. Jakobsson H, Farmaki K, Sakinis A, Ehn O, Johannsson G, Ragnarsson O. Adrenal venous sampling: the learning curve of a single interventionalist with 282 consecutive procedures. *Diagn Intervent. Radiol.* (2018) 24(2):89. doi: 10.5152/dir.2018.17397

12. Fuss CT, Treitl M, Rayes N, Podrabsky P, Fenske WK, Heinrich DA, et al. Radiation exposure of adrenal vein sampling: a German Multicenter Study. *Eur J Endocrinol.* (2018) 179(4):261–7. doi: 10.1530/EJE-18-0328

13. Kempers MJ, Lenders JW, van Outheusden L, van der Wilt GJ, Schultze Kool LJ, Hermus AR, et al. Systematic review: diagnostic procedures to differentiate unilateral from bilateral adrenal abnorMality in primary aldosteronism. *Ann Intern Med* (2009) 151(5):329–37. doi: 10.7326/0003-4819-151-5-200909010-00007

14. Zhou Y, Wang D, Jiang L, Ran F, Chen S, Zhou P, et al. Diagnostic accuracy of adrenal imaging for subtype diagnosis in primary aldosteronism: systematic review and meta-analysis. *BMJ Open* (2020) 10(12):e038489. doi: 10.1136/bmjopen-2020-038489

15. Lim V, Guo Q, Grant CS, Thompson GB, Richards ML, Farley DR, et al. Accuracy of adrenal imaging and adrenal venous sampling in predicting surgical cure of primary aldosteronism. *J Clin Endocrinol Metab* (2014) 99(8):2712–9. doi: 10.1210/jc.2013-4146

16. Riester A, Fischer E, Degenhart C, Reiser MF, Bidlingmaier M, Beuschlein F, et al. Age below 40 or a recently proposed clinical prediction score cannot bypass adrenal venous sampling in primary aldosteronism. *J Clin Endocrinol Metab* (2014) 99 (6):E1035–E9. doi: 10.1210/jc.2013-3789

17. Funder JW, Carey RM, Mantero F, Murad MH, Reincke M, Shibata H, et al. The management of primary aldosteronism: case detection, diagnosis, and treatment: an endocrine society clinical practice guideline. *J Clin Endocrinol Metab* (2016) 101 (5):1889–916. doi: 10.1210/jc.2015-4061

18. Naruse M, Katabami T, Shibata H, Sone M, Takahashi K, Tanabe A, et al. Japan Endocrine Society clinical practice guideline for the diagnosis and management of primary aldosteronism 2021. *Endocr J* (2022) 69(4):327–59. doi: 10.1507/endocrj.EJ21-0508

19. Akai H, Yasaka K, Kunimatsu A, Ohtomo K, Abe O, Kiryu S. Application of CT texture analysis to assess the localization of primary aldosteronism. *Sci Rep* (2020) 10 (1):472. doi: 10.1038/s41598-020-57427-7

20. Lambin P, Rios-Velazquez E, Leijenaar R, Carvalho S, Van Stiphout RG, Granton P, et al. Radiomics: extracting more information from medical images using advanced feature analysis. *Eur J cancer* (2012) 48(4):441–6. doi: 10.1016/j.ejca.2011.11.036

21. Lambin P, Leijenaar RTH, Deist TM, Peerlings J, de Jong EEC, van Timmeren J, et al. Radiomics: the bridge between medical imaging and personalized medicine. *Nat Rev Clin Oncol* (2017) 14(12):749–62. doi: 10.1038/nrclinonc.2017.141

22. van Timmeren JE, Cester D, Tanadini-Lang S, Alkadhi H, Baessler B. Radiomics in medical imaging-"how-to" guide and critical reflection. *Insights Imaging* (2020) 11 (1):91. doi: 10.1186/s13244-020-00887-2

23. Rogers W, Thulasi Seetha S, Refaee TAG, Lieverse RIY, Granzier RWY , Ibrahim A, et al. Radiomics: from qualitative to quantitative imaging. *Br J Radiol* (2020) 93(1108):20190948. doi: 10.1259/bjr.20190948

24. Rossi GP, Barisa M, Allolio B, Auchus RJ, Amar L, Cohen D, et al. The Adrenal Vein Sampling International Study (AVIS) for identifying the major subtypes of primary aldosteronism. *J Clin Endocrinol.* (2012) 97(5):1606–14. doi: 10.1210/jc.2011-2830

25. Lee J, Kang B, Ha J, Kim M-H, Choi B, Hong T-H, et al. Clinical outcomes of primary aldosteronism based on lateralization index and contralateral suppression index after adrenal venous sampling in real-world practice: a retrospective cohort study. *BMC Endocr. Disord* (2020) 20(1):1–10. doi: 10.1186/s12902-020-00591-8

26. Zwanenburg A, Vallières M, Abdalah MA, Aerts HJ, Andrearczyk V, Apte A, et al. The image biomarker standardization initiative: standardized quantitative radiomics for high-throughput image-based phenotyping. *Radiology* (2020) 295 (2):328–38. doi: 10.1148/radiol.2020191145

27. Rossi GP, Bernini G, Caliumi C, Desideri G, Fabris B, Ferri C, et al. A prospective study of the prevalence of primary aldosteronism in 1,125 hypertensive patients. *J Am Coll Cardiol* (2006) 48(11):2293–300. doi: 10.1016/j.jacc.2006.07.059

28. Wang K, Qiao Z, Zhao X, Li X, Wang X, Wu T, et al. Individualized discrimination of tumor recurrence from radiation necrosis in glioma patients using an integrated radiomics-based model. *Eur J Nucl Med Mol Imaging* (2020) 47(6):1400–11. doi: 10.1007/s00259-019-04604-0

29. Shi S, Tian Y, Ren Y, Li L, Yu M, Wang J, et al. A new machine learning-based prediction model for subtype diagnosis in primary aldosteronism. *Front Endocrinol* (2022) 13. doi: 10.3389/fendo.2022.1005934

30. Tamaru S, Suwanai H, Abe H, Sasaki J, Ishii K, Iwasaki H, et al. Machine learning approach to predict subtypes of primary aldosteronism is helpful to estimate indication of adrenal vein sampling. *High Blood Pressure Cardiovasc Prev* (2022) 29(4):375–83. doi: 10.1007/s40292-022-00523-8

31. He K, Zhang Z-T, Wang Z-H, Wang Y, Wang Y-X, Zhang H-Z, et al. A clinical-radiomic nomogram based on unenhanced computed tomography for predicting the risk of aldosterone-producing adenoma. *Front Oncol* (2021) 1189. doi: 10.3389/fonc.2021.634879

32. Nagano H, Kono T, Saiga A, Kubota Y, Fujimoto M, Felizola SJ, et al. Aldosterone reduction rate after saline infusion test may be a novel prediction in patients with primary aldosteronism. *J Clin Endocrinol Metab* (2020) 105(3):e319–e27. doi: 10.1210/clinem/dgz092

33. Leung AA, Symonds CJ, Hundemer GL, Ronksley PE, Lorenzetti DL, Pasieka JL, et al. Performance of confirmatory tests for diagnosing primary aldosteronism: a systematic review and meta-analysis. *Hypertension* (2022) 79(8):1835–44. doi: 10.1161/HYPERTENSIONAHA.122.19377

34. Burrello J, Burrello A, Pieroni J, Sconfienza E, Forestiero V, Rabbia P, et al. Development and validation of prediction models for subtype diagnosis of patients with primary aldosteronism. *J Clin Endocrinol Metab* (2020) 105(10):e3706–e17. doi: 10.1210/clinem/dgaa379

35. Dekkers T, Prejbisz A, Kool L, Groenewoud H, Velema M, Spiering W, et al. SPARTACUS Investigators Adrenal vein sampling versus CT scan to determine treatment in primary aldosteronism: An outcome-based randomised diagnostic trial. *Lancet Diabetes Endocrinol* (2016) 4(9):739–46. doi: 10.1016/S2213-8587(16)30100-0

36. Williams TA, Gong S, Tsurutani Y, Tezuka Y, Thuzar M, Burrello J, et al. Adrenal surgery for bilateral primary aldosteronism: an international retrospective cohort study. *Lancet Diabetes Endocrinol* (2022). doi: 10.1016/S2213-8587(22)00253-4

37. Meyer LS, Handgriff L, Lim JS, Udager AM, Kinker I-S, Ladurner R, et al. Single-center prospective cohort study on the histopathology, genotype, and postsurgical outcomes of patients with primary aldosteronism. *Hypertension* (2021) 78(3):738–46. doi: 10.1161/HYPERTENSIONAHA.121.17348

38. Wu X, Senanayake R, Goodchild E, Bashari WA, Salsbury J, Cabrera CP, et al. [11C] metomidate PET-CT versus adrenal vein sampling for diagnosing surgically curable primary aldosteronism: a prospective, within-patient trial. *Nat Med* (2023) 29 (1):190–202. doi: 10.1038/s41591-022-02114-5

39. Rizzo S, Botta F, Raimondi S, Origgi D, Fanciullo C, Morganti AG, et al. Radiomics: the facts and the challenges of image analysis. *Eur Radiol experimental* (2018) 2(1):1–8. doi: 10.1186/s41747-018-0068-z

frontiers | Frontiers in Endocrinology

TYPE Case Report
PUBLISHED 08 September 2023
DOI 10.3389/fendo.2023.1115893

OPEN ACCESS

EDITED BY
Marta Araujo-Castro,
Ramón y Cajal University Hospital, Spain

REVIEWED BY
Robert Galagan,
Tulane University, United States
Carolina Victor,
University of São Paulo, Brazil

*CORRESPONDENCE
Shao-Ling Zhang
zhshaol@mail.sysu.edu.cn
Zhi-Hua Li
lzhdoct@163.com

†These authors have contributed equally to this work

RECEIVED 04 December 2022
ACCEPTED 18 August 2023
PUBLISHED 08 September 2023

CITATION
Weng Y, Wang L, Wang X-Y, Fan X-X, Yan L, Li Z-H and Zhang S-L (2023) Case report: Remarkable response to a novel combination of mitotane, etoposide, paraplatin, and sintilimab in a patient with metastatic adrenocortical carcinoma. *Front. Endocrinol.* 14:1115893. doi: 10.3389/fendo.2023.1115893

Case report: Remarkable response to a novel combination of mitotane, etoposide, paraplatin, and sintilimab in a patient with metastatic adrenocortical carcinoma

Yan Weng[1†], Lin Wang[2†], Xiao-Yi Wang[1], Xin-Xiang Fan[3], Li Yan[1], Zhi-Hua Li[4*] and Shao-Ling Zhang[1*]

[1]Department of Endocrinology, Sun Yat-sen Memorial Hospital, Sun Yat-sen University, Guangzhou, China, [2]Department of Pathology, Sun Yat-sen Memorial Hospital, Sun Yat-sen University, Guangzhou, China, [3]Department of Urology, Sun Yat-sen Memorial Hospital, Sun Yat-sen University, Guangzhou, China, [4]Department of Oncology, Sun Yat-sen Memorial Hospital, Sun Yat-sen University, Guangzhou, China

Background: Adrenocortical carcinoma (ACC) is a rare malignancy with a poor prognosis and limited treatment options for metastases. However, new effective regimens are emerging for specific conditions in metastatic ACC.

Case presentation: We report a case of a 36-year-old man diagnosed with metastatic ACC who had a large left adrenal mass (158 mm × 112 mm) and multiple metastases in the liver and lungs. Genetic testing revealed a microsatellite instability-high (MSI-H) tumor, a splice mutation in MLH1, and a high tumor mutational burden (TMB). After the left adrenalectomy, he received sequential treatment with a combination of mitotane, etoposide, paraplatin (EP-M), and sintilimab. His condition has been assessed as a stable disease since the sixth cycle of the combined regimen.

Conclusion: This case highlights the remarkable response of our patient's ACC with MSI-H tumor, MLH1 spice mutation, and high TMB to treatment with a novel combination of EP-M and sintilimab. Our findings suggest a promising therapeutic option for patients with similar molecular profiles.

KEYWORDS

adrenocortical carcinoma, MSI-H, MLH1, tumor mutational burden, PD-1

Background

Adrenocortical carcinoma (ACC) is a rare malignancy with an incidence of 0.5–2 per million person-years. Although ACC is typically an aggressive tumor, its prognosis is largely dependent on tumor staging (1). The 5-year survival of ACC rapidly decreases with advancing oncology stages: stage I (66% to 82%), stage II (58% to 64%), stage III (24% to 50%), and stage IV (0% to 17%) (2).

Treatment options for advanced ACC are limited. In general, first-line therapy in patients with metastatic ACC is mitotane alone or mitotane plus chemotherapy (3). Surgery may be used to control tumor growth and hypersecretion-related symptoms and prolong survival in selected patients. Mitotane and chemotherapy have limited effectiveness in treating advanced ACC (1). However, new effective regimens are emerging, particularly in cases of ACC with specific gene mutations. Currently, immunotherapy (such as antiprogrammed cell death protein 1 (PD-1)/antiprogrammed cell death ligand-1 (PD-L1) agents) has changed the treatment paradigm for certain cancers, including melanoma, lung cancer, and renal cancer (4). Patients with malignant tumors who carry specific genetic mutations in DNA mismatch repair (MMR) enzymes or have high TMB are expected to have better outcomes with immunotherapy (5, 6).

Case presentation

We present the case of a 36-year-old man from Hunan Province, China, with severe hypertension and hypokalemia and without any history of glucocorticoid exposure. Clinically, the patient had a 7-year duration of hypertension (160–180/90–110 mmHg) with an elevated body mass index (25.6 kg/m^2). Physical examination revealed no manifestations of Cushing's syndrome, such as the moon face and the buffalo neck. No family history of hypertension, endocrine tumors, or Lynch disorder was found.

The patient's blood, urine, stool tests, and renal and liver functions were normal. Biochemical tests showed marked autonomous adrenocorticotrophic hormone-independent hypercortisolemia. Plasma cortisol was 705.21 nmol/L at 8 a.m. and 680.50 nmol/L at 24 p.m. (reference range: 118.60–610.00 nmol/L), plasma adrenocorticotropic hormone (ACTH) was < 5 pg/mL (reference range: 0–46 pg/mL), indicating excessive cortisol and disturbed rhythm (Figure 1A). The patient's late-night salivary cortisol was 53.84 nmol/L (reference range: 0.00–10.40 nmol/L), and his urinary free cortisol was 3,211.2 nmol/24 h (reference range: 153.2–789.4 nmol/24 h). Furthermore, plasma cortisol was not suppressed by 1 mg of dexamethasone (725.77 nmol/L) administered overnight. The patient's serum potassium was 2.3 mmol/L, plasma renin activity was 0.78 ng/mL/h (reference range: 0.10–6.56 ng/mL/h), and plasma aldosterone concentration was 1,460.0 ng/L (reference range: 70.0–300.0 ng/L). The patient underwent a captopril challenge test; premedication plasma aldosterone concentration was 676.0 ng/L and plasma renin activity was 0.94 ng/mL/h; postmedication plasma aldosterone concentration was 799.0 ng/L and plasma renin activity was 0.61 ng/mL/h. Vanillic amygdalin assay in the urine during a 24-h period was 10.2 mg/24 h (reference range: 0–12.0 mg/24 h), metanephrine was 0.06 nmol/L (reference range: ≤ 0.60 nmol/L), and methoxynorepinephrine was 0.14 nmol/L (reference range: ≤ 0.90 nmol/L). The thyroid function test reported that the level of thyroid-stimulating hormone (TSH) was 2.047 mU/L (reference range: 0.550–4.780 mU/L), free triiodothyronine (FT3) was 5.58 pmol/L (reference range: 3.50–6.50 pmol/L), and free thyroxine (FT4) was 15.03 pmol/L (reference range: 11.50–22.70 pmol/L). His plasma testosterone was 5.67 nmol/L (reference range: 6.07–27.10 nmol/L) and dehydroepiandrosterone-sulfate was 80.88 μg/dL (reference range: 88.90–427.00 μg/dL). An analysis of the patient's plasma steroid metabolites by liquid chromatography-tandem mass spectrometry revealed an elevated secretion of 11-deoxycorticosterone and 11-deoxycortisol.

Magnetic resonance imaging (MRI) showed a large left adrenal mass (158 mm × 112 mm) compressing the left kidney, with multiple liver and lung metastases. MRI also showed partially high density on T2-emphasizing phase images and low density on T1-emphasizing phase images (Figure 2). There were 14 metastases in the liver, and the largest metastasis was about 44 mm in diameter. Multiple metastases were visible in both lungs, with a maximum lesion of about 15 mm (Figures 1B, C). Fluorodeoxyglucose positron emission tomography showed a strong accumulation in the left adrenal mass (SUV max of 8.8, Figure 3A) and metastatic lesions in the lung (SUV max of 8.7, Figure 3B) and liver (SUV max of 17.1, Figure 3C), but no lesions were detected in the bone or lymph nodes.

The patient had such resistant hypertension that five antihypertensives daily were required to maintain blood pressure between 173 and 200/100 and 130 mmHg. After 26 g of potassium chloride supplementation, the serum potassium was corrected to 3.2 mmol/L. When the patient's general condition improved, he then underwent the palliative left adrenalectomy on 22nd April 2021, and a subsequent tumor biopsy confirmed the diagnosis of ACC (Figure 4A), with a Weiss score of 7 points. The pathological results revealed vascular invasion with a Ki-67% of 75% and a mitotic count of 40/50 high-power field (Figure 4B). Immunohistochemical results indicated that α-inhibin (+), CD56 (+), Syn (partially+), Melan-A (+), CgA (−), NSE (partially+), and S-100 (−) were present. Thus, the patient was diagnosed with ACC of the left adrenal gland, with multiple metastases in the liver and both lungs (stage IV, T4N0M1).

Additionally, the patient's genetic test identified an MLH1 nonsense mutation and an NF1 frameshift mutation, along with a synonymous variant in exon 4 of the *TP53* gene. The patient also had a microsatellite instability-high (MSI-H) tumor with a TMB of 19.9 mut/Mb.

After surgery, the patient was initially administered mitotane at 0.5 g/day, which was gradually increased to 4 g/day within a month and then decreased to 1 g/day after combination therapy (Table 1). From 8 May 2021 to 3 November 2021, the patient received eight cycles of chemotherapy with etoposide and paraplatin (EP regime: etoposide 200 mg Days 1–3 + paraplatin 500 mg Day 1). After the first cycle of EP-M, he was assessed as having progressive disease (PD): the maximum size of the liver lesions grew to 64 mm and that of the lung lesion grew to 16 mm (Figures 1D, E). Thus, the patient began an add-on therapy with programmed death-1 (PD-1) immunotherapy using sintilimab (200 mg once a month) on 1st

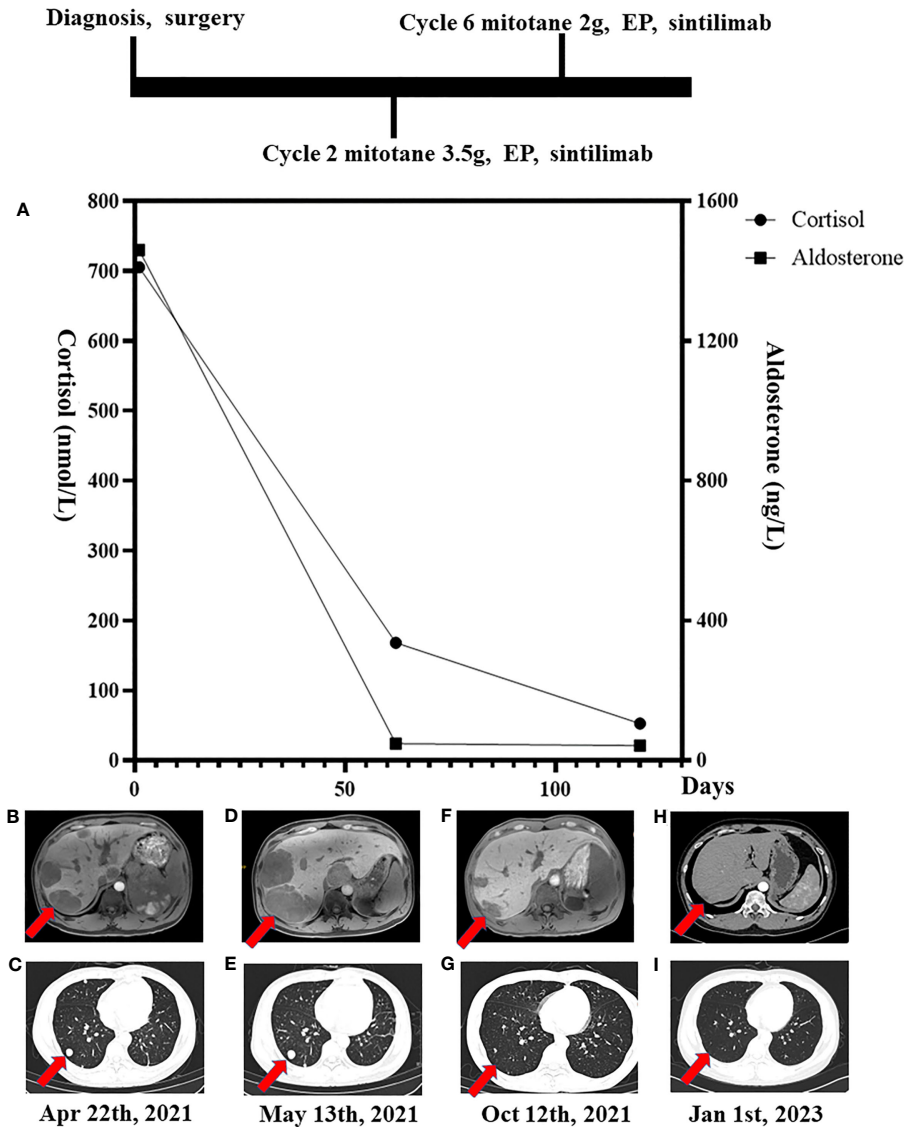

FIGURE 1
Timeline of laboratory results. **(A)** The cortisol and aldosterone concentrations plotted against time. Magnetic resonance imaging and computerized tomography showed multiple metastases in both the liver **(B, D, F, H)** and lungs **(C, E, G, I)** at diagnosis and following initiation of therapy.

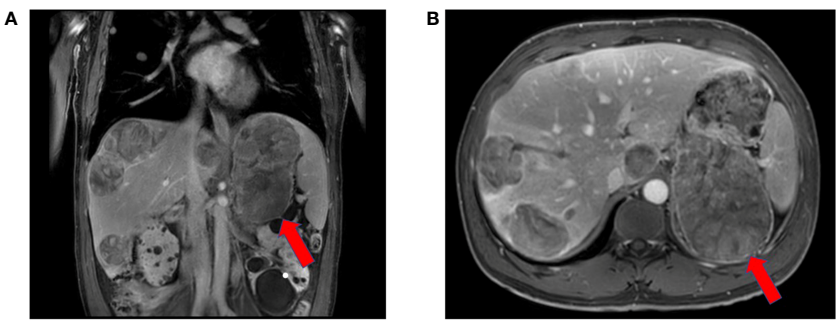

FIGURE 2
Red arrowheads indicate the primary tumor at diagnosis. Contrast-enhanced magnetic resonance imaging revealed a 158 mm × 112 mm heterogeneously enhanced left suprarenal mass with necrosis.

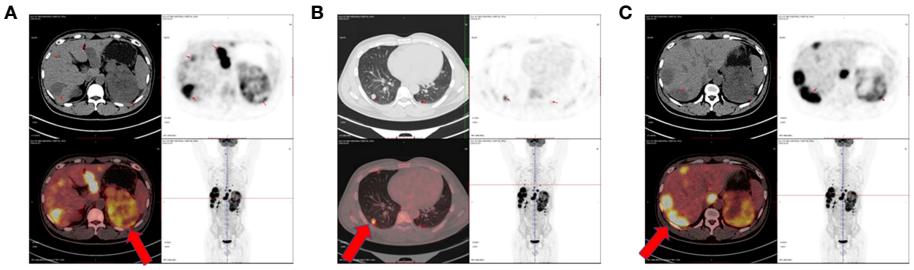

FIGURE 3
Positron emission tomography-computed tomography showed primary tumor in the left adrenal gland **(A)** and multiple metastases in both lungs **(B)** and liver **(C)** before treatment. The red arrowheads showed the primary lesion of the left adrenal gland and the metastatic lesions of the lungs and liver.

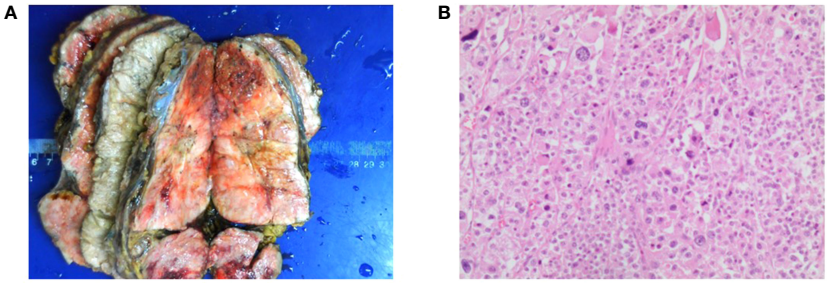

FIGURE 4
Presentation of the resected adrenocortical carcinoma (ACC) tumor tissue. **(A)** Resected (ACC) tumors. The size of the tumor is 17 cm × 10 cm × 8 cm. **(B)** Representative hematoxylin and eosin-stained photomicrograph of ACC (scale bar = 200 μm).

TABLE 1 Timeline of the treatment.

Starting date	Treatment	Side effects
22nd April 2021	Left adrenalectomy	
1st May 2021	Adjuvant mitotane at 0.5 g	
8th May 2021	Adjuvant mitotane at 1.5 g, EP	
1st June 2021	Adjuvant mitotane at 4 g, EP, sintilimab	
24th June 2021	Adjuvant mitotane at 3.5 g, EP, sintilimab	
25th July 2021	Adjuvant mitotane at 3 g, EP sintilimab	Hypothyroidism and hypoadrenocorticism
20th August 2021	Adjuvant mitotane at 2 g, EP, sintilimab	
15th September 2021	Adjuvant mitotane at 1 g, EP, sintilimab	
12th October 2021	Adjuvant mitotane at 1 g, EP, sintilimab	
3rd November 2021	Adjuvant mitotane at 1 g, EP, sintilimab	
17th December 2021	Adjuvant mitotane at 1 g, sintilimab	
13th January 2022	Adjuvant mitotane at 1g, sintinimab	
10th February 2022	Adjuvant mitotane at 1 g, sintinimab	
8th March 2022	Adjuvant mitotane at 1 g, sintinimab	
11th April 2022	Adjuvant mitotane at 1 g, sintinimab	

(Continued)

TABLE 1 Continued

Starting date	Treatment	Side effects
9th May 2022	Adjuvant mitotane at 1 g, sintinimab	
9th June 2022	Adjuvant mitotane at 1 g, sintinimab	
5th July 2022	Adjuvant mitotane at 1 g, sintinimab	
28th July 2022	Adjuvant mitotane at 1 g, sintinimab	
22nd August 2022	Adjuvant mitotane at 1 g, sintinimab	
20th September 2022	Sintinimab	
26th October 2022	Sintinimab	
26th November 2022	Sintinimab	
11th January 2023	Sintinimab	
8th February 2023	Sintinimab	
8th March 2023	Sintinimab	

EP, etoposide and paraplatin.

June 2021. After four cycles of EP-M and sintilimab, the metastatic lesions continued to shrink, and the patient's condition was assessed as stable disease (SD) at the sixth cycle, the maximum size of the liver lesion decreased to 24 mm and that of the lung lesion decreased to 4 mm (Figures 1F, G). Following eight cycles of EP, the patient continued to receive sintilimab and mitotane only, and eventually, sintilimab monotherapy was used to maintain SD (Table 1). The computed tomography (CT) scan on 1st January 2023 showed a reduction of ACC metastases both in the liver and lungs. The original maximum liver lesion was approximately 17 mm in diameter and the original maximum lung lesion disappeared. Moreover, neither relapsed disease at the primary site nor new metastases were detected (Figures 1H, I). On 20th July 2022, his blood pressure was stabilized in a normal range without antihypertensives, and the hypokalemia was corrected without potassium supplements.

On 24th June 2021, the patient's plasma aldosterone and cortisol decreased to 48 ng/L and 168 nmol/L, respectively (Figure 1A). He tolerated treatment except for the occurrence of endocrine adverse events. At the third cycle of a combination of EP-M and sintilimab, he developed hypoadrenocorticism and hypothyroidism, characterized by an elevated ACTH level of 522 pg/mL and an elevated TSH level of 5.953 mU/L (accompanied by FT3 level of 4.84 pmol/L and FT4 level of 11.36 pmol/L). Thus, a hormone replacement regimen (80 mg hydrocortisone and 50 μg L-thyroxine/day) was prescribed. Plasma cortisol levels maintained at 14.15–28.49 nmol/L, and TSH, FT3, and FT4 levels were normal throughout his subsequent treatment.

Discussion

Here, we describe a patient with metastatic ACC who demonstrated long-term stability following cytoreductive surgery and a combination of EP-M and sintilimab.

Surgery is considered the most effective initial treatment for ACC, as evidenced by a previous study demonstrating reduced mortality in patients with metastatic ACC following cytoreductive surgery (7). In this case, the patient underwent palliative surgery to remove the primary lesion, and the pathological result confirmed the diagnosis of ACC.

Despite the patient's highly aggressive pathology, with vascular invasion, a Ki-67% of 75%, and a mitotic count of 40/50 high-power field, the combination of chemotherapy with mitotane was selected as the initial regimen after surgery following the ESMO Guidelines. To avoid the cardiotoxic effect of doxorubicin, we modified the EDP chemotherapy regimen to EP, which was shown to have comparable efficacy with advanced ACC (8, 9). The patient's response to treatment was initially disappointing, with metastatic lesions in the liver and lungs increasing in size after only 1 month.

Reports of the genetic analysis from tumor tissue and blood came out with informative data, showing that this patient had an MSI-H tumor, a splice mutation in DNA MMR machinery (MLH1), and a high TMB. Tumor MSI-H and/or MMR-deficient status is a known predictive biomarker of response to immune-based therapies (5, 10). Earlier observations demonstrated an increased response of ACC to the PD-1 inhibitor pembrolizumab in the presence of MSI-H or MMR deficiency (11). Hence, high TMB status is regarded as a potential biomarker for predicting the efficacy and response rate of immunotherapy (12, 13). After multidiscipline consultation of the above predictors of response to immunotherapy in ACC, we began to add sintilimab to the EP and mitotane regimen on 1 June 2021.

While immunotherapy is the latest evolution in ACC therapy, its efficacy varies widely (14). A phase 1b expansion cohort involving 50 metastatic ACC patients who received avelumab showed an objective response rate of 6.0% and a partial response (PR) in three patients over a median of 16.5 months (15). In a phase 2 clinical trial using pembrolizumab monotherapy in 16 metastatic ACC patients, two patients had PR, seven patients had SD, and five

patients had PD, resulting in an objective response rate of 14% (16). In a small trial, only two out of 10 metastatic ACC patients had SD during the treatment with nivolumab (17). This evidence reveals that immunotherapy is effective for ACC with metastases in some patients. Recent evidence suggests that immunotherapy also provides clinically meaningful and durable antitumor activity even in patients with advanced ACC that is MSI-stable compared to those with MSI-H (18).

Sintilimab, a novel human IgG4 antibody targeting PD-1, binds 10–50-fold more strongly compared to pembrolizumab (19). Based on our institute's experience, we selected sintilimab as the immunotherapy drug for this patient. We speculated that the exceptional effects of sintilimab were possibly associated with MSI-H and the high TMB observed in this patient, although there are different views on the use of immunotherapy for ACC. In addition, the combination of sintilimab and mitotane might be synergistic, as mitotane is the adrenolytic agent leading to steroid reduction, which can make the tumors more susceptible to checkpoint inhibitor therapy. Hypercortisolemia, whatever endogenous (due to tumor secretion) and exogenous glucocorticoid administrations, has been inversely associated with immune infiltration and has the potential to impair immunotherapy efficacy in ACC patients (20). Steroid hormone secretion was inversely associated with immune infiltration, so treatment with glucocorticoid inhibitor drugs may enhance the response to immunotherapy. Considering that high levels of glucocorticoids affect the effectiveness of immunotherapy, we administered mitotane to suppress the patient's cortisol levels.

In conclusion, we report the first case of a stage IV ACC patient with metastatic lesions in both the lungs and liver who was treated with a combination of EP-M and sintilimab and has maintained long-term stable diseases. In summary, our patient's unique gene mutations may be targets for amending treatment of advanced ACC to achieve longer survival with tolerable morbidity.

Data availability statement

The original contributions presented in the study are included in the article/supplementary material. Further inquiries can be directed to the corresponding authors.

Ethics statement

Written informed consent was obtained from the individual(s) for the publication of any potentially identifiable images or data included in this article.

Author contributions

S-LZ conceived the idea of this manuscript. YW, X-YW, X-XF, Z-HL, and S-LZ clinically followed up on the patient. YW, LW, and Z-HL collected and interpreted the patient clinical data. YW wrote the manuscript. S-LZ revised the manuscript. LY and S-LZ were responsible for the supervision. All authors contributed to the article and approved the submitted version.

Funding

This work was supported by the National Natural Science Foundation of China (81970683), the National Development Plan from China's Ministry of Science and Technology (2021YFC2501600, 2021YFC2501603), and the Natural Science Foundation of Guangdong Province (2020A1515010245) to Shao-Ling Zhang.

Conflict of interest

The authors declare that the research was conducted in the absence of any commercial or financial relationships that could be construed as a potential conflict of interest.

Publisher's note

All claims expressed in this article are solely those of the authors and do not necessarily represent those of their affiliated organizations, or those of the publisher, the editors and the reviewers. Any product that may be evaluated in this article, or claim that may be made by its manufacturer, is not guaranteed or endorsed by the publisher.

References

1. Fassnacht M, Assie G, Baudin E, Eisenhofer G, de la Fouchardiere C, Haak HR, et al. Adrenocortical carcinomas and Malignant phaeochromocytomas: ESMO-EURACAN Clinical Practice Guidelines for diagnosis, treatment and follow-up. *Ann Oncol* (2020) 31:1476–90. doi: 10.1016/j.annonc.2020.08.2099

2. Libé R. Adrenocortical carcinoma (ACC): diagnosis, prognosis, and treatment. *Front Cell Dev Biol* (2015) 3:45. doi: 10.3389/fcell.2015.00045

3. Berruti A, Grisanti S, Pulzer A, Claps M, Daffara F, Loli P, et al. Long-term outcomes of adjuvant mitotane therapy in patients with radically resected adrenocortical carcinoma. *J Clin Endocrinol Metab* (2017) 102:1358–65. doi: 10.1210/jc.2016-2894

4. Drake CG, Lipson EJ, Brahmer JR. Breathing new life into immunotherapy: review of melanoma, lung and kidney cancer. *Nat Rev Clin Oncol* (2014) 11:24–37. doi: 10.1038/nrclinonc.2013.208

5. Le DT, Uram JN, Wang H, Bartlett BR, Kemberling H, Eyring AD, et al. PD-1 blockade in tumors with mismatch-repair deficiency. *N Engl J Med* (2015) 372:2509–20. doi: 10.1056/NEJMoa1500596

6. Goodman AM, Kato S, Bazhenova L, Patel SP, Frampton GM, Miller V, et al. Tumor mutational burden as an independent predictor of response to immunotherapy in diverse cancers. *Mol Cancer Ther* (2017) 16(11):2598–608. doi: 10.1158/1535-7163.MCT-17-0386

7. Srougi V, Bancos I, Daher M, Lee JE, Graham PH, Karam JA, et al. Cytoreductive surgery of the primary tumor in metastatic adrenocortical carcinoma: Impact on patients' survival. *J Clin Endocrinol Metab* (2022) 107:964–71. doi: 10.1210/clinem/dgab865

8. Fassnacht M, Terzolo M, Allolio B, Baudin E, Haak H, Berruti A, et al. Combination chemotherapy in advanced adrenocortical carcinoma. *N Engl J Med* (2012) 366:2189–97. doi: 10.1056/NEJMoa1200966

9. Bonacci R, Gigliotti A, Baudin E, Wion-Barbot N, Emy P, Bonnay M, et al. Cytotoxic therapy with etoposide and cisplatin in advanced adrenocortical carcinoma. *Br J Cancer*. (1998) 78:546–9. doi: 10.1038/bjc.1998.530

10. Le DT, Durham JN, Smith KN, Wang H, Bartlett BR, Aulakh LK, et al. Mismatch repair deficiency predicts response of solid tumors to PD-1 blockade. *Science* (2017) 357:409–13. doi: 10.1126/science.aan6733

11. Mota JM, Sousa LG, Braghiroli MI, Siqueira LT, Neto JEB, Chapchap P, et al. Pembrolizumab for metastatic adrenocortical carcinoma with high mutational burden: two case reports. *Med (Baltimore)* (2018) 97:e13517. doi: 10.1097/MD.0000000000013517

12. Fumet JD, Truntzer C, Yarchoan M, Ghiringhelli F. Tumour mutational burden as a biomarker for immunotherapy: Current data and emerging concepts. *Eur J Cancer*. (2020) 131:40–50. doi: 10.1016/j.ejca.2020.02.038

13. Marabelle A, Fakih M, Lopez J, Shah M, Shapira-Frommer R, Nakagawa K, et al. Association of tumour mutational burden with outcomes in patients with advanced solid tumours treated with pembrolizumab: prospective biomarker analysis of the multicohort, open-label, phase 2 KEYNOTE-158 study. *Lancet Oncol* (2020) 21 (10):1353–65. doi: 10.1016/S1470-2045(20)30445-9

14. Araujo-Castro M, Pascual-Corrales E, Molina-Cerrillo J, Alonso-Gordoa T. Immunotherapy in adrenocortical carcinoma: predictors of response, efficacy, safety, and mechanisms of resistance. *Biomedicines* (2021) 9:304. doi: 10.3390/biomedicines9030304

15. Le Tourneau C, Hoimes C, Zarwan C, Wong DJ, Bauer S, Claus R, et al. Avelumab in patients with previously treated metastatic adrenocortical carcinoma: phase 1b results from the JAVELIN solid tumor trial. *J Immunother Cancer*. (2018) 6:111. doi: 10.1186/s40425-018-0424-9

16. Habra MA, Stephen B, Campbell M, Hess K, Tapia C, Xu M, et al. Phase II clinical trial of pembrolizumab efficacy and safety in advanced adrenocortical carcinoma. *J Immunother Cancer*. (2019) 7:253. doi: 10.1186/s40425-019-0722-x

17. Carneiro BA, Konda B, Costa RB, Costa RLB, Sagar V, Gursel DB, et al. Nivolumab in metastatic adrenocortical carcinoma: results of a phase 2 trial. *J Clin Endocrinol Metab* (2019) 104(12):6193–200. doi: 10.1210/jc.2019-00600

18. Raj N, Zheng Y, Kelly V, Katz SS, Chou J, Do RKG, et al. PD-1 blockade in advanced adrenocortical carcinoma. *J Clin Oncol* (2020) 38(1):71–80. doi: 10.1200/JCO.19.01586

19. Zhang H, Deng M, Lin P, Liu J, Liu C, Strohl WR, et al. Frontiers and opportunities: highlights of the 2nd annual conference of the chinese antibody society. *Antib Ther* (2018) 1(2):65–74. doi: 10.1093/abt/tby009

20. Karwacka I, Obołończyk Ł, Kaniuka-Jakubowska S, Sworczak K. The role of immunotherapy in the treatment of adrenocortical carcinoma. *Biomedicines* (2021) 9:98. doi: 10.3390/biomedicines9020098

frontiers | Frontiers in Endocrinology

TYPE Review
PUBLISHED 22 September 2023
DOI 10.3389/fendo.2023.1257078

OPEN ACCESS

EDITED BY
Piotr Glinicki,
Centre of Postgraduate Medical Education, Poland

REVIEWED BY
Takao Ando,
Nagasaki University Hospital, Japan
Lakshmi Kannan,
University of Pikeville Kentucky College of Osteopathic Medicine, United States

*CORRESPONDENCE
Everardo Josué Díaz-López
everardodiaz2@gmail.com
Rocio Villar-Taibo
rotaibo22@gmail.com

RECEIVED 11 July 2023
ACCEPTED 28 August 2023
PUBLISHED 22 September 2023

CITATION
Díaz-López EJ, Villar-Taibo R, Rodriguez-Carnero G, Fernandez-Pombo A, Garcia-Peino R, Blanco-Freire MN, Pena-Dubra A, Prado-Moraña T, Fernández-Xove I, Pérez-Béliz E, Cameselle-Teijeiro JM, Hermida-Ameijeiras A and Martinez-Olmos MA (2023) Should we suspect primary aldosteronism in patients with hypokalaemic rhabdomyolysis? A systematic review. *Front. Endocrinol.* 14:1257078. doi: 10.3389/fendo.2023.1257078

Should we suspect primary aldosteronism in patients with hypokalaemic rhabdomyolysis? A systematic review

Everardo Josué Díaz-López[1,2*], Rocio Villar-Taibo[1*], Gemma Rodriguez-Carnero[1,3], Antia Fernandez-Pombo[1,2], Roberto Garcia-Peino[1], Manuel Narciso Blanco-Freire[4], Alberto Pena-Dubra[1], Teresa Prado-Moraña[1,2], Irea-Fernández-Xove[1], Edurne Pérez-Béliz[5], Jose Manuel Cameselle-Teijeiro[5,6], Alvaro Hermida-Ameijeiras[7] and Miguel Angel Martinez-Olmos[1,8,9]

[1]Division of Endocrinology and Nutrition, University Clinical Hospital of Santiago de Compostela, Santiago de Compostela, Spain, [2]Unidad de Enfermedades Tiroideas e Metabólicas (UETeM)-Molecular Pathology Group. Department of Psychiatry, Radiology, Public Health, Nursing and Medicine, Health Research Institute of Santiago de Compostela (IDIS)-Center for Research in Molecular Medicine and Chronic Diseases (CIMUS), University of Santiago de Compostela, Santiago de Compostela, Spain, [3]Division of Epigenomics in Endocrinology and Nutrition Group-Health Research Institute of Santiago de Compostela (IDIS), University of Santiago de Compostela, Santiago de Compostela, Spain, [4]Division of Surgery, University Clinical Hospital of Santiago de Compostela, Santiago de Compostela, Spain, [5]Division of Pathology, University Clinical Hospital of Santiago de Compostela, Santiago de Compostela, Spain, [6]Medical Faculty, University of Santiago de Compostela, Santiago de Compostela, Spain, [7]Division of Internal Medicine, University Clinical Hospital of Santiago de Compostela, Santiago de Compostela, Spain, [8]Molecular Endocrinology Group-Health Research Institute of Santiago de Compostela (IDIS), University of Santiago de Compostela, Santiago de Compostela, Spain, [9]CIBER Pathophysiology of Obesity and Nutrition (CIBEROBN), Carlos III Health Institute, Madrid, Spain

Severe hypokalaemia causing rhabdomyolysis (RML) in primary aldosteronism (PA) is a rare entity, and only a few cases have been reported over the last four decades. This systematic review and case report aims to gather all published data regarding a hypokalaemic RML as presentation of PA in order to contribute to the early diagnosis of this extremely rare presentation. With the use of PubMed Central, EMBASE, and Google Scholar, a thorough internet-based search of the literature was conducted to identify articles and cases with RML secondary to hypokalaemia due to PA between June 1976 and July 2023. The case study concerns a 68-year-old male patient with hypokalaemic RML at presentation of PA. In the systematic review of the literature, 37 cases of RML secondary to hypokalaemia due to PA have been reported to date. In summary, the median age was 47.5 years, the male/female ratio was 17/21, all patients presented symptoms (weakness and/or myalgia), all the patients were hypertensive, and only four patients had complications with acute kidney injury (AKI). Although PA rarely presents with RML, it should be suspected when marked hypokalaemia and hypertension are also present. Early detection and management are essential to reduce the frequency of manifestations such as AKI.

KEYWORDS

rhabdomyolysis, hypokalaemia, hypokalaemic rhabdomyolysis, primary aldosteronism, acute kidney injury

10.3389/fendo.2023.1257078

1 Introduction

Primary aldosteronism (PA), also known as Conn's syndrome, is the most common and treatable cause of endocrine-related hypertension, with a prevalence of 5%–10% among patients with hypertension in primary care and 20% among patients with resistant hypertension (1). PA results from the excessive production of aldosterone independently of renin and angiotensin II and leads to increased renal tubular resorption of sodium and volume expansion, resulting in increased blood pressure and hypokalaemia.

Although hypokalaemia is common in this disorder, severe hypokalaemia causing rhabdomyolysis (RML) in PA is a rare entity, and only a few cases have been reported over the last four decades (2, 3).

RML is a syndrome characterised by the destruction of striated muscle, which triggers the consequent release of intracellular elements such as electrolytes, myoglobin, creatine kinase (CK), and aldolase (4, 5). The effects are recognised as a clinical syndrome of muscle injury that is associated with the development of myoglobinuria, electrolyte abnormalities, and often acute kidney injury (AKI) (6, 7). RML has been described in patients with electrolyte disorders and endocrine disorders such as hypothyroidism and hyperthyroidism, hyperaldosteronism, diabetes mellitus, and diabetic ketoacidosis (4). One of the most intriguing causes of RML is potassium deficiency (8). The mechanism of hypokalaemia-induced RML is still not clear. Profound hypokalaemia (serum potassium <2.5 mEq/L) might play an important role in muscle damage secondary to i) contraction of capillaries with reduced muscle blood supply and resulting in lysing muscle cells, ii) suppression of synthesis and storage of glycogen, and iii) deranged ion transport across the cell membrane (2, 9).

We present a case report and systematic review aimed at collecting and summarising the published data regarding hypokalaemic RML as a form of presentation of PA in order to contribute to the early diagnosis of this extremely rare presentation.

2 Case report

A 68-year-old man with a history of schizophrenia, type 2 diabetes mellitus, and uncontrolled hypertension of 8 years was evaluated in the emergency department due to a fall after an episode acute of muscle weakness in the lower limbs while walking.

He received home antihypertensive treatment with a beta-blocker, mineralocorticoid receptor antagonists (MRAs), and angiotensin-converting enzyme (ACE) inhibitors.

His blood pressure was 183/101 mmHg with a heart rate of 40 beats/minute. He presented a body mass index of 29.8 kg/m^2. Laboratory tests showed severe hypokalaemia with serum potassium of 2.1 mmol/L, glycaemia of 459 mg/dL, creatinine of 2.1 mg/dL, myoglobinaemia with serum myoglobin of 10,453 ng/mL, and CK of 3,616 IU/L. An electrocardiogram presented a prolongation of the QT interval.

Four months earlier, he presented with serum potassium of 3.9 mmol/L and creatinine of 0.97 mg/dL.

His clinical records were reviewed, and 4 months earlier, his levels of potassium and creatinine were normal. He also presented a 10-mm right adrenal nodule on an abdominal computed tomography (CT) scan 11 years previously, which was unknown at the time of admission.

With the clinical suspicion of primary hyperaldosteronism, the patient underwent a hormonal analysis, which showed high levels of plasma aldosterone (188.0 ng/dL [upper limit of normal, 39.2 ng/dL]) and low plasma renin activity (0.18 ng/mL/h) with an aldosteronetorenin ratio (ARR) of 1,074.3 ng/dL. His corresponding potassium was 4.1 mmol/L. Plasma cortisol, testosterone, dehydroepiandrosterone sulfate, 24-hour urine cortisol, and metanephrine levels were normal. A new adrenal CT was requested, observing a 27-mm nodule in the right adrenal gland, which showed attenuation of less than 10 Hounsfield units (Figure 1).

After stabilisation, the decision was taken to discharge the patient due to clinical improvement and normalisation of renal function, serum potassium, CK, and electrocardiogram alterations. Antihypertensives were changed to others that do not interfere with renin and aldosterone measurements in order to request a new hormonal study after 6 weeks.

During follow-up in the outpatient clinic, he presented an ARR of 866.7 ng/dL. Due to the presence of overt PA, no confirmatory studies were deemed necessary since this pattern is not observed in other entities (10).

The patient was evaluated by the Endocrine Tumour Committee at our hospital and scheduled for right posterior retroperitoneoscopic adrenalectomy. An adrenalectomy specimen with abundant adjacent

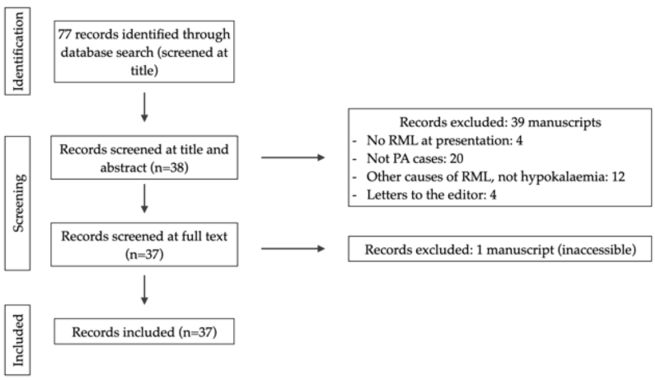

FIGURE 1
Preferred Reporting Items for Systematic Reviews and Meta-Analyses (PRISMA) flow chart for the identification of inclusion and exclusion of studies.

adipose tissue was obtained, weighing 79.7 g and occupying a combined area of 10.8 × 4.2 cm. After the serial cuts, an adrenal gland with conventional characteristics was identified in an area of up to 4.0 × 2.2 cm. The gland included a solid, well-delimited, yellowish nodule measuring 2.6 × 2.3 × 2.0 cm in diameter, compressing the residual adrenal tissue. A diagnosis of cortical adenoma was confirmed, pathologically consistent with aldosterone production. The adjacent adipose tissue did not present notable alterations (Figure 2). A 4.0-cm-diameter cortical adenoma was confirmed, pathologically consistent with aldosterone production. As an incidental finding, the tumour included spironolactone bodies (Figure 3).

Fifteen days after surgery, there was a clinical improvement in strength, and antihypertensive treatment (only with amlodipine 5 mg) was reduced due to good control of blood pressure. Potassium and aldosterone levels normalised without the need for oral potassium supplementation. The patient is currently fully recovered and is being monitored in primary care.

3 Research design and methods

3.1 Literature search and screening

The reported systematic review follows the Preferred Reporting Items for Systematic Reviews and Meta-Analyses (PRISMA) guidelines. The protocol was registered on PROSPERO International Prospective Register of Systematic Reviews, with registration ID CRD42023439678.

With the use of PubMed Central, EMBASE, and Google Scholar, a thorough internet-based search of the literature was carried out to identify articles and cases with RML secondary to hypokalaemia due to PA between June 17, 1976, and July 2, 2023. The search strategy was as follows: [(rhabdomyolysis) OR (hypokalaemia) OR (hypokalaemic rhabdomyolysis) OR (primary aldosteronism AND (hypokalaemia OR rhabdomyolysis)] OR (hypokalaemic rhabdomyolysis) OR (Conn's syndrome).

3.2 Study selection and data management

Regarding study selection, data from the retrieved articles (title, authors, date of publication, journal, abstract, and keywords) were gathered from the major scientific platforms and transferred into Zotero (www.zotero.org) to identify and eliminate duplicate articles. Two independent reviewers (EJDL and RVT) initially screened the eligibility of studies based on the title/abstract content of each study identified. Studies that clearly did not satisfy the inclusion criteria were discarded with any disagreements being resolved by consensus or, if necessary, via consultation with a third reviewer (GRC). When

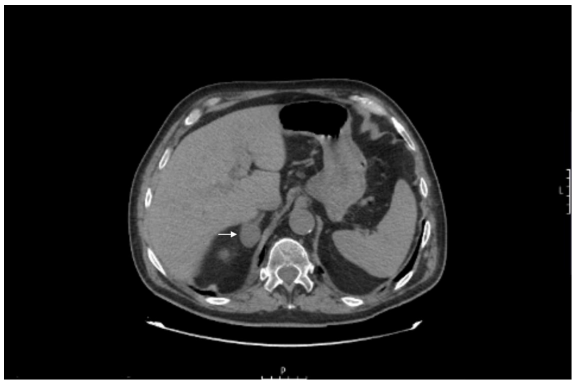

FIGURE 2
Adrenal computed tomography of the case study. White arrow showing a 27-mm nodule in the right adrenal gland.

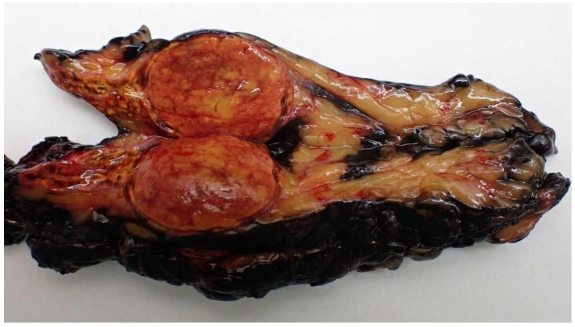

FIGURE 3
Aldosterone-producing adrenal cortical adenoma. The tumour is a solid, yellowish nodule that is well-demarcated by a thin rim of normal adrenal cortex.

no agreement was reached, a third reviewer (GRC) was involved to make the final decision.

All potentially eligible articles from this screening were downloaded as full text and distributed to the reviewers for verification that they fulfilled all the inclusion criteria and none of the exclusion criteria. Only cases or case series with hypokalaemic RML as presentation of PA were considered. Cases with no RML as presentation or other causes of RML not related to hypokalaemia were excluded. No restrictions on language or search period were included. In addition to the relevant articles, the articles referenced in the retrieved publications were also manually scrutinised.

General information from each article, such as first author or year of publication, was noted. Specific epidemiological data were also registered, including age and sex. The following clinical and biochemical variables were recorded: initial symptoms, antihypertensive drugs, presence of AKI, serum potassium (mmol/L), and creatinine (u/L). The treatment for PA and the anatomopathological diagnosis were also recorded.

Written informed consent was obtained from the patient for the publication of this article.

4 Results of the systematic review

In the systematic review of the literature, 37 cases of RML secondary to hypokalaemia due to PA reported to date were identified. The flow chart of studies included is presented in Figure 4.

Clinical features, diagnosis data, treatment, and outcomes of all cases (including our patient) are presented in Table 1. In summary, the median age was 47.5 years, the male/female ratio was 17/21, all patients presented symptoms (weakness and/or myalgia), all the patients were hypertensive, and only four patients had complications with AKI.

5 Discussion

Here, we present a patient who was suspected of having RML secondary to PA due to the presence of resistant hypertension and hypokalaemia, although this is a very rare presentation of PA, and it is more common for patients with RML to present hyperkalaemia due to the release of intracellular metabolites (potassium, phosphates, and urate) and intracellular proteins to the extracellular space and circulation (42).

The diagnosis of RML was based on the clinical presentation and the very high levels of CK and myoglobin. The myoglobinuria was detected by the presence of dark-coloured urine, with a positive urine dipstick test for blood without evidence of red blood cells on microscopy. This is a clue to the presence of RML, as myoglobin will also react with the orthotolidine test reagent (7).

A confirmatory test for PA was not required in this patient considering that current guidelines suggest bypassing such tests in patients with a particularly severe clinical phenotype (overt PA), i.e., patients with hypokalaemia, undetectable plasma renin, and plasma aldosterone concentrations higher than 20 ng/dL (555 pmol/L) (43).

In the systematic review, 21 out of 38 of the cases presented in women (55%), the majority of the patients (30/38) were younger than 60 years, and all the patients manifested symptoms (weakness and/or myalgias). In the Chinese biomedical literature database, 13 cases have been reported of PA being related to hypokalaemic RML. In this series, the epidemiological characteristics of the patients were similar, with a predominance of cases in women (69%), most of whom were under 60 years of age (84.6%). All 13 patients had a history of hypertension and weakness and/or myalgias. Twelve out of 13 patients had blood potassium lower than 2.5 mmol/L, 11 had adrenal adenoma, and none had renal failure (8). In a review of the English literature, 22 cases of PA related to hypokalaemic RML were summarised. Among these cases, nine patients were male and 13 were female (59%), five were 60 years of age or older and 17 were younger, 21 had symptoms of fatigue, and 20 had hypertension (2).

Regarding the levels of hypokalaemia related to RML occurrence, severe muscle weakness or RML usually occurs if serum potassium is below 2.5 mmol/L (44). In this review of cases, there are 35 patients who developed rhabdomyolysis with serum potassium below 2.1 mmol/L.

In the cases described, acute renal injury was very rare, being observed in only four patients (12, 16, 21). It was intensively managed with fluid therapy and intravenous potassium, with rapid clinical and analytical improvement. Intravenous fluids should be initiated as soon as possible, preferably within the first 6 hours after muscle injury (45).

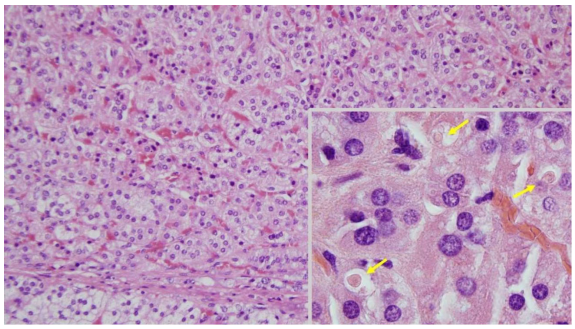

FIGURE 4
Adrenal histology of the case study. The adenoma is well-vascularised and composed of trabeculae of monomorphic cells with weakly eosinophilic cytoplasm, which contrasts with the clearer appearance of the cytoplasm of adjacent normal cells (bottom). At higher magnification (inset), spironolactone bodies can be seen (arrows); (hematoxylin and eosin, ×200; inset, ×1,000).

10.3389/fendo.2023.1257078

TABLE 1 Clinical features, diagnosis data, treatment, and outcomes of all cases with hypokalaemic RML due to PA as a form of presentation.

Case/year (reference)	Country	Age (years)/ sex	Initial symptoms	HT	Antihypertensive drugs	AKI	K^+ (mmol/ L)	CK (U/ L)	Treatment	Subtype
1/1976 (11)	Canada	68/M	Weakness	Yes	HCTZ	No	0.6	3,250	UN	UN
2/1978 (12)	United States	49/M	Weakness	Yes	HCTZ	Yes	2.5	12,030	Surgical	Adenoma
3/1979 (13)	Japan	55/M	Weakness	Yes	Furosemide	No	1.8	2,000	Surgical	Adenoma
4/1981 (14)	United Kingdom	60/M	Weakness	Yes	Metoprolol	UN	1.4	36,000	UN	UN
5/1990 (15)	United States	32/F	Weakness	Yes	Beta-blocker, HCTZ	No	2.0	10,000	Surgical	Adenoma
6/1997 (16)	Canada	70/M	Weakness	Yes	Beta-blocker, amlodipine	Yes	1.8	2,800	Surgical	Adenoma
7/1998 (17)	France	64/M	Weakness	Yes	Enalapril, atenolol, nifedipine, HCTZ	No	1.3	2,997	Surgical	Adenoma
8/2002 (18)	Germany	30/F	Weakness	Yes	Fosinopril, amlodipine, HCTZ, furosemide	No	1.3	1,751	Surgical	Adenoma
9/2005 (19)	Turkey	44/F	Weakness	Yes	ACE inhibitor, verapamil	No	1.2	6,133	Surgical	Adenoma
10/2007 (20)	Poland	50/F	Weakness	Yes	Amlodipine	No	1.95	9,546	Surgical	Unilateral hyperplasia
11/2007 (21)	Greece	36/F	Weakness	Yes	Atenolol, chlorthalidone	Yes	2.2	2,860	Medical	NA
12/2008 (22)	Taiwan	28/F	Weakness	Yes	None	No	1.8	12,147	Surgical	Adenoma
13/2009 (23)	Germany	52/M	Weakness	Yes	Ramipril, Bisoprolol, HCTZ, clonidine	No	1.9	10,615	Surgical	Adenoma
14/2009 (24)	Greece	76/F	Weakness	Yes	Amlodipine	No	1.6	7,463	Surgical	Unilateral hyperplasia
15/2009 (25)	Turkey	14/F	None	Yes	None	UN	1.7	3,375	Surgical	Adenoma
16/2009 (26)	Japan	55/M	Weakness	Yes	Amlodipine, valsartan, HCTZ	No	1.4	15,760	Surgical	Adenoma
17/2009 (27)	Spain	46/F	Weakness and myalgias	Yes	None	No	1.3	21,000	Surgical	Adenoma
18/2012 (28)	Taiwan	49/F	Weakness	Yes	Amlodipine, valsartan	No	1.8	1,753	Medical	Bilateral nodular hyperplasia
19/2013 (29)	Austria	60/M	Weakness and myalgias	Yes	None	No	1.7	1,522	Surgical	Adenoma
20/2013 (30)	India	45/F	Weakness and myalgias	Yes	Nifedipine, atenolol, losartan	No	2.0	11,347	Surgical	Adenoma
21/2013 (31)	China	44/F	Weakness	Yes	UN	No	1.98	8,531	Surgical	Adenoma
22/2013 (31)	China	45/F	Weakness	Yes	Nitrendipine, captopril	No	1.38	4,907	Surgical	Adenoma
23/2015 (32)	China	38/M	Weakness and myalgias	Yes	Metoprolol, nifedipine	No	2.8	2,974	Surgical	Adenoma
24/2015 (33)	Japan	43/F	Weakness	Yes	Amlodipine, candesartan	No	1.8	6,929	Medical	Adenoma
25/2015 (2)	Italia	40/F	Weakness and myalgias	Yes	Irbesartan, HCTZ	No	1.66	9,122	Medical	Bilateral nodular hyperplasia
26/2015 (34)	Korea	54/M	Weakness	Yes	Felodipine, losartan, atenolol, HCTZ	No	2.0	2,982	Surgical	Adenoma
27/2017 (35)	Mexico	35/F	Weakness	Yes	Losartan, amlodipine	No	1.4	3,694	Surgical	Adenoma

(Continued)

10.3389/fendo.2023.1257078

TABLE 1 Continued

Case/year (reference)	Country	Age (years)/ sex	Initial symptoms	HT	Antihypertensive drugs	AKI	K^+ (mmol/ L)	CK (U/ L)	Treatment	Subtype
28/2017 (36)	Albania	47/F	Weakness and myalgias	Yes	Amlodipine, valsartan	No	1.4	8,559	Surgical	NA
29/2018 (37)	Austria	55/F	Weakness and myalgias	Yes	Amlodipine, HCTZ, ARB, alpha- and beta-blockers	No	1.5	2,900	Surgical	Adenoma
30/2019 (38)	Taiwan	46/M	Weakness	Yes	Acebutolol, amlodipine, valsartan.	No	1.7	4,532	Medical	NA
31/2019 (39)	Russia	61/M	Weakness	Yes	ACE inhibitor, indapamide, bisoprolol	No	2.08	11,307	Medical	NA
32/2021 (3)	India	38/F	Weakness	Yes	MRA	No	1.9	1,015	Surgical	Adenoma
33/2021 (40)	Turkey	48/F	Weakness and myalgias	Yes	Valsartan, bisoprolol	No	1.3	14,248	Surgical	Adenoma
34/2021 (41)	Philippines	45/M	Weakness	Yes	Amlodipine	No	2.1	1,579	Surgical	Adenoma
35/2021 (9)	Taiwan	46/M	Weakness	Yes	Valsartan, HCTZ	No	1.9	1,626	Surgical	Adenoma
36/2021 (9)	Taiwan	53/M	Weakness and myalgias	Yes	Amlodipine, valsartan, HCTZ	No	2.1	1,593	Surgical	Adenoma
37/2022 (8)	China	65/F	Weakness and myalgias	No	None	No	1.8	18,370	Surgical	Adenoma
38/2023 (present case)	Spain	68/M	Weakness	Yes	Beta-blocker, ACE inhibitor, MRA	Yes	2.1	3,250	Surgical	Adenoma

M, male; F, female; UN, unknown; HCTZ, hydrochlorothiazide; NA, not applicable; HT, hypertension; AKI, acute kidney injury; ACE, angiotensinconverting enzyme; MRA, mineralocorticoid receptor antagonist; ARB, angiotensin receptor blocker; RML, rhabdomyolysis; PA, aldosteronism.

In this review, 85% of the patients received surgery as the treatment for PA. The pathological diagnosis was adrenal adenomas in 93% of the cases. Of those who received definitive medical treatment (n = 5), three patients did not accept surgery, and two did not meet the criteria due to bilateral nodular hyperplasia. As an incidental finding, in our case, spironolactone bodies were detected. The incidence of spironolactone bodies within the adrenal gland in patients taking spironolactone or eplerenone is unknown. Patel et al., in a retrospective study, detected inclusions in only 33% of patients with PA treated with spironolactone and/or eplerenone (46). In this review, there were no cases other than our case describing this finding.

In conclusion, after reviewing the cases published in the literature, it can be concluded that hypokalaemic RML due to PA is a rare condition. It presents mostly in young patients (<60 years of age) with a certain predominance among women. It should be suspected in subjects with hypertension and mild hypokalaemia. Early diagnosis and management can lead to a better evolution of the patient, reducing the frequency of RML and complications such as AKI.

Author contributions

ED-L: Conceptualization, Methodology, Supervision, Visualization, Writing – original draft, Writing – review & editing. RV-T: Conceptualization, Methodology, Supervision, Writing – review & editing. GR-C: Conceptualization, Writing – review & editing. AF-P: Supervision, Writing – review & editing. RG-P: Writing – review & editing. MB-F: Writing – review & editing. AP-D: Writing – review & editing. TP-M: Writing – review & editing. IF-X: Writing – review & editing. EP-B: Writing – review & editing. JC-T: Writing – review & editing. AH-A: Supervision, Writing – review & editing. MM-O: Writing – review & editing.

Funding

The authors declare financial support was received for the research, authorship, and/or publication of this article. AF-P receives funding from the Fundació;n Alfonso Martí;n Escudero.

Conflict of interest

The authors declare that the research was conducted in the absence of any commercial or financial relationships that could be construed as a potential conflict of interest.

Publisher's note

References

1. Parra Ramí;rez P, Rojas-Marcos PM, Paja Fano M, González Boillos M, Pascual-Corrales E, Garcí;a-Cano A, et al. Differences in the presentation and evolution of primary aldosteronism in elderly (≥65 years) and young patients (<65 years)(2022). Available at: https://ec.bioscientifica.com/view/journals/ec/11/6/EC-22-0169.xml (Accessed 2023 Jun 17).

2. Zavatto A, Concistrè A, Marinelli C, Zingaretti V, Umbro I, Fiacco F, et al. Hypokalemic rhabdomyolysis: a rare manifestation of primary aldosteronism. *Eur Rev Med Pharmacol Sci* (2015) 19(20):3910–6.

3. Kollipara S, Ravindra S, Pai K, Shetty S. Quadriplegia and rhabdomyolysis as a presenting feature of Conn's syndrome. *BMJ Case Rep* (2021) 14(1):e234686. doi: 10.1136/bcr-2020-234686

4. Młynarska E, Krzemińska J, Wronka M, Franczyk B, Rysz J, Rhabdomyolysis-Induced AKI. (RIAKI) including the role of COVID-19. *Int J Mol Sci* (2022) 23 (15):8215. doi: 10.3390/ijms23158215

5. Baeza-Trinidad R. Rhabdomyolysis: A syndrome to be considered(2022). Available at: https://linkinghub.elsevier.com/retrieve/pii/S2387020622000961 (Accessed 2023 Apr 10).

6. Gupta A, Thorson P, Penmatsa KR, Gupta P. Rhabdomyolysis: revisited. *Ulster Med J* (2021) 90(2):61–9.

7. Zimmerman JL, Shen MC. Rhabdomyolysis(2013). Available at: https://linkinghub.elsevier.com/retrieve/pii/S0012369213606261 (Accessed 2023 Jun 4).

8. Han R, Jiang X. Hypokalemia-induced rhabdomyolysis as the first symptom of primary aldosteronism: a case report and literature review. *Ann Palliat Med* (2022) 11 (8):2778–84. doi: 10.21037/apm-21-3010

9. Chen CT, Wang YC, Lin CM. Hypokalemia-induced rhabdomyolysis caused by adrenal tumor-related primary aldosteronism: A report of 2 cases. *Am J Case Rep* (2021) 22:e929758. doi: 10.12659/AJCR.929758

10. Araujo-Castro M, Parra-Ramí;rez P. Diagnó;stico del hiperaldosteronismo primario(2022). Available at: https://linkinghub.elsevier.com/retrieve/pii/S0025775321006564 (Accessed 2023 Jun 16).

11. Crawhall JC, Tolis G, Roy D. Elevation of serum creatine kinase in severe hypokalemic hyperaldosteronism. *Clin Biochem* (1976) 9(5):237–40. doi: 10.1016/S0009-9120(76)80067-7

12. Dominic JA, Koch M, Guthrie GP, Galla JH. Primary aldosteronism presenting as myoglobinuric acute renal failure. *Arch Intern Med* (1978) 138(9):1433–4. doi: 10.1001/archinte.1978.03630340099036

13. Atsumi T, Ishikawa S, Miyatake T, Yoshida M. Myopathy and primary aldosteronism: electronmicroscopic study. *Neurology.* (1979) 29(10):1348–53. doi: 10.1212/WNL.29.10.1348

14. SChady W, Yuill GM. Myopathy and primary hyperaldosteronism. *Neurology.* (1981) 31(2):225–6. doi: 10.1212/WNL.31.2.225-b

15. Mahdyoon H, Mermiges DN, Wisgerhof M. Conn's syndrome with rhabdomyolysis mimicking deep vein thrombophlebitis. *South Med J* (1990) 83 (3):346–7. doi: 10.1097/00007611-199003000-00024

16. Chow CP, Symonds CJ, Zochodne DW. Hyperglycemia, lumbar plexopathy and hypokalemic rhabdomyolysis complicating Conn's syndrome. *Can J Neurol Sci J Can Sci Neurol* (1997) 24(1):67–9. doi: 10.1017/S0317167100021132

17. Mourad JJ, Milliez P, Blacher J, Safar M, Girerd X. [Conn adenoma manifesting as reversible tetraparesis and rhabdomyolysis]. *Rev Med Interne.* (1998) 19(3):203–5. doi: 10.1016/S0248-8663(97)80722-9

18. Ozgür B, Kürsat S. Hypokalemic rhabdomyolysis aggravated by diuretics complicating Conn's syndrome without acute renal failure. *Clin Nephrol.* (2002) 57 (1):89–91. doi: 10.5414/cnp57089

19. Kaşifoğlu T, Korkmaz C, Paşaoğlu O. Conn's syndrome (primary hyperaldosteronism) simulating polymyositis. *Rheumatol Int* (2005) 25(2):133–4. doi: 10.1007/s00296-004-0462-0

20. Gonerska-Szadkowska A, Wittych-Długosz J, Makarewicz J, Szmidt M, Lewiński A. Rhabdomyolysis following severe hypokalemia caused by Conn's syndrome. *Arch Med Sci* (2007) 3(3):274–7.

21. Petidis K, Douma S, Aslanidis S, Papaefthimiou P, Kartali N, Zamboulis C. Hypertension associated with rhabdomyolysis. *J Clin Hypertens Greenwich Conn.* (2007) 9(1):60–2. doi: 10.1111/j.1524-6175.2007.05811.x

22. Chuang TH, Wang CH, Tseng BY, Hsu YH, Tsai JP, Hsu BG, et al. syndrome with an unusual presentation of rhabdomyolysis secondary to severe hypokalemia. *Conn's* (2008) (Accessed 2023 May 29).

23. Etgen T, Gräbert C. Tetraparesis with hypertensive crisis: hypokalemic rhabdomyolysis in primary hyperaldosteronism. *Nervenarzt.* (2009) 80(6):717–9. doi: 10.1007/s00115-009-2676-6

24. Kotsaftis P, Savopoulos C, Agapakis D, Ntaios G, Tzioufa V, Papadopoulos V, et al. Hypokalemia induced myopathy as first manifestation of primary hyperaldosteronism - an elderly patient with unilateral adrenal hyperplasia: a case report. *cases J* (2009) 2:6813. doi: 10.4076/1757-1626-2-6813

25. Karagüzel G, Bahat E, Imamoğlu M, Ahmetoğlu A, Yildiz K, Okten A. An unusual case of an aldosterone-producing adrenocortical adenoma presenting with rhabdomyolysis. *J Pediatr Endocrinol Metab JPEM.* (2009) 22(11):1087–90. doi: 10.1515/jpem.2009.22.11.1087

26. Goto A, Takahashi Y, Kishimoto M, Minowada S, Aibe H, Hasuo K, et al. Primary aldosteronism associated with severe rhabdomyolysis due to profound hypokalemia. *Intern Med Tokyo Jpn* (2009) 48(4):219–23. doi: 10.2169/internalmedicine.48.1444

27. Martí;nez JJA, Oliveira CL, Meneses AL, Rodrí;guez SA, Corrales PP, Ló;pez AH, et al. Rhabdomyolysis due to primary hyperaldosteronism(2009) (Accessed 2023 May 29).

28. Tsai WT, Chen YL, Yang WS, Lin HD, Chien CC, Lin CL. Primary aldosteronism associated with severe hypokalemic rhabdomyolysis. *Horm Athens Greece.* (2012) 11(4):505–6. doi: 10.14310/horm.2002.1385

29. Finsterer J, Lässer S. Severe hypokalemic paralysis as a manifestation of a mitochondrial disorder. *Tohoku J Exp Med* (2013) 231(1):9–12. doi: 10.1620/tjem.231.9

30. Cooray MSA, Bulugahapitiya US, Peiris DN. Rhabdomyolysis: A rare presentation of aldosterone-producing adenoma. *Indian J Endocrinol Metab* (2013) 17(Suppl 1):S237–239. doi: 10.4103/2230-8210.119583

31. Wen Z, Chuanwei L, Chunyu Z, Hui H, Weimin L. Rhabdomyolysis presenting with severe hypokalemia in hypertensive patients: a case series. *BMC Res Notes.* (2013) 6:155. doi: 10.1186/1756-0500-6-155

32. Yao B, Qin Z, Tan Y, He Y, Yan J, Liang Q, et al. Rhabdomyolysis in primary aldosteronism: A case report and review of the literature(2015) (Accessed 2023 May 29).

33. Eguchi T, Miyauchi S. A case of primary aldosteronism with secondary hyperparathyroidism and bilateral adrenal tumors. *Endocrinol Diabetes Metab Case Rep* (2015) 2015:15–0029. doi: 10.1530/EDM-15-0029

34. Lee JH, Kim E, Chon S. Hypokalemia-induced rhabdomyolysis by primary aldosteronism coexistent with sporadic inclusion body myositis. *Ann Rehabil Med* (2015) 39(5):826–32. doi: 10.5535/arm.2015.39.5.826

35. Martí;nez-Ruiz EE, Paz-Manifacio S, Sánchez-Dí;az S, Cruz E. Rhabdomyolysis due to hypokalemia: an atypical manifestation of Conn's syndrome. *Med Interna Mex.* (2017) 33:826–34. doi: 10.24245/mim.v33i6.1417

36. Dyrmishi B, Olldashi T, Rista E, Fureraj T, Ylli D, Ylli A. Severe Hypokalemia Induced Rhabdomyolysis By Primary Hyperaldosteronism Coexistent With Recurrent Bilateral Renal Calculi. *Acta Endocrinol Buchar Rom 2005.* (2017) 13(2):228–31. doi: 10.4183/aeb.2017.228

37. Pecnik P, Müller P, Vrabel S, Windpessl M. Two cases of hypokalaemic rhabdomyolysis: same but different(2018) (Accessed 2023 Apr 10).

38. Wang SC, Chiu KY. Primary hyperaldosteronism manifested by rhabdomyolysis. *Open J Clin Med Case Rep* (2019) 5(3):1519.

39. Skaletsky K, Kosmacheva E, Kizhvatova N, Porhanov V. Primary aldosteronism complicated by hypokalemic rhabdomyolysis (2019) (Accessed 2023 May 29).

40. Sirkeci O, Sirkeci EE, Kucukciloglu Y. Severe hypokalemia and rhabdomyolysis caused by conn syndrome. *Clin Ter.* (2021) 172(5):407–9. doi: 10.32322/jhsm.844053

41. Maung AC, Kerwen AK, Ching LP. Hypokalaemic rhabdomyolysis as initial presentation of primary aldosteronism. *J R Coll Physicians Edinb.* (2021) 51(2):149–52. doi: 10.4997/jrcpe.2021.211

42. Bosch X, Poch E, Grau JM. Rhabdomyolysis and acute kidney injury. *N Engl J Med* (2009) 361(1):62–72. doi: 10.1056/NEJMra0801327

43. Burrello J, Amongero M, Buffolo F, Sconfienza E, Forestiero V, Burrello A, et al. Development of a prediction score to avoid confirmatory testing in patients with suspected primary aldosteronism. *J Clin Endocrinol Metab* (2021) 106(4):e1708–16. doi: 10.1210/clinem/dgaa974

44. Maung AC, Kerwen AK, Ching LP. Hypokalaemic rhabdomyolysis as initial presentation of primary aldosteronism (Accessed 2023 Apr 10).

45. Scharman EJ, Troutman WG. Prevention of kidney injury following rhabdomyolysis: a systematic review. *Ann Pharmacother.* (2013) 47(1):90–105. doi: 10.1345/aph.1R215

46. Patel KA, Calomeni EP, Nadasdy T, Zynger DL. Adrenal gland inclusions in patients treated with aldosterone antagonists (Spironolactone/Eplerenone): incidence, morphology, and ultrastructural findings(2014) (Accessed 2023 Jun 17).

frontiers | Frontiers in Endocrinology

TYPE Original Research
PUBLISHED 16 November 2023
DOI 10.3389/fendo.2023.1265790

OPEN ACCESS

EDITED BY
Marta Araujo-Castro,
Ramón y Cajal University Hospital, Spain

REVIEWED BY
Jingshan Gong,
Jinan University, China
Davide De Sio,
Catholic University of the Sacred Heart, Italy

*CORRESPONDENCE
Yangang Zhang
urozyg@163.com

†These authors have contributed equally to this work

RECEIVED 23 July 2023
ACCEPTED 03 November 2023
PUBLISHED 16 November 2023

CITATION
Sun S, Yao W, Wang Y, Yue P, Guo F, Deng X and Zhang Y (2023) Development and validation of machine-learning models for the difficulty of retroperitoneal laparoscopic adrenalectomy based on radiomics. *Front. Endocrinol.* 14:1265790. doi: 10.3389/fendo.2023.1265790

Development and validation of machine-learning models for the difficulty of retroperitoneal laparoscopic adrenalectomy based on radiomics

Shiwei Sun[1†], Wei Yao[1†], Yue Wang[1†], Peng Yue[1], Fuyu Guo[1], Xiaoqian Deng[1] and Yangang Zhang[1,2,3*]

[1]Third Hospital of Shanxi Medical University, Shanxi Bethune Hospital, Shanxi Academy of Medical Sciences, Tongji Shanxi Hospital, Taiyuan, China, [2]Shanxi Bethune Hospital, Shanxi Academy of Medical Sciences, Tongji Shanxi Hospital, Third Hospital of Shanxi Medical University, Taiyuan, China, [3]Tongji Hospital, Tongji Medical College, Huazhong University of Science and Technology, Wuhan, China

Objective: The aim is to construct machine learning (ML) prediction models for the difficulty of retroperitoneal laparoscopic adrenalectomy (RPLA) based on clinical and radiomic characteristics and to validate the models.

Methods: Patients who had undergone RPLA at Shanxi Bethune Hospital between August 2014 and December 2020 were retrospectively gathered. They were then randomly split into a training set and a validation set, maintaining a ratio of 7:3. The model was constructed using the training set and validated using the validation set. Furthermore, a total of 117 patients were gathered between January and December 2021 to form a prospective set for validation. Radiomic features were extracted by drawing the region of interest using the 3D slicer image computing platform and Python. Key features were selected through LASSO, and the radiomics score (Rad-score) was calculated. Various ML models were constructed by combining Rad-score with clinical characteristics. The optimal models were selected based on precision, recall, the area under the curve, F1 score, calibration curve, receiver operating characteristic curve, and decision curve analysis in the training, validation, and prospective sets. Shapley Additive exPlanations (SHAP) was used to demonstrate the impact of each variable in the respective models.

Results: After comparing the performance of 7 ML models in the training, validation, and prospective sets, it was found that the RF model had a more stable predictive performance, while xGBoost can significantly benefit patients. According to SHAP, the variable importance of the two models is similar, and both can reflect that the Rad-score has the most significant impact. At the same time, clinical characteristics such as hemoglobin, age, body mass index, gender, and diabetes mellitus also influenced the difficulty.

Conclusion: This study constructed ML models for predicting the difficulty of RPLA by combining clinical and radiomic characteristics. The models can help surgeons evaluate surgical difficulty, reduce risks, and improve patient benefits.

KEYWORDS

adrenal tumor, laparoscopy, retroperitoneal space, machine learning, radiomics, random forest, extreme gradient boosting

1 Introduction

Adrenal tumors (ATs) are a rare type of tumor that usually occurs in the cortex or medulla of the adrenal gland (1). Depending on their type and size, these tumors can be benign or malignant (2). ATs can cause many symptoms, including high blood pressure, palpitations, headaches, insomnia, anxiety, and obesity (3). In some cases, these symptoms may be mistaken for symptoms of other diseases, so further testing is needed to determine the diagnosis (4–6).

Treatment for AT includes surgery, radiation therapy, and chemotherapy. Surgery is the most common treatment method and can altogether remove the tumor (7). The gold standard treatment for AT is laparoscopic surgery, which can be divided into two main approaches: transperitoneal laparoscopic adrenalectomy (TPLA) and retroperitoneal laparoscopic adrenalectomy (RPLA) (8). The RPLA involves entering the retroperitoneal cavity through laparoscopic surgery, avoiding interference with abdominal organs, and reducing surgical trauma and recovery time. Compared with traditional open surgery, this technique has fewer complications and faster recovery (6, 9, 10).

In the field of medicine, machine learning (ML) has wide-ranging applications (3). For example, ML can be used for medical image recognition to help doctors diagnose diseases. It can also be used to predict the health status of patients, assisting doctors to develop better treatment plans. In addition, ML can be used for drug development and clinical trials to speed up the development and launch of new drugs (11). For example, a study has used ML to differentiate between adrenal pheochromocytoma and adrenocortical adenoma (12).

Radiomics is an emerging field of medicine that combines computer science, mathematics, and medical imaging to understand better and diagnose diseases (13, 14). Radiomics analyzes large amounts of medical imaging data to extract useful information, helping doctors make more accurate diagnoses and treatment decisions (15).

This study aimed to collect data retrospectively from patients with AT who underwent RPLA at Shanxi Bethune Hospital from August 2014 to December 2020. The study utilized ML to analyze their clinical and radiomics features and develop a predictive model for the difficulty of RPLA. The goal was to improve preoperative preparation, reduce surgical risks, and enhance patient benefits.

2 Method

2.1 General information

We retrospectively collected data from patients with AT treated at Shanxi Bethune Hospital between August 2014 and December 2020. A model was established using this data and prospectively validated with AT patients treated from January 2021 to December 2021. Inclusion criteria: 1) abdominal Computed Tomography (CT) examination confirming the presence of an AT within 15 days before surgery, 2) preoperative routine laboratory tests to determine the hormonal activity of AT, and 3) treatment of AT with laparoscopic surgery. Exclusion criteria: 1) patients who did not undergo surgery, 2) patients who underwent multiple surgeries concurrently, 3) patients treated for AT with other surgical methods, and 4) patients with incomplete preoperative radiological examination. A total of 396 patients were included in the study, and an additional 117 patients were collected for prospective validation (Figure 1A). All surgical procedures are performed by a cohesive team within the same department at a single center, led by an expert surgeon with 35 years of experience.

2.2 Research method

Referring to previous studies (9, 10, 16–20) and combining practical experience, we defined cases with serious surgical difficulty if any of the following conditions were met: 1) operation time ≥ P_{75}

Abbreviations: AT, Adrenal tumor; ANOVA, Analysis of variance; AUC, Area under the curve; BMI, Body Mass Index; CART, Classification and Regression Trees; CT, Computed Tomography; DCA, Decision curve analysis; DICOM, Digital Imaging and Communications in Medicine; xGBoost, EXtreme Gradient Boosting; GLCM, Gray Level Co-occurrence Matrix; GLDM, Gray Level Dependence Matrix; GLRLM, Gray Level Run Length Matrix; GLSZM, Gray Level Size Zone Matrix; Hb, Hemoglobin; IDI, Integrated Discrimination Improvement; ICC, Intraclass correlation coefficient; KNN, K-Nearest Neighbors; LASSO, Least Absolute Shrinkage and Selection Operator; ML, Machine learning; NB, Naive Bayes; NGTDM, Neighboring Gray Tone Difference Matrix; NRI, Net Classification Index; Rad-score, Radiomics scores; RF, Random Forest; ROC, Receiver operating characteristic; ROI, Region of interest; RPLA, Retroperitoneal laparoscopic adrenalectomy; SHAP, Shapley Additive exPlanations; SVM, Support Vector Machine; TPLA, Transperitoneal laparoscopic adrenalectomy

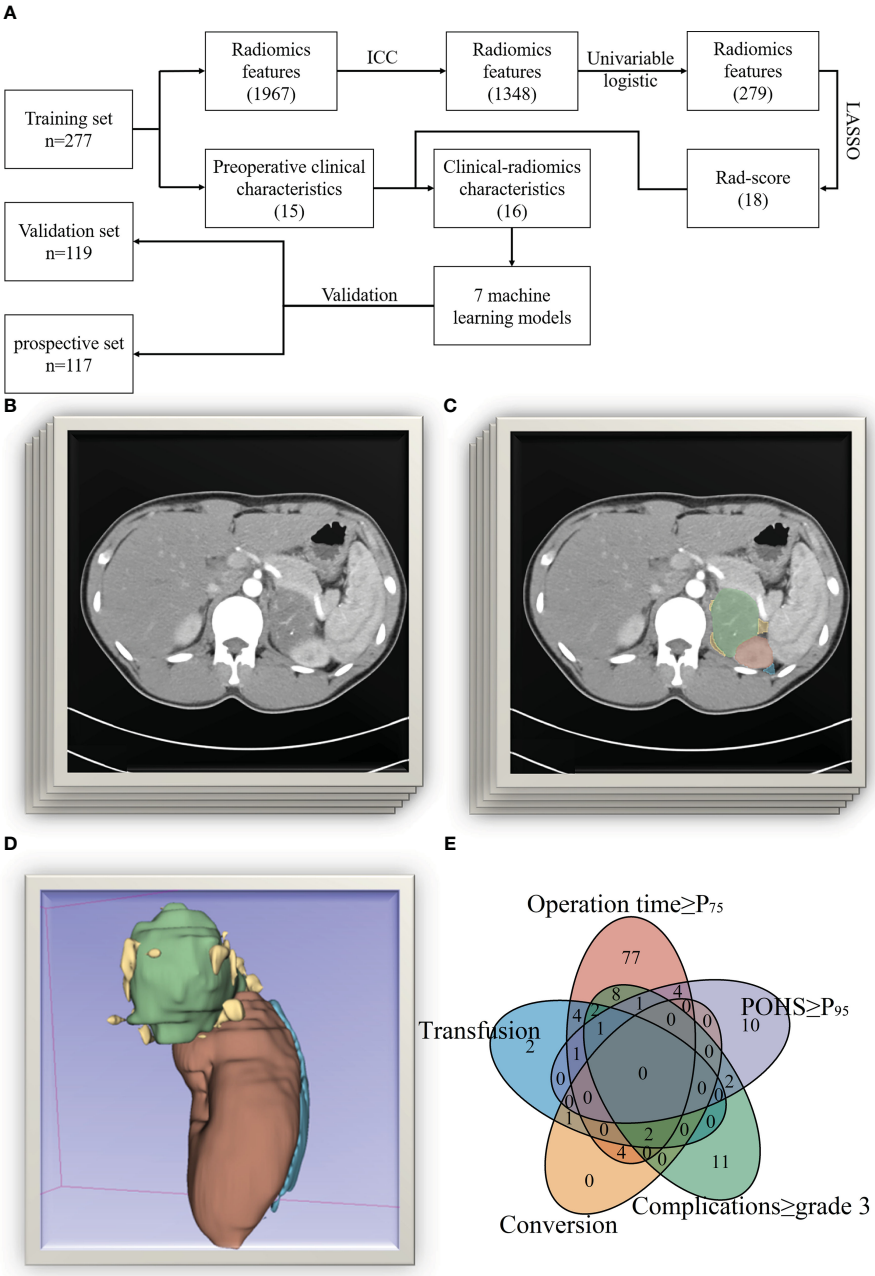

FIGURE 1
The process of this study. (**A** Flowchart of this study; **(B)** Original CT images; **(C)** Drawing of regions of interest [ROIs]; **(D)** 3D reconstruction of the ROIs; **(E)** Venn plot of the reasons for the difficulty of surgery).

(150 min), 2) intraoperative injury to organs or vessels requiring blood transfusion, 3) conversion from minimally invasive to open surgery, 4) postoperative complications of Clavien-Dindo classification (21) greater than or equal to grade 3, 5) Postoperative hospital stay ≥ P_{95} (15 days).

The Siemens Somatom Definition Flash or Force dual-source CT scanner (manufactured by Siemens AG in Munich, Germany) was utilized for the purpose of scanning and reconstructing thin-slice images. DICOM format was used to export the images. Using the 3D Slicer image computing platform (version 5. 0. 2), two radiology-trained urologists independently identified the region of interest (ROI) in arterial-enhanced images. Python 3. 7. 1 (Python Software Foundation) was utilized to extract radiomics features from the images (Figures 1B–D). The included image types are Original, Wavelet, Laplacian of Gaussian, Square, Square Root, Logarithm, Exponential, Gradient, Local Binary Pattern 2D, and Local Binary Pattern 3D. The feature types consisted of First Order Features, Shape Features (3D), Shape Features (2D), Gray Level Co-occurrence Matrix (GLCM) Features, Gray Level Size Zone Matrix (GLSZM) Features, Gray Level Run Length Matrix (GLRLM) Features, Neighboring Gray Tone Difference Matrix (NGTDM) Features, Gray Level Dependence Matrix (GLDM) Feature. A total

of 1967 radiomics features were extracted (Figure 2). Data on patients' clinical conditions and treatment were obtained from the computerized physician order entry and medical record management system (Winning Health Technology Group Co., Ltd., Shanghai, China).

Patients were randomly divided into a training set and a validation set at a ratio of 7:3. The training set was used for model construction, and the validation set was used for model validation.

2.3 Statistical methods

Data were further analyzed using R 4. 2. 3 (Vienna Statistical Computing Foundation, Austria). All continuous variables were non-normally distributed and were presented as median [interquartile range]; categorical variables were presented as frequency and percentage (%). Analysis of variance (ANOVA) was used to compare differences between sets in the training set, validation set, and prospective set. The consistency of the regions of interest (ROIs) drawn by the two urologists was evaluated using the intraclass correlation coefficient (ICC), excluding features with a correlation below 0. 75. Radiomics features were subjected to univariable logistic regression analysis using the "glmnet" package. Factors with a P-value greater than 0. 05 were considered unrelated and subsequently excluded. Key features were selected using the Least Absolute Shrinkage and Selection Operator (LASSO), and the radiomics score (Rad-score) was calculated based on the results. Using the "mlr3" package, seven ML models were developed by combining the Rad-score with clinical characteristics. These models included Classification and Regression Trees (CART), K-Nearest Neighbors (KNN), LASSO, Naive Bayes (NB), Random Forest (RF), Support Vector Machine (SVM), and Extreme Gradient Boosting (xGBoost). The optimal models were selected based on precision, recall, area under the curve (AUC), F1 score, calibration curve, Receiver Operating Characteristic (ROC) curve, and decision curve analysis (DCA) in the training set, validation set, and prospective set. Shapley Additive exPlanations (SHAP) value demonstrated the impact of each variable in the respective model (22).

3 Results

3.1 General information

A total of 396 patients were included in the study. Patients were randomly divided into a training set and a validation set at a ratio of 7:3. Baseline patient characteristics are shown in Table 1. A total of 130 patients were considered to have high surgical difficulty due to meeting one or more criteria, with specific reasons shown in Figure 1E. An additional 117 patients were collected and regarded as a prospective set. ANOVA showed no statistically significant differences in baseline characteristics between sets.

3.2 Radiomics feature selection

Consistency was assessed using ICC, excluding 619 radiomics features with consistency lower than 0.75 to eliminate the interference of human factors on the model. Univariable logistic analysis was performed, excluding 1069 variables with $P > 0.05$. The remaining 279 features underwent dimensionality reduction using LASSO and ten-fold cross-validation. As the logarithm of the harmonic parameter (λ) changed on the horizontal axis, the AUC on the vertical axis also changed. The corresponding number of

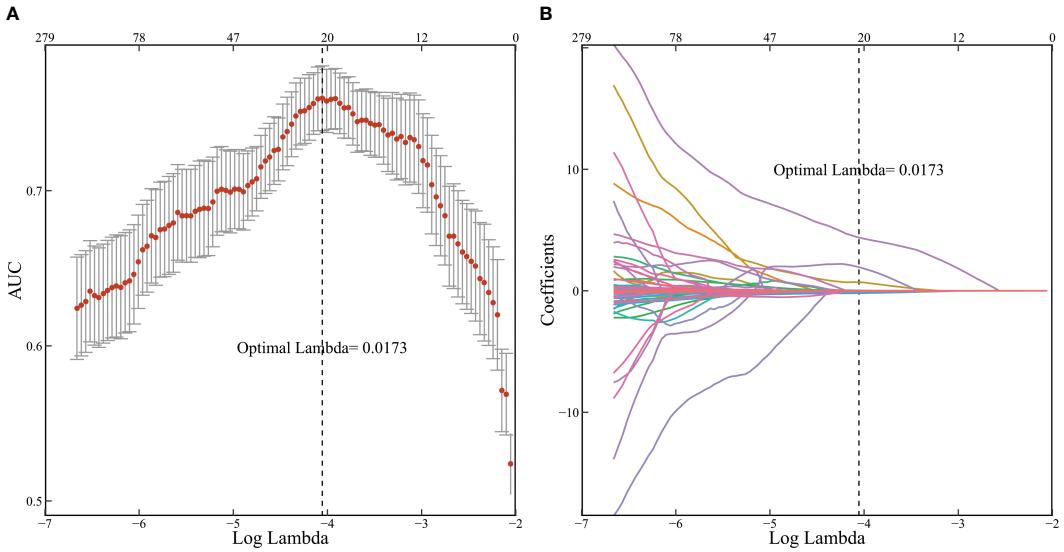

FIGURE 2
Radiomic features selected by LASSO. (**A** 10-fold cross-validation corresponding AUC results; **(B)** 279 feature screening adjoint coefficient changes).

10.3389/fendo.2023.1265790

TABLE 1 Baseline clinical and radiomics characteristics of patients.

Characteristics	Training set	Validation set	Prospective set	F	P
Radiomics characteristics					
Rad score	8.87[8.76,9.00]	8.87[8.74,8.97]	8.87[8.77,8.97]	1.030	0.358
Clinical characteristics					
Preoperative					
Gender				0.732	0.482
Male	125(45.1)	53(44.5)	60(51.3)		
Female	152(54.9)	66(55.5)	57(48.7)		
Age (year)	50.00[40.00,59.00]	51.00[42.00,58.00]	51.00[39.00,58.00]	0.047	0.954
BMI (kg/m^2)	24.72[22.68,27.51]	24.57[23.10,27.36]	25.95[23.44,28.32]	2.430	0.089
Side				1.130	0.324
Left	161(58.1)	77(64.7)	65(55.6)		
Right	116(41.9)	42(35.3)	52(44.4)		
Hypertension				0.417	0.660
No	58(20.9)	27(22.7)	21(17.9)		
Yes	219(79.1)	92(77.3)	96(82.1)		
Diabetes mellitus				1.446	0.236
No	229(82.7)	92(77.3)	89(76.1)		
Yes	48(17.3)	27(22.7)	28(23.9)		
Scoliosis				1.108	0.331
No	264(95.3)	113(95.0)	115(98.3)		
Yes	13(4.7)	6(5.0)	2(1.7)		
Coronary disease				1.673	0.189
No	249(89.9)	107(89.9)	98(83.8)		
Yes	28(10.1)	12(10.1)	19(16.2)		
Cerebral infarction				0.965	0.382
No	254(91.7)	104(87.4)	107(91.5)		
Yes	23(8.3)	15(12.6)	10(8.5)		
Hyperlipidemia				0.393	0.675
No	245(88.4)	108(90.8)	102(87.2)		
Yes	32(11.6)	11(9.2)	15(12.8)		
History of malignancy				2.129	0.120
No	270(97.5)	113(95.0)	109(93.2)		
Yes	7(2.5)	6(5.0)	8(6.8)		
History of operation				0.436	0.647
No	202(72.9)	84(70.6)	80(68.4)		
Yes	75(27.1)	35(29.4)	37(31.6)		
Infectious disease				0.262	0.769
No	272(98.2)	118(99.2)	115(98.3)		
Yes	5(1.8)	1(0.8)	2(1.7)		

(Continued)

TABLE 1 Continued

Characteristics	Training set	Validation set	Prospective set	F	P
Radiomics characteristics					
Rad score	8.87[8.76,9.00]	8.87[8.74,8.97]	8.87[8.77,8.97]	1.030	0.358
Previous antiplatelet use				2.567	0.078
No	268(96.8)	116(97.5)	108(92.3)		
Yes	9(3.2)	3(2.5)	9(7.7)		
Hb (g/L)	137.0[126.0,145.0]	138.0[127.5,147.0]	137.0[127.0,146.0]	0.065	0.937
Intraoperative and postoperative					
Range				0.475	0.622
Partial	253(91.3)	105(88.2)	105(89.7)		
Radical	24(8.7)	14(11.8)	12(10.3)		
Operation time (min)	110.0[90.0,150.0]	110.0[90.0,149.0]	98.0[76.0,130.0]	4.130	0.017
Blood loss (ml)	20.0[0.0,50.0]	20.0[0.0,50.0]	15.0[0.0,25.0]	0.264	0.768
POHS	8.0[6.0,9.0]	7.0[6.5,9.0]	6.0[2.0,7.0]	15.966	<0.001
Conversion				0.558	0.573
No	273(98.6)	116(97.5)	116(99.1)		
Yes	4(1.4)	3(2.5)	1(0.9)		
Transfusion				0.078	0.925
No	268(96.8)	115(96.6)	114(97.4)		
Yes	9(3.2)	4(3.4)	3(2.6)		
Complications				0.122	0.885
None	248(89.5)	107(89.9)	105(89.7)		
1	9(3.2)	2(1.7)	4(3.4)		
2	2(0.7)	1(0.8)	0(0.0)		
3a	1(0.4)	0(0.0)	3(2.6)		
3b	0(0.0)	1(0.8)	0(0.0)		
4	17(6.1)	8(6.7)	5(4.3)		
Pathology				1.330	0.265
NFAT	107(38.6)	51(42.9)	38(32.5)		
Aldosteronoma	79(28.5)	33(27.7)	43(36.8)		
Cushing's syndrome	25(9.0)	16(13.4)	17(14.5)		
Paraganglioma	26(9.4)	7(5.9)	7(6.0)		
Myelolipoma	10(3.6)	5(4.2)	4(3.4)		
Cyst	13(4.7)	3(2.5)	3(2.6)		
Malignant tumor	5(1.8)	1(0.8)	2(1.7)		
Ganglioneuroma	2(0.7)	2(1.7)	2(1.7)		
Others	10(3.6)	1(0.8)	1(0.9)		

BMI, body mass index; NFAT, non-function adrenal tumor; Others(pathology) include eosinophil tumor, teratoma, schwannoma, hematoma, tuberculoma, foreign body granuloma, retroperitoneal bronchial cyst, hemangioma.

selected variables is shown in Figure 2A. A risk factor classifier was constructed using LASSO (Figure 2B), with 18 features selected (Table 2). The optimal λ value was 0.0173, with a logarithm of -4.055.

Based on the LASSO results (Table 3), Rad-score was calculated. The specific calculation formula is provided in the Supplementary Data.

3.3 Construction of clinical-radiomics machine learning models

The Rad-score calculated above was combined with clinical characteristics to construct CART, KNN, LASSO, NB, RF, SVM, and xGBoost models (Table 2). Additionally, we constructed a clinical model for comparison using stepwise logistic regression based on the clinical characteristics of the patients. All models demonstrated high predictive ability in the training set, with acceptable consistency in the validation and prospective sets (Figures 3A, B).

A comprehensive evaluation of precision, F1 score, ROC curve, and AUC values in the training, validation, and prospective sets revealed that the RF model had a more stable predictive performance, followed by xGBoost and LASSO (Figures 3C–E). According to DCA, it is evident that xGBoost can significantly benefit patients (Figure 3F).

The SHAP value and SHAP plot were used to display the importance of each variable in the RF and xGBoost models. According to the SHAP, the variable importance of the two models is similar, and both can reflect that the Rad-score has the most significant impact. At the same time, other clinical characteristics such as Hemoglobin (Hb), age, Body Mass Index (BMI), gender, and diabetes mellitus also influenced the difficulty (Figure 4).

4 Discussion

AT has become a hot topic in the medical field, and surgery is the primary treatment method. TPLA and RPLA were proposed in

TABLE 2 Comparison of machine learning model performance.

Model	Set	AUC	Sensitivity	Specificity	Precision	F1-score
CART	Training	0.866	0.667	0.901	0.780	0.719
CART	Validation	0.421	0.235	0.776	0.296	0.262
CART	Prospective	0.356	0.393	0.809	0.393	0.393
KNN	Training	0.983	0.698	0.978	0.944	0.802
KNN	Validation	0.579	0.147	0.835	0.263	0.189
KNN	Prospective	0.588	0.286	0.798	0.308	0.296
LASSO	Training	0.824	0.417	0.956	0.833	0.556
LASSO	Validation	0.631	0.294	0.918	0.588	0.392
LASSO	Prospective	0.720	0.321	0.921	0.562	0.409
NB	Training	0.779	0.458	0.834	0.595	0.518
NB	Validation	0.696	0.441	0.776	0.441	0.441
NB	Prospective	0.662	0.536	0.730	0.385	0.448
RF	Training	0.994	0.885	0.994	0.988	0.934
RF	Validation	0.681	0.353	0.835	0.462	0.400
RF	Prospective	0.724	0.536	0.820	0.484	0.508
SVM	Training	0.917	0.688	0.950	0.880	0.772
SVM	Validation	0.677	0.294	0.847	0.435	0.351
SVM	Prospective	0.617	0.286	0.775	0.286	0.286
xGBoost	Training	0.914	0.750	0.917	0.828	0.787
xGBoost	Validation	0.615	0.353	0.706	0.324	0.338
xGBoost	Prospective	0.710	0.500	0.764	0.400	0.444
Clinical	Training	0.660	0.719	0.514	0.439	0.545
Clinical	Validation	0.621	0.735	0.431	0.357	0.481
Clinical	Prospective	0.658	0.821	0.461	0.324	0.465

TABLE 3 Radiomic features selected by LASSO.

Image types	Feather types	Feathers	Coefficients
Logarithm	GLCM	Imc1	-0.197
Square	GLSZM	SizeZoneNonUniformityNormalized	-0.134
Wavelet.LLH	Firstorder	Mean	-0.060
Wavelet.LLL	Firstorder	Kurtosis	-0.049
Original	GLSZM	SizeZoneNonUniformityNormalized	-0.034
Log.sigma.4.mm.3D	Firstorder	90Percentile	-0.012
Log.sigma.5.mm.3D	Firstorder	90Percentile	-0.001
Squareroot	GLSZM	LargeAreaEmphasis	$9.721*10^{-11}$
Wavelet.LLL	GLDM	DependenceEntropy	0.001
Original	Shape	Maximum3DDiameter	0.003
Wavelet.HHL	GLRLM	LongRunLowGrayLevelEmphasis	0.006
Wavelet.HLL	GLRLM	LongRunLowGrayLevelEmphasis	0.011
Logarithm	Firstorder	InterquartileRange	0.014
Log.sigma.5.mm.3D	Firstorder	Kurtosis	0.022
Log.sigma.4.mm.3D	GLDM	LowGrayLevelEmphasis	0.031
Lbp.3d.k	GLDM	DependenceNonUniformityNormalized	0.714
Wavelet.HLH	GLCM	DifferenceEntropy	1.949
Wavelet.HLL	GLCM	Imc1	4.384

1992 (8, 23), respectively, and have continuously improved. The advantage of RPLA is that it results in less surgical trauma and bleeding, faster recovery, and fewer complications. Moreover, it is also suitable for some cases that traditional surgery finds challenging, such as obesity and complex AT. There are some relatively objective analysis systems for the surgical difficulty of TPLA, while there is less analysis on RPLA (10, 17).

This study retrospectively analyzed 396 patients who underwent RPLA for AT. The LASSO analysis of radiomics features was used to calculate the Rad-score. By combining the Rad-score with preoperative clinical characteristics, ML models such as CART, KNN, LASSO, NB, RF, SVM, and xGBoost were constructed and compared. It was found that RF had a more stable prediction accuracy, while xGBoost could bring more significant benefits to patients. The ML model suggested that in addition to the most influential Rad-score, the clinical characteristics such as Hb, age, BMI, gender, and diabetes mellitus also greatly influenced surgical difficulty. Through the validation of the validation set and prospective set, it was found that the ML models had high predictive ability. Through the comprehensive comparison of different models, it was found that the RF model exhibits the best prediction performance, thus making it our recommended model. Furthermore, in comparison to clinical models in previous study (16), our RF model exhibited superiority as evidenced by 2000 Bootstrap tests ($D = 7.155$, $P < 0.001$). The discrimination power of models can be effectively compared using two measures: the Net Classification Index (NRI) and the Integrated Discrimination Improvement (IDI). In comparison to previous studies, the RF model in this study demonstrated an NRI of 0.308 (95% CI: 0.194-0.422, $p < 0.001$) and an IDI of 0.165 (95% CI: 0.119-0.210, $p < 0.001$).

The Rad-score calculated based on LASSO significantly impacts the surgical difficulty of RPLA. When performing univariate logistic regression, 279 features were statistically significant. After LASSO, 18 variables were retained and used to construct the Rad-score. The final retained variables included "Shape Features" like "Maximum3DDiameter". Moreover, many studies have generally confirmed that the maximum diameter of the tumor is an essential factor affecting the difficulty of removing AT (9, 10, 16–20). In addition, "First Order Features", which are linearly correlated with the CT value of the tumor, such as "90Percentile" were also included. Malignant and benign AT have different degrees of enhancement during arterial enhancement, which increases the risk of bleeding during surgery (18, 24, 25). It may also be because lipid-rich AT has lower CT values and requires more attention during surgery to prevent breaking the capsule, which prolongs the operation time (9, 16, 20). "DifferenceEntropy" in "GLCM Features" measures the randomness or complexity of differences between pixel intensity values. It was included because malignant tumors, such as metastases, exhibit more randomness or complexity between pixel intensity values, while their removal is more challenging than benign tumors (18).

Some clinical characteristics of patients also affect the difficulty of RPLA. Patients with diabetes mellitus are more likely to have perirenal fat adhesions, which affect surgical difficulty (26). Studies by Chen (17) and Takeda (27) have also shown that diabetes mellitus

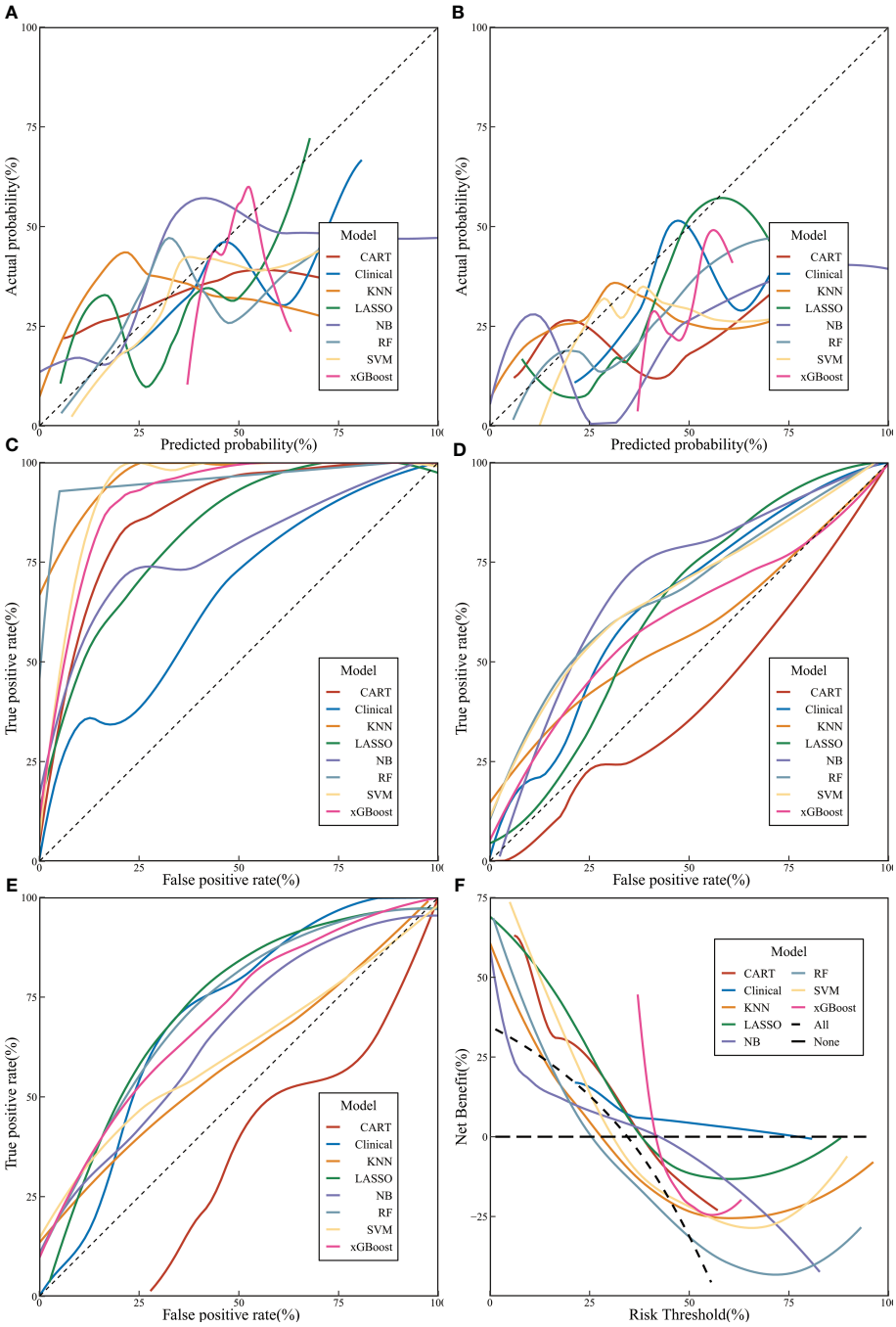

FIGURE 3
The performance of machine learning models. (**A** Calibration curve of validation set; **(B)** Calibration curve of prospective set; **(C)** Receiver operating characteristic [ROC] curves of machine learning models in training set; **(D)** ROC curves of machine learning models in validation set; **(E)** ROC curves of machine learning models in prospective set; **(F)** decision curve analysis curves of machine learning models).

significantly affects it. Some studies also suggest that a history of hypertension and coronary heart disease affects surgical difficulty (28, 29). BMI is used to assess the degree of obesity and also affects it. However, it mainly reflects the overall body fat composition, while the distribution of visceral fat, especially perirenal fat, may differ (9, 16). Therefore, there is still controversy over BMI prediction of surgical difficulty. Some studies believe that measuring visceral fat would be more accurate (10, 25, 29).

Hb reflects the patient's blood reserve and blood oxygen reserve situation (30). If it is too low, it will affect the surgery. Age affects almost all tumor surgeries and prognoses because older patients often have poorer nutrition and tolerance. Moreover, diseases tend to be more malignant in older patients (31, 32). In addition, some researchers believe that males may have more dangerous lifestyles (such as smoking), and there are differences in hormone levels between men and women, which may lead to poorer physical

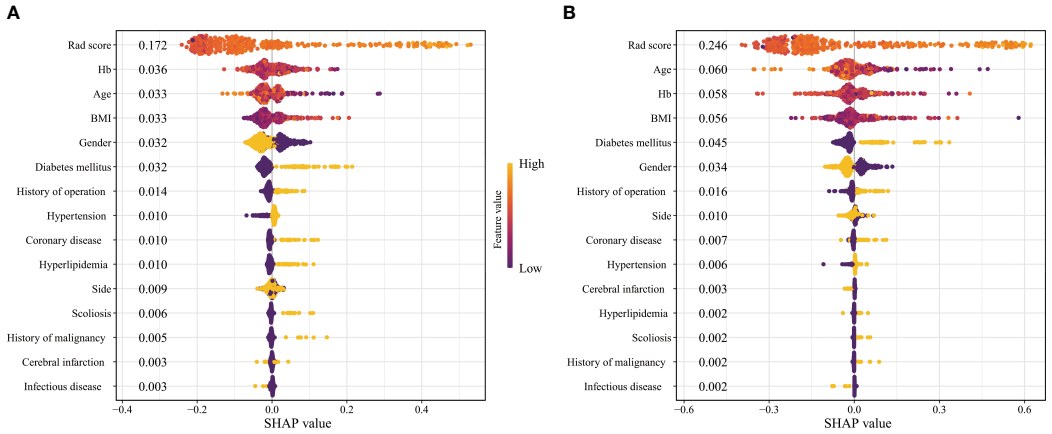

FIGURE 4
The SHAP plots of machine learning models. (**A** Random Forest; **(B)** Extreme Gradient Boosting).

conditions and more incredible surgical difficulty in male patients (33, 34).

This study established ML models for predicting the difficulty of RPLA based on preoperative radiomics and clinical characteristics. It was validated internally and prospectively to prove that the ML models can significantly improve patients' net benefit rate.

There needs to be more accurate prediction models for the difficulty of RPLA. The innovation of this study lies in combining ML with radiomics to analyze the risk factors for the difficulty of RPLA and establish prediction models for it, then conduct internal validation and prospective validation to make the model more meaningful. Moreover, this study is currently one of the largest cohorts using radiomics to predict the difficulty of RPLA.

The prospects of this study include: external validation to confirm its stability and accuracy further; using radiomics to analyze the tumor's surrounding environment while analyzing AT and optimizing the model through more ML algorithms. Some studies have proposed that magnetic resonance imaging has multiple weighted sequences, which may have better effects when applied to radiomics than CT. Although the accuracy of this study's models is high, the time cost of drawing ROI is high. If further promotion or clinical transformation is needed, combining deep learning to train artificial intelligence to draw ROI is necessary. Some studies have successfully trained artificial intelligence to draw ROIs for pancreatic duct tumors and predicted lymph node metastasis and prognosis based on them. Its sensitivity and specificity are superior to clinical and radiomics models (35).

In conclusion, Rad-score, Hb, age, BMI, gender, and diabetes mellitus affect RPLA surgical difficulty. The ML prediction model established based on patient clinical characteristics and Rad-score using RF and xGBoost has good predictive performance. Through the above model, surgeons can effectively evaluate the difficulty of RPLA, thereby reducing surgical risks and improving patient benefits.

Data availability statement

The raw data supporting the conclusions of this article will be made available by the authors, without undue reservation.

Ethics statement

The studies involving humans were approved by Ethics Committee of the Shanxi Bethune Hospital. The studies were conducted in accordance with the local legislation and institutional requirements. Written informed consent for participation was not required from the participants or the participants' legal guardians/next of kin in accordance with the national legislation and institutional requirements.

Author contributions

SS: Conceptualization, Data curation, Methodology, Project administration, Validation, Visualization, Writing – original draft. WY: Data curation, Validation, Visualization, Writing – original draft. YW: Data curation, Validation, Writing – original draft. PY: Data curation, Writing – original draft. FG: Data curation, Writing – original draft. XD: Data curation, Writing – original draft. YZ: Conceptualization, Methodology, Project administration, Supervision, Writing – review & editing.

Funding

The author(s) declare that no financial support was received for the research, authorship, and/or publication of this article.

Conflict of interest

The authors declare that the research was conducted in the absence of any commercial or financial relationships that could be construed as a potential conflict of interest.

Publisher's note

All claims expressed in this article are solely those of the authors and do not necessarily represent those of their affiliated organizations, or those of the publisher, the editors and the reviewers. Any product that may be evaluated in this article, or claim that may be made by its manufacturer, is not guaranteed or endorsed by the publisher.

Supplementary material

The Supplementary Material for this article can be found online at: https://www.frontiersin.org/articles/10.3389/fendo.2023.1265790/full#supplementary-material

References

1. Chung R, Garratt J, Remer EM, Navin P, Blake MA, Taffel MT, et al. Adrenal neoplasms: lessons from adrenal multidisciplinary tumor boards. *Radiographics* (2023) 43(7):e220191. doi: 10.1148/rg.220191

2. Martinelli S, Amore F, Canu L, Maggi M, Rapizzi E. Tumour microenvironment in pheochromocytoma and paraganglioma. *Front Endocrinol (Lausanne)* (2023) 14:1137456. doi: 10.3389/fendo.2023.1137456

3. Pamporaki C, Berends AMA, Filippatos A, Prodanov T, Meuter L, Prejbisz A, et al. Prediction of metastatic pheochromocytoma and paraganglioma: A machine learning modelling study using data from a cross-sectional cohort. *Lancet Digit Health* (2023) 5(9):e551–9. doi: 10.1016/S2589-7500(23)00094-8

4. Reincke M, Bancos I, Mulatero P, Scholl UI, Stowasser M, Williams TA. Diagnosis and treatment of primary aldosteronism. *Lancet Diabetes Endocrinol* (2021) 9(12):876–92. doi: 10.1016/S2213-8587(21)00210-2

5. Zelinka T, Eisenhofer G, Pacak K. Pheochromocytoma as a catecholamine producing tumor: implications for clinical practice. *Stress* (2007) 10(2):195–203. doi: 10.1080/10253890701395896

6. Chang Z, Shang J, Yang S, Qin W, Cui H. Co-occurrence of pheochromocytoma and paraganglioma of the organ of zuckerkandl resected simultaneously by laparoscopy: A rare case report and literature review. *J Int Med Res* (2023) 51 (3):3000605231161211. doi: 10.1177/03000605231161211

7. Gaujoux S, Mihai R. joint working group of E, Ensat. European Society of Endocrine Surgeons (Eses) and European Network for the Study of Adrenal Tumours (Ensat) Recommendations for the Surgical Management of Adrenocortical Carcinoma. *Br J Surg* (2017) 104(4):358–76. doi: 10.1002/bjs.10414

8. Gaur DD. Laparoscopic operative retroperitoneoscopy: use of a new device. *J Urol* (1992) 148(4):1137–9. doi: 10.1016/s0022-5347(17)36842-8

9. Rah CS, Kim WW, Lee YM, Chung KW, Koh JM, Lee SH, et al. New predictive factors for prolonged operation time of laparoscopic posterior retroperitoneal adrenalectomy; retrospective cohort study. *Int J Surg* (2021) 94:106113. doi: 10.1016/j.ijsu.2021.106113

10. Alberici L, Paganini AM, Ricci C, Balla A, Ballarini Z, Ortenzi M, et al. Development and validation of a preoperative "Difficulty score" for laparoscopic transabdominal adrenalectomy: A multicenter retrospective study. *Surg Endosc* (2022) 36(5):3549–57. doi: 10.1007/s00464-021-08678-6

11. Robinson-Weiss C, Patel J, Bizzo BC, Glazer DI, Bridge CP, Andriole KP, et al. Machine learning for adrenal gland segmentation and classification of normal and adrenal masses at ct. *Radiology* (2023) 306(2):e220101. doi: 10.1148/radiol.220101

12. Liu H, Guan X, Xu B, Zeng F, Chen C, Yin HL, et al. Computed tomography-based machine learning differentiates adrenal pheochromocytoma from lipid-poor adenoma. *Front Endocrinol (Lausanne)* (2022) 13:833413. doi: 10.3389/fendo.2022.833413

13. Dunn B, Pierobon M, Wei Q. Automated classification of lung cancer subtypes using deep learning and ct-scan based radiomic analysis. *Bioengineering (Basel)* (2023) 10(6):690. doi: 10.3390/bioengineering10060690

14. Yang Z, Gong J, Li J, Sun H, Pan Y, Zhao L. The gap before real clinical application of imaging-based machine-learning and radiomic models for chemoradiation outcome prediction in esophageal cancer: A systematic review and meta-analysis. *Int J Surg* (2023) 109(8):2451–66. doi: 10.1097/JS9.0000000000000441

15. Kong J, Zheng J, Wu J, Wu S, Cai J, Diao X, et al. Development of a radiomics model to diagnose pheochromocytoma preoperatively: A multicenter study with prospective validation. *J Transl Med* (2022) 20(1):31. doi: 10.1186/s12967-022-03233-w

16. Sun S, Wang J, Yang B, Wang Y, Yao W, Yue P, et al. A nomogram for evaluation and analysis of difficulty in retroperitoneal laparoscopic adrenalectomy: A single-center study with prospective validation using lasso-logistic regression. *Front Endocrinol (Lausanne)* (2022) 13:1004112. doi: 10.3389/fendo.2022.1004112

17. Chen Y, Scholten A, Chomsky-Higgins K, Nwaogu I, Gosnell JE, Seib C, et al. Risk factors associated with perioperative complications and prolonged length of stay after laparoscopic adrenalectomy. *JAMA Surg* (2018) 153(11):1036–41. doi: 10.1001/jamasurg.2018.2648

18. Natkaniec M, Dworak J, Pedziwiatr M, Pisarska M, Major P, Dembinski M, et al. Patients criteria determining difficulty of the laparoscopic lateral transperitoneal adrenalectomy. *A Retrospective Cohort Study. Int J Surg* (2017) 43:33–7. doi: 10.1016/j.ijsu.2017.05.032

19. Wang J, Yang B, Sun S, Zhang Y. Perioperative factors influencing the difficulty of retroperitoneal laparoscopic adrenalectomy: A single-center retrospective study. *BMC Urol* (2022) 22(1):22. doi: 10.1186/s12894-022-00976-y

20. Yuan Y, Feng H, Kang Z, Xie Y, Zhang X, Zhang Y. Mayo adhesive probability score is associated with perioperative outcomes in retroperitoneal laparoscopic adrenalectomy. *ANZ J Surg* (2022) 92(12):3273–7. doi: 10.1111/ans.17983

21. Clavien PA, Barkun J, de Oliveira ML, Vauthey JN, Dindo D, Schulick RD, et al. The clavien-dindo classification of surgical complications: five-year experience. *Ann Surg* (2009) 250(2):187–96. doi: 10.1097/SLA.0b013e3181b13ca2

22. Lundberg SM, Erion G, Chen H, DeGrave A, Prutkin JM, Nair B, et al. From local explanations to global understanding with explainable ai for trees. *Nat Mach Intell* (2020) 2(1):56–67. doi: 10.1038/s42256-019-0138-9

23. Gagner M, Lacroix A, Bolte E. Laparoscopic adrenalectomy in cushing's syndrome and pheochromocytoma. *N Engl J Med* (1992) 327(14):1033. doi: 10.1056/NEJM199210013271417

24. Pisarska M, Dworak J, Natkaniec M, Malczak P, Przeczek K, Wysocki M, et al. Risk factors for prolonged hospitalization in patients undergoing laparoscopic adrenalectomy. *Wideochir Inne Tech Maloinwazyjne* (2018) 13(2):141–7. doi: 10.5114/wiitm.2018.73357

25. Vidal O, Saavedra-Perez D, Martos JM, de la Quintana A, Rodriguez JI, Villar J, et al. Risk factors for open conversion of lateral transperitoneal laparoscopic adrenalectomy: retrospective cohort study of the spanish adrenal surgery group (Sasg). *Surg Endosc* (2020) 34(8):3690–5. doi: 10.1007/s00464-019-07264-1

26. Yanishi M, Kinoshita H, Koito Y, Taniguchi H, Mishima T, Sugi M, et al. Adherent perinephric fat is a surgical risk factor in laparoscopic single-site donor nephrectomy: analysis using mayo adhesive probability score. *Transplant Proc* (2020) 52(1):84–8. doi: 10.1016/j.transproceed.2019.11.027

27. Takeda T, Hakozaki K, Yanai Y, Masuda T, Yasumizu Y, Tanaka N, et al. Risk factors for haemodynamic instability and its prolongation during laparoscopic adrenalectomy for pheochromocytoma. *Clin Endocrinol (Oxf)* (2021) 95(5):716–26. doi: 10.1111/cen.14557

28. Brunaud L, Nguyen-Thi PL, Mirallie E, Raffaelli M, Vriens M, Theveniaud PE, et al. Predictive factors for postoperative morbidity after laparoscopic adrenalectomy for pheochromocytoma: A multicenter retrospective analysis in 225 patients. *Surg Endosc* (2016) 30(3):1051–9. doi: 10.1007/s00464-015-4294-7

29. BiLiGe W, Wang C, Bao J, Yu D, Min A, Hong Z, et al. Predicting factors related with uncured hypertension after retroperitoneal laparoscopic adrenalectomy for unilateral primary aldosteronism. *Med (Baltimore)* (2019) 98(30):e16611. doi: 10.1097/MD.0000000000016611

30. Premont RT, Reynolds JD, Zhang R, Stamler JS. Role of nitric oxide carried by hemoglobin in cardiovascular physiology: developments on a three-gas respiratory cycle. *Circ Res* (2020) 126(1):129–58. doi: 10.1161/CIRCRESAHA.119.315626

31. Miller KD, Fidler-Benaoudia M, Keegan TH, Hipp HS, Jemal A, Siegel RL. Cancer statistics for adolescents and young adults, 2020. *CA Cancer J Clin* (2020) 70 (6):443–59. doi: 10.3322/caac.21637

32. Lin L, Li Z, Yan L, Liu Y, Yang H, Li H. Global, regional, and national cancer incidence and death for 29 cancer groups in 2019 and trends analysis of the global cancer burden, 1990-2019. *J Hematol Oncol* (2021) 14(1):197. doi: 10.1186/s13045-021-01213-z

33. Costa AR, Lanca de Oliveira M, Cruz I, Goncalves I, Cascalheira JF, Santos CRA. The sex bias of cancer. *Trends Endocrinol Metab* (2020) 31(10):785–99. doi: 10.1016/j.tem.2020.07.002

34. Haupt S, Caramia F, Klein SL, Rubin JB, Haupt Y. Sex disparities matter in cancer development and therapy. *Nat Rev Cancer* (2021) 21(6):393–407. doi: 10.1038/s41568-021-00348-y

35. Chu LC, Fishman EK. Artificial intelligence outperforms radiologists for pancreatic cancer lymph node metastasis prediction at ct. *Radiology* (2023) 306 (1):170–1. doi: 10.1148/radiol.222012

frontiers | Frontiers in Endocrinology

TYPE Systematic Review
PUBLISHED 28 November 2023
DOI 10.3389/fendo.2023.1278007

OPEN ACCESS

EDITED BY
Marta Araujo-Castro,
Ramón y Cajal University Hospital, Spain

REVIEWED BY
Leonardo Rossi,
University of Pisa, Italy
Ioannis Koutelidakis,
Aristotle University of Thessaloniki, Greece
Simone Sforza,
University of Florence, Italy

*CORRESPONDENCE
Bo Liao
boyedlover@sina.com

†These have authors contributed equally to this work

RECEIVED 15 August 2023
ACCEPTED 06 November 2023
PUBLISHED 28 November 2023

CITATION
Li Y-g, Chen X-b, Wang C-m, Yu X-d, Deng X-z and Liao B (2023) Robotic posterior retroperitoneal adrenalectomy versus laparoscopic posterior retroperitoneal adrenalectomy: outcomes from a pooled analysis. *Front. Endocrinol.* 14:1278007. doi: 10.3389/fendo.2023.1278007

Robotic posterior retroperitoneal adrenalectomy versus laparoscopic posterior retroperitoneal adrenalectomy: outcomes from a pooled analysis

Yu-gen Li[1†], Xiao-bin Chen[1†], Chun-mei Wang[2], Xiao-dong Yu[1], Xian-zhong Deng[1] and Bo Liao[1*]

[1]Department of Urology, Affiliated Hospital of North Sichuan Medical College, Nan chong, China, [2]Physical Examination Center, Affiliated Hospital of North Sichuan Medical College, Nan chong, China

Background: The comparative advantages of robotic posterior retroperitoneal adrenalectomy (RPRA) over laparoscopic posterior retroperitoneal adrenalectomy (LPRA) remain a topic of ongoing debate within the medical community. This systematic literature review and meta-analysis aim to assess the safety and efficacy of RPRA compared to LPRA, with the ultimate goal of determining which procedure yields superior clinical outcomes.

Methods: A systematic search was conducted on databases including PubMed, Embase, Web of Science, and the Cochrane Library database to identify relevant studies, encompassing both randomized controlled trials (RCTs) and non-RCTs, that compare the outcomes of RPRA and LPRA. The primary focus of this study was to evaluate perioperative surgical outcomes and complications. Review Manager 5.4 was used for this analysis. The study was registered with PROSPERO (ID: CRD42023453816).

Results: A total of seven non-RCTs were identified and included in this study, encompassing a cohort of 675 patients. The findings indicate that RPRA exhibited superior performance compared to LPRA in terms of hospital stay (weighted mean difference [WMD] -0.78 days, 95% confidence interval [CI] -1.46 to -0.10; p = 0.02). However, there were no statistically significant differences observed between the two techniques in terms of operative time, blood loss, transfusion rates, conversion rates, major complications, and overall complications.

Conclusion: RPRA is associated with a significantly shorter hospital stay compared to LPRA, while demonstrating comparable operative time, blood loss, conversion rate, and complication rate. However, it is important to note that further research of a more comprehensive and rigorous nature is necessary to validate these findings.

Systematic review registration: https://www.crd.york.ac.uk/prospero/display_record.php?RecordID=453816, identifier CRD42023453816.

KEYWORDS

robotic, laparoscopic, posterior, adrenalectomy, meta-analysis

1 Introduction

Laparoscopic transperitoneal adrenalectomy (LTA) was first elucidated by Gagner et al. in 1992 (1). Subsequent empirical evidence has unequivocally unveiled a spectrum of advantages inherently associated with LTA, transcending those of conventional open adrenalectomy. These encompass a notable reduction in estimated blood loss, abbreviated hospitalization periods, alleviated postoperative discomfort, and a diminished incidence of complications (2, 3). In the year 1995, Mercan et al. introduced the laparoscopic posterior retroperitoneal adrenalectomy (LPRA), an innovative surgical paradigm that has since been methodically established as both a practicable and secure operative approach (4–6). From an anatomical vantage point, LPRA presents a more direct conduit to reach the adrenal gland, obviating the necessity for the mobilization of contiguous structures. This tactical approach concomitantly mitigates the potential for complications entailed in peritoneal cavity ingress. Noteworthy is LPRA's specific commendation for patients harboring bilateral tumors and grappling with abdominal adhesions (7). However, juxtaposed against LTA, LPRA does encounter certain limitations stemming from its confined surgical arena, rigid instrumentation, and plausible interactions with neighboring anatomical architecture (8).

In the realm of surgical innovation, propelled by advancements in technology, robotic posterior retroperitoneal adrenalectomy (RPRA) has ascended as a preeminent surgical modality. RPRA affords an array of advantages, including heightened visual acuity through three-dimensional optics and an expanded panoramic canvas of the operative field. This is coupled with a broader range of maneuverability, encompassing seven degrees of freedom compared to the conventional four, thereby enhancing the ergonomic milieu for surgical practitioners (9, 10). However, it is imperative to acknowledge the attendant limitations inherent in robotic surgical systems, encompassing the requisites of setup, the intricacies of instrumentation, augmented expenses, and an extended surgical duration. As a result, the quest for the optimal surgical paradigm within the constricted confines of the retroperitoneal space remains a matter of ongoing scholarly discourse.

Therefore, the aim of this study is to amalgamate data derived from comparative studies and evaluate the efficacy and safety of RPRA and LPRA. The results of this study are intended to function as an all-encompassing guide for clinical decision-making, thereby assisting physicians in the discernment of the most fitting surgical approach for their patients.

2 Methods

This study was executed in strict adherence to the protocols delineated within the Preferred Reporting Items for Systematic Reviews and Meta-Analyses (PRISMA) statement [13]. Furthermore, it underwent registration within the PROSPERO database (ID: CRD42023453816) in accordance with established practices.

2.1 Literature search strategy, study selection and data collection

A thorough and exhaustive electronic survey of the academic databases, encompassing PubMed, Embase, Web of Science, and the Cochrane Library, was meticulously conducted. The data collection process was finalized in July 2023. The search strategy seamlessly integrated pertinent terms concerning the intervention and patient demographics, culminating in the formulation of the subsequent search query: ((Laparoscopic OR Robot-assisted OR Minimally invasive) AND (Retroperitoneoscopic OR Retroperitoneal OR Direct posterior OR Posterior) AND (Adrenalectomy)). Additionally, a comprehensive manual inquiry and scrupulous assessment of pertinent studies were undertaken to ensure the preemptive mitigation of potential oversights. It is noteworthy that the search was specifically delimited to publications presented in the English language. In instances of discordance, a consensus was judiciously attained through deliberation or, when deemed necessary, through consultation with a third reviewer.

The criteria for inclusion were delineated utilizing the PICOS methodology. P (patients): Patients aged 18 years or older who were due to undergo adrenalectomy for any indication. I (intervention): Encompassing patients subjected to RPRA. C (comparator): LPRA was employed as the comparative modality. O (outcome): The primary objective of this inquiry was to evaluate one or more of the ensuing outcomes: perioperative ramifications, surgical outcomes, and associated complications. S (study type): This investigation encompassed randomized controlled trials (RCTs), alongside both retrospective and prospective comparative analyses. Exclusionary criteria were employed as follows: (1) Studies bereft of comparative designs were systematically excluded. (2) Editorial commentaries, epistolary exchanges with the editor, abstracts from meetings, and singular case reports were not integrated into the analytical framework. (3) Studies that did not undertake an evaluation of the stipulated outcome metrics were purposefully excluded from consideration.

Following that, two independent reviewers meticulously extracted the subsequent dataset from the incorporated studies: (1) General manuscript details encompassing the year of publication, lead author, and country of origin. (2) Characteristics of the study population including sample size, age distribution, and body mass index (BMI). (3) Attributes specific to the tumors under investigation: tumor diameter, tumor site, and oncologic outcomes. (4) Perioperative effectiveness metrics: procedural duration, volume of blood loss, duration of hospitalization, rate of conversions, and frequency of transfusions. (5) Considerations regarding perioperative safety: overall complications (as defined by Clavien grade ≥ 1) and major complications (as defined by Clavien grade ≥ 3) (11). The process of data extraction was autonomously executed by the two reviewers to ensure meticulousness and uniformity.

In order to assess the quality of the literature, a comprehensive evaluation was conducted on the studies incorporated in the analysis, employing the "risk of bias in non-randomized studies of interventions" (ROBINS-I) framework (12). This assessment was executed independently by two evaluators (Y.L. and X.C.), who conducted a meticulous scrutiny of the studies for potential biases,

encompassing confounding factors or other potential sources of systematic deviation. Any inconsistencies or differences that emerged during the assessment process were resolved through in-depth discourse.

2.2 Statistical analysis

For the purpose of data analysis within this study, we used the Cochrane Collaborative RevMan 5.4 software. Odds ratios (OR) were applied to assess dichotomous outcomes, while weighted mean differences (WMD) were employed to quantify continuous outcomes, accompanied by 95% confidence intervals (CI) for all evaluated measures. The evaluation of inter-study heterogeneity was accomplished using the I^2 test (13). Given the anticipated existence of inter-trial heterogeneity, we adopted the random-effects model for all analyses, and statistical significance was determined at a significance threshold of $p < 0.05$. In instances where substantial heterogeneity was observed among outcomes ($I^2 > 75\%$), sensitivity analyses were undertaken to ascertain the origin of inter-study variability and to verify the robustness of our findings. However, sensitivity analyses could not be conducted for outcomes predicated on three or fewer studies.

2.3 Subgroup analysis

We performed a subgroup analysis considering several factors, such as age, BMI, sample size, and tumor diameter.

2.4 Publication bias

To evaluate the possibility of publication bias, we employed Begg's method funnel plot.

3 Results

3.1 Baseline characteristics

The applied search algorithm initially identified a total of 139 studies within the databases. Following an extensive review of full-text materials and a meticulous screening process, seven studies, comprising 675 patients in total, were deemed suitable for inclusion in the comprehensive meta-analysis (Figure 1) (14–20). All seven investigations adopted the posterior retroperitoneal adrenalectomy approach. The succinct overview in Table 1 offers a synopsis of fundamental patient characteristics, accompanied by the corresponding interventions and associated preoperative variables (including sample size, age, BMI, surgical approach, tumor diameter, and location). These studies were conducted across diverse countries, including China, the United States, and Korea, and were published between 2012 and 2023. Table 2 delineates perioperative and surgical outcomes, encompassing pivotal parameters such as operative duration, blood loss, hospitalization duration, conversion rate, transfusion frequency, and occurrences of complications. The compendious summation of oncologic outcomes is presented in Table 3.

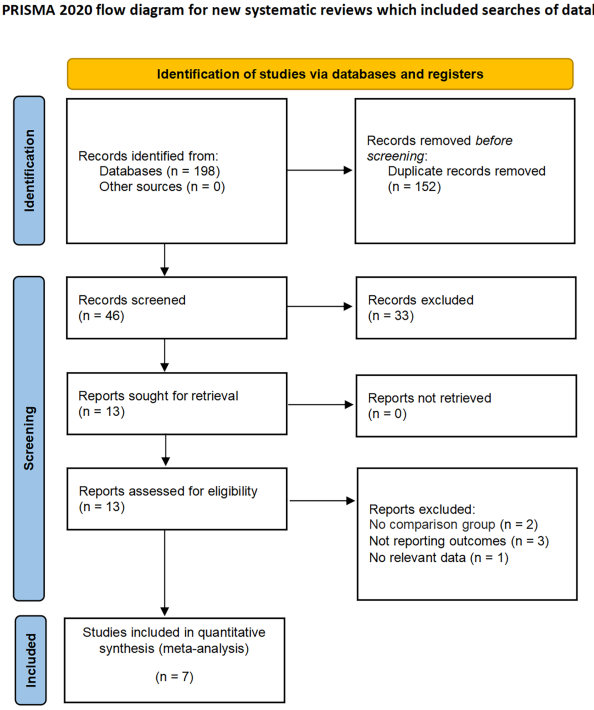

FIGURE 1
PRISMA flow diagram for the systematic review.

TABLE 1 The trials included in the systemic review.

Reference	Year	Country	Age(y)		BMI (kg/m^2)		Patients		Tumor diameter (cm)		Tumor site (Lt / Rt)		Surgical approach
			RPRA	LPRA	RPRA	LPRA	RPRA	LPRA	RPRA	LPRA	RPRA	LPRA	
Isiktas	2023	USA	53.9 (19.3)	51.6 (10.22)	37.9(2)	38.2 (2.74)	15	24	3.58 (1.63)	2.80 (2.19)	06-Sep	18/6	Retroperitoneal
Ma	2021	China	45 (14.82)	49(13.33)	23.53 (3.43)	23.62 (3.22)	79	79	3.5 (1.63)	3.2 (1.48)	47/32	46/33	Retroperitoneal
Fu	2020	China	44 (9.062)	47.53 (14.048)	26.64 (3.82)	25.84 (4.45)	19	32	8(2.22)	7.65 (1.76)	10-Sep	16/16	Retroperitoneal
Kim	2019	Korea	46.5 (11.6)	50.1(13.4)	24.8(3.5)	24.8(3.9)	61	169	3.7(2.5)	3.4(2.2)	35/26	81/88	Retroperitoneal
Lairmore	2016	USA	56.5	52.9	28.5	31.23	17	72	2.4(1.3)	2.38 (1.2)	11-Jun	40/36	Retroperitoneal
Dickson	2013	USA	52(10.3)	52(13)	31.6(6.1)	30(6)	23	23	3.8(1.6)	2.8(1.2)	13/10	11-Dec	Retroperitoneal
Agcaoglu	2012	USA	52.5 (12.81)	53.2 (11.14)	27.5(3.9)	30.3 (4.45)	31	31	3.1 (1.11)	3(1.11)	16/15	19-Dec	Retroperitoneal

RPRA, robotic posterior retroperitoneal adrenalectomy; LPRA, laparoscopic posterior retroperitoneal adrenalectomy; Mean (SD).

3.2 Assessment of quality

No randomized controlled trials (RCTs) comparing RPRA to LPRA were identified. The current meta-analysis meticulously scrutinized a cumulative of seven meticulously chosen investigations, with six of these displaying a discernible, moderate proclivity for bias, while only a study exhibited a notably diminished susceptibility to bias (14). Notably, each of the incorporated studies executed a meticulous comparative scrutiny, as elucidated in Table S1.

3.3 Outcome analysis

3.3.1 Perioperative effectiveness

Following the amalgamation of findings from seven studies, no statistically significant distinction emerged in operative time between the RPRA and LPRA approaches (p = 0.22) (14–20). Upon pooling data from six distinct studies, the RPRA cohort exhibited a diminished duration of hospitalization compared to their LPRA counterparts (WMD -0.78 days, 95% CI -1.46 to -0.10; p = 0.02) (14–16, 18–20) (Figure 2).

TABLE 2 Surgical outcomes.

Reference	operative time (mins)		blood loss (ml)		hospital stay (days)		conversion (n)		transfusion (n)		complications (n)	
	RPRA	LPRA	RPRA	LPRA	RPRA	LPRA	RPRA	LPRA	RPRA	LPRA	RPRA	LPRA
Isiktas	170.6 (80.7)	188 (101.85)	NA		1.1(0.5)	3.1(0.5)	0	0	NA		overall:0	overall:1
Ma	163 (56.23)	165.7 (52.89)	50 (59.26)	50(66.67)	3(0.74)	4(1.48)	0	0	0	2	major:0	overall:2 major:0
Fu	166.3 (54.0)	165(69.5)	100 (111.1)	200 (162.96))	5(0.74)	6(1.48)	NA	NA	1	7	overall:6 major:1	overall:9 major:2
Kim	138 (54.5)	110(50.9)	NA		NA		0	0	NA		NA	
Lairmore	177.3 (50.1)	105.33 (29.60)	46.5 (25.4)	78.4 (141.5)	1.53 (0.87)	1.85 (1.5)	0	3	0	1	major:1	overall:1 major:1
Dickson	154(43)	131(41)	28.3 (50.9)	20(37.4)	1.3(0.6)	1.4(0.7)	NA	NA	NA		NA	
Agcaoglu	163 (56.23)	165.7 (52.89)	25.3 (57.35)	35.6 (55.12)	NA	NA	0	0	NA		major:0	major:0

RPRA, robotic posterior retroperitoneal adrenalectomy; LPRA, laparoscopic posterior retroperitoneal adrenalectomy; Mean (SD).

10.3389/fendo.2023.1278007

TABLE 3 Oncologic outcomes.

Reference	RPRA	LPRA
Isiktas	Pheochromocytoma:3; Aldosteronism:5 Cushing syndrome:4; Other:3	Pheochromocytoma:3; Aldosteronism:5 Cushing syndrome:12; Other:4
Ma	Pheochromocytoma:19; Aldosteronism:5 Cushing syndrome:25; Other:30	Pheochromocytoma:18; Aldosteronism:5 Cushing syndrome:25; Other:31
Fu	Pheochromocytoma:19	Pheochromocytoma:32
Kim	Pheochromocytoma:24; Aldosteronism:9 Cushing syndrome:22; Other:6	Pheochromocytoma:54; Aldosteronism:42 Cushing syndrome:47; Other:26
Lairmore	Pheochromocytoma:20; Aldosteronism:23; Cushing syndrome:20; Other:26	
Dickson	Pheochromocytoma:8; Aldosteronism:3 Cushing syndrome:8; Other:4	NA
Agcaoglu	Pheochromocytoma:6; Aldosteronism:6 Cushing syndrome:13; Other:6	Pheochromocytoma:7; Aldosteronism:8 Cushing syndrome:13; Other:3

RPRA, robotic posterior retroperitoneal adrenalectomy; LPRA, laparoscopic posterior retroperitoneal adrenalectomy.

The cumulative revealed no statistically significant disparity in the occurrence of blood loss (five studies; p = 0.25) (15, 16, 18–20). Likewise, no substantial difference emerged in the prevalence of transfusion rate between RPRA and LPRA (p = 0.14, three studies) (Figure 3) (15, 16, 18). The frequency of conversion to open surgery was documented in five studies. However, the aggregated analysis did not reveal any statistically significant disparities in the reduction of conversion to open surgery between RPRA and LPRA (p = 0.71) (Figure 4) (14, 15, 17, 18, 20).

3.3.2 Complications

The collective incidence of overall complications was 9.2% (12 out of 130 cases) for RPRA and 10.6% (22 of 207 cases) for LPRA (14–16, 18). Notably, no substantial disparities emerged in the prevalence of postoperative overall complications (graded as Clavien ≥1) (p = 0.99). Moreover, the rates of major complications were 1.3% (2 out of 146 cases) for RPRA and 1.4% (3 of 214 cases) for LPRA. Similarly, no statistically significant differences were identified in the occurrence of major complications between RPRA and LPRA (four studies; p = 0.57) (Figure 5) (15–18).

3.3.3 Subgroup

We undertook a subgroup analysis through the stratification of data according to age, BMI, sample size, and tumor diameter. This rigorous analysis encompassed pivotal outcomes, including operative time, length of hospitalization, and blood loss, all of which are presented in Table 4.

All subgroup analyses consistently indicated no significant disparity in operative time between the two groups. The heterogeneity across studies concerning length of hospital stay was found to be influenced by both age and tumor diameter. Specifically, within the subset of studies involving individuals aged < 50 years, RPRA exhibited a markedly reduced length of stay compared to LPRA (p < 0.00001). In contrast, within the subgroup of studies encompassing individuals aged ≥ 50 years, no significant variance in length of stay was observed between the two groups (p = 0.22). Furthermore, within the subgroup characterized

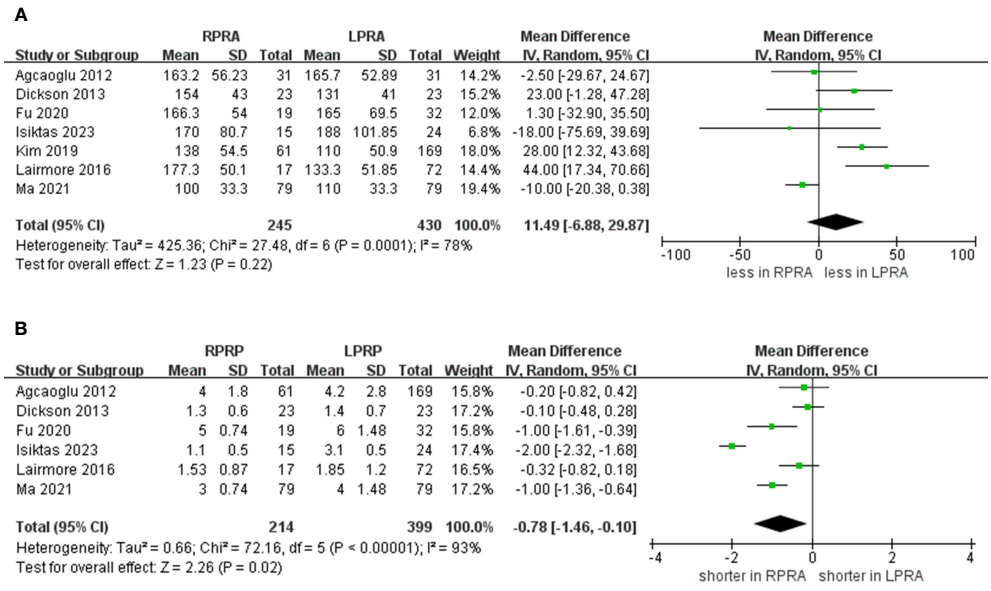

FIGURE 2
Forest plots of perioperative outcomes for RPRA versus LPRA. **(A)** operative time, **(B)** length of hospital stay.

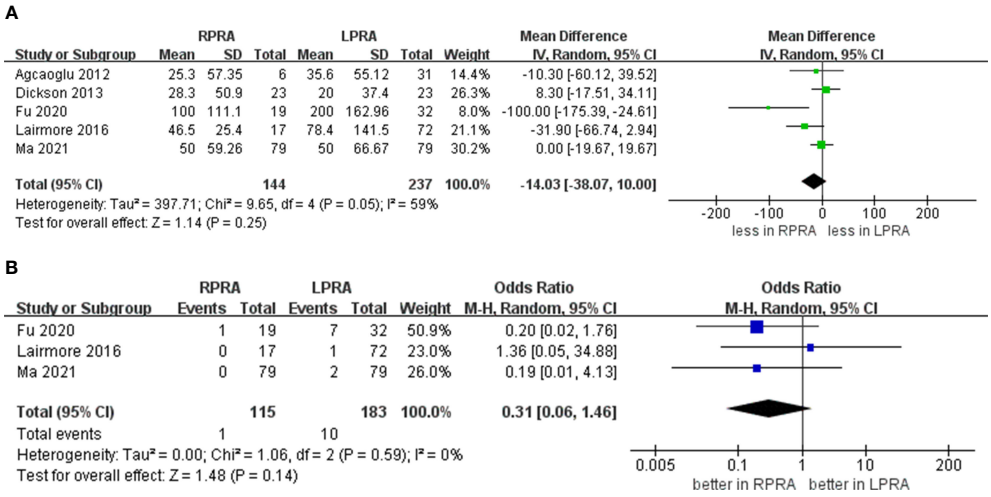

FIGURE 3
Forest plots of perioperative outcomes for RPRA versus LPRA. **(A)** blood loss, **(B)** transfusion rates.

by a tumor diameter ≥ 5 cm, patients who underwent RPRA displayed a significantly shorter length of hospital stay compared to those who underwent LPRA (p = 0.001). Conversely, no noteworthy distinction was noted within the subgroup of cases with a tumor diameter < 5 cm (p = 0.07).

Our analysis revealed tumor diameter as a substantive source of heterogeneity concerning blood loss. In particular, within the subset characterized by a tumor diameter ≥ 5 cm, RPRA exhibited an association with diminished blood loss in contrast to LPRA (p = 0.009), whereas in the subgroup marked by a mean tumor diameter < 5 cm, no noteworthy distinction was evident (p = 0.6).

3.4 Heterogeneity

A prevailing trend toward low to moderate heterogeneity was evident in most of the findings. Even with the incorporation of studies of intermediate and high quality, substantial variability was discerned in two of the outcomes (operative time, I^2 = 78%; length of hospital stay, I^2 = 93%).

3.5 Sensitivity analysis

Within the context of this study, the evident heterogeneity present in factors such as operative time and hospital stay prompted the implementation of a sensitivity analysis. This analytical endeavor aimed to unveil the fundamental origins of the heterogeneity while also evaluating the robustness and steadfastness of the study's outcomes. The findings of this comprehensive analysis unveiled a lack of substantial shifts in the extent of heterogeneity, signifying the enduring consistency of the underlying heterogeneity sources in both operative time and hospital stay over the course of the study.

3.6 Publication bias

To ascertain the potential for publication bias within the examined studies, an analysis was conducted involving operative time, and length of stay as variables. Our findings revealed that the distribution among the studies exhibited an almost symmetrical pattern, suggesting a minimal probability of publication bias (Figure 6).

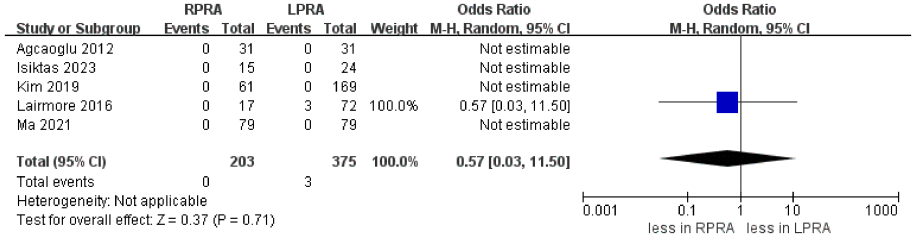

FIGURE 4
Forest plots of perioperative outcomes for RPRA versus LPRA. Conversion to open.

10.3389/fendo.2023.1278007

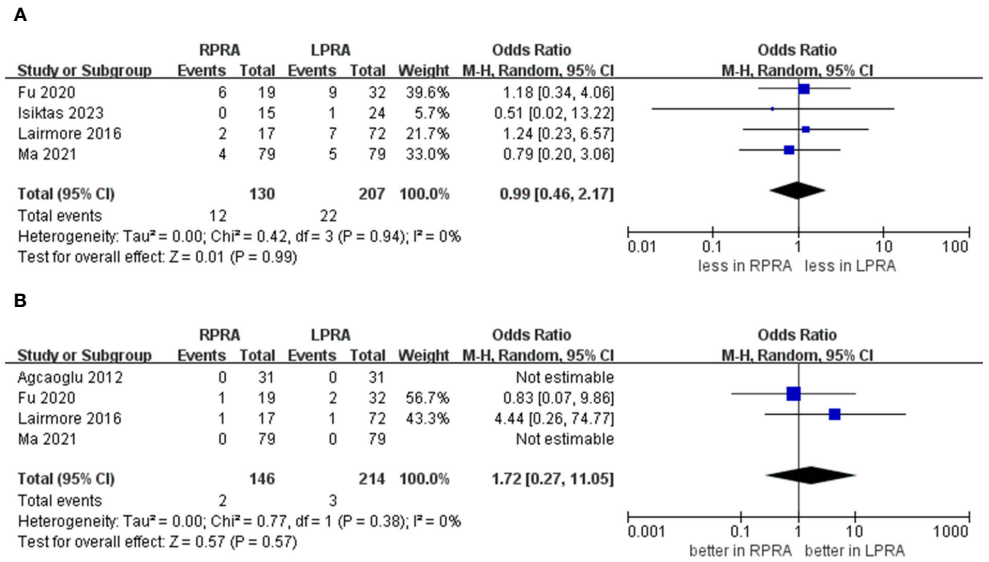

FIGURE 5
Forest plots of complication for MIPN versus OPN. **(A)** overall complication, **(B)** major complications.

TABLE 4 Subgroup analysis of perioperative and oncologic outcomes for RPRA and LPRA.

Group	Subgroups	Studies (n)	MD/OR (95% CI)	I^2 (%)	*P*
Operative time					
Age	Mean age < 50 years	3	6.58 (-21.73, 34.90)	87	0.65
	Mean age ≥ 50 years	4	16.65 (-7.60, 40.89)	60	0.18
BMI	BMI < 30 kg/m2	5	11.90 (-10.44, 34.24)	84	0.3
	BMI ≥ 30 kg/m2	2	11.19 (-25.19, 47.58)	39	0.55
Sample size	Sample size < 80	4	7.45 (-7.97, 22.87)	0	0.34
	Sample size ≥ 80	3	19.17 (-13.84, 52.18)	92	0.26
Tumor diameter	Tumor diameter < 5 cm	5	12.85 (-7.74, 33.43)	82	0.22
	Tumor diameter ≥ 5 cm	1	-1.30 (-32.90, 35.50)	0	0.94
Length of stay					
Age	Mean age < 50 years	2	-1.00 (-1.31, -0.69)	0	< 0.00001
	Mean age ≥ 50 years	4	-0.67 (-1.72, 0.39)	96	0.22
BMI	BMI < 30 kg/m2	4	-0.65 (-1.08, -0.23)	64	0.003
	BMI ≥ 30 kg/m2	2	-0.78 (-2.15, 0.60)	97	0.27
Sample size	Sample size < 80	4	-0.83 (-1.89, 0.22)	95	0.12
	Sample size ≥ 80	2	-0.68 (-1.35, -0.02)	79	0.04
Tumor diameter	Tumor diameter < 5 cm	5	-0.74 (-1.52, 0.05)	94	0.07
	Tumor diameter ≥ 5 cm	1	-1.00 (-1.61, -0.39)	0	0.001
Blood loss					
Age	Mean age < 50 years	2	-43.11 (-140.17, 53.96)	84	0.38
	Mean age ≥ 50 years	3	-9.03 (-35.22, 17.17)	40	0.5

(Continued)

TABLE 4 Continued

Group	Subgroups	Studies (n)	MD/OR (95% CI)	I^2 (%)	*P*
BMI	BMI < 30 kg/m2	4	-24.08 (-56.07, 7.92)	62	0.14
	BMI ≥ 30 kg/m2	1	8.30 (-17.51, 34.11)	0	0.53
Sample size	Sample size < 80	3	-23.82 (-76.05, 28.41)	72	0.37
	Sample size ≥ 80	2	-12.58 (-43.13, 17.98)	59	0.42
Tumor diameter	Tumor diameter < 5 cm	4	-4.11 (-19.62, 11.40)	15	0.6
	Tumor diameter ≥ 5 cm	1	-100.00 (-175.39, -24.61)	0	0.009

4 Discussion

This represents the first systematic review and meta-analysis examining the comparative outcomes between RPRA and LPRA. Several pivotal discoveries within this study merit comprehensive elucidation and discourse.

Seven studies were encompassed in the analysis of operative duration. No statistically significant difference was observed in operative time between RPRA and LPRA. Nevertheless, earlier investigations revealed a substantial elongation in the procedural duration for robotic-assisted posterior retroperitoneoscopic adrenalectomy in contrast to its posterior retroperitoneoscopic counterpart (21, 22). After establishing pneumoperitoneum, three to four robotic ports are typically positioned two finger-widths below the rib edge. Additionally, there are instances where it becomes necessary to create an initial auxiliary opening near the border of the rectus muscle to facilitate retraction or suction (23, 24). The surgeon's preparatory actions, encompassing the orchestration of the operative field, calibration of camera perspectives, and manipulative proficiency, may have exerted influence on the temporal course of RPRA procedures. Furthermore, the variable levels of surgical expertise possessed by individual practitioners bore impact on the operative time within the aggregate studies. In light of recent investigations, as surgeons traverse the learning curve, the temporal demands associated with the robotic approach are anticipated to diminish. In addition, the favorable outcomes observed in robotic urology surgeries conducted by RPRA surgeons may be ascribed to their expertise gained through previous experience in other robotic procedures, such as robotic prostatectomy and nephrectomy (1). An explicable conjecture could attribute this phenomenon to the prevalence of more contemporary RPRA interventions, a manifestation likely stemming from the evolutionary aspects of the surgical technique. Hence, it is conceivable that the surgeon's navigation through the learning curve could inadvertently protract the operative duration (8, 25). Indeed, within the recent inclusions, RPRA has demonstrated a notably reduced operative time in comparison to LPRA. The integration of robotic articulatory instruments with a more robust camera platform and the provision of high-definition 3D visualizations have the potential to expedite the dissection process. Therefore, it remains conceivable that RPRA may have the potential to necessitate a reduced operative duration compared to LARP in subsequent periods (26, 27). Accordingly, a more substantial body of high-caliber evidence is imperative to substantiate our findings. No statistically significant disparity surfaced in the conversion rate between RPRA and LARP. A prior investigation documented a RPRA conversion rate reaching a magnitude of 40%, thereby unveiling an elevated conversion propensity within the RPRA domain as juxtaposed with LARP (28). Concomitant with the accumulated proficiency of individual surgeons utilizing the robotic platform, the conversion rates exhibited a parallel reduction akin to the corresponding levels observed within the LARP frame (29).

Notwithstanding the divergent findings reported in antecedent studies regarding hospital stay (20, 30), our conducted meta-analysis tends to corroborate that RPRA was linked to a briefer hospitalization interval in comparison to LPRA. The variance in hospital stay can be elucidated through the subsequent rationales. Primarily, this variance could potentially stem from the advantages intrinsic to the robotic platform. The benefits conferred by robotic technology encompass high-resolution three-dimensional optics, augmented dexterity, and improved ergonomics, enabling quiver-free and meticulous movements (31). Additionally, the sensitivity analysis indicates the robustness of the estimations. Secondly, bearing in mind the consistent demonstration in prior research of the pivotal role played by institutional caseload and surgeon expertise as crucial determinants influencing the outcomes of minimally invasive procedures, RPRA and LARP are not exempt from this paradigm (32). Hence, exercising prudence is imperative while appraising the hospitalization period following RPRA and LPRA.

Blood loss stands as a pivotal metric for assessing surgical quality. While a statistically significant discrepancy in blood loss between the two groups was not observed, the majority of the encompassed studies exhibited that the RPRA cohort manifested a diminished transfusion incidence and reduced blood loss in contrast to the LARP cohort. The variance in estimated blood loss can be explicated through the ensuing rationales. The adaptability of the robotic flexible arm coupled with the enhanced precision afforded by magnified high-definition stereoscopic vision facilitates the identification and management of intraoperative bleeding and the precise delineation of intricate anatomical structures and separations (33). However, what is worth our attention is that estimate blood loss is not a relevant parameter to assess the surgical efficacy, because of a difference of few ml may not be clinically significant. Furthermore, it is essential to consider that the postoperative blood transfusion rate among patients may be contingent on the surgical expertise of the healthcare professionals

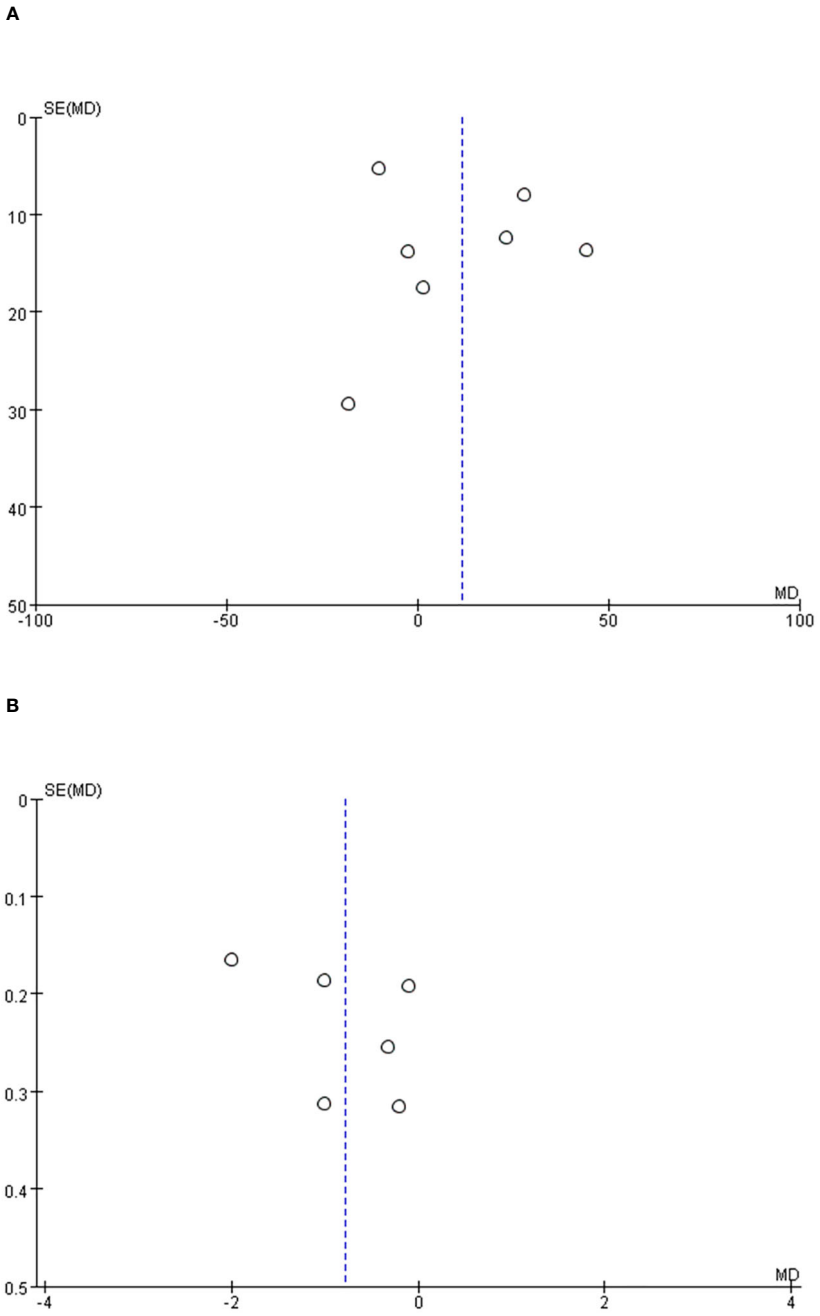

FIGURE 6
Funnel plot of the studies represented in the meta-analysis. **(A)** operative time, **(B)** length of hospital stay.

involved and the specific blood transfusion protocols adhered to by the hospitals (34). In forthcoming times, a deeper reservoir of research focusing on blood loss is requisite to further corroborate this assertion.

Regarding morbidity, no noteworthy distinction emerged between RPRA and LARP in relation to both overall and major complications. A precedent meta-analysis substantiated that RPRA exhibited a higher incidence of complications in contrast to LPRA (35). Nonetheless, contemporary investigations have demonstrated a lack of significant divergence between the two groups concerning complication rates (36). The variance in complication rates can be elucidated through the subsequent rationales. Primarily, the accumulated surgeon expertise in robotic utilization has contributed to the reduction in RPRA-associated complications. Secondly, the abbreviated hospital stay and mitigated blood loss appear to equilibrate the physiological strain endured by the surgical patient, thereby culminating in commensurate complication rates.

Given that the elevated cost associated with robotic surgery constitutes a drawback of the procedure, cost assumes a pivotal role in the contemplation of robotic utilization. Several studies have indicated that robotic surgery has been documented to be 1.3 -3.2

times pricier compared to laparoscopy (28, 37). On one hand, the depreciation of the robotic system and augmenting the annual volume of robotic cases employed proved more efficacious in cost mitigation. On the other hand, patients' selection of an approach was influenced by their individual financial capacity. Hence, cost may not be deemed a salient determinant impacting outcomes. Nevertheless, it exerted influence on infrastructure and medical insurance provisions. It is incumbent upon us to deliberate upon which patients are suitable candidates for the robotic approach, taking into account the social and economic costs.

A subgroup analysis was conducted to ascertain the patient cohort that could potentially derive advantages from RPRA as opposed to LPRA. Certain studies have posited that LTA for tumors surpassing the 5 cm threshold is both secure and feasible under the supervision of a seasoned practitioner. Despite the anticipation of lengthier operative durations associated with LPRA in comparison to LTA, select research endeavors have indicated that the employment of a robotic platform could potentially truncate the procedural chronometry for adrenal tumors > 5 cm (9, 38). Nevertheless, our study did not disclose statistically significant disparities in operative time. Despite the subgroup analysis unveiling a shorter postoperative hospitalization duration within the RPRA cohort, no marked distinctions between the two surgical methodologies were discerned in relation to other outcomes. This could potentially be attributed to the diminutive sample size. Given the inherent advantages of robotic platforms, some surgeons may opt for robotic methods to manage more challenging cases, such as larger tumors or patients with higher BMI (39). Consequently, additional investigations are imperative to facilitate a comprehensive comparison of the advantages intrinsic to both approaches within these cases. Upon stimulation, pheochromocytomas can exude catecholamines, precipitating hemodynamic fluctuations that may culminate in severe complications or morbidity. Consequently, adrenalectomy for pheochromocytoma presents a substantial challenge for operators. In recent years, several studies have postulated that the robotic platform confers superior therapeutic efficacy in the context of adrenal tumors with pheochromocytoma (40, 41). Particularly for pheochromocytomas, neoplasms characterized by a profuse vascular supply, precision in surgical execution holds paramount significance for efficacious hemostatic management. With the exception of operative time, no significant distinctions were observed between the two groups. In light of the paucity of data within our study, circumspection is warranted while appraising the outcomes differential between RPRA and LPRA in the context of pheochromocytoma. Furthermore, Li et al. (42) conducted a meticulous meta-analysis to comprehensively assess the safety and efficacy of partial adrenalectomy (PA) in comparison to total adrenalectomy (TA), with a focus on perioperative and functional outcomes. Their analysis reveals that surgical outcomes in both TA and PA procedures are indeed comparable. The robotic system appears exceptionally well-suited for this technology, owing to its remarkable capacity for achieving precise operations. This is primarily attributed to its multi-degree-of-freedom articulated wrist and the advantage of 3D magnified vision (24). However, further research is imperative to corroborate this conclusion. We have added these relevant findings in the current manuscript.

The current study bears certain limitations that necessitate acknowledgment prior to the interpretation of our findings. First and foremost, the composition of non-randomized controlled trials (non-RCTs) with intermediate methodological quality engenders susceptibility to potential misclassification bias and latent confounding variables. Moreover, a subset of the incorporated studies exhibited diminutive sample sizes. Secondly, albeit the utilization of subgroup analysis, it is noteworthy that the amalgamated studies encompass diverse clinical diagnoses for tumors, a factor that potentially introduces confounding elements into the results. Thirdly, the preponderance of outcomes is contingent upon a selection of the seven studies, precipitated by a dearth of data within the remaining studies. This aspect conspicuously underscores the limitations inherent in the comparison. A substantial portion of the studies are characterized by limited sample sizes and inadequate statistical power.

5 Conclusions

The outcomes of this meta-analysis provide encouragement for the adoption of RPRA within the retroperitoneal space. Specifically, RPRA exhibited a reduced hospitalization duration and diminished invasiveness. Furthermore, the study indicates comparable perioperative outcomes and complication rates when juxtaposed with LPRA. Given that the encompassed studies were characterized by non-randomized controlled trials (non-RCTs) with intermediate methodological quality, the substantiation of RPRA's superiority and identification of the patients most predisposed to gain from RPRA mandate the execution of prospective randomized controlled trials (RCTs) with extended follow-up periods and elevated-level evidence.

Data availability statement

The original contributions presented in the study are included in the article/Supplementary Material. Further inquiries can be directed to the corresponding author.

Author contributions

Y-GL: Conceptualization, Data curation, Formal analysis, Funding acquisition, Investigation, Methodology, Project administration, Resources, Software, Supervision, Validation, Visualization, Writing – original draft, Writing – review & editing. X-BC: Conceptualization, Formal analysis, Resources, Visualization, Writing – original draft, Writing – review &

editing. C-MW: Conceptualization, Data curation, Formal analysis, Project administration, Supervision, Validation, Writing – original draft, Writing – review & editing. X-DY: Formal analysis, Investigation, Visualization, Writing – original draft, Writing – review & editing. X-ZD: Conceptualization, Formal analysis, Writing – original draft, Writing – review & editing. BL: Conceptualization, Data curation, Formal analysis, Funding acquisition, Methodology, Writing – original draft, Writing – review & editing.

Funding

The author(s) declare financial support was received for the research, authorship, and/or publication of this article. This study was supported by the City and College Technology Strategic Cooperation Project of Nanchong (18SXHZ0576); City and College Technology Strategic Cooperation Project of Nanchong (22SXQT0215); Project of North Sichuan Medical College (CBY21-QA38); Five-Year Plan" for Social Science Research in Nanchong City (NC2018B035).

Conflict of interest

The authors declare that the research was conducted in the absence of any commercial or financial relationships that could be construed as a potential conflict of interest.

Publisher's note

Supplementary material

The Supplementary Material for this article can be found online at: https://www.frontiersin.org/articles/10.3389/fendo.2023.1278007/full#supplementary-material

References

1. Gagner M, Lacroix A, Bolté E. Laparoscopic adrenalectomy in Cushing's syndrome and pheochromocytoma. *N Engl J Med* (1992) 327(14):1033. doi: 10.1056/nejm199210013271417

2. Gonzalez R, Smith CD, McClusky DA 3rd, Ramaswamy A, Branum GD, Hunter JG, et al. Laparoscopic approach reduces likelihood of perioperative complications in patients undergoing adrenalectomy. *Am Surg* (2004) 70(8):668–74. doi: 10.1177/000313480407000803

3. Hazzan D, Shiloni E, Golijanin D, Jurim O, Gross D, Reissman P. Laparoscopic vs open adrenalectomy for benign adrenal neoplasm. *Surg Endosc* (2001) 15(11):1356–8. doi: 10.1007/s004640080052

4. Mercan S, Seven R, Ozarmagan S, Tezelman S. Endoscopic retroperitoneal adrenalectomy. *Surgery* (1995) 118(6):1071–5. doi: 10.1016/s0039-6060(05)80116-3

5. Barczyński M, Konturek A, Nowak W. Randomized clinical trial of posterior retroperitoneoscopic adrenalectomy versus lateral transperitoneal laparoscopic adrenalectomy with a 5-year follow-up. *Ann Surg* (2014) 260(5):740–7. doi: 10.1097/sla.0000000000000982

6. Arezzo A, Bullano A, Cochetti G, Cirocchi R, Randolph J, Mearini E, et al. Transperitoneal versus retroperitoneal laparoscopic adrenalectomy for adrenal tumours in adults. *Cochrane Database Syst Rev* (2018) 12(12):Cd011668. doi: 10.1002/14651858.CD011668.pub2

7. Koehne EL, Bajic P, Gupta GN. Robotic-assisted laparoscopic retroperitoneal adrenalectomy. *Surg Oncol* (2019) 31:7. doi: 10.1016/j.suronc.2019.06.005

8. Berber E, Mitchell J, Milas M, Siperstein A. Robotic posterior retroperitoneal adrenalectomy: operative technique. *Arch Surg* (2010) 145(8):781–4. doi: 10.1001/archsurg.2010.148

9. Agcaoglu O, Aliyev S, Karabulut K, Mitchell J, Siperstein A, Berber E. Robotic versus laparoscopic resection of large adrenal tumors. *Ann Surg Oncol* (2012) 19(7):2288–94. doi: 10.1245/s10434-012-2296-4

10. Karabulut K, Agcaoglu O, Aliyev S, Siperstein A, Berber E. Comparison of intraoperative time use and perioperative outcomes for robotic versus laparoscopic adrenalectomy. *Surgery* (2012) 151(4):537–42. doi: 10.1016/j.surg.2011.09.047

11. Dindo D, Demartines N, Clavien PA. Classification of surgical complications: a new proposal with evaluation in a cohort of 6336 patients and results of a survey. *Ann Surg* (2004) 240(2):205–13. doi: 10.1097/01.sla.0000133083.54934.ae

12. Sterne JA, Hernán MA, Reeves BC, Savović J, Berkman ND, Viswanathan M, et al. ROBINS-I: a tool for assessing risk of bias in non-randomised studies of interventions. *Bmj* (2016) 355:i4919. doi: 10.1136/bmj.i4919

13. Higgins JP, Thompson SG, Deeks JJ, Altman DG. Measuring inconsistency in meta-analyses. *Bmj* (2003) 327(7414):557–60. doi: 10.1136/bmj.327.7414.557

14. Isiktas G, Avci SN, Erten O, Ergun O, Krishnamurthy V, Shin J, et al. Laparoscopic versus robotic adrenalectomy in severely obese patients. *Surg Endosc* (2023) 37(2):1107–13. doi: 10.1007/s00464-022-09594-z

15. Ma W, Mao Y, Dai J, Alimu P, Zhuo R, He W, et al. Propensity score matched analysis comparing robotic-assisted with laparoscopic posterior retroperitoneal adrenalectomy. *J Invest Surg* (2021) 34(11):1248–53. doi: 10.1080/08941939.2020.1770377

16. Fu SQ, Zhuang CS, Yang XR, Xie WJ, Gong BB, Liu YF, et al. Comparison of robot-assisted retroperitoneal laparoscopic adrenalectomy versus retroperitoneal laparoscopic adrenalectomy for large pheochromocytoma: a single-centre retrospective study. *BMC Surg* (2020) 20(1):227. doi: 10.1186/s12893-020-00895-5

17. Kim WW, Lee YM, Chung KW, Hong SJ, Sung TY. Comparison of robotic posterior retroperitoneal adrenalectomy over laparoscopic posterior retroperitoneal adrenalectomy: A single tertiary center experience. *Int J Endocrinol* (2019), 9012910. doi: 10.1155/2019/9012910

18. Lairmore TC, Folek J, Govednik CM, Snyder SK. Improving minimally invasive adrenalectomy: selection of optimal approach and comparison of outcomes. *World J Surg* (2016) 40(7):1625–31. doi: 10.1007/s00268-016-3471-8

19. Dickson PV, Alex GC, Grubbs EG, Jimenez C, Lee JE, Perrier ND. Robotic-assisted retroperitoneoscopic adrenalectomy: making a good procedure even better. *Am Surg* (2013) 79(1):84–9.

20. Agcaoglu O, Aliyev S, Karabulut K, Siperstein A, Berber E. Robotic vs laparoscopic posterior retroperitoneal adrenalectomy. *Arch Surg* (2012) 147(3):272–5. doi: 10.1001/archsurg.2011.2040

21. Tang K, Li H, Xia D, Yu G, Guo X, Guan W, et al. Robot-assisted versus laparoscopic adrenalectomy: a systematic review and meta-analysis. *J Laparoendosc Adv Surg Tech A* (2015) 25(3):187–95. doi: 10.1089/lap.2014.0431

22. Pineda-Solís K, Medina-Franco H, Heslin MJ. Robotic versus laparoscopic adrenalectomy: a comparative study in a high-volume center. *Surg Endosc* (2013) 27(2):599–602. doi: 10.1007/s00464-012-2496-9

23. Nomine-Criqui C, Germain A, Ayav A, Bresler L, Brunaud L. Robot-assisted adrenalectomy: indications and drawbacks. *Updates Surg* (2017) 69(2):127–33. doi: 10.1007/s13304-017-0448-6

24. Materazzi G, Rossi L. Robot-assisted adrenalectomy: state of the art. *Updates Surg* (2021) 73(3):1131–46. doi: 10.1007/s13304-020-00915-2

25. Gu L, Ma X, Wang B, Xie Y, Li X, Gao Y, et al. Laparoscopic vs robot-assisted partial nephrectomy for renal tumours of >4 cm: a propensity score-based analysis. *BJU Int* (2018) 122(3):449–55. doi: 10.1111/bju.14386

26. Asher KP, Gupta GN, Boris RS, Pinto PA, Linehan WM, Bratslavsky G. Robot-assisted laparoscopic partial adrenalectomy for pheochromocytoma: the National Cancer Institute technique. *Eur Urol* (2011) 60(1):118–24. doi: 10.1016/j.eururo.2011.03.046

27. Boris RS, Gupta G, Linehan WM, Pinto PA, Bratslavsky G. Robot-assisted laparoscopic partial adrenalectomy: initial experience. *Urology* (2011) 77(4):775–80. doi: 10.1016/j.urology.2010.07.501

28. Morino M, Benincà G, Giraudo G, Genio GMD, Rebecchi F, Garrone C. Robot-assisted vs laparoscopic adrenalectomy: a prospective randomized controlled trial. *Surg Endosc* (2004) 18(12):1742–6. doi: 10.1007/s00464-004-9046-z

29. Mishra K, Maurice MJ, Bukavina L, Abouassaly R. Comparative efficacy of laparoscopic versus robotic adrenalectomy for adrenal Malignancy. *Urology* (2019) 123:146–50. doi: 10.1016/j.urology.2018.08.037

30. Melquist JJ, Redrow G, Delacroix S, Park A, Faria EE, Karam JA, et al. Comparison of single-docking robotic-assisted and traditional laparoscopy for retroperitoneal lymph node dissection during nephroureterectomy with bladder cuff excision for upper-tract urothelial carcinoma. *Urology* (2016) 87:216–23. doi: 10.1016/j.urology.2015.07.070

31. Mack MJ. Minimally invasive and robotic surgery. *Jama* (2001) 285(5):568–72. doi: 10.1001/jama.285.5.568

32. Fleming ND, Axtell AE, Lentz SE. Operative and anesthetic outcomes in endometrial cancer staging via three minimally invasive methods. *J Robot Surg* (2012) 6(4):337–44. doi: 10.1007/s11701-011-0319-y

33. Takagi T, Kondo T, Tachibana H, Iizuka J, Omae K, Kobayashi H, et al. Robot-assisted laparoscopic versus open partial nephrectomy in patients with chronic kidney disease: A propensity score-matched comparative analysis of surgical outcomes. *Int J Urol* (2017) 24(7):505–10. doi: 10.1111/iju.13363

34. Li KP, Chen SY, Wang CY, Yang L. Comparison between minimally invasive partial nephrectomy and open partial nephrectomy for complex renal tumors: a systematic review and meta-analysis. *Int J Surg* (2023) 109(6):1769–82. doi: 10.1097/js9.0000000000000397

35. Brandao L, Zargar H, Autorino R, Economopoulos KP, Stamou A, Sergentanis TN, et al. Robotic versus laparoscopic adrenalectomy: a systematic review and meta-analysis. *Eur Urol* (2014)67(2):1154–61e33–4. doi: 10.1016/j.eururo.2014.09.053

36. Perivoliotis K, Baloyiannis I, Sarakatsianou C, Tzovaras G. Comparing the efficacy and safety of laparoscopic and robotic adrenalectomy: a meta-analysis and trial sequential analysis. *Langenbecks Arch Surg* (2020) 405(2):125–35. doi: 10.1007/s00423-020-01860-9

37. Winter JM, Talamini MA, Stanfield CL, Chang DC, Hundt JD, Dackiw AP, et al. Thirty robotic adrenalectomies: a single institution's experience. *Surg Endosc* (2006) 20 (1):119–24. doi: 10.1007/s00464-005-0082-0

38. Brunaud L, Bresler L, Ayav A, Zarnegar R, Raphoz AL, Levan T, et al. Robotic-assisted adrenalectomy: what advantages compared to lateral transperitoneal laparoscopic adrenalectomy? *Am J Surg* (2008) 195(4):433–8. doi: 10.1016/j.amjsurg.2007.04.016

39. Sforza S, Minervini A, Tellini R, Ji C, Bergamini C, Giordano A, et al. Perioperative outcomes of robotic and laparoscopic adrenalectomy: a large international multicenter experience. *Surg Endosc* (2021) 35(4):1801–7. doi: 10.1007/s00464-020-07578-5

40. Manny TB, Pompeo AS, Hemal AK. Robotic partial adrenalectomy using indocyanine green dye with near-infrared imaging: the initial clinical experience. *Urology* (2013) 82(3):738–42. doi: 10.1016/j.urology.2013.03.074

41. Pahwa M, Pahwa AR, Batra R, Abraham RR, Chawla A, Kathuria S, et al. Robotic assisted laparoscopic adrenalectomy: Initial experience from a tertiary care centre in India. *J Minim Access Surg* (2015) 11(1):83–6. doi: 10.4103/0972-9941.147704

42. Li KP, Duan X, Yang XS, Huang J, Wu T. Partial versus total adrenalectomy for the treatment of unilateral aldosterone-producing adenoma: a systematic review and meta-analysis. *Updates Surg* (2021) 73(6):2301–13. doi: 10.1007/s13304-021-01116-1

frontiers | Frontiers in Endocrinology

TYPE Original Research
PUBLISHED 30 November 2023
DOI 10.3389/fendo.2023.1265794

OPEN ACCESS

EDITED BY
Piotr Glinicki,
Centre of Postgraduate Medical Education, Poland

REVIEWED BY
Rosario Pivonello,
University of Naples Federico II, Italy
Pietro Locantore,
Catholic University of the Sacred Heart, Italy
Filippo Ceccato,
University of Padua, Italy
Nadia Cherradi,
INSERM U1292 Biology and Biotechnologies for Health, France
Mark Stevenson,
University of Oxford, United Kingdom
Felicia Alexandra Hanzu,
Hospital Clinic of Barcelona, Spain

*CORRESPONDENCE
Sharmilee Vetrivel
sharmilee.vetrivel@med.uni-muenchen.de

RECEIVED 23 July 2023
ACCEPTED 07 November 2023
PUBLISHED 30 November 2023

CITATION
Vetrivel S, Tamburello M, Oßwald A, Zhang R, Khan A, Jung S, Baker JE, Rainey WE, Nowak E, Altieri B, Detomas M, Watts D, Williams TA, Wielockx B, Beuschlein F, Reincke M, Sbiera S and Riester A (2023) PPARG dysregulation as a potential molecular target in adrenal Cushing's syndrome.
Front. Endocrinol. 14:1265794.
doi: 10.3389/fendo.2023.1265794

PPARG dysregulation as a potential molecular target in adrenal Cushing's syndrome

Sharmilee Vetrivel[1]*, Mariangela Tamburello[2,3], Andrea Oßwald[1], Ru Zhang[1], Ali Khan[2], Sara Jung[1], Jessica E. Baker[4], William E. Rainey[4], Elisabeth Nowak[1], Barbara Altieri[2], Mario Detomas[2], Deepika Watts[5], Tracy Ann Williams[1], Ben Wielockx[5], Felix Beuschlein[1,6], Martin Reincke[1], Silviu Sbiera[2] and Anna Riester[1]

[1]Department of Medicine IV, LMU University Hospital, LMU Munich, Munich, Germany, [2]Division of Endocrinology and Diabetes, Department of Internal Medicine I, University Hospital, University of Würzburg, Würzburg, Germany, [3]Section of Pharmacology, Department of Molecular and Translational Medicine, University of Brescia, Brescia, Italy, [4]Department of Molecular and Integrative Physiology, University of Michigan Medical School, Ann Arbor, MI, United States, [5]Institute of Clinical Chemistry and Laboratory Medicine, Technische Universität Dresden (TUD)/Universitätsklinikum Carl Gustav Carus Dresden (UKD), Dresden, Germany, [6]Department of Endocrinology, Diabetology and Clinical Nutrition, University Hospital Zurich (USZ) and University of Zurich (UZH), Zurich, Switzerland

Background: We performed a transcriptomic analysis of adrenal signaling pathways in various forms of endogenous Cushing's syndrome (CS) to define areas of dysregulated and druggable targets.

Methodology: Next-generation sequencing was performed on adrenal samples of patients with primary bilateral macronodular adrenal hyperplasia (PBMAH, n=10) and control adrenal samples (n=8). The validation groups included cortisol-producing adenoma (CPA, n=9) and samples from patients undergoing bilateral adrenalectomy for Cushing's disease (BADX-CD, n=8). *In vivo* findings were further characterized using three adrenocortical cell-lines (NCI-H295R, CU-ACC2, MUC1).

Results: Pathway mapping based on significant expression patterns identified PPARG (peroxisome proliferator-activated receptor gamma) pathway as the top hit. Quantitative PCR (QPCR) confirmed that *PPARG* (l2fc<-1.5) and related genes – *FABP4* (l2fc<-5.5), *PLIN1* (l2fc<-4.1) and *ADIPOQ* (l2fc<-3.3) – were significantly downregulated (p<0.005) in PBMAH. Significant downregulation of *PPARG* was also found in BADX-CD (l2fc<-1.9, p<0.0001) and CPA (l2fc<-1.4, p<0.0001). *In vitro* studies demonstrated that the PPARG activator rosiglitazone resulted in decreased cell viability in MUC1 and NCI-H295R (p<0.0001). There was also a significant reduction in the production of aldosterone, cortisol, and cortisone in NCI-H295R and in Dihydrotestosterone (DHT) in MUC1 (p<0.05), respectively.

Outcome: This therapeutic effect was independent of the actions of ACTH, postulating a promising application of *PPARG* activation in endogenous hypercortisolism.

KEYWORDS

transcriptome, hypercortisolism, rosiglitazone, adrenocortical cell line, steroidome, cortisol, primary bilateral macronodular hype

1 Introduction

Enhanced adrenal cell proliferation clinically translates into a high incidence of adrenal incidentaloma occurring in 2–10% of the population worldwide (1). One third of these patients have mild autonomous cortisol secretion without typical Cushing stigmata but associated with an elevated cardiometabolic morbidity (2–4). Comparatively, endogenous cortisol excess resulting in Cushing's syndrome (CS) has an incidence of 0.2–5.0 per million people per year (5). In the majority of patients with overt CS, endogenous hypercortisolism is due to adrenocorticotropic hormone (ACTH) secretion by corticotroph adenomas of the pituitary gland resulting in Cushing's disease (CD) (6). In approximately 20% of cases cortisol is secreted autonomously by the adrenal cortex. Adrenal CS is mostly caused by unilateral cortisol-producing adenomas (CPA). Primary bilateral macronodular adrenocortical hyperplasia (PBMAH) represents another specific subtype of adrenal CS characterized morphologically by bilateral nodular enlargement with a grape-like appearance. PBMAH accounts for less than 2% of patients with endogenous CS (7). Genomic approaches led to the identification of germline *ARMC5* mutations in approximately 20-25% of PBMAH patients, and germline *KDM1A* mutations in 90% of patients who have food-dependent CS (8). *PRKACA* gene mutations are detected in approximately 40% of cortisol-producing adenomas (9).

Despite the advances in genomic analyses, the medical management of CS remains controversial. Uni- or bilateral adrenalectomy is the first line treatment in overt CS. Patients after bilateral adrenalectomy require lifetime steroid replacement with risk of life-threatening adrenal crises (10, 11). Medical therapy in CS consists of steroid synthesis inhibitors and glucocorticoid receptor antagonists (12, 13). However, long term control of hypercortisolism with the available drugs has been afflicted with various side effects on gastrointestinal, neural and hepatic systems (14).

In this study our aim was to define altered cell signaling pathways in CS through PBMAH transcriptome and identify new pharmacological targets using the following experimental approach:

(1) Untargeted transcriptome analysis of PBMAH samples of the discovery cohort.
(2) Pathway analysis and preliminary validation of the next generation sequencing (NGS) results using QPCR.
(3) Validation of the candidate pathway genes including Peroxisome proliferator-activated receptor gamma (*PPARG*) pathway in an independent validation cohort.
(4) *In vivo* analyses of the effect of ACTH on *Pparg* expression
(5) *In vitro* experiments to assess the therapeutic effect of PPARG pathway modulation.

The overarching aim of our study was to have a comprehensive transcriptomics-based discovery dataset from patient samples that allows *in vitro* confirmatory studies. For this purpose, the unique genetic mutations and the increasing prevalence/missed diagnosis of PBMAH (13) make it an intriguing subtype of CS for the discovery cohort analyses. Further, by focusing on PBMAH, we aimed to identify previously unexplored therapeutic mechanisms for the CS pathology.

2 Materials and methods

2.1 Sample collection and ethics approval

The patients were registered as part of ongoing registries and biobanks (European Network for the Study of Adrenal Tumor [ENS@T, www.ensat.org] and Excellence Network for Neuroendocrine Tumors [NeoExNet]). The study was approved by the Ethics Committees of the University of Munich and Würzburg. Written informed consent was obtained from all enrolled patients, and the experiments were performed according to relevant guidelines and protocols.

For NGS a total of 18 cryo-preserved adrenal samples were used. The discovery cohort consisted of PBMAH (n=10) and adjacent normal adrenal cortex from patients with pheochromocytoma (controls, n=8).

Additional QPCR validation was performed in RNA extracted from cryo-preserved tissue from the following samples: cortisol producing adenoma (CPA, n=9), and adrenal samples from patients undergoing bilateral adrenalectomy for persistent Cushing's disease (BADX-CD, n=8). Normal adrenals from patients who underwent kidney surgery (normal adrenals, n=10), and adrenal samples from patients with aldosterone producing adenoma (APA, n=10) were used as controls for validation. Furthermore, the results were validated with data from 3'RNA sequencing of RNA extracted from FFPE tissues on an independent PBMAH cohort (PBMAH-FFPE, n=11).

The clinical characteristics of the groups are given in Table 1. In total, four PBMAH patients carried *ARMC5* mutations (2/10 PBMAH samples used in the discovery and 2/11 used in the validation cohort), and one patient from the validation cohort carried a *KDM1A* mutation.

2.2 Total RNA extraction from cryo and FFPE tissues

The adrenal tissues were stored at -80°C. Total RNA isolation was carried out from all adrenal cortex samples using the RNeasy Tissue Kit (Qiagen, Germany). The isolated RNA was kept frozen at –80°C until further use. RNA yield and purity were measured using NanoDrop (Thermofisher Scientific, Germany). Quality control of the isolated RNA, RNA library preparation, and sequencing was performed by QIAGEN (Zymo Research, Irvine, US). In case of RNA from FFPE material, the tumor area was marked and 10 µm sections from five serial slides were collected under a stero microscope (Motic). Total RNA was extracted from the collected tumor using the AllPrep DNA/RNA FFPE kit (Qiagen) according to the manufacturer's instructions. The RNA quantity and quality were determined using NanoDrop 2000 spectrophotometer (Thermo Fisher).

10.3389/fendo.2023.1265794

TABLE 1 Clinical characteristics of the patient groups.

	N	Age at diagnosis [years]	Sex [% female]	baseline ACTH [pmol/L]	Cortisol 24h Urine [nmol/day]	midnight Cortisol [nmol/L]	Cortisol after 1 mg Dexamethasone [nmol/L]	methods	preservation of the tissue
Normal Range				0.9-13.4	138-414	<4.1	< 50		
Discovery cohort									
Controls (normal adrenals)	8	53 [48;58]	50	NA	NA	NA	NA	RNA Seq, QPCR	cryo
PBMAH	10	61 [59;68]	60	0.6 [0.4;0.7]	994 [619;1256]	15.6 [9.3;21.1]	250 [206;481]	RNA Seq, QPCR	cryo
Validation cohort									
CPA	7	52 [40;57]	62	0.4 [0.4;0.8]	1684 [1449;2120]	16.0 [12.7;24.3]	386 [326;431]	QPCR	cryo
BADX-CD	8	42 [37;52]	75	10.5 [7.8;12.1]	2211 [1949;2338]	21.1 [12.0;27.3]	373 [233;622]	QPCR	cryo
APA	10	47 [43;52]	70	NA	NA	NA	NA	QPCR	cryo
Normal adrenals	10	NA	NA	NA	NA	NA	NA	QPCR	cryo
PBMAH	11	58 [56;62]	100	0.6 [0.5;0.9]	458 [254; 530]	12.6 [8.2; 15.9]	155 [110;373]	3′ RNA Seq	FFPE

Data are given as median with 25th and 75th percentile in brackets. APA, Aldosterone producing adenoma; CPA, cortisol producing adenoma; BADX-CD, Bilateral adrenalectomized patients with persistent Cushing's Disease. PBMAH, Primary Bilateral Macronodular Hyperplasia.

2.3 RNA sequencing

RNA-seq from frozen adrenal samples was performed at Qiagen, Hilden, Germany and sequencing from FFPE samples was done at the SysMed Core Facility, Würzburg. Briefly, RNA integrity and the absence of contaminating DNA were confirmed by Bioanalyzer RNA Nano (Agilent Technologies) and by Qubit DNA High sensitivity kits, respectively. QIAseq Stranded RNA Library Kits was used for library preparation. Sequencing was performed on Illumina NextSeq (single end read, 75 bp). Adapter and quality trimming were performed by the "Trim Reads" tool from CLC Genomics Workbench. Further, reads were trimmed based on quality scores. The QC reports were generated by the "QC for Sequencing Reads" tool from CLC Genomics Workbench. Read mapping and gene quantification were performed by the "RNA-seq Analysis" tool from CLC Genomics Workbench (15). In case of FFPE derived RNA, sequencing libraries were prepared using the QuantSeq 3' mRNA-Seq protocol (Lexogen, Vienna, Austria), from 100 to 500 ng RNA. Single read sequencing (1 ×75bp) was performed on a NextSeq 550 platform (Illumina, San Diego, CA, USA). For RNA extracted from FFPE samples, sequencing libraries were constructed using the QuantSeq 3' mRNA-Seq protocol from Lexogen (Vienna, Austria). The libraries were prepared using 100 to 500 ng of RNA. Subsequently, single-read sequencing with a read length of 75 bases (1 × 75bp) was carried out on a NextSeq 550 platform from Illumina (San Diego, CA, USA) (16).

2.4 Validation of RNA expression of related pathway genes

Differentially expressed RNAs identified through NGS were validated by QPCR. RNA concentration was assessed using a NanoDrop 2000 spectrophotometer (Thermo Fisher Scientific), and reverse transcription was performed on 50 ng of RNA using Superscript VILO reverse transcriptase (Thermo Fisher Scientific) according to the manufacturer's instructions. The selection of a suitable housekeeping gene was carried out using the BestKeeper tool to determine the most stably expressed housekeeping gene (p-value <0.001) (15). In frozen adrenal samples of the discovery cohort, controls (n=8) and PBMAH (n=10), housekeeping genes *ACTB*, *GAPDH*, and *PPIA* were evaluated. For adrenocortical cell lines (NCI-H295R; n=10, CU-ACC2; n=10, and MUC1; n=10), the housekeeping genes *ACTB* and *PPIA* were assessed. *PPIA* was identified as the most stable reference gene for human adrenal samples, while *ACTB* was chosen as the reference gene for adrenocortical cell lines (Figure S1). QPCR was conducted using TaqMan Fast Universal PCR Master Mix (Thermo Fisher Scientific) on a Quantstudio 7 Flex Real-Time PCR System (Thermo Fisher Scientific), following the manufacturer's TaqMan mRNA assay protocol. TaqMan probes used are listed in Table S1, and negative control reactions lacked cDNA templates. Each QPCR reaction used 5 ng of cDNA and was analyzed in technical triplicates. The PCR was carried out in a 20 µL mixture, with

10µL of Master Mix, 1 µL of TaqMan probes, 5 µL of cDNA, and 4 µL of nuclease-free water. The qPCR was performed following the recommended thermocycling conditions on the Quantstudio 7 Flex Real-Time PCR System (Thermo Fisher Scientific) under the Fast mode, with an initial activation at 95°C for 20 sec and 40 cycles of 95°C for 1 sec and 60°C for 20 sec. Gene expression levels were quantified using the relative quantification method (17), normalized to the reference gene, to enable easier comparisons.

2.5 *In vivo* ACTH stimulation

ACTH stimulation tests were performed in 16 female mice (C57BL/6). Briefly, Jfemale mice representing each time point of injection). Briefly, 13-week-old mice were intraperitoneally injected with 1mg/kg of ACTH (Sigma Aldrich, Germany) and adrenals collected after 10, 30, and 60 min of injections (4 mice per time point). In addition, control adrenals were collected from mice at baseline conditions (0 min). Details of the experiment are published in (18). *Gapdh* was used as housekeeping gene in the QPCR. All mice were maintained in accordance with facility guidelines on animal welfare and approved by Landesdirektion Sachsen, Germany.

2.6 *In vitro* assays to evaluate pathway activation

The identified *PPARG* pathway was further characterized *in vitro* using three adrenocortical cell-lines (NCI-H295R, CU-ACC2 and MUC1), derived from patients with malignant adrenocortical carcinoma (ACC). The human NCI-H295R cell line, derived from a primitive ACC in a female patient, was obtained from the American Type Culture Collection (ATCC) and cultured as indicated by ATCC. MUC-1 cell line, established from a neck metastasis of an EDP-M-treated (etoposide, doxorubicin and cisplatin plus oral mitotane) male patient, was kindly given by Dr. Hantel and cultured as suggested (19). CU-ACC2 cell lines were obtained from Dr. Katja Kiseljak-Vassiliades (20). A detailed description of these cell lines can be found in Sigala et al. (21). The activation of *PPARG* in the cell lines was assayed for cell viability, gene expression changes and effect on steroidogenesis. Rosiglitazone, which is a known drug in diabetes therapy, was used as a *PPARG* activator.

2.7 Cell viability assay, hormones measurements and gene expression

Cells (50.000 cells/well) were seeded in 96-wells-plates and treated with increasing concentrations of ACTH (2.5–20 nM; Alfasigma), solubilized in water, and rosiglitazone (5–40 µM; Cayman Chemical). Rosiglitazone was solubilized and serially diluted using DMSO. The drug solutions were prepared 200 times more concentrated to dilute the DMSO at a ratio of 1:200 in the well. Both compounds were tested alone and in combination. Cell viability was evaluated by WST-1 assay according to the manufacturer protocol (Roche). All the subsequent sets of experiments were conducted treating the cells for 48h in serum-free medium. For treatments on CU-ACC2 cell line also the hydrocortisone has been removed.

Cells ($1.5x10^6$ cells/well) were seeded in 6-wells-plates and treated with ACTH (2.5 nM), and 5, 10, 20 µM of rosiglitazone in a final volume of 3 ml. These doses were chosen based on the cell viability results. After 48h the media were collected and stored at -20°C until analysis performed using liquid chromatography tandem mass spectrometry (LC-MS/MS) as described by Schweitzer et al. (22). The cells were scraped from the bottom of the wells to isolate the mRNA using the Maxwell RSC Simply RNA Kit (Promega). RNA concentration was determined using a NanoDrop 2000 spectrophotometer (Thermo Fisher) and 1000 ng RNA were reverse transcribed with the High-Capacity cDNA Reverse Transcription Kit, Applied Biosystems). QPCR was performed using TaqMan gene expression probes (Thermo Fisher Scientific) for *PPARG* (Hs01115513) and for ACTH receptor, also known as the melanocortin receptor 2 (*MC2R*), (Hs00300820). Endogenously expressed *ACTB* (Hs99999903) was used as housekeeping gene for normalization. For each QPCR reaction, 5 ng cDNA were used, and each sample was analyzed in technical triplicates. All transcripts were amplified using TaqMan Gene Expression Master Mix (Thermo Fisher) using the CFX96 real-time thermocycler (Bio-rad) and the Bio-rad CFX Manager 2.0 software. Cycling conditions were 95°C for 3 min, followed by 39 cycles of 95°C for 30 s, 60°C for 30 s, and 72°C for 30 s. Fold change was calculated using the delta cycle threshold (dCt) method, normalized to housekeeping gene *ACTB*.

2.8 Bioinformatic and statistical analyses

R version 4.2.0 was used for statistical analyses of NGS data. To identify RNAs differentially expressed, generalized linear model (GLM, a flexible generalization of ordinary linear regression that allows for variables that have distribution patterns other than a normal distribution) in the software package edgeR (Empirical Analysis of DGE in R) was employed to calculate *p*-values (23, 24). *P*-values were adjusted with the Benjamini–Hochberg false discovery rate (FDR) procedure (25). GraphPad Prism Version 8 was used for statistical analysis of QPCR. To identify RNAs differentially expressed in QPCR, the dCt method (target gene's Ct minus housekeeping RNA's Ct) was used in Microsoft Excel 2016 (Microsoft, Redmond, WA, USA). For intergroup comparison of QPCR data, ANOVA test with Benjamini–Hochberg false discovery rate (FDR) procedure was used (26). $P<0.05$ and $FDR<0.05$ were considered significant. Pathway mapping for the significant genes was performed using the ShinyGO program (27).

3 Results

3.1 PBMAH transcriptome

Transcriptome analyses of PBMAH adrenal samples (n=10) identified a total of 1104 genes to be significantly differentially

expressed in comparison to the control group (n=8) in the discovery cohort (|2fc>|2|, FDR<0.05). Almost 70% of the genes were downregulated (769 genes), indicating an overall transcriptionally repressed state in PBMAH samples (Figure 1, Table S2). Hierarchical clustering based on the top upregulated significant genes was performed and revealed a good discrimination between (27)en PBMAH samples and controls. Interestingly, PBMAH samples with *ARMC5* mutations clustered together while the *ARMC5*^{wt} PBMAH samples clustered separately and were further divided in two additional clusters (Figure S2).

3.2 Pathway mapping

To better understand the transcriptional profile of PBMAH, all significant genes (n=1104 genes) were used for pathway mapping to identify which genes are enriched in different pathways (Figure 2A). This pathway mapping analysis is grounded in the concept of fold enrichment (Figure 2A), wherein fold enrichment is computed as the percentage of genes in the input list relative to the corresponding background percentage. This calculation serves as a metric of the statistical significance of pathway dysregulation. Overall, the top pathway hits from the PBMAH transcriptome generated two major pathway clusters (Figure 2B) (1): "peroxisome proliferator-activated receptors" (PPARs) signaling, which is widely acknowledged for its anti-glycemic and anti-lipolytic effects (28), and (2) pathways related to neuronal function and diseases including "nicotine addiction" and "neuroactive ligand-receptor interaction". To validate the pathway enrichment based on the transcriptome data, the significantly altered *PPARG* and its top downregulated target genes (*ADIPOQ*, *APOA1*, *FABP4*, *PCK1* and *PLIN1*) were chosen. A significant (p<0.01) downregulation of *PPARG* and its target genes *ADIPOQ*, *FABP4* and *PLIN1* was found in the PBMAH samples in comparison to controls (Figure 3). For the neuronal pathway cluster, five genes (*DRD2*, *GRIA2*, *GRIA4*, *GRIN2A* and *SCTR*) shared most among the pathways were chosen for further analyses but failed to show significant dysregulation (Figure S3).

3.3 Validation of PPARG pathway dysregulation

The observed downregulation of *PPARG* and its target genes by QPCR and NGS were further validated in two ways. In the first step, DESeq2 based gene expression analyses from FFPE RNA from an independent PBMAH cohort (n=11) (Table 2) showed that *PPARG* and its target genes were consistently downregulated in the

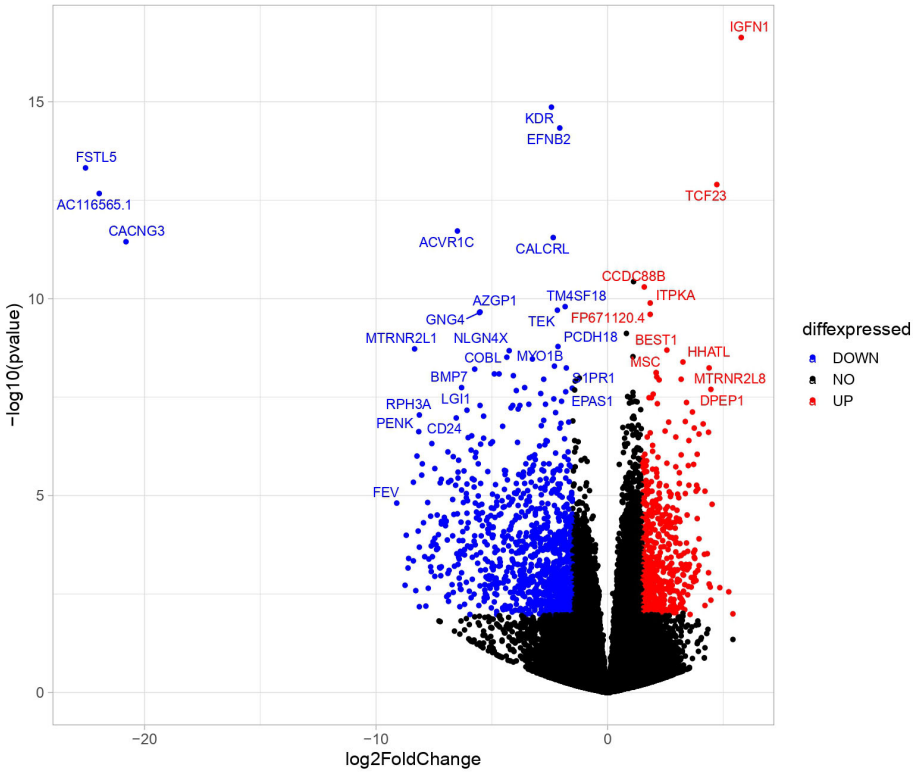

FIGURE 1
Differentially expressed significant genes in NGS between in adrenals of PBMAH vs. controls. Volcano plot showing the relationship between fold change (log2foldchange) and statistical significance (-log10pvalue). The red points represent significantly upregulated genes while blue points represent significantly downregulated genes. The top 32 altered genes are labelled (24 downregulated and 10 upregulated).

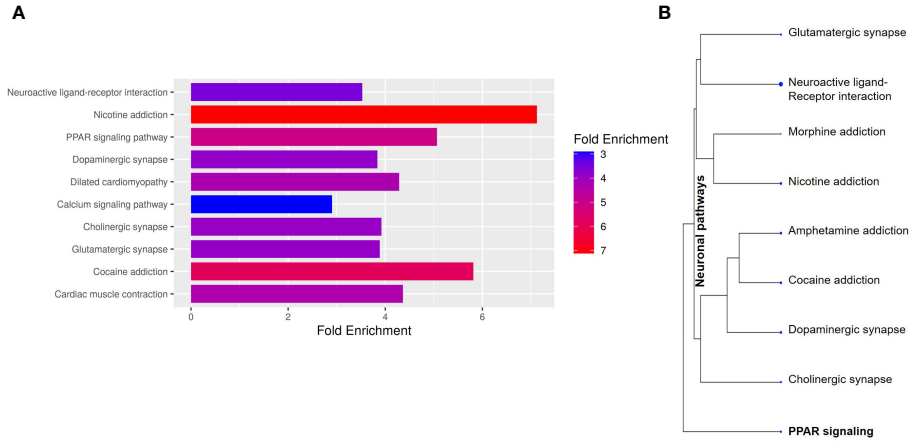

FIGURE 2
Pathway analyses of the significant genes from NGS. The significantly expressed genes were shortlisted (log2FC > abs (2), p<0.05). **(A)** The shortlisted genes were used for KEGG pathway mapping using ShinyGO online analyses tool. **(A)** Barplot representation of the top significant pathway hits. Higher fold enrichment refers to higher representation of the genes in the pathway. The pathways are sorted by FDR, with higher significant pathways at the top. **(B)** Hierarchical clustering of significant pathways: The pathway genes were clustered based on the genes shared amongst the different pathways.

validation cohort of PBMAH. In the second step, the expression of *PPARG* and its target genes was verified in adrenal samples from other types of CS, normal adrenals and APAs (Figure 4). Significant downregulation of *PPARG* was observed in all the CS samples in comparison to both controls, APAs and normal adrenals (Figure 4A). Interestingly, significant downregulation of *PPARG* and its target genes, *ADIPOQ* (Figure 4B) and *FABP4* (Figure 4C) was also observed in APA in comparison to normal adrenals, but not as pronounced as in CS subtypes. In contrast, the significant downregulation of *PLIN1* was specific to CS groups (Figure 4D). Taken together, the candidate PPARG pathway downregulation observed in the adrenal samples of PBMAH by NGS could be validated in all adrenals with cortisol excess.

3.4 *In vivo* analyses of *Pparg*

To analyze whether *Pparg* expression is influenced by ACTH, an ACTH stimulation study was done in mice and *Pparg* expression was assayed at different timepoints. No changes in *Pparg* expression were found in any of the timepoints (Figure 5).

3.5 *In vitro* analysis of the PPARG dependent pathway activation

Next, the effect of ACTH stimulation on *MC2R* mRNA expression was tested in adrenocortical cell lines. Only NCI-

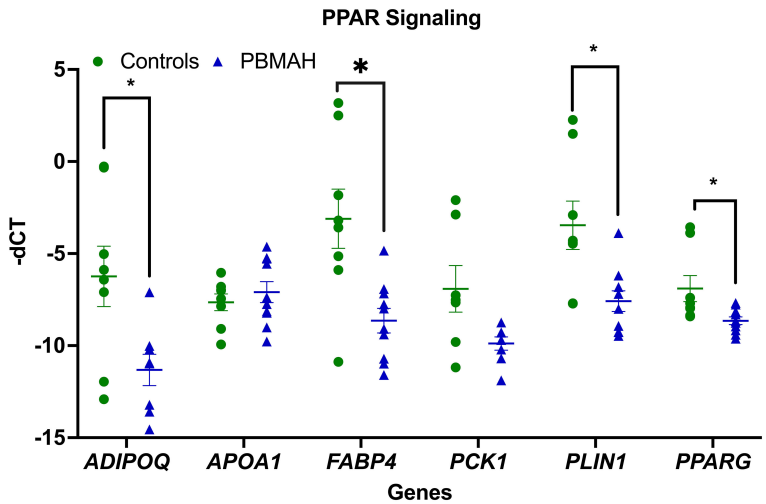

FIGURE 3
QPCR analyses of the significant genes from pathway analyses. Expression analysis of the pathway genes from PPARG signaling. Data are represented as mean ± standard error of mean (SEM) of -dCT values. Housekeeping gene: *Ppia*. *p-value <0.05 and FDR<0.05. PBMAH, Primary Bilateral Macronodular Hyperplasia.

10.3389/fendo.2023.1265794

TABLE 2 Comparison of significant log2Fold Change (p<0.05) of PPARG and its target genes in the validation and discovery cohort of PBMAH in comparison to controls.

PBMAH vs Controls	Discovery Cohort (PBMAH)		Validation Cohort (PBMAH-FFPE)
Gene	NGS	QPCR	NGS
ADIPOQ	-5.8	-5.0	-8.4
FABP4	-2.3	-5.5	-6.1
PLIN1	-2.9	-4.1	-9.1
PPARG	-2.0	-1.7	-7.3

H295R cells were found to show a decrease in *MC2R* expression upon ACTH treatment (Figure 6). The activation of PPARG in the cell lines was assayed for cell viability, gene expression changes, and effect on steroidogenesis. Rosiglitazone, an insulin sensitizer formerly used in diabetes therapy, was used as a PPARG activator.

3.5.1 Cell viability

Cell viability was assessed under varying ACTH and rosiglitazone concentrations. Rosiglitazone impaired NCI-H295R and MUC1 cell viability (Figures 7A, B): a trend of decreased cell viability was found using 5μM with significant reductions at the consecutive doses of 10, 20 and 40μM. ACTH stimulation did not interfere with the apoptotic effect of rosiglitazone as significant reduction in cell viability was found over all ACTH concentrations. In CU-ACC2 cells, rosiglitazone did not have any effect on cell viability in presence or absence of ACTH (Figure 7C).

3.5.2 PPARG activation

PPARG and *MC2R* expression were assessed in the absence or presence of ACTH (2.5nM), to understand whether the observed loss in cell viability was a direct effect of *PPARG* activation (Figure 8). In the absence of ACTH, all tested cell lines showed *PPARG* expression to increase with increasing doses of rosiglitazone. Briefly, significant increased *PPARG* expression was found at 10 and 20μM of rosiglitazone in NCI-H295R (Figure 8A), at 20μM of rosiglitazone in MUC1 (Figure 8B), and at 10 and 20μM of rosiglitazone in CU-ACC2 (Figure 8C). In the presence of ACTH, a more pronounced *PPARG* activation was found with significantly increased *PPARG* expression at all analyzed doses (Figures 8A–C). In case of *MC2R*, the cell lines showed varying results: In NCI-H295R, rosiglitazone treatment led to significantly downregulated *MC2R* expression, both in presence and absence of ACTH (Figure 8D). MUC1 cells showed upregulated *MC2R* expression both in the presence and absence of ACTH (Figure 8E). In CU-ACC2 cells, no changes in *MC2R* expression were found in the absence of ACTH. However, in the presence of ACTH, rosiglitazone at 20μM was found to significantly increase *MC2R* expression (Figure 8F).

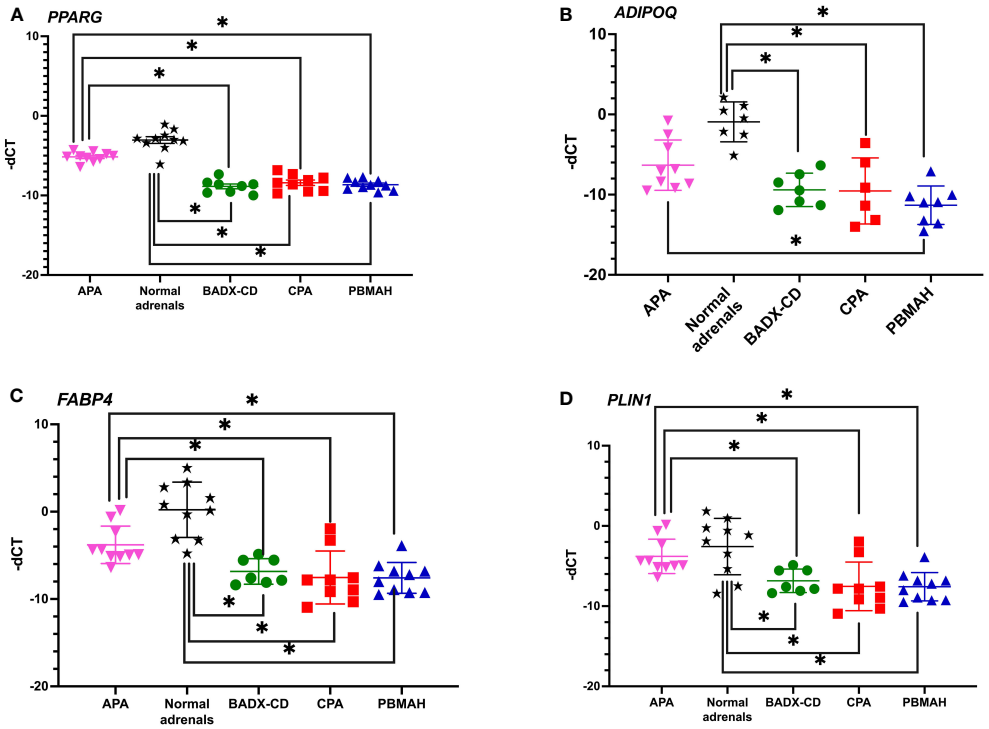

FIGURE 4
QPCR analyses of the significantly altered PPARG pathway genes in CS subtypes. The expression of significantly altered *PPARG* **(A)** and its target genes *ADIPOQ* **(B)**, *FABP4* **(C)**, *PLIN1* **(D)** were tested in CS subtypes of CD and CPA including additional controls of APA and normal adrenals. Data are represented as mean ± SEM of -dCT values. Housekeeping gene: *Ppia*. *p-value <0.05 and FDR<0.05. APA, Aldosterone producing adenoma; CPA, cortisol producing adenoma; BADX-CD, Bilateral adrenalectomized patients with persistent Cushing's Disease.

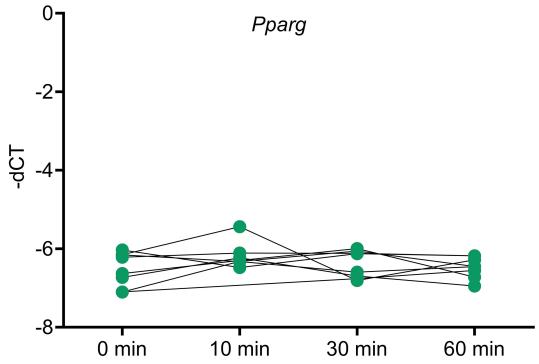

FIGURE 5
Pparg expression in ACTH stimulated murine adrenals. Mice were injected with ACTH and adrenals were collected at different timepoints after ACTH stimulation to assess the impact of ACTH on *Pparg* expression. Housekeeping gene: *Gapdh*. * <0.05 and FDR<0.05 (*).

3.5.3 Steroidome

Based on these findings, the rosiglitazone treatment of 20μM was chosen to estimate the effect of rosiglitazone on steroidogenesis in all cell lines. Briefly, LC-MS/MS analyses revealed that rosiglitazone treatment led to a 30% reduction in cortisol levels in NCI-H295R cells, from a mean value of 3.32 ± 0.42 μg/dl to 1.00 ± 0.19 μg/dl(Figure 9A). The reduction was maintained in the presence of ACTH stimulation with a reduction from 3.24 ± 0.24 μg/dl to 1.181 ± 0.19 μg/dl. Rosiglitazone was also found to significantly reduce cortisone (Figure 9B), aldosterone (Figure 9C), and 21-deoxycortisol (21-df; (Figure 9D) levels in NCI-H295R. In NCI-H295R, no other significant changes were observed (Figures 9E–I, S4, S5). In case of MUC1, no detectable levels of cortisol, cortisone, aldosterone, 21-deoxycortisol and 11-deoxycortisol were seen (Figures 9A–E). However, a significant increase in DHEA levels coupled with a significant reduction in DHT levels was found upon rosiglitazone treatment (Figures 9H, I). The significant change was also maintained in the presence of ACTH in MUC1. There was no change in the other androgens and precursor levels (Figure S5), including testosterone (Figure 9G). Interestingly, CU-ACC2 cells had higher cortisol and cortisone levels compared to both MUC1 and NCI-H295R, but without changes upon rosiglitazone and/or ACTH treatment (Figures 9A, B). The observation was confirmed to be a property of the CU-ACC2 cells and not affected by the hydrocortisone in the media by repeating the experiment with medium containing no hydrocortisone (data not shown).

3.5.4 PPARG target genes

Finally, the expression of PPARG target genes was analyzed at 20μM rosiglitazone concentration in comparison to the controls (0μM rosiglitazone), in presence and absence of ACTH (2.5nmACTH). Interestingly, no expression of *ADIPOQ* was found in any of the cell lines (no amplification by QPCR, data not shown). Expression of *FABP4* was observed only in NCI-H295R and in CU-ACC2 on a low level but with no major changes upon rosiglitazone treatment (Figure S6). In case of *PLIN1*, expression was observed in all the cell lines, however, significant activation by rosiglitazone was observed only in NCI-H295R (Figure 10).

4 Discussion

Previous molecular approaches on the pathology of PBMAH have been directed primarily towards molecular heterogeneity (29) and genetic predispositions involving *ARMC5* (30) and

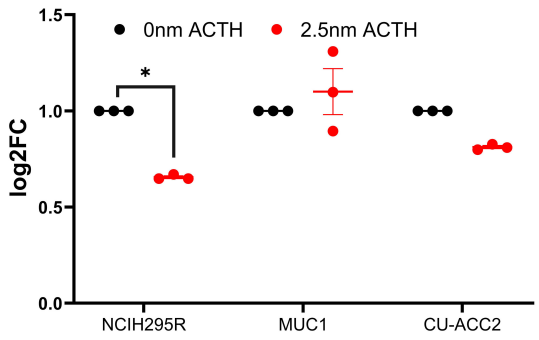

FIGURE 6
Effect of ACTH treatment on *MC2R* expression in adrenocortical cell lines. Data are represented as mean ± SEM of log2Fold Change (log2FC) expression values normalized to the control samples. Housekeeping gene: *ACTB*. *p-value <0.05 and FDR<0.01.

10.3389/fendo.2023.1265794

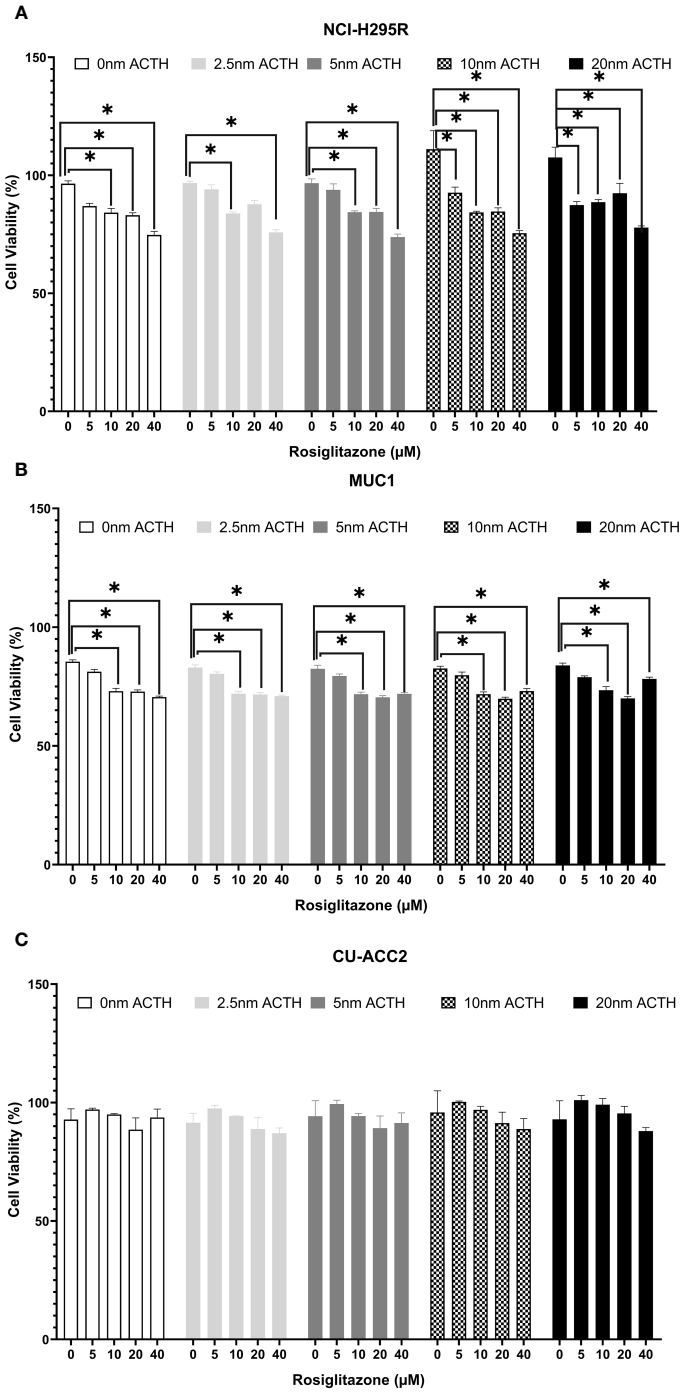

FIGURE 7
Effect of rosiglitazone and ACTH treatment on cell viability in three different adrenocortical cell lines: NCI-H295R **(A)**, MUC1 **(B)** and CU-ACC2 **(C)**. Cell viability was evaluated by WST-1 assay (n=8 in each group). The cells were treated with increasing concentrations of rosiglitazone (0, 5, 10, 20 and 40 μM) and ACTH (0, 2.5,5,10 and 20 nm). The average absorbance values of each treatment group were normalized to background control group. Data are represented as percentage mean ± SEM of the normalized absorbance values. *p-value <0.0005 and FDR<0.01.

KDM1A (11). Herein, we present a transcriptomic profile of PBMAH in comparison to controls. This enabled a targeted characterization of the molecular factors that are dysregulated in genes attest to this point. The highly different transcriptome profile with more than 1000 dysregulated genes attest to this point. Interestingly, the top dysregulated genes included *IGFN1* (l2fc=5.7, pvalue<0.005) and *TCF23* (l2fc=5.2, p-value<0.005) that had been previously identified by Di Dalmazi, Altieri et al. (31) in RNAseq analyses of CPA. In the same study neuronal pathways were found to be differentially expressed in mild autonomous producing adrenocortical adenomas and ACC, which is in line with our findings. Taken together, it could be speculated that neuronal pathway genes could represent a major differentially regulated pathway group in adrenal pathology. Validation of the

10.3389/fendo.2023.1265794

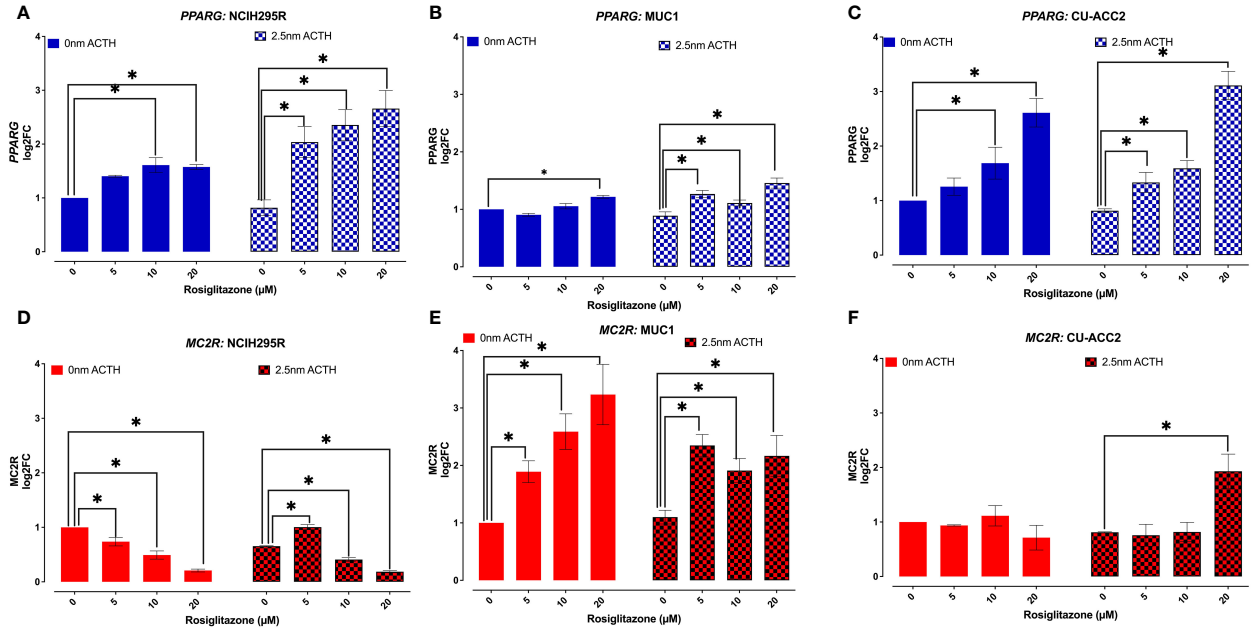

FIGURE 8
Effect of rosiglitazone and ACTH treatment on *PPARG* and *MC2R* expression in adrenocortical cell lines. The cells were treated with increasing concentrations of rosiglitazone (0,5,10,20 and 40 μM) and the expression was checked in the presence (2.5nm) and absence of ACTH. Data are represented as mean ± SEM of log2Fold Change (log2FC) expression values normalized to the control samples. Housekeeping gene: *ACTB*. *p-value <0.05 (*).

pathway by QPCR identified a trend towards downregulation but it was not found to be significant.

Interestingly, the druggable pathway of PPARG signaling was identified as another top hit. *PPARG* downregulation is known to occur in pituitary corticotropic cells of CD patients (32), however, this is the first identification of its dysregulation in adrenals of CS patients. The pathway dysregulation was validated in the PBMAH samples of the discovery cohort as well as in additional cohorts of tumors associated with hypercortisolism such as CPA and BADX-CD. Also, in adrenal samples of APA, downregulation of *PPARG* and its target genes were found. This is in line with previous findings from Williams et al. (33). However, downregulation of *PPARG* pathway and its target genes were much more pronounced in the adrenal samples of CPA, BADX-CD and PBMAH in comparison to APA.

Since the first clinical application of PPARG agonists, thiazolidinediones (TZD) in 1997, there have been various studies exploiting the activation of PPARG pathway in various pathologies, including CD, regulation of steroidogenesis and adrenocortical tumors with varying results (34). Therefore, a comprehensive analysis of PPARG activation was done in three different adrenocortical cell lines – NCI-H295R, MUC1 and CU-ACC2 – varying concentrations of ACTH and rosiglitazone. These adrenocortical cell lines were chosen for experimentation due to the absence of established benign *in vitro* models for CS. Interestingly, none of the cell lines used in our study were to show upregulated *MC2R* expression, characteristic of adrenocortical cells to increase steroidogenesis via This MC2R mediated activation initiates a signaling cascade of. 3′,5′-cyclic AMP, protein kinase A, hormone-sensitive lipase, and steroidogenic acute regulatory protein (10). Rather, the NCIH295R cells showed a downregulation of *MC2R* upon ACTH stimulation (Figure 6) with no accompanying changes in steroidogenesis (Figure 10). Interestingly, downregulated *MC2R* expression have been observed in cortisol secreting adrenocortical carcinomas (35–37) and studies in canine models of ACC have suggested that cortisol regulates interrenal expression of *MC2R* in response to ACTH in a negative short-loop feedback (36, 38, 39). It could be speculated that the downregulated *MC2R* expression we found in the NCIH295R cells could be an indication of this negative short-loop feedback and with respect to this reaction in presence of ACTH, the NCIH295R cells could be said to be ACTH responsive. However, it should be noted that further mechanistic elaboration of the response is beyond the scope of the current study. In NCI-H295R cells rosiglitazone treatment decreased cell viability (Figure 7A) and transcriptionally activated *PPARG* at all ACTH concentrations (Figure 8A). The *PPARG* activation was also found to modulate *MC2R* expression, leading to its downregulation, both in the presence and absence of ACTH (Figure 8A). It could be hypothesized that in NCI-H295R, rosiglitazone reduces the *MC2R* expression to counteract the effects of ACTH mediated cortisol production. Furthermore, among the PPARG target genes only *PLIN1* was found to show upregulated expression upon rosiglitazone treatment in the cell line (Figure 10). Similarly, the downregulation of *PLIN1* was found to be specific only to CS, in contrast to *ADIPOQ* and *FABP4*, which were also downregulated significantly in APA (Figure 4). Interestingly, PLIN1 has been characterized to have a critical role in lipolysis (40) and has been associated with cholesteryl ester droplets in steroidogenic

10.3389/fendo.2023.1265794

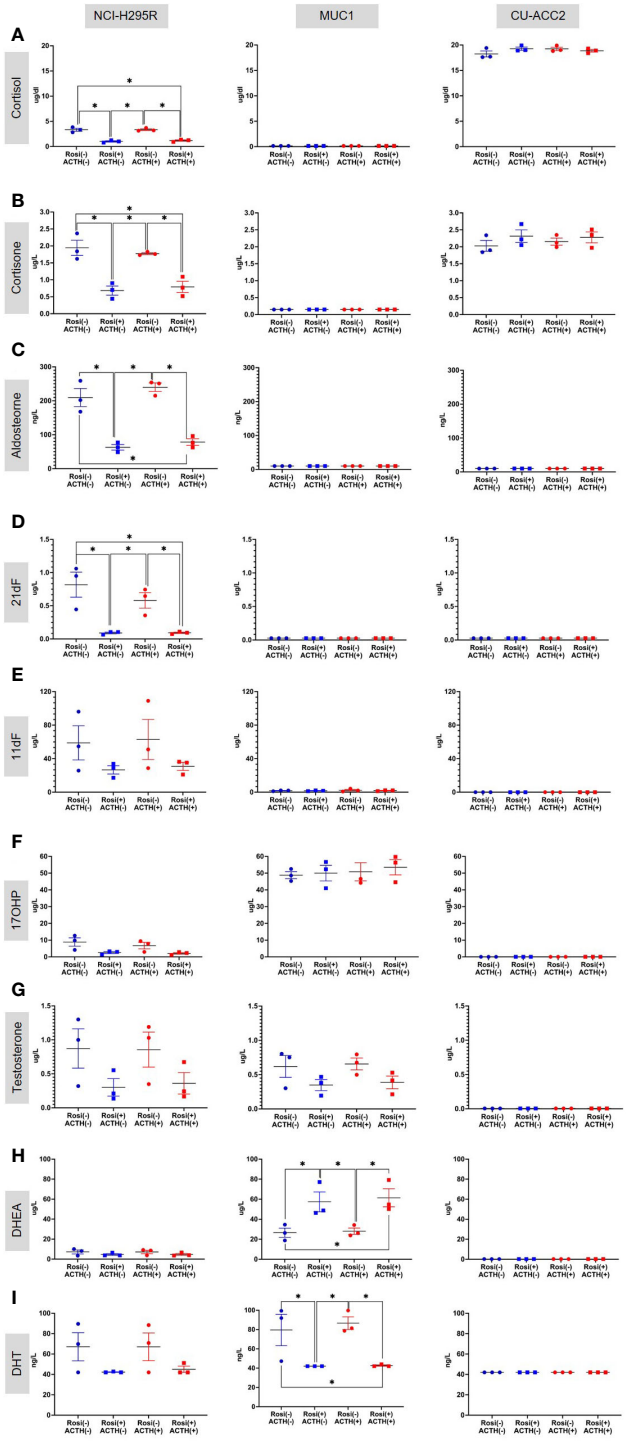

FIGURE 9
Effect of rosiglitazone (20μM) and ACTH (2.5 nm) treatment on the steroidome of adrenocortical cell lines. LC-MS/MS was used to quantify the steroidome in the supernatant of cells treated with rosiglitazone and ACTH and their respective controls. Importantly, the levels of glucocorticoids – cortisol **(A)**, cortisone **(B)** and aldosterone **(C)**, precursors of cortisol – 21-deoxycortisol [21-dF;**(D)**], 11-deoxycortisol [11-dF; **(E)**] and 17-hydroxyprogesterone [17OHP;**(F)**], androgens – testosterone **(G)**, DHEA **(H)** and dihydrotestosterone [DHT;**(I)**] were quantified. Data are represented as mean ± SEM of individual concentration values (μg/L). *p-value <0.05 and FDR<0.05 (*).

adrenocortical cells (41). In summary, PPARG activation by rosiglitazone in NCI-H295R cells alleviates hypercortisolism by cell death, via *MC2R* and the target gene of *PLIN1*. Considering the complex interplay among *PPARG*, *MC2R*, and *PLIN1*, it could be hypothesized that the modulation of PPARG by rosiglitazone could reduce suppressed lipid-mediated signaling. This could be particularly relevant in conditions characterized by suppressed inflammatory responses, such as CS and adrenocortical cancer.

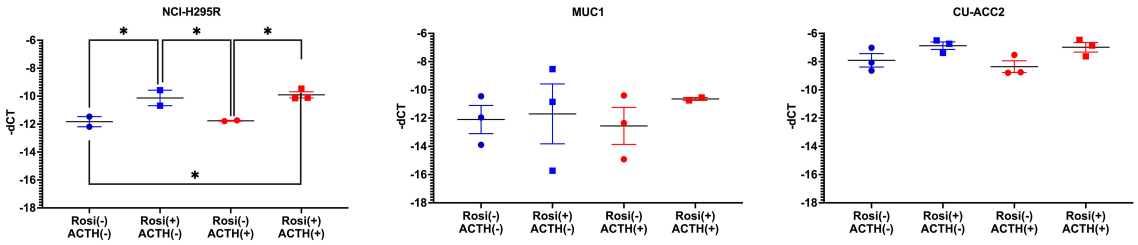

FIGURE 10
Expression of *PLIN1*, PPARG target gene, in adrenocortical cell lines treated with rosiglitazone (20μM) and ACTH (2.5 nm). Data are represented as mean ± SEM of -dCT values. Housekeeping gene: *ACTB*. *represents p-value <0.05 and FDR<0.05 (*).

In comparison to the promising effects in NCI-H295R, MUC1 and CU-ACC2 cells showed varying results in response to rosiglitazone treatment, where we observed a loss in cell viability only in MUC1 (Figure 7B) accompanied by an upregulation of *MC2R* and *PPARG* expression (Figures 8C, D). Interestingly, in one of the earlier studies performed on the primary NCI cell strains, rosiglitazone was also found to increase *MC2R* expression, decrease cell viability and promote steroidogenesis (42). Steroidome analyses showed that MUC1 cells have altered levels of DHT and DHEA upon rosiglitazone treatment. The effect of rosiglitazone treatment on DHT, DHEA levels in MUC1 combined with altered aldosterone and cortisone levels in NCI-H295R hint at an extended therapeutic effect of rosiglitazone on a range of adrenocortical steroids including cortisol. Contrarily, CU-ACC2 cells secrete cortisol but did not show any significant cell death or reduction in cortisol levels in response to rosiglitazone treatment (Figure 7C). Of note, CU-ACC2 cells had generally higher levels of cortisol and cortisone as NCI-H295R, however, no detectable level of their precursors (Figure 9). Therefore, this discrepancy in the modulation effects induced by rosiglitazone in the steroidogenically active NCI-H295R and CU-ACC2 could be the result of a suppressed classical cortisol synthesis pathway in CU-ACC2. The variability in cortisol secretion among the cell lines could also be explained by the varied malignant genetic background of the cell lines (43). Therefore, the consistently observed *PPARG* and *MC2R* regulation by rosiglitazone in the adrenocortical cell lines holds potential for prospective CS therapies.

In summary, we found the PPARG pathway to be prominently downregulated in adrenals in different CS subtypes including CPA and CD. The dysregulation was observed in all samples, irrespective of the mutational status, indicating that it is strongly linked to hypercortisolism and not to the specific genetic backgrounds found in CS. The *in vitro* activation using rosiglitazone yielded promising results with significant effects on cell viability, gene expression and steroidogenesis depending on the adrenocortical carcinoma cells used (Table 3). Therefore, rosiglitazone therapy has the potential of providing a therapeutic for a subset of adrenal CS patients as well, including PBMAH. This aligns with the findings from clinical trials in Cushing's disease (CD), where rosiglitazone demonstrated the ability to reduce cortisol levels in a subgroup of patients (44, 45). Nevertheless, it is imperative to emphasize that additional research is essential to validate this potential fully. Given that Cushing is a metabolic disorder, our established *in vitro* models may not encompass all the necessary elements to comprehensively investigate the therapeutic effects of PPARG pathway. Therefore, the incorporation of primary cultures derived from CS patients could offer a valuable alternative for future investigations. Moreover, a targeted therapy designed for ectopic receptors in PBMAH (46), can be combined with rosiglitazone to potentially augment treatment outcomes. Furthermore, conducting mechanistic studies to elucidate the interplay between the PPARG pathway and pathological processes like inflammation and cortisol synthesis would provide a more comprehensive understanding of rosiglitazone's application as a therapy for CS.

TABLE 3 Cumulative analyses of the effect of rosiglitazone treatment on adrenocortical cell lines.

Effects of Rosiglitazone treatment on	NCI-H295R	MUC1	ACC2
Cell viability	Reduced	Reduced	No change
ACTH responsiveness	Responsive	No change	No change
PPARG expression	Activated	Activated	Activated
MC2R expression	Downregulated	Upregulated	Upregulated (2.5nm ACTH)
Steroidogenesis	aldosterone, cortisol and cortisone levels decreased	No cortisol production	dihydrotestosterone (DHT) levels decreases
Target genes	Perilipin-1 activated	No change/ low expression	No change/low expression

Data availability statement

Table of the significant genes from the NGS data are deposited Ain the supplementary data (Table S2). As Cushing, being a rare disease, the sequence information provided could be traced back to the patients and therefore, not readily available because of data protection. However, reasonable requests (for research purpose) to access the complete datasets should be directed to the corresponding author.

Ethics statement

The study was conducted according to the guidelines of the Declaration of Helsinki and approved by the Ethics Committee of the Ludwig Maximilian University, Munich (protocol code 379-10, 152-10 and 20 July 2021). Informed consent was obtained from all subjects involved in the study. The studies were conducted in accordance with the local legislation and institutional requirements. The participants provided their written informed consent to participate in this study. All mice were maintained in accordance with facility guidelines on animal welfare and approved by Landesdirektion Sachsen, Germany. The studies were conducted in accordance with the local legislation and institutional requirements. Written informed consent was obtained from the owners for the participation of their animals in this study. Written informed consent was obtained from the individual(s) for the publication of any potentially identifiable images or data included in this article.

Author contributions

SV: Formal Analysis, Methodology, Software, Supervision, Writing – original draft, Conceptualization, Visualization, Data curation, Investigation. MT: Investigation, Methodology, Validation, Writing – review & editing. AO: Writing – review & editing. RZ: Writing – review & editing. AK: Methodology, Writing – review & editing. SJ: Methodology, Writing – review & editing. JB: Methodology, Writing – review & editing. WR: Validation, Writing – review & editing. EN: Investigation, Writing – review & editing. BA: Investigation, Writing – review & editing. MD: Investigation, Writing – review & editing. DW: Investigation, Writing – review & editing. TW: Investigation, Resources, Writing – review & editing. BW: Resources, Writing – review & editing. FB: Writing – review & editing. MR: Funding acquisition, Resources, Writing – review & editing. SS: Conceptualization, Funding acquisition, Resources, Validation, Writing – original draft, Writing – review & editing. AR: Conceptualization, Data curation, Funding acquisition, Project administration, Resources, Supervision, Validation, Writing – original draft, Writing – review & editing.

Funding

The author(s) declare financial support was received for the research, authorship, and/or publication of this article. This work was supported by a grant from the Deutsche Forschungsgemeinschaft (DFG) (within the CRC/Transregio 205/1 "The Adrenal: Central Relay in Health and Disease") to TW, BW, FB, MR, SS and AR and individual grant SB 52/1-1 to SS. This work is part of the German Cushing's Registry CUSTODES and has been supported by a grant from the Else Kröner-Fresenius Stiftung to MR (2012_A103 and 2015_A228).

Acknowledgments

We thank S. Zopp for her technical support.

Conflict of interest

The authors declare that the research was conducted in the absence of any commercial or financial relationships that could be construed as a potential conflict of interest.

The author(s) declared that they were an editorial board member of Frontiers, at the time of submission. This had no impact on the peer review process and the final decision.

Publisher's note

Supplementary material

The Supplementary Material for this article can be found online at: https://www.frontiersin.org/articles/10.3389/fendo.2023.1265794/full#supplementary-material

References

1. Marquardt A, Landwehr LS, Ronchi CL, Di Dalmazi G, Riester A, Kollmannsberger P, et al. Identifying new potential biomarkers in adrenocortical tumors based on mRNA expression data using machine learning. *Cancers* (2021) 13:4671. doi: 10.3390/cancers13184671

2. Kelsall A, Iqbal A, Newell-Price J. Adrenal incidentaloma: cardiovascular and metabolic effects of mild cortisol excess. *Gland Surg* (2020) 9:94. doi: 10.21037/gs.2019.11.19

3. Oreglia M, Sbiera S, Fassnacht M, Guyon L, Denis J, Cristante J, et al. Early postoperative circulating miR-483-5p is a prognosis marker for adrenocortical cancer. *Cancers (Basel)* (2020) 12:724. doi: 10.3390/cancers12030724

4. Fassnacht M, Arlt W, Bancos I, Dralle H, Newell-Price J, Sahdev A, et al. Management of adrenal incidentalomas: European Society of Endocrinology Clinical Practice Guideline in collaboration with the European Network for the Study of Adrenal Tumors. *Eur J Endocrinol* (2016) 175:G1–G34. doi: 10.1530/EJE-16-0467

5. Braun LT, Riester A, Oßwald-Kopp A, Fazel J, Rubinstein G, Bidlingmaier M, et al. Toward a diagnostic score in cushing's syndrome. *Front Endocrinol (Lausanne)* (2019) 10:766. doi: 10.3389/fendo.2019.00766

6. Stratakis C. Cushing syndrome caused by adrenocortical tumors and hyperplasias (corticotropin-independent Cushing syndrome). *Endocr Dev* (2008) 13:117–32. doi: 10.1159/000134829

7. Stratakis CA, Boikos SA. Genetics of adrenal tumors associated with Cushing's syndrome: A new classification for bilateral adrenocortical hyperplasias. *Nat Clin Pract Endocrinol Metab* (2007) 3:748–57. doi: 10.1038/ncpendmet0648

8. Cavalcante IP, Berthon A, Fragoso MC, Reincke M, Stratakis CA, Ragazzon B, et al. Primary bilateral macronodular adrenal hyperplasia: definitely a genetic disease. *Nat Rev Endocrinol* (2022) 18:699–711. doi: 10.1038/s41574-022-00718-y

9. Beuschlein F, Fassnacht M, Assié G, Calebiro D, Stratakis CA, Osswald A, et al. Constitutive activation of PKA catalytic subunit in adrenal Cushing's syndrome. *N Engl J Med* (2014) 370:1019–28. doi: 10.1056/NEJMoa1310359

10. Heinrich DA, Adolf C, Holler F, Lechner B, Schneider H, Riester A, et al. Adrenal insufficiency after unilateral adrenalectomy in primary aldosteronism: long-term outcome and clinical impact. *J Clin Endocrinol Metab* (2019) 104:5658–64. doi: 10.1210/jc.2019-00996

11. Vaczlavik A, Bouys L, Violon F, Giannone G, Jouinot A, Armignacco R, et al. KDM1A inactivation causes hereditary food-dependent Cushing syndrome. *Genet Med* (2022) 24:374–83. doi: 10.1016/j.gim.2021.09.018

12. Feelders RA, Newell-Price J, Pivonello R, Nieman LK, Hofland LJ, Lacroix A. Advances in the medical treatment of Cushing's syndrome. *Lancet Diabetes Endocrinol* (2019) 7:300–12. doi: 10.1016/S2213-8587(18)30155-4

13. Vassiliadi DA, Tsagarakis S. Diagnosis and management of primary bilateral macronodular adrenal hyperplasia. *Endocr Relat Cancer* (2019) 26:R567–81. doi: 10.1530/ERC-19-0240

14. Feelders RA, Hofland LJ, De Herder WW. Medical treatment of cushing's syndrome: adrenal-blocking drugs and ketaconazole. *Neuroendocrinology* (2010) 92:111–5. doi: 10.1159/000314292

15. Liu CH, Di YP. Analysis of RNA sequencing data using CLC genomics workbench. *Methods Mol Biol* (2020) 2102:61–113. doi: 10.1007/978-1-0716-0223-2_4

16. Jouinot A, Lippert J, Sibony M, Violon F, Jeanpierre L, De Murat D, et al. Transcriptome in paraffin samples for the diagnosis and prognosis of adrenocortical carcinoma. *Eur J Endocrinol* (2022) 186:607. doi: 10.1530/EJE-21-1228

17. Livak KJ, Schmittgen TD. Analysis of relative gene expression data using real-time quantitative PCR and the 2–ΔΔCT method. *Methods* (2001) 25:402–8. doi: 10.1006/meth.2001.1262

18. Vetrivel S, Zhang R, Engel M, Oßwald A, Watts D, Chen A, et al. Characterization of adrenal miRNA-based dysregulations in cushing's syndrome. *Int J Mol Sci* (2022) 23:7676. doi: 10.3390/ijms23147676

19. Hantel C, Shapiro I, Poli G, Chiapponi C, Bidlingmaier M, Reincke M, et al. Targeting heterogeneity of adrenocortical carcinoma: Evaluation and extension of preclinical tumor models to improve clinical translation. *Oncotarget* (2016) 7:79292–304. doi: 10.18632/oncotarget.12685

20. Kiseljak-Vassiliades K, Zhang Y, Bagby SM, Kar A, Pozdeyev N, Xu M, et al. Development of new preclinical models to advance adrenocortical carcinoma research. *Endocr Relat Cancer* (2018) 25:437–51. doi: 10.1530/ERC-17-0447

21. Sigala S, Bothou C, Penton D, Abate A, Peitzsch M, Cosentini D, et al. A comprehensive investigation of steroidogenic signaling in classical and new experimental cell models of adrenocortical carcinoma. *Cells* (2022) 11:1439. doi: 10.3390/cells11091439

22. Schweitzer S, Kunz M, Kurlbaum M, Vey J, Kendl S, Deutschbein T, et al. Plasma steroid metabolome profiling for the diagnosis of adrenocortical carcinoma. *Eur J Endocrinol* (2019) 180:117–125. doi: 10.1530/EJE-18-0782

23. Love MI, Huber W, Anders S. Moderated estimation of fold change and dispersion for RNA-seq data with DESeq2. *Genome Biol* (2014) 15:550. doi: 10.1186/s13059-014-0550-8

24. Robinson MD, McCarthy DJ, Smyth GK. edgeR: A Bioconductor package for differential expression analysis of digital gene expression data. *Bioinformatics* (2009) 26:139–40. doi: 10.1093/bioinformatics/btp616

25. Hu Z, Gao S, Lindberg D, Panja D, Wakabayashi Y, Li K, et al. Temporal dynamics of miRNAs in human DLPFC and its association with miRNA dysregulation in schizophrenia. *Transl Psychiatry* (2019) 9:1–17. doi: 10.1038/s41398-019-0538-y

26. Esteva-Socias M, Gómez-Romano F, Carrillo-Ávila JA, Sánchez-Navarro AL, Villena C. Impact of different stabilization methods on RT-qPCR results using human lung tissue samples. *Sci Rep* (2020) 10:1–11. doi: 10.1038/s41598-020-60618-x

27. Ge SX, Jung D, Yao R. ShinyGO: a graphical gene-set enrichment tool for animals and plants. *Bioinformatics* (2020) 36:2628–9. doi: 10.1093/bioinformatics/btz931

28. Vázquez-Carrera M, Wahli W. PPARs as key mediators in the regulation of metabolism and inflammation. *Int J Mol Sci* (2022) 23:5025. doi: 10.3390/ijms23095025

29. Drougat L, Espiard S, Bertherat J. Genetics of primary bilateral macronodular adrenal hyperplasia: A model for early diagnosis of Cushing's syndrome? *Eur J Endocrinol (BioScientifica Ltd.)* 2015 173(4): M121–31. doi: 10.1530/EJE-15-0532

30. Kamilaris CDC, Stratakis CA, Hannah-Shmouni F. Molecular genetic and genomic alterations in cushing's syndrome and primary aldosteronism. *Front Endocrinol (Lausanne)* (2021) 12:142. doi: 10.3389/fendo.2021.632543

31. Di Dalmazi G, Altieri B, Scholz C, Sbiera S, Luconi M, Waldman J, et al. RNA-sequencing and somatic mutation status of adrenocortical tumors: novel pathogenetic insights. *J Clin Endocrinol Metab* (2020) 105(12):dgaa616. doi: 10.1530/endoabs.70.YI3

32. Mannelli M, Cantini G, Poli G, Mangoni M, Nesi G, Canu L, et al. Role of the PPAR-γ System in normal and tumoral pituitary corticotropic cells and adrenal cells. *Neuroendocrinology* (2010) 92:23–7. doi: 10.1159/000314312

33. Williams TA, Monticone S, Urbanet R, Bertello C, Giraudo G, Vettor R, et al. Genes implicated in insulin resistance are down-regulated in primary aldosteronism patients. *Mol Cell Endocrinol* (2012) 355:162–8. doi: 10.1016/j.mce.2012.02.007

34. Heaney AP. PPAR-γ in cushing's disease. *Pituitary* (2004) 7:265–9. doi: 10.1007/s11102-005-1430-8

35. Tacon LJ, Soon PS, Gill AJ, Chou AS, Clarkson A, Botling J, et al. The glucocorticoid receptor is overexpressed in Malignant adrenocortical tumors. *J Clin Endocrinol Metab* (2009) 94:4591–9. doi: 10.1210/jc.2009-0546

36. Agulleiro MJ, Sánchez E, Leal E, Cortés R, Fernández-Durán B, Guillot R, et al. Molecular characterization and functional regulation of melanocortin 2 receptor (MC2R) in the sea bass. A putative role in the adaptation to stress. *PloS One* (2013) 8:e65450. doi: 10.1371/journal.pone.0065450

37. Gummow BM, Scheys JO, Cancelli VR, Hammer GD. Reciprocal regulation of a glucocorticoid receptor-steroidogenic factor-1 transcription complex on the Dax-1 promoter by glucocorticoids and adrenocorticotropic hormone in the adrenal cortex. *Mol Endocrinol* (2006) 20:2711–23. doi: 10.1210/me.2005-0461

38. Galac S, Kool MMJ, Naan EC, Daminet S, Mol JA, Kooistra HS. Expression of the ACTH receptor, steroidogenic acute regulatory protein, and steroidogenic enzymes in canine cortisol-secreting adrenocortical tumors. *Domest Anim Endocrinol* (2010) 39:259–67. doi: 10.1016/j.domaniend.2010.07.001

39. Sanders K, Mol JA, Kooistra HS, Galac S. Melanocortin 2 receptor antagonists in canine pituitary-dependent hypercortisolism: in *vitro* studies. *Vet Res Commun* (2018) 42:283. doi: 10.1007/s11259-018-9737-x

40. Tansey JT, Sztalryd C, Hlavin EM, Kimmel AR, Londos C. The central role of perilipin a in lipid metabolism and adipocyte lipolysis. *IUBMB Life* (2004) 56:379–85. doi: 10.1080/15216540400009968

41. Servetnick DA, Brasaemle DL, Gruia-Gray J, Kimmel AR, Wolff J, Londos C. Perilipins are associated with cholesteryl ester droplets in steroidogenic adrenal cortical and Leydig cells. *J Biol Chem* (1995) 270:16970–3. doi: 10.1074/jbc.270.28.16970

42. Betz MJ, Shapiro I, Fassnacht M, Hahner S, Reincke M, Beuschlein F. Peroxisome proliferator-activated receptor-gamma agonists suppress adrenocortical tumor cell proliferation and induce differentiation. *J Clin Endocrinol Metab* (2005) 90:3886–96. doi: 10.1210/jc.2004-1267

43. Nanba K, Blinder AR, Rainey WE. Primary cultures and cell lines for *in vitro* modeling of the human adrenal cortex. *Tohoku J Exp Med* (2021) 253:217–32. doi: 10.1620/tjem.253.217

44. Ambrosi B, Dall'Asta C, Cannavò S, Libè R, Vigo T, Epaminonda P, et al. Effects of chronic administration of PPAR-gamma ligand rosiglitazone in Cushing's disease. *Eur J Endocrinol* (2004) 151:173–8. doi: 10.1530/eje.0.1510173

45. Giraldi FP, Scaroni C, Arvat E, De Martin M, Giordano R, Albiger N, et al. Effect of protracted treatment with rosiglitazone, a PPARgamma agonist, in patients with Cushing's disease. *Clin Endocrinol (Oxf)* (2006) 64:219–24. doi: 10.1111/j.1365-2265.2006.02452.x

46. Albiger NM, Ceccato F, Zilio M, Barbot M, Occhi G, Rizzati S, et al. An analysis of different therapeutic options in patients with Cushing's syndrome due to bilateral macronodular adrenal hyperplasia: a single-centre experience. *Clin Endocrinol (Oxf)* (2015) 82:808–15. doi: 10.1111/cen.12763

frontiers | Frontiers in Endocrinology

TYPE Original Research
PUBLISHED 07 December 2023
DOI 10.3389/fendo.2023.1279828

OPEN ACCESS

EDITED BY
Silvia Monticone,
University of Turin, Italy

REVIEWED BY
Sergei Tevosian,
University of Florida, United States
Mark Stevenson,
University of Oxford, United Kingdom

*CORRESPONDENCE
Marta Araujo-Castro
marta.araujo@salud.madrid.org

RECEIVED 18 August 2023
ACCEPTED 16 October 2023
PUBLISHED 07 December 2023

CITATION
Araujo-Castro M, García Sanz I, Mínguez Ojeda C, Hanzu F, Mora M, Vicente A, Blanco Carrera C, de Miguel Novoa P, López García MC, Lamas C, Manjón-Miguélez L, del Castillo Tous M, Rodríguez de Vera P, Barahona San Millán R, Recasens M, Tomé Fernández-Ladreda M, Valdés N, Gracia Gimeno P, Robles Lazaro C, Michalopoulou T, Álvarez Escolá C, García Centeno R, Barca-Tierno V, Herrera-Martínez AD and Calatayud M (2023) Local recurrence and metastatic disease in pheochromocytomas and sympathetic paragangliomas. *Front. Endocrinol.* 14:1279828. doi: 10.3389/fendo.2023.1279828

Local recurrence and metastatic disease in pheochromocytomas and sympathetic paragangliomas

Marta Araujo-Castro [1,2*], Iñigo García Sanz [3], César Mínguez Ojeda [4], Felicia Hanzu [5], Mireia Mora [5], Almudena Vicente [6], Concepción Blanco Carrera [7], Paz de Miguel Novoa [8], María del Carmen López García [9], Cristina Lamas [9], Laura Manjón-Miguélez [10], María del Castillo Tous [11], Pablo Rodríguez de Vera [11], Rebeca Barahona San Millán [12], Mónica Recasens [12], Mariana Tomé Fernández-Ladreda [13], Nuria Valdés [14], Paola Gracia Gimeno [15], Cristina Robles Lazaro [16], Theodora Michalopoulou [17], Cristina Álvarez Escolá [18], Rogelio García Centeno [19], Verónica Barca-Tierno [20], Aura D. Herrera-Martínez [21] and María Calatayud [22] and Adrenal Group of the Spanish Society of Endocrinology Nutrition (SEEN)

[1]Endocrinology & Nutrition Department, Hospital Universitario Ramón y Cajal, Madrid, Spain, [2]Instituto de Investigación Biomédica Ramón y Cajal (IRYCIS), Madrid, Spain, [3]General & Digestive Surgery Department, Hospital Universitario de La Princesa, Madrid, Spain, [4]Urology Department, Hospital Universitario Ramón y Cajal, Madrid, Spain, [5]Endocrinology & Nutrition Department, Hospital Clinic, Barcelona, Spain, [6]Endocrinology & Nutrition Department, Hospital Universitario de Toledo, Toledo, Spain, [7]Endocrinology & Nutrition Department, Hospital Universitario Príncipe de Asturias, Madrid, Spain, [8]Endocrinology & Nutrition Department, Hospital Clínico San Carlos, Madrid, Spain, [9]Endocrinology & Nutrition Department, Hospital Universitario de Albacete, Albacete, Spain, [10]Endocrinology & Nutrition Department, Hospital Universitario Central de Asturias, Oviedo, Spain & Instituto de Investigación Sanitaria del Principado de Asturias (ISPA), Oviedo, Spain, [11]Endocrinology & Nutrition Department, Hospital Universitario Virgen de la Macarena, Sevilla, Spain, [12]Endocrinology & Nutrition Department, Institut Català de la Salut Girona, Girona, Spain, [13]Endocrinology & Nutrition Department, Hospital Universitario de Puerto Real, Cádiz, Spain, [14]Endocrinology & Nutrition Department, Hospital Universitario Cruces, Biobizkaia, Bizkaia, Spain, [15]Endocrinology & Nutrition Department, Hospital Royo Villanueva, Zaragoza, Spain, [16]Endocrinology & Nutrition Department, Hospital Universitario de Salamanca, Salamanca, Spain, [17]Department of Endocrinology and Nutrition, Joan XXIII University Hospital, Tarragona, Spain, [18]Endocrinology & Nutrition Department, Hospital Universitario La Paz, Madrid, Spain, [19]Endocrinology & Nutrition Department, Hospital Universitario Gregorio Marañón, Madrid, Spain, [20]Genetic Department, Hospital Universitario Ramón y Cajal, Madrid, Spain, [21]Endocrinology & Nutrition Department, Hospital Reina Sofía, Córdoba, Spain, [22]Endocrinology & Nutrition Department, Hospital Universitario Doce de Octubre, Madrid, Spain

Purpose: To evaluate the rate of recurrence among patients with pheochromocytomas and sympathetic paragangliomas (PGLs; together PPGLs) and to identify predictors of recurrence (local recurrence and/or metastatic disease).

Methods: This retrospective multicenter study included information of 303 patients with PPGLs in follow-up in 19 Spanish tertiary hospitals. Recurrent disease was defined by the development of local recurrence and/or metastatic disease after initial complete surgical resection.

Results: A total of 303 patients with PPGLs that underwent 311 resections were included (288 pheochromocytomas and 15 sympathetic PGLs). After a median follow-up of 4.8 years (range 1-19), 24 patients (7.9%) had recurrent disease (3 local recurrence, 17 metastatic disease and 4 local recurrence followed by metastatic disease). The median time from the diagnosis of the PPGL to the recurrence was of 11.2 months (range 0.5-174) and recurrent disease cases distributed uniformly during the follow-up period. The presence of a pathogenic variant in *SDHB* gene (hazard ratio [HR] 13.3, 95% CI 4.20-41.92), higher urinary normetanephrine levels (HR 1.02 per each increase in standard deviation, 95% CI 1.01-1.03) and a larger tumor size (HR 1.01 per each increase in mm, 95% CI 1.00-1.02) were independently associated with disease recurrence.

Conclusion: The recurrence of PPGLs occurred more frequently in patients with *SDHB* mutations, with larger tumors and with higher urinary normetanephrine levels. Since PPGL recurrence may occur at any time after the initial PPGL diagnosis is performed, we recommend performing a strict follow-up in all patients with PPGLs, especially in those patients with a higher risk of recurrent disease.

KEYWORDS

adrenal tumor, SDHB gene, recurrent disease, metastatic PPGL, catecholamines

1 Introduction

Pheochromocytomas and paragangliomas (PGLs) –together PPGLs– are neuroendocrine tumors derived from chromaffin cells of the adrenal medulla or extra-adrenal paraganglionic tissue, respectively (1). They are considered rare tumors, occurring in about 0.05% to 0.1% of patients with sustained hypertension. It is estimated that the joint annual incidence of PPGL is of 2–8 cases per million inhabitants (1). Although they are rare tumors, they are considered one of the most frequent inherited tumors since about one tumor in four are linked to a genetic disease (2). The most common hereditary syndromes are those associated with pathogenic variants in the different subunits of *SDH* (15–20%), in the *VHL* gene (9%), in the *RET* proto-oncogene (5%) and in the *NF1* gene (2%). Currently, targeted Next Generation Sequencing (NGS) is the recommended approach to enable the testing of all relevant genes potentially associated with PPGL development in a single panel (3). The characterization of the genetic status of PPGL is of paramount importance given the well-known genotype-phenotype correlation in these tumors. This correlation includes associated biochemical profile, tumor location, malignant potential, and overall prognosis. In addition, genetic identification provides valuable information for establishing a treatment plan and procures the rational for an appropriate guidance for follow-up surveillance (4).

PPGLs are usually curable with the removal of the catecholamine secreting tumor. However, both pheochromocytomas and PGLs may recur as a benign or malignant tumor. In this sense, it is estimated that about 5% to 20% of PPGLs exhibit recurrence, and it can occur even after several decades after primary tumor resection (5–8). This fact justifies the need of a long-term follow-up for all patients with PPGLs who have undergone surgery (9). Surgery after local recurrence of PPGLs represents a major technical challenge and the only curative option for these patients. Although laparoscopic resection is possible in selected cases, it may be limited by the presence of multiple associated neoplasms and the impossibility of lymph node clearance (7). Another, even more challenging situation, is the development of metastatic disease, since therapeutic options for metastatic disease are limited; thus the management of all of these cases should be carried out by a multidisciplinary reference team (10). In this context, some factors, including genetic status, tumor size and location, among others, have been associated to a higher likelihood of metastatic PPGLs development (11–17). In this regard, some studies found that plasma methoxytyramine is the most accurate biomarker for discriminating patients with and without metastases, with a plasma methoxytyramine 4.7-fold higher in patients with than without metastases (11). Other authors describe larger increases of norepinephrine in malignant than in benign disease (14). A higher malignant risk associated with tumors due to mutations of *SDHB* gene or arising from extra-adrenal locations has been reported by several series (12, 15). Most studies also agree that there is an association between tumor size and the risk of malignancy in PPGLs (15–17). Other authors identified as risk factors of metastatic disease, an early onset postoperative hypertension, higher plasma or urine metadrenaline and the expression of the 3 angiogenesis related genes *VEGF*, *COX-2* and *MVD* (17). Thus, in general, there is no clear consensus on which are the risk factors for metastatic disease in PPGLs. In addition, the available data on the natural history of pheochromocytomas and PGLs after radical surgery are heterogeneous and discordant. Moreover, most of these studies are unicentric and include a limited number of cases. Thus, considering this background, the aim of our study was to find clinical predictors of recurrence (including local recurrence and metastatic

disease) in patients with pheochromocytomas and sympathetic PGLs that underwent radical surgery.

2 Methods

2.1 Study design

A Spanish multicentric retrospective study of patients who underwent surgical resection of a PPGL between 1998 and 2022 in 19 tertiary hospitals was carried out. As we have previously described (18), the following criteria should be met to enter in the PHEO-PARA risk study: i) an age at diagnosis of the PPGL older than 17 years old; ii) histological diagnostic confirmation of PPGL, iii) available clinical, biochemical, and radiological information at the diagnosis of the PPGL and during follow-up and iv) absence of evidence of metastatic disease at the time of the diagnosis. Among all patients, 303 patients with PPGLs who underwent to 311 resections met the inclusion criteria and were included (288 pheochromocytomas and 15 sympathetic PGLs) (Figure 1).

The Ethics Committee of Hospital Universitario Ramón y Cajal has reviewed and approved the study on 22nd of April 2021, ACTA 411.

PPGL: pheochromocytomas and sympathetic paragangliomas. After a median follow-up of 4.8 years (range 1 to 19), 24 patients (7.9%) had recurrent disease (3 local recurrence, 17 metastatic disease and 4 local recurrence followed by metastatic disease).

2.2 Clinical evaluation and definitions

The diagnosis of PPGL was based on the recommendations of the current clinical guidelines (9, 19). Catecholamine hypersecretion was assessed by the determination of plasma-free metanephrines, 24-h urinary fractionated metanephrines and/or 24-h urinary catecholamines. Considering that different normal ranges were applied for these determinations in the different local laboratories, the number of times (standard deviations: SD) above the upper limit of normal for each value was calculated and used for the analysis.

Hereditary PPGL diagnosis was based on the presence of a pathogenic germline variant in known susceptibility genes. As we have previously described (18), in all patients with a negative genetic study, at least the following genes have been sequenced: *NF1, RET, VHL, SDHA, SDHB, SDHC*, and *SDHD*. In addition, most of the centers tested also other genes, including *SDHAF2, SDHAF1, MAX, HIF1A, HIF2A, TMEM127, HRAS, KRAS, GOT2, FH, MDH2, SLC25A11, DNMT3A, DLST, MERTK, IDH1, IDH2, CSED1, EGLN1, EGLN2, BRAF, MET, FGFR1, KIF1B,CDKN1B, MEN1, PTEN, H3F3a, ATRX*, and the promoter region of *TER*. Positive genetic study was based on the demonstration of a pathogenic variant in at least one of these genes; those cases with variants of uncertain significance (VUS) were excluded. Cardiovascular disease was defined as the presence of ischemic and/or hypertensive heart disease, heart failure, cardiac arrhythmias and/or valvular disease. Obesity was defined as a body mass index ≥ 30 kg/m^2 and diabetes definition was based on the last American Diabetes Association (ADA) recommendations (20). As we have previously reported (21), hypertensive PPGL was defined when systolic blood pressure was > 140 mmHg and/or diastolic blood pressure > 90 mmHg before surgery, or the patient was under medical treatment with antihypertensive drugs.

Recurrent disease was defined as the development of a local and/or metastatic disease during follow-up after the confirmation of surgical cure. Local recurrence was diagnosed when a local relapse occurred; and we considered metastatic PPGLs when recurrence occurred at sites where chromaffin tissue is normally absent. Follow-up period was defined as the time between the date of the PPGL diagnosis to the last available follow-up visit in the Endocrinology Department in patients with non-recurrent disease, and between the date of the PPGL diagnosis to the date of the diagnosis of recurrent disease in patients with recurrent PPGL. All patients were followed-up annually with hormonal values and with CT/MRI associated with nuclear medicine imaging if there were suspicions of tumor recurrence.

2.3 Statistical analysis

The statistical analysis was performed using STATA.15 (StataCorp LLC, College Station, Texas, USA). Continuous variables were described as means ± SD for normally distributed data or medians and interquartile ranges for non-normal distributions and compared using two-tailed t test. Categorical variables were expressed as percentage and absolute numbers and were compared using the chi2 test. To describe the timing of recurrence, the cumulative incidence was estimated using the Kaplan–Meier method. Statistical significance ($p < 0.05$) of differences in the cumulative incidence of recurrence between groups was tested using

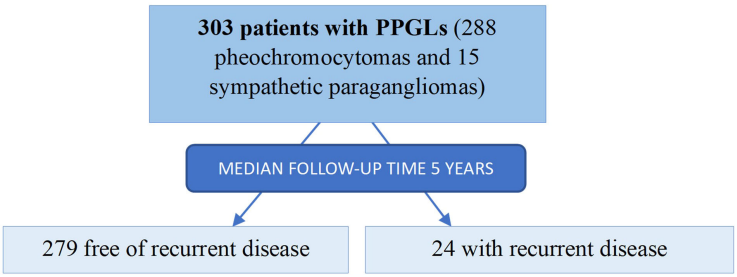

FIGURE 1
Study population.

10.3389/fendo.2023.1279828

the log-rank test for homogeneity. A univariant Cox proportional hazard model was employed to estimate the crude hazard ratios (HRs) and the multivariant Cox proportional hazard model for the estimation of multivariable-adjusted HRs with 95% confidence intervals (CIs) and to evaluate possible predictors of recurrence.

3 Results

3.1 Baseline characteristics

A total of 303 patients with PPGLs that underwent 311 resections were included (288 pheochromocytomas and 15 sympathetic PGLs). Open surgery was performed in 41 PPGLs (including thoracotomy in 2 sympathetic PGL) and in the rest of the cases laparoscopic surgery was performed. Hereditary PPGL was confirmed by genetic analysis in 93 out of the 265 patients (35.1%) with available genetic results (in the remaining 38 patients, genetic study was not performed, or results were still pending). The most common pathogenic variant was in the *RET* gene causing MEN2A syndrome (n=45), followed by in the *NF1* gene (n=19), in the *SDHB* gene (n=14) and in the *VHL* gene (n=6). The pathogenic variant on these genes is not known in all cases, but for the RET pathogenic variant this information was available in 14 cases, being the mutation in exon 11 at codon 634 (p.Cys634Phe; TGC-TTC; n=8) and at codon 618 (p.Cys618Arg;:TGC>CGC; n=5) the most common pathogenic variants. One patient had a mutation at codon 634 (p.Cys634Tyr; TGC>TAC), and the information was lacking for the remaining patients. Personal and clinical characteristics of the patients at the time of the diagnosis are shown in Table 1.

TABLE 1 Baseline patient´s characteristics.

Variable	Patients (n=303)
Female sex	51.8% (n=157)
Age (years)	52 (range 18-81)
Hereditary PPGL [n=265]	35.1% (n=93)
Hypertension	72.3% (n=219)
Systolic blood pressure at diagnosis (mmHg)	133 (range 96-220)
Diastolic blood pressure at diagnosis (mmHg)	80 (range 50-135)
Diabetes	26.4% (n=80)
Fasting plasma glucose levels (mg/dL)	101 (range 70-283)
Obesity	16.2% (n=49)
Body mass index, kg/m2 [n=272]	25.7 (range 17.6-43.9)
Cardiovascular disease	13.2% (n=40)
Cerebrovascular disease [n=301]	4.7% (n=14)
Smoker [n=265]	25.3% (n=67)
Glomerular filtration rate (ml/min/ 1.73m^2)	85 (range 38-165)
Catecholamine phenotype [n=223]	32.7% noradrenergic; 17.9% adrenergic; 48.4% mixed and 1% dopaminergic
Urine metanephrine (SD) [n=175]	1.4 (range 0-85)
Urine normetanephrine (SD) [n=153]	2.4 (range 0.1-70)
Urine epinephrine (SD) [n=203]	1.4 (range 0-42)
Urine norepinephrine (SD) [n=212]	1.6 (range 0.1-46.5)
Urine dopamine (SD) [n=164]	0.5 (range 0-8.4)
Plasmatic metanephrine (SD) [n=68]	1.5 (range 0-31.6)
Plasmatic normetanephrine (SD) [n=67]	3.4 (range 0.3-35.9)
Tumor size (mm) [n=292]	42 (range 10-136)
Tumor >40 mm [n=292]	51.0% (n=149)
Bilateral tumor	4.6% (n=14)

PPGL, pheochromocytomas and sympathetic paragangliomas; SD, standard deviations. Normal range for systolic blood pressure at diagnosis: <140 mmHg; for diastolic blood pressure: <90 mmHg; for fasting plasma glucose: <100 mg/dL; for glomerular filtration rate: >90 ml/min/1.73m^2. *For variables with missing data, the number of patients with available data is described in brackets.

3.2 Recurrent disease and survival analysis

After a median follow-up of 4.8 years (range 1 to 19), 24 patients (7.9%) had recurrent disease (3 local recurrence, 17 metastatic disease and 4 local recurrence followed by metastatic disease). The most common site of metastasis was the bone (n=9) and the lymph nodes (n=8), followed by the liver (n=5), lungs (n=5), retroperitoneum (n=4), peritoneum (n=2) and neck (n=1); 9 patients having metastasis in two or more sites. The median time from the diagnosis of the PPGL to the diagnosis of the recurrent disease was of 11.2 months (range 0.5 to 174), and the cases of recurrent disease distributed uniformly during the follow-up period (Figure 2). However, the higher cumulative incidence of new cases of recurrence was observed in the period of 0 to 2 years of follow-up (hazard function of 0.03, 95% CI 0.01 to 0.04) (Table 2). In addition, the overall follow-up time was longer in those patients who had recurrence compared with patients free of recurrence (8.1 ± 5.68 vs. 6.0 ± 4.63 years, P=0.040).

The cases of recurrence of the PPGL occurred progressively during the follow-up period, even after 10 years of follow-up. However, the higher risk of recurrence was observed in the period of 0 to 2 years (hazard: 0.026; 95% CI 0.013-0.040).

A total of 12 patients died during follow-up (18.2% of the patients with recurrent disease vs. 2.9% of benign PPGLs, P<0.001). The survival time was significantly lower in those patients with recurrent disease in comparison with those without recurrence (Log-rank test for equality of survivor functions, X^2 18.1, P<0.0001) (Figure 3).

The survival time was lower in those patients with recurrent disease than in those without recurrence (Log-rank test for equality of survivor functions, X2 18.1, P<0.0001).

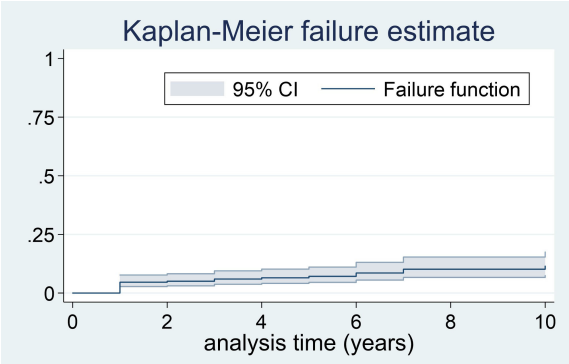

FIGURE 2
Failure curve for recurrent disease in PPGL.

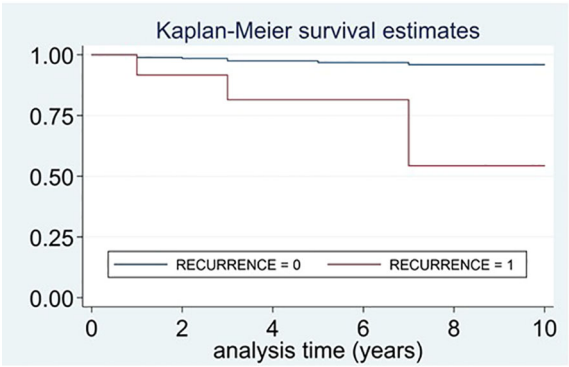

FIGURE 3
Survival curves of patients who died and had recurrent disease vs. patients who died and did not have recurrence.

3.3 Predictors of recurrent disease

In the univariant analysis, a hereditary PPGL, harboring a *SDHB* pathogenic variant, a higher excretion of urine normetanephrine and lower of urine epinephrine, a larger tumor size and having a sympathetic PGL were identified as predictors of recurrent disease (Table 3). *SDHB* mutation was the strongest predictive factor of recurrent disease. Moreover, patients with *SDHB* who had recurrence, developed the recurrence earlier than patients with recurrence without *SDHB* pathogenic variants (1.2 ± 1.67 vs. 3.8 ± 3.95 years, P=0.034). The number of recurrences was significantly higher in *SDHB* mutated PPGLs than in those without the mutation (events expected 23.1% vs. 0.9%, log-rank test; *X2* 63.0, P<0.0001). The median time free of recurrence was significantly higher in PPGL without pathogenic variants in SDHB than in those carrying the pathogenic variants (Figure 4). In fact, the association of recurrent disease and hereditary PPGL disappeared after adjusting by *SDHB* mutational status (adjusted HR 1.29 [0.46-3.66]). Similarly, the association between sympathetic PGL and risk of recurrence disappeared after adjusting by *SDHB* mutational status (adjusted HR 2.64 [0.43-16.46]). The variables that were independently associated with recurrence (in the multivariant analysis) were the presence of *SDHB* pathogenic variant (HR 13.3, 95% CI 4.20-41.92), higher levels of urinary normetanephrine (HR 1.02 per each increase in standard deviation, 95% CI 1.01-1.03) and a larger tumor size (HR 1.01 per each increase in mm, 95% CI 1.00-1.02). In addition, those patients operated by an open approach had a four-fold higher risk of recurrence than those operated laparoscopically (HR 3.62, 95% CI 1.58-8.29). These differences continued being statistically significant after adjusting by tumor size (HR 3.15, 95% CI 1.34-7.41), but disappeared after adjusting by *SDHB* mutational status (adjusted HR 2.01, 95% CI 0.81-4.98).

The mean time free of recurrence was of 5.2 ± 3.47 years in patients with pathogenic variants in *SDHB* and of 3.1 ± 2.73 years in those harboring *SDHB* pathogenic variants (P=0.024).

4 Discussion

Recurrence of PPGL after its resection occurred in 8% of our patients after a mean follow-up of 5 years, with a rate of local recurrence of 2.3% and of metastatic disease of 7%. Nevertheless, the reported rates of recurrence (local and metastatic together) widely range between 6 to 22% in other series (6, 8, 22, 23). Specifically, local recurrence is reported in 0% of a series of 135 pheochromocytomas after a median follow-up time of 10 years (24) and in 6% of pheochromocytomas after a median follow-up of 4 years in a series of 52 cases (6). Neumann series of pediatric patients described local recurrence in 50% of the patients after 30 years of follow-up (25). An intermediate rate has been described in Amar L series that included 176 cases of PPGL at risk of recurrence, reporting local recurrence of 8% but after a larger follow-up period, of 9 years (8). In this same series, metastases occurred in 15 out of the 176 PPGLs (8.5%). Nevertheless, only 3% of the

TABLE 2 Cumulative incidence of recurrent disease by intervals (years).

Interval (years)	Patients in follow-up	Cumulative incidence	Hazard	95% Confident interval
0-2	303	0.051	0.026	0.013-0.040
2-4	229	0.065	0.007	0.000-0.016
4-6	177	0.077	0.007	0.000-0.016
6-8	131	0.110	0.018	0.000-0.035
8-10	93	0.110	0.000	Not calculable
10-12	68	0.135	0.015	0.000-0.044

10.3389/fendo.2023.1279828

TABLE 3 Predictors of recurrent disease in PPGLs.

Variable	Recurrent disease (n=24)	Free of recurrent disease (n=279)	Hazard ratio [95% CI], p value
Male sex	62.5% (n=15)	47.0% (n=131)	1.87 [0.82-4.27], 0.131
Age	46.8 ± 13.52	51.6 ± 16.15	0.99* [0.96-1.01], 0.244
Age < 35 years	16.7% (n=4)	17.2% (n=48)	0.89 [0.30.2.59], 0.824
Hereditary PPGL [n=265]	60.9% (n=14/23)	32.6% (n=79/249)	2.72 [1.17-6.31], 0.018†
SDHB mutation	33.3% (n=8/24)	2.2% (n=6/279)	15.46 [6.45-36.80], <0.0001†
Hypertension	83.3% (n=20)	71.3% (n=199)	2.21 [0.75-6.47], 0.116
Diabetes	30.4% (n=7)	26.2% (n=73)	1.56 [0.64-3.79], 0.346
Obesity	12.5% (n=3)	16.5% (n=46)	0.75 [0.22-2.51], 0.628
Cardiovascular disease	4.2% (n=1)	14.0% (n=39)	0.32 [0.04-2.39], 0.184
Cerebrovascular disease [n=301]	4.2% (n=1)	4.7 (n=13)	0.79 [0.11-5.85], 0.811
Smoker [n=265]	17.4% (n=4)	26.1% (n=63)	0.61 [0.21-1.80], 0.346
Systolic blood pressure at diagnosis	135.9 ± 28.48	138.2 ± 25.57	1.00* [0.98-1.02], 0.754
Diastolic blood pressure at diagnosis	80.5 ± 14.59	82.0 ± 16.22	1.00* [0.97-1.02], 0.741
Secretory phenotype [n=223] -Only adrenaline -Only norepinephrine -Mixed			0.51 [0.12-2.23], 0.331 2.39 [0.95-6.04], 0.069 0.51 [0.19-1.36], 0.165
Urine metanephrine (SD)	6.7± 21.72	6.6± 15.20	1.00* [0.97-1.03], 0.908
Urine normetanephrine (SD)	32.8± 66.7	5.5± 8.66	1.02* [1.01-1.03], <0.0001†
Urine epinephrine (SD)	0.6 ± 0.37	4.9± 8.84	0.37* [0.16-0.89], <0.0001†
Urine norepinephrine (SD)	6.5± 9.15	4.7 ± 12.66	1.00* [0.98-1.04], 0.606
Plasmatic metanephrine (SD)	3.2 ± 5.19	4.9 ± 6.50	0.95* [0.83-1.08], 0.381
Plasmatic normetanephrine (SD)	7.7 ± 9.22	4.5 ± 5.60	1.04* [0.98-1.11], 0.282
Tumour size (mm)	65.7 ± 7.85	46.3 ± 31.27	1.10 per each 10 mm [1.04-1.17], 0.018†
Tumour >40 mm	69.6% (n=16/23)	49.3% (n=132/268)	2.34 [0.96-5.70], 0.050
Bilateral tumors	0%	5.0% (n=14)	Not calculable
Sympathetic paraganglioma	33.3% (n=8)	2.5% (n=7)	11.9 [5.02-28.08], <0.0001
Open adrenalectomy	37.5% (n=9)	11.1% (n=31)	3.62 [1.58-8.29], <0.003
PASS score [n=70]	3.8 ± 3.25	2.9 ± 2.50	1.27 per each increase in unit [0.91-1.77], 0.158

PASS, Pheochromocytoma of the Adrenal gland Scaled Score; PPGL, pheochromocytomas and sympathetic paragangliomas; SD, standard deviations; *refers to each increase in unit; † refers to statistically significant results; **for variables with missing data, the number of patients with available data is described in brackets.

patients of the O'Dwyer PJ study developed metastasis after a median follow-up of 10 years (24) and as high as 24% in patients with PGLs in other different study (26). The differences described across these studies may be explained by several factors, including differences in the duration of the follow-up period (for example of 30 years in Neumann series (25) and 4 years in Johnston PC study (6)), the inclusion criteria (for example, in series that include extraadrenal tumors the rate of recurrence is higher (8), also in pediatric patients, who have a higher rate of hereditary disease, e.g of 80% of the patients in Neumann series were hereditary), the definitions used for recurrent disease and the diagnosis method employed.

Importantly, despite that in our cohort the median time from the diagnosis to the recurrence was only of 11.2 months, the cases of recurrent disease distributed uniformly during the follow-up period, and they can occur even after 10 years of follow-up. In this line, in the Johnston CP series, all cases or local recurrence occurred at least after 8 years of the surgery for the primary pheochromocytoma (6). In contrast, a meta-analysis of 13 studies, described a lower rate of local recurrence (3%) and a larger mean time to local recurrence (4 years, ranging from 0.5 to 12 years) (27). In addition, in the recent study of Pamporaki (28), 29% of all patients with recurrent sporadic PPGL, were diagnosed with recurrence at least 10 years after primary tumor diagnosis. For

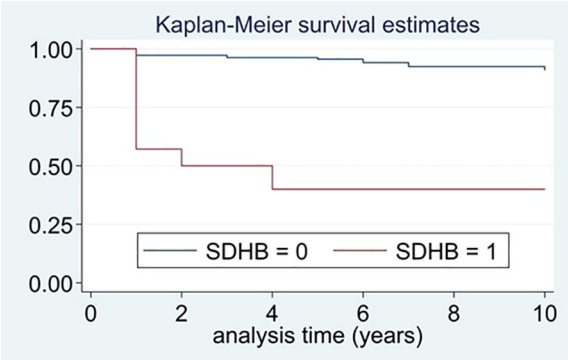

FIGURE 4
Differences in time free of recurrence between patients with and without pathogenic variants in *SDHB*.

these reasons and given the limitations to predict the development of recurrent disease, the current recommendation is an extended long-term follow-up for all patients with PPGLs (9).

We identified as the strongest predictor of recurrence the presence of a pathogenic variant in the *SDHB* gene (HR 13.3, 95% CI 4.20-41.92). According with our results, a recent study found that *SDHB* immunohistochemistry is an important predictive factor of recurrence for PPGL, specifically, in a prospective evaluation they found that 18.8% (3/16) of participants in the *SDHB* (-) group had progressive tumors compared with 3.6% (7/197) in the *SDHB* (+) group (RR: 5.28, 95% CI: 1.51-18.47) (23). In the same line, in a study of 44 malignant PPGLs and 113 benign PPGLs, all 11 patients with germline *SDHB* mutations had malignant disease (29). In agreement with these information, it has been reported that the prevalence of recurrence among patients with sporadic PPGL (14.7%) is lower (P<0.001) than for patients with pathogenic variants that activate pseudohypoxia pathways (47.5%), but similar to those with variants that activate kinase pathways (14.9%) (28). *SDHB* is also a predictive factor of survival in patients with metastatic PPGL, the relative risk of mortality (SDHB mutated vs non-mutated) is of 2.7; [95% confidence interval 1.2 to 6.4] in the Plouin PF study (26). In agreement with these results, we observed that recurrent disease occurred earlier in *SDHB* mutated patients in comparison with those without the mutation, suggesting a more aggressive disease in the former. The same observation was reported in the Plouin PF study: the median time from the diagnosis of primary tumor to the documentation of a first metastasis was 4 months in patients with *SDHB* mutations and 20 months in patients without (26). Thus, when a *SDHB* pathogenic variant is detected, we recommend performing a strict biochemical and radiological follow-up with a special attention for any data that may suggest recurrence development, including an increase in 3-methoxytyramine levels or indeterminate radiological findings. Moreover, the type of *SDHB* pathogenic variants may also be useful to indicate the potential risk for metastatic disease development (30). We also observed that patients with sympathetic PGLs had a higher risk of recurrent disease, but these differences disappeared after adjusting by *SDHB* mutation. This fact may be explained because the clinical behavior of the PGL vary depending on if the case is sporadic or if genetic. Moreover, the clinical behavior of the PGL depends on the underlying pathogenic variant; for example for *SDHD* mutations the risk of malignancy is estimated to be of 4% whereas for *SDHB* mutation, the risk is of up to 50% (10).

A higher urinary normetanephrine excretion was an independently factor of recurrence (HR 1.02 per each increase in standard deviation above the upper limit of normality). In addition, we observed that those patients who developed recurrence tended to have lower urinary epinephrine excretion than those without recurrence. These results are in line with the recently reported by Pamporaki C. et al. (28). In this study, a noradrenergic/dopaminergic phenotype (HR 2.73; 95% CI, 1.55-4.80), larger size (HR 1.82; 95% CI, 1.11-2.96) and extra-adrenal location (HR 1.79; 95% CI, 1.00-3.19) were independent predictors of recurrence in sporadic PPGL. In accordance with these results, the rate of noradrenergic/dopaminergic tumors in recurrent disease was higher than in non-recurrent PPGLs (67.1% vs 32.8%, P<0.001). Moreover, several years ago a retrospective study of 83 PPGLs described those patients with higher levels of dopamine, norepinephrine and aromatic l-amino acid decarboxylase, as well as lower ratios of epinephrine/epinephrine+norepinephrine, had significantly shorter metastases-free intervals (31). Furthermore Eisenhofer et al. (28) conducted a study on 365 PPGLs patients and demonstrated higher norepinephrine, normetanephrine, and 3-methoxytyramine levels in metastatic PPGLs. They found that 3-methoxytyramine was the most accurate biomarker of metastatic disease because plasma methoxytyramine was 4.7 times higher in patients with metastases compared to patients without metastases, and high plasma methoxytyramine was associated with SDHB mutations and extra-adrenal disease, both recognized risk factors of metastatic disease.

In our cohort, large tumor size increased the risk of recurrence during follow-up (HR 1.01 per each increase in mm, 95%CI 1.00-1.02), this finding agrees with several previous studies (16, 32, 33). Tumor size of 5-5.5 cm has been proposed as the most sensitive threshold to differentiate patients with low and high risk of developing recurrent disease (11, 32), additionally, tumor size < 4 cm has been linked to a lower risk of metastatic disease after 7.3 years according to the Dhir M. study (29). Moreover, tumor size is a prognosis factor for metastatic PPGL (16, 32). In this line, a series of 152 patients with pheochromocytoma, including 5 with metastasis at the time of the initial surgical excision and 12 who developed metastasis during follow-up, described a greater overall 5-year progression free survival rate in patients with smaller tumors (≤5.5 vs. >5.5 cm; 90.6% vs. 81.2%, p=0.025) (32). Similar results were reported by Ayala-Ramirez M et al. (16, 34), in which tumor size was significantly associated with worse overall survival (HR = 1.08; 95% CI = 1.04–1.13; P = 0.0003) while adjusting for age, gender, and tumor location.

We also found that patients who underwent surgery using an open approach presented a risk of recurrence three times higher than those who were operated laparoscopically. The open approach is preferred when there is a clinical suspicion or concern for an invasive malignant pheochromocytoma. In addition, larger tumors are at a higher risk for tumor rupture, which may lead to

pheochromocytomatosis. However, we observed that even after adjusting by tumor size, open approach was associated with a higher risk of recurrence. Nevertheless, when open approach was adjusted by SDHB mutational status, these differences disappeared. An open adrenalectomy approach may be justified in patients with SDHB mutations due to the higher rate of metastatic disease in this group (35).

Histopathological information may also be useful to predict the development of metastatic disease. However, we did not find differences in the score obtained in the Pheochromocytoma of the Adrenal gland Scaled Score (PASS) system between patients who developed recurrence and those who remained without recurrence. Specifically the Grading System for Adrenal Pheochromocytoma and Paraganglioma (GAPP) criteria include six variables: histological pattern, cellularity, comedo-type necrosis, capsular/vascular invasion, Ki67 labelling index and catecholamine type (36) or the PASS score (37) based on 12 histologic features such as diffuse growth, high cellularity, cellular monotony, tumor cell spindling, mitotic figures [3/10 HPF, atypical mitoses, profound nuclear pleomorphism and nuclear hyperchromasia. However, several of the features are associated with inter- and intra-observer variability and histologic features have not been shown to reliably predict malignancy in PPGLs (38). Other authors have proposed the application of compositive predictive scores combining different clinical and histological variables for the prediction of the progression-free survival (PFS) and metastatic behavior of PPGLs. In this regard, Pierre et al. (39) proposed a new prognostic score called COPPS that combines the variables tumor size, necrosis, vascular invasion and the losses of PS100 and *SDHB* immunostaining to predict the risk of metastasis. Cho et al. (40) proposed another integrated risk score for recurrence prediction called ASES-score, using the variables age ≤35 years, tumor size ≥ 6.0 cm, extra-adrenal localization, and norepinephrine-secretory type. The negative predictive value of this system was 96.5% for a cut-off point of 2. Other similar models have been reported by other authors (41).

We are aware that this is a retrospective study with associated limitations, including cases selection and referral bias. In addition, we have analyzed the predictive value of histological characteristics for development of recurrent disease in few patients, so the power of this analysis to detect differences it is low. Nevertheless, we included a large sample size and a long mean follow-up period, which is one of the main strengths of the study. Furthermore, we have evaluated the influence of several characteristics in the risk of development both metastatic and local recurrent disease, including clinical, genetic, hormonal and radiological data.

5 Conclusion

Disease recurrence of PPGLs occurs more frequently in patients with mutations in *SDHB*, with larger tumors and higher levels of urinary normetanephrine. PPGL recurrence may occur after the initial PPGL diagnosis is performed, thus, we recommend genetic testing in all patients with PPGL and a strict follow-up, especially in those patients with a higher risk of recurrent disease.

Data availability statement

The raw data supporting the conclusions of this article will be made available by the authors, without undue reservation.

Ethics statement

All procedures performed in the participants of the study were in accordance with the ethical standards of the institutional research committee and with the 1964 Helsinki declaration and its later amendments or comparable ethical standards. The study has been approved by the Ethical Committee of the Hospital Universitario La Princesa and Hospital Universitario Ramón y Cajal. This retrospective multicenter study was approved, and waiver of informed consent was granted by the Hospital Universitario Ramón y Cajal Ethics' Committee.

Author contributions

MA-C: Conceptualization, Investigation, Writing – original draft, Writing – review & editing. IG: Writing – review & editing. CM: Writing – review & editing. FH: Writing – review & editing. MM: Writing – review & editing. AV: Writing – review & editing. CB: Writing – review & editing. PN: Writing – review & editing. ML: Writing – review & editing. CL: Writing – review & editing. LM-M: Writing – review & editing. MC: Writing – review & editing. PR: Writing – review & editing. RB: Writing – review & editing. MR: Writing – review & editing. MT: Writing – review & editing. NV: Writing – review & editing. PG: Writing – review & editing. CR: Writing – review & editing. TM: Writing – review & editing. CA: Writing – review & editing. RG: Writing – review & editing. VB-T: Methodology, Writing - review & editing. AH-M: Writing – review & editing. MC: Writing – review & editing.

Funding

The author(s) declare financial support was received for the research, authorship, and/or publication of this article. Spanish Society of Endocrinology & Nutrition (SEEN).

Conflict of interest

The authors declare that the research was conducted in the absence of any commercial or financial relationships that could be construed as a potential conflict of interest.

Publisher's note

References

1. Garcia-Carbonero R, Matute Teresa F, Mercader-Cidoncha E, Mitjavila-Casanovas M, Robledo M, Tena I, et al. Multidisciplinary practice guidelines for the diagnosis, genetic counseling and treatment of pheochromocytomas and paragangliomas. *Clin Transl Oncol* (2021) 23:1995–2019. doi: 10.1007/s12094-021-02622-9

2. Kantorovich V, Pacak K. New insights on the pathogenesis of paraganglioma and pheochromocytoma. *F1000Research* (2018) 7. doi: 10.12688/F1000RESEARCH.14568.1/DOI

3. Araujo-Castro M, Pascual-Corrales E, Nattero Chavez L, Martínez Lorca A, Alonso-Gordoa T, Molina-Cerrillo J, et al. Protocol for presurgical and anesthetic management of pheochromocytomas and sympathetic paragangliomas: a multidisciplinary approach. *J Endocrinol Invest* (2021) 44:2545–55. doi: 10.1007/s40618-021-01649-7

4. Alrezk R, Suarez A, Tena I, Pacak K. Update of pheochromocytoma syndromes: genetics, biochemical evaluation, and imaging. *Front Endocrinol (Lausanne)* (2018) 9:515. doi: 10.3389/fendo.2018.00515

5. Parasiliti-Caprino M, Lucatello B, Lopez C, Burrello J, Maletta F, Mistrangelo M, et al. Predictors of recurrence of pheochromocytoma and paraganglioma: a multicenter study in Piedmont, Italy. *Hypertens Res* (2020) 43:500–10. doi: 10.1038/s41440-019-0339-y

6. Johnston PC, Mullan KR, Atkinson AB, Eatock FC, Wallace H, Gray M, et al. Recurrence of phaeochromocytoma and abdominal paraganglioma after initial surgical intervention. *Ulster Med J* (2015) 84(2):102–6.

7. Van Slycke S, Caiazzo R, Pigny P, Cardot-Bauters C, Arnalsteen L, D'Herbomez M, et al. Local-regional recurrence of sporadic or syndromic abdominal extra-adrenal paraganglioma: incidence, characteristics, and outcome. *Surgery* (2009) 146:986–92. doi: 10.1016/J.SURG.2009.10.055

8. Amar L, Servais A, Gimenez-Roqueplo AP, Zinzindohoue F, Chatellier G, Plouin PF. Year of diagnosis, features at presentation, and risk of recurrence in patients with pheochromocytoma or secreting paraganglioma. *J Clin Endocrinol Metab* (2005) 90:2110–6. doi: 10.1210/jc.2004-1398

9. Lenders JWM, Duh QY, Eisenhofer G, Gimenez-Roqueplo AP, Grebe SKG, Murad MH, et al. Pheochromocytoma and paraganglioma: An endocrine society clinical practice guideline. *Endocr Soc* (2014) 99:1915–42. doi: 10.1210/jc.2014-1498

10. Araujo-Castro M, Nattero Chavez L, Martínez Lorca A, Molina-Cerrillo J, Alonso-Gordoa T, Pascual-Corrales E. Special situations in pheochromocytomas and paragangliomas: pregnancy, metastatic disease, and cyanotic congenital heart diseases. *Clin Exp Med* (2022) 22:359–70. doi: 10.1007/S10238-021-00763-3

11. Eisenhofer G, Lenders JWM, Siegert G, Bornstein SR, Friberg P, Milosevic D, et al. Plasma methoxytyramine: a novel biomarker of metastatic pheochromocytoma and paraganglioma in relation to established risk factors of tumour size, location and SDHB mutation status. *Eur J Cancer* (2012) 48:1739–49. doi: 10.1016/J.EJCA.2011.07.016

12. Brouwers FM, Eisenhofer G, Tao JJ, Kant JA, Adams KT, Linehan WM, et al. High frequency of SDHB germline mutations in patients with Malignant catecholamine-producing paragangliomas: implications for genetic testing. *J Clin Endocrinol Metab* (2006) 91:4505–9. doi: 10.1210/JC.2006-0423

13. Hescot S, Curras-Freixes M, Deutschbein T, Van Berkel A, Vezzosi D, Amar L, et al. Prognosis of Malignant pheochromocytoma and paraganglioma (MAPP-ProNO study): A European network for the study of adrenal tumors retrospective study. *J Clin Endocrinol Metab* (2019) 104:2367–74. doi: 10.1210/jc.2018-01968

14. Fangwen RAO, Keiser HR, O'Connor DT. Malignant and benign pheochromocytoma: chromaffin granule transmitters and the response to medical and surgical treatment. *Ann N Y Acad Sci* (2002) 971:530–2. doi: 10.1111/J.1749-6632.2002.TB04519.X

15. John H, Ziegler WH, Hauri D, Jaeger P. Pheochromocytomas: Can Malignant potential be predicted? *Urology* (1999) 53:679–83. doi: 10.1016/S0090-4295(98)00612-8

16. Ayala-Ramirez M, Feng L, Johnson MM, Ejaz S, Habra MA, Rich T, et al. Clinical risk factors for Malignancy and overall survival in patients with pheochromocytomas and sympathetic paragangliomas: primary tumor size and primary tumor location as prognostic indicators. *J Clin Endocrinol Metab* (2011) 96:717–25. doi: 10.1210/JC.2010-1946

17. *Predictive factors for Malignant pheochromocytoma: analysis of 136 patients*. (Accessed September 10, 2023).

18. Araujo-Castro M, Mínguez Ojeda C, García Sanz I, Calatayud M, Hanzu F, Mora M, et al. Genetic study in pheochromocytoma ¿is it possible to stratify the risk of hereditary pheochromocytoma? *Neuroendocrinology* (2023) 113(6)657–66. doi: 10.1159/000529319

19. Lenders JWM, Kerstens MN, Amar L, Prejbisz A, Robledo M, Taieb D, et al. Genetics, diagnosis, management and future directions of research of phaeochromocytoma and paraganglioma: A position statement and consensus of the Working Group on Endocrine Hypertension of the European Society of Hypertension. *J Hypertens* (2020) 38:1443–56. doi: 10.1097/HJH.0000000000002438

20. ElSayed NA, Aleppo G, Aroda VR, Bannuru RR, Brown FM, Bruemmer D, et al. 2. Classification and diagnosis of diabetes: standards of care in diabetes-2023. *Diabetes Care* (2023) 46:S19–40. doi: 10.2337/DC23-S002

21. Araujo-Castro M, García Sanz I, Mínguez Ojeda C, Calatayud M, Hanzu F, Mora M, et al. Differences in intraoperative and surgical outcomes between normotensive pheochromocytomas and sympathetic paragangliomas (PPGLs) and hypertensive PPGLs: results from the PHEO-RISK STUDY. *J Endocrinol Invest* (2023) 46:805–14. doi: 10.1007/s40618-022-01954-9

22. Plouin PF, Chatellier G, Fofol I, Corvol P. Tumor recurrence and hypertension persistence after successful pheochromocytoma operation. *Hypertension* (1997) 29:1133–9. doi: 10.1161/01.HYP.29.5.1133

23. Su T, Yang Y, Jiang L, Xie J, Zhong X, Wu L, et al. SDHB immunohistochemistry for prognosis of pheochromocytoma and paraganglioma: A retrospective and prospective analysis. *Front Endocrinol (Lausanne)* (2023) 14:1121397. doi: 10.3389/FENDO.2023.1121397

24. O'Dwyer PJ, Chew C, Zino S, Serpell MG. Long-term follow-up of patients undergoing laparoscopic surgery for phaeochromocytoma. *BJS Open* (2022) 6. doi: 10.1093/BJSOPEN/ZRAC076

25. Bausch B, Wellner U, Bausch D, Schiavi F, Barontini M, Sanso G, et al. Long-term prognosis of patients with pediatric pheochromocytoma. *Endocr Relat Cancer* (2013) 21:17–25. doi: 10.1530/ERC-13-0415

26. Amar L, Baudin E, Burnichon N, Peyrard S, Silvera S, Bertherat J, et al. Succinate dehydrogenase B gene mutations predict survival in patients with Malignant pheochromocytomas or paragangliomas. *J Clin Endocrinol Metab* (2007) 92:3822–8. doi: 10.1210/jc.2007-0709

27. Holscher I, Van Den Berg TJ, Dreijerink KMA, Engelsman AF, Nieveen Van Dijkum EJM. Recurrence rate of sporadic pheochromocytomas after curative adrenalectomy: A systematic review and meta-analysis. *J Clin Endocrinol Metab* (2021) 106:588–97. doi: 10.1210/CLINEM/DGAA794

28. Li M, Prodanov T, Meuter L, Kerstens MN, Bechmann N, Prejbisz A, et al. Recurrent disease in patients with sporadic pheochromocytoma and paraganglioma. *J Clin Endocrinol Metab* (2023) 108:397–404. doi: 10.1210/CLINEM/DGAC563

29. Dhir M, Li W, Hogg ME, Bartlett DL, Carty SE, McCoy KL, et al. Clinical predictors of Malignancy in patients with pheochromocytoma and paraganglioma. *Ann Surg Oncol* (2017) 24:3624–30. doi: 10.1245/S10434-017-6074-1/FIGURES/3

30. Davidoff DF, Benn DE, Field M, Crook A, Robinson BG, Tucker K, et al. Surveillance improves outcomes for carriers of SDHB pathogenic variants: A multicenter study. *J Clin Endocrinol Metab* (2022) 107:E1907–16. doi: 10.1210/CLINEM/DGAC019

31. van der Harst E, de Herder WW, de Krijger RR, Bruining HA, Bonjer HJ, Lamberts SWJ, et al. The value of plasma markers for the clinical behaviour of phaeochromocytomas. *Eur J Endocrinol* (2002) 147:85–94. doi: 10.1530/EJE.0.1470085

32. Park J, Song C, Park M, Yoo S, Park SJ, Hong S, et al. Predictive characteristics of Malignant pheochromocytoma. *Korean J Urol* (2011) 52:241–6. doi: 10.4111/KJU.2011.52.4.241

33. Press D, Akyuz M, Dural C, Aliyev S, Monteiro R, Mino J, et al. Predictors of recurrence in pheochromocytoma. *Surgery* (2014) 156:1523–8. doi: 10.1016/J.SURG.2014.08.044

34. Assadipour Y, Sadowski SM, Alimchandani M, Quezado M, Steinberg SM, Nilubol N, et al. SDHB mutation status and tumor size but not tumor grade are important predictors of clinical outcome in pheochromocytoma and abdominal paraganglioma. *Surgery* (2017) 161:230–9. doi: 10.1016/J.SURG.2016.05.050

35. Neumann HPH, Pawlu C, Pęczkowska M, Bausch B, McWhinney SR, Muresan M, et al. Distinct clinical features of paraganglioma syndromes associated with SDHB and SDHD gene mutations. *JAMA* (2004) 292:943–51. doi: 10.1001/JAMA.292.8.943

36. Kimura N, Takayanagi R, Takizawa N, Itagaki E, Katabami T, Kakoi N, et al. Pathological grading for predicting metastasis in phaeochromocytoma and paraganglioma. *Endocr Relat Cancer* (2014) 21:405–14. doi: 10.1530/ERC-13-0494

37. Thompson LDR. Pheochromocytoma of the adrenal gland scaled score (PASS) to separate benign from Malignant neoplasms: A clinicopathologic and immunophenotypic study of 100 cases. *Am J Surg Pathol* (2002) 26:551–66. doi: 10.1097/00000478-200205000-00002

38. Korevaar TIM, Grossman AB. Pheochromocytomas and paragangliomas: assessment of Malignant potential. *Endocrine* (2011) 40:354–65. doi: 10.1007/S12020-011-9545-3

39. Pierre C, Agopiantz M, Brunaud L, Battaglia-Hsu SF, Max A, Pouget C, et al. COPPS, a composite score integrating pathological features, PS100 and SDHB losses, predicts the risk of metastasis and progression-free survival in pheochromocytomas/paragangliomas. *Virchows Arch* (2019) 474:721–34. doi: 10.1007/S00428-019-02553-5

40. Cho YY, Kwak MK, Lee SEH, Ahn SH, Kim H, Suh S, et al. A clinical prediction model to estimate the metastatic potential of pheochromocytoma/paraganglioma: ASES score. *Surgery* (2018) 164:511–7. doi: 10.1016/j.surg.2018.05.001

41. Parasiliti-Caprino M, Bioletto F, Lopez C, Maletta F, Caputo M, Gasco V, et al. Development and internal validation of a predictive model for the estimation of pheochromocytoma recurrence risk after radical surgery. *Eur J Endocrinol* (2022) 186:399–406. doi: 10.1530/EJE-21-0370

frontiers | Frontiers in Endocrinology

TYPE Original Research
PUBLISHED 10 January 2024
DOI 10.3389/fendo.2023.1320722

OPEN ACCESS

EDITED BY
Nadia Sawicka-Gutaj,
Poznan University of Medical Sciences, Poland

REVIEWED BY
Henrik Ryberg,
Sahlgrenska University Hospital, Sweden
Marija M. Janjic,
University of Belgrade, Serbia

*CORRESPONDENCE
Letizia Canu
letizia.canu@unifi.it

RECEIVED 12 October 2023
ACCEPTED 14 December 2023
PUBLISHED 10 January 2024

CITATION
Canu L, Sparano C, Naletto L, De Filpo G, Cantini G, Rapizzi E, Martinelli S, Ercolino T, Cioppi F, Fantoni A, Zanatta L, Terreni A, Mannelli M, Luconi M, Maggi M and Lotti F (2024) Hypogonadism and sexual function in men affected by adrenocortical carcinoma under mitotane therapy.
Front. Endocrinol. 14:1320722.
doi: 10.3389/fendo.2023.1320722

Hypogonadism and sexual function in men affected by adrenocortical carcinoma under mitotane therapy

Letizia Canu [1,2,3,4]*, Clotilde Sparano [1,2], Lara Naletto [1], Giuseppina De Filpo [1], Giulia Cantini [1,3,4], Elena Rapizzi [3,4,5], Serena Martinelli [1,3,4], Tonino Ercolino [2,3,4], Francesca Cioppi [5], Alessandro Fantoni [1], Lorenzo Zanatta [1,2], Alessandro Terreni [6], Massimo Mannelli [1,3,4], Michaela Luconi [1,3,4], Mario Maggi [1,2,3,4] and Francesco Lotti [7]

[1]Endocrinology Unit, Department of Experimental and Clinical Biomedical Sciences "Mario Serio", University of Florence, Florence, Italy, [2]Endocrinology Unit, Careggi University Hospital (AOUC), Florence, Italy, [3]Centro di Ricerca e Innovazione sulle Patologie Surrenaliche, AOU Careggi, Florence, Italy, [4]Center of Excellence of European Network for the Study of Adrenal Tumors (ENS@T), Florence, Italy, [5]Department of Experimental and Clinical Medicine, University of Florence, Florence, Italy, [6]Department of Laboratory, Careggi University Hospital (AOUC), Florence, Italy, [7]Andrology, Female Endocrinology and Gender Incongruence Unit, Department of Experimental and Clinical Biomedical Sciences "Mario Serio", University of Florence, Florence, Italy

Purpose: Adrenocortical carcinoma (ACC) is a rare and aggressive tumor. ACC male patients under adjuvant mitotane therapy (AMT) frequently develop hypogonadism, however sexual function has never been assessed in this setting. The aim of this retrospective study was to evaluate in AMT treated ACC patients the changes in Luteinizing hormone (LH), Sex Hormone Binding Globulin (SHBG), total testosterone (TT) and calculated free testosterone (cFT), the prevalence and type of hypogonadism and sexual function, the latter before and after androgen replacement therapy (ART).

Methods: LH, SHBG, TT and cFT were assessed in ten ACC patients at baseline (T0) and six (T1), twelve (T2), and eighteen (T3) months after AMT. At T3, ART was initiated in eight hypogonadal patients, and LH, SHBG, TT and cFT levels were evaluated after six months (T4). In six patients, sexual function was evaluated before (T3) and after (T4) ART using the International Index of Erectile Function-15 (IIEF-15) questionnaire.

Results: Under AMT we observed higher SHBG and LH and lower cFT levels at T1-T3 compared to T0 (all $p<0.05$). At T3, hypergonadotropic hypogonadism and erectile dysfunction (ED) were detected in 80% and 83.3% of cases. At T4, we observed a significant cFT increase in men treated with T gel, and a significant improvement in IIEF-15 total and subdomains scores and ED prevalence (16.7%) in men under ART.

Conclusion: AMT was associated with hypergonatropic hypogonadism and ED, while ART led to a significant improvement of cFT levels and sexual function in the hypogonadal ACC patients. Therefore, we suggest to evaluate LH, SHBG, TT and cFT and sexual function during AMT, and start ART in the hypogonadal ACC patients with sexual dysfunction.

KEYWORDS

adrenocortical carcinoma, mitotane, hypergonadotropic hypogonadism, androgen replacement therapy, sexual dysfunction

Introduction

Adrenocortical carcinoma (ACC) is a rare tumor (0.7–2.0 cases per million persons/year) (1, 2), with a slight female preponderance (M:F 1.0:1.2) (3). The relative peak of incidence is in the fourth and fifth decades of life (4). ACC is associated with a poor prognosis and with an average 5-years survival rate of 50%, which dramatically drops to 6.9 – 13.0% in patients with documented distant metastases (5, 6). Currently, surgery represents the only curative approach for ACC patients (7). However, the complete tumor resection is often not curative due to the high risk of recurrence (8). For this reason, international guidelines recommend adjuvant therapies after surgery (9).

In particular, the latest guidelines of the European Network for the Study of Adrenal Tumors (ENSAT) recommend mitotane as an adjuvant therapy for at least two years after surgery in patients with a high risk of recurrence (ENSAT stage III, or R1 resection, or Ki67 > 10%) (9). Mitotane is a synthetic derivative of dichloro-diphenyl-trichloroethane (DDT) with a direct cytotoxic effect on the adrenal cortex (10–12), and has been approved by the European Medicines Agency (EMA) as therapy for ACC patients with advanced inoperable, or metastatic, or cortisol secreting masses. Recent evidences confirmed that adjuvant mitotane therapy (AMT) reduces the risk of recurrence and death (13). In addition, a high mitotane "time in target range" (TTR, months with mitotane levels 14-20 mg/l) was associated with a reduced risk of ACC recurrence in an adjuvant setting (14) and of death in a palliative group (15).

Nevertheless, mitotane has several side effects that are responsible of a limited tolerability (16). In males, one of the most frequent adverse effects is hypogonadism, which has been reported in 35.6% of men (17). The main reason suggested for AMT-related hypogonadism is that mitotane causes a rise in the hepatic SHBG synthesis and release (18) which can lead to a reduction in cFT levels. Despite this evidence, the hormonal status in ACC patients under AMT has been evaluated only in four studies (19–22), with partially discordant results, which might in part be due to differences in mitotane regimen, timing of blood sampling and laboratory methods for mitotane measurement, as well as in the circulating levels of the drug.

On the other hand, it is well known that hypogonadism, as well as malignancies *per se*, are associated with sexual dysfunction (23). However, no study evaluated the sexual function and the impact of androgen replacement therapy (ART) on sexuality in surgically treated ACC men under AMT.

The aim of the present study was to evaluate in surgically treated ACC patients under AMT: (i) the changes in LH, SHBG, TT, and cFT levels and the prevalence and type of hypogonadism during AMT, as well as (ii), for the first time, the sexual function before and after ART in patients with hypogonadism.

Materials and methods

Patients

We studied retrospectively ten surgically treated ACC male patients attending the Endocrinology Unit of the University Hospital of Florence. In particular, we included in this study a consecutive series of patients affected by histologically confirmed ACC treated with AMT between January 1st, 2013 and December 31, 2020. A comprehensive anamnesis (including age, smoking habit and alcohol consumption), as well as a general (body mass index, waistline, systolic and diastolic arterial blood pressure) and andrological (including testis volume and male breast assessment) physical examination were performed according to a previous study (24).

AMT was initiated after radical surgery with the intention of at least two years of therapy, although an individual approach was adopted considering the patients' compliance and the side effect tolerability (9). In particular, AMT was started with a minimum daily dose of 1000 mg and was increased up to the maximally tolerated dose. We evaluated the minimum and maximum daily dose of mitotane, the mean and maximum levels reached and the "time in target range" (TTR) corresponding to the number of months in which mitotane concentrations were between 14 and 20 mg/l (15). The mitotane levels were evaluated every month until the achievement of 14 mg/l and then every two-three months. We also registered the start date and type of any supportive/

replacement therapy (glucocorticoid, fludrocortisone, levothyroxine, lipid lowering, ART) initiated due to ACC or ACC surgery-related hormonal deficiencies/metabolic abnormalities. In particular, ART was offered to patients with hypogonadism in different forms based on the presence or not of gynecomastia. Subjects with hypogonadism and gynecomastia were treated with 2.5% transdermal dihydrotestosterone (DHT) gel, a non-aromatizable ART, at the daily dose of 2 applications on each breast (one in the morning and one in the evening). Patients with hypogonadism without gynecomastia were treated with 2% testosterone (T) gel at the daily dose of 50 mg (five puffs/day). We preferred the use of gel to avoid any additional liver load in subjects already under the liver-affecting mitotane treatment, and because the gel manageability and rapid suspension in case of side effects.

LH, SHBG, TT, and cFT were assessed in all patients at baseline (T0) and 6 (T1), 12 (T2) and 18 (T3) months after AMT start (see below). In addition, TT, SHBG, cFT, and LH and sexual function were evaluated in eight and six men, respectively, before (T3) and six months after (T4) ART (see below).

Biochemical evaluation

Biochemical evaluation was performed in single reference laboratory, the General Laboratory of Careggi Hospital. The Laboratory is part of AOUC (Azienda Ospedaliero-Universitaria Careggi), is certificated by the Tuscany region, and works according to ISO 9001:2015. Internal quality controls (IQC) are periodically reviewed by the direction of the Laboratory and External Quality Assessment (EQA) schemes are provided and evaluated by third part institution QualiMedLab (CNR, Pisa) and Reference Regional Centre for EQA (CRRVEQ).

Blood samples were drawn in the morning, after an overnight fast, and were immediately centrifuged at 3.000 rpm for 20 minutes. In particular, at T4 (after six months of ART), blood samples were drawn two hours after the application of T or DHT gel (see above) according to the Endocrine Society guidelines (25). LH, TT and SHBG were measured by electrochemiluminescence (ECLIA) method on COBAS 6000 (Roche Diagnostic, Mannheim, Germany). In particular, TT was evaluated by the electrochemiluminescence immunoassay "ECLIA", intended for use on Elecsys Testosterone II and cobas e immunoassay analyzers; for details see https://labogids.sintmaria.be/sites/default/files/files/testosteron_ii_2017-11_v9.pdf) standardized via ID–GC/MS ("Isotope Dilution - Gas Chromatography/Mass Spectrometry") (26, 27), which shows good agreement with mass spectrometry in the distribution of results for TT (28). To ensure day-to-day consistency of an analytical process, two levels Bio-Rad internal IQC samples were processed before and after the sample measurements. An External Quality Assurance (EQA) systems to evaluate accuracy and bias was adopted by laboratory using QualiMedLab (CNR, Pisa) EQA controls. A one-year EQA schemes coefficients of variation (CVs) for these methods were 6.0%, 9.0% and 5.6% for LH, TT and SHBG, respectively. EQA sample at cut-off concentration (300 ng/dL) showed a CV and u% of 4.3% and 0.48%, respectively. LH, TT and SHBG assay sensitivity are 0.2 IU/L, 0.42 nmol/l and 0.35 nmol/l, respectively, with a Limit of Quantitation of TT of 0.416 nmoli/l. Calculated free testosterone (cFT) was derived according to the Vermeulen's formula (available at http://www.issam.ch/freetesto.htm).

Since patients under AMT show a relevant increase in SHBG levels (19–22), in our study, hypogonadism was diagnosed using cFT instead of TT, to increase the specificity of T deficiency detection (low cFT levels) even in men with apparent normal TT levels. A cFT < 225 pmol/l was considered to define hypogonadism (29), while a LH cut-off of 9.4 U/l was used to distinguish between hypo- and hyper-gonadotropic hypogonadism. According to the largely accepted definition derived from the European Male Ageing Study (30), LH < 9.4 U/l defines "secondary or hypogonadotropic hypogonadism", while LH ≥ 9.4 U/l defines "hypergonadotropic hypogonadism". In addition, the contemporary presence of LH ≥ 9.4 U/l and cFT ≥ 225 pmol/L defines "compensated hypogonadism" (31). Finally, the presence of hypo- and/or hyper-gonadotropic hypogonadism was defined as "overt hypogonadism", excluding eugonadism and/or "compensated" hypogonadism.

Plasma mitotane concentration was measured by the Lysosafe service provided by HRA Pharma (http://www.lysosafe.com) at Cochin Hospital Laboratory (Paris, France). Quantification of mitotane plasma concentrations was performed using a validated liquid chromatography method coupled with UV-detection. Mitotane and its internal standard (p,p'DDE) were extracted using a one-step extraction method (protein precipitation). The calibration was linear in the range 0.5-25 mg/L. The intra and inter-precision for the four internal quality controls (0.7, 4, 12.5 and 20 mg/L) were below 4.4 and 9.7%, respectively; and the intra and inter-accuracy ranged from 92.8 to 109.7%. The accuracy of the method was also ensured by the participation to an external quality assessment Scheme including five French Hospital Laboratories.

Evaluation of sexual function

A standard question "Do you agree to be investigated about your sexuality?" was raised to all patients. The "yes" responders were asked to complete the International Index of Erectile Function-15 (IIEF-15) (32), in its Italian form. The domains investigated by the IIEF-15 are: erectile function, orgasmic function, sexual desire, intercourse satisfaction and overall satisfaction. Erectile function was assessed using the IIEF-15-erectile function domain (EFD) (33). According to the IIEF-15-EFD score, the severity of erectile dysfunction (ED) can be categorized as: no ED (score 30-26), mild ED (score 25-22), mild-to-moderate ED (score 21-17), moderate ED (score 16-11) and severe ED (score 10-6) (33). Since scores between 25 and 22 suggest "very mild" ED, it is not likely to be a major problem for men in engaging coitus, whereas threshold of 22, identifying a more severe problem, can be considered as indicative of a more relevant clinical ED (34). Hence, in our study, ED was defined for an IIEF-15-EFD score < 22.

Statistical analysis

To summarize patients' clinical characteristics, we used descriptive statistics. Continuous data were expressed as mean ± standard deviation (SD) when normally distributed, or as medians (quartiles) for non-normal distribution, while categorical data were indicated as percentages, unless otherwise specified. Correlations were assessed using Spearman's or Pearson's method, whenever appropriate. One-way ANOVA test for repeated measures was used to compare more than two groups, i.e. hormonal (TT, SHBG, cFT and LH) levels at baseline (T0), T1, T2 and T3. The paired two-sided Student's *t*-test was used to compare hormonal (LH, SHBG, TT and cFT) levels in two groups and IIEF-15 total and subdomains scores at T3 and T4.

Statistical analysis was performed with SPSS (SPSS, Inc., Chicago, IL, USA) for Windows 27, GraphPad Prism version 9.0.0 for Windows, GraphPad Software, San Diego, California USA, http://www.graphpad.com, and Origin version 6.1 for Windows.

A p-value < 0.05 was considered significant.

All the figures were prepared using GraphPad Prism version 9.0.0 for Windows, GraphPad Software, San Diego, California USA, http://www.graphpad.com and Origin version 6.1 for Windows.

Results

Clinical and hormonal characteristics of the entire patients' cohort at baseline

Patients surgically treated for ACC who underwent AMT (n=10) had a mean age of 43.0 ± 14.2 years. The main clinical and hormonal baseline characteristics of the patients, as well as the main ACC features, are summarized in Table 1. At baseline, secondary hypogonadism and gynecomastia were detected in three patients (30%) (Table 1), while no patient complained of sexual dysfunction.

Adjuvant mitotane therapy (AMT)

Table 2 shows the mitotane minimum and maximum daily dose, the mean and maximum levels reached and the TTR in each patient and in the entire cohort. The mitotane plasma mean concentration during AMT was 12.5 ± 2.6 mg/L. The mean TTR in the whole sample was 14.2 ± 13.4 months. Out of ten patients, two never reached the target range.

LH, SHBG, TT, cFT levels and hypogonadal status during AMT

Figure 1 shows the mean levels of LH, SHBG, TT and cFT at baseline (T0) and 6 (T1), 12 (T2) and 18 (T3) months after the

TABLE 1 Main clinical, hormonal and oncological features of the sample at baseline.

			N = 10
	%	Mean values	Median values
Clinical parameters			
Age (years)		43.0 ± 14.2	47.0 [29-51.75]
Current smokers (%)	0.0%		
Past smokers (%)	0.0%		
Daily alcohol consumption (%)	0.0%		
Body mass index (kg/m^2)		27.8 ± 4.5	28.2 [23.4-33.3]
Waistline (cm)		110.9 ± 11.6	102.0 [89.8-115.1]
Systolic blood pressure (mmHg)		131.0 ± 19.0	132.5 [117.5-140.0]
Diastolic blood pressure (mmHg)		81.5 ± 12.7	85.0 [75.0-90.0]
Mean testis volume (Prader) (ml)		13.6 ± 2.0	14.0 [12.0-15.2]
Gynecomastia (%)	30%		
Hypogonadism[a] (%)	30%		
Current medications[b] (%)			
- **Hydrocortisone/ cortisone acetate**	100%		
- **Fludrocortisone**	20%		
- **Levothyroxine**	70%		
- **Lipid-lowering therapy**	50%		
Hormonal parameters			
LH (U/l)		3.3 ± 1.8	4.0 [3.3-4.4]
Total testosterone (nmol/l)		14.6 ± 4.8	14.6 [10.5-18.9]
Sex hormone binding globulin (nmol/l)		36.6 ± 13.2	33.3 [27.2-43.7]
Calculated free testosterone (pmol/l)		296.4 ± 135.4	271.5 [187.2-364.2]
Tumour related parameters			
Tumour size (cm)		10.8 ± 5.2	9.2 [4.3-15.5]
ENSAT tumour stage at the start of AMT (%)			
Stage I	20%		
Stage II	50%		
Stage III	20%		
Stage IV	10%		
Hormonal secretion (%)			
Cortisol	50%		
Non functional tumors	30%		
Cortisol and androgens	10%		
Androgens	10%		

(Continued)

10.3389/fendo.2023.1320722

TABLE 1 Continued

			N = 10
	%	Mean values	Median values
Weiss score (%)			
4	10%		
5	10%		
6	20%		
7	20%		
8	40%		

[a]All the hypogonadal patients showed secondary hypogonadism at baseline.
[b]Supportive/replacement treatments. AMT, adjuvant mitotane therapy.

initiation of AMT in all patients. Compared to baseline, at all the follow-up time points we observed significantly higher levels of LH and SHBG, which showed a progressive increase, and lower cFT levels (all $p < 0.05$; Figures 1A, B, D, respectively), while no significant change in TT levels were observed (Figure 1C). Of note, no significant difference in physical examination-related parameters, including body mass index and waistline, was observed in each patient at different time points (not shown).

On the basis of cFT and LH levels at T0, three patients (30%) showed hypogonadotropic hypogonadism and seven (70%) eugonadism. At T1, five patients (50%) showed hypergonadotropic hypogonadism, three (30%) hypogonadotropic hypogonadism and two (20%) eugonadism. At T2, eight patients (80%) showed hypergonadotropic hypogonadism and two (20%) eugonadism. At T3, eight patients (80%) showed hypergonadotropic hypogonadism and two (20%) compensated hypogonadism. Compared to T0, the prevalence of overt hypogonadism, as well as of hypergonadotropic hypogonadism, was higher at all-time points (T1, T2, T3) after AMT initiation (all $p < 0.05$) (Figure 2A).

Interestingly, we found no associations between AMT-related parameters (minimum and maximum mitotane daily doses, mean and maximum mitotane levels and TTR) and hormonal (TT, cFT, SHBG and LH) levels at any time (T1, T2, T3) (not shown).

Evaluation of LH, SHBG, TT, and cFT levels and sexual function before and after ART

At T3, ART was offered to subjects with overt hypogonadism (n=8) (Table 3). In particular, three patients with overt hypogonadism and gynecomastia (cases #3, #4, #5) underwent treatment with DHT gel, while five patients with overt hypogonadism and without gynecomastia (cases #1, #6, #8, #9, #10) underwent treatment with T gel (Table 3; see Methods section). Comparing hormonal levels before (T3) and after six months (T4) of ART, no significant differences in LH and SHBG levels were observed (Figures 3A, B). Conversely, in the five T-gel-treated patients, after six months of T replacement therapy a significant increase in cFT levels was observed (Figure 3D), as well as a trend toward a significant increase in TT levels (Figure 3C). Obviously, in those patients under DHT-treatment, TT and cFT levels were not considered. In addition, out of the five patients who showed overt hypogonadism at T3, and therefore started T gel-treatment, two switched to compensated hypogonadism at T4, with a statistical trend ($p = 0.089$) toward the reduction of overt hypogonadism frequency (Figure 2B).

In the six patients from whom sexuality was investigated, sexual function data were available starting from T3 (see Supplementary Table 1). At T3, five out of six patients (83.3%) had ED (IIEF-15-EFD score < 22) (Figure 2C). All the six patients started ART, three (#3, #4, #5) with DHT gel and three (#1, #6, #8) with T gel (Table 3). At T4,

TABLE 2 Mitotane daily dose, mitotane levels and time in target range (TTR).

Patients	Minimum mitotane daily dose	Maximum mitotane daily dose	Mitotane maximum levels	Mitotane mean levels	TTR
	mg/day	mg/day	mg/L	mg/L	months
1	2000	3000	13.60	10.22	0
2	2000	4500	24.33	11.15	5.5
3	1500	2500	26.76	14.89	42.2
4	2000	3000	18.80	13.47	16.4
5	2000	3000	17.12	7.39	0
6	1500	2500	25.16	14.44	5.2
7	3000	3000	13.60	10.53	0
8	2000	4000	18.50	13.20	23.7
9	2000	3000	18.80	13.47	18.3
10	1000	3000	32.00	16.05	33.3
Overall	1900 ± 516.4	3150 ± 625.8	20.7 ± 6.3	12.5 ± 2.6	14.2 ±13.4

10.3389/fendo.2023.1320722

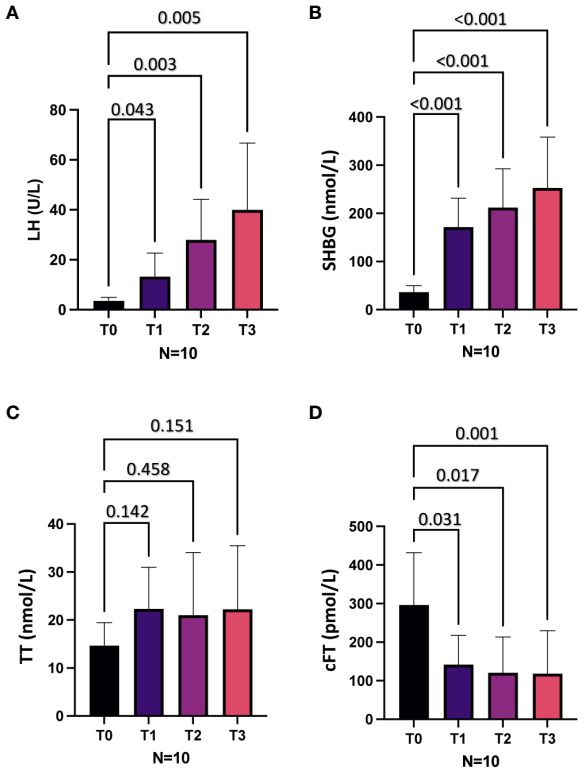

FIGURE 1
Hormonal parameters at baseline (T0) and after 6 (T1), 12 (T2) and 18 (T3) months of mitotane therapy in the whole cohort. **(A)**, Luteinizing hormone (LH) levels. **(B)**, Sex hormone binding globulin (SHBG) levels. **(C)**, Total testosterone (TT) levels. **(D)**, Calculated free testosterone (cFT) levels.

after six months of ART, we observed a significant decrease in ED prevalence (83.3% at T3 *vs.* 16.7% at T4, p = 0.040) (Figure 2C) associated with a significant increase in the all IIEF-15 subdomains and total score (Figures 2D, Supplementary Figures 1A-E). Supplementary Table 1 reports the starting (at T3) and the final (at T4) values of the IIEF-15 total and subdomains scores for each patient.

Discussion

Main findings of the study

In this study LH, SHBG, TT and cFT variations as well as the prevalence and type of hypogonadism before and after AMT were evaluated in ten surgically treated ACC male patients under AMT. In addition, we evaluated the changes in LH, SHBG, TT, and cFT levels after six months of ART administered in patients who showed overt hypogonadism (n=8). In six patients who had agreed to be investigated about their sexuality, we further investigated the sexual function before and after six months of ART by using the IIEF-15 questionnaire. Essentially, we found that during AMT, patients showed lower cFT levels as well as higher SHBG and LH levels compared to baseline, without significant variations in TT levels over time, most probably because of SHBG increase. At 12 and 18 months-treatment with AMT, 80% of the patients showed overt hypergonadotropic hypogonadism. ART treatment with T gel of the hypogonadal patients subgroup resulted in a significant increase in cFT levels. When evaluating ED in AMT-treated patients, its prevalence (IIEF-15-EFD-defined) was 83.3% eighteen months of treatment. In addition, in six months ART (T or DHT gel)-treated hypogonadal patients, we observed a significant improvement in IIEF-15 total and subdomains scores, (including the EFD score), with an overall significant decrease in ED prevalence to 16.7%.

Adjuvant mitotane therapy (AMT) and LH, SHBG, TT, and cFT levels changes over time

In the present study, we reported LH, SHBG, TT, and cFT levels changes over time during AMT. In particular, we found that during

TABLE 3 Presence of overt hypogonadism and gynecomastia after 18 months of mitotane therapy (T3), patients treated with androgen replacement therapy (ART) and type of ART, and patients who agreed to be investigated about their sexuality.

Patients	Gynecomastia	Overt hypogonadism	Androgen replacement therapy (ART)	Patients who agreed to be investigated about sexuality
1	No	Yes	T gel 2 %	Yes
2	No	No	–	No
3	Yes	Yes	DHT gel 2.5%	Yes
4	Yes	Yes	DHT gel 2.5%	Yes
5	Yes	Yes	DHT gel 2.5%	Yes
6	No	Yes	T gel 2 %	Yes
7	No	No	–	No
8	No	Yes	T gel 2%	Yes
9	No	Yes	T gel 2%	No
10	No	Yes	T gel 2%	No

T, Testosterone; DHT, Dihydrotestosterone.

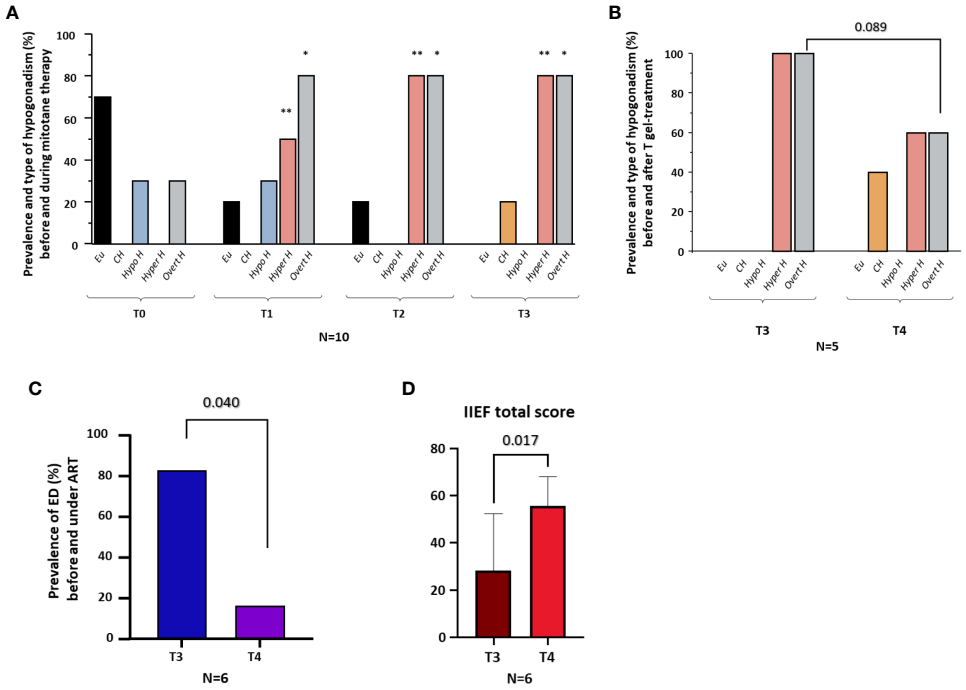

FIGURE 2
Prevalence and type of hypogonadism before (T0) and during (T1-T3) mitotane therapy; prevalence and type of hypogonadism before (T3) and six months after (T4) T gel therapy; prevalence of erectile dysfunction (ED) before (T3) and six months after (T4) androgen replacement therapy (ART); IIEF total score. **(A)**, Prevalence of eugonadism (Eu), compensated hypogonadism (CH), hypogonadotropic hypogonadism (Hypo H), hypergonadotropic hypogonadism (Hyper H) and overt hypogonadism (Overt H) in the whole cohort at baseline (T0) and 6 (T1), 12 (T2) and 18 (T3) months after the initiation of mitotane therapy. **(B)**, Prevalence of eugonadism (Eu), compensated hypogonadism (CH), hypogonadotropic hypogonadism (Hypo H), hypergonadotropic hypogonadism (Hyper H), and overt hypogonadism (Overt H) in five men before (T3) and after six months (T4) of T gel therapy. **(C)**, Prevalence of erectile dysfunction (ED) in six men before (T3) and after six months (T4) of androgen replacement therapy (ART, including patients under T gel [n=3] and DHT gel [n=3] therapy). **(D)**, Total score of International Index of Erectile Function-15 (IIEF-15) in six men before (T3) and after six months (T4) of ART. *p <0.05, comparing the prevalence of overt hypogonadism at T1, T2 and T3 *vs.* T0. **p <0.05, comparing the prevalence of hypergonadotropic hypogonadism at T1, T2 and T3 *vs.* T0.

AMT, patients showed lower cFT levels as well as higher SHBG and LH levels compared to baseline, without significant variations in TT levels over time. It has been demonstrated that mitotane causes a rise in the hepatic SHBG synthesis and release (18) that can lead to a reduction in cFT levels, despite frequent normal or elevated TT levels, and a compensatory elevation of LH. The increase in LH can, in turn, compensate the cFT reduction in some cases, leading to compensated hypogonadism. Since physical examination-related parameters, including body mass index and waistline, did not change in each patient at different time points, SHBG increase, and related cFT reduction, can be mainly attributed to AMT, excluding possible variations of SHBG and testosterone levels related to changes in fat mass, being SHBG and testosterone inversely associated with body mass index (35). The hormonal status in ACC patients under AMT has been evaluated previously only in four studies (17–20), with partially discordant results. A first study (17) reported a significant surge of sex hormone binding globulin (SHBG) levels associated with an initial rise in total testosterone (TT) levels, followed by a reduction, and with a decrease in calculated free testosterone (cFT) levels, with no changes in gonadotropins levels. A second study (18) reported a significant increase in SHBG, a decrease in cFT, but no change in TT levels and gonadotropins. A third study (19) reported an increase in TT but not in cFT levels, along with an increased level of luteinizing hormone (LH). A most recent study reported a cumulative prevalence of hypogonadism of 87.5%, however LH levels were not assessed and the type of hypogonadism was not evaluated (20). Of note, the difference in results reported in previous studies might in part be due to differences in mitotane regimen, timing of blood sampling and laboratory methods for mitotane measurement, as well as in the circulating levels of the drug.

Adjuvant mitotane therapy (AMT) and prevalence and type of hypogonadism

In the present study, we reported a high prevalence of overt hypogonadism in AMT male patients, timely associated with AMT duration, reaching 80% of cases after twelve and eighteen months of AMT. The time dependent SHBG and LH increase associated with lower cFT levels with no significant changes in TT levels observed in our patients might explain the higher prevalence of hypogonadism detected respect to a previous study, reporting hypogonadism in about one out of three patients under mitotane therapy (16). Of

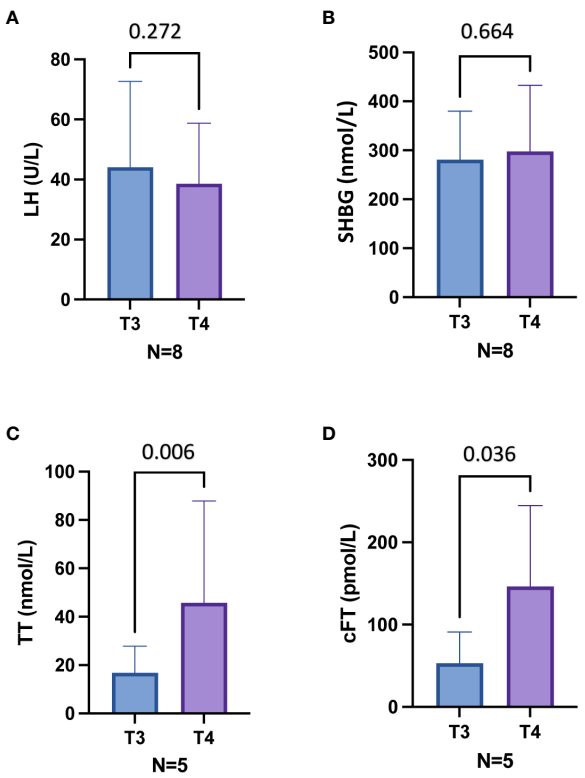

FIGURE 3
Hormonal parameters before (T3) and six months after (T4) androgen replacement therapy (ART) in eight patients with overt hypogonadism **(A, B)** and in five patients treated with T gel **(C, D)**. Out of eight patients, five have been treated with T gel and three with DHT gel. **(A)**, Luteinizing hormone (LH) levels in eight patients treated with ART. **(B)**, Sex hormone binding globulin (SHBG) levels in eight patients treated with ART. **(C)**, Total testosterone (TT) levels in five patients treated with T gel. **(D)**, Calculated free testosterone (cFT) levels in five patients treated with T gel. T3, 18 months after mitotane therapy; T4, 24 months after mitotane therapy and treated with ART since the last 6 months.

note, patients with overt hypogonadism showed a hypergonadotropic form.

At baseline, we observed that 30% of patients already had hypogonadism but with a hypogonadotropic form. This form of hypogonadism could be due either to the excess of cortisol if present, and/or to the tumor-related cachectic condition (24). After twelve and eighteen months of AMT, 80% of patients showed hypergonadotropic hypogonadism, and, at eighteen months, the remaining 20% showed compensated hypogonadism (high LH with normal cFT levels). The induction of hypergonadotropic hypogonadism was timely associated with AMT duration. However, no association was found between the onset of hypogonadism and mitotane levels or with TTR, in agreement with a previous study (20). Differently, other authors reported an inverse correlation between mitotane and TT levels (22). The present report of hypergonadotropic hypogonadism in surgically treated ACC patients under AMT is a new finding. In fact, two previous studies reported the onset of hypogonadotropic hypogonadism in patients treated with mitotane (19, 20), while one study found an increase in LH values without the development of overt hypogonadism (21). As reported above, the differences between the results of these studies could be in part related to the different mitotane concentration reached, time of evaluation and the laboratory methods used.

In our study, the number of patients that reached a mitotane level higher than 14 mg/l is in line with the literature data (36). As reported above, mitotane causes a rise in SHBG levels (18) that can lead to a reduction in cFT levels and a compensatory elevation of LH. The increase in LH can, in turn, compensate the cFT reduction. The compensatory elevation of LH levels can explain the two cases of compensated hypogonadism observed in our study, while a direct testicular damage of mitotane might explain the lack of compensation and the induction of a hypergonadotropic hypogonadism observed in most of the cases. Accordingly, a previous case report (37) showed that a patient affected by a cortisol-secreting ACC treated with mitotane developed hypergonadotropic hypogonadism associated with ED (37). The patient underwent a testicular biopsy which demonstrated a mitotane-related direct testicular toxicity. This is not surprising because mitotane is toxic for the steroid-producing cells, present not only in the adrenal gland but also as Leydig cells in the testis. The causative role of AMT in the aforementioned alterations was supported by the gradual improvement of libido observed in the patient after therapy discontinuation (37). Regarding this case report (37), two different aspects should be underlined. First, in the presence of hypercortisolism in a patient affected by a cortisol-secreting ACC, a hypogonatropic hypogonadism is expected, while the high levels of gonadotropins observed in that patient strengthen the hypothesis of a crucial negative effect of mitotane at testicular level. Second, the patient was treated with a very high dose of mitotane (6000 mg every 12 hours) which was interrupted due to gastrointestinal and central nervous system side effects (37). Hence, further investigations at the testicular level are needed in patients treated with mitotane in an adjuvant setting.

Androgen replacement therapy (ART) and LH, SHBG, TT, and cFT levels changes

Considering ART, in the subset of hypogonadal men treated with T gel we observed a significant increase in cFT levels and a trend toward an increase in TT levels after six months of treatment, and a shift of two out of five patients from hypergonadotropic to compensated hypogonadism. Conversely, no significant differences in LH and SHBG levels were observed in all patients treated with ART before and after therapy. Our findings, if supported by future studies, could suggest the use of higher doses of testosterone than those currently used foe the replacement therapy (TRT) in mitotane-induced hypogonadism. A limitation of our study is that we have not measured the DHT levels but is possible that the above considerations for TRT should be extended also to the DHT therapy.

Sexual function of ACC patients under AMT before and after ART

Regarding sexual function, six patients agreed to be investigated after eighteen months from the initiation of AMT using the IIEF-15 questionnaire. Interestingly, among them, 83.3% of the patients complained of clinically significant ED, as derived from the IIEF-15-EFD score. Upon ART, a significant reduction to 16.7% in ED prevalence was observed along with an overall improvement of sexual function. It could be hypothesized that the increased cFT levels, observed in men under T gel treatment, and/or the increased androgen receptor stimulation by T or DHT are responsible for the amelioration of sexual functions in the treated patients.

A previous study reported no significant clinical effects of TRT in surgically treated ACC patients under AMT (21), while another study observed an improvement in strength, mood and sexual desire in four out of seven treated patients (19). Larger studies comparing treated and non-treated patients as well as treatment with T or DHT gel are necessary to evaluate the real role of ART therapy in ACC patients treated with mitotane. Furthermore, the evaluation of bone assessment could clarify the role of TRT therapy in this setting.

Limitations and strengths of the study

This study has some limitations, including the retrospective nature and the limited number of patients studied, partly justified by the fact that ACC is a rare cancer. Hence, larger prospective studies are needed to confirm our results. Another limiting point is the use of the electrochemiluminescence method to evaluate TT levels instead of mass spectrometry. However, TT was assessed using the electrochemiluminescence immunoassay "ECLIA" (see above in the Methods section; https://labogids.sintmaria.be/sites/default/files/files/testosteron_ii_2017-11_v9.pdf), standardized via ID–GC/MS ("Isotope Dilution - Gas Chromatography/Mass Spectrometry") (26, 27), which has previously been demonstrated to show a good agreement with mass spectrometry in the distribution of TT results (28). However, mass spectrometry assays are considered to have the highest specificity and are preferred, but immunoassays are regarded to possess the ability to discriminate between hypogonadism and eugonadism. A further source of heterogeneity is associated to ART: in fact, five out of eight patients received T gel while three received DHT gel, because of symptomatic gynecomastia. In addition, cutaneous absorption of the gel can vary, despite the standardization of the dosage and the time interval between applications.

The present study has also some strengths. In particular, this study evaluated LH, SHBG, TT, and cFT changes at different times as well as, for the first time, sexual function before and after ART. Furthermore, LH, SHBG, TT, and cFT assessment was performed in a single reference laboratory (General laboratory of Careggi Hospital). Finally, this is the first study focused on the andrological assessment of ACC patients treated with mitotane and considering the prevalence and type of hypogonadism as primary aim, and assessing sexual function through a standardized questionnaire as the IIEF-15.

Conclusions

AMT is associated with a high prevalence of hypergonadotropic hypogonadism in ACC male patients, regardless of mitotane levels and TTR reached. Primary hypogonadism is essentially due to a rise in SHBG and to the absence of LH-related compensatory increase in T synthesis, likely resulting from a mitotane-induced direct damage to the Leydig cells. Patients who underwent surgery for ACC and subsequent AMT showed a high prevalence of sexual dysfunction, that could be ameliorated by ART. Hence, we suggest a periodic LH, SHBG, TT and cFT monitoring during AMT, as well as an assessment of sexual function, to identify those patients with sexual dysfunction who might benefit from ART to, at least partially, improve their quality of life.

Data availability statement

The raw data supporting the conclusions of this article will be made available by the authors, without undue reservation.

Ethics statement

Ethical approval was not required for the studies involving humans because we have the approval to collect samples of patients affected by adrenal diseases: Ethics Committee of University Hospital of Florence protocol code 59/11 version 1.3 date 05/04/2019. Informed consent was obtained from all subjects involved in the study. The studies were conducted in accordance with the local legislation and institutional requirements. The human samples used in this study were acquired from primarily isolated as part of your previous study for which ethical approval was obtained. Written informed consent to participate in this study was not required from the participants or the participants' legal guardians/next of kin in accordance with the national legislation and the institutional requirements.

Author contributions

LC: Writing – original draft, Writing – review & editing, Conceptualization, Methodology. CS: Data curation, Formal analysis, Methodology, Software, Writing – review & editing. LN: Data curation, Investigation, Writing – review & editing. GDF: Data curation, Investigation, Writing – review & editing. GC: Data curation, Methodology, Writing – review & editing. ER: Data curation, Writing – review & editing. SM: Data curation, Writing – review & editing. TE: Data curation, Writing – review & editing. FC: Data curation, Writing – review & editing. AF: Data curation, Writing – review & editing. LZ: Data curation, Writing – review & editing. AT: Writing – original draft, Writing – review & editing, Data curation. MMan: Supervision, Writing – review & editing. ML: Supervision, Writing – review & editing. MMag: Supervision, Writing – review & editing. FL: Conceptualization, Data curation, Writing – original draft, Writing – review & editing, Methodology.

Funding

The author(s) declare that no financial support was received for the research, authorship, and/or publication of this article.

Acknowledgments

This work is generated within the European Network for rare Endocrine Conditions (Endo-ERN) and ERN- EURACAN. We thank HRA Pharma and Section of Pharmacology and Toxicology of Hospital Cochin for quantification of mitotane plasma concentrations.

Conflict of interest

The authors declare that the research was conducted in the absence of any commercial or financial relationships that could be construed as a potential conflict of interest.

The author(s) declared that they were an editorial board member of Frontiers, at the time of submission. This had no impact on the peer review process and the final decision.

Publisher's note

Supplementary material

The Supplementary Material for this article can be found online at: https://www.frontiersin.org/articles/10.3389/fendo.2023.1320722/full#supplementary-material

SUPPLEMENTARY FIGURE 1
Subdomains scores of the International Index of Erectile Function-15 (IIEF-15) before (T3) and after six months (T4) of androgen replacement therapy (ART) in six patients who agreed to be investigated about their sexuality. Out of six patients, three have been treated with T gel and three with DHT gel **(A)**, IIEF-15-erectile function domain (EFD) scores. **(B)**, IIEF-15-intercourse satisfaction domain scores. **(C)**, IIEF-15-orgasmic function domain scores. **(D)**, IIEF-15-sexual desire domain scores. **(E)**, IIEF-15-overall satisfaction domain scores. T3, 18 months after mitotane therapy; T4, 24 months after mitotane therapy and treated with ART since the last 6 months.

References

1. Kerkhofs TM, Verhoeven RH, van der Zwan JM, Dieleman J, Kerstens MN, Links TP, et al. Adrenocortical carcinoma: a population-based study on incidence and survival in the Netherlands since 1993. *Eur J Cancer.* (2013) 49(11):2579–86. doi: 10.1016/j.ejca.2013.02.034

2. Stigliano A, Chiodini I, Giordano R, Faggiano A, Canu L, Della Casa S, et al. Management of adrenocortical carcinoma: A consensus statement of the Italian Society of Endocrinology (SIE). *J Endocrinological Invest* (2016) 39(1):103–21. doi: 10.1007/s40618-015-0349-9

3. Kebebew E, Reiff E, Duh QY, Clark OH, McMillan A. Extent of disease at presentation and outcome for adrenocortical carcinoma: have we made progress? *World J Surg* (2006) 30(5):872–8. doi: 10.1007/s00268-005-0329-x

4. Else T, Kim AC, Sabolch A, Raymond VM, Kandathil A, Caoili EM, et al. Adrenocortical carcinoma. *Endocr Rev* (2014) 35(2):282–326. doi: 10.1210/er.2013-1029

5. Fassnacht M, Johanssen S, Quinkler M, Bucsky P, Willenberg HS, Beuschlein F, et al. Limited prognostic value of the 2004 International Union Against Cancer staging classification for adrenocortical carcinoma: proposal for a Revised TNM Classification. *Cancer.* (2009) 115(2):243–50. doi: 10.1002/cncr.24030

6. Lughezzani G, Sun M, Perrotte P, Jeldres C, Alasker A, Isbarn H, et al. The European Network for the Study of Adrenal Tumors staging system is prognostically superior to the international union against cancer-staging system: a North American validation. *Eur J Cancer.* (2010) 46(4):713–9. doi: 10.1016/j.ejca.2009.12.007

7. De Filpo G, Mannelli M, Canu L. Adrenocortical carcinoma: current treatment options. *Curr Opin Oncol* (2021) 33(1):16–22. doi: 10.1097/CCO.0000000000000695

8. Glenn JA, Else T, Hughes DT, Cohen MS, Jolly S, Giordano TJ, et al. Longitudinal patterns of recurrence in patients with adrenocortical carcinoma. *Surgery.* (2019) 165(1):186–95. doi: 10.1016/j.surg.2018.04.068

9. Fassnacht M, Dekkers OM, Else T, Baudin E, Berruti A, de Krijger R, et al. European Society of Endocrinology Clinical Practice Guidelines on the management of adrenocortical carcinoma in adults, in collaboration with the European Network for the Study of Adrenal Tumors. *Eur J Endocrinol* (2018) 179(4):G1–G46. doi: 10.1530/EJE-18-0608

10. Hescot S, Amazit L, Lhomme M, Travers S, DuBow A, Battini S, et al. Identifying mitotane-induced mitochondria-associated membranes dysfunctions: metabolomic and lipidomic approaches. *Oncotarget.* (2017) 8(66):109924–40. doi: 10.18632/oncotarget.18968

11. Hescot S, Slama A, Lombès A, Paci A, Remy H, Leboulleux S, et al. Mitotane alters mitochondrial respiratory chain activity by inducing cytochrome c oxidase defect in human adrenocortical cells. *Endocr Relat Cancer.* (2013) 20(3):371–81. doi: 10.1530/ERC-12-0368

12. Sbiera S, Leich E, Liebisch G, Sbiera I, Schirbel A, Wiemer L, et al. Mitotane inhibits sterol-O-acyl transferase 1 triggering lipid-mediated endoplasmic reticulum stress and apoptosis in adrenocortical carcinoma cells. *Endocrinology.* (2015) 156(11):3895–908. doi: 10.1210/en.2015-1367

13. Tang Y, Liu Z, Zou Z, Liang J, Lu Y, Zhu Y. Benefits of adjuvant mitotane after resection of adrenocortical carcinoma: A systematic review and meta-analysis. *BioMed Res Int* (2018) 2018:9362108. doi: 10.1155/2018/9362108

14. Puglisi S, Calabrese A, Basile V, Ceccato F, Scaroni C, Simeoli C, et al. Mitotane concentrations influence the risk of recurrence in adrenocortical carcinoma patients on adjuvant treatment. *J Clin Med* (2019) 8(11). doi: 10.3390/jcm8111850

15. Puglisi S, Calabrese A, Basile V, Ceccato F, Scaroni C, Altieri B, et al. Mitotane concentrations influence outcome in patients with advanced adrenocortical carcinoma. *Cancers (Basel)* (2020) 12(3). doi: 10.3390/cancers12030740

16. Paragliola RM, Torino F, Papi G, Locantore P, Pontecorvi A, Corsello SM. Role of mitotane in adrenocortical carcinoma - review and state of the art. *Eur Endocrinol* (2018) 14(2):62–6. doi: 10.17925/EE.2018.14.2.62

17. Bianchini M, Puliani G, Chiefari A, Mormando M, Lauretta R, Appetecchia M. Metabolic and endocrine toxicities of mitotane: A systematic review. *Cancers (Basel).* (2021) 13(19). doi: 10.3390/cancers13195001

18. Nader N, Raverot G, Emptoz-Bonneton A, Déchaud H, Bonnay M, Baudin E, et al. Mitotane has an estrogenic effect on sex hormone-binding globulin and corticosteroid-binding globulin in humans. *J Clin Endocrinol Metab* (2006) 91(6):2165–70. doi: 10.1210/jc.2005-2157

19. Daffara F, De Francia S, Reimondo G, Zaggia B, Aroasio E, Porpiglia F, et al. Prospective evaluation of mitotane toxicity in adrenocortical cancer patients treated adjuvantly. *Endocr Relat Cancer.* (2008) 15(4):1043–53. doi: 10.1677/ERC-08-0103

20. Basile V, Puglisi S, Calabrese A, Pia A, Perotti P, Berruti A, et al. Unwanted hormonal and metabolic effects of postoperative adjuvant mitotane treatment for adrenocortical cancer. *Cancers (Basel)* (2020) 12(9). doi: 10.3390/cancers12092615

21. Vikner ME, Krogh J, Daugaard G, Andreassen M. Metabolic and hormonal side effects of mitotane treatment for adrenocortical carcinoma: A retrospective study in 50 Danish patients. *Clin Endocrinol (Oxf).* (2021) 94(2):141–9. doi: 10.1111/cen.14345

22. Delbarba A, Cosentini D, Facondo P, Laganà M, Pezzaioli LC, Cremaschi V, et al. Androgen serum levels in male patients with adrenocortical carcinoma given mitotane therapy: A single center retrospective longitudinal study. *Front Endocrinol (Lausanne).* (2023) 14:1128061. doi: 10.3389/fendo.2023.1128061

23. Lotti F, Maggi M. Sexual dysfunction and male infertility. *Nat Rev Urol.* (2018) 15(5):287–307. doi: 10.1038/nrurol.2018.20

24. Lotti F, Frizza F, Balercia G, Barbonetti A, Behre HM, Calogero AE, et al. The European Academy of Andrology (EAA) ultrasound study on healthy, fertile men: clinical, seminal and biochemical characteristics. *Andrology.* (2020) 8(5):1005–20. doi: 10.1111/andr.12808

25. Bhasin S, Brito JP, Cunningham GR, Hayes FJ, Hodis HN, Matsumoto AM, et al. Testosterone therapy in men with hypogonadism: an endocrine society clinical practice guideline. *J Clin Endocrinol Metab* (2018) 103(5):1715–44. doi: 10.1210/jc.2018-00229

26. Thienpont LM, De Brabandere VI, Stöckl D, De Leenheer AP. Use of cyclodextrins for prepurification of progesterone and testosterone from human serum prior to determination with isotope dilution gas chromatography/mass spectrometry. *Anal Chem* (1994) 66(22):4116–9. doi: 10.1021/ac00094a041

27. Thienpont L, Franzini C, Kratochvila J, Middle J, Ricós C, Siekmann L, et al. Analytical quality specifications for reference methods and operating specifications for networks of reference laboratories. discussion paper from the members of the external quality assessment (EQA) Working Group B1) on target values in EQAS. *Eur J Clin Chem Clin Biochem* (1995) 33(12):949–57.

28. Huhtaniemi IT, Tajar A, Lee DM, O'Neill TW, Finn JD, Bartfai G, et al. Comparison of serum testosterone and estradiol measurements in 3174 European men using platform immunoassay and mass spectrometry; relevance for the diagnostics in aging men. *Eur J Endocrinol* (2012) 166(6):983–91. doi: 10.1530/EJE-11-1051

29. Wang C, Nieschlag E, Swerdloff R, Behre HM, Hellstrom WJ, Gooren LJ, et al. ISA, ISSAM, EAU, EAA and ASA recommendations: investigation, treatment and monitoring of late-onset hypogonadism in males. *Int J Impot Res* (2009) 21(1):1–8.

30. Tajar A, Forti G, O'Neill TW, Lee DM, Silman AJ, Finn JD, et al. Characteristics of secondary, primary, and compensated hypogonadism in aging men: evidence from the European Male Ageing Study. *J Clin Endocrinol Metab* (2010) 95(4):1810–8. doi: 10.1210/jc.2009-1796

31. Rastrelli G, Corona G, Tarocchi M, Mannucci E, Maggi M. How to define hypogonadism? Results from a population of men consulting for sexual dysfunction. *J Endocrinol Invest.* (2016) 39(4):473–84. doi: 10.1007/s40618-015-0425-1

32. Rosen RC, Riley A, Wagner G, Osterloh IH, Kirkpatrick J, Mishra A. The international index of erectile function (IIEF): a multidimensional scale for assessment of erectile dysfunction. *Urology.* (1997) 49(6):822–30. doi: 10.1016/S0090-4295(97)00238-0

33. Cappelleri JC, Rosen RC. Reply to 'The sexual health inventory for men (IIEF-5)' by JA Vroege. *Int J Impot Res* (1999) 11(6):353–4. doi: 10.1038/sj.ijir.3900481

34. Lotti F, Corona G, Rastrelli G, Forti G, Jannini EA, Maggi M. Clinical correlates of erectile dysfunction and premature ejaculation in men with couple infertility. *J Sex Med* (2012) 9(10):2698–707. doi: 10.1111/j.1743-6109.2012.02872.x

35. Marriott RJ, Murray K, Adams RJ, Antonio L, Ballantyne CM, Bauer DC, et al. Factors associated with circulating sex hormones in men : individual participant data meta-analyses. *Ann Intern Med* (2023) 176(9):1221–34. doi: 10.7326/M23-0342

36. Terzolo M, Fassnacht M, Perotti P, Libé R, Kastelan D, Lacroix A, et al. Adjuvant mitotane versus surveillance in low-grade, localised adrenocortical carcinoma (ADIUVO): an international, multicentre, open-label, randomised, phase 3 trial and observational study. *Lancet Diabetes Endocrinol* (2023) 11(10):720–30. doi: 10.1016/S2213-8587(23)00193-6

37. Sparagana M. Primary hypogonadism associated with o,p' DDD (mitotane) therapy. *J Toxicol Clin Toxicol* (1987) 25(6):463–72. doi: 10.3109/15563658708992649

frontiers | Frontiers in Endocrinology

TYPE Original Research
PUBLISHED 01 March 2024
DOI 10.3389/fendo.2024.1336306

OPEN ACCESS

EDITED BY
Roberta Giordano,
University of Turin, Italy

REVIEWED BY
Sergei Tevosian,
University of Florida, United States
Avinaash Vickram Maharaj,
Queen Mary University of London,
United Kingdom

*CORRESPONDENCE
Marta Araujo-Castro
marta.araujo@salud.madrid.org

RECEIVED 10 November 2023
ACCEPTED 06 February 2024
PUBLISHED 01 March 2024

CITATION
Araujo-Castro M, Parra P, Martín Rojas-Marcos P, Paja Fano M, González Boillos M, Pascual-Corrales E, García Cano AM, Ruiz-Sanchez JG, Vicente Delgado A, Gómez Hoyos E, Ferreira R, García Sanz I, Recasens Sala M, Barahona San Millan R, Picón César MJ, Díaz Guardiola P, Perdomo CM, Manjón-Miguélez L, García Centeno R, Rebollo Román Á, Gracia Gimeno P, Robles Lázaro C, Morales-Ruiz M, Calatayud M, Furio Collao SA, Meneses D, Sampedro Nuñez M, Escudero Quesada V, Mena Ribas E, Sanmartín Sánchez A, Gonzalvo Diaz C, Lamas C, del Castillo Tous M, Serrano Gotarredona J, Michalopoulou Alevras T, Moya Mateo EM and Hanzu FA (2024) Differences in the clinical and hormonal presentation of patients with familial and sporadic primary aldosteronism.
Front. Endocrinol. 15:1336306.
doi: 10.3389/fendo.2024.1336306

Differences in the clinical and hormonal presentation of patients with familial and sporadic primary aldosteronism

Marta Araujo-Castro [1,2*], Paola Parra [3], Patricia Martín Rojas-Marcos [3], Miguel Paja Fano [4,5], Marga González Boillos [6], Eider Pascual-Corrales [1,2], Ana María García Cano [7], Jorge Gabriel Ruiz-Sanchez [8], Almudena Vicente Delgado [9], Emilia Gómez Hoyos [10], Rui Ferreira [11], Iñigo García Sanz [12], Mònica Recasens Sala [13], Rebeca Barahona San Millan [13], María José Picón César [14,15], Patricia Díaz Guardiola [16], Carolina M. Perdomo [17], Laura Manjón-Miguélez [18,19], Rogelio García Centeno [20], Ángel Rebollo Román [21], Paola Gracia Gimeno [22], Cristina Robles Lázaro [23], Manuel Morales-Ruiz [24], María Calatayud [25], Simone Andree Furio Collao [25], Diego Meneses [6], Miguel Sampedro Nuñez [26], Verónica Escudero Quesada [27], Elena Mena Ribas [28], Alicia Sanmartín Sánchez [28], Cesar Gonzalvo Diaz [29], Cristina Lamas [29], María del Castillo Tous [30], Joaquín Serrano Gotarredona [31], Theodora Michalopoulou Alevras [32], Eva María Moya Mateo [33] and Felicia A. Hanzu [34]

[1]Endocrinology and Nutrition Department, Hospital Universitario Ramón y Cajal, Madrid, Spain, [2]Instituto de Investigación Biomédica Ramón y Cajal (IRYCIS), Madrid, Spain, [3]Endocrinology and Nutrition Department, Hospital Universitario La Paz, Madrid, Spain, [4]Endocrinology and Nutrition Department, OSI Bilbao-Basurto, Hospital Universitario de Basurto, Bilbao, Spain, [5]Medicine Department, Basque Country University, Bilbao, Spain, [6]Endocrinology and Nutrition Department, Hospital Universitario de Castellón, Castellón, Spain, [7]Biochemistry Department, Hospital Universitario Ramón y Cajal, Madrid, Spain, [8]Endocrinology and Nutrition Department, Hospital Universitario Fundación Jiménez Díaz, Madrid, Spain, [9]Endocrinology and Nutrition Department, Hospital Universitario de Toledo, Toledo, Spain, [10]Endocrinology and Nutrition Department, Hospital Universitario de Valladolid, Valladolid, Spain, [11]Endocrinology and Nutrition Department, Hospital Universitario Rey Juan Carlos, Madrid, Spain, [12]General and Digestive Surgery Department, Hospital Universitario de La Princesa, Madrid, Spain, [13]Endocrinology and Nutrition Department, Hospital De Girona Doctor Josep Trueta, Girona, Spain, [14]Endocrinology and Nutrition Department, Hospital Universitario Virgen de la Victoria de Málaga, IBIMA, Malaga, Spain, [15]CIBEROBN, Madrid, Spain, [16]Endocrinology and Nutrition Department, Hospital Universitario Infanta Sofía, Madrid, Spain, [17]Endocrinology and Nutrition Department, Clínica Universidad de Navarra, Pamplona, Spain, [18]Endocrinology and Nutrition Department, Hospital Universitario Central de Asturias, Oviedo, Spain, [19]Instituto de Investigación Sanitaria del Principado de Asturias (ISPA), Oviedo, Spain, [20]Endocrinology and Nutrition Department, Hospital Universitario Gregorio Marañón, Madrid, Spain, [21]Endocrinology and Nutrition Department, Hospital Reina Sofía, Córdoba, Spain, [22]Endocrinology and Nutrition Department, Hospital Royo Villanova, Zaragoza, Spain, [23]Endocrinology and Nutrition Department, Complejo Universitario de Salamanca, Salamanca, Spain, [24]Biochemistry and Molecular Genetics Department-CDB, Hospital Clinic, IDIBAPS, CIBERehd, Barcelona, Spain, [25]Endocrinology and Nutrition Department, Hospital Doce de Octubre, Madrid, Spain, [26]Endocrinology and Nutrition Department, Hospital Universitario La Princesa, Madrid, Spain, [27]Nephrology Department, Hospital

Universitario Doctor Peset, Valencia, Spain, [28]Endocrinology and Nutrition Department, Hospital Universitario Son Espases, Palma de Mallorca, Spain, [29]Endocrinology and Nutrition Department, Hospital Universitario De Albacete, Albacete, Spain, [30]Endocrinology and Nutrition Department, Hospital Universitario Virgen Macarena, Sevilla, Spain, [31]Endocrinology and Nutrition Department, Hospital General Universitario de Alicante, Alicante, Spain, [32]Endocrinology and Nutrition Department, Hospital Joan XXIII, Tarragona, Spain, [33]Internal Medicine, Hospital Universitario Infanta Leonor, Madrid, Spain, [34]Endocrinology and Nutrition Department, Hospital Clinic, IDIPAS, Barcelona, Spain

Purpose: To compare the clinical and hormonal characteristics of patients with familial hyperaldosteronism (FH) and sporadic primary aldosteronism (PA).

Methods: A systematic review of the literature was performed for the identification of FH patients. The SPAIN-ALDO registry cohort of patients with no suspicion of FH was chosen as the comparator group (sporadic group).

Results: A total of 360 FH (246 FH type I, 73 type II, 29 type III, and 12 type IV) cases and 830 sporadic PA patients were included. Patients with FH-I were younger than sporadic cases, and women were more commonly affected (P = 0.003). In addition, the plasma aldosterone concentration (PAC) was lower, plasma renin activity (PRA) higher, and hypokalemia (P < 0.001) less frequent than in sporadic cases. Except for a younger age (P < 0.001) and higher diastolic blood pressure (P = 0.006), the clinical and hormonal profiles of FH-II and sporadic cases were similar. FH-III had a distinct phenotype, with higher PAC and higher frequency of hypokalemia (P < 0.001), and presented 45 years before sporadic cases. Nevertheless, the clinical and hormonal phenotypes of FH-IV and sporadic cases were similar, with the former being younger and having lower serum potassium levels.

Conclusion: In addition to being younger and having a family history of PA, FH-I and III share other typical characteristics. In this regard, FH-I is characterized by a low prevalence of hypokalemia and FH-III by a severe aldosterone excess causing hypokalemia in more than 85% of patients. The clinical and hormonal phenotype of type II and IV is similar to the sporadic cases.

KEYWORDS

primary aldosteronism, familial hyperaldosteronism, genetic study, pathogenic variant, plasma aldosterone concentration

1 Introduction

Primary aldosteronism (PA) is the most common cause of secondary hypertension, accounting for 10% of hypertensive patients in the general setting and of 20% in patients with refractory hypertension (1). Approximately 95% of these cases are sporadic, with the remaining 5% caused by a pathogenic variant in genes that result in an increase in the transcription and expression of CYP11B2, which is responsible for aldosterone synthesis (familial hyperaldosteronism (FH) types II, III, and IV) or a fusion of the *CYP11B2* and *CYP11B1* genes, which is responsible for FH-I or glucocorticoid-remediable PA (GRA) (2).

Sutherland et al. described the familial occurrence of PA for the first time in 1966 (3). Lifton et al. (4) demonstrated the genetic basis of this familial form: GRA caused by a hybrid gene composed of ACTH-regulated 11b-hydroxylase (CYP11B1) regulatory sequences and aldosterone synthase (CYP11B2) coding sequences. Following that, a number of FH type I cases have been described in the literature (5–29). Gordon et al. (30) described the first case of FH type II several years after the discovery of FH-I. Since its first description, more than 80 cases have been reported in the literature (6, 31–41). More recently, two additional kinds of genetic PA have been identified: type III caused by a pathogenic mutation in *KCNJ5* (42) and type IV caused by a *CACNA1H* pathogenic variant (43).

However, few studies have directly compared the clinical and hormonal aspects of the familial and sporadic PA cases (11, 33), despite the well-known description of the familial cases. Michael Stowasser (33) was the first to compare 88 consecutive PA patients and 13 FH type II patients. There were no differences in age at presentation, sex incidence, and biochemical parameters between both groups. Another series comparing family members with positive (n = 21) and negative (n = 18) study for FH-I found that body mass index (BMI) was lower and plasma aldosterone concentration (PAC) higher in FH-I; however, the control group did not have PA in this study (26). This study design was comparable with the Litchfield study (25). A subsequent study matched 79 GRA-positive patients and 114 GRA-negative unilateral PA patients by age, gender, and BMI. They found that being younger and having a lower PAC were associated with a higher probability of FH-I (11). Nevertheless, the majority of these studies contained a small number of patients and only evaluated the differences between sporadic PA cases and FH type I and type II cases.

Considering this background, the aim of our study was to identify the clinical and hormonal features linked to FH by comparing a large cohort of FH patients to a group of sporadic PA cases. Based on that information, we will aim to determine which PA patients should be genetically tested.

2 Methods

2.1 Patients

The control group of sporadic cases was extracted from the Spanish Primary Aldosteronism (SPAIN-ALDO) Registry of the Spanish Endocrinology and Nutrition Society (SEEN). As previously described (44), this is a multicenter collaborative study involving patients with a diagnosis of PA who were followed up in 35 Spanish tertiary hospitals between January 2018 and July 2023. At the time of data analysis (11/08/2023), the registry contained 855 patients with PA.

We excluded the following patients from the sporadic group: (i) those patients with a positive genetic study (n = 1); (ii) those with familial history of PA and no available negative genetic study for FH (n = 13); (iii) patients who underwent genetic testing due to high suspicion and whose results were pending (n = 7); and (iv) patients diagnosed of PA before the age of 30 and no available negative genetic study for FH (n = 4). Thus, 830 cases were included. Of these 830 patients, only 18 underwent genetic study for FH, with negative results (Figure 1).

For the diagnosis of FH, we followed the following criteria: Diagnosis of FH-I was performed by long-PCR amplification of the hybrid gene (*CYP11B1/CYP11B2*); diagnosis of FH-II was made when a mutation in *CLCN2* was detected or when there was a family history of PA in at least two family members; diagnosis of FH-III when a pathogenic variant in *KCNJ5* was demonstrated and FH-IV if a pathogenic variant in *CACNA1H* was detected.

2.2 Definitions

PA diagnosis was made following the recommendations of the clinical international guidelines for PA (45, 46). Blood samples for plasma renin activity (PRA) and/or concentration (PRC) and PAC were collected from all patients. As we have previously described (47), those patients (n = 340) who did not meet the criteria of overt PA (hypokalemia, PAC >18 ng/dL and pathological aldosterone-to-renin ratio) underwent at least one of the following confirmatory tests: oral sodium loading, saline infusion test, captopril challenge test, and/or fludrocortisone suppression test.

The findings of the adrenal venous sampling (AVS) and/or the outcomes after adrenalectomy were used to differentiate between unilateral and bilateral PA. A total of 326 out of 830 patients underwent AVS, with 190 being successful. Unilateral disease was assumed if the lateralization index of the aldosterone to cortisol ratio was ≥4.0 on the dominant vs. non-dominant side during ACTH stimulation or at least two times higher under unstimulated conditions (1, 6). In patients without successful AVS, unilateral disease was assumed if a complete biochemical cure after surgery was obtained (n = 186). The PASO classification criteria were used to define biochemical and clinical cure for PA after adrenalectomy (48).

2.3 Search strategy for the identification of FH cases

The FH cases were identified using the SANRA scale (49). The search strategy was conducted in PubMed without a date filter until 12/08/2023. The following keywords were used in the search: familial primary aldosteronism [TI]: 136 results; familial hyperaldosteronism [TI]: 61 results; hereditary aldosteronism [title]: 18 results; inherited primary aldosteronism [TI]: 16 results; dexamethasone-suppressible aldosteronism: 2 results; and glucocorticoid-remediable aldosteronism [TI]: 49 results. Potentially relevant articles were retrieved after reading the title, abstract, or whole article, and we discarded repeated articles. Only articles written in English were considered. The articles found through these searches as well as the pertinent references listed in those papers were reviewed. After that, 53 original articles were included: 25 articles about FH-I (5–29), 12 about FH-II (6, 31–41), 13 about FAH-III (32, 42, 50–60), and 3 about FAH-IV (43, 61, 62) (Figure 2).

2.4 Statistical analysis

All statistical analyses were conducted with STATA.15. Shapiro–Wilk's test was used to assess the normality of continuous variables. All data are expressed as the mean and standard deviation for normally distributed variables and the median (and range) for non-normally distributed variables. Student's t-test was used to compare quantitative variables and

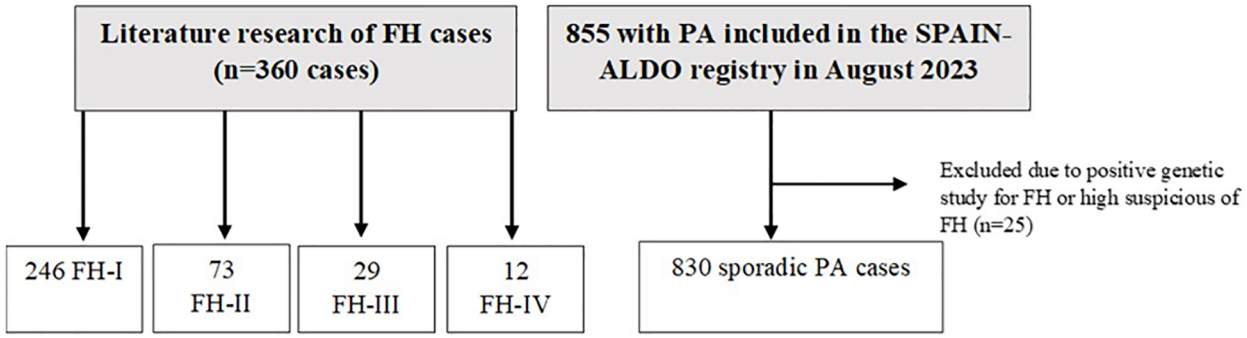

FIGURE 1
Study population. PA, primary aldosteronism; FH, familial hyperaldosteronism.

the X^2 test for qualitative variables between two groups. In all cases, a two-tailed P value < 0.05 was considered statistically significant.

3 Results

3.1 Differences between FH-I and sporadic cases

A total of 246 patients with confirmed FH-I were compared with 830 cases of sporadic PA. Patients with FH-I were found to be younger than sporadic cases, and women were more commonly affected than men. On the other hand, sporadic cases had higher PAC and lower PRA than FH-I. Besides, hypokalemia was uncommon (12%) in FH-I patients, but it reached a prevalence of 60% in sporadic cases. 40.3% of the FH-I patients (n = 77/129) were normotensive. No other differences were detected between the two groups (Table 1).

3.2 Differences between FH-II and sporadic cases

We compared 73 FH-II patients to 830 sporadic PA patients. The clinical and hormonal profiles were similar, except for a younger age and higher diastolic blood pressure in the group of FH-II (Table 2).

3.3 Differences between FH-III and IV and sporadic cases

The 29 cases of FH type III and the 12 cases of FH-IV were compared with the sporadic cases. FH-III showed a distinct phenotype, with higher PAC, lower PRA, lower serum potassium levels, and a younger age at PA diagnosis, presenting 45 years earlier than the sporadic cases (Table 3). Due to problems in achieving proper blood pressure control, 17 of the 29 patients with FH-III underwent bilateral adrenalectomy.

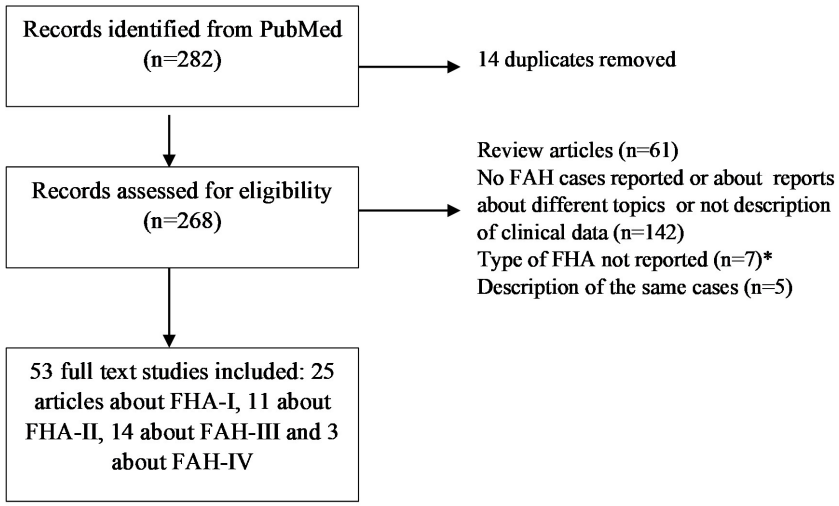

FIGURE 2
Flow-chart for identification of FAH cases. FH, familial hyperaldosteronism.

10.3389/fendo.2024.1336306

TABLE 1 Differences between FH-I and sporadic PA cases.

Variable	FH-I (n = 246)	Sporadic PA (n = 830)	P value
Age, years	33.6 ± 18.07	56.5 ± 4.76	<0.001
% women	51.9% (n = 126)	41.3% (n = 342)	0.003
Systolic blood pressure, mmHg	151.0 ± 20.05	150.3 ± 21.86	0.689
Diastolic blood pressure, mmHg	92.5 ± 10.44	89.7 ± 13.52	0.007
Hypokalemia, %	11.6% (n = 17/146)	59.6% (n = 486/816)	<0.001
Serum K levels (mEq/L)	3.9 ± 0.50	3.8 ± 1.67	0.304
PAC (ng/dL)	29.5 ± 15.03	44.4 ± 78.85	0.005
PRA (ng/mL/h)	1.3 ± 6.81	0.4 ± 0.86	0.004

FH, familiar hyperaldosteronism; PA, primary aldosteronism; PAC, plasma aldosterone concentration; PRA, plasma renin activity. Normal ranges for serum K levels: 3.5 mEq/mL–4.5 mEq/mL.

The clinical and hormonal phenotypes of FH type IV and sporadic cases were similar, except for lower age and serum potassium levels and higher PRA at presentation in the former (Table 3).

4 Discussion

The most consistent finding in FH patients was the younger age of the four types when compared with sporadic PA cases. Because

TABLE 2 Differences between FH-II and sporadic PA cases.

Variable	FH-II (n = 73)**	Sporadic PA (n = 830)	P value
Age, years	33.6 ± 19.65	56.5 ± 4.76	<0.001
% women	51.4% (n = 37)	41.3% (n = 342)	0.097
Systolic blood pressure, mmHg	154.6 ± 31.05	150.3 ± 21.86	0.230
Diastolic blood pressure, mmHg	97.3 ± 21.16	89.7 ± 13.52	0.006
Hypokalemia, %	53.9% (n = 35/65)	59.6% (n = 486/816)	0.373
Serum K levels (mEq/L)	3.5 ± 0.56	3.8 ± 1.67	0.164
PAC (ng/dL)	43.3 ± 45.4	44.4 ± 78.85	0.226
PRA (ng/mL/h)	0.82 ± 1.40	0.4 ± 0.86	0.017

FH, familiar hyperaldosteronism; PA, primary aldosteronism; PAC, plasma aldosterone concentration; PRA, plasma renin activity. Normal ranges for serum K levels: 3.5 mEq/mL–4.5 mEq/mL.

**FH-II was genetically demonstrated in 18 out of the 73 patients (pathogenic variant in the *CCLN2* gene); in the other 55 patients, the diagnosed was based on the presence of ≥2 members of the same family with confirmed PA (6).

TABLE 3 Differences between FH-III and IV and sporadic PA cases.

Variable	FH-III (n = 29)	FH-IV (n = 12)	Sporadic PA (n = 830)
Age, years	7.42 ± 11.51*	23.3 ± 20.41*	56.5 ± 4.76
% women	75.9% (n = 7)*	33.3% (n = 4)	41.3% (n = 342)
Systolic blood pressure, mmHg	154.4 ± 27.85	151.6 ± 20.08	150.3 ± 21.86
Diastolic blood pressure, mmHg	99.4 ± 19.36*	98.8 ± 17.56	89.7 ± 13.52
Hypokalemia, %	89.3% (n = 25/28)*	58.3% (n = 7/12)	59.6% (n = 486/816)
Serum K levels (mEq/L)	2.6 ± 0.74*	3.1 ± 0.71*	3.8 ± 1.67
PAC (ng/dL)	101.5 ± 80.73*	44.1 ± 31.22	44.4 ± 78.85
PRA (ng/mL/h)	0.18 ± 1.40*	1.3 ± 1.31*	0.4 ± 0.86

FH, familiar hyperaldosteronism; PA, primary aldosteronism; PAC, plasma aldosterone concentration; PRA, plasma renin activity. Normal ranges for serum K levels: 3.5 mEq/mL–4.5 mEq/mL.

* symbol refers to statistically significant differences between FAH cases when comparing with sporadic cases.

FH is transmitted by autosomal dominant inheritance, the history of other members of the family with PA is another key indicator to infer hereditary PA (63). In fact, the current general recommendation for screening hereditary PA is for patients with early onset and a positive family history of PA (64).

When we compared FH type I and sporadic cases, we found that, in addition to being younger, FH-I had more severe hypertension than in sporadic PA patients. In this regard, it has been previously reported that severe hypertension in infancy and early adulthood is the most typical presentation of GRA (5). Nevertheless, some cases are just moderately hypertensive, if at all (65). According to this, we found that 40% of the FH-I patients had normal blood pressure levels and were classed as normotensive. However, even in normotensive FH-I patients, the aldosterone excess is associated with increased left ventricular wall thickness and reduced diastolic function when compared with normotensive subjects without GRA (23). Another notable feature of FH-I cases in our study was the low prevalence of hypokalemia, which occurred in less than 12% of the cases. Accordingly, a prevalence of 13% was described in the PATOGEN study (6) and in the Aglony et al. series (5). The real cause of hypokalemia in individuals with PA is due to the fact that the *CYP11B1/CYP11B2* hybrid gene is unknown; however, it may be connected to the fact that aldosterone secretion is regulated by ACTH instead of angiotensin II. Thus, the mineralocorticoid effect may be expected to be reduced. This hypothesis is supported by the observation that PRA was less suppressed in FH-I than in sporadic cases. Considering our results, it is important to take into account that FH-I may be hypokalemic or normokalemic. Thus, the presence of normal serum potassium

levels does not discount genetic testing particularly in families where the penetrance of hypertension is inevitably variable.

In relation to FH type II, we found that the clinical and hormonal profile was comparable with sporadic cases, apart from a younger age and slightly higher diastolic blood pressure in the group of FH-II. Type II FH is caused by a pathogenic mutation in the *CLCN2* gene, leading to elevated intracellular Ca^{2+} concentration, which triggers depolarization and aldosterone secretion (43). The only previous study that compared sporadic and FH-II cases described that both groups had similar potassium levels and blood pressure levels. In addition, since the prevalence of aldosterone producing adenomas was not significantly different in FH-II and sporadic PA patients, the former group may have had radiological features similar to sporadic cases (6). Considering that the clinical picture does not allow to differentiate it from sporadic cases and taking into account that FH-II is the most common form of hereditary PA (6), the most recent Endocrinology PA guidelines recommend screening for familial FH type II in all hypertensive patients who have relatives with FH (66). However, we are aware that some patients classified as FH-II may be sporadic cases coexisting within the same family since until the discovery of the underlying genetic cause of FH-II, all cases with two or more positive cases of primary aldosteronism in the same family were classified as FH type II.

Type III FH is a severe form of PA characterized by extensive adrenocortical hyperplasia and hybrid steroid synthesis (42). The genetic defect is located in the *KCNJ5* gene. Women are disproportionately afflicted, accounting for more than 75% of all cases described in the literature. A higher prevalence of women has also been described in those sporadic PA patients who harbor a somatic pathogenic variant in *KCNJ5* (67). As we found, FH-III is frequently detected at a very young age and PAC reached double values than in sporadic cases. In addition, serum potassium levels are typically low, with a prevalence of hypokalemia nearing 90%. In fact, over 60% of these patients required a bilateral adrenalectomy to achieve adequate blood pressure control. Nevertheless, the severity of the PA varies depending on the *KCNJ5* pathogenic variant; for example, p.T158A, p.I157S, p.E145Q, and p.G151R are associated with early-onset severe PA (68) whereas p.G151E and p.Y152C present with mild PA (50, 59).

Only few cases of FH-IV have been reported in the literature (43). FH-IV is caused by germline defects in *CACNA1H*. Type IV, like FH-III, manifests at a very young age but later than the FH III cases. When compared with sporadic cases, serum potassium levels are also lower, but the degree of decline seems to be less severe than in FH type III. Patients with a family history of FH and early diagnosis of PA should be screened for familial FH type IV. Thus, the indications are identical to those for FH-III (45). In fact, if there is a suspicion of genetic PA, it is recommended that all genes be tested.

We are aware that our study has some limitations. The main limitation is that the definition of sporadic in the control group of sporadic patients was based on the epidemiological and clinical characteristics since the majority of patients in the SPAIN-ALDO did not undergo genetic testing. Nevertheless, cases with any suspicion of familial origin were excluded. Second, we have included all the cases reported in the literature following our strategy research that have available clinical and hormonal data, including patients from all over the world. Thus, we know that ethnic differences may also play a role in the many clinical and hormonal phenotypes detected. Thus, specific studies comparing sporadic and familial cases of the same ethnicity should be conducted. However, despite these limitations, this is the largest study comparing all the patients with FH of different types as well as sporadic PA cases.

5 Conclusion

In addition to being younger and having a family history of PA, FH-I and III share other typical characteristics. In this regard, FH-I is characterized by a low prevalence of hypokalemia and FH-III by a severe aldosterone excess causing hypokalemia in more than 85% of patients. The clinical and hormonal phenotype of types II and IV is similar to the sporadic cases. However, all genes should be tested if there is a possibility of genetic PA.

Data availability statement

The raw data supporting the conclusions of this article will be made available by the authors, without undue reservation.

Ethics statement

The studies involving humans were approved by CEIm Hospital Ramón y Cajal, Madrid. The studies were conducted in accordance with the local legislation and institutional requirements. The ethics committee/institutional review board waived the requirement of written informed consent for participation from the participants or the participants' legal guardians/next of kin because Retrospective nature of the study.

Author contributions

MA: Conceptualization, Data curation, Formal analysis, Investigation, Methodology, Writing – original draft, Writing – review & editing. PP: Writing – review & editing. PR: Writing – review & editing. MF: Writing – review & editing. MB: Writing – review & editing. EP: Writing – review & editing. AC: Writing – review & editing. JR: Writing – review & editing. AD: Writing – review & editing. EH: Writing – review & editing. RF: Writing – review & editing. IS: Writing – review & editing. MS: Writing – review & editing. RM: Writing – review & editing. MC: Writing – review & editing. PG: Writing – review & editing. CP: Writing – review & editing. LM: Writing – review & editing. RC: Writing – review & editing. ÁR: Writing – review & editing. PG: Writing – review & editing. CL: Writing – review & editing. MM:

Writing – review & editing. MC: Writing – review & editing. SC: Writing – review & editing. DM: Writing – review & editing. MN: Writing – review & editing. VQ: Writing – review & editing. ER: Writing – review & editing. AS: Writing – review & editing. CD: Writing – review & editing. CO: Writing – review & editing. MT: Writing – review & editing. JG: Writing – review & editing. TM: Writing – review & editing. EM: Writing – review & editing. FH: Writing – review & editing.

Funding

The author(s) declare that no financial support was received for the research, authorship, and/or publication of this article.

Conflict of interest

The authors declare that the research was conducted in the absence of any commercial or financial relationships that could be construed as a potential conflict of interest.

Publisher's note

References

1. Pilz S, Grubler MR, Theiler-Schwetz V, Malle O, Trummer C. The unrecognized prevalence of primary aldosteronism. *Ann Intern Med*. (2020) 173:682. doi: 10.7326/L20-1094

2. Araujo-Castro M, Martín Rojas-Marcos P, Parra Ramírez P. Familial forms and molecular profile of primary hyperaldosteronism. *Hipertens y Riesgo Vasc*. (2022) 39:167–73. doi: 10.1016/J.HIPERT.2022.05.007

3. Sutherland DJ, Ruse JL, Laidlaw JC. Hypertension, increased aldosterone secretion and low plasma renin activity relieved by dexamethasone. *Can Med Assoc J*. (1966) 95:1109–19.

4. Lifton RP, Dluhy RG, Powers M, Rich GM, Cook S, Ulick S, et al. A chimaeric llβ-hydroxylase/aldosterone synthase gene causes glucocorticoid-remediable aldosteronism and human hypertension. *Nature*. (1992) 355:262–5. doi: 10.1038/355262a0

5. Aglony M, Martínez-Aguayo A, Carvajal CA, Campino C, García H, Bancalari R, et al. Frequency of familial hyperaldosteronism type 1 in a hypertensive pediatric population: clinical and biochemical presentation. *Hypertens (Dallas Tex 1979)*. (2011) 57:1117–21. doi: 10.1161/HYPERTENSIONAHA.110.168740

6. Mulatero P, Tizzani D, Viola A, Bertello C, Monticone S, Mengozzi G, et al. Prevalence and characteristics of familial hyperaldosteronism: The PATOGEN study (Primary aldosteronism in TOrino-GENetic forms). *Hypertension*. (2011) 58:797–803. doi: 10.1161/HYPERTENSIONAHA.111.175083

7. Sanga V, Lenzini L, Seccia TM, Rossi GP. Familial hyperaldosteronism type 1 and pregnancy: successful treatment with low dose dexamethasone. *Blood Press*. (2021) 30:133–7. doi: 10.1080/08037051.2020.1863771

8. Carvajal CA, Campino C, Martinez-Aguayo A, Tichauer JE, Bancalari R, Valdivia C, et al. A new presentation of the chimeric CYP11B1/CYP11B2 gene with low prevalence of primary aldosteronism and atypical gene segregation pattern. *Hypertens (Dallas Tex 1979)*. (2012) 59:85–91. doi: 10.1161/HYPERTENSIONAHA.111.180513

9. Shahrrava A, Moinuddin S, Boddu P, Shah R. A case of glucocorticoid remediable aldosteronism and thoracoabdominal aneurysms. *Case Rep Endocrinol*. (2016) 2016:1–4. doi: 10.1155/2016/2017571

10. Methe H, Pehlivanli S. Glucocorticoid-remediable aldosteronism in a young adult with a family history of Conn's syndrome. *Clin Case Rep*. (2018) 6:416–9. doi: 10.1002/CCR3.1377

11. Cheng CY, Liao HW, Peng KY, Chen TH, Lin YH, Chueh JS, et al. Characteristics and outcomes in primary aldosteronism patients harboring glucocorticoid-remediable aldosteronism. *Biomedicines*. (2021) 9. doi: 10.3390/BIOMEDICINES9121816

12. Carvajal CA, Stehr CB, González PA, Riquelme EM, Montero T, Santos MJ, et al. A *de novo* unequal cross-over mutation between CYP11B1 and CYP11B2 genes causes familial hyperaldosteronism type I. *J Endocrinol Invest*. (2011) 34:140–4. doi: 10.1007/BF03347044

13. Kamrath C, Maser-Gluth C, Haag C, Schulze E. Diagnosis of glucocorticoid-remediable aldosteronism in hypertensive children. *Horm Res Paediatr*. (2011) 76:93–8. doi: 10.1159/000326524

14. Yokota K, Ogura T, Kishida M, Suzuki J, Otsuka F, Mimura Y, et al. Japanese family with glucocorticoid-remediable aldosteronism diagnosed by long-polymerase chain reaction. *Hypertens Res*. (2001) 24:589–94. doi: 10.1291/HYPRES.24.589

15. Dluhy RG, Anderson B, Harlin B, Ingelfinger J, Lifton R. Glucocorticoid-remediable aldosteronism is associated with severe hypertension in early childhood. *J Pediatr*. (2001) 138:715–20. doi: 10.1067/MPD.2001.112648

16. Campino C, Trejo P, Carvajal CA, Vecchiola A, Valdivia C, Fuentes CA, et al. Pregnancy normalized familial hyperaldosteronism type I: a novel role for progesterone? *J Hum Hypertens*. (2015) 29:138–9. doi: 10.1038/JHH.2014.49

17. Lee IS, Kim SY, Jang HW, Kim MK, Lee JH, Lee YH, et al. Genetic analyses of the chimeric CYP11B1/CYP11B2 gene in a Korean family with glucocorticoid-remediable aldosteronism. *J Korean Med Sci*. (2010) 25:1379–83. doi: 10.3346/JKMS.2010.25.9.1379

18. Gill JR, Bartter FC. Overproduction of sodium-retaining steroids by the zona glomerulosa is adrenocorticotropin-dependent and mediates hypertension in dexamethasone-suppressible aldosteronism. *J Clin Endocrinol Metab*. (1981) 53:331–7. doi: 10.1210/JCEM-53-2-331

19. Fallo F, Sonino N, Armanini D, Luzzi T, Pedini F, Pasini C, et al. A new family with dexamethasone-suppressible hyperaldosteronism: aldosterone unresponsiveness to angiotensin II. *Clin Endocrinol (Oxf)*. (1985) 22:777–85. doi: 10.1111/j.1365-2265.1985.tb00168.x

20. Seeman T, Widimský J, Hampf M, Bernhardt R. Abolished nocturnal blood pressure fall in a boy with glucocorticoid-remediable aldosteronism. *J Hum Hypertens*. (1999) 13:823–8. doi: 10.1038/SJ.JHH.1000918

21. Liu X, Jin L, Zhang H, Ma W, Song L, Zhou X, et al. A Chinese pedigree with glucocorticoid remediable aldosteronism. *Hypertens Res*. (2021) 44:1428–33. doi: 10.1038/S41440-021-00685-3

22. Fallo F, Pilon C, Williams TA, Sonino N, Morra Di Cella S, Veglio F, et al. Coexistence of different phenotypes in a family with glucocorticoid-remediable aldosteronism. *J Hum Hypertens*. (2004) 18:47–51. doi: 10.1038/SJ.JHH.1001636

23. Stowasser M, Sharman J, Leano R, Gordon RD, Ward G, Cowley D, et al. Evidence for abnormal left ventricular structure and function in normotensive individuals with familial hyperaldosteronism type I. *J Clin Endocrinol Metab*. (2005) 90:5070–6. doi: 10.1210/jc.2005-0681

24. Stowasser M, Huggard PR, Rossetti TR, Bachmann AW, Gordon RD. Biochemical evidence of aldosterone overproduction and abnormal regulation in normotensive individuals with familial hyperaldosteronism type I. *J Clin Endocrinol Metab*. (1999) 84:4031–6. doi: 10.1210/JCEM.84.11.6159

25. Litchfield WR, New MI, Coolidge C, Lifton RP, Dluhy RG. Evaluation of the dexamethasone suppression test for the diagnosis of glucocorticoid-remediable aldosteronism. *J Clin Endocrinol Metab*. (1997) 82:3570–3. doi: 10.1210/JCEM.82.11.4381

26. Mulatero P, Di Cella SM, Williams TA, Milan A, Mengozzi G, Chiandussi L, et al. Glucocorticoid remediable aldosteronism: low morbidity and mortality in a four-generation italian pedigree. *J Clin Endocrinol Metab*. (2002) 87:3187–91. doi: 10.1210/JCEM.87.7.8647

27. Al Romhain B, Young AMH, Battacharya JJ, Suttner N. Intracranial aneurysm in a patient with glucocorticoid-remediable aldosteronism. *Br J Neurosurg*. (2015) 29:715–7. doi: 10.3109/02688697.2015.1023775

28. Vonend O, Altenhenne C, Büchner NJ, Dekomien G, Maser-Gluth C, Weiner SM, et al. A German family with glucocorticoid-remediable aldosteronism. *Nephrol Dial Transplant*. (2007) 22:1123–30. doi: 10.1093/NDT/GFL706

29. Lin YF, Peng KY, Chang CH, Hu YH, Wu VC, Chueh JS, et al. Adrenalectomy completely cured hypertension in patients with familial hyperaldosteronism type I who had somatic KCNJ5 mutation. *J Clin Endocrinol Metab*. (2019) 104:5462–6. doi: 10.1210/JC.2019-00689

30. Gordon RD, Stowasser M, Tunny TJ, Klemm SA, Finn WL, Krek AL. Clinical and pathological diversity of primary aldosteronism, including a new familial variety. *Clin Exp Pharmacol Physiol*. (1991) 18:283–6. doi: 10.1111/j.1440-1681.1991.tb01446.x

31. Lafferty AR, Torpy DJ, Stowasser M, Taymans SE, Lin JP, Huggard P, et al. A novel genetic locus for low renin hypertension: familial hyperaldosteronism type II maps to chromosome 7 (7p22). *J Med Genet*. (2000) 37:831–5. doi: 10.1136/JMG.37.11.831

32. Fernandes-Rosa FL, Daniil G, Orozco IJ, Göppner C, El Zein R, Jain V, et al. A gain-of-function mutation in the CLCN2 chloride channel gene causes primary aldosteronism. *Nat Genet*. (2018) 50:355–61. doi: 10.1038/S41588-018-0053-8

33. Stowasser M, Gordon RD, Tunny TJ, Klemm SA, Finn WL, Krek AL. Familial hyperaldosteronism type II: five families with a new variety of primary aldosteronism. *Clin Exp Pharmacol Physiol*. (1992) 19:319–22. doi: 10.1111/j.1440-1681.1992.tb00462.x

34. Scholl UI, Stölting G, Schewe J, Thiel A, Tan H, Nelson-Williams C, et al. CLCN2 chloride channel mutations in familial hyperaldosteronism type II. *Nat Genet*. (2018) 50:349–54. doi: 10.1038/s41588-018-0048-5

35. Sukor N, Mulatero P, Gordon RD, So A, Duffy D, Bertello C, et al. Further evidence for linkage of familial hyperaldosteronism type II at chromosome 7p22 in Italian as well as Australian and South American families. *J Hypertens*. (2008) 26:1577–82. doi: 10.1097/HJH.0B013E3283028352

36. Malagon-Rogers M. Non-glucocorticoid-remediable aldosteronism in an infant with low-renin hypertension. *Pediatr Nephrol*. (2004) 19:235–6. doi: 10.1007/S00467-003-1339-2

37. Torpy DJ, Gordon RD, Lin JP, Huggard PR, Taymans SE, Stowasser M, et al. Familial hyperaldosteronism type II: description of a large kindred and exclusion of the aldosterone synthase (CYP11B2) gene. *J Clin Endocrinol Metab*. (1998) 83:3214–8. doi: 10.1210/JCEM.83.9.5086

38. Pallauf A, Schirpenbach C, Zwermann O, Fischer E, Morak M, Holinski-Feder E, et al. The prevalence of familial hyperaldosteronism in apparently sporadic primary aldosteronism in Germany: a single center experience. *Horm Metab Res*. (2012) 44:215–20. doi: 10.1055/S-0031-1299730

39. Elphinstone MS, Gordon RD, So A, Jeske YWA, Stratakis CA, Stowasser M. Genomic structure of the human gene for protein kinase A regulatory subunit R1-beta (PRKAR1B) on 7p22: no evidence for mutations in familial hyperaldosteronism type II in a large affected kindred. *Clin Endocrinol (Oxf)*. (2004) 61:716–23. doi: 10.1111/j.1365-2265.2004.02155.x

40. Ise T, Shimoda A, Takakuwa H, Kato T, Izumiya Y, Shimizu K, et al. A chimeric CYP11B1/CYP11B2 gene in glucocorticoid-insuppressible familial hyperaldosteronism. *Clin Endocrinol (Oxf)*. (2001) 55:131–4. doi: 10.1046/j.1365-2265.2001.01192.x

41. Somekh NN, Finkielstein D. A mother/daughter case of familial hyperaldosteronism. *Clin Cardiol*. (2010) 33:E68–9. doi: 10.1002/CLC.20654

42. Geller DS, Zhang J, Wisgerhof MV, Shackleton C, Kashgarian M, Lifton RP. A novel form of human mendelian hypertension featuring nonglucocorticoid-remediable aldosteronism. *J Clin Endocrinol Metab*. (2008) 93:3117–23. doi: 10.1210/JC.2008-0594

43. Scholl UI, Stölting G, Nelson-Williams C, Vichot AA, Choi M, Loring E, et al. Recurrent gain of function mutation in calcium channel CACNA1H causes early-onset hypertension with primary aldosteronism. *Elife*. (2015) 4:e06315. doi: 10.7554/eLife.06315

44. Ruiz-Sánchez JG, Paja-Fano M, González Boillos M, Pla Peris B, Pascual-Corrales E, García Cano AM, et al. Impact of obesity on clinical characteristics of Primary Aldosteronism patients at diagnosis and post-surgical response. *J Clin Endocrinol Metab*. (2023) 109(1):e379–88. doi: 10.1210/CLINEM/DGAD400

45. Funder JW, Carey RM, Mantero F, Murad MH, Reincke M, Shibata H, et al. The management of primary aldosteronism: Case detection, diagnosis, and treatment: An endocrine society clinical practice guideline. *J Clin Endocrinol Metab*. (2016) 101:1889–916. doi: 10.1210/jc.2015-4061

46. Monticone S, Sconfienza E, D'Ascenzo F, Buffolo F, Satoh F, Sechi LA, et al. Renal damage in primary aldosteronism: A systematic review and meta-analysis. *J Hypertens*. (2020) 38(1):3–12. doi: 10.1097/HJH.0000000000002216

47. Parra Ramírez P, Martín Rojas-Marcos P, Paja Fano M, González Boillos M, Peris BP, Pascual-Corrales E, et al. Is adrenal venous sampling always necessary to differentiate between unilateral and bilateral primary aldosteronism? Lesson from the SPAIN-ALDO register. *Endocrine*. (2023). doi: 10.1007/s12020-023-03609-y

48. Williams TA, Lenders JWM, Mulatero P, Burrello J, Rottenkolber M, Adolf C, et al. Outcomes after adrenalectomy for unilateral primary aldosteronism: an international consensus on outcome measures and analysis of remission rates in an international cohort. *Lancet Diabetes Endocrinol*. (2017) 5:689–99. doi: 10.1016/S2213-8587(17)30135-3

49. Baethge C, Goldbeck-Wood S, Mertens S. SANRA-a scale for the quality assessment of narrative review articles. *Res Integr Peer Rev*. (2019) 4. doi: 10.1186/S41073-019-0064-8

50. Mulatero P, Tauber P, Zennaro MC, Monticone S, Lang K, Beuschlein F, et al. KCNJ5 mutations in European families with nonglucocorticoid remediable familial hyperaldosteronism. *Hypertension*. (2012) 59:235–40. doi: 10.1161/HYPERTENSIONAHA.111.183996

51. Takizawa N, Tanaka S, Nishimoto K, Sugiura Y, Suematsu M, Ohe C, et al. Familial hyperaldosteronism type 3 with a rapidly growing adrenal tumor: an *in situ* aldosterone imaging study. *Curr Issues Mol Biol*. (2021) 44:128–38. doi: 10.3390/CIMB44010010

52. Tamura A, Nishimoto K, Seki T, Matsuzawa Y, Saito J, Omura M, et al. Somatic KCNJ5 mutation occurring early in adrenal development may cause a novel form of juvenile primary aldosteronism. *Mol Cell Endocrinol*. (2017) 441:134–9. doi: 10.1016/J.MCE.2016.07.031

53. Adachi M, Muroya K, Asakura Y, Sugiyama K, Homma K, Hasegawa T. Discordant genotype-phenotype correlation in familial hyperaldosteronism type III with KCNJ5 gene mutation: a patient report and review of the literature. *Horm Res Paediatr*. (2014) 82:138–42. doi: 10.1159/000358197

54. Greco RG, Carroll JE, Morris DJ, Grekin RJ, Melby JC. Familial hyperaldosteronism, not suppressed by dexamethasone. *J Clin Endocrinol Metab*. (1982) 55:1013–6. doi: 10.1210/JCEM-55-5-1013

55. Gomez-Sanchez CE, Qi X, Gomez-Sanchez EP, Sasano H, Bohlen MO, Wisgerhof M. Disordered zonal and cellular CYP11B2 enzyme expression in familial hyperaldosteronism type 3. *Mol Cell Endocrinol*. (2017) 439:74–80. doi: 10.1016/J.MCE.2016.10.025

56. Tong A, Liu G, Wang F, Jiang J, Yan Z, Zhang D, et al. A novel phenotype of familial hyperaldosteronism type III: concurrence of aldosteronism and Cushing's syndrome. *J Clin Endocrinol Metab*. (2016) 101:4290–7. doi: 10.1210/JC.2016-1504

57. Pons Fernández N, Moreno F, Morata J, Moriano A, León S, De Mingo C, et al. Familial hyperaldosteronism type III a novel case and review of literature. *Rev Endocr Metab Disord*. (2019) 20:27–36. doi: 10.1007/S11154-018-9481-0

58. Charmandari E, Sertedaki A, Kino T, Merakou C, Hoffman DA, Hatch MM, et al. A novel point mutation in the KCNJ5 gene causing primary hyperaldosteronism and early-onset autosomal dominant hypertension. *J Clin Endocrinol Metab*. (2012) 97. doi: 10.1210/JC.2012-1334

59. Monticone S, Hattangady NG, Penton D, Isales CM, Edwards MA, Williams TA, et al. a Novel Y152C KCNJ5 mutation responsible for familial hyperaldosteronism type III. *J Clin Endocrinol Metab*. (2013) 98:E1861-5. doi: 10.1210/JC.2013-2428

60. Maria AG, Suzuki M, Berthon A, Kamilaris C, Demidowich A, Lack J, et al. Mosaicism for KCNJ5 causing early-onset primary aldosteronism due to bilateral adrenocortical hyperplasia. *Am J Hypertens*. (2020) 33:124–30. doi: 10.1093/AJH/HPZ172

61. Wulczyn K, Perez-Reyes E, Nussbaum RL, Park M. Primary aldosteronism associated with a germline variant in CACNA1H. *BMJ Case Rep*. (2019) 12:e229031. doi: 10.1136/BCR-2018-229031

62. Daniil G, Fernandes-Rosa FL, Chemin J, Blesneac I, Beltrand J, Polak M, et al. CACNA1H mutations are associated with different forms of primary aldosteronism. *EBioMedicine*. (2016) 13:225–36. doi: 10.1016/J.EBIOM.2016.10.002

63. Karwacka I, Obołończyk Ł, Kaniuka-Jakubowska S, Bohdan M, Sworczak K. Progress on genetic basis of primary aldosteronism. *Biomedicines*. (2021) 9:1708. doi: 10.3390/BIOMEDICINES9111708

64. Mulatero P, Monticone S, Deinum J, Amar L, Prejbisz A, Zennaro MC, et al. Genetics, prevalence, screening and confirmation of primary aldosteronism: a position statement and consensus of the Working Group on Endocrine Hypertension of The European Society of Hypertension. *J Hypertens*. (2020) 38:1919–28. doi: 10.1097/HJH.0000000000002510

65. Stowasser M, Bachmann AW, Huggard PR, Rossetti TR, Gordon RD. Severity of hypertension in familial hyperaldosteronism type I: relationship to gender and degree of biochemical disturbance. *J Clin Endocrinol Metab*. (2000) 85:2160–6. doi: 10.1210/JCEM.85.6.6651

66. Funder JW. Primary aldosteronism: Mutations, mechanisms, prevalence, and public health. *Hypertension*. (2019) 74:458–66. doi: 10.1161/HYPERTENSIONAHA.119.12935

67. Pitsava G, Faucz FR, Stratakis CA, Hannah-Shmouni F. Update on the genetics of primary aldosteronism and aldosterone-producing adenomas. *Curr Cardiol Rep*. (2022) 24:1189–95. doi: 10.1007/s11886-022-01735-z.

68. Choi M, Scholl UI, Yue P, Björklund P, Zhao B, Nelson-Williams C, et al. K+ channel mutations in adrenal aldosterone-producing adenomas and hereditary hypertension. *Science (80-)*. (2011) 331:768–72. doi: 10.1126/science.1198785

frontiers | Frontiers in Endocrinology

TYPE Original Research
PUBLISHED 08 April 2024
DOI 10.3389/fendo.2024.1336128

OPEN ACCESS

EDITED BY
Piotr Glinicki,
Centre of Postgraduate Medical Education, Poland

REVIEWED BY
Wasineenart Mongkolpun,
Mahidol University, Thailand
Alice Helena Dutra Violante,
Federal University of Rio de Janeiro, Brazil

*CORRESPONDENCE
Bo Long
longbo_27@163.com

†These authors have contributed equally to this work

RECEIVED 10 November 2023
ACCEPTED 25 March 2024
PUBLISHED 08 April 2024

CITATION
Liu L, Shang L, Zhuang Y, Su X, Li X, Sun Y and Long B (2024) Exploration of factors affecting hemodynamic stability following pheochromocytoma resection - cohort study. *Front. Endocrinol.* 15:1336128. doi: 10.3389/fendo.2024.1336128

Exploration of factors affecting hemodynamic stability following pheochromocytoma resection - cohort study

Lidan Liu†, Lihua Shang†, Yimeng Zhuang, Xiaojing Su, Xue Li, Yumeng Sun and Bo Long*

Department of Anesthesiology, Shengjing Hospital of China Medical University, Shenyang, China

Purpose: Surgery is the only way to cure pheochromocytoma; however, postoperative hemodynamic instability is one of the main causes of serious complications and even death. This study's findings provide some guidance for improved clinical management.

Patients and methods: This study was to investigate the factors leading to postoperative hemodynamic instability in the postoperative pathology indicated pheochromocytoma from May 2016 to May 2022. They were divided into two groups according to whether vasoactive drugs were used for a median number of days or more postoperatively. The factors affecting the postoperative hemodynamics in the perioperative period (preoperative, intraoperative, and postoperative) were then evaluated.

Results: The median number of days requiring vasoactive drug support postoperatively was three in 234 patients, while 118 (50.4%) patients required vasoactive drug support for three days or more postoperatively. The results of the multivariate analysis indicated more preoperative colloid use (odds ratio [OR] =1.834, confidence interval [CI]:1.265–2.659, P=0.001), intraoperative use of vasoactive drug (OR=4.174, CI:1.882–9.258, P<0.001), and more postoperative crystalloid solution input per unit of body weight per day (ml/kg/d) (OR=1.087, CI:1.062–1.112, P<0.001) were risk factors for predicting postoperative hemodynamic instability. The optimal cutoff point of postoperative crystalloid use were 42.37 ml/kg/d.

Conclusion: Hemodynamic instability is a key issue for consideration in the perioperative period of pheochromocytoma. The amount of preoperative colloid use, the need for intraoperative vasoactive drugs, and postoperative crystalloid solution are risk factors for predicting postoperative hemodynamic instability (registration number: ChiCT2300071166).

KEYWORDS

haemodynamic instability, pheochromocytoma, postoperative hypotension, vasoactive drug, perioperative management

Introduction

Pheochromocytomas are endocrine tumors of adrenal medullary origin, characterized by the secretion of catecholamines, including norepinephrine, epinephrine, and dopamine. Subsequently, severe cardiovascular disease is induced, including severe hypertensive crisis, arrhythmias, myocardial infarction, and acute heart failure (1, 2). While surgical resection is the only cure for this disease, the presence of hemodynamic fluctuations in the perioperative period seriously endangers the patient's life. For example, tracheal intubation, change of position, the establishment of pneumoperitoneum, and touching the tumor will cause massive secretion of catecholamines and a dramatic increase in blood pressure, while a sudden decrease in catecholamines following tumor removal will result in persistent intractable hypotension and hypoglycemia (3).

The predictors of intraoperative hemodynamic instability in pheochromocytoma have been reported to include preoperative blood pressure control level, tumor size, preoperative catecholamine level, and surgical approach (4, 5), while the predictors of postoperative hypotension include preoperative beta-blocker use (6), type of preoperative alpha-blocker use (7), catecholamine secretion level (7), and tumor size (8). In fact, various studies have reported that tumor size is not an influencing factor in predicting hemodynamic instability; however, this was likely because the size of the tumor in these studies was comparatively small (7). Meanwhile, studies have also reported no difference in the effect of different surgical approaches (9, 10).

Most current studies focus on preoperative and intraoperative management, with few studies focusing on postoperative management. Both the hemodynamic effects of large intraoperative catecholamine release and the dramatic decrease in catecholamine levels following tumor resection may persist into the postoperative period, and the investigation of postoperative management should not be neglected in view of reducing hemodynamic fluctuations. The aim of this study was to explore the factors affecting the use of vasoactive drugs in the postoperative period.

Materials and methods

Study design and patient selection

The study has been reported in line with the STROCSS criteria (11) and ethical approval was granted, which applied for a waiver of informed consent. The study has been registered in the Chinese Clinical Trial Registry. This was a single-center retrospective study conducted between May 2016 and 2022. A total of 254 adrenalectomy patients from the same surgical group of operators with postoperative pathology of pheochromocytoma were included.20 were excluded. Among them, five were excluded due to bilateral pheochromocytoma, and fifteen were excluded due to incomplete data. The final 234 patients were included in the statistical analysis and were divided into two groups according to the median time(whether it is≥3 days) of the postoperative use of vasoactive drugs (Figure 1).

Preoperative management

Preoperative treatment with terazosin or other antihypertensive agents is required for patients with biochemical parameters, clinical symptoms, or imaging suspicion of pheochromocytoma. The need for beta-adrenergic receptor blockers to control the heart rate is determined by the presence of tachycardia. For patients with severe preoperative clinical symptoms and a large tumor size, as determined via imaging, appropriate volume expansion therapy (crystalloid/colloid/albumin/plasma/erythrocytes) should be administered 2–3 days prior to surgery. Here, the preoperative control criteria were orthostatic hypotension of <130/80 mm Hg and a heart rate of <90/min.

Outcomes

The basic preoperative information (gender, age, weight, body mass index [BMI]), the presence of diabetes, coronary heart disease comorbidity, American Society of Anesthesiologists classification, tumor size, preoperative blood pressure, preoperative medication, preoperative ionic disturbances, preoperative fluid replacement, blood transfusion and albumin transfusion were recorded. The mode of surgery, the duration of surgery, whether intraoperative vasoactive drugs were used, the amount of norepinephrine used, intraoperative blood and fluid transfusion, intraoperative urine volume, the amount of tachyphylaxis used were also recorded. In addition, whether the patients were admitted to the intensive care unit following surgery, as well as information related to postoperative blood transfusion, albumin transfusion, amount of rehydration fluid, postoperative 24 h urine volume, tachyphylaxis use, and postoperative hospitalization time were examined.

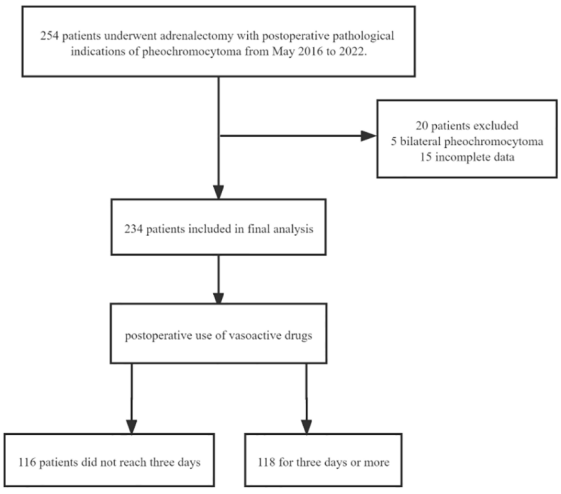

FIGURE 1
Flow diagram of the study.

Statistical analysis

The statistical analysis was conducted using IBM SPSS Statistics for Windows, Version 25.0. The normality of the continuous variables was determined using the Shapiro–Wilk test, with the variables following normal distribution expressed as mean ± standard deviation (SD). The non-normally distributed continuous variables were presented in terms of median (interquartile range). The means of two continuous normally distributed variables were compared using the independent samples Student's t-test, while the Mann–Whitney U-test was used to compare two continuous non-normally distributed variables. The categorical variables were presented in terms of quantity (percentage), with a chi-square test and Fisher's exact test used to compare these variables.

To ascertain the association between duration of use and the preoperative, intraoperative, and postoperative factors, univariate analysis was performed in terms of patients who used norepinephrine for a number of days at or above the median and those who did not. Factors with a P-value of <0.1 in the univariate analysis were included in a multivariate binary logistic regression model. Variance inflation factors (VIFs) were used to evaluate the collinearity, and any variables with severe collinearity (VIF≥10) were excluded from the multivariate analysis. Multivariate logistic regression analysis was performed to determine the predictors of postoperative norepinephrine use reaching and exceeding the median number of days, with the variables selected using a forward approach. The cutoff values and the area under the curve values for the continuous variables that were independent risk factors for norepinephrine use reaching and exceeding the median number of days were calculated using receiver operating characteristic curve analysis. A P-value of <0.05 was considered to be statistically significant.

Results

Among the included 234 patients, the median time to postoperative need for norepinephrine for hypotension was three days, and compared with the patients who did not reach three days of vasoactive drug use, those who reached or exceeded this point had a lower BMI (23.1 vs. 24.2 kg/m2, P=0.012), a larger tumor (5.0 vs. 4.4 cm, P=0.003), lowerer doses preoperative doxazosin use (4.5 vs. 5 mg, P=0.001), more preoperative crystalloid solution (1225 vs. 0 ml, P<0.001), and higher colloid use (500 vs. 0 ml, P<0.001). There was no significant difference in age and sex between the two groups. The detailed intraoperative information is provided in Table 1.

Compared with the patients who did not reach the median number of days of postoperative vasopressor use, a higher proportion of patients who received intraoperative vasopressor treatment required vasoactive drug support to meet or exceed the median number of days after surgery (85.6% vs. 46.6%, P<0.001), as well as higher intraoperative norepinephrine use (0.6 vs. 0 mg, P<0.001) and more intraoperative fluid infusions (3000 vs. 2,500 ml, P=0.001). The detailed intraoperative information is provided in Table 2. The patients who reached or exceeded the median number of days of postoperative crystalloid solution input (57.4 vs. 26.2 ml/kg/d, P<0.001) had a longer postoperative hospital stay compared with those who did not reach the median number of days of postoperative booster use (ten vs. seven days P<0.001). Detailed information is provided in Table 3.

All variables with a P-value of <0.1 were included in the multivariate regression analysis (Table 4). The logistic regression analysis results indicated that the amount of preoperative colloid use (odds ratio [OR]=1.834, confidence interval [CI]:1.265–2.659, P=0.001), intraoperative booster use (OR=4.174, CI:1.882–9.258, P<0.001), and postoperative crystalloid solution input (ml/kg/d) (OR=1.087, CI:1.062–1.112, P<0.001) were risk factors for predicting postoperative hemodynamic instability (Table 4).

In addition, the optimal cutoff point of the amount of postoperative crystalloid solution used were 42.37 ml/kg/d, which were analyzed using the receiver operating characteristic curve method (Figure 2).

Discussion

There is no clear uniform definition of hemodynamic instability (12). In this study, the need for vasoactive drugs for a median number of days postoperatively was defined as hemodynamic instability in view of investigating the factors affecting hemodynamic stability following surgery.

Postoperative hemodynamic instability mainly refers to the postoperative development of hypotension, which requires the use of vasoactive drugs to maintain the blood pressure levels. According to current reports, the common causes of postoperative hypotension include a sudden drop in catecholamine levels following tumor resection or decreased vascular tone due to vascular insensitivity to catecholamines, decreased myocardial function that cannot compensate for peripheral vasodilation, relative fluid deficiency, residual effects of the preoperative use of alpha-adrenergic receptor blockers, or excessive intraoperative blood loss (8, 13). Various studies have suggested that the incidence of postoperative hypotension is approximately 30%–60%, which is consistent with the results of the present study (8, 14).

The results of the present study indicated that the intraoperative use of vasoactive drugs during pheochromocytoma resection is 3.174 times more likely to be a risk factor for the development of hemodynamic instability following surgery than the non-use of these drugs. In our study, intraoperative vasoactive drugs were used in 85.6% of the patients, and more than two-thirds of these patients had an intraoperative episode of hypotension requiring treatment. Previous studies have reported intraoperative hypotension requiring vasoactive drug as an independent risk factor for postoperative cardiovascular morbidity (15). Li et al. (16) also suggested that the presence of intraoperative hypotension is an independent risk factor for complications, while Pisarska-Adamczyk et al. (15) suggested that intraoperative treatment of hypotension with vasoactive drugs was the only risk factor for the development of postoperative hypotension. These findings are similar to those obtained in the present study.

The persistence of high levels of catecholamines in the body preoperatively may result in desensitization of the adrenergic

TABLE 1 Demographics and perioperative data between two groups.

Variables	Vasopressor use <3d N=116	Vasopressor use ≥3d N=118	Total N=234	P-value
Female	58 (50.0%)	61 (51.7%)	119 (50.9%)	0.795
Age (years)	54.5 (45.3-62.0)	53.0 (45.8-62.0)	52.5 (45.8-62.0)	0.715
Body weight (kg)	67.1 ± 10.3	62.5 ± 11.0	64.8 ± 10.9	0.645
BMI (kg/m2)	24.2 (21.8-25.4)	23.1 (20.8-24.6)	23.6 (21.4-24.8)	0.012
Diabetes mellitus	32 (27.6%)	38 (32.2%)	70 (29.9%)	0.441
Coronary artery disease	15 (12.9%)	12 (10.2%)	27 (11.5%)	0.509
Hypertension	49 (42.2%)	50 (42.4%)	99 (42.3%)	0.984
Maximal size (cm)	4.4 (3.0-6.0)	5.0 (4.0-6.8)	4.9 (3.5-6.0)	0.003
ASA				<0.001
II	81 (69.8%)	75 (63.6%)	156 (66.7%)	
III	35 (30.2%)	43 (36.4%)	78 (33.3%)	
terazosin (mg)	5 (0-8)	4.5 (0-22)	2 (0-16)	0.001
other antihypertensive agents	29 (25.0%)	31 (26.3%)	60 (25.6%)	0.824
low potassium	9 (7.8%)	7 (5.9%)	16 (6.8%)	0.580
crystal (ml)	0 (0-1500)	1225 (0-2500)	1000 (0-2000)	<0.001
colloid (ml)	0 (0-500)	500 (0-1500)	250 (0-1000)	<0.001
RBC (U)	0 (0-0)	0 (0-0)	0 (0-0)	0.199
Plasma (ml)	0 (0-0)	0 (0-0)	0 (0-0)	0.010
albumin (g)	0 (0-0)	0 (0-10)	0 (0-0)	<0.001

Continuous variables with normal distribution were reported as the mean ± standard deviation (SD); non-normal continuous variables were expressed as median (interquartile range); categorical variables were reported as number(percentage).
BMI, body mass index; ASA, American Society of Anesthesiologists.

TABLE 2 Intraoperative data of patients between two groups.

Variables	Vasopressor use <3d N=116	Vasopressor use ≥3d N=118	Total N=234	P-value
Laparoscopy	101 (87.0%)	103 (87.3%)	204 (87.2%)	0.960
Intraoperative vasopressor support	54 (46.6%)	101 (85.6%)	155 (66.2%)	<0.001
Duration of surgery (minutes)	150 (120-180)	169 (120-210)	150 (120-205.2)	0.072
Total infusion volume (ml)	2500 (1725-3300)	3000 (2200-3800)	2600 (2000-3500)	0.001
Crystal (ml)	1775 (1300-2500)	2000 (1500-2800)	2000 (1400-2700)	0.018
Colloid (ml)	500 (500-1000)	750 (500-1000)	500 (500-1000)	0.003
RBC (U)	0 (0-0)	0 (0-2)	0 (0-0)	0.001
Plasma (ml)	0 (0-0)	0 (0-0)	0 (0-0)	0.001
Urine output (ml)	500 (280-700)	680 (400-1000)	600 (350-800)	<0.001
Furosemide (mg)	0 (0-0)	0 (0-0)	0 (0-0)	0.664
Estimated blood loss (ml)	100 (30-200)	150 (50-500)	100 (50-237)	0.003
Goal-directed fluid therapy	11 (9.5%)	14 (11.9%)	25 (10.7%)	0.555
Norepinephrine (mg)	0 (0-0.2)	0.6 (0.1-2.1)	0.2 (0-0.8)	<0.001

TABLE 3 Postoperative data between two groups.

Variables	Vasopressor use <3天 N=116	Vasopressor use≥3天 N=118	TOTAL N=234	P-value
ICU	27 (23.3%)	41 (34.7%)	68 (29.1%)	0.053
Crystal (ml/kg/d)	26.2 (18.8-38.8)	57.4 (43.8-70.8)	42.4 (25.5-60.2)	<0.001
RBC (U)	0 (0-0)	0 (0-0)	0 (0-0)	0.252
Plasma (ml)	0 (0-0)	0 (0-0)	0 (0-0)	0.189
24 h urine output (ml)	2150 (1500-2882)	2630 (2000-3400)	2400 (1752-3100)	<0.001
Furosemide (mg)	0 (0-0)	0 (0-20)	0 (0-0)	<0.001
Albumin (g)	0 (0-0)	0 (0-10)	0 (0-0)	<0.001
Hospital stay after Surgery(days)	7.0 (6.0-9.0)	10.0 (8.0-12.0)	8.0 (7.0-11.0)	<0.001

receptors, which reduces the affinity of catecholamines for these receptors or decreases the number of cell surface receptors (17, 18). At this point, while the patient will likely have high levels of catecholamines in the body, they may not present the corresponding clinical manifestations and can be easily overlooked. Intraoperative ligation of tumor veins followed by catecholamine receptor desensitization or a dramatic decrease in catecholamines and the persistence of the effects of preoperative antihypertensive drugs may be possible causes of chronic vascular paralysis hypotension following a tumor resection requiring the use of vasoactive drugs to maintain the blood pressure (19).

Increased preoperative colloid input is also a predictor of the development of hemodynamic instability in the postoperative period, and this study's findings revealed that for every 1,000-ml increase in the amount of colloid infused preoperatively, there is a 0.834-fold increase in the risk of developing hemodynamic instability in the postoperative period. It has been demonstrated that preoperative failure to enter crystalloid solution or colloids is an independent risk factor for postoperative cardiovascular morbidity (20). Recently, it has been recommended that all patients with a high preoperative suspicion of pheochromocytoma should be treated with appropriate infusion for volume expansion to avoid hemodynamic instability in the perioperative period (21, 22). However, there are differing views, with Hao et al. (23) suggesting that in patients undergoing pheochromocytoma resection, preoperative intravenous fluid replacement does not prevent perioperative hemodynamic changes, while Niederle et al. (24) performed goal-directed fluid therapy in patients undergoing pheochromocytoma resection using esophageal Doppler ultrasound to ascertain that the cause of postoperative hypotension was vascular paralysis, rather than true hypovolemia.

The results of this study indicated that the higher the postoperative crystalloid solution input, the higher the risk of postoperative hemodynamic instability. Thompson et al. (6) reported that the appearance of postoperative hypotension was transient and did not have serious consequences for postoperative outcomes, but was associated with increased intravenous input during the first 24 h postoperatively. The amount of crystal input in our study was calculated by comparing the amount per unit of body weight per day, and the results indicated that a higher amount of crystalloid solution input per unit of body weight per day postoperatively was associated with hemodynamic instability. On the one hand, due to the high function of the tumor, which causes vascular paralysis, more vasoactive drugs and fluid expansion are needed, while on the other, the patient's surgical stress response and

TABLE 4 Multivariable analysis for predictors of postoperative norepinephrine use reaching and exceeding the median number of days.

Variables	Odds ratio (95% CI)	P-value
preoperative colloid (ml)	1.834 (1.265-2.659)	0.001
Intraoperative vasopressor support	4.174 (1.882-9.258)	<0.001
postoperation crystal (ml/kg/d)	1.087 (1.062-1.112)	<0.001

CI, confidence interval.

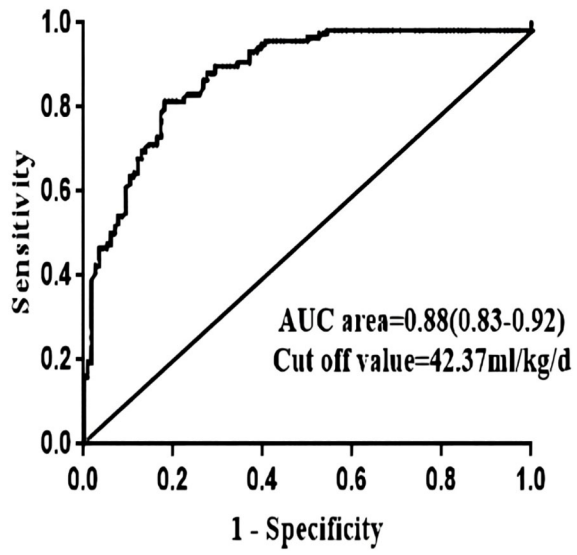

FIGURE 2
ROC curve of continuous independent risk factors (postoperative crystals) of norepinephrine use reaching and exceeding the median number of days. AUC, area under the curve.

violent circulatory fluctuations may lead to intimal damage and capillary leakage, with <5% of the fluid volume remaining in the vessels after 1 h of infusion (25). Furthermore, the large amount of fluid input will aggravate any tissue interstitial edema. Fluid overload with excess volume may lead to decreased cardiac function (26, 27), increased intra-abdominal pressure (26–28), and increased renal venous congestion (29, 30). Elevated intra-abdominal pressure decreases renal perfusion (28) and venous return, with the decreased venous return leading to decreased cardiac output (31) and consequently exacerbating the onset of hypotension.

Fluid input and the use of vasoactive drugs are considered to be the main measures for treating postoperative hemodynamic instability in patients. A growing number of studies have proposed that preoperative volume expansion does not reduce the perioperative hemodynamic fluctuations or the occurrence of related complications, and does not improve the patient's prognosis (32–35). This is largely because crystalloid fluid is free to cross the semi-permeable capillary intima and ends up being stored in the vasculature with only one-fifth of the input volume. While colloidal fluid has a stronger volume expansion effect, this effect only lasts for 24 h (36).

Meanwhile, the hazards associated with volume overload are gradually being appreciated. These hazards include slow repair of acute kidney injury, slow wound healing, prolonged mechanical ventilation (28, 37, 38), acute pulmonary edema, acute respiratory distress syndrome (38–43), and impaired cardiac function (44). Due to the low incidence of pheochromocytoma, most of the relevant studies are currently small-sample single-center retrospective studies. Among them, Niederle et al. (24) conducted a prospective study using minimally invasive hemodynamic monitoring for intraoperative goal-directed fluid therapy and found that patients do not benefit from the use of free fluid infusion and that perioperative volume overload should be avoided. However, the sample in this study was too small and this aspect must be further explored using larger-sample prospective studies.

Conclusion and limitations

This study involved a number of limitations. First, while the factors affecting the intraoperative and postoperative hemodynamic stability of pheochromocytoma resection were comprehensively explored, the low incidence and the difficulty of preoperative diagnosis confirmation made it difficult to complete a randomized prospective study with a small sample size and limited reference space. Second, this study included patients who had a pathological indication of pheochromocytoma in our hospital over the last seven years, and both perioperative management and the surgical techniques have been constantly updated and the level of medical progress has been rapid, meaning the impact of these changes on the results is difficult to estimate. Third, urinary or plasma catecholamine monitoring was not performed, and its effect on hemodynamic instability could not be predicted. Fourth, since this was a retrospective study, all the data were obtained from electronic medical records, which may have resulted in a loss of accuracy and comprehensiveness of the assessment and documentation. While our study included cases of intraoperative goal-directed fluid therapy, it did not reveal a significant difference in terms of the improvement in postoperative hemodynamic instability. This may have been partly due to the limited number of cases and partly because our data were obtained from retrospective electronic medical records without a rigorous prospective study.

In conclusion, the instability and variability of perioperative blood flow in pheochromocytoma and the potential for dramatic intraoperative blood pressure fluctuations, even with adequate preoperative preparation, both surgery and anesthesia for pheochromocytoma should be performed by experienced surgeons who are constantly refining and updating their perioperative management strategies, further prospective randomized controlled studies must be conducted.

Data availability statement

The raw data supporting the conclusions of this article will be made available by the authors, without undue reservation.

Ethics statement

The studies involving humans were approved by Ethics Committee of Shengjing Hospital affiliated to China Medical University. The studies were conducted in accordance with the local legislation and institutional requirements. The participants provided their written informed consent to participate in this study. Written informed consent was obtained from the individual(s) for the publication of any potentially identifiable images or data included in this article.

Author contributions

BL: Conceptualization, Writing – review & editing. LL: Data curation, Investigation, Methodology, Software, Supervision, Writing – original draft. LS: Data curation, Investigation, Methodology, Project administration, Software, Supervision, Validation, Writing – original draft. YZ: Formal analysis, Writing – review & editing. XS: Data curation, Writing – review & editing. XL: Data curation, Writing – review & editing. YS: Data curation, Writing – review & editing.

Funding

The author(s) declare that no financial support was received for the research, authorship, and/or publication of this article.

Conflict of interest

The authors declare that the research was conducted in the absence of any commercial or financial relationships that could be construed as a potential conflict of interest.

Publisher's note

References

1. Lenders JWM, Kerstens MN, Amar L, Prejbisz A, Robledo M, Taieb D, et al. Genetics, diagnosis, management and future directions of research of phaeochromocytoma and paraganglioma: a position statement and consensus of the Working Group on Endocrine Hypertension of the European Society of Hypertension. *J Hypertens*. (2020) 38:1443–56. doi: 10.1097/HJH.0000000000002438

2. Prejbisz A, Lenders JW, Eisenhofer G, Januszewicz A. Cardiovascular manifestations of phaeochromocytoma. *J Hypertens*. (2011) 29:2049–60. doi: 10.1097/HJH.0b013e32834a4ce9

3. Ramakrishna H. Pheochromocytoma resection: Current concepts in anesthetic management. *J Anaesthesiol Clin Pharmacol*. (2015) 31:317–23. doi: 10.4103/0970-9185.161665

4. Kinney MA, Warner ME, vanHeerden JA, Horlocker TT, Young WF Jr, Schroeder DR, et al. Perianesthetic risks and outcomes of pheochromocytoma and paraganglioma resection. *Anesth Analg*. (2000) 91:1118–23. doi: 10.1097/00000539-200011000-00013

5. Gaujoux S, Bonnet S, Lentschener C, Thillois J-M, Duboc D, Bertherat J, et al. Preoperative risk factors of hemodynamic instability during laparoscopic adrenalectomy for pheochromocytoma. *Surg Endosc*. (2016) 30:2984–93. doi: 10.1007/s00464-015-4587-x

6. Thompson JP, Bennett D, Hodson J, Asia M, Ayuk J, O'Reilly MW, et al. Incidence, risk factors and clinical significance of postoperative haemodynamic instability after adrenalectomy for phaeochromocytoma. *Gland Surg*. (2019) 8:729–39. doi: 10.21037/gs

7. Kim JH, Lee HC, Kim SJ, Yoon SB, Kong SH, Yu HW, et al. Perioperative hemodynamic instability in pheochromocytoma and sympathetic paraganglioma patients. *Sci Rep*. (2021) 11:18574. doi: 10.1038/s41598-021-97964-3

8. Namekawa T, Utsumi T, Kawamura K, Kamiya N, Imamoto T, Takiguchi T, et al. Clinical predictors of prolonged postresection hypotension after laparoscopic adrenalectomy for pheochromocytoma. *Surgery*. (2016) 159:763–70. doi: 10.1016/j.surg.2015.09.016

9. Ma L, Shen L, Zhang X, Huang YG. Predictors of hemodynamic instability in patients with pheochromocytoma and paraganglioma. *J Surg Oncol*. (2020) 122:803–8. doi: 10.1002/jso.26079

10. Bruynzeel H, Feelders RA, Groenland TH, Meiracker AH, Eijck CHJ, Lange JF, et al. Risk factors for hemodynamic instability during surgery for pheochromocytoma. *J Clin Endocrinol Metab*. (2010) 95:678–85. doi: 10.1210/jc.2009-1051

11. Mathew G, Agha R, Albrecht J, Goel P, Mukherjee I, Pai P, et al. STROCSS 2021: Strengthening the reporting of cohort, cross-sectional and case-control studies in surgery. *Int J Surg*. (2021) 96:106165. doi: 10.1016/j.ijso.2021.100430

12. Dindo D, Demartines N, Clavien PA. Classification of surgical complications: a new proposal with evaluation in a cohort of 6336 patients and results of a survey. *Ann Surg*. (2004) 240:205–13. doi: 10.1097/01.sla.0000133083.54934.ae

13. Olson SW, Deal LE, Piesman M. Epinephrine-secreting pheochromocytoma presenting with cardiogenic shock and profound hypocalcemia. *Ann Intern Med*. (2004) 140:849–51. doi: 10.7326/0003-4819-140-10-200405180-00033

14. Kong H, Li N, Tian J, Li X-Y. Risk predictors of prolonged hypotension after open surgery for pheochromocytomas and paragangliomas. *World J Surg*. (2020) 44:3786–94. doi: 10.1007/s00268-020-05706-9

15. Pisarska-Adamczyk M, Zawadzka K, Więckowski K, Przęczek K, Major P, Wysocki M, et al. Risk factors for hemodynamic instability during laparoscopic pheochromocytoma resection: a retrospective cohort study. *Gland Surg*. (2021) 10:892–900. doi: 10.21037/gs

16. Li N, Kong H, Li SL, Zhu SN, Zhang Z, Wang DX, et al. Intraoperative hypotension is associated with increased postoperative complications in patients undergoing surgery for pheochromocytoma-paraganglioma: a retrospective cohort study. *BMC Anesthesiol*. (2020) 20:147. doi: 10.1186/s12871-020-01066-y

17. Tsujimoto G, Manger WM, Hoffman BB. Desensitization of beta-adrenergic receptors by pheochromocytoma. *Endocrinology*. (1984) 114:1272–8. doi: 10.1210/endo-114-4-1272

18. Tsujimoto G, Honda K, Hoffman BB, Hashimoto K. Desensitization of postjunctional alpha 1- and alpha 2-adrenergic receptor-mediated vasopressor responses in rat harboring pheochromocytoma. *Circ Res*. (1987) 61:86–98. doi: 10.1161/01.RES.61.1.86

19. Ramachandran R, Rewari V. Current perioperative management of pheochromocytomas. *Indian J Urol*. (2017) 33:19–25. doi: 10.4103/0970-1591.194781

20. Bai S, Yao Z, Zhu X, Li ZD, Jiang YZ, Wang RZ, et al. Risk factors for postoperative cardiovascular morbidity after pheochromocytoma surgery: a large single center retrospective analysis. *Endocr J*. (2019) 66:165–73. doi: 10.1507/endocrj.EJ18-0402

21. Lenders JW, Duh QY, Eisenhofer G, Gimenez-Roqueplo AP, Grebe S, Murad MH, et al. Pheochromocytoma and paraganglioma: an endocrine society clinical practice guideline. *J Clin Endocrinol Metab*. (2014) 99:1915–42. doi: 10.1210/jc.2014-1498

22. Pacak K. Preoperative management of the pheochromocytoma patient. *J Clin Endocrinol Metab*. (2007) 92:4069–79. doi: 10.1210/jc.2007-1720

23. Kong H, Yang JN, Tian J, Li N, Zhang YX, Ye PC, et al. Preoperative intravenous rehydration for patients with pheochromocytomas and paragangliomas: is it necessary? *A propensity score matching analysis. BMC Anesthesiol*. (2020) 20:294. doi: 10.1186/s12871-020-01212-6

24. Niederle MB, Fleischmann E, Kabon B, Niederle B. The determination of real fluid requirements in laparoscopic resection of pheochromocytoma using minimally invasive hemodynamic monitoring: a prospectively designed trial. *Surg Endosc*. (2020) 34:368–76. doi: 10.1007/s00464-019-06777-z

25. Sánchez M, Jiménez-Lendínez M, Cidoncha M, Asensio MJ, Herrerot E, Collado A, et al. Comparison of fluid compartments and fluid responsiveness in septic and non-septic patients. *Anaesth Intensive Care*. (2011) 39:1022–9. doi: 10.1177/0310057X1103900607

26. Micek ST, McEvoy C, McKenzie M, Hampton N, Doherty JA, Kollef MH. Fluid balance and cardiac function in septic shock as predictors of hospital mortality. *Crit Care*. (2013) 17:R246. doi: 10.1186/cc13072

27. Han MJ, Park KH, Shin JH, et al. Influence of daily fluid balance prior to continuous renal replacement therapy on outcomes in critically ill patients. *J Korean Med Sci*. (2016) 31:1337–44. doi: 10.3346/jkms.2016.31.8.1337

28. Malbrain ML, Marik PE, Witters I, et al. Fluid overload, de-resuscitation, and outcomes in critically ill or injured patients: a systematic review with suggestions for clinical practice. *Anaesthesiol Intensive Ther*. (2014) 46:361–80. doi: 10.5603/AIT.2014.0060

29. Schefold JC, Filippatos G, Hasenfuss G, et al. Heart failure and kidney dysfunction: epidemiology, mechanisms and management. *Nat Rev Nephrol*. (2016) 12:610–23. doi: 10.1038/nrneph.2016.113

30. Bielecka-Dabrowa A, Godoy B, Schefold JC, et al. Decompensated heart failure and renal failure: what is the current evidence? *Curr Heart Fail Rep*. (2018) 15:224–38. doi: 10.1007/s11897-018-0397-5

31. Papavramidis TS, Marinis AD, Pliakos I, et al. Abdominal compartment syndrome - Intra-abdominal hypertension: Defining, diagnosing, and managing. *J Emerg Trauma Shock*. (2011) 4:279–91. doi: 10.4103/0974-2700.82224

32. Pheochromocytoma: current concepts of diagnosis and treatment. Combined clinical staff conference at the National Institutes of Health. *Ann Intern Med*. (1966) 65:1302–26. doi: 10.7326/0003-4819-65-6-1302

33. Lentschener C, Gaujoux S, Thillois JM, et al. Increased arterial pressure is not predictive of haemodynamic instability in patients undergoing adrenalectomy for phaeochromocytoma. *Acta Anaesthesiol Scand*. (2009) 53:522–7. doi: 10.1111/j.1399-6576.2008.01894.x

34. Mallat J, Pironkov A, Destandau MS, et al. Systolic pressure variation (Deltadown) can guide fluid therapy during pheochromocytoma surgery. *Can J Anaesth*. (2003) 50:998–1003. doi: 10.1007/BF03018362

35. Iijima T, Takagi T, Iwao Y. An increased circulating blood volume does not prevent hypotension after pheochromocytoma resection. *Can J Anaesth*. (2004) 51:212–5. doi: 10.1007/BF03019097

36. Westphal M, James MF, Kozek-Langenecker S, et al. Hydroxyethyl starches: different products–different effects. *Anesthesiology*. (2009) 111:187–202. doi: 10.1097/ALN.0b013e3181a7ec82

37. Salahuddin N, Sammani M, Hamdan A, et al. Fluid overload is an independent risk factor for acute kidney injury in critically Ill patients: results of a cohort study. *BMC Nephrol*. (2017) 18:45. doi: 10.1186/s12882-017-0460-6

38. Bouchard J, Soroko SB, Chertow GM, et al. Fluid accumulation, survival and recovery of kidney function in critically ill patients with acute kidney injury. *Kidney Int*. (2009) 76:422–7. doi: 10.1038/ki.2009.159

39. Goldstein SL, Currier H, Graf C, et al. Outcome in children receiving continuous venovenous hemofiltration. *Pediatrics*. (2001) 107:1309–12. doi: 10.1542/peds.107.6.1309

40. Goldstein SL, Somers MJ, Baum MA, et al. Pediatric patients with multi-organ dysfunction syndrome receiving continuous renal replacement therapy. *Kidney Int*. (2005) 67:653–8. doi: 10.1111/j.1523-1755.2005.67121.x

41. Gillespie RS, Seidel K, Symons JM. Effect of fluid overload and dose of replacement fluid on survival in hemofiltration. *Pediatr Nephrol*. (2004) 19:1394–9. doi: 10.1007/s00467-004-1655-1

42. National Heart L and Blood Institute Acute Respiratory Distress Syndrome Clinical Trials N, Wiedemann HP, et al. Comparison of two fluid-management strategies in acute lung injury. *N Engl J Med*. (2006) 354:2564–75. doi: 10.1056/NEJMoa062200

43. Brandstrup B, Tønnesen H, Beier-Holgersen R, et al. Effects of intravenous fluid restriction on postoperative complications: comparison of two perioperative fluid regimens: a randomized assessor-blinded multicenter trial. *Ann Surg*. (2003) 238:641–8. doi: 10.1097/01.sla.0000094387.50865.23

44. Beaubien-Souligny W, Bouchard J, Desjardins G, et al. Extracardiac signs of fluid overload in the critically ill cardiac patient: A focused evaluation using bedside ultrasound. *Can J Cardiol*. (2017) 33:88–100. doi: 10.1016/j.cjca.2016.08.012

Frontiers in Endocrinology

Explores the endocrine system to find new therapies for key health issues

The second most-cited endocrinology and metabolism journal, which advances our understanding of the endocrine system. It uncovers new therapies for prevalent health issues such as obesity, diabetes, reproduction, and aging.

Discover the latest Research Topics

See more →

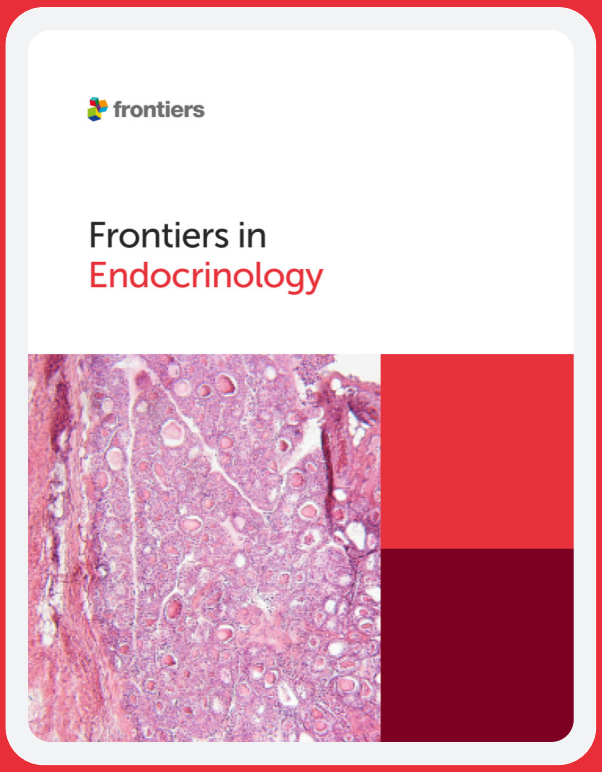

Frontiers

Avenue du Tribunal-Fédéral 34
1005 Lausanne, Switzerland
frontiersin.org

Contact us

+41 (0)21 510 17 00
frontiersin.org/about/contact